DOUBLE SIDE BLADE: NICHE IN STEM CELL POTENCY AND POTENTIAL APPLICATION

EDITED BY: Rita Yen-Hua Huang, Cheng Ming Chuong and Stephanie Ma
PUBLISHED IN: Frontiers in Cell and Developmental Biology

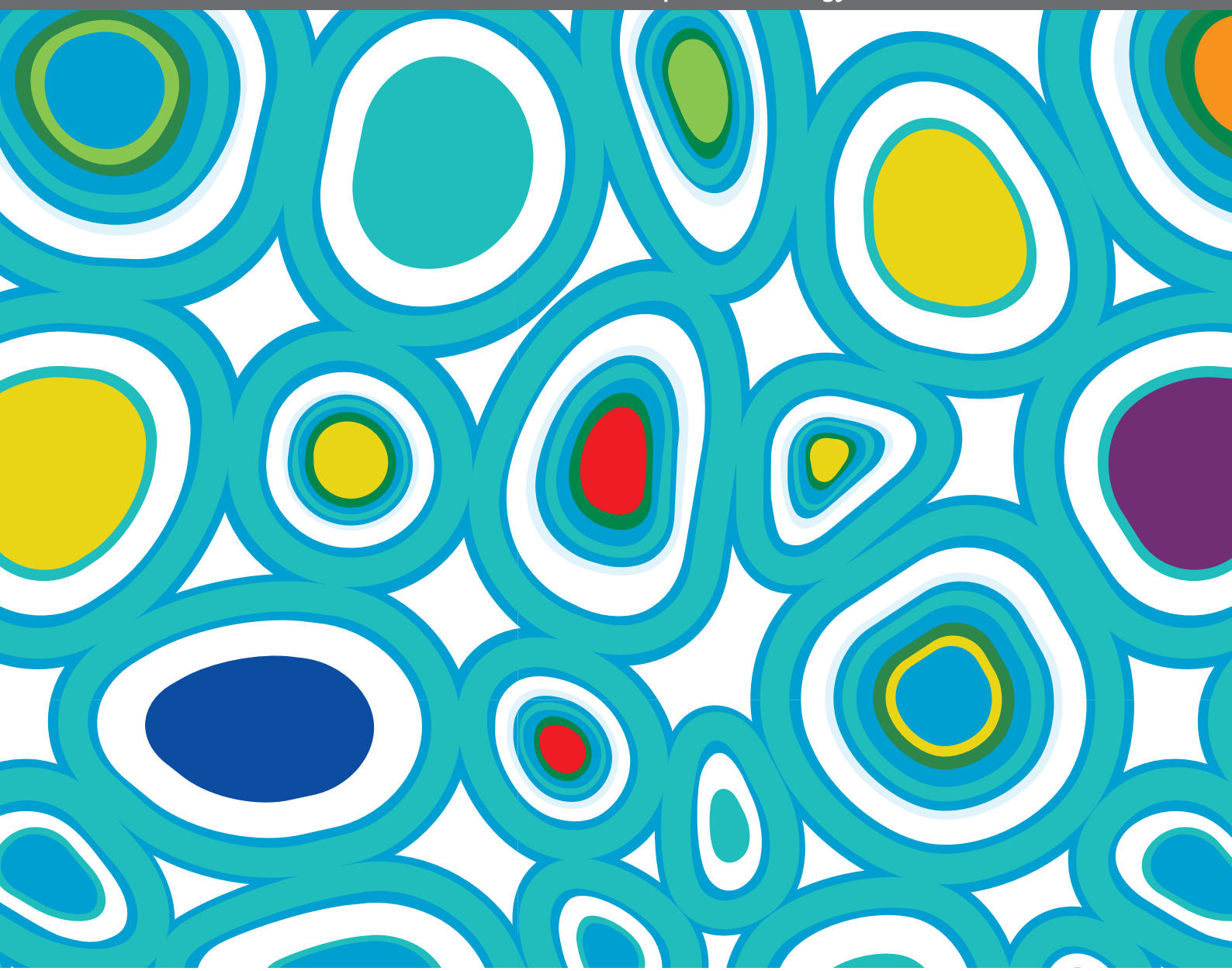

frontiers Research Topics

ISSN 1664-8714
ISBN 978-2-83250-126-9
DOI 10.3389/978-2-83250-126-9

About Frontiers

Frontiers is more than just an open-access publisher of scholarly articles: it is a pioneering approach to the world of academia, radically improving the way scholarly research is managed. The grand vision of Frontiers is a world where all people have an equal opportunity to seek, share and generate knowledge. Frontiers provides immediate and permanent online open access to all its publications, but this alone is not enough to realize our grand goals.

Frontiers Journal Series

The Frontiers Journal Series is a multi-tier and interdisciplinary set of open-access, online journals, promising a paradigm shift from the current review, selection and dissemination processes in academic publishing. All Frontiers journals are driven by researchers for researchers; therefore, they constitute a service to the scholarly community. At the same time, the Frontiers Journal Series operates on a revolutionary invention, the tiered publishing system, initially addressing specific communities of scholars, and gradually climbing up to broader public understanding, thus serving the interests of the lay society, too.

Dedication to Quality

Each Frontiers article is a landmark of the highest quality, thanks to genuinely collaborative interactions between authors and review editors, who include some of the world's best academicians. Research must be certified by peers before entering a stream of knowledge that may eventually reach the public - and shape society; therefore, Frontiers only applies the most rigorous and unbiased reviews.
Frontiers revolutionizes research publishing by freely delivering the most outstanding research, evaluated with no bias from both the academic and social point of view. By applying the most advanced information technologies, Frontiers is catapulting scholarly publishing into a new generation.

What are Frontiers Research Topics?

Frontiers Research Topics are very popular trademarks of the Frontiers Journals Series: they are collections of at least ten articles, all centered on a particular subject. With their unique mix of varied contributions from Original Research to Review Articles, Frontiers Research Topics unify the most influential researchers, the latest key findings and historical advances in a hot research area! Find out more on how to host your own Frontiers Research Topic or contribute to one as an author by contacting the Frontiers Editorial Office: frontiersin.org/about/contact

DOUBLE SIDE BLADE: NICHE IN STEM CELL POTENCY AND POTENTIAL APPLICATION

Topic Editors:
Rita Yen-Hua Huang, Taipei Medical University, Taiwan
Cheng Ming Chuong, University of Southern California, United States
Stephanie Ma, The University of Hong Kong Pokfulam, SAR China

Citation: Huang, R. Y.-H., Chuong, C. M., Ma, S., eds. (2022). Double Side Blade: Niche in Stem Cell Potency and Potential Application. Lausanne: Frontiers Media SA. doi: 10.3389/978-2-83250-126-9

Table of Contents

frontiers in Cell and Developmental Biology

REVIEW
published: 12 January 2021
doi: 10.3389/fcell.2020.625943

Niche Modulation of IGF-1R Signaling: Its Role in Stem Cell Pluripotency, Cancer Reprogramming, and Therapeutic Applications

Pei-Chin Chen[1,2,3], *Yung-Che Kuo*[4], *Cheng-Ming Chuong*[5]* and *Yen-Hua Huang*[2,4,6,7,8,9,10,11]*

[1] Department of Education, Taipei Medical University Hospital, Taipei Medical University, Taipei, Taiwan, [2] Department of Biochemistry and Molecular Cell Biology, School of Medicine, College of Medicine, Taipei Medical University, Taipei, Taiwan, [3] Department of Internal Medicine, Taipei Medical University Hospital, Taipei Medical University, Taipei, Taiwan, [4] TMU Research Center of Cell Therapy and Regeneration Medicine, Taipei Medical University, Taipei, Taiwan, [5] Department of Pathology, Keck School of Medicine, University of Southern California, Los Angeles, CA, United States, [6] International Ph.D. Program for Cell Therapy and Regeneration Medicine, College of Medicine, Taipei Medical University, Taipei, Taiwan, [7] Graduate Institute of Medical Sciences, College of Medicine, Taipei Medical University, Taipei, Taiwan, [8] TMU Research Center of Cancer Translational Medicine, Taipei Medical University, Taipei, Taiwan, [9] Center for Reproductive Medicine, Taipei Medical University Hospital, Taipei Medical University, Taipei, Taiwan, [10] Comprehensive Cancer Center of Taipei Medical University, Taipei, Taiwan, [11] PhD Program for Translational Medicine, College of Medical Science and Technology, Taipei Medical University, Taipei, Taiwan

Stem cells work with their niches harmoniously during development. This concept has been extended to cancer pathology for cancer stem cells (CSCs) or cancer reprogramming. IGF-1R, a classical survival signaling, has been shown to regulate stem cell pluripotency, CSCs, or cancer reprogramming. The mechanism underlying such cell fate determination is unclear. We propose the determination is due to different niches in embryo development and tumor malignancy which modulate the consequences of IGF-1R signaling. Here we highlight the modulations of these niche parameters (hypoxia, inflammation, extracellular matrix), and the targeted stem cells (embryonic stem cells, germline stem cells, and mesenchymal stem cells) and CSCs, with relevance to cancer reprogramming. We organize known interaction between IGF-1R signaling and distinct niches in the double-sided cell fate with emerging trends highlighted. Based on these new insights, we propose that, through targeting IGF-1R signaling modulation, stem cell therapy and cancer stemness treatment can be further explored.

Keywords: IGF-1R, niche, stem cells, cancer stemness, hypoxia, inflammation, extracellular matrix

OPEN ACCESS

Edited by:
Katiucia Batista Silva Paiva, University of São Paulo, Brazil

Reviewed by:
Peter Polverini, University of Michigan, United States
Maria Fernanda Rodrigues, Universidade Nove de Julho, Brazil

***Correspondence:**
Yen-Hua Huang
rita1204@tmu.edu.tw
Cheng-Ming Chuong
cmchuong@usc.edu

Specialty section:
This article was submitted to Stem Cell Research, a section of the journal Frontiers in Cell and Developmental Biology

Received: *04 November 2020*
Accepted: *15 December 2020*
Published: *12 January 2021*

Citation:
Chen P-C, Kuo Y-C, Chuong C-M and Huang Y-H (2021) Niche Modulation of IGF-1R Signaling: Its Role in Stem Cell Pluripotency, Cancer Reprogramming, and Therapeutic Applications. Front. Cell Dev. Biol. 8:625943. doi: 10.3389/fcell.2020.625943

INTRODUCTION

The development of an embryo requires delicate and precise control over cellular mechanisms to establish a structural and functional organism from the stem cells. Recent advances in stem cell research have revealed the detailed processes of embryogenesis, stem cell differentiation, and cell reprogramming. In contrast to embryogenesis, cancer is considered a dysregulated cellular process. Notably, cancer growth use many of the machinery originally used in the development processes, but they are deregulated for cancer growth and metastasis (Reya et al., 2001; Afify and Seno, 2019).

Today, the cancer stemness are thought to derive from direct mutations of stem/progenitor cells (cancer stem cell (CSC) model) or the de-differentiation of cancer cells (cancer reprogramming model) (Bjerkvig et al., 2005). Because of their unlimited self-renewal ability and potential plasticity, the cancer cells with stemness properties are also considered responsible for tumor recurrence, drug resistance, and distant metastasis (Clevers, 2011).

Notably, as researchers have continued to explore the essential signaling pathways that regulate stem cell features in stem cells, these pathways have also been found to control cancer initiation, progression as well as the metastasis of CSCs or cancer cells with stemness-related properties (Taipale and Beachy, 2001; Mishra et al., 2005). For example, Wnt signaling is essential for maintaining the structure and homeostasis of intestinal crypts, and its surrounding mesenchymal cells are the major provider of Wnt ligands, which assist in the functional orchestration of intestinal tissue (Mah et al., 2016). Moreover, excessive Wnt signaling activation is the main trigger of colon cancer initiation, and it is highly expressed in colon CSCs (Basu et al., 2016). In addition, transforming growth factor β (TGF-β) signaling plays a major role in regulating self-renewal and pluripotency in stem cells. It was also proven to be susceptible to hijacking by CSCs to maintain cancer stemness (Sakaki-Yumoto et al., 2013). Nevertheless, the underlying mechanism that switches the role of the same signaling-mediated stemness features between stem cell and cancer reprogramming has been less discussed.

Insulin-like growth factor-1 receptor (IGF-1R) signaling was recently shown to regulate stem cell characteristics during embryogenesis and tumorigenesis (Chang T.S. et al., 2015; Kuo et al., 2018). Interestingly, the interaction between IGF-1R signaling and the niche environment has been shown to modulate IGF-1R signaling itself and the IGF-1R-mediated cellular responses. Here, we review the interaction between IGF-1R signaling and niche environment with specific focus on niche hypoxia, niche inflammation, and the interaction between cell and extracellular matrix, and further explore how such interaction modulates stemness in various stem cells and CSCs (**Figure 1**). These insights might provide greater understanding in finding therapeutic opportunities in stem cell therapy and cancer treatment. In the following sections, we target IGF-1R signaling as a basis to explore how key signaling pathways are modulated in diverse conditions as well as the possible switches in controlling the double-bladed role of IGF-1R signaling in stem cells, CSCs, or cancer reprogramming. We also develop a niche modulation concept to explain this conundrum.

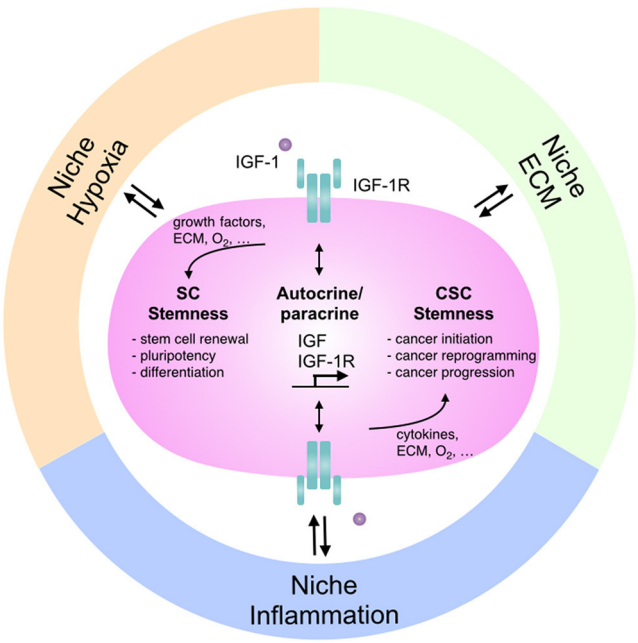

FIGURE 1 | The interactions between IGF-1R signaling and niches: the regulation in stem cells and cancer stemness. Niche microenvironment differs in various physiological and pathological conditions and modulates cellular signaling as well as tissue function accordingly. Different niches affect IGF-1R signaling to regulate stem cell features and control the dual roles of IGF-1R-mediated stemness in stem cell pluripotency and cancer stemness. SC, stem cell; CSC, cancer stem cell; ECM, extracellular matrix.

IGF-1R SIGNALING AND NICHE INTERACTION

IGF-1R is a transmembrane protein in the receptor tyrosine kinase family. It consists of two subunits, namely IGF-1R-α and IGF-1R-β. IGF-1, IGF-2, and insulin are the three ligands of IGF-1R, among which IGF-1 has the highest affinity. Upon ligand stimulation, IGF-1R-β undergoes autophosphorylation and phosphorylates adaptor proteins such as IRS1/2, SHC, and 14-3-3; subsequently, it activates downstream PI3K/AKT, RAS/MAPK, and JAK/STAT signaling, which modulate gene expressions in apoptosis as well as protein synthesis and cell proliferation [reviewed in Girnita et al. (2014)]. Physiologically, IGF-1R signaling is indispensable during normal development. For example, IGF signaling plays a crucial role in regulating organ size. On a large scale, the growth hormone (GH)/IGF-1 axis is essential for postnatal growth. GH insufficiency and deficiency result in smaller body size during an individual's teenage and adult stages; furthermore, IGF-1 expression in GH-deficient mice reverses the decreased body size caused by GH deficiency, suggesting that GH exerts its pro-growth function through IGF-1 (Kaplan and Cohen, 2007; Velloso, 2008). The IGF-1R pathway has also been linked to cancer progression in multiple cancer types, including liver, lung, breast, and colorectal cancers (Dallas et al., 2009; Chang et al., 2013; Chen et al., 2014; Chang T.S. et al., 2015). Given the importance of IGF-1R signaling as a core pathway in regulating multiple cellular responses, more and more studies explore the mechanism of how IGF-1R signaling is modulated. Niche (microenvironment) has been known to modulate cellular signaling through various parameters. The following subsections outline the interaction between different niche properties and IGF-1R signaling and how such interaction affects IGF-1R-mediated cellular responses. We specifically focused on the interaction between IGF-1R and extracellular

matrix, niche hypoxia, as well as niche inflammation, and gave a brief review on nuclear IGF-1R, a possible modulator of IGF-1R signaling that was recently reported (**Figure 2**).

Niche Extracellular Matrix (ECM) and Integrins

ECM and integrins have been demonstrated to modulate IGF-1R signaling directly through the IGF-1R activation (Girnita et al., 2014). In response to the ECM which contains proteins and glycoproteins, the integrins will induce the intracellular signaling to promote cell proliferation and mobility.

Decorin, an extracellular proteoglycan, shows to bind to both IGF-1 and IGF-1R to repress the IGF-1R activation. Therefore, the downregulation of decorin in bladder cancer results in decreased migration ability and mobility (Iozzo et al., 2011). Mechanical stress and ECM binding enhance the IGF-1/IGF-1R signaling through recruiting integrins and integrin-associated downstream adaptor proteins to the IGF-1R (Tahimic et al., 2016). Supportively, the activation of integrin was shown to transactivate the IGF-1R through adaptor proteins (Girnita et al., 2014). In addition, Takada et al. demonstrated that IGF-1 is able to bind both the IGF-1R and integrins to form a tertiary complex that strengthens the IGF-1R signaling. This observation was further verified by the use of mutant IGF-1, which is defective in integrin-IGF-1R tertiary complex formation, can suppress IGF-1-mediated tumorigenesis *in vivo* in breast cancer and skin squamous cell carcinoma (Fujita et al., 2013; Takada et al., 2017).

Insulin-like growth factor binding proteins (IGFBPs) are proteins secreted by cells to modulate the bioavailability of IGFs [reviewed in Baxter (2014)]. They comprise six main proteins—IGFBP-1 to IGFBP-6—most of which limit the access of IGFs to IGF-1R. IGFBPs participate in various cellular processes, such as cell proliferation, survival, and motility. For example, IGFBP-3 is degraded by matrix metalloproteinase-3 to release IGF-1, activating IGF-1R signaling and cell proliferation (Fowlkes et al., 2004). However, the effect of IGFBP-3 seems to be cell type

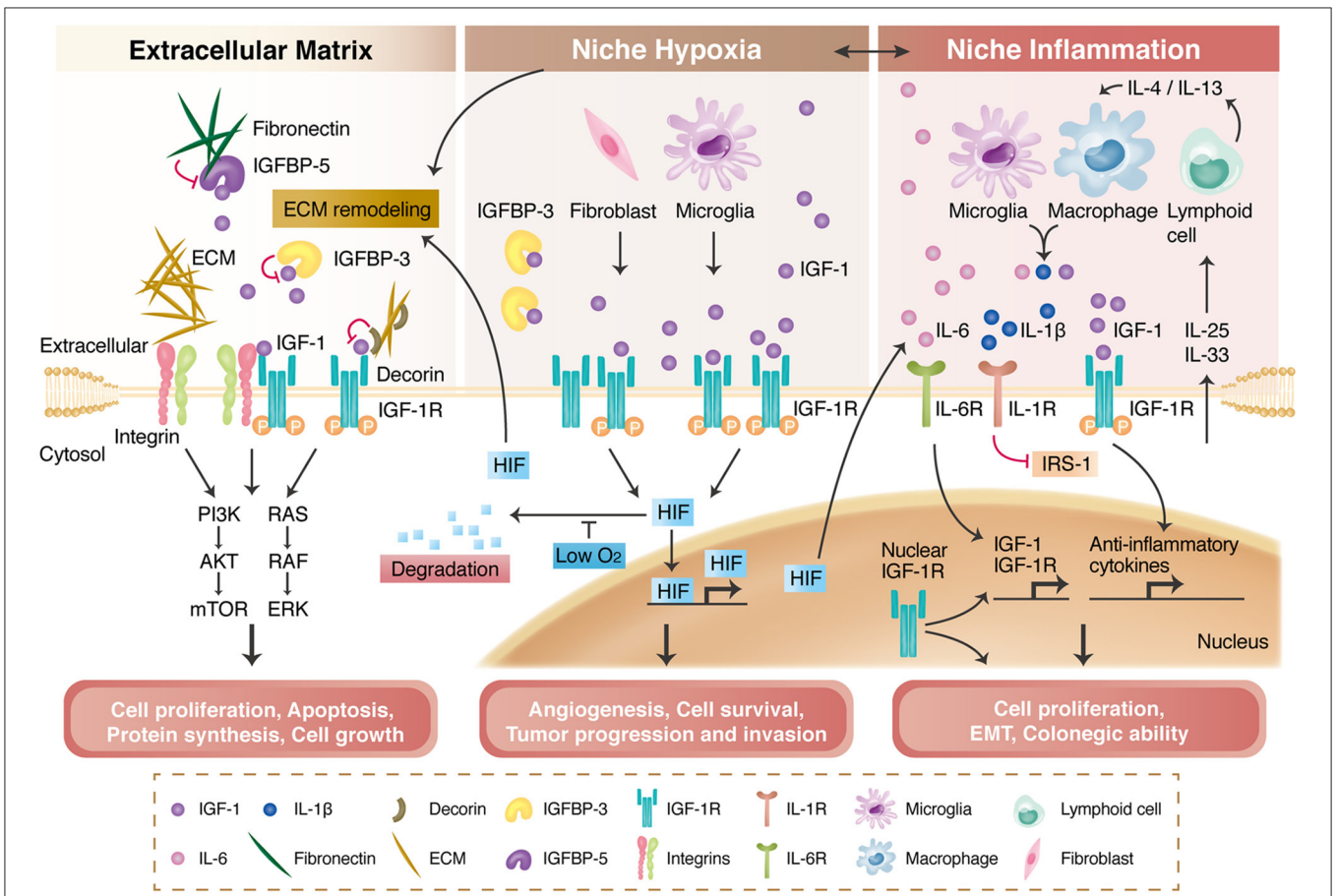

FIGURE 2 | IGF-1R signaling and its modulation by the extracellular matrix (ECM), niche hypoxia, niche inflammation, and nuclear translocation. The ECM and integrins regulate IGF-1R signaling activation through direct binding, transactivation, and the formation of a tertiary complex with IGF-1R. The ECM also interacts with insulin-like growth factor binding proteins (IGFBPs) to modulate IGF-1R signaling (left panel). Niche hypoxia affects IGF-1R signaling by affecting IGFBPs and increasing IGF secretion from niche cells. Hypoxia also stabilizes hypoxia-induced factors (HIFs), enabling HIF-mediated angiogenesis and tumor progression (middle panel). IGF-1R signaling is regulated by niche immune cells in the inflammation process and further modulates local inflammatory responses or tumor progression (right panel). Nuclear-translocated IGF-1R can bind to DNA; can increase *IGF-1R*, *CYCLIN D1*, *AXIN2*, and *SNAI2* expression; and is associated with cancer stem cell properties.

dependent. In one study, IGFBP-3 exerted a pro-apoptotic effect on doxorubicin-induced endothelial cell death but inhibited apoptosis in serum-starved endothelial cells (Granata et al., 2004). The amount of IGFBPs is also regulated by the ECM. IGFBP-5 was reported to enhance the IGF-1-mediated cell migration of mouse embryonic cells, but this effect was abolished upon fibronectin binding because of the increased proteolysis of IGFBP-5 (Xu et al., 2004).

Niche Hypoxia

Cells receive diverse signals from extracellular microenvironment and respond accordingly. Among different microenvironment factors, niche hypoxia is one of the most common conditions. Physiologically, hypoxia in the early embryonic stage is crucial in stem cell functions, pluripotency, and organ development (Simon and Keith, 2008; Fathollahipour et al., 2018; Kuo et al., 2018) Pathologically, Eliasz et al. demonstrated that hypoxia-activated Notch 1 can increase IGF-1R expression by binding to the IGF-1R promoter, thereby enhancing IGF-1R-mediated antiapoptosis in lung adenocarcinoma (Eliasz et al., 2010). Moreover, in the pathophysiology of pulmonary hypertension, hypoxic condition will enhance the IGF-1 secretion from the arterial smooth muscle cells, by which to affect pulmonary vessel remodeling (Sun et al., 2016). Meanwhile, it was reported that niche hypoxia in pulmonary hypertension reduces the expression of miR-223 in the lung and right ventricle regions. Decreased expression of miR-223 results in the upregulation of IGF-1R and enhances IGF-1/IGF-1R signaling that mediates right ventricular hypertrophy in the pathophysiology of pulmonary hypertension (Shi et al., 2016).

Niche hypoxia also affects the niche cell interactions, IGFBPs, and exosomes to regulate the IGF-1R signaling. In pancreatic cancer, hypoxic conditions both induce IGF-1 expression in cancer-associated fibroblasts (CAFs) and the IGF-1R expression in pancreatic cancer cells, and such IGF-1R signaling promotes cell mobility (Hirakawa et al., 2016). Furthermore, the secretion of IGF-1 from microglia increases under hypoxia, which eventually enhances VEGFR expression in endothelial cells to promote retinal angiogenesis (Yin et al., 2017). IGFBP-1 phosphorylation is also increased by hypoxia, resulting in limited IGF-1 bioavailability (Shehab et al., 2017). Moreover, hypoxia increases the secretion of IGFBP-3 from cardiomyocytes, which reduces cellular survival through the reduction of IGF-1 bioavailability (Chang R.L. et al., 2015). The exosomes and miRNAs may involve in the underlying mechanism. The miR-29a targeted by exosomal circHIPK3 could upregulate IGF-1 expression in hypoxic endothelial cells, thereby reducing cellular apoptosis (Wang et al., 2019).

Niche Inflammation

Niche inflammation plays a prominent role in the body's frequent responses to foreign attacks. IGF-1R signaling is involved in the inflammatory responses in the inflammatory microenvironment. For example, IGF-1 is overexpressed in the inflammatory niche of diabetic nephropathy, and the inhibition of IGF-1R relieves both inflammation and fibrosis in diabetic kidneys (Li et al., 2018). In a model of asthma, a well-known inflammatory disease, Shao et al. demonstrated that miR-133a is downregulated in this inflammatory niche and activates IGF-1R signaling, which is responsible for airway remodeling in asthma (Shao et al., 2019). IGF-1R deletion reduces the infiltration of immune cells as well as the expression of inflammation markers in the lung tissues in a murine model of asthma (Pineiro-Hermida et al., 2017). In addition, niche inflammation modulates IGF-1R signaling and affects local cellular responses. Upon allergen exposure, pulmonary epithelial cells activate certain lymphoid cells to secrete interleukin-4 (IL-4) and IL-13, further inducing the secretion of IGF-1 from macrophages. IGF-1 then binds with IGF-1R to reduce the allergic inflammatory response of pulmonary epithelial cells by promoting microvesicle uptake and anti-inflammatory cytokine release (Han et al., 2016). In rheumatic arthritis, an inflammatory disease affecting multiple organs, including the joints and nervous system, increased IL-6 level and number of activated microglia were observed in the serum and hippocampus, respectively (Andersson et al., 2018). Microglia secrete IL-1β in response to an inflammatory environment, and this secretion is associated with increased IGF-1R expression. This correlates with inhibitory IRS phosphorylation in the neurons and impairs IGF-1R-mediated neurogenesis in the hippocampus regions (Andersson et al., 2018). Niche inflammation is also highly correlated with IGF-IR signal activation and cancer formation. For example, in colorectal cancer, tumor growth and niche inflammation are both attenuated by the dual inhibition of IGF-1R signaling and the STAT3 pathway, resulting in much smaller tumor sizes in both primary and metastatic tumors (Sanchez-Lopez et al., 2016).

Nuclear IGF1R

The traditional concept of membrane receptors has been challenged as an increasing number of studies have suggested that they can be found, with or without their ligands, in cell nuclei. Nuclear IGF-1R was first detected in hamster kidneys and later in cancer cells and highly proliferative non-malignant tissues (Chen and Roy, 1996; Aleksic et al., 2010). After ligand treatment, activated IGF-1R undergoes clathrin-mediated endocytosis before connecting to microtubules and motor protein dynein through the $p150^{Glued}$ subunit of dynactin, which targets nuclei (Aleksic et al., 2010; Packham et al., 2015). As IGF-1R approaches a nucleus, it is sumoylated by RanBP2 before translocating to the nucleus through importin-β/Ran GTPase (Packham et al., 2015). Regarding its function, nuclear IGF-1R possesses a specific DNA binding capacity and seems to be enriched in intergenic regions, suggesting its role in the regulation of gene transcription through the modulation of enhancers as a transcription factor or coactivator (Sehat et al., 2010). Studies have shown that IGF-1R can bind with the transcriptional coactivator of LEF1/TCF to upregulate the gene expression of *cyclin D1* and *axin2* (Warsito et al., 2012) and that it autoregulates its own gene expression (Sarfstein et al., 2012). More surprisingly, nuclear IGF-1R is associated with RNA polymerase II (Aleksic et al., 2010, 2018) and can phosphorylate histone H3 at the Tyr41 position. This modification can stabilize

and recruit the chromatin-remodeling protein Brg1 and further induce *SNAI2* expression (Warsito et al., 2016). Physiologically, it was proposed that nuclear IGF-1R might increase cell proliferation while the traditional AKT and ERK pathways promote cell differentiation and survival (Lin et al., 2017). Nuclear IGF-1R in cancers is positively correlated with tumor stage and presents higher protein levels in metastatic cancer (Codony-Servat et al., 2017; Aleksic et al., 2018). High levels of nuclear IGF-1R were detected in PDGFRα^{high}/IGF-1R^{high} murine alveolar rhabdomyosarcoma cells and were associated with greater anchorage-independent colony formation ability (Aslam et al., 2013). Furthermore, the amount of nuclear IGF-1R serves as an effective predictor of anti-IGF-1R therapy in sarcoma (Asmane et al., 2012) and of drug resistance in liver cancer cells and colorectal cancers (Bodzin et al., 2012; Codony-Servat et al., 2017). Collectively, nuclear IGF-1R exerts transcriptional regulation activity, and its newly discovered role in cancer provides a novel mechanism in IGF1R-mediated cancer progression and can serve as a new biomarker for predicting clinical prognosis.

NICHE AND IGF-1R-MEDIATED STEMNESS EXPRESSIONS IN STEM CELLS AND CANCERS

The fact that IGF-1R signaling promotes and maintains stemness in both stem cells and CSCs or cancer reprogramming raises the following questions: What transforms IGF-1R signaling from a traditional pathway to being central to the regulation of stem cell properties? Furthermore, how is the dual role of IGF-1R-mediated stemness controlled between the development of embryos and cancers? As mentioned earlier, the interaction between IGF-1R signaling and the niche microenvironment has a crucial role in affecting IGF-1R activation and IGF-1R-mediated cellular responses. Many researches have implicated the importance of niche in controlling stem cell properties, stem cell fate, and lineage differentiation (Morrison and Spradling, 2008; Chacon-Martinez et al., 2018). A similar interplay was also noted between CSCs and cancer niche. We propose that the communication between niche microenvironment and stem cells switches the cell fate into stem cell pluripotency, CSCs, or cancer reprogramming in different stem cells within distinct surrounding niches. Additionally, in normal and malignant cells, interior stimulation could be attributed to the distinct epigenetic signatures of DNA methylation and histone modification at gene promoters. Epigenetic signatures have been proven to change as stem cells differentiate, and the disruption of epigenetic regulation leads to cancer development (Spivakov and Fisher, 2007; Toh et al., 2017). In the following section, we instanced several kinds of stem cell and CSCs to explore how the niche microenvironment modulates the roles of IGF-1R-mediated stemness regulation (**Figure 3**).

IGF-1R-Mediated Stemness in Stem Cells

Embryonic Stem Cells

ESCs are cells that originate from the inner cell mass and contribute to all cell types of the body. Although many factors have been shown to sustain ESC populations, little is known regarding cell surface receptor activation required for ESC self-renewal. Wang et al. demonstrated that IGF-1R could be activated in human ESCs when the cells were cultured in a mouse embryonic fibroblast (MEF)-derived condition medium (Wang et al., 2007). Furthermore, IGF-1R was coexpressed with the stem cell markers OCT4, SSEA4, and SSEA3 in human ESCs. Blocking IGF-1R activation by using specific antibodies and knocking down IGF-1R in human ESCs limited ESC expansion and induced differentiation (Wang et al., 2007). IGFs, fibroblast growth factor (FGF), and heregulin (HRG) in feeder-, serum-, and KSR-free defined medium are required for the colony formation of human ESCs. Furthermore, human ESCs cultured in this defined media exhibit high resemblance to ESCs cultured in MEF-condition media in terms of global transcriptional expression, micro-RNA expression, and genome methylation profile (Wang et al., 2007). Moreover, IGF/IGF-1R signaling together with HRG/ERBB2 signaling promotes the self-renewal of ESCs and prevents their apoptosis through the PI3K pathway (Wang et al., 2007). Another study of human ESCs also showed that IGF-2/IGF-1R is required for their self-renewal (Bendall et al., 2007). IGF-2 sustains ESC expansion and prevents apoptosis (Bendall et al., 2007). Moreover, the IGF-1R pathway participates in regulating pluripotency in stem cells by promoting and maintaining the expression of pluripotency genes. In mouse ESCs, IGF-1/IGF-1R signaling promotes NANOG expression through the PI3K/AKT pathway, and IGF-1R expression is positively associated with stronger expression of alkaline phosphatase (AP), an undifferentiated ESC marker (Chen and Khillan, 2010). Notably, the promoter of pluripotency genes such as OCT4 and NANOG is unmethylated in ESCs, which might facilitate IGF-1R signaling in promoting pluripotency gene expression (Altun et al., 2010). ESCs themselves can form a microenvironment comprising colony-forming ESCs and ESC-derived fibroblasts (Bendall et al., 2007). These fibroblasts secreted IGF-2 and TGF-β in response to ESC-secreted FGFs. These results demonstrated that IGF-2/IGF-1R signaling supports ESC self-renewal and prevents their apoptosis and that their interaction with the surrounding microenvironment sustains their pluripotent stem cell status and prevents differentiation.

Germline Stem Cells

Mouse germline stem cells are responsible for gamete formation during embryogenesis. Our previous study established a serum-free culture system to investigate the defined component of the pluripotency regulation of pluripotent germline stem cells (Huang et al., 2009). Germline stem cells present integrin $\alpha6^+/AP^+/OCT4^+$ and are capable of differentiating into hepatocyte- and neuron-like cells as well as forming embryonic chimeras; thus, they were designated as AP^+ germline stem cells (AP^+ GSCs). We found that IGF-1R signaling supported the pluripotency gene expression of *OCT4*, *SOX2*, and *NANOG* in AP^+ GSCs. Moreover, IGF-1 was secreted by AP^+ GSCs as well as testicular stromal Leydig cells to form an autocrine and paracrine signaling loop. Notably, laminin enhanced the colony-forming ability of AP^+ GSCs, indicating the role of the ECM in assisting IGF-1R-mediated stemness.

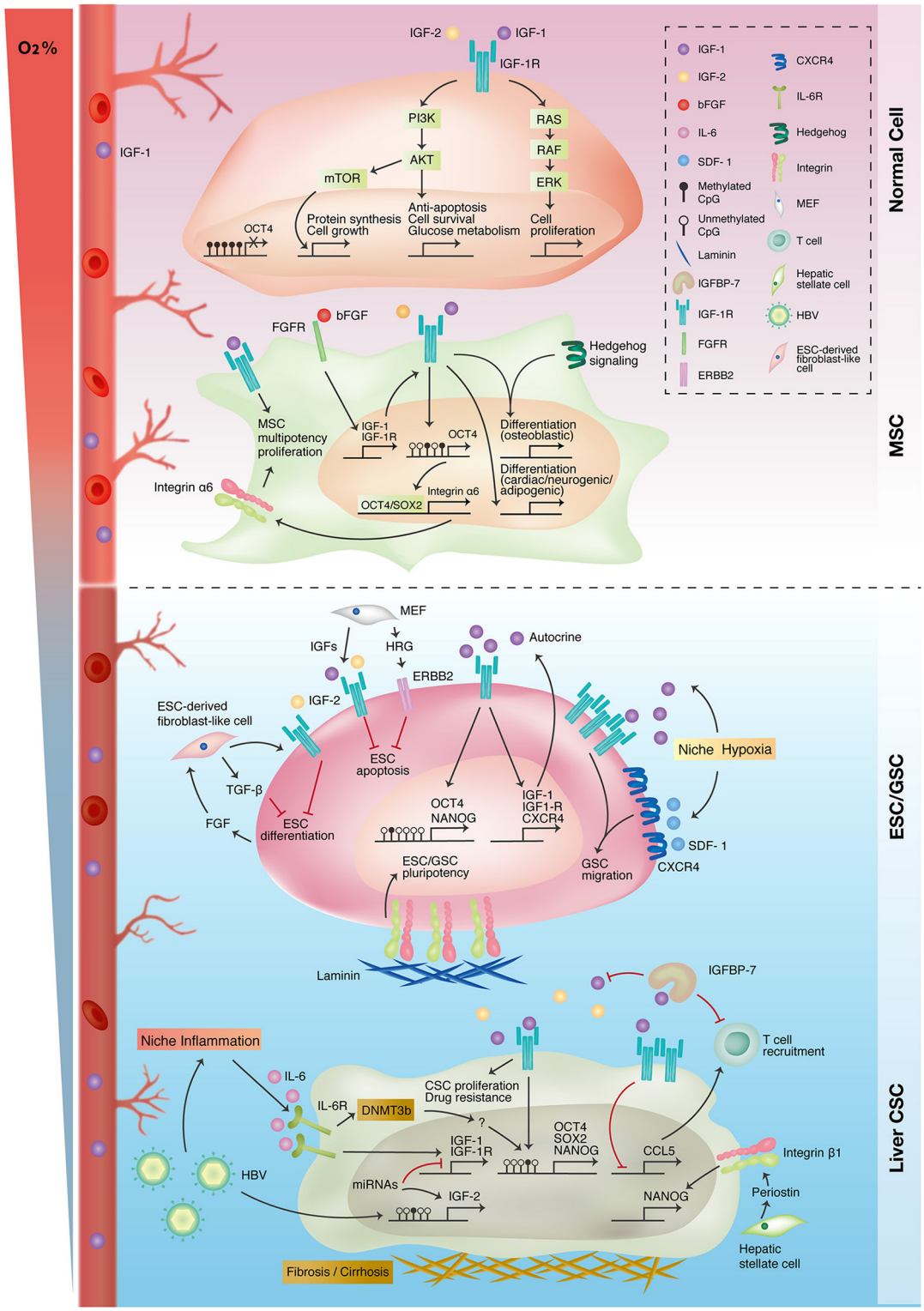

FIGURE 3 | Interplay of IGF-1R-related signaling and niche microenvironment in stemness expressions of different cell types. Traditional IGF-1R signaling promotes cell proliferation, growth, and survival in differentiated normal cells (upper panel). Autocrine IGF-1R signaling promotes mesenchymal stem cell (MSC) proliferation and multiple lineage differentiation through interacting with other signaling pathways (upper-middle panel). In embryonic and germline stem cells (ESC/GSC), niche cells maintain embryonic stem cell survival and pluripotency status through autocrine/paracrine IGF-1R signaling. Niche hypoxia activates both IGF-1R and CXCR4 signaling in promoting the self-renewal and migration of germline stem cells (lower-middle panel). IGF-1R signaling is upregulated in liver cancer because of epigenetic alterations and niche inflammation. The IGF-1R pathway also promotes stemness in liver cancer stem cells (liver CSC) and niche inflammation (lower panel).

During embryogenesis, hypoxia is a natural process involved in the development of multiple organs through HIFs. Hypoxia is also an active member of the niche microenvironment in regulating stem cell activities (Mohyeldin et al., 2010). Regarding gamete formation, primordial germ cells, a gamete precursor, migrate from the hindgut to the embryonic genital ridge under a hypoxic environment. Notably, hypoxic conditions enhanced the self-renewal ability and OCT4 expression in mouse GSCs. Studies have revealed that IGF-1/IGF-1R expression is induced and IGF-1R signaling is activated by niche hypoxia to synergistically support the proliferation and OCT4 maintenance of GSCs through the PI3K/AKT/mTOR/HIF-2α pathway (Huang et al., 2009, 2014). Interestingly, niche hypoxia is also essential in supporting the migratory potential of GSCs by promoting SDF1/CXCR4 expression and activation. Of relevance here is that hypoxia-activated IGF-1R signaling not only induces SDF1/CXCR4 expression and activation but also transactivates CXCR4 signaling to collectively enhance hypoxia-mediated GSC migration (Kuo et al., 2018). These findings indicate that during embryogenesis, niche hypoxia governs stem cell features through IGF-1R signaling. Taken together, although the IGF-1R pathway is central to the regulation of the stem cell features of self-renewal and pluripotency, it also supports other cellular processes required for precise and organized embryonic development.

Mesenchymal Stem Cells

In addition to its role in pluripotent stem cells, IGF-1R signaling has also been shown to be involved in maintaining the self-renewal ability of multipotent and less potent stem cells. MSCs, as previously mentioned, are multipotent adult stem cells with great potential for differentiating into cells such as adipocytes, osteocytes, and neurons. The IGF-1/IGF-1R autocrine loop induces stem cell proliferation and prevents apoptosis through the AKT/GSK-3β/P70S6K pathway in umbilical cord–derived MSCs (UC-MSCs) (Wang et al., 2018). IGF/IGF-1R is activated by basic FGFs (bFGF) to maintain MSC multipotency, and disruption of the IGF-1R pathway with specific molecular inhibitors reduces OCT4/NANOG/SOX2 expression (Park et al., 2009). OCT4/SOX2 can bind to the promoter region of integrin α6 (also known as CD49f or ITGA6) and enhance its expression, and integrin α6 promotes multipotency and stemness in MSCs through the PI3K/AKT/p53 pathway (Yu et al., 2012).

IGF-1R signaling is shown to regulate the differentiation of MSCs. A comparison of gene expression profiles between bone marrow–derived MSCs (BM-MSCs) and BM-MSC-derived adipocytes revealed that IGF-1R signaling was highly involved during the adipogenic differentiation of BM-MSCs (Xu X. et al., 2016). Supplementation of IGF-1 in adipocyte-induction medium promoted the adipogenesis of BM-MSCs by stimulating peroxisome proliferator-activated receptor-γ (PPAR-γ) expression and lipid accumulation (Scavo et al., 2004). Moreover, blockage of IGF-1R activation resulted in less adipogenesis of human UC-MSCs (Park et al., 2009).

In addition to adipogenesis, IGF-1R signaling partakes in osteogenic differentiation (Shi et al., 2015). The IGF/IGF-1R autocrine loop in human BM-MSCs is activated and upregulated by hedgehog signaling, a well-established pathway that is essential for osteoblast differentiation during embryonic skeletal development. IGF-1R and its downstream AKT/mTOR cascade stabilize hedgehog-induced transcription effector Gli2 protein, thereby enhancing a hedgehog-mediated effect on osteoblast differentiation (Shi et al., 2015). Xian et al. also reported that the osteoclast-mediated bone resorption microenvironment contains IGF-1 and TGF-β during bone remodeling. TGF-β attracts BM-MSCs to the sites of bone remodeling, where IGF-1/IGF-1R signaling induces osteoblast differentiation of cells through the PI3K/AKT/mTOR pathway, which preserves bone mass and skeletal microarchitecture. Therefore, IGF-1R knockdown reduces bone mineral density and causes loss of trabecular bone volume in an osteoblast differentiation factor Osx1-expressing cell (Xian et al., 2012). Some studies have also demonstrated that IGF-1R activation induces the expression of osteo/odontogenic markers (such as *OCN*, *OSX*, *DSPP*, *RUNX2*, *ALP*, *COL-1*, and *DMP1*) through the JNK/p38 MAPK pathway in dental pulp–derived MSCs (Liu et al., 2018). Additionally, IGF-1R signaling is essential not only for the induction of neurogenesis in adipose tissue–derived MSCs (AD-MSCs) but also for cardiomyocyte differentiation from BM-MSCs (Ning et al., 2008; Gong et al., 2017).

IGF-1R-Mediated Stemness in Cancer Stem Cells

IGF-1R signaling had also been demonstrated to regulate the cancer stemness in various cancer stem cell models, such as colorectal cancer and breast cancer (Dallas et al., 2009; Chang et al., 2013). We take lung and liver cancer stem cells as an example to explain our concept of niche-specific effect on IGF-1R-mediated cancer stemness.

Liver Cancer Stem Cells

Because studies on embryogenesis have suggested that the niche plays a role in the regulation of stem cell characteristics, we further extended this concept to cancer reprogramming to investigate the role of niche microenvironments in hijacking IGF-1R signaling to promote stemness properties in cancers. IGF/IGF-1R is upregulated in hepatocellular carcinoma (HCC) and is associated with tumorigenesis (Martinez-Quetglas et al., 2016). IGF-1R and FGFR are continuously activated in sorafenib-resistant HCC, and these sorafenib-resistant tumor cells exhibit greater tumor-initiating capacity *in vivo* (Tovar et al., 2017). IGF-1R induces the Ras/Raf/Erk-kinase cascade and reduces cellular apoptosis in sorafenib resistance. IGF-1R knockdown in sorafenib-resistant cells increases sorafenib sensitivity, whereas IGF-1R inhibition in naïve cells limits the emergence of drug-resistant cells (Xu Y. et al., 2016).

Emerging evidence has revealed the role of inflammation in carcinogenesis. Chronic inflammation and liver cirrhosis are the predisposing factors in the development of HCC. Hepatitis B virus (HBV) infection was reported to increase the expression of IGF-2 through IGF-1R/MEK/ERK signaling (Ji et al., 2018). Decreases in IGFBP-7 expression increase IGF/IGF-1R signaling, which facilitates the proliferation of HCC and creates a proinflammatory microenvironment (Akiel et al., 2017). IGF-1R inhibition also increases chemokine ligand 5 expression, which

is essential for T cell recruitment (Wang et al., 2017). Hepatic stellate cells are responsible for the cirrhotic change and would induce Nanog expression through integrin β1 (Zhang et al., 2017). We previously found that IGF-1R signaling promotes the expression of the pluripotency genes OCT4 and NANOG in hepatitis B virus (HBV^+)-infected HCC patients. Histological staining of IGF-1R in patients with HBV^+ HCC is positively correlated with pluripotency gene expression and worse clinical outcomes. Furthermore, expression of OCT4/NANOG in tumor cells is positively correlated with the amount of infiltrated immune cells within the tumor region. Inflammation-condition medium derived from lipopolysaccharide-stimulated HBV^+ HCC induces the expression of stemness gene OCT4 and NANOG through an IGF-1R-dependent mechanism, suggesting the possible role of active inflammation in controlling IGF-1R-mediated cancer stemness (Chang et al., 2016). Moreover, the serum level of the inflammatory cytokine interleukine-6 (IL-6) is highly elevated in patients with HBV^+ HCC. Activation of the IL-6/STAT3 pathway induces the expression of IGF-1/IGF-1R, thereby initiating the IGF-1/IGF-1R autocrine and paracrine loop within tumor bulk to induce stemness-related gene expression. Disruption of IGF-1R signaling abolishes IL-6-mediated tumorigenesis *in vitro* and *in vivo*. The coexpression of IL-6, phosphorylated IGF-1R, OCT4, and NANOG corresponds to the worst clinical outcomes for HCC (Chang T.S. et al., 2015).

Epigenetic dysregulation also affects IGF-1R signaling-mediated stemness. IGF-2 is upregulated in HCC due to promoter hypomethylation and higher IGF-2 levels are correlated with the upregulation of hepatic progenitor and angiogenesis markers (Martinez-Quetglas et al., 2016). IGF-1R expression level is modulated by IGF-1R-targeted micro-RNA such as miR122 in HCC (Xu Y. et al., 2016). The concept of epigenetic mechanisms also accords with the re-expression of pluripotency genes in somatic cancer cells. The promoter regions of pluripotency genes OCT4, NANOG, and SOX2 are hypomethylated in HCC compared with normal hepatocytes (Wang et al., 2013). Moreover, niche inflammatory factor IL-6 level positively correlated with IGF-1R, OCT4, and DNA-methyltransferase 3b level in HBV^+ HCC. This indicates the possible role of epigenetics in controlling IGF-1R-mediated stemness in tumorigenesis under inflammatory niche (Chang T.S. et al., 2015; Lai et al., 2019).

Lung Cancer Stem Cells

In lung cancer, IGF-1R signaling regulates CSC activities through the activation of different downstream cascades and cross-talk with the surrounding microenvironment. Xu et al. discovered that IGF-1R expression is highly associated with lung CSC markers CD133 and ALDH1A1 in lung adenocarcinoma. Closer investigation revealed that IGF-1/IGF-1R activates the PI3K/AKT/GSK3β/β-catenin pathway and induces expression of the pluripotency gene OCT4. OCT4 later formed a transcriptional complex with β-catenin that promoted NANOG expression, which is essential for tumorigenesis *in vitro* and *in vivo* for CSCs. Moreover, clinical findings of patient tissue immunostaining have indicated that colocalization of IGF-1R, β-catenin, and OCT4 is strongly correlated with poor prognosis (Xu et al., 2013). IGF-1R also regulates cancer stemness through other downstream pathways. In non–small-cell lung cancer (NSCLC), the IGF-1R/Tescalcin/c-Src complex mediates the STAT3 pathway to induce ALDH1 expression, which preserves CSC features (Lee et al., 2018). In addition, the CD74-NRG1 oncogenic fusion gene activates the PI3K/AKT/NF-κB pathway in lung adenocarcinoma and induces activation of the IGF-2/IGF-1R autocrine loop. Disruption of the IGF-2/IGF-1R circuit abolishes CD74-NRG1-mediated tumor-initiating ability (Murayama et al., 2016). In NSCLC, the IGF-1R pathway is activated by APBB1 and stabilizes SNAIL1 through the PI3K/AKT/GSK3β pathway. This cascade also prevents β-catenin from degradation, thereby promoting the expression of the CSC marker ALDH1 (Lee et al., 2017).

In addition, IGF-1R is regulated by the ECM in controlling epithelial-to-mesenchymal transition (EMT). Fibulin-3 is an extracellular glycoprotein expressed in various tissues and involved in embryonic development (Zhang and Marmorstein, 2010). Suppression of fibulin-3 in lung adenocarcinoma stem cells enhances EMT-associated gene expression. Further data revealed that fibulin-3 competitively inhibits IGF/IGF-1R interaction, and therefore, the loss of fibulin-3 promotes IGF-1R signaling to induce EMT in lung CSCs (Kim I.G. et al., 2014). Chen et al. reported that IGF-2/IGF-1R paracrine signaling between NSCLC and CAFs is essential for sustaining CSCs' features. Fibroblasts isolated from the tumors of patients with NSCLC were used as feeder cells and could maintain an *in vitro* culture system of CSC. IGF-2 secreted from CAFs supported stemness features in CSCs through activation of the IGF-1R/PI3K/AKT pathway, which eventually induced NANOG expression and was responsible for the cells' tumorigenic ability. Depletion of CAFs from the culture system reduced the expression of stemness markers OCT4/SOX2/NANOG and the anchor-independent capacity in CSCs, whereas it increased the expression of differentiation markers such as adenocarcinoma and squamous carcinoma markers (thyroid transcription factor 1, CK7, CK20, p63, and keratin 5/6). Notably, re-coculturing these differentiated cancer cells with CAFs reversed this pattern, suggesting that the microenvironment may be involved in the reprogramming of cancer cells to their CSC state (Chen et al., 2014).

TARGETING IGF-1R SIGNALING IN STEM CELL THERAPY AND CANCER WITH STEMNESS-RELATED PROPERTIES

IGF-1R Signaling in Stem Cell Therapy

Regenerative medicine provides novel and promising means for recovering organ damage and tissue injury caused by trauma, disease, or age. Because of stem cells' self-renewal ability and pluripotency, they are considered one of the finest tools for treating or preventing diseases and injuries. Stem cells have the ability to interact with and affect adjacent cells and their surrounding microenvironment, forming a niche that might be beneficial for healing and regeneration. For example, emerging evidence shows that stem cells might secrete cytokines and

TABLE 1 | Ongoing clinical trials of IGF-1R inhibitors in cancers.

Drug	Combination therapy	Indicated diseases	Phase	NCT number	Status[#]
Ganitumab (AMG479)	-	Metastatic or recurrent sarcoma	1	NCT04199026	NR
	Combination chemotherapy	Newly diagnosed metastatic Ewing sarcoma	3	NCT02306161	Ac/NR
	Dasatinib	Rhabdomyosarcoma	1/2	NCT03041701	R
	Metformin	Breast cancer	2	NCT01042379	R
	Palbociclib	Ewing sarcoma	2	NCT04129151	R
Cixutumumab (IMC-A12)	Paclitaxel	Metastatic esophageal cancer or gastroesophageal junction cancer	2	NCT01142388	Ac/NR

[#]*R, recruiting; Ac/NR, active not recruiting; NR, not yet recruiting.*

exosomes and play an anti-inflammatory role in injured regions (Vakhshiteh et al., 2019). They may also be recruited to damaged areas by local signals and differentiate into much more mature cells that participate in healing and reconstruction.

One of the most promising possible applications of regenerative medicine is in treating or curing devastating neurological diseases, such as brain stroke, spinal cord injuries, and degenerative neurological diseases. Stroke causes ischemic and hypoxic changes in affected brains. Intravenous injection of human BM-MSCs improved functional outcomes in a rat stroke model of middle cerebral artery occlusion (Zhang et al., 2004). Human MSC administration was detected in ischemic regions, and it increased IGF-1 expression as well as local IGF-1/IGF-1R expression; these increases in expression corresponded with increased cell proliferation and neural progenitor cell recruitment at the damage sites (Zhang et al., 2004). Jeon et al. reported that human BM-MSCs secreted IGFBP-6, which in turn increased extracellular IGF-1 levels in reactive oxygen species (ROS)-induced neuron injury. This IGF-1/IGF-1R signaling protects neural cell death from ROS-mediated toxicity through the PI3K/AKT pathway (Jeon et al., 2017). The survival and migration of neural stem cells were also reported to be regulated by IGF-1R when transplanted into an injured spinal cord, and their survival and migration could be augmented through treadmill training (Hwang et al., 2018). Human dental pulp–derived MSCs with higher expression of IGF-1R exhibited a greater antiapoptotic effect and neural differentiation capacity in a cerebral ischemic rat model. Rats with intracerebral transplantation of IGF-1R$^+$ MSCs exhibited improved neurological prognosis and cerebral blood flow (Lee et al., 2016). Additionally, the IGF-1/IGF-1R axis promoted migration potential and neural differentiation in human spinal stem cells without affecting its terminal differentiation. This was used in a phase 1 trial in which human spinal stem cells were injected into cervical, thoracic, and lumbar spinal cord regions to treat amyotrophic lateral sclerosis (ALS), and promising results were reported. Overexpression of IGF-1 in human spinal stem cells enhanced their neuroprotection from excitotoxicity, which enhances the understanding and future prospects of stem cell therapy in ALS (Lunn et al., 2015).

In addition, cardiovascular diseases such as myocardial infarction may benefit from stem cell therapy. Jackson et al. found that after myocardial infarction, IGF-1R expression was upregulated in the ischemic and paraischemic regions of the heart. They then isolated cardiac stem cells from patients with myocardial infarction and overexpressed IGF-1 in the CD90$^+$ cardiac stem cell subset (which is thought to have little effect on myocardial repair) through lentiviral transduction. This IGF-1/IGF-1R signaling in cardiac stem cells promotes stem cell survival and protects surrounding cardiomyocytes from apoptosis after infarction. Intramyocardial transplantation of these IGF-1-overexpressing cardiac stem cells in the infarcted area also preserves stem cells in the damaged region and increases myocardial regeneration without affecting its differentiation into cardiomyocytes, smooth muscle, or endothelial cells (Jackson et al., 2015).

In the muscular-skeletal system, stem cell therapy is widely applied for ligament and muscle sprain as well as osteoarthritis and other muscular-skeletal diseases. In an *in vivo* study of the use of AD-MSCs to treat rotator cuff injury, IGF-1R was found to be highly expressed in transplanted AD-MSCs and associated with myocyte differentiation marker myosin heavy chain expression (Kim S.H. et al., 2014). Furthermore, overexpression of IGF-1 in BM-MSCs overcomes the decreased proliferation and osteogenic potential caused by aging (Chen et al., 2017). Taken together, these findings indicate that IGF-1R signaling is involved in repairing and restoring dysfunctional tissue damage and also participates in stem cell therapy. More solid evidence demonstrating IGF-1R signaling manipulation is warranted to provide enhanced strategies for applying stem cell therapy in regenerative medicine.

IGF-1R Signaling as a Therapeutic Target of Cancer With Stemness-Related Properties

The IGF-1R pathway has been implicated as participating in the regulation of cell proliferation and antiapoptosis in cancers. This raises the possibility of targeting IGF-1R signaling in cancer treatment. However, despite the promising evidence from preclinical studies and early phase 1 trials, larger clinical trials targeting IGF-1R have experienced great setbacks. Some trials were terminated early due to lack of efficiency, while other completed trials showed no improvement in patient outcomes. Many argued that the failure in the phase 2 and 3 trials was largely due to unselected patients and the lack of studies that actually investigated the patient prognosis based on various biomarkers. Pharmaceutical companies have been closing up their project on IGF-1R and only few drugs are now under clinical

evaluation (**Table 1**) (Beckwith and Yee, 2015; Werner et al., 2019).

Another way to target IGF-1R signaling in cancer could be eliminating cancer stemness or CSCs by inhibiting IGF-1R given that the IGF-1R pathway plays a crucial role in supporting stemness activities in cancer cells with stemness-related properties. For example, in colorectal cancer, IGF-1R signaling enriches the side-population cell (cells that are best at effluxing the dyes and have been referred to as CSCs) but not the non-side-population cells, indicating the role of IGF-1R in CSC features. Targeting IGF-1R with figitumumab reduces side population cells and $ALDH^+$ populations and also inhibits xenograft tumor growth (Hart et al., 2011). Dual inhibitors targeting IGF-1R and other key signaling pathways represent another approach. The co-inhibition of IGF-1R and EGFR inhibits tumor-initiating potential and increases sensitivity to radiation therapy in pancreatic CSCs (Urtasun et al., 2015). The co-inhibition of IGF-1R and EGFR might also render cancer cells sensitive to other combined therapies. However, as indicated in previous clinical trials, specific biomarkers for selecting suitable patients and precise targeting of IGF-1R in CSCs are required. In support of this, Huang et al. demonstrated that the precise targeting of IGF-1R in sarcomas is feasible through the bioengineering of patient-derived chimeric antigen receptor (CAR)-T cells. The authors designed IGF-1R-targeting CAR-T cells and revealed that they selectively exerted their cytotoxicity against sarcoma cells in localized and disseminated xenografts model and extended overall survival (Huang et al., 2015). Further studies should be conducted to identify definitive biomarkers for clinical use and to enhance specific therapeutic targeting of IGF-1R.

CONCLUSION AND PERSPECTIVES

In this review, we highlight the modulation interplay between IGF-1R signaling and microenvironments as well as how this interaction modulates IGF-1R-mediated stemness in stem cells, CSCs, and cancer reprogramming. The implications are 2-folds. The first is about IGF-1R. Given the consequences of the interaction between IGF-1R signaling and niche microenvironments, we reviewed the importance of IGF-1R signaling in regenerative medicine and cancer treatment in terms of stem cell therapy and therapeutic targets toward the cancers with stemness-related properties. Future research will focus on unraveling how IGF-1R signaling regulates stem cell features and to explore the underlying factors that control the dual consequences of IGF1R-mediated stemness. The second is about niche modulation perspective. We contemplate that niche properties can be modulated by adjusting parameters such as extracellular matrix, oxygen tension, cytokines, in different physiological and pathological conditions. The outcome is mediated through selective hub pathways such as IGF-1R signaling in this case, but can be Wnt/beta-catenin in other cases. It is speculative, but we hope more discussions and future investigations along this line can enrich our understanding of stem cell – niche interactions in the future.

AUTHOR CONTRIBUTIONS

P-CC, Y-CK, C-MC, and Y-HH: conception and design, writing, review, and/or revision of the manuscript. Y-HH and C-MC: study supervision. All authors contributed to the article and approved the submitted version.

FUNDING

This work was financially supported by research grants from the Ministry of Science and Technology, Taiwan (Grant numbers: MOST 107-2321-B-038-002, MOST 107-2314-B-038-061, MOST 108-2321-B-038-003, MOST109-2314-B-038-135, and MOST 109-2321-B-038-003); Health and Welfare Surcharge of Tobacco Products (Grant numbers: MOHW108-TDU-B-212-124014 and MOHW109-TDU-B-212-134014); Taipei Medical University (Grant number: TMU109-AE1-B02); Ministry of Education, Taiwan (Grant number: DP2-109-21121-01-T-03-02).

ACKNOWLEDGMENTS

The authors acknowledge the academic and science graphic illustration service provided by the Office of Research and Development at Taipei Medical University. This manuscript was edited by Wallace Academic Editing.

REFERENCES

Afify, S. M., and Seno, M. (2019). Conversion of stem cells to cancer stem cells: undercurrent of cancer initiation. *Cancers (Basel)* 11:E345. doi: 10.3390/cancers11030345

Akiel, M., Guo, C., Li, X., Rajasekaran, D., Mendoza, R. G., Robertson, C. L., et al. (2017). IGFBP7 deletion promotes hepatocellular carcinoma. *Cancer Res.* 77, 4014–4025. doi: 10.1158/0008-5472.CAN-16-2885

Aleksic, T., Chitnis, M. M., Perestenko, O. V., Gao, S., Thomas, P. H., Turner, G. D., et al. (2010). Type 1 insulin-like growth factor receptor translocates to the nucleus of human tumor cells. *Cancer Res.* 70, 6412–6419. doi: 10.1158/0008-5472.CAN-10-0052

Aleksic, T., Gray, N., Wu, X., Rieunier, G., Osher, E., Mills, J., et al. (2018). Nuclear IGF1R interacts with regulatory regions of chromatin to promote rna polymerase II recruitment and gene expression associated with advanced tumor stage. *Cancer Res.* 78, 3497–3509. doi: 10.1158/0008-5472.CAN-17-3498

Altun, G., Loring, J. F., and Laurent, L. C. (2010). DNA methylation in embryonic stem cells. *J. Cell. Biochem.* 109, 1–6. doi: 10.1002/jcb.22374

Andersson, K. M. E., Wasen, C., Juzokaite, L., Leifsdottir, L., Erlandsson, M. C., Silfversward, S. T., et al. (2018). Inflammation in the hippocampus affects IGF1 receptor signaling and contributes to neurological sequelae in rheumatoid arthritis. *Proc. Natl. Acad. Sci. U. S. A.* 115, E12063–E12072. doi: 10.1073/pnas.1810553115

Aslam, M. I., Hettmer, S., Abraham, J., Latocha, D., Soundararajan, A., Huang, E. T., et al. (2013). Dynamic and nuclear expression of PDGFRalpha and IGF-1R in alveolar rhabdomyosarcoma. *Mol. Cancer Res.* 11, 1303–1313. doi: 10.1158/1541-7786.MCR-12-0598

Asmane, I., Watkin, E., Alberti, L., Duc, A., Marec-Berard, P., Ray-Coquard, I., et al. (2012). Insulin-like growth factor type 1 receptor (IGF-1R) exclusive nuclear staining: a predictive biomarker for IGF-1R monoclonal antibody (Ab) therapy in sarcomas. *Eur. J. Cancer* 48, 3027–3035. doi: 10.1016/j.ejca.2012.05.009

Basu, S., Haase, G., and Ben-Ze'ev, A. (2016). Wnt signaling in cancer stem cells and colon cancer metastasis. *F1000Res.* 5:F1000 Faculty Rev. doi: 10.12688/f1000research.7579.1

Baxter, R. C. (2014). IGF binding proteins in cancer: mechanistic and clinical insights. *Nat. Rev. Cancer* 14, 329–341. doi: 10.1038/nrc3720

Beckwith, H., and Yee, D. (2015). Minireview: were the IGF Signaling Inhibitors All Bad? *Mol. Endocrinol.* 29, 1549–1557. doi: 10.1210/me.2015-1157

Bendall, S. C., Stewart, M. H., Menendez, P., George, D., Vijayaragavan, K., Werbowetski-Ogilvie, T., et al. (2007). IGF and FGF cooperatively establish the regulatory stem cell niche of pluripotent human cells *in vitro*. *Nature* 448, 1015–1021. doi: 10.1038/nature06027

Bjerkvig, R., Tysnes, B. B., Aboody, K. S., Najbauer, J., and Terzis, A. J. (2005). Opinion: the origin of the cancer stem cell: current controversies and new insights. *Nat. Rev. Cancer* 5, 899–904. doi: 10.1038/nrc1740

Bodzin, A. S., Wei, Z., Hurtt, R., Gu, T., and Doria, C. (2012). Gefitinib resistance in HCC mahlavu cells: upregulation of CD133 expression, activation of IGF-1R signaling pathway, and enhancement of IGF-1R nuclear translocation. *J. Cell. Physiol.* 227, 2947–2952. doi: 10.1002/jcp.23041

Chacon-Martinez, C. A., Koester, J., and Wickstrom, S. A. (2018). Signaling in the stem cell niche: regulating cell fate, function and plasticity. *Development* 145:dev165399. doi: 10.1242/dev.165399

Chang, R. L., Lin, J. W., Hsieh, D. J., Yeh, Y. L., Shen, C. Y., Day, C. H., et al. (2015). Long-term hypoxia exposure enhanced IGFBP-3 protein synthesis and secretion resulting in cell apoptosis in H9c2 myocardial cells. *Growth Factors* 33, 275–281. doi: 10.3109/08977194.2015.1077824

Chang, T. S., Chen, C. L., Wu, Y. C., Liu, J. J., Kuo, Y. C., Lee, K. F., et al. (2016). Inflammation promotes expression of stemness-related properties in HBV-related hepatocellular carcinoma. *PLoS ONE* 11:e0149897. doi: 10.1371/journal.pone.0149897

Chang, T. S., Wu, Y. C., Chi, C. C., Su, W. C., Chang, P. J., Lee, K. F., et al. (2015). Activation of IL6/IGFIR confers poor prognosis of HBV-related hepatocellular carcinoma through induction of OCT4/NANOG expression. *Clin. Cancer Res.* 21, 201–210. doi: 10.1158/1078-0432.CCR-13-3274

Chang, W. W., Lin, R. J., Yu, J., Chang, W. Y., Fu, C. H., Lai, A., et al. (2013). The expression and significance of insulin-like growth factor-1 receptor and its pathway on breast cancer stem/progenitors. *Breast Cancer Res.* 15:R39. doi: 10.1186/bcr3423

Chen, C. W., and Roy, D. (1996). Up-regulation of nuclear IGF-I receptor by short term exposure of stilbene estrogen, diethylstilbestrol. *Mol. Cell. Endocrinol.* 118, 1–8. doi: 10.1016/0303-7207(96)03751-3

Chen, C. Y., Tseng, K. Y., Lai, Y. L., Chen, Y. S., Lin, F. H., and Lin, S. (2017). Overexpression of insulin-like growth factor 1 enhanced the osteogenic capability of aging bone marrow mesenchymal stem cells. *Theranostics* 7, 1598–1611. doi: 10.7150/thno.16637

Chen, L., and Khillan, J. S. (2010). A novel signaling by vitamin A/retinol promotes self renewal of mouse embryonic stem cells by activating PI3K/Akt signaling pathway via insulin-like growth factor-1 receptor. *Stem Cells* 28, 57–63. doi: 10.1002/stem.251

Chen, W. J., Ho, C. C., Chang, Y. L., Chen, H. Y., Lin, C. A., Ling, T. Y., et al. (2014). Cancer-associated fibroblasts regulate the plasticity of lung cancer stemness via paracrine signalling. *Nat. Commun.* 5:3472. doi: 10.1038/ncomms4472

Clevers, H. (2011). The cancer stem cell: premises, promises and challenges. *Nat. Med.* 17, 313–319. doi: 10.1038/nm.2304

Codony-Servat, J., Cuatrecasas, M., Asensio, E., Montironi, C., Martinez-Cardus, A., Marin-Aguilera, M., et al. (2017). Nuclear IGF-1R predicts chemotherapy and targeted therapy resistance in metastatic colorectal cancer. *Br. J. Cancer* 117, 1777–1786. doi: 10.1038/bjc.2017.279

Dallas, N. A., Xia, L., Fan, F., Gray, M. J., Gaur, P., van Buren, G. II, et al. (2009). Chemoresistant colorectal cancer cells, the cancer stem cell phenotype, and increased sensitivity to insulin-like growth factor-I receptor inhibition. *Cancer Res.* 69, 1951–1957. doi: 10.1158/0008-5472.CAN-08-2023

Eliasz, S., Liang, S., Chen, Y., De Marco, M. A., Machek, O., Skucha, S., et al. (2010). Notch-1 stimulates survival of lung adenocarcinoma cells during hypoxia by activating the IGF-1R pathway. *Oncogene* 29, 2488–2498. doi: 10.1038/onc.2010.7

Fathollahipour, S., Patil, P. S., and Leipzig, N. D. (2018). Oxygen regulation in development: lessons from embryogenesis towards tissue engineering. *Cells Tissues Organs* 205, 350–371. doi: 10.1159/000493162

Fowlkes, J. L., Serra, D. M., Bunn, R. C., Thrailkill, K. M., Enghild, J. J., and Nagase, H. (2004). Regulation of insulin-like growth factor (IGF)-I action by matrix metalloproteinase-3 involves selective disruption of IGF-I/IGF-binding protein-3 complexes. *Endocrinology* 145, 620–626. doi: 10.1210/en.2003-0636

Fujita, M., Ieguchi, K., Cedano-Prieto, D. M., Fong, A., Wilkerson, C., Chen, J. Q., et al. (2013). An integrin binding-defective mutant of insulin-like growth factor-1 (R36E/R37E IGF1) acts as a dominant-negative antagonist of the IGF1 receptor (IGF1R) and suppresses tumorigenesis but still binds to IGF1R. *J. Biol. Chem.* 288, 19593–19603. doi: 10.1074/jbc.M113.470872

Girnita, L., Worrall, C., Takahashi, S., Seregard, S., and Girnita, A. (2014). Something old, something new and something borrowed: emerging paradigm of insulin-like growth factor type 1 receptor (IGF-1R) signaling regulation. *Cell. Mol. Life Sci.* 71, 2403–2427. doi: 10.1007/s00018-013-1514-y

Gong, H., Wang, X., Wang, L., Liu, Y., Wang, J., Lv, Q., et al. (2017). Inhibition of IGF-1 receptor kinase blocks the differentiation into cardiomyocyte-like cells of BMSCs induced by IGF-1. *Mol. Med. Rep.* 16, 787–793. doi: 10.3892/mmr.2017.6639

Granata, R., Trovato, L., Garbarino, G., Taliano, M., Ponti, R., Sala, G., et al. (2004). Dual effects of IGFBP-3 on endothelial cell apoptosis and survival: involvement of the sphingolipid signaling pathways. *FASEB J.* 18, 1456–1458. doi: 10.1096/fj.04-1618fje

Han, C. Z., Juncadella, I. J., Kinchen, J. M., Buckley, M. W., Klibanov, A. L., Dryden, K., et al. (2016). Macrophages redirect phagocytosis by non-professional phagocytes and influence inflammation. *Nature* 539, 570–574. doi: 10.1038/nature20141

Hart, L. S., Dolloff, N. G., Dicker, D. T., Koumenis, C., Christensen, J. G., Grimberg, A., et al. (2011). Human colon cancer stem cells are enriched by insulin-like growth factor-1 and are sensitive to figitumumab. *Cell Cycle* 10, 2331–2338. doi: 10.4161/cc.10.14.16418

Hirakawa, T., Yashiro, M., Doi, Y., Kinoshita, H., Morisaki, T., Fukuoka, T., et al. (2016). Pancreatic Fibroblasts stimulate the motility of pancreatic cancer cells through IGF1/IGF1R signaling under hypoxia. *PLoS ONE* 11:e0159912. doi: 10.1371/journal.pone.0159912

Huang, X., Park, H., Greene, J., Pao, J., Mulvey, E., Zhou, S. X., et al. (2015). IGF1R- and ROR1-specific CAR T cells as a potential therapy for high risk sarcomas. *PLoS ONE* 10:e0133152. doi: 10.1371/journal.pone.0133152

Huang, Y. H., Chin, C. C., Ho, H. N., Chou, C. K., Shen, C. N., Kuo, H. C., et al. (2009). Pluripotency of mouse spermatogonial stem cells maintained by IGF-1-dependent pathway. *FASEB J.* 23, 2076–2087. doi: 10.1096/fj.08-121939

Huang, Y. H., Lin, M. H., Wang, P. C., Wu, Y. C., Chiang, H. L., Wang, Y. L., et al. (2014). Hypoxia inducible factor 2alpha/insulin-like growth factor receptor signal loop supports the proliferation and Oct-4 maintenance of mouse germline stem cells. *Mol. Hum. Reprod.* 20, 526–537. doi: 10.1093/molehr/gau016

Hwang, D. H., Park, H. H., Shin, H. Y., Cui, Y., and Kim, B. G. (2018). Insulin-like growth factor-1 receptor dictates beneficial effects of treadmill training by regulating survival and migration of neural stem cell grafts in the injured spinal cord. *Exp. Neurobiol.* 27, 489–507. doi: 10.5607/en.2018.27.6.489

Iozzo, R. V., Buraschi, S., Genua, M., Xu, S. Q., Solomides, C. C., Peiper, S. C., et al. (2011). Decorin antagonizes IGF receptor I (IGF-IR) function by interfering with IGF-IR activity and attenuating downstream signaling. *J. Biol. Chem.* 286, 34712–34721. doi: 10.1074/jbc.M111.262766

Jackson, R., Tilokee, E. L., Latham, N., Mount, S., Rafatian, G., Strydhorst, J., et al. (2015). Paracrine engineering of human cardiac stem cells with insulin-like growth factor 1 enhances myocardial repair. *J. Am. Heart Assoc.* 4:e002104. doi: 10.1161/JAHA.115.002104

Jeon, H. J., Park, J., Shin, J. H., and Chang, M. S. (2017). Insulin-like growth factor binding protein-6 released from human mesenchymal stem cells confers neuronal protection through IGF-1R-mediated signaling. *Int. J. Mol. Med.* 40, 1860–1868. doi: 10.3892/ijmm.2017.3173

Ji, Y., Wang, Z., Chen, H., Zhang, L., Zhuo, F., and Yang, Q. (2018). Serum from chronic hepatitis B patients promotes growth and proliferation via the IGF-II

/IGF-IR/MEK/ERK signaling pathway in hepatocellular carcinoma cells. *Cell. Physiol. Biochem.* 47, 39–53. doi: 10.1159/000489744

Kaplan, S. A., and Cohen, P. (2007). The somatomedin hypothesis 2007: 50 years later. *J. Clin. Endocrinol. Metab.* 92, 4529–4535. doi: 10.1210/jc.2007-0526

Kim, I. G., Kim, S. Y., Choi, S. I., Lee, J. H., Kim, K. C., and Cho, E. W. (2014). Fibulin-3-mediated inhibition of epithelial-to-mesenchymal transition and self-renewal of ALDH+ lung cancer stem cells through IGF1R signaling. *Oncogene* 33, 3908–3917. doi: 10.1038/onc.2013.373

Kim, S. H., Chung, S. W., and Oh, J. H. (2014). Expression of insulin-like growth factor type 1 receptor and myosin heavy chain in rabbit's rotator cuff muscle after injection of adipose-derived stem cell. *Knee Surg. Sports Traumatol. Arthrosc.* 22, 2867–2873. doi: 10.1007/s00167-013-2560-6

Kuo, Y. C., Au, H. K., Hsu, J. L., Wang, H. F., Lee, C. J., Peng, S. W., et al. (2018). IGF-1R promotes symmetric self-renewal and migration of alkaline phosphatase(+) germ stem cells through HIF-2alpha-OCT4/CXCR4 loop under hypoxia. *Stem Cell Rep.* 10, 524–537. doi: 10.1016/j.stemcr.2017.12.003

Lai, S. C., Su, Y. T., Chi, C. C., Kuo, Y. C., Lee, K. F., Wu, Y. C., et al. (2019). DNMT3b/OCT4 expression confers sorafenib resistance and poor prognosis of hepatocellular carcinoma through IL-6/STAT3 regulation. *J. Exp. Clin. Cancer Res.* 38:474. doi: 10.1186/s13046-019-1442-2

Lee, H. T., Chang, H. T., Lee, S., Lin, C. H., Fan, J. R., Lin, S. Z., et al. (2016). Role of IGF1R(+) MSCs in modulating neuroplasticity via CXCR4 cross-interaction. *Sci. Rep.* 6:32595. doi: 10.1038/srep32595

Lee, J. H., Choi, S. I., Kim, R. K., Cho, E. W., and Kim, I. G. (2018). Tescalcin/c-Src/IGF1Rbeta-mediated STAT3 activation enhances cancer stemness and radioresistant properties through ALDH1. *Sci. Rep.* 8:10711. doi: 10.1038/s41598-018-29142-x

Lee, J. H., Kim, J. Y., Kim, S. Y., Choi, S. I., Kim, K. C., Cho, E. W., et al. (2017). APBB1 reinforces cancer stem cell and epithelial-to-mesenchymal transition by regulating the IGF1R signaling pathway in non-small-cell lung cancer cells. *Biochem. Biophys. Res. Commun.* 482, 35–42. doi: 10.1016/j.bbrc.2016.11.030

Li, J., Dong, R., Yu, J., Yi, S., Da, J., Yu, F., et al. (2018). Inhibitor of IGF1 receptor alleviates the inflammation process in the diabetic kidney mouse model without activating SOCS2. *Drug Des. Devel. Ther.* 12, 2887–2896. doi: 10.2147/DDDT.S171638

Lin, Y., Liu, H., Waraky, A., Haglund, F., Agarwal, P., Jernberg-Wiklund, H., et al. (2017). SUMO-modified insulin-like growth factor 1 receptor (IGF-1R) increases cell cycle progression and cell proliferation. *J. Cell. Physiol.* 232, 2722–2730. doi: 10.1002/jcp.25818

Liu, G. X., Ma, S., Li, Y., Yu, Y., Zhou, Y. X., Lu, Y. D., et al. (2018). Hsa-let-7c controls the committed differentiation of IGF-1-treated mesenchymal stem cells derived from dental pulps by targeting IGF-1R via the MAPK pathways. *Exp. Mol. Med.* 50:25. doi: 10.1038/s12276-018-0048-7

Lunn, J. S., Sakowski, S. A., McGinley, L. M., Pacut, C., Hazel, T. G., Johe, K., et al. (2015). Autocrine production of IGF-I increases stem cell-mediated neuroprotection. *Stem Cells* 33, 1480–1489. doi: 10.1002/stem.1933

Mah, A. T., Yan, K. S., and Kuo, C. J. (2016). Wnt pathway regulation of intestinal stem cells. *J. Physiol. (Lond).* 594, 4837–4847. doi: 10.1113/JP271754

Martinez-Quetglas, I., Pinyol, R., Dauch, D., Torrecilla, S., Tovar, V., Moeini, A., et al. (2016). IGF2 is up-regulated by epigenetic mechanisms in hepatocellular carcinomas and is an actionable oncogene product in experimental models. *Gastroenterology* 151, 1192–1205. doi: 10.1053/j.gastro.2016.09.001

Mishra, L., Derynck, R., and Mishra, B. (2005). Transforming growth factor-beta signaling in stem cells and cancer. *Science* 310, 68–71. doi: 10.1126/science.1118389

Mohyeldin, A., Garzon-Muvdi, T., and Quinones-Hinojosa, A. (2010). Oxygen in stem cell biology: a critical component of the stem cell niche. *Cell Stem Cell* 7, 150–161. doi: 10.1016/j.stem.2010.07.007

Morrison, S. J., and Spradling, A. C. (2008). Stem cells and niches: mechanisms that promote stem cell maintenance throughout life. *Cell* 132, 598–611. doi: 10.1016/j.cell.2008.01.038

Murayama, T., Nakaoku, T., Enari, M., Nishimura, T., Tominaga, K., Nakata, A., et al. (2016). Oncogenic fusion gene CD74-NRG1 confers cancer stem cell-like properties in lung cancer through a IGF2 autocrine/paracrine circuit. *Cancer Res.* 76, 974–983. doi: 10.1158/0008-5472.CAN-15-2135

Ning, H., Lin, G., Fandel, T., Banie, L., Lue, T. F., and Lin, C. S. (2008). Insulin growth factor signaling mediates neuron-like differentiation of adipose-tissue-derived stem cells. *Differentiation* 76, 488–494. doi: 10.1111/j.1432-0436.2007.00240.x

Packham, S., Warsito, D., Lin, Y., Sadi, S., Karlsson, R., Sehat, B., et al. (2015). Nuclear translocation of IGF-1R via p150(Glued) and an importin-beta/RanBP2-dependent pathway in cancer cells. *Oncogene* 34, 2227–2238. doi: 10.1038/onc.2014.165

Park, S. B., Yu, K. R., Jung, J. W., Lee, S. R., Roh, K. H., Seo, M. S., et al. (2009). bFGF enhances the IGFs-mediated pluripotent and differentiation potentials in multipotent stem cells. *Growth Factors* 27, 425–437. doi: 10.3109/08977190903289875

Pineiro-Hermida, S., Alfaro-Arnedo, E., Gregory, J. A., Torrens, R., Ruiz-Martinez, C., Adner, M., et al. (2017). Characterization of the acute inflammatory profile and resolution of airway inflammation after Igf1r-gene targeting in a murine model of HDM-induced asthma. *PLoS ONE* 12:e0190159. doi: 10.1371/journal.pone.0190159

Reya, T., Morrison, S. J., Clarke, M. F., and Weissman, I. L. (2001). Stem cells, cancer, and cancer stem cells. *Nature* 414, 105–111. doi: 10.1038/35102167

Sakaki-Yumoto, M., Katsuno, Y., and Derynck, R. (2013). TGF-beta family signaling in stem cells. *Biochim. Biophys. Acta* 1830, 2280–2296. doi: 10.1016/j.bbagen.2012.08.008

Sanchez-Lopez, E., Flashner-Abramson, E., Shalapour, S., Zhong, Z., Taniguchi, K., Levitzki, A., et al. (2016). Targeting colorectal cancer via its microenvironment by inhibiting IGF-1 receptor-insulin receptor substrate and STAT3 signaling. *Oncogene* 35, 2634–2644. doi: 10.1038/onc.2015.326

Sarfstein, R., Pasmanik-Chor, M., Yeheskel, A., Edry, L., Shomron, N., Warman, N., et al. (2012). Insulin-like growth factor-I receptor (IGF-IR) translocates to nucleus and autoregulates IGF-IR gene expression in breast cancer cells. *J. Biol. Chem.* 287, 2766–2776. doi: 10.1074/jbc.M111.281782

Scavo, L. M., Karas, M., Murray, M., and Leroith, D. (2004). Insulin-like growth factor-I stimulates both cell growth and lipogenesis during differentiation of human mesenchymal stem cells into adipocytes. *J. Clin. Endocrinol. Metab.* 89, 3543–3553. doi: 10.1210/jc.2003-031682

Sehat, B., Tofigh, A., Lin, Y., Trocme, E., Liljedahl, U., Lagergren, J., et al. (2010). SUMOylation mediates the nuclear translocation and signaling of the IGF-1 receptor. *Sci Signal.* 3:ra10. doi: 10.1126/scisignal.2000628

Shao, Y., Chong, L., Lin, P., Li, H., Zhu, L., Wu, Q., et al. (2019). MicroRNA-133a alleviates airway remodeling in asthtama through PI3K/AKT/mTOR signaling pathway by targeting IGF1R. *J. Cell. Physiol.* 234, 4068–4080. doi: 10.1002/jcp.27201

Shehab, M. A., Biggar, K., Singal, S. S., Nygard, K., Shun-Cheng Li, S., Jansson, T., et al. (2017). Exposure of decidualized HIESC to low oxygen tension and leucine deprivation results in increased IGFBP-1 phosphorylation and reduced IGF-I bioactivity. *Mol. Cell. Endocrinol.* 452, 1–14. doi: 10.1016/j.mce.2017.04.005

Shi, L., Kojonazarov, B., Elgheznawy, A., Popp, R., Dahal, B. K., Bohm, M., et al. (2016). miR-223-IGF-IR signalling in hypoxia- and load-induced right-ventricular failure: a novel therapeutic approach. *Cardiovasc. Res.* 111, 184–193. doi: 10.1093/cvr/cvw065

Shi, Y., Chen, J., Karner, C. M., and Long, F. (2015). Hedgehog signaling activates a positive feedback mechanism involving insulin-like growth factors to induce osteoblast differentiation. *Proc. Natl. Acad. Sci. U. S. A.* 112, 4678–4683. doi: 10.1073/pnas.1502301112

Simon, M. C., and Keith, B. (2008). The role of oxygen availability in embryonic development and stem cell function. *Nat. Rev. Mol. Cell Biol.* 9, 285–296. doi: 10.1038/nrm2354

Spivakov, M., and Fisher, A. G. (2007). Epigenetic signatures of stem-cell identity. *Nat. Rev. Genet.* 8, 263–271. doi: 10.1038/nrg2046

Sun, M., Ramchandran, R., Chen, J., Yang, Q., and Raj, J. U. (2016). Smooth muscle insulin-like growth factor-1 mediates hypoxia-induced pulmonary hypertension in neonatal mice. *Am. J. Respir. Cell Mol. Biol.* 55, 779–791. doi: 10.1165/rcmb.2015-0388OC

Tahimic, C. G., Long, R. K., Kubota, T., Sun, M. Y., Elalieh, H., Fong, C., et al. (2016). Regulation of ligand and shear stress-induced insulin-like growth factor 1 (IGF1) signaling by the integrin pathway. *J. Biol. Chem.* 291, 8140–8149. doi: 10.1074/jbc.M115.693598

Taipale, J., and Beachy, P. A. (2001). The Hedgehog and Wnt signalling pathways in cancer. *Nature* 411, 349–354. doi: 10.1038/35077219

Takada, Y., Takada, Y. K., and Fujita, M. (2017). Crosstalk between insulin-like growth factor (IGF) receptor and integrins through direct integrin binding to IGF1. *Cytokine Growth Factor Rev.* 34, 67–72. doi: 10.1016/j.cytogfr.2017.01.003

Toh, T. B., Lim, J. J., and Chow, E. K. (2017). Epigenetics in cancer stem cells. *Mol. Cancer* 16:29. doi: 10.1186/s12943-017-0596-9

Tovar, V., Cornella, H., Moeini, A., Vidal, S., Hoshida, Y., Sia, D., et al. (2017). Tumour initiating cells and IGF/FGF signalling contribute to sorafenib resistance in hepatocellular carcinoma. *Gut* 66, 530–540. doi: 10.1136/gutjnl-2015-309501

Urtasun, N., Vidal-Pla, A., Perez-Torras, S., and Mazo, A. (2015). Human pancreatic cancer stem cells are sensitive to dual inhibition of IGF-IR and ErbB receptors. *BMC Cancer* 15:223. doi: 10.1186/s12885-015-1249-2

Vakhshiteh, F., Atyabi, F., and Ostad, S. N. (2019). Mesenchymal stem cell exosomes: a two-edged sword in cancer therapy. *Int. J. Nanomedicine* 14, 2847–2859. doi: 10.2147/IJN.S200036

Velloso, C. P. (2008). Regulation of muscle mass by growth hormone and IGF-I. *Br. J. Pharmacol.* 154, 557–568. doi: 10.1038/bjp.2008.153

Wang, L., Schulz, T. C., Sherrer, E. S., Dauphin, D. S., Shin, S., Nelson, A. M., et al. (2007). Self-renewal of human embryonic stem cells requires insulin-like growth factor-1 receptor and ERBB2 receptor signaling. *Blood* 110, 4111–4119. doi: 10.1182/blood-2007-03-082586

Wang, Q., Zhang, F., and Hong, Y. (2018). Blocking of autocrine IGF-1 reduces viability of human umbilical cord mesenchymal stem cells via inhibition of the Akt/Gsk-3beta signaling pathway. *Mol. Med. Rep.* 17, 4681–4687. doi: 10.3892/mmr.2018.8445

Wang, X., Liu, S., Cao, L., Zhang, T., Yue, D., Wang, L., et al. (2017). miR-29a-3p suppresses cell proliferation and migration by downregulating IGF1R in hepatocellular carcinoma. *Oncotarget* 8, 86592–86603. doi: 10.18632/oncotarget.21246

Wang, X. Q., Ng, R. K., Ming, X., Zhang, W., Chen, L., Chu, A. C., et al. (2013). Epigenetic regulation of pluripotent genes mediates stem cell features in human hepatocellular carcinoma and cancer cell lines. *PLoS ONE* 8:e72435. doi: 10.1371/journal.pone.0072435

Wang, Y., Zhao, R., Liu, W., Wang, Z., Rong, J., Long, X., et al. (2019). Exosomal circHIPK3 released from hypoxia-pretreated cardiomyocytes regulates oxidative damage in cardiac microvascular endothelial cells via the miR-29a/IGF-1 pathway. *Oxid. Med. Cell. Longev.* 2019:7954657. doi: 10.1155/2019/7954657

Warsito, D., Lin, Y., Gnirck, A. C., Sehat, B., and Larsson, O. (2016). Nuclearly translocated insulin-like growth factor 1 receptor phosphorylates histone H3 at tyrosine 41 and induces SNAI2 expression via Brg1 chromatin remodeling protein. *Oncotarget* 7, 42288–42302. doi: 10.18632/oncotarget.9785

Warsito, D., Sjostrom, S., Andersson, S., Larsson, O., and Sehat, B. (2012). Nuclear IGF1R is a transcriptional co-activator of LEF1/TCF. *EMBO Rep.* 13, 244–250. doi: 10.1038/embor.2011.251

Werner, H., Sarfstein, R., and Bruchim, I. (2019). Investigational IGF1R inhibitors in early stage clinical trials for cancer therapy. *Expert Opin. Investig. Drugs* 28, 1101–1112. doi: 10.1080/13543784.2019.1694660

Xian, L., Wu, X., Pang, L., Lou, M., Rosen, C. J., Qiu, T., et al. (2012). Matrix IGF-1 maintains bone mass by activation of mTOR in mesenchymal stem cells. *Nat. Med.* 18, 1095–1101. doi: 10.1038/nm.2793

Xu, C., Xie, D., Yu, S. C., Yang, X. J., He, L. R., Yang, J., et al. (2013). beta-Catenin/POU5F1/SOX2 transcription factor complex mediates IGF-I receptor signaling and predicts poor prognosis in lung adenocarcinoma. *Cancer Res.* 73, 3181–3189. doi: 10.1158/0008-5472.CAN-12-4403

Xu, Q., Yan, B., Li, S., and Duan, C. (2004). Fibronectin binds insulin-like growth factor-binding protein 5 and abolishes Its ligand-dependent action on cell migration. *J. Biol. Chem.* 279, 4269–4277. doi: 10.1074/jbc.M311586200

Xu, X., Li, X., Yan, R., Jiang, H., Wang, T., Fan, L., et al. (2016). Gene expression profiling of human bone marrow-derived mesenchymal stem cells during adipogenesis. *Folia Histochem. Cytobiol.* 54, 14–24. doi: 10.5603/FHC.a2016.0003

Xu, Y., Huang, J., Ma, L., Shan, J., Shen, J., Yang, Z., et al. (2016). MicroRNA-122 confers sorafenib resistance to hepatocellular carcinoma cells by targeting IGF-1R to regulate RAS/RAF/ERK signaling pathways. *Cancer Lett.* 371, 171–181. doi: 10.1016/j.canlet.2015.11.034

Yin, J., Xu, W. Q., Ye, M. X., Zhang, Y., Wang, H. Y., Zhang, J., et al. (2017). Up-regulated basigin-2 in microglia induced by hypoxia promotes retinal angiogenesis. *J. Cell. Mol. Med.* 21, 3467–3480. doi: 10.1111/jcmm.13256

Yu, K. R., Yang, S. R., Jung, J. W., Kim, H., Ko, K., Han, D. W., et al. (2012). CD49f enhances multipotency and maintains stemness through the direct regulation of OCT4 and SOX2. *Stem Cells* 30, 876–887. doi: 10.1002/stem.1052

Zhang, J., Li, Y., Chen, J., Yang, M., Katakowski, M., Lu, M., et al. (2004). Expression of insulin-like growth factor 1 and receptor in ischemic rats treated with human marrow stromal cells. *Brain Res.* 1030, 19–27. doi: 10.1016/j.brainres.2004.09.061

Zhang, R., Yao, R. R., Li, J. H., Dong, G., Ma, M., Zheng, Q. D., et al. (2017). Activated hepatic stellate cells secrete periostin to induce stem cell-like phenotype of residual hepatocellular carcinoma cells after heat treatment. *Sci. Rep.* 7:2164. doi: 10.1038/s41598-017-01177-6

Zhang, Y., and Marmorstein, L. Y. (2010). Focus on molecules: fibulin-3 (EFEMP1). *Exp. Eye Res.* 90, 374–375. doi: 10.1016/j.exer.2009.09.018

Conflict of Interest: The authors declare that the research was conducted in the absence of any commercial or financial relationships that could be construed as a potential conflict of interest.

frontiers in Cell and Developmental Biology

BRIEF RESEARCH REPORT
published: 26 May 2021
doi: 10.3389/fcell.2021.675411

Oncostatin M Maintains Naïve Pluripotency of mESCs by Tetraploid Embryo Complementation (TEC) Assay

Xiaoying Ye[1,2†], Chenglei Tian[1,2,3†], Linlin Liu[1,2], Guofeng Feng[1,2], Kairang Jin[1,2], Haiying Wang[1,2], Jiyu Chen[1,2] and Lin Liu[1,2*]*

[1] State Key Laboratory of Medicinal Chemical Biology, Nankai University, Tianjin, China, [2] Department of Cell Biology and Genetics, College of Life Sciences, Nankai University, Tianjin, China, [3] Novo Nordisk Foundation Center for Stem Cell Biology (DanStem), University of Copenhagen, Copenhagen, Denmark

OPEN ACCESS

Edited by:
Rita Yen-Hua Huang,
Taipei Medical University, Taiwan

Reviewed by:
Yuhua Sun,
Institute of Hydrobiology (CAS), China
Evangelos Delivopoulos,
University of Reading,
United Kingdom

***Correspondence:**
Xiaoying Ye
nkxy10@nankai.edu.cn
Lin Liu
liulin@nankai.edu.cn

† These authors have contributed equally to this work and share first authorship

Specialty section:
This article was submitted to Stem Cell Research, a section of the journal Frontiers in Cell and Developmental Biology

Received: 03 March 2021
Accepted: 03 May 2021
Published: 26 May 2021

Citation:
Ye X, Tian C, Liu L, Feng G, Jin K, Wang H, Chen J and Liu L (2021) Oncostatin M Maintains Naïve Pluripotency of mESCs by Tetraploid Embryo Complementation (TEC) Assay. Front. Cell Dev. Biol. 9:675411. doi: 10.3389/fcell.2021.675411

It has been well established that leukemia inhibitory factor (LIF) is essential for maintaining naïve pluripotency of embryonic stem cells (ESCs). Oncostatin M (OSM) is a member of the IL-6 family of cytokines which share gp130 as a receptor subunit, and the OSM-gp130 complex can recruit either LIF receptor β or OSM receptor β. Here we show that OSM can completely replace LIF to maintain naïve pluripotency of ESCs. Mouse ESCs (mESCs) cultured in the presence of LIF or OSM not only express pluripotency genes at similar levels but also exhibit the same developmental pluripotency as evidenced by the generation of germline competent chimeras, supporting previous findings. Moreover, we demonstrate by tetraploid embryo complementation assay, the most stringent functional test of authentic pluripotency that mESCs cultured in OSM produce viable all-ESC pups. Furthermore, telomere length and telomerase activity, which are also crucial for unlimited self-renewal and genomic stability of mESCs, do not differ in mESCs cultured under OSM or LIF. The transcriptome of mESCs cultured in OSM overall is very similar to that of LIF, and OSM activates Stat3 signaling pathway, like LIF. Additionally, OSM upregulates pentose and glucuronate interconversion, ascorbate and aldarate metabolism, and steroid and retinol metabolic pathways. Although the significance of these pathways remains to be determined, our data shows that OSM can maintain naïve pluripotent stem cells in the absence of LIF.

Keywords: oncostatin M (OSM), LIF, ESC, naïve pluripotency, TEC mice, telomere, 2C-genes, Stat3

INTRODUCTION

Mouse embryonic stem cells (mESCs) derived from the inner cell mass of preimplantation embryos are known to be in a state of naïve pluripotency. This condition is underscored by the derivation of healthy adult mice if the cells are introduced into a tetraploid donor blastocyst (Nagy et al., 1993). Leukemia inhibitory factor (LIF) is typically added to the culture medium to inhibit autonomous differentiation of mESCs, mainly by activating the Jak/Stat3 pathway (Niwa et al., 1998; Raz et al., 1999). Novel condition 2i (inhibitors of Mek and Gsk3β signaling) medium reportedly could retain self-renewal and multilineage commitment of embryoid bodies independent of LIF and Stat3 (Ying et al., 2008). Addition of LIF to 2i medium (2i/L medium) was reported to elevate the development potential of mESCs by completed-ESC pups, although the

pups failed to survive to adulthood due to irreversible global DNA hypomethylation and impaired telomere function for long-term culture (Choi et al., 2017; Yagi et al., 2017; Guo et al., 2018). More specifically, LIF has been shown to play an essential role in underpinning the naïve pluripotency of mESCs not only in conventional serum medium but also in chemically defined 2i medium. Thus far, however, there have been no reports of a complete replacement for LIF in mESC cultures.

Oncostatin M (OSM) is a member of the interleukin (IL)-6 family and was originally characterized for its ability to promote differentiation of histiocytic lymphoma cells (Zarling et al., 1986). Of note, OSM has been reported to be structurally and functionally related to LIF, sharing both the transducer gp130 and LIF receptor beta (LIFRβ) (Gearing and Bruce, 1992; Gearing et al., 1992). Notably, mESCs cultured in OSM were shown to resemble, in morphology and expression of pluripotency markers, to mESCs grown in LIF-supplemented medium (Rose et al., 1994). Moreover, OSM was found to retain mESCs in pluripotency, as revealed by the detection of chimeras that were competent for germline transmission (Nichols et al., 1994). However, it remains elusive whether OSM could completely substitute LIF in maintaining the mESCs in naïve pluripotency by tetraploid embryo complementation, which is considered the most stringent test for complete developmental potential (Eggan et al., 2002).

In the present study, we demonstrate that OSM could maintain mESCs in naïve pluripotency, as validated by the generation of healthy adult mice from mESCs cultured in OSM for up to 10 passages using the TEC method. mESCs in OSM-supplemented medium exhibited equivalent pluripotency and 2-cell gene expression levels, telomere length, telomerase activity, overall transcriptome profile, efficiency of germline competent chimera, and generation of TEC mice, compared with mESCs cultured in LIF. In addition to activating the Jak/Stat3 signaling pathway, OSM was also found to upregulate pentose and glucuronate interconversion, ascorbate and aldarate metabolism, and steroid and retinol metabolic pathways, which might be involved in the self-renewal and maintenance of naïve pluripotency. However, this needs further investigation.

MATERIALS AND METHODS

Mice and Cell Culture

Mice were housed in the College Animal Facility and the use of mice for this research was approved by the Institutional Animal Care and Use Committee at Nankai University. Balb/c and ICR mice were purchased from Beijing Vital River Laboratory Animal Technology Co., Ltd.

The mouse ES cell line used in this study was derived from the C57BL/6 × 129S6 blastocyte based on the method described (Huang et al., 2008). The mESCs were cultured on mitomycin C-inactivated MEF feeder cells in serum and LIF based conventional ESC culture medium for five passages. Then the mESCs were transferred to different conditions including ESC basic medium (-LIF medium), ESC basic medium with 1,000 U/mL LIF (Millipore) (LIF medium), and ESC basic medium with OSM (GenScript) (OSM medium), for another 5 (P5) and 10 (P10) passages. ESC culture medium was changed daily and cells routinely passaged every 2 days. Count the cells during passaging for proliferation curve. The ESC basic medium consisted of knockout DMEM (Invitrogen), 20% ESC-quality FBS (Hyclone), 0.1 mM non-essential amino acids (Sigma), 0.1 mM β-mercaptoethanol (Invitrogen), 1 mM L-glutamine (Invitrogen), penicillin (50 U/mL) and streptomycin (50 U/mL) (Invitrogen).

Immunofluorescence Microscopy

Mouse ESCs were fixed in 3.7% paraformaldehyde in PBS for 30 min at 4°C, washed once in PBS then permeabilized in 0.1% Triton X-100 in blocking solution (3% goat serum plus 0.1% BSA in PBS) for 30 min at room temperature, washed once with PBS, and left in blocking solution for 2 h. Cells were incubated overnight at 4°C with primary antibodies against Oct4 (sc5279, Santa Cruz), Nanog (A300-397A, Bethyl), SSEA-1 (MAB4301, Millipore). ESCs were washed three times (each for 15 min) with blocking solution, and incubated for 2 h with secondary antibodies at room temperature. Goat Anti-Mouse IgG (H + L) FITC (115-095-003, Jackson) and Goat Anti-Rabbit IgG (H + L) Alexa Fluor® 594 (111-585-003, Jackson), diluted 1:200 with blocking solution, were used. Samples were washed and counterstained with 0.5 μg/mL DAPI in Vectashield mounting medium (Vector Laboratories). Fluorescence was detected and imaged using Confocal laser scanning microscope LSM710 (Carl Zeiss).

Gene Expression Analysis by Real-Time qPCR

Total RNA of mESCs at P10 was extracted with RNeasy Mini Kit (Qiagen), according to manufacturer's instructions. The cDNA was generated from 2 μg total RNA using M-MLV Reverse Transcriptase (Invitrogen). Real-time quantitative PCR (qPCR) reactions were set up in duplicate with the FS Universal SYBR Green Master (Roche) and run on an iCycler MyiQ2 Detection System (Bio-Rad). Each sample was repeated three times and normalized using Gapdh as the internal control. The amplification was performed for primary denaturation at 95°C for 10 min, then 40 cycles of denaturation at 95°C for 15 s, annealing and elongation at 58°C for 1 min, and the last cycle under 55–95°C for the dissociation curve. Relative quantitative evaluation of the target gene was determined by comparing the threshold cycles. The primers are listed in **Supplementary Table 1**.

Western Blot

Mouse ESCs were collected and lysed in cell lysis buffer on ice for 30 min and then sonicated for 1 min at 60 of amplitude at 2 s intervals. After centrifugation at 10,000 *g* at 4°C for 10 min, the supernatant was collected. The protein samples were boiled in SDS sample buffer at 95°C for 10 min then was resolved by 10% Acr-Bis SDS-PAGE and transferred to polyvinylidene difluoride membranes (PVDF, Millipore). Non-specific binding was blocked by incubation in 5% non-fat milk or 5% BSA solution

for 2 h. Blots were then probed with primary antibodies overnight by incubation at 4°C with Oct4 (sc5279, Santa Cruz), Nanog (ab80892, Abcam), Lin28a (3978S, CST), Stat3 (ab76315, Abcam), pStat3 (#9131S, Cell Signaling), H3K4me3 (Abcam, ab213224), H3K27me3 (Abcam, ab177178), H3 (Abcam, ab1791), or β-Actin (P30002, Abmart) served as the loading control. Secondary antibodies HRP conjugated goat anti-rabbit IgG (NA934V, GE Healthcare) or goat anti-mouse IgG (H + L) (ZB2305, ZSGB-BIO) were used for incubation at room temperature for 2 h. Protein bands were visualized using Chemiluminescent HRP substrate (WBKLS0500, Millipore).

FACS Analysis

For the FACS analysis of Zscan4 expression profile, mESCs at P10 were collected and washed with cold PBS, then fixed in cold 70% ethanol, permeabilized in 0.1% Triton X-100 in blocking solution (3% goat serum in PBS) for 30 min, washed three times, and left in blocking solution for 1 h. ESCs were incubated with primary antibody against Zscan4 (AB4340, Millipore) for 1.5 h, washed three times, and incubated for 1 h with secondary antibody Alex a Fluor 488 Goat Anti-Rabbit IgG (H + L) (A11008, Life) diluted 1:200 with blocking solution. Samples were washed three times with PBS and FACS analysis was performed using a Flow Cytometer (BD Biosciences).

Telomere Measurement by Q-FISH

Telomere length was estimated by telomere Q-FISH as described previously (Herrera et al., 1999; Huang et al., 2011). Telomeres were denatured at 80°C for 3 min and hybridized with Cy3-labeled $(CCCTAA)_3$ peptide nucleic acid (PNA) probe at 0.5 μg/mL (F1002, Panagene). Chromosomes were stained with 0.5 μg/mL DAPI. Fluorescence from chromosomes and telomeres were digitally imaged on a Zeiss microscope with Cy3/DAPI using AxioCam and AxioVision software 4.6. Telomere length showed as telomere fluorescence intensity was integrated using the TFL-TELO program (a gift kindly provided by P. Lansdorp).

Telomerase Activity by TRAP Assay

Telomerase activity was determined by the Stretch PCR method according to manufacturer's instruction using the TeloChaser Telome-rase assay kit (T0001, MD Biotechnology). About 2.5×10^4 mESCs at P10 from each sample were lysed. Lysis buffer served as negative controls. PCR products of cell lysate were separated on non-denaturing TBE-based 12% polyacrylamide gel electrophoresis and visualized by ethidium bromide (EB) staining.

Telomerase Assay by ELISA Assay

Telomerase level was determined by ELISA method according to the manufacturer's instruction using Mouse Telomerase (TE) ELISA kit (CSB-E08022m, CUSABIO).

Chimera Generation, Tetraploid Complementation, and Genotyping

To produce chimeric mice, 10–15 mESCs were injected into four or eight-cell embryos collected from Balb/c mice, using a piezo-actuated microinjection pipette. Injected embryos were cultured overnight in KSOM medium. Blastocysts were transplanted into the uterus of 2.5 dpc pseudo-pregnant ICR mice. For tetraploid embryo complementation assay, tetraploid embryos were first produced by electrofusion of two-cell stage embryos collected from ICR mice. Approximate 15 ESCs at P10 were subsequently injected into the cavity of the tetraploid blastocysts. The tetraploid complemented embryos were transplanted into the uterus of pseudo-pregnant ICR mice. Surrogate mother delivered pups naturally on approximately day 17.5 of gestation. DNA microsatellite genotyping analysis was performed using D12Mit136 and D8Mit4. The PCR primer sequences (**Supplementary Table 2**) were obtained from the Mouse Genome Informatics website.

Library Preparation and RNA-Sequencing

Library Preparation and RNA-Sequencing mRNA was purified from total RNA extracted from mESCs at P10 using poly-T oligo-attached magnetic beads. Fragmentation was carried out using divalent cations under elevated temperature in NEB Next First Strand Synthesis Reaction Buffer (5×). First strand cDNA was synthesized using random hexamer primer and M-MLV Reverse Transcriptase (RNase H). Second strand cDNA synthesis was subsequently performed using DNA Polymerase I and RNase H. Remaining overhangs were converted into blunt ends via exonuclease/polymerase activities. After adenylation of 30 ends of DNA fragments, NEB Next Adaptors with hairpin loop structure were ligated to prepare for hybridization. To select cDNA fragments of preferentially 150–200 bp in length, the library fragments were purified with AMPure XP system (Beckman Coulter, Beverly, United States). Then 3 mL USER Enzyme (NEB, United States) was used with size-selected and cDNA adaptor ligated at 37°C for 15 min followed by 5 min at 95°C prior to PCR. PCR was performed with Phusion High-Fidelity DNA polymerase, Universal PCR primers and Index Primer. At last, PCR products were purified using AMPure XP system and library quality assessed on the Agilent Bioanalyzer 2100 system. Cluster of the index-coded samples was performed on a cBot Cluster Generation System using TruSeq PE Cluster Kit (Illumina) according to the manufacturer's instructions. After cluster generation, the library preparations were sequenced on an Illumina Hiseq platform.

Bioinformatics Analysis

Clean reads were mapped to the mouse reference mm10 reference genome using Hisat2 (Kim et al., 2015). Reads were assigned and counted to genes using the Featurecounts (Liao et al., 2014). The read counts were then loaded into RStudio (R version 3.5), and DESeq2 was used to identify differentially expressed genes. Functional enrichments (GO annotation or KEGG) of differential genes were performed using clusterProfiler (Yu et al., 2012). The heat-maps were drawn by the function "pheatmap" of R packages, correlation coefficients were calculated by the function "cor" in R. Scatterplots were generated using the "ggplot2" package to graphically reveal genes that differ significantly between two

groups. Corrected *P*-value of 0.05 and $\log_2$ (fold change) of 1 were set as the threshold for significantly differential gene expression.

Quantification and Statistical Analysis

Statistics were analyzed using the GraphPad Prism. Data were analyzed using two-tailed unpaired Student's *t*-test to compare two groups or ANOVA to compare more than two groups and expressed as Mean ± SEM. *P*-values less than 0.05 were considered significant ($^*P < 0.05$, $^{**}P < 0.01$ or $^{***}P < 0.001$). In addition, data of TFU is expressed as Mean ± SD in **Figure 2B**. FACS data were analyzed by FlowJo. TFU of telomere Q-FISH was quantified by TFL-TELO program. Graphs were generated using GraphPad Prism or R package ggplot2 and other R packages described in the method details.

RESULTS

OSM Activates the Stat3 Pathway and Sustains Expression of Pluripotency Genes

It is known that LIF binds to the gp130/LIFRβ cell-surface receptor complex, which intracellularly bound to Jak1 to initiate activation of the Stat3 signaling cascade and the core pluripotency circuitry (Niwa et al., 2009). Activation of Stat3 is known to be critical for the maintenance of pluripotency in ESCs (Raz et al., 1999). We thus investigated whether the Stat3 pathway was activated by OSM and aimed to confirm the optimal concentration for this activation.

We used naïve mESCs at passage 5 in these experiments. Using western blot analysis, we measured the protein levels of Stat3 and pStat3 (phosphorylated Stat3) in the mESCs treated with different concentrations of OSM (5, 10, and 20 ng/mL) for 24 h. We also used mESCs cultured in LIF and LIF-free ESC culture medium as positive and negative controls, respectively. As expected, based on the shared receptors with LIF, we found that OSM activated Stat3 at concentrations of 5, 10, and 20 ng/mL. We also observed that phosphorylation of Stat3 reached its maximum level at 10 ng/mL OSM (**Figure 1D**). Based on this finding, we cultured mESCs in medium supplemented with 10 ng/mL OSM in all subsequent experiments. To determine the time required for OSM-triggered activation of Stat3, we treated mESCs with 10 ng/mL OSM for different periods (0, 1 2, 3, and 4 h). Our western blot analysis showed that after 1 h of incubation with OSM, the level of pStat3 increased, reaching its maximum level at 3 h, after which it decreased to a relatively stable level (**Figure 1E**).

Mouse ESCs were then cultured for another 5 (P5) and 10 (P10) passages in the ESC culture medium supplemented with 10 ng/mL OSM (OSM-ESCs) or 1,000 units/mL LIF (LIF-ESCs), with mESCs cultured in the absence of either LIF or OSM (-LIF-ESCs) serving as the control. We observed that morphologically, both LIF and OSM could sustain the undifferentiated cell state (characterized by compact domed cell colonies). In contrast, only differentiated clones (characterized by large, flat cells) could be observed in the -LIF-ESCs at the same passages (**Figure 1A**). Furthermore, immunofluorescent staining indicated that the expression of pluripotency-associated proteins (Oct4, Nanog, SSEA1) did not differ in mESCs cultured in either OSM or LIF at either P5 or P10, whereas they were dramatically decreased in -LIF-ESCs, suggesting that these cells underwent dramatic cellular differentiation (**Figure 1B**). This result was further validated by western blot analysis for Oct4, Nanog, and Lin28 (**Figure 1C**).

OSM Facilitates Normal Telomere Function and Heterogeneity in 2-Cell Gene Expression

Mammalian telomeres consist of $TTAGGG_n$ repeat sequences at the end of chromosomes that are known to protect genomic stability, with the telomere length being maintained primarily by the action of telomerase (Blackburn et al., 2015; Liu, 2017). Telomere lengths have been highly correlated with the developmental pluripotency of mESCs (Huang et al., 2011). Therefore, we measured telomere length of mESCs chromosomes by telomere quantitative fluorescence *in situ* hybridization (Q-FISH). We observed that mESCs cultured under the three conditions described above exhibited normal karyotypes at P10 (**Figure 2A**). Moreover, telomere length (represented as telomere fluorescence intensity (TFU) in OSM-ESCs (83.56 ± 30.00 TFU) were similar to those of LIF-ESCs (81.89 ± 21.43 TFU). In contrast, we note that telomeres dramatically shortened in -LIF-ESCs (76.32 ± 38.40 TFU) over passages *in vitro* (**Figure 2B**), which is associated with the differentiating phenotype. Using quantitative real-time PCR (qRT-PCR), we found that the expression of *Tert* was significant at a higher level in OSM-ESCs than in -LIF-ESCs, though lower than in LIF-ESCs. There were no significant differences in the expression levels of *Terc* telomerase subunits in -LIF-ESCs, OSM-ESCs and LIF-ESCs (**Figure 2C**). To directly assess the telomerase activity, we performed both telomeric repeat amplification protocol (TRAP) and enzyme-linked aptamer sorbent assay (ELISA). The TRAP assay did not reveal any noticeable differences among -LIF-ESCs, LIF-ESCs, and OSM-ESCs in terms of their telomerase activity. For ELISA assay, we used the A49*Terc*-knockout ES cell line as the negative control, and the N33 wild-type ES cell line as the positive control. We observed that both OSM-ESCs and LIF-ESCs exhibited significant higher telomerase activity than -LIF-ESCs, whereas telomerase activity in OSM-ESCs was lower than in LIF-ESCs (**Figures 2D,E**). Together, these results indicated that OSM retained the length of telomeres and a relatively high telomerase activity to maintain the capacity of ESCs for indefinite self-renewal.

Naïve mESC cultures are known to be a heterogeneous mixture of metastable cells with fluctuating activation of 2-cell embryo specific genes (2C-genes), such as *Zscan4* (Falco et al., 2007), *Tcstv1/3* (Cerulo et al., 2014) and *MERVL* elements (Macfarlan et al., 2012). These 2C-like cells have been reported to exhibit an extended development ability, contributing to both embryonic and extraembryonic tissues, thus mimicking their *in vivo* counterparts, the totipotent 2-cell embryos. To determine whether OSM facilitates expression of 2C-genes, we analyzed the transcripts of *Zscan4*, *Tcstv1*, and *Tcstv3* by qRT-PCR. We did not observe any significant differences in the expression

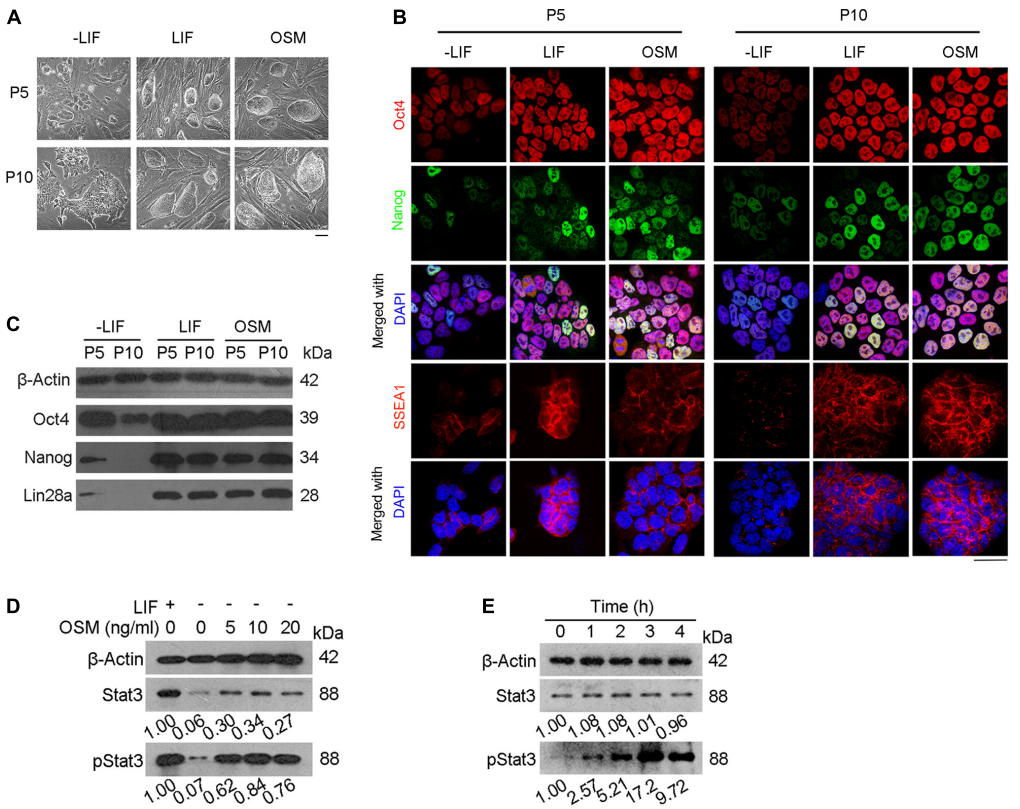

FIGURE 1 | OSM activates Stat3 pathway and sustains expression of pluripotency genes. **(A)** Morphology of mESCs cultured in ESC basic medium (-LIF), ESC basic medium with LIF (LIF) and ESC basic medium with OSM (OSM). Scale bar, 100 μm. **(B,C)** Expression of pluripotency genes cultured in -LIF, LIF and OSM medium at P5 and P10 by immunofluorescence **(B)** and western blot **(C)**. Scale bar, 20 μm. **(D)** Western blot analysis of Stat3 activated by treatment with different concentrations of OSM for 24 h. **(E)** Western blot analysis of Stat3 activated by treatment with 10 ng/mL OSM for different lengths of time.

levels of these three genes between OSM-ESCs and LIF-ESCs. In contrast, their expression was dramatically decreased in ESCs grown without LIF or OSM (**Figure 2F**). Typically, mESC cultures (~5% of cell population) are known to express *Zscan4*, facilitating telomere elongation by telomere-sister chromatid exchange (T-SCE) (Zalzman et al., 2010). Immunofluorescence microscopy quantification and flow cytometry analysis confirmed the occurrence of a proper proportion of Zscan4-positive ($Zscan4^+$) cells maintained in OSM-ESCs, similar to those in LIF-ESCs (**Figures 2G–I**).

OSM Supports Efficient Production of Germline Transmission Mice and TEC Mice

To assess the developmental potential of mESCs cultured in OSM, we performed injections of 4–8-cell embryos. We noted that the mESCs cultured in OSM and LIF exhibited similar efficiency in generating chimeras with germline competence (**Figures 3A,B,D**). Microsatellite genotyping analysis verified that these mESCs contributed to the generation and development of various tissues including the heart, liver, spleen, lungs, brain, kidneys, and gonads (**Figure 3C**). To firmly demonstrate their naïve pluripotency, we performed TEC experiment, the most stringent functional test of pluripotency (Eggan et al., 2002). Surrogate female mice naturally delivered TEC pups on approximately day 17.5 of gestation. We found that the mESCs cultured in OSM and LIF achieved similar efficiency in producing TEC pups, and all pups were able to grow healthily into adulthood, being fertile (**Figures 3E,F**). Microsatellite genotyping analysis confirmed that the examined tissues were molecularly of an ESCs origin (**Figure 3G**). Both chimera and TEC experiments demonstrated that naïve ESCs cultured in OSM based medium robustly contribute to three germ layers including brain from ectoderm, kidney, heart from mesoderm, and liver, lungs and spleen from endoderm, revealed by microsatellite genotyping analysis (**Figures 3C,G**). These results verified that OSM was equivalent to LIF in maintaining the naïve pluripotency of ESCs in the TEC assay.

Transcriptome Profile and Signaling Pathways Regulated by OSM

To illustrate the mechanism underlying the maintenance of naïve pluripotency by OSM, we compared the transcriptomes of mESCs cultured in OSM, LIF, and -LIF medium at P10, using RNA-seq analysis. The tSNE and correlation analyses showed that OSM-ESCs clustered closely together with LIF-ESCs, and were

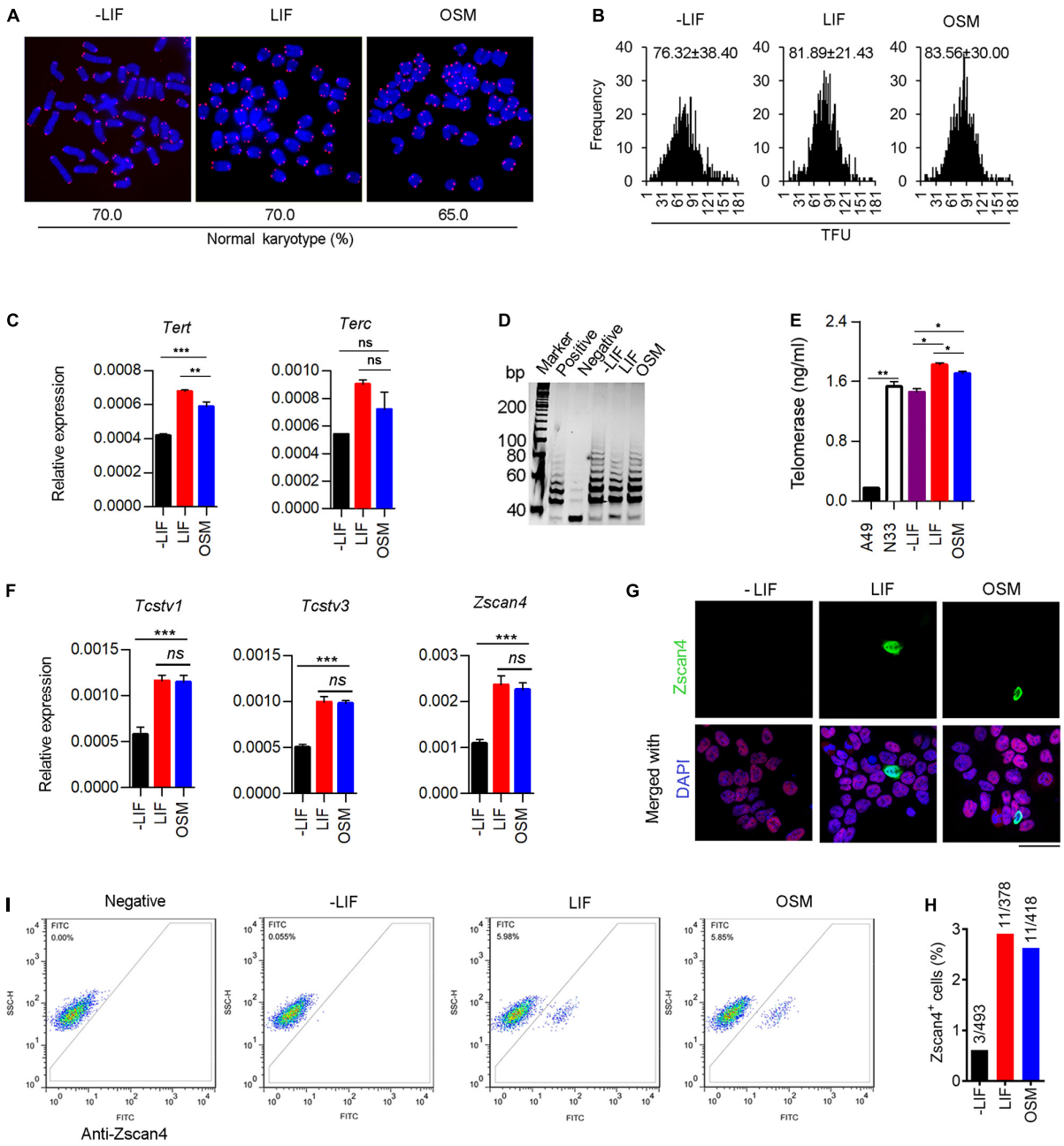

FIGURE 2 | OSM maintains telomere elongation, telomerase activity and heterogeneity in 2-cell gene expression. **(A)** Representative images displaying telomere Q-FISH of mESCs cultured in -LIF, LIF, and OSM medium. Blue, chromosomes stained with DAPI; Red dots, telomeres. Bottom panel, the ratio of normal karyotype in the three culture conditions. **(B)** Telomere Q-FISH assay showing telomere length distribution by telomere fluorescence unit (TFU). Data shown as Mean ± SD. **(C)** Expression of telomerase-related genes: *Tert* and *Terc* in mESCs cultured in -LIF, LIF and OSM medium. $^{**}p < 0.01$; $^{***}p < 0.001$; ns, no significant difference. **(D)** Telomerase activity measured by TRAP assay. Lysis buffer served as negative control. **(E)** Telomerase activity measured by ELISA assay. A49 mESCs (*Terc*$^{-/-}$ G4 ESCs) and N33 mESCs (wild type ESCs) served as negative control and positive control, respectively. $^{*}p < 0.05$; $^{**}p < 0.01$. **(F)** Relative expression of 2-cell genes including *Tcstv1*, *Tcstv3*, and *Zscan4* in ESCs cultured in -LIF, LIF, and OSM medium. $^{***}p < 0.001$; ns, no significant difference. **(G)** Immunofluorescence staining of Zscan4 (green) and Oct4 (red) in ESCs cultured in -LIF, LIF, and OSM medium. Blue, DAPI. Scale bar, 20 μm. **(H)** Percentage of Zscan4^{+} cells (number of mESCs counted in immunofluorescence staining assay). **(I)** Flow cytometry diagram indicating percentage of Zscan4^{+} cells in mESCs cultured in -LIF, LIF, and OSM medium. Samples lacking the antibody served as a negative control.

obviously separated from -LIF-ESCs (**Figures 4A,B**). The global gene expression profile revealed substantial similarities between OSM- and LIF-ESCs, compared to -LIF-ESCs (**Figures 4C,D**). We also observed that pluripotency genes, such as *Oct4*, *Nanog*, *Tbx3*, *Sox2*, *Esrrb,* and *Nr0b1,* were expressed at higher levels in both OSM-ESCs and LIF-ESCs than in -LIF-ESCs

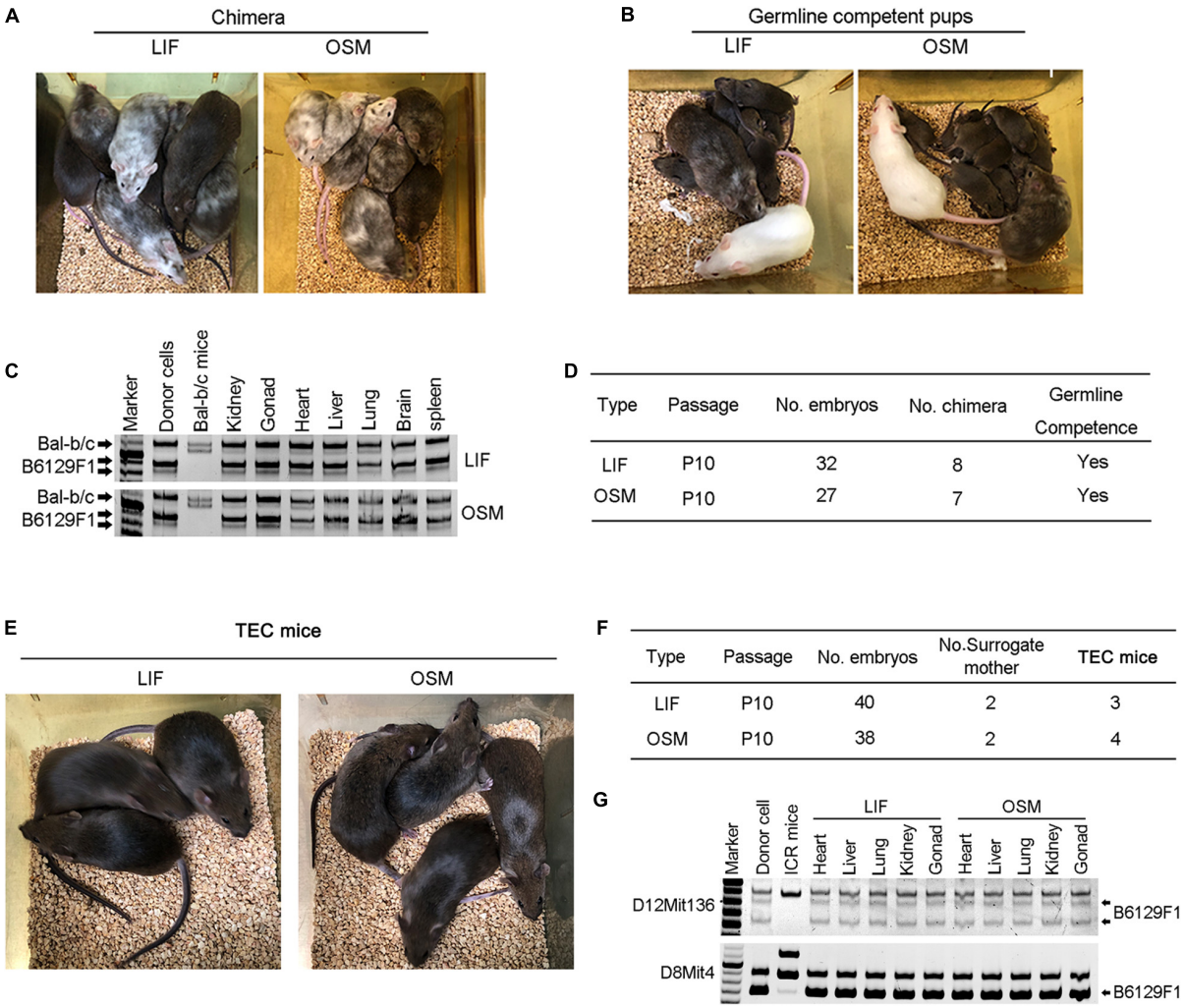

FIGURE 3 | Germline competence chimera and viable tetraploid complementation mice generated from ESCs cultured in OSM medium. **(A,B)** Chimera **(A)** and germline competency **(B)** of mESCs cultured in LIF and OSM medium by 4–8-cell embryo injection. Germline offspring was produced by mating chimeras with albino ICR mice. Albino Balb/c mice served as embryo donors, and pseudo-pregnant albino ICR mice as surrogate mother. **(C)** Genotyping analysis of chimeras by microsatellite primers D12Mit136. **(D)** Summary of 4–8-cell embryo injection of mESCs cultured in LIF and OSM medium. **(E)** Full-ESC mice generated from mESCs cultured in LIF and OSM medium by tetraploid complementation (TEC mice). **(F)** Summary of tetraploid embryo injection of mESCs cultured in LIF and OSM medium. **(G)** Genotyping analysis of TEC mice by microsatellite primers D12Mit136 and D8mit4.

(**Figures 4D,E**), consistent with our immunofluorescence and western blotting data (**Figures 1B,C**). Moreover, genes regulated DNA methylation and histone methylation and acetylation showed no significant differences between LIF-ESCs and OSM-ESCs except for Dnmt3b and Dnmt3l (**Supplementary Figures 1A,B**).

Using KEGG pathway and GO term analysis, we found that the genes expressed equivalently in both OSM-ESCs and LIF-ESCs were enriched in pathways including PI3K-Akt signaling (Paling et al., 2004), cell cycle, stem cell maintenance, and proliferation-associated molecular functions, suggesting that these signaling pathways were likely involved in self-renewal and pluripotency maintenance by OSM, as with LIF (**Figure 4F**). We also examined the differentially expressed genes (DEGs) between OSM-ESCs and LIF-ESCs. Compared to LIF-ESCs, the number of upregulated and downregulated genes in OSM-ESCs were 169 and 87, respectively (**Figure 4G** and **Supplementary Figure 1C**). The genes upregulated in OSM-ESCs were enriched in pentose and glucuronate interconversion, ascorbate and aldarate metabolism, and steroid and retinol metabolism (**Figure 4H**). The genes downregulated in OSM-ESCs were enriched in carbohydrate metabolism, such as fructose and mannose metabolism and galactose metabolism. The role of retinol in supporting the self-renewal of ESCs by elevating the expression of Nanog and Oct4, which are known to be the critical transcription factors for the maintenance of pluripotency of ESCs, has been previously reported (Chen et al., 2007; Chen and Khillan, 2008, 2010). In addition, ascorbate (vitamin C) has been shown to improve the efficiency of generation and quality of induced pluripotent stem cells by modulating histone

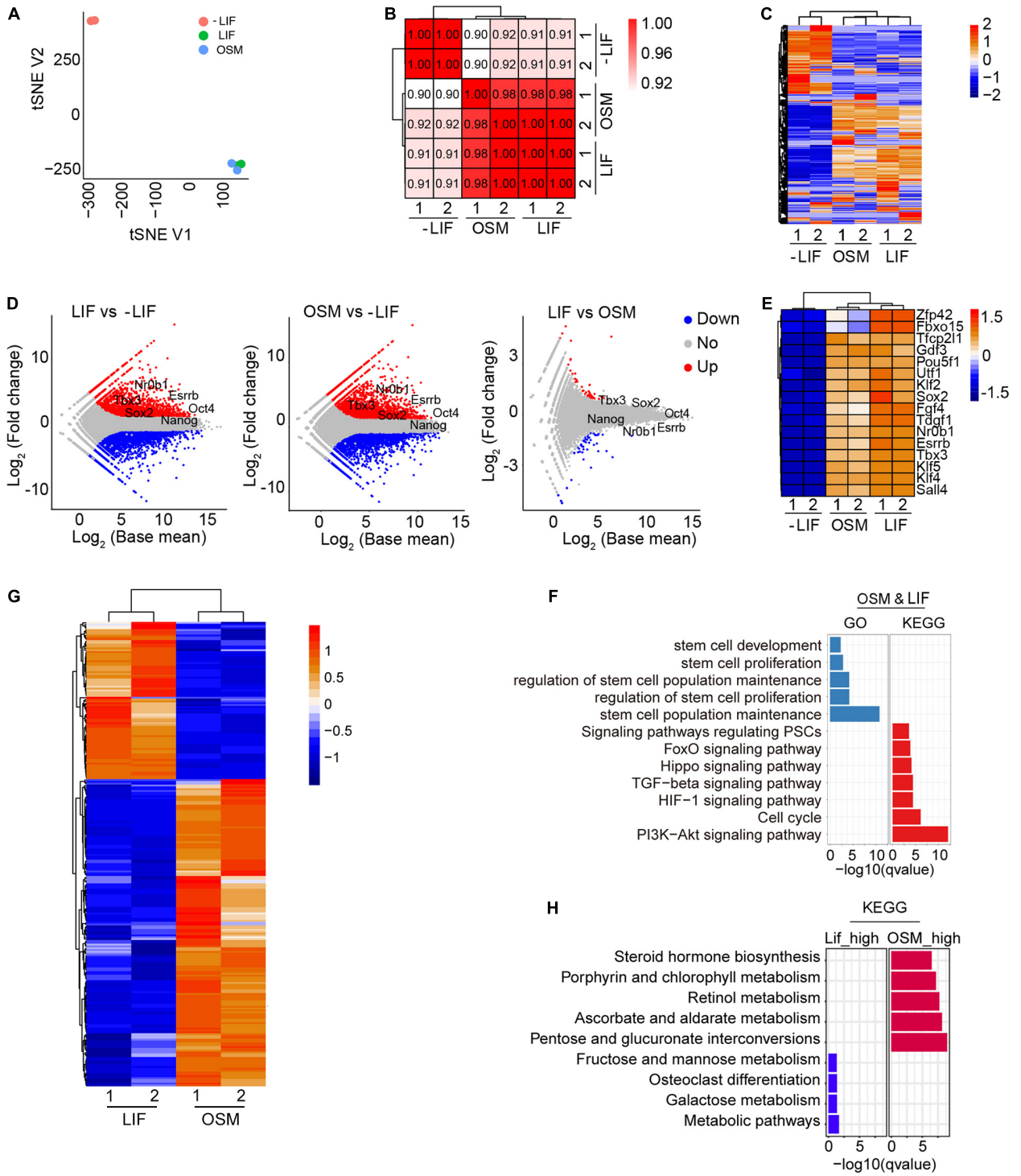

FIGURE 4 | Transcriptome and signal pathways in ESCs cultured in OSM medium. **(A)** tSNE analysis of ESCs cultured in -LIF, LIF, and OSM medium by RNA-seq. **(B)** Pearson's correlation coefficient graph of mESCs cultured in -LIF, LIF, and OSM medium. The value of 1.0 represents perfect positive correlation and 0 represents no correlation between the two samples. **(C)** Heatmap displaying global gene expression profile of mESCs cultured in -LIF, LIF, and OSM medium. Color key from red to blue represents the relative gene expression level from high to low. **(D)** Scatter-plots showing the differential expression genes in mESCs cultured in -LIF, LIF, and OSM medium. Parallel diagonal lines indicate twofold threshold in expression difference ($P < 0.05$). **(E)** Heatmap of expression profile of pluripotent genes in ESCs cultured in -LIF, LIF, and OSM medium. **(F)** GO and KEGG analysis of genes expressed without differences (fold change < 1.5) in LIF-ESCs and OSM-ESCs. **(G)** Heatmap illustrating differentially expressed genes (DEGs) between mESCs cultured with LIF and with OSM. Two biological replicates were analyzed per group. Genes with ≥0.5-fold expression changes, *P*-value < 0.05 were chosen for heatmap. **(H)** KEGG analysis of upregulated genes in mESCs cultured in OSM medium and those in LIF medium, respectively.

demethylation (Esteban et al., 2010; Wang et al., 2011; Esteban and Pei, 2012; Chen et al., 2013). To illustrate whether vitamin C (Vc) associated histone modifications might play roles in pluripotency maintenance by OSM, we assessed protein levels of H3K4me3 and H3K27me3 in mESCs cultured in LIF, OSM and LIF medium supplemented with 50 μg/mL Vc. By western blot, level of H3K4me3 did not differ among LIF-ESCs, OSM-ESCs and LIF + Vc-ESCs, but level of H3K27me3 was decreased in OSM-ESCs, and addition of Vc slightly decreased H3K27me3 level of ESCs compared to LIF medium but with no significant differences (**Supplementary Figure 2A**). Moreover, genomic 5 mC level decreased in OSM-ESCs compared to that of LIF-ESCs by dot blot assay (**Supplementary Figure 2B**). By real-time qPCR of relative expression levels of selective genes associated with the metabolism, *Ugt1a1* and *Ugt1a6a*, upregulated in OSM-ESCs by RNA-seq, also were expressed at higher levels in OSM-ESCs than in LIF-ESCs (**Supplementary Figure 2C**). Together, these upregulated metabolic pathways might be involved in the regulation of naïve pluripotency by OSM, but this requires further investigation.

DISCUSSION

Pluripotent ESCs can differentiate into all cell types in the body and thus have great potential for cell replacement therapy in regenerative medicine, but their culturing requires LIF, a very expensive reagent, to maintain stemness. This expense has limited the number of labs that can participate in stem cell research and has encouraged efforts to find a viable alternative. Several studies have shown that dimethyl sulfoxide (DMSO) (Yi et al., 2020), salvianolic acid B (Liu et al., 2014), and cordycepin (Wang et al., 2020) could maintain the expression of pluripotency markers in mESCs cultured in the absence of LIF; however, the developmental pluripotency of these mESCs was elusive.

That OSM could maintain pluripotency of mESCs has been reported either through morphological criteria (Rose et al., 1994) or through the generation of chimeras (Nichols et al., 1994). The method they used for generation of germline-competent chimeric mice by injecting mESCs into diploid blastocysts provided a valuable but less stringent test of pluripotency (Jaenisch and Young, 2008). Whether OSM could maintain the authentic pluripotency of mESCs through the most stringent tetraploid complementation needed to be addressed. This study reports the first instance of successfully generated all-ESC mice by using the TEC method. In addition, we further examined the effects of OSM on telomere function, 2-cell gene expression, and global gene transcription in naïve mESCs.

Cell metabolism has been shown to be closely related to the pluripotency of ESCs (Gu et al., 2016; Li et al., 2020). We found OSM upregulates ascorbate and retinol metabolic pathways. Future study on these pathways' function in OSM-maintained pluripotency will expand our understanding of the mechanisms underlying pluripotency. In addition, longer *in vitro* culture is required to confirm the role of OSM in mESC maintenance.

In summary, we demonstrated that OSM can maintain full pluripotency of mESCs in the absence of LIF. This study demonstrates the potential of OSM to completely substitute LIF in mESC cultures, which would be a cost-effective strategy in mESC maintenance.

DATA AVAILABILITY STATEMENT

The accession number for the RNA-seq data used in this study is GEO: GSE165292 and the other datasets generated during the current study are available from the corresponding author on reasonable request.

ETHICS STATEMENT

The animal study was reviewed and approved by the Institutional Animal Care and Use Committee at Nankai University.

AUTHOR CONTRIBUTIONS

XY and CT conducted the experiments and prepared the manuscript. LlL analyzed the RNA-seq data. GF, KJ, HW, and JC conducted part of experiments or provided reagents. LL conceived the project, designed the experiments, wrote, and revised the manuscript. All authors contributed to the article and approved the submitted version.

FUNDING

This work was supported by the National Key R&D Program of China (2018YFA0107000 and 2018YFC1003004) and the National Natural Science Foundation of China (91749129), and PCSIRT (No. IRT13023).

SUPPLEMENTARY MATERIAL

The Supplementary Material for this article can be found online at: https://www.frontiersin.org/articles/10.3389/fcell.2021.675411/full#supplementary-material

REFERENCES

Blackburn, E. H., Epel, E. S., and Lin, J. (2015). Human telomere biology: a contributory and interactive factor in aging, disease risks, and protection. *Science* 350, 1193–1198. doi: 10.1126/science.aab3389

Cerulo, L., Tagliaferri, D., Marotta, P., Zoppoli, P., Russo, F., Mazio, C., et al. (2014). Identification of a novel gene signature of ES cells self-renewal fluctuation through system-wide analysis. *PLoS One* 9:e83235. doi: 10.1371/journal.pone.0083235

Chen, J., Liu, H., Liu, J., Qi, J., Wei, B., Yang, J., et al. (2013). H3K9 methylation is a barrier during somatic cell reprogramming into iPSCs. *Nat. Genet.* 45, 34–42. doi: 10.1038/ng.2491

Chen, L., and Khillan, J. S. (2008). Promotion of feeder-independent self-renewal of embryonic stem cells by retinol (vitamin A). *Stem Cells* 26, 1858–1864.

Chen, L., and Khillan, J. S. (2010). A novel signaling by vitamin A/retinol promotes self renewal of mouse embryonic stem cells by activating PI3K/Akt signaling pathway via insulin-like growth factor-1 receptor. *Stem Cells* 28, 57–63. doi: 10.1002/stem.251

Chen, L., Yang, M., Dawes, J., and Khillan, J. S. (2007). Suppression of ES cell differentiation by retinol (vitamin A) via the overexpression of Nanog. *Differentiation* 75, 682–693. doi: 10.1111/j.1432-0436.2007.00169.x

Choi, J., Huebner, A. J., Clement, K., Walsh, R. M., Savol, A., Lin, K., et al. (2017). Prolonged Mek1/2 suppression impairs the developmental potential of embryonic stem cells. *Nature* 548, 219–223. doi: 10.1038/nature23274

Eggan, K., Rode, A., Jentsch, I., Samuel, C., Hennek, T., Tintrup, H., et al. (2002). Male and female mice derived from the same embryonic stem cell clone by tetraploid embryo complementation. *Nat. Biotechnol.* 20, 455–459. doi: 10.1038/nbt0502-455

Esteban, M. A., and Pei, D. (2012). Vitamin C improves the quality of somatic cell reprogramming. *Nat. Genet.* 44, 366–367. doi: 10.1038/ng.2222

Esteban, M. A., Wang, T., Qin, B., Yang, J., Qin, D., Cai, J., et al. (2010). Vitamin C enhances the generation of mouse and human induced pluripotent stem cells. *Cell Stem Cell* 6, 71–79. doi: 10.1016/j.stem.2009.12.001

Falco, G., Lee, S. L., Stanghellini, I., Bassey, U. C., Hamatani, T., and Ko, M. S. (2007). Zscan4: a novel gene expressed exclusively in late 2-cell embryos and embryonic stem cells. *Dev. Biol.* 307, 539–550. doi: 10.1016/j.ydbio.2007.05.003

Gearing, D. P., and Bruce, A. G. (1992). Oncostatin M binds the high-affinity leukemia inhibitory factor receptor. *New Biol.* 4, 61–65.

Gearing, D. P., Comeau, M. R., Friend, D. J., Gimpel, S. D., Thut, C. J., McGourty, J., et al. (1992). The IL-6 signal transducer, gp130: an oncostatin M receptor and affinity converter for the LIF receptor. *Science* 255, 1434–1437. doi: 10.1126/science.1542794

Gu, W., Gaeta, X., Sahakyan, A., Chan, A. B., Hong, C. S., Kim, R., et al. (2016). Glycolytic metabolism plays a functional role in regulating human pluripotent stem cell state. *Cell Stem Cell* 19, 476–490. doi: 10.1016/j.stem.2016.08.008

Guo, R., Ye, X., Yang, J., Zhou, Z., Tian, C., Wang, H., et al. (2018). Feeders facilitate telomere maintenance and chromosomal stability of embryonic stem cells. *Nat. Commun.* 9:2620. doi: 10.1038/s41467-018-05038-2

Herrera, E., Samper, E., Martín-Caballero, J., Flores, J. M., Lee, H. W., and Blasco, M. A. (1999). Disease states associated with telomerase deficiency appear earlier in mice with short telomeres. *EMBO J.* 18, 2950–2960. doi: 10.1093/emboj/18.11.2950

Huang, J., Deng, K., Wu, H., Liu, Z., Chen, Z., Cao, S., et al. (2008). Efficient production of mice from embryonic stem cells injected into four- or eight-cell embryos by piezo micromanipulation. *Stem Cells* 26, 1883–1890. doi: 10.1634/stemcells.2008-0164

Huang, J., Wang, F., Okuka, M., Liu, N., Ji, G., Ye, X., et al. (2011). Association of telomere length with authentic pluripotency of ES/iPS cells. *Cell Res.* 21, 779–792. doi: 10.1038/cr.2011.16

Jaenisch, R., and Young, R. (2008). Stem cells, the molecular circuitry of pluripotency and nuclear reprogramming. *Cell* 132, 567–582. doi: 10.1016/j.cell.2008.01.015

Kim, D., Langmead, B., and Salzberg, S. L. (2015). HISAT: a fast spliced aligner with low memory requirements. *Nat. Methods* 12, 357–360. doi: 10.1038/nmeth.3317

Li, L., Chen, K., Wang, T., Wu, Y., Xing, G., Chen, M., et al. (2020). Glis1 facilitates induction of pluripotency via an epigenome-metabolome-epigenome signalling cascade. *Nat. Metab.* 2, 882–892. doi: 10.1038/s42255-020-0267-9

Liao, Y., Smyth, G. K., and Shi, W. (2014). Featurecounts: an efficient general purpose program for assigning sequence reads to genomic features. *Bioinformatics* 30, 923–930. doi: 10.1093/bioinformatics/btt656

Liu, C. H., Shyu, W. C., Fu, R. H., Huang, S. J., Chang, C. H., Huang, Y. C., et al. (2014). Salvianolic acid B maintained stem cell pluripotency and increased proliferation rate by activating Jak2-Stat3 combined with EGFR-Erk1/2 pathways. *Cell Transplant.* 23, 657–668. doi: 10.3727/096368914X678391

Liu, L. (2017). Linking telomere regulation to stem cell pluripotency. *Trends Genet.* 33, 16–33. doi: 10.1016/j.tig.2016.10.007

Macfarlan, T. S., Gifford, W. D., Driscoll, S., Lettieri, K., Rowe, H. M., Bonanomi, D., et al. (2012). Embryonic stem cell potency fluctuates with endogenous retrovirus activity. *Nature* 487, 57–63. doi: 10.1038/nature11244

Nagy, A., Rossant, J., Nagy, R., Abramow-Newerly, W., and Roder, J. C. (1993). Derivation of completely cell culture-derived mice from early-passage embryonic stem cells. *Proc. Natl. Acad. Sci. U.S.A.* 90, 8424–8428. doi: 10.1073/pnas.90.18.8424

Nichols, J., Chambers, I., and Smith, A. (1994). Derivation of germline competent embryonic stem cells with a combination of interleukin-6 and soluble interleukin-6 receptor. *Exp. Cell Res.* 215, 237–239. doi: 10.1006/excr.1994.1338

Niwa, H., Burdon, T., Chambers, I., and Smith, A. (1998). Self-renewal of pluripotent embryonic stem cells is mediated via activation of STAT3. *Genes Dev.* 12, 2048–2060. doi: 10.1101/gad.12.13.2048

Niwa, H., Ogawa, K., Shimosato, D., and Adachi, K. (2009). A parallel circuit of LIF signalling pathways maintains pluripotency of mouse ES cells. *Nature* 460, 118–122. doi: 10.1038/nature08113

Paling, N. R., Wheadon, H., Bone, H. K., and Welham, M. J. (2004). Regulation of embryonic stem cell self-renewal by phosphoinositide 3-kinase-dependent signaling. *J. Biol. Chem.* 279, 48063–48070. doi: 10.1074/jbc.M406467200

Raz, R., Lee, C. K., Cannizzaro, L. A., d'Eustachio, P., and Levy, D. E. (1999). Essential role of STAT3 for embryonic stem cell pluripotency. *Proc. Natl. Acad. Sci. U.S.A.* 96, 2846–2851. doi: 10.1073/pnas.96.6.2846

Rose, T. M., Weiford, D. M., Gunderson, N. L., and Bruce, A. G. (1994). Oncostatin M (OSM) inhibits the differentiation of pluripotent embryonic stem cells in vitro. *Cytokine* 6, 48–54. doi: 10.1016/1043-4666(94)90007-8

Wang, C. H., Chang, C. H., Lin, T. L., Fu, R. H., Huang, Y. C., Chen, S. Y., et al. (2020). The novel application of cordycepin in maintaining stem cell pluripotency and increasing iPS cell generation efficiency. *Sci. Rep.* 10:2187. doi: 10.1038/s41598-020-59154-5

Wang, T., Chen, K., Zeng, X., Yang, J., Wu, Y., Shi, X., et al. (2011). The histone demethylases Jhdm1a/1b enhance somatic cell reprogramming in a vitamin-C-dependent manner. *Cell Stem Cell* 9, 575–587. doi: 10.1016/j.stem.2011.10.005

Yagi, M., Kishigami, S., Tanaka, A., Semi, K., Mizutani, E., Wakayama, S., et al. (2017). Derivation of ground-state female ES cells maintaining gamete-derived DNA methylation. *Nature* 548, 224–227. doi: 10.1038/nature23286

Yi, J. K., Park, S., Ha, J. J., Kim, D. H., Huang, H., Park, S. J., et al. (2020). Effects of dimethyl sulfoxide on the pluripotency and differentiation capacity of mouse embryonic stem cells. *Cell. Reprogram.* 22, 244–253. doi: 10.1089/cell.2020.0006

Ying, Q. L., Wray, J., Nichols, J., Batlle-Morera, L., Doble, B., Woodgett, J., et al. (2008). The ground state of embryonic stem cell self-renewal. *Nature* 453, 519–523. doi: 10.1038/nature06968

Yu, G., Wang, L. G., Han, Y., and He, Q. Y. (2012). clusterProfiler: an R package for comparing biological themes among gene clusters. *OMICS* 16, 284–287. doi: 10.1089/omi.2011.0118

Zalzman, M., Falco, G., Sharova, L. V., Nishiyama, A., Thomas, M., Lee, S. L., et al. (2010). Zscan4 regulates telomere elongation and genomic stability in ES cells. *Nature* 464, 858–863. doi: 10.1038/nature08882

Zarling, J. M., Shoyab, M., Marquardt, H., Hanson, M. B., Lioubin, M. N., and Todaro, G. J. (1986). Oncostatin M: a growth regulator produced by differentiated histiocytic lymphoma cells. *Proc. Natl. Acad. Sci. U.S.A.* 83, 9739–9743. doi: 10.1073/pnas.83.24.9739

Conflict of Interest: The authors declare that the research was conducted in the absence of any commercial or financial relationships that could be construed as a potential conflict of interest.

frontiers in Cell and Developmental Biology

REVIEW
published: 21 June 2021
doi: 10.3389/fcell.2021.692940

Cancer Stem Cells: Emerging Key Players in Immune Evasion of Cancers

Martina Mang Leng Lei[1] *and Terence Kin Wah Lee*[1,2]*

[1] *Department of Applied Biology and Chemical Technology, The Hong Kong Polytechnic University, Kowloon, Hong Kong,* [2] *State Key Laboratory of Chemical Biology and Drug Discovery, The Hong Kong Polytechnic University, Kowloon, Hong Kong*

Cancer stem cells (CSCs) are subpopulations of undifferentiated cancer cells within the tumor bulk that are responsible for tumor initiation, recurrence and therapeutic resistance. The enhanced ability of CSCs to give rise to new tumors suggests potential roles of these cells in the evasion of immune surveillance. A growing body of evidence has described the interplay between CSCs and immune cells within the tumor microenvironment (TME). Recent data have shown the pivotal role of some major immune cells in driving the expansion of CSCs, which concurrently elicit evasion of the detection and destruction of various immune cells through a number of distinct mechanisms. Here, we will discuss the role of immune cells in driving the stemness of cancer cells and provide evidence of how CSCs evade immune surveillance by exerting their effects on tumor-associated macrophages (TAMs), dendritic cells (DCs), myeloid-derived suppressor cells (MDSCs), T-regulatory (Treg) cells, natural killer (NK) cells, and tumor-infiltrating lymphocytes (TILs). The knowledge gained from the interaction between CSCs and various immune cells will provide insight into the mechanisms by which tumors evade immune surveillance. In conclusion, CSC-targeted immunotherapy emerges as a novel immunotherapy strategy against cancer by disrupting the interaction between immune cells and CSCs in the TME.

Keywords: cancer, cancer stem cells, immune cells, tumor microenvironment, immune evasion

OPEN ACCESS

Edited by:
Stephanie Ma,
The University of Hong Kong, Hong Kong

Reviewed by:
Gianpaolo Papaccio,
Second University of Naples, Italy
Kwan Ho Tang,
New York University, United States

****Correspondence:***
Terence Kin Wah Lee
terence.kw.lee@polyu.edu.hk

Specialty section:
This article was submitted to Stem Cell Research, a section of the journal Frontiers in Cell and Developmental Biology

Received: *09 April 2021*
Accepted: *31 May 2021*
Published: *21 June 2021*

Citation:
Lei MML and Lee TKW (2021) Cancer Stem Cells: Emerging Key Players in Immune Evasion of Cancers. Front. Cell Dev. Biol. 9:692940. doi: 10.3389/fcell.2021.692940

Abbreviations: ADCC, antibody-dependent cellular cytotoxicity; CSC, cancer stem cell; CCL, C-C motif chemokine ligand; CAR, chimeric antigen receptor; CHI3L1, chitinase 3–like 1; CXCR, C-X-C motif chemokine receptor; CXCL, C-X-C motif ligand; CTL, cytotoxic T cell; CTLA-4, cytotoxic T-lymphocyte-associated protein-4; DC, dendritic cell; EMT, epithelial–mesenchymal transition; FTO, fat mass and obesity-associated protein; HCC, hepatocellular carcinoma; HMA, hypomethylating agents; IFN-γ, interferon gamma; gMDSC, granulocytic MDSC; IL, interleukin; MSC, mesenchymal stem cell; mMDSC, monocytic MDSC; MDSC, myeloid-derived suppressor cell; m6A, N6-methyladenosine; NK, natural killer; NF-κB, nuclear factor-κB; NFAT, nuclear factor of activated T-cells; PD-1, programmed cell death protein; PD-L1, programmed death-ligand 1; PGE2, prostaglandin E2; Siglec-10, sialic-acid-binding Ig-like lectin 10; SIPRα, signal regulatory protein alpha; STAT3, signal transducer and activator of transcription 3; TIM-3, T cell immunoglobulin and mucin domain-containing protein-3; Th cell, T helper cell; TGF-β, transforming growth factor beta; Treg, T regulatory; TAM, tumor associated macrophage; TIL, tumor-infiltrating lymphocyte; TME, tumor microenvironment; TNF-α, tumor necrosis factor-alpha; VEGF, vascular endothelial growth factor.

INTRODUCTION

Cancer stem cells (CSCs) are subsets of cancer cells enriched with stem cell-like characteristics, including self-renewal ability and multilineage differentiation (Bhatia and Kumar, 2016). The CSC theory of tumor progression presents the tumor microenvironment (TME) as a hierarchically organized tissue with a CSC subpopulation ranked at the top level, which generates more differentiated cancer cells with lower or limited proliferative potential. CSCs are often defined by the expression of surface stem cell markers such as CD24, CD34, CD44, CD47, CD133, and CD90, along with side populations that can be isolated and enriched *in vitro* and *in vivo* without stem cell surface markers (Taniguchi et al., 2019). Epithelial-to-mesenchymal transition (EMT) is well known to be an inducer of CSC phenotypes via epigenetic regulation (Bocci et al., 2019). Its activation allows CSCs to drive resistance to conventional therapy and thus leads to treatment relapse and tumor reoccurrence (Shibue and Weinberg, 2017).

A substantial body of literature has extensively described the interactions of tumor bulks with the immune system; however, investigations have only begun to elucidate the relationship of CSCs and immune cells within the TME, paving the way for the development of rational therapeutic strategies to explore CSC-immune dynamics. The capability of CSCs in tumor initiation in partly immunocompromised mice e.g., SCID or NOD/SCID mice (T, B cells defect but NK cells present) suggests that these cells are empowered with the definitive ability to evade immune detection and surveillance, whereas non-CSCs require a higher extent of deficiency in immune system for generating tumors in NSG mice (lack of T, B, and NK cells) (Tsuchiya and Shiota, 2021). Increasing evidence has demonstrated that there is a reciprocal interaction between CSCs and various immune cells. Major immune cells within the TME drive CSC expansion and concurrently elicit protumorigenic immune cell activities, promoting CSC-specific avoidance of immune detection and destruction. In this section, we will discuss the emerging knowledge of the role of tumor-associated macrophages (TAMs), dendritic cells (DCs), myeloid-derived suppressor cells (MDSCs), T regulatory (Treg) cells, natural killer (NK) cells, and tumor-infiltrating lymphocytes (TILs) in driving cancer stemness and how CSCs evade the immune surveillance of these cells. Finally, we will discuss the potential of CSC-targeted immunotherapy to eradicate cancer.

TUMOR-ASSOCIATED MACROPHAGES

Macrophages can be classified into two subtypes: pro-inflammatory M1 and anti-inflammatory M2 macrophages (Chen et al., 2019). TAMs usually express an M2 phenotype, which executes immunosuppressive and pro-tumor functions and is thus closely related to cancer progression and recurrence (Lewis and Pollard, 2006; Malfitano et al., 2020).

Developing findings support the hypothesis that CSCs influence the immune TME via the recruitment of macrophages and the promotion of their pro-tumor properties, while TAMs, in turn, are crucial for the self-renewal ability and maintenance of CSCs in primary tumors through the coupling between STAT3 and NF-κB signaling cascades (Sainz et al., 2016). It has been proposed that CSCs have an intrinsic immunosuppressive program involving recruiting macrophages and driving them toward M2 polarization at the tumor site (Brissette et al., 2012). This ability of CSCs is commonly found in ovarian, glioblastoma, liver, breast and lung cancers through activating the signal transducer and activator of transcription 3 (STAT3) and nuclear factor-κB (NF-κB) pathways and cytokines such as interleukin (IL)-8 and IL-10 (Iliopoulos et al., 2009; Ginestier et al., 2010; Mitchem et al., 2013; Fang et al., 2014). For example, in hepatocellular carcinoma (HCC), $CD133^+$ cells induce M2 polarization of TAMs through secretion of IL-8 (Xiao et al., 2018). In glioblastoma, CSCs generate higher levels of the chemoattractants C-C motif chemokine ligand 2 (CCL2), CCL5, vascular endothelial growth factor-A (VEGF-A), and neurotensin than the bulk of the glioma (Yi et al., 2011). The extracellular matrix protein periostin is preferentially expressed on $CD133^+CD15^+$ glioma CSCs and recruits macrophages through integrin αvβ3 from the peripheral blood to the brain (Zhou et al., 2015). Depletion of periostin in glioma CSCs leads to a reduction in the M2 population and alleviates tumor growth in glioblastoma xenografts. In breast cancer, $Sox2^+$ cancer cells, via activation of nuclear factor of activated T-cells (NFAT), STAT3 and NF-κB, express chemokines CCL3 and ICAM-1 and thus recruit TAMs into the TME (Yang et al., 2013; Mou et al., 2015). These findings suggest that CSCs play an important role in TAM recruitment and M2 polarization by secreting macrophage chemoattractants.

Subsequent to TAM recruitment to the TME, TAMs are deployed as a "niche" to support CSC growth. Infiltrating TAMs, by activating the NF-κB signaling pathway, secrete the inflammatory cytokines IL-1β, IL-6, IL-10, transforming growth factor beta (TGF-β), and MFG-E8 (Jinushi et al., 2011; Li et al., 2012; Fang et al., 2014; Wan et al., 2014; Yang et al., 2019). These tumor-promoting cytokines bind to their receptors, further stimulating STAT3 activation in adjacent CSCs. This results in a vicious cycle of NF-κB activation as well as stemness maintenance of cancer cells. For example, treatment of breast cancer cells with conditioned medium of TAMs leads to increments in the stem cell markers Sox-2, Oct3/4 and Nanog with enhanced ALDH1 activity in a mouse model (Nnv and Kundu, 2018). The abrogation of STAT3 confirmed the role of JAK/STAT pathway in mediating TAM regulation on CSC enrichment. In coculture systems, recruited TAMs promote liver CSC expansion through IL-6/STAT3, Wnt/β-catenin and TGF-β signaling pathways (Fang et al., 2014; Wan et al., 2014; Chen et al., 2019). TAMs preferentially secrete TGF-β to stimulate CSC-like properties by inducing EMT, while TAM-derived IL-6 induces $CD44^+$ HCC stem cell expansion by activating STAT3, thus promoting tumor development through CSC growth. Blockade of IL-6 with tocilizumab and STAT3 knockdown attenuated $CD44^+$ sphere formation and tumor growth of patient-derived HCC as well as breast xenografts (Wan et al., 2014; Wang et al., 2018a).

To facilitate communication, TAMs establish direct adhesion with $CD90^+$ CSCs through EphA/ephrin A signaling and

promote tumor initiation in breast cancer tissue (Lu et al., 2014). The EMT program first induces the expression of the surface ligands Thy1 and EphA4, which enable more frequent cell-cell interactions between TAMs and CSCs. Upregulated TAM-CSC contact thus activates the EphA4 receptor on CSCs and its downstream Src and NF-κB pathways (Iliopoulos et al., 2009; Lu et al., 2014). NF-κB activation positively reinforces the secretion of cytokines, including IL-6, IL-8, and GM-CSF, which are crucial for CSC self-renewal and stemness state maintenance (Rinkenbaugh and Baldwin, 2016; Choi et al., 2019). Interestingly, proinflammatory M1 macrophages were also found to play a role in breast CSC formation due to their activation of the STAT3 and NF-κB pathways by $CD44^{high}/CD24^{-/low}$ or $ALDH1^{+}$ CSCs, while M2 macrophages maintained a higher population of $ALDH^{+}$ cells (Guo et al., 2019). There is a possibility that M1 macrophages, through M2-mediated signaling, modulate CSC formation and regulate tumor initiation. Other signaling pathways, such as PTN/β-catenin, Notch1 and p38-MAPK, are also involved in stimulating CSC self-renewal in lymphoma, lung and ovarian cancers via the preferential secretion of IL-10 and IL-17 by TAMs (Xiang et al., 2015; Wei X. et al., 2019; Yang et al., 2019). Taken together, TAMs, through activating STAT3 and NF-κB signaling cascades and cytokines IL-1β, IL-6, IL-8, IL-10, and IL-17 and growth factor TGF-β, play an important role in the self-renewal and chemoresistance of CSCs.

Numerous studies have demonstrated the direct regulation of CSC self-renewal and proliferation by TAMs. CSCs also take advantage of TAM immunosuppressive functions to escape immune surveillance. In HCC, TAMs provide a "safe" environment for CSCs by overexpressing SIPRα, which interacts with CD47 that in turn acts as a "Don't eat me" signal and protects CSCs from being phagocytosed. Recently, CD24, one of the liver CSC markers, was identified to be another "Don't eat me" signal to macrophages by binding to inhibitory receptor sialic-acid-binding Ig-like lectin 10 (Siglec-10) (Lee et al., 2014; Barkal et al., 2019). Liver CSCs may also escape the clearance of macrophages by interacting with their surface Siglec-10 receptor. TAMs also influence T-cell cytotoxic activity by stimulating immune checkpoint molecules such as programmed death-ligand 1 (PD-L1) in cancer cells and T cell immunoglobulin and mucin domain-containing protein 3 (TIM-3), programmed cell death protein-1 (PD-1) and cytotoxic T-lymphocyte-associated protein-4 (CTLA-4) on the T cell surface, leading to an impaired immune response (Cassetta and Kitamura, 2018; Liu et al., 2018; Xiao et al., 2018). Interestingly, it has been proposed that leukemic CSCs secure their survival by overexpressing TIM-3, which promotes MDSCs and subsequent differentiation into TAMs in the leukemic stem cancer niche (Kikushige et al., 2010; Gao et al., 2014; Raggi et al., 2016). The relationship between TIM-3 expression and CSCs has also been shown in melanoma, osteosarcoma, as well as liver, lung, and ovarian cancers (Fourcade et al., 2010; Gao et al., 2012). To protect themselves from being targeted, deterioration in the antigen-presenting ability of TAMs also minimizes macrophage stimulation of T-cell and NK cell cytotoxicity activity (Lewis and Pollard, 2006).

In summary, complicated STAT3/NF-κB crosstalk is established between CSCs and TAMs in the TME, in which CSCs attract, re-educate, and put macrophages into their service to support primary tumor growth.

DENDRITIC CELLS

Dendritic cells are antigen-presenting cells that elicit innate or adaptive immune responses (Ma et al., 2013). Immature DCs capture tumor-derived antigens and present them on their cell surface to immune cells with proper costimulatory molecules, resulting in an antigen-specific immune response and the formation of T and B cell memories (Ravindran et al., 2019). Nevertheless, DCs exert antitumor or pro-tumor immune responses in accordance with their distinct morphologies and phenotypes.

A growing number of research studies have demonstrated the importance of CSCs in immune evasion by changing DC phenotypes and impeding their recruitment to the TME. CSCs are responsible for influencing the functional differentiation and activation of DCs, turning DCs to become tolerogenic or limiting them to activate T cells (Jachetti et al., 2015; Zhong et al., 2019). $CD133^{+}$ CSCs impair the function of DCs by reducing the quantity of activated DCs in colorectal cancer (Szarynska et al., 2018). The $EpCAM^{+}$ HCC subtype has stemness properties and induces AFP expression, which hinders DC differentiation, maturation and T cell proliferation (Yamashita et al., 2009; Pardee et al., 2014). CSCs also produce immunosuppressive cytokines IL-4, IL-10, IL-13, and TGF-β, and express higher levels of coinhibitory molecules such as PD-L1, B7-H3, and IDO1 (Shipitsin et al., 2007; Todaro et al., 2007). These molecules play crucial roles in accumulating immunosuppressive DCs, which hamper the antitumor response by inducing T cell tolerance and T reg cell recruitment (Boks et al., 2012; Pardee et al., 2014). TGF-β is known for its negative effect on immune response; in terms of DCs, TGF-β inhibits DC activation by suppressing the expressions of its costimulatory molecules CD80 and CD86 and MHC class II (Kobie et al., 2003; Fainaru et al., 2007). Defective RIG-I liver CSCs reduce DC population and induce immunotolerance by upregulating TGF-β signaling (Zhong et al., 2019). Additionally, TGF-β promotes Wnt/β-catenin activation and thus impairs the recruitment of $BATF3^{+}$ DCs, which is correlated with $CD8^{+}$ T cell infiltration (Spranger et al., 2017). Via β-catenin activation, TGF-β impairs T cell mediated immune surveillance and subsides DC recruitment to the tumor site, consequently incurring HCC immune escape and resistance to anti-PD1 treatment (Ruiz de Galarreta et al., 2019). Moreover, TGF-β encourages the development of PD-L1-expressing immunosuppressive DCs, resulting in weakened $CD8^{+}$ T cell activity in a metastatic ovarian cancer model (Cubillos-Ruiz et al., 2010; Krempski et al., 2011).

In the TME, cancer and stromal cells also express C-X-C motif chemokine receptor 4 (CXCR4) and produce its ligand C-X-C motif ligand 12 (CXCL12) to sustain CSC self-renewal and to recruit regulatory DCs. These DCs produce CXCL12 themselves in an autocrine manner and employ a feed-forward mechanism for maintaining CSC stemness (Sultan et al., 2017). Similar to TAM-mediated escape from phagocytic killing,

overexpressed CD47 on CSC surface elicits "Don't eat me" signal by binding to signal regulatory protein alpha (SIPRα), which acts in phagocytosis signaling pathway of DCs (Liu et al., 2017). Although recent findings showed CSCs hijack immune responses by impairing DC functions and recruiting immunosuppressive DC subsets, more investigations are necessary to shed light on the interactions between these two cell types, especially on how DCs alternately regulate CSC stemness properties.

MYELOID-DERIVED SUPPRESSOR CELLS

Myeloid-derived suppressor cells are a heterogeneous subset of myeloid-originated progenitor cells. In humans, these cells are defined by $CD11b^{+}CD14^{-}CD33^{+}$, while in mice, they are characterized by $CD11b^{+}Gr1^{+}$ (Kusmartsev et al., 2004; Nagaraj and Gabrilovich, 2010). MDSCs have been used as a prognostic indicator for patients' responsiveness to immunotherapy and their survival, as they account for the majority of cells that promote an immunosuppressive environment in the TME (Ai et al., 2018). MSDCs can be classified into two main populations according to their different nuclear morphologies: monocytic-MDSC (mMDSC) and granulocytic-MDSC (gMDSC). They are endowed with different immunosuppressive molecules: mMDSC contains both arginase-1 and iNOS, while g-MDSC contains high levels of arginase-1; therefore, are suggested to exert distinct spatiotemporal regulations on tumor plasticity (Ouzounova et al., 2017). Both mMDSC-derived iNOS and NO, and gMDSC-induced ROS and arginase-1, can lead to TCR peroxynitration and T cell apoptosis (Nagaraj and Gabrilovich, 2010). In addition, MDSCs produce the immunosuppressive cytokines IL-10 and TGF-β as well as PD-L1, which together suppress T cell activity and recruit Tregs (Ostrand-Rosenberg, 2010). They also convey their immunosuppressive functions to macrophages, NK cells and DCs via crosstalk.

Myeloid-derived suppressor cell accumulation in the TME is facilitated by the secretion of cytokines, including IL-1β, IL-6, G-CSF, M-CSF, GM-CSF, macrophage MIF, and TGF-1β, and chemokines CCL1, CCL2, CCL5, CCL22, CXCL2, CXCL5, and CXCL12. The quantity of infiltrating MDSCs is positively associated with CSCs in cancer patients. In a synergistic mammary tumor model, CSCs enhance G-CSF, which is responsible for recruiting MDSCs to the tumor site (Welte et al., 2016). Activation of IL-6/STAT3 signaling has been reported to promote the differentiation of monocytes to MDSCs (Panni et al., 2014). Reciprocally, MDSCs promote the stemness and mesenchymal properties of cancer cells through NOTCH/STAT3 signaling, forming a positive feedback loop with crosstalk between MDSCs and CSCs (Welte et al., 2016; Ouzounova et al., 2017). Via secretion of prometastatic molecules such as MMP9 and chitinase 3–like 1 (CHI3L1), recruited MDSCs enhance stem cell features to promote tumorigenesis and metastasis in triple-negative breast cancer (Kumar et al., 2018). MDSCs also enrich breast cancer cells with stem-like properties by activating IL-6/STAT3 and NO/NOTCH signaling pathways with NO, leading to suppression of T cell activation (Peng et al., 2016). Intriguingly, MDSCs play an additional important role beyond just IL-6-induced transient STAT3 activation. Cell-derived IL-6 further increases IL-6 and IL6Rα in MDSCs, thus allowing MDSCs to prolong STAT3 signaling activation and maintain STAT3 phosphorylation. IL-6-derived MDSC regulation of CSC expansion and immunosuppressive activity is present in both breast and liver cancers (Peng et al., 2016; Xu et al., 2017).

In addition, MDSCs influence cancer stemness via modulation of RNA interference as well as epigenetic regulation. MDSCs trigger miR-101 expression in ovarian cancer, thus inhibit the co-repressor CtBP2 from repressing the transcription of stem cell core genes, leading to an upregulation of stemness markers and tumor growth (Cui et al., 2013). In a co-culture setup, gMDSCs are found to enhance expression of stemness genes and CSC phenotypes of multiple myeloma cell lines through piRNA-823 and subsequent activation of DNA methyltransferases DNMT3B (Ai et al., 2019). MDSCs also increase stem-like properties in ovarian CSCs by upregulating prostaglandin E2 (PGE2) and PD-L1 expressions (Komura et al., 2020). Under hypoxic conditions where liver CSCs are enriched, MDSCs migrate to the tumor site through ENTPD2/CD39 L1 signaling. These MDSCs further promote HCC progression and reduce the efficacy of PD1 therapy (Chiu et al., 2017). Interestingly, depletion of MDSCs leads to sensitization of HCC cells to 5-FU (Xu et al., 2017). Reduction of MDSCs by Listeria bacteria or herpes simplex virus expressing 15-PGDH can attenuate tumor growth and metastasis in breast cancer (Walker et al., 2011; Chandra et al., 2013). All of these findings emphasize the role of MDSCs in reshaping stemness in breast, ovarian and liver cancers and demonstrate the possibility of targeting MDSCs along with CSC eradication in future immunotherapy.

REGULATORY T CELLS

Regulatory T cells (Tregs) are a group of $CD4^{+}$ T cells with tumor-promoting effects, usually defined by the $Foxp3^{+}CD25^{+}CD4^{+}$ T cell subpopulation (Sakaguchi et al., 2010). Tregs abolish host defense mechanisms and exert their functions by inhibiting effector T cells and other immune cells by secreting immunosuppressive cytokines such as IL-10, IL-35, and TGF-β.

A positive correlation has been observed between the presence of CSCs and Tregs in cancers, suggesting possible crosstalk between these cell populations in promoting an immunosuppressive milieu (Yu et al., 2012; Napoletano et al., 2016; Solis-Castillo et al., 2020). In glioblastoma, CSCs induce Treg cell infiltration mediated by the costimulatory molecule PD-L1, soluble Galectin-3, and TGF-β secretion (Wei et al., 2010, 2011), whereas $ABCB5^{+}$ melanoma cells induce Treg cell infiltration via a B7-2-dependent mechanism (Schatton et al., 2010). Chemokines such as CC17, CCL22, and CCL28 are also produced by various cancers to attract $Foxp3^{+}$ Treg cells.

CSCs have been suggested to affect the Th17/Treg balance by altering the production of cytokines such as IL-6 and IL-8 and chemokine CCL5 in the TME (Yu et al., 2012). Treg/Th17 homeostasis has been implicated in its dual effect

on the promotion or suppression of cancer (Maniati et al., 2010; Marshall et al., 2016; Knochelmann et al., 2018). A study on Treg and Th17 cells demonstrated STAT3 was a pivotal transcription factor in Th17 differentiation and Treg inhibition, whereas STAT3 is significantly activated in gastric CSCs (Wei et al., 2008; Rezalotfi et al., 2019). Therefore, STAT3 may act as a key factor in modulating CSC stemness and expansion as well as Th17/Treg homeostasis. Yang et al. (2011) demonstrated that IL-17 Tregs stimulate the development of colorectal cancer-related stemness markers, including CD44, CD133, CD166, EpCAM, and ALDH, in bone marrow-derived mononuclear cells and drive cells to become CSCs, indicating the ability of Tregs to induce CSC development. In addition, Tregs release PGE2, which promotes colorectal CSC expansion and metastasis in a mouse model through NF-κB activation (Wang et al., 2015). Indirect interactions between Tregs and CSCs act on the regulation of angiogenesis, TGF-β signaling and macrophage-associated EMT (Mima et al., 2012; Yu et al., 2012; Liu et al., 2021). Under hypoxic conditions, Tregs, which are an important source of VEGF expression, release TGF-β and indirectly regulate CSC expansion by mediating angiogenesis (Facciabene et al., 2011). Additionally, VEGF signaling was found to promote CSC stemness and expansion in melanoma (Beck et al., 2011). Depletion of Tregs lowers VEGF-A and decreases vascularization in tumors. Blockade of VEGFR2 leads to a shrunken CSC population and impaired self-renewal. Similar results have been demonstrated in brain tumors, where the vascular niche directly correlates with CSC generation (Treps et al., 2017). Blockade of angiogenesis signaling significantly inhibits brain CSCs due to reduced blood vasculature in tumors. In line with clinical data, metastatic renal cancer patients who receive antiangiogenic therapy have an overall survival strongly correlated with the reduction in Treg numbers (Brodaczewska et al., 2018). Additionally, the angiogenetic situation is aggravated by TAM preferential secretion of VEGF and IL-8, doubling the effect on promoting CSC proliferation (Werno et al., 2010). Apart from angiogenesis, Tregs also promote CSC expansion by TAM-mediated EMT induction via the expression of CTLA-4, IL-10, and TGF-β (Yu et al., 2012).

Overall, CSCs induce Treg infiltration via costimulatory molecules and STAT3 signaling in the TME, while Tregs alternately regulate CSC proliferation and expansion directly via secretion of IL-17 and PGE2 or indirectly through TGF-β-mediated angiogenesis and EMT.

NATURAL KILLER CELLS

Natural killer cells represent a population of cytotoxic lymphocytes with an innate immune response and are responsible for eradicating tumor cells. High cytotoxic activity of NK cells is correlated with a lowered cancer risk (Imai et al., 2000). Approximately 95% of peripheral blood NK cells are $CD56^{dim}CD16^{+}$, which exert strong cytotoxic activity.

Beside antibody-dependent cellular cytotoxicity (ADCC) via Fc receptors bound to target cells, NK cells recognize target cells in cell-cell interactions through a variety of activating and inhibitory receptors. Activating receptors, including NKG2C, NKG2D, and NCR, as well as inhibitory receptors, such as Ly49, bind to MHC or HLA class I molecules and cellular stress ligands, leading to the NK cell response (Zhang et al., 2020a). In response to exposure to cancer cells, preferential NK killing of CSCs has been demonstrated in oral squamous carcinoma, human colon carcinoma, melanoma and glioblastoma (Castriconi et al., 2009; Pietra et al., 2009; Tseng et al., 2010; Tallerico et al., 2013; Pan et al., 2015). Specific killing of CSCs with the stem cell markers $CD24^{+}$, $CD133^{+}$, and $ALDH^{+}$ confirms the role of NK cells in effectively targeting and eradicating CSCs. This selective recognition of CSCs has been proposed to be mediated through NKG2D-, DNAM-1- and NKp30-activating receptors (Tallerico et al., 2016). In line with these findings, different types of CSCs express or overexpress the corresponding ligands of those activating receptors with low expression of MHC class I on the surface, leading to effective NK cytotoxicity activity.

However, the preferential tumorigenic capability of CSCs in NOD/SCID mice suggests that there are underlying immunosuppressive mechanisms for CSCs to dodge from NK cell specific killing (Al-Hajj et al., 2003; Tsuchiya and Shiota, 2021). It has been reported that CSCs escape NK-mediated cytotoxicity via various mechanisms by tuning NK receptors. In lung cancer, tumor-derived mesenchymal stem cells (MSCs) alter the NK cell phenotype by downregulating activating receptor expression and inhibiting interferon gamma (IFN-γ) secretion, whereas abortion of PGE2 and restoration of IL-6 activity reverse the tumor-derived MSC-mediated immunosuppression activities (Galland et al., 2017). $CD34^{+}CD38^{-}$ leukemic stem cells were shown to be resistant to allogenic NK-mediated killing (She et al., 2012). Breast $ALDH^{+}$ CSCs escape NK cells by reducing the expression of NKG2D ligands MICA and MICB through miR20a modulation (Wang et al., 2014). Downregulation of MICA/B expression supports CSC resistance to NK cell cytotoxicity and increases their metastatic capacity *in vivo*. Recent research also revealed the dual immunoinhibitory role of PCNA in upregulating the stemness of pancreatic and colon $CD44^{+}CD133^{+}$ CSCs, as well as participating in immune evasion from NK cytotoxicity by engaging with the inhibitory receptor NKp44 (Malaer and Mathew, 2020). Blockade of the PCNA-NKp44 interaction changes IFN-γ secretion and NK cytotoxicity, suggesting a potential immunotherapeutic target for NK cell-mediated attack. The interaction of NK cell coinhibitory receptors, such as PD-1, with their ligands on tumor cells, also suppresses NK cell-mediated glioma CSC eradication (Huang et al., 2015).

As most NK cell-mediated immune responses occur in tumor cells with low levels of MHC-I, melanoma cancer cells may escape NK cells by upregulating MHC-I on their surface. Interestingly, Huergo-Zapico et al. (2018) suggested that NK cells may release tumor necrosis factor-alpha (TNF-α) and IFN-γ and induce melanoma cells to undergo EMT, pushing them toward invasive phenotypes. EMT induction endows melanoma cells with upregulated stemness markers and enhances their invasive capability. Moreover, EMT favors immune escape by suppressing activating receptors or HLA class-I (Chen et al., 2015). In contrast, some reports have demonstrated that EMT

induction promotes NKG2D-L expression on colorectal cells and upregulates NK cell-mediated immunosurveillance in lung cancer (Lopez-Soto et al., 2013; Chockley et al., 2018). This finding suggests that the disparity of the EMT-derived NK cell immune response is dependent on the cancer type.

In summary, NK-mediated killing plays an important role in immune response in diminishing CSCs through the assistance of various activating and inhibitory receptors. Nevertheless, CSCs may escape specific targeting by modulating the expression of these receptors. A novel study also pointed out that NK cells may clash with their classical cytotoxic activity by promoting EMT in CSCs, dependent on the cancer type (Huergo-Zapico et al., 2018).

TUMOR-INFILTRATING LYMPHOCYTES

Tumor-infiltrating lymphocytes represent all lymphocytic cell populations, including $CD4^+$, $CD8^+$, and a small portion of B and NK cells that infiltrate the TME. TILs have been observed in the majority of solid tumors, such as breast, liver and lung cancers (Biller and Dow, 2007). These cells exert diverse effects on the immune response toward the tumor and are correlated with tumor aggressiveness, metastasis, treatment response rate and tumor recurrence. Subsequent to antigen stimulation by APCs, activated helper ($CD4^+$) T cells (Th) support the antitumor immune response by further activating cytotoxic ($CD8^+$) T cells (CTLs) and recruiting innate immune cells. Th cells stimulate CTLs by IL-2 secretion and cell-cell interactions through costimulatory molecules, including MHC-II, CD27 and CD134 (Giuntoli et al., 2002). Cancer cells, by producing CCL18, recruit Tregs that promote tumor formation and impact other immune cells (Paluskievicz et al., 2019). Bone marrow-derived MSCs have been reported to recruit and maintain Tregs via TGF-β secretion, leading to a negative regulation on T cell proliferation (Di Ianni et al., 2008; Papaccio et al., 2017). Moreover, tumor-derived TGF-β, TNF-α, and IFN-γ induce the differentiation of IL-17^{hi} Th17 cells, which supports angiogenesis and enhances protumor transcription factors (Maniati et al., 2010).

The presence of TILs frequently represents a good prognosis for cancer patients (Fridman et al., 2011; Dieci et al., 2014; Idos et al., 2020). Tumor-specific $CD8^+$ T cells induced by CSCs *in vitro* demonstrated an effective antitumor response, including inhibiting tumor growth and metastasis with prolonged survival in pancreatic and lung cancer mouse models (Visvader and Lindeman, 2008; Luo et al., 2014). Nevertheless, CSCs are capable of attenuating the action of these cells directly by altering their PD-L1 expression. Elevated stromal TILs and their PD-L1 expression in inflammatory breast cancer and lung adenocarcinoma have been reported to be significantly associated with CSC markers (Mansour et al., 2020; Zhang et al., 2020b). By analyzing PD-L1 expression in a large cohort of HCC patients, Kurebayashi et al. (2018) and others showed that PD-L1 expression in tumor infiltrates is associated with the progenitor subtype of HCC, marked by CK19 and SALL4 expression (Calderaro et al., 2016). High expression levels of PD-L1 are also observed in $CD133^+CD44^+$ colorectal CSCs and CSC-enriched tumor spheres. Hsu et al. (2018) suggested that PD-L1 enrichment in CSCs is mediated by β-catenin/STT3 signaling through glycosylation modulation and PD-L1 stabilization. Based on the clinical correlation between IL-6 and PD-L1 in HCC patient samples, Chan et al. (2019) showed that IL-6 activated JAK1 signaling cascade-induced N-glycosylation and the stabilization of PD-L1. Notch3/mTOR pathway activation is also reported to mediate PD-L1 overexpression on breast CSCs (Mansour et al., 2020). Altered PD-L1 expression, in turn, facilitates colorectal CSC self-renewal with upregulated stemness genes and promotes CSC expansion by activating HMGA1-dependent signaling pathways (Wei F. et al., 2019). PI3K/Akt pathway activation has also been reported to participate in PD-L1-derived promotion of stemness in CSCs (Almozyan et al., 2017).

In addition, interaction with nonlytic $CD8^+$ T cells leads to CSC expansion by cell-cell contact in primary breast cancer cell cultures (Stein et al., 2019). The induction of stemness properties in CSCs was confirmed by enhanced tumorigenesis in immunodeficient mice, and the resulting tumors were endowed with a higher cell density and an increased proliferation rate, as well as an elevated chance of lymphoid metastasis. Taken together, these findings showed that the ineffective cytotoxic activity of tumor infiltrates not only fails to eradicate malignancy but also conversely facilitates immune evasion by promoting CSC stemness, proliferation and tumorigenesis of cancer cells. The interaction between various immune cells and CSCs was summarized in **Figure 1**.

DEVELOPMENT OF CSC-TARGETED IMMUNOTHERAPY

Immune checkpoint CTLA-4 and PD-1 inhibitors revolutionized cancer research in the last decade and brought immunology back to the spotlight in therapeutic development. As immunotherapy relies on the immune system to recognize and attack tumor cells, it takes into account not only the tumor cells but also the TME as a therapeutic target to induce a powerful antitumor response. It is clear that CSCs and differentiated tumor cells exhibit distinct gene expression and functions in the tumor bulk, and therefore immunological targeting of the tumor bulk will be biased toward more differentiated tumor cells that express differentiated antigens (Pan et al., 2015). Effective targeting of CSCs may require highly specific identification of the CSC population. Currently, immunological targets of CSCs in therapeutic development have now been focused on three major approaches: CSC-associated antigens, phenotypes and niches.

The innate immune response, including NK and DC cells, exhibits cytotoxic activities toward tumor cells when they are exposed to foreign antigens in the normal immune system. The innate effector and antigen-presenting properties of NK and DC cells empower them to be suitable candidates for immunotherapy. Furthermore, several studies demonstrated that chemotherapy or radiation therapy increased MICA and MICB expression on CSCs, accompanied with CSC expansion (Ames et al., 2015b). This highlights the prospective use of NK cell therapy in combination with traditional therapies in

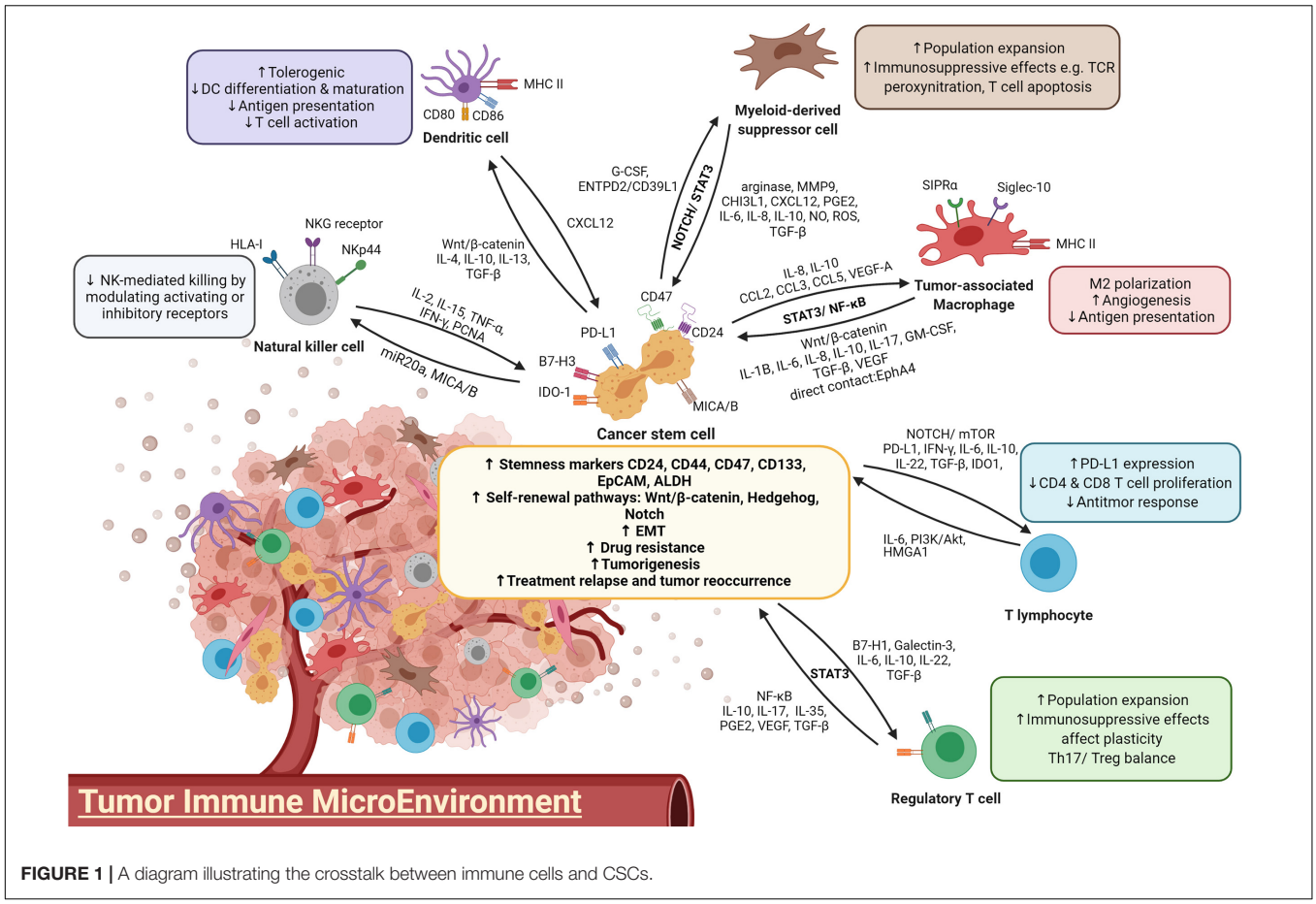

FIGURE 1 | A diagram illustrating the crosstalk between immune cells and CSCs.

eradicating CSCs. Currently, several clinical trials using NK cells infusion (NCT04162158 and NCT03592706) or in combination therapies (NCT03319459) to treat advanced solid tumors are ongoing. Adoptive NK cell therapy aims to strengthen and reinforce the antitumor functions of NK cells from autologous and allogeneic sources (Wang et al., 2021). After exposure to cytokines such as IL-2 and IL-5, NK cells prolong their activation and exhibit increased cytotoxicity. IL-2- and IL-15-activated NK cells have been shown to be able to eradicate human breast, colon, glioblastoma and melanoma CSCs (Castriconi et al., 2009; Ames et al., 2015a; Yin et al., 2016). A phase I clinical trial using allogeneic NK cells to target CSCs in advanced biliary tract cancer was conducted (NCT03358849). However, the administration of the activating cytokine IL-2 may also lead to the expansion of other immunosuppressive immune cells, including Treg cells (Koreth et al., 2016). In addition, to consistently activate NK cells, the trafficking and maintenance of engineered cytokines such as mbIL-15 and mbIL-21 will also need to be modified during the development of NK cell therapy (Pittari et al., 2015).

Sipuleucel-T is the first FDA-approved DC vaccine against advanced prostate cancer, ensuring DCs as a promising therapeutic strategy in immunotherapy (Cheever and Higano, 2011). DC vaccination has been confirmed to have effective immunologic activities in several preclinical studies. Stimulating DCs with CSC-designated antigens is believed to facilitate CSC eradication with high specificity and effectively resolve CSC-mediated tumor relapse and metastasis (Pang et al., 2019). However, clinical trials reported only a 10 to 15% response to DC vaccination by several cancer types (Anguille et al., 2014). One of the problems leading to low efficacy is the immunosuppressive effect from the upregulation of immune checkpoints (Shi et al., 2018). Recently, CSC-targeted DC vaccines have been reported to enhance the elimination of melanoma CSCs in a mouse tumor model with a combination of PD-L1 and CTLA-4 blockades, with an enhanced $CD8^+$ T cell response, increased IFN-γ and inhibited TGF-β expression (Zheng et al., 2018). This finding demonstrates the potential of CSC-based DC vaccines in combinational therapy.

The FDA has approved the use of chimeric antigen receptor (CAR)-T cell therapies targeting CD19 in treating lymphoma since 2017 (FDA, 2017). Increasing numbers of preclinical studies have demonstrated effective immunological control of CAR-T cells in inhibiting cancer growth and prolonging host survival (Chong et al., 2017; Foster et al., 2017; Heczey et al., 2017; Kloss et al., 2018; Zhang et al., 2019). As CAR-T therapy has been in use with a high success rate in treating lymphoma and leukemia, it has also been proposed for targeting CSCs. CSC-related markers such as CD133, EpCAM, and CD90 have been identified as targeted antigens for CAR-T cells (Guo et al., 2018).

TABLE 1 | Therapeutic strategies targeting the CSC niche and their development progress.

Trial description	Drug name	Molecular targets	Mechanism of action	Phase of drug development	References
CSC-associated molecules					
NK cell therapy		HLA	NK cell killing	I/II	NCT04162158;
				II/III	NCT03592706;
	FAKE-NK100			I	NCT03319459;
	SMT-NK			I	NCT03358849
CAR-T cell therapy	CARTEPC	EpCAM	T cell cytotoxicity	I/II	NCT03013712
		CD133		I/II	NCT02541370
Pathways					
iL-6/JAK/STAT	AZD-1480	JAK1/2	Inhibition of JAK1/2	I	NCT01112397
	Celecoxib (FDA approved)	STAT3	Inhibition of STAT3	III	NCT00087256
	Pyrimethamine (FDA approved)	STAT3	Inhibition of STAT3	I/II	NCT01066663
	Tocilizumab	IL-6	IL-6R monoclonal antibody	II	NCT03999749
	Siltuximab	IL-6	IL-6R monoclonal antibody	II	NCT03315026
IL-8	Reparixin	CXCR1	Inhibition of CXCR1	II	NCT01861054;
				II	NCT02370238
NF-kB					
	Acalabrutinib	BTK	Inhibition of BTK	III	NCT04008706
	Ibudilast (MN-166)	TLR4	TLR4 antagonist	II	NCT03782415
	LCL-161	c-IAP	Inhibition of c-IAP	II	NCT01617668;
				I/II	NCT02649673
TGF-β					
	Fresolimumab	TGF-β1/2/3	Neutralizing antibody	II	NCT01472731;
				I/II	NCT02581787
	Galunisertib	TGF-βR1	Inhibition of TGF-βR1	II	NCT02688712;
				II	NCT02538471;
				II	NCT01246986
	Lucanix	TGF-β2	Antisense oligonucleotide	II	NCT01058785;
				III	NCT00676507
	M7824	TGF-β/PD-L1	Ligand trap	III	NCT04066491
Wnt/β-catenin					
	Ipafricept (OMP-54F28)	FZD receptor	FZD8 decoy receptor	I	NCT01608867;
				I	NCT02050178;
				I	NCT02092363;
				I	NCT02069145
	Vantictumab (OMP-18R5)	FZD receptor	Monoclonal antibody against FZD receptors	I	NCT01957007;
				I	NCT01973309;
				I	NCT01345201;
				I	NCT02005315
	PRI-724	CBP/β-catenin	Antagonist	II	NCT01302405
	WNT974	PORCN	Inhibition of PORCN	II	NCT02649530;
				I/II	NCT02278133;
				I	NCT01351103
Notch					
	AL101	γ-Secretase	Inhibition of S3 cleavage	II	NCT03691207
	MK-0752	γ-Secretase	Inhibition of S3 cleavage	I	NCT00106145;
				I	NCT01098344
	Nirogacestat (PF-03084014)	γ-Secretase	Inhibition of S3 cleavage	II	NCT02109445;
				II	NCT02299635
	Demicizumab (OMP-21 M18)	DLL4	Blockade of DLL4	II	NCT02259582
	Enoticumab (REGN421)	DLL4	Monoclonal antibody against DLL4	I	NCT00871559
VEGF					
	Axitinib	VEGFR	Inhibition of VEGFR	I	NCT02853331

(Continued)

TABLE 1 | Continued

Trial description	Drug name	Molecular targets	Mechanism of action	Phase of drug development	References
	Bevacizumab (FDA approved)	VEGFR	Inhibition of VEGF binding to receptor	II	NCT02226289;
				III	NCT02420821;
				III	NCT03434379
Immune cells					
TAMs	Zoledronate acid	Mevalonate pathway	Elimination	I/II	NCT00588913;
				III	NCT02622607
	BMS-813160	CCR2/5	Inhibition of macrophage recruitment	II	NCT04123379;
				I/II	NCT03767582;
				I/II	NCT03496662;
				II	NCT02996110
	BL-8040	CXCR4	Antagonist	II	NCT02826486;
				II	NCT02907099
	Pexidartinib	CSF-1R	Inhibition of CSF-1R	I	NCT02777710
	AMG820	CSF-1R	Monoclonal antibody against CSF-1R	I/II	NCT02713529
	ALX148	CD47/SIRPα	Blockade of CD47	I	NCT03013218
	IBI322	CD47/SIRPα	CD47/PD-L1 bispecific antibody	I	NCT04328831
	Hu5F9-G4	CD47/SIRPα	Monoclonal antibody against CD47	I	NCT02216409
MDSCs	INCB001158	Arginase	Inhibition of arginase	I/II	NCT02903914
	Decitabine	Arginase	Differentiation	I	NCT00030615
	Entinostat	Arginase	Elimination	I	NCT02453620
NK cells	Lirilumab	KIR	Blockade of inhibitory signal of NK cells	I/II	NCT03532451;
					NCT01714739
	Monalizumab (IPH2201)	NKG2A	Inhibition of immune checkpoint	I/II	NCT03822351;
					NCT03833440
Tregs	Ontak (Denileukin diftitox)	CD25	Induction of apoptosis	II	NCT00726037

Zhu et al. (2015) successfully eliminated $CD133^+$ CSCs derived from glioblastoma patients; however, T cell aging marker CD57 was induced as a side effect. Recently, a phase I clinical trial (NCT02541370) using autologous CD133-targeted CAR-T cells to treat 23 patients with advanced $CD133^+$ tumors resulted in a benefit of 5-month median progression-free survival, with controllable toxicity (Wang et al., 2018b). Zhang et al. (2019) also reported that adoptive transfer of EpCAM-targeted CAR-T cells significantly reduced tumor growth in a xenograft model without safety issues. An EpCAM-targeted CAR-T cell clinical trial (NCT03013712) is in progress for targeting $EpCAM^+$ cancers. To minimize the toxicity to normal cells, targeting these CSC markers can be coupled with an inhibitory receptor with specificity for normal tissue antigens.

Yet, more investigations are necessary to overcome the challenges of using CAR-T cells to eliminate CSCs. One of the limitations in developing CAR-T cells targeting CSCs is the diverse treatment response due to the distinct CSCs plasticity and heterogenicity in patients (Alhabbab, 2020). Common immunotherapy hurdles, including acquired resistance as well as upregulation of immune checkpoints are also observed in T cell immunotherapies. Miao et al. (2019) demonstrated that TGF-β-enriched CSCs dampened the cytotoxicity of adoptive T cells by promoting the exhaustion state through CD80-CTLA4 interaction in squamous cell carcinoma. The findings of adaptive immune resistance raised from CSCs against immunotherapy echoes with the previously proposed immunosuppressing feature of CSC, and furthermore emphases CSC as the root of tumor relapse (Tsuchiya and Shiota, 2021).

In addition to direct targeting CSC phenotype and markers, researchers have also targeted the CSC niche, which contributes to CSC self-renewal and immune escape. This includes CSC-associated pathways, cytokines and immune cells (**Table 1**). As mentioned above, CSCs maintain their self-renewal by generating a positive feedback loop with immunosuppressive cells such as TAMs through JAK/STAT3, Wnt/β-catenin, and NF-κB crosstalk activation, with the expression of inhibitory cytokines such as IL-6, IL-8, and TGF-β. Wnt/ β-catenin-targeted therapies such as anti-FZD receptors monoclonal antibody (Vantictumab), β-catenin inhibitors PRI-724, as well as small-molecule porcupine inhibitor WNT974 are currently in clinical trials. Wnt-targeted treatments are proposed to be implemented as combinational therapies with immune checkpoint inhibitors such as nivolumab and ipilimumab or tyrosine kinase inhibitors, in order to pinpoint the immune evasive ability of CSCs in Wnt-driven cancers (Katoh, 2017). Blockade of IL-6 was previously

proven to affect non-small cell lung cancer tumorigenesis and the proliferation of H460 lung CSCs (Yi et al., 2012). The IL-6 receptor monoclonal antibody tocilizumab has been reported to suppress the premetastatic ability of breast CSCs and potentiate the cytotoxicity of cisplatin against triple-negative breast cancer (Alraouji et al., 2020). The drug has been approved by the FDA for treating rheumatoid arthritis and is now under phase II study for curing advanced melanoma in combination with the immune checkpoint inhibitors nivolumab and ipilimumab (NCT03999749). Blockade of the IL-8 receptor CXCR1 using small molecule Reparixin successfully attenuated the CSC population and induced massive apoptosis in a breast cancer cell line. The result of phase I clinical trial showed that Reparixin is safe and well tolerated, in combination of paclitaxel (Schott et al., 2017). Phase II study of this drug showed a $\geq$20% reduction in CSC markers $ALDH^+$ and $CD24^-/CD44^+$ in HER-2-negative breast patients with no serious adverse reactions (Goldstein et al., 2020). Due to the limited number of CSC in primary breast cancer, another clinical trial (NCT02370238) with alternative evaluation endpoint, for example, measurement of metastasis, has been set for assessing the effectiveness of reparixin on CSC eradication (Ruffini, 2019).

The roles of angiogenesis in supporting immunosuppressive TME and self-renewal of CSCs have been extensively studied, thus the combination use with VEGF inhibitor provides a novel direction for immunotherapy. A phase III clinical trial (NCT03434379) of bevacizumab with PD-L1 inhibitor atezolizumab showed a superior outcome in overall and progression-free survival than sorafenib in advanced HCC cases (Finn et al., 2020). Due to this encouraging result, FDA approved the combined use of bevacizumab and atezolizumab as the first-line treatment for unresectable HCC patients (Yang et al., 2020). A recent report on targeting aberrant mRNA modification in leukemia has highlighted another potential therapeutic approach to suppress fat mass and obesity-associated protein (FTO), an RNA N6-methyladenosine (m6A) demethylase (Su et al., 2020). M6A RNA modification has been implicated in self-renewal and tumorigenesis in various cancers, thus is proposed to be a novel therapeutic target against CSCs (Ma and Ji, 2020). Using small molecule inhibitors CS1 and CS2, inhibition of FTO attenuates self-renewal ability of leukemic stem cells via reducing MYC and CEBPA expressions. Targeting FTO also suppresses the immune checkpoint gene LILRB4, and thus sensitizes the cancer cells to T cell cytotoxicity (Su et al., 2020). Thus, the combination of FTO inhibitors and hypomethylating agents (HMA) is recommended for future clinical trials, in order to overcome the adaptive immune resistance induced by HMA treatment in leukemia patients with high FTO.

Direct targeting of immunosuppressive cells such as TAMs with zoledronic acid successfully inhibited the growth of cervical cancer cell-derived CSCs by reducing their stemness properties and inducing apoptosis (Wang et al., 2019). The drug is now undergoing phase III clinical trials to examine its preventive effect on bone metastasis in patients with advanced lung cancer (NCT02622607). CD47-targeting antibodies also overcome a key immune escape mechanism, the CD47/SIRPα-mediated "Don't eat me" signal. ALX148, which is a CD47 blocking protein, was well tolerated in combination with anticancer antibodies and conventional chemotherapy in patients with advanced cancers (NCT03013218). Hu5F9-G4, an anti-CD47 antibody, also shows excellent tolerability and promising effects in leukemia stem cells in combination with Azacitidine (NCT03248479). These findings suggest that targeting CD47 with conventional cancer treatment may be a powerful strategy to address CSC-derived immune evasion. Ontak, a fusion protein comprized of human IL-2 and diphtheria toxin, targets $CD25^+$ Treg cells by inducing apoptotic cell death (Cheung et al., 2019). A pilot study was carried out to evaluate its inhibitory effect on Tregs in metastatic pancreatic cancer patients (NCT00726037). This drug is designed to integrate DC vaccine administration for treating unresectable pancreatic cancer. Several clinical trials aiming at other immunotherapeutic targets, such as MDSCs and NK cells, are also ongoing (**Table 1**).

While direct CSC-targeted treatments such as NK, CAR-T therapies and DC vaccines are still being studied, targeting the CSC niche might be a feasible immunological therapeutic approach to eradicate cancer, considering several encouraging preclinical results. Similarly, much effort will be required to resolve the side effects such as the resistance or diverse treatment responses that most immunotherapies may arouse. Additionally, basic research on the crosstalk between CSCs and their niche is also necessary for identifying a biomarker that can monitor the treatment response, as well as novel therapeutic targets for the development of effective treatments.

AUTHOR CONTRIBUTIONS

ML: conception and design, writing, review, and/or revision of the manuscript. TL: study supervision. Both authors contributed to the article and approved the submitted version.

FUNDING

The study was supported by the RGC General Research Fund (15102020), Collaborative Research Fund (C7026-18G), Health and Medical Research Fund (05161216), and Research Impact Fund (R5050-18F).

REFERENCES

Ai, L., Mu, S., Sun, C., Fan, F., Yan, H., Qin, Y., et al. (2019). Myeloid-derived suppressor cells endow stem-like qualities to multiple myeloma cells by inducing piRNA-823 expression and DNMT3B activation. *Mol. Cancer* 18:88. doi: 10.1186/s12943-019-1011-5

Ai, L., Mu, S., Wang, Y., Wang, H., Cai, L., Li, W., et al. (2018). Prognostic role of myeloid-derived suppressor cells in cancers: a systematic review and meta-analysis. *BMC Cancer* 18:1220. doi: 10.1186/s12885-018-5086-y

Alhabbab, R. Y. (2020). Targeting cancer stem cells by genetically engineered chimeric antigen receptor T cells. *Front. Genet.* 11:312. doi: 10.3389/fgene.2020.00312

Al-Hajj, M., Wicha, M., Benito-Hernandez, A., Morrison, S., and Clarke, M. (2003). Prospective identification of tumorigenic breast cancer cells. *Proc. Natl. Acad. Sci. U.S.A.* 100, 3983–3988. doi: 10.1073/pnas.1231735100

Almozyan, S., Colak, D., Mansour, F., Alaiya, A., Al-Harazi, O., Qattan, A., et al. (2017). PD-L1 promotes OCT4 and Nanog expression in breast cancer stem cells by sustaining PI3K/AKT pathway activation. *Int. J. Cancer* 141, 1402–1412. doi: 10.1002/ijc.30834

Alraouji, N. N., Al-Mohanna, F. H., Ghebeh, H., Arafah, M., Almeer, R., Al-Tweigeri, T., et al. (2020). Tocilizumab potentiates cisplatin cytotoxicity and targets cancer stem cells in triple-negative breast cancer. *Mol. Carcinog.* 59, 1041–1051. doi: 10.1002/mc.23234

Ames, E., Canter, R. J., Grossenbacher, S. K., Mac, S., Chen, M., Smith, R. C., et al. (2015a). NK Cells preferentially target tumor cells with a cancer stem cell phenotype. *J. Immunol.* 195, 4010–4019. doi: 10.4049/jimmunol.1500447

Ames, E., Canter, R. J., Grossenbacher, S. K., Mac, S., Smith, R. C., Monjazeb, A. M., et al. (2015b). Enhanced targeting of stem-like solid tumor cells with radiation and natural killer cells. *Oncoimmunology* 4:e1036212. doi: 10.1080/2162402X.2015.1036212

Anguille, S., Smits, E. L., Lion, E., van Tendeloo, V. F., and Berneman, Z. N. (2014). Clinical use of dendritic cells for cancer therapy. *Lancet Oncol.* 15, e257–e267. doi: 10.1016/s1470-2045(13)70585-0

Barkal, A. A., Brewer, R. E., Markovic, M., Kowarsky, M., Barkal, S. A., Zaro, B. W., et al. (2019). CD24 signalling through macrophage Siglec-10 is a target for cancer immunotherapy. *Nature* 572, 392–396. doi: 10.1038/s41586-019-1456-0

Beck, B., Driessens, G., Goossens, S., Youssef, K. K., Kuchnio, A., Caauwe, A., et al. (2011). A vascular niche and a VEGF-Nrp1 loop regulate the initiation and stemness of skin tumours. *Nature* 478, 399–403. doi: 10.1038/nature10525

Bhatia, A., and Kumar, Y. (2016). Cancer stem cells and tumor immunoediting: putting two and two together. *Expert Rev. Clin. Immunol.* 12, 605–607. doi: 10.1586/1744666X.2016.1159133

Biller, B., and Dow, S. (2007). *Immunotherapy of Cancer. Withrow & MacEwen's Small Animal Clinical Oncology*. St. Louis: Elsevier. 211–235.

Bocci, F., Levine, H., Onuchic, J. N., and Jolly, M. K. (2019). Deciphering the dynamics of epithelial-mesenchymal transition and cancer stem cells in tumor progression. *Curr. Stem Cell Rep.* 5, 11–21. doi: 10.1007/s40778-019-0150-3

Boks, M. A., Kager-Groenland, J. R., Haasjes, M. S., Zwaginga, J. J., van Ham, S. M., and ten Brinke, A. (2012). IL-10-generated tolerogenic dendritic cells are optimal for functional regulatory T cell induction–a comparative study of human clinical-applicable DC. *Clin. Immunol.* 142, 332–342. doi: 10.1016/j.clim.2011.11.011

Brissette, M. J., Lepage, S., Lamonde, A. S., Sirois, I., Groleau, J., Laurin, L. P., et al. (2012). MFG-E8 released by apoptotic endothelial cells triggers anti-inflammatory macrophage reprogramming. *PLoS One* 7:e36368. doi: 10.1371/journal.pone.0036368

Brodaczewska, K. K., Szczylik, C., and Kieda, C. (2018). Immune consequences of anti-angiogenic therapyin renal cell carcinoma. *Contemp. Oncol. (Pozn)* 22, 14–22. doi: 10.5114/wo.2018.73878

Calderaro, J., Rousseau, B., Amaddeo, G., Mercey, M., Charpy, C., Costentin, C., et al. (2016). Programmed death ligand 1 expression in hepatocellular carcinoma: relationship With clinical and pathological features. *Hepatology* 64, 2038–2046. doi: 10.1002/hep.28710

Cassetta, L., and Kitamura, T. (2018). Targeting tumor-associated macrophages as a potential strategy to enhance the response to immune checkpoint inhibitors. *Front. Cell Dev. Biol.* 6:38. doi: 10.3389/fcell.2018.00038

Castriconi, R., Daga, A., Dondero, A., Zona, G., Poliani, P. L., Melotti, A., et al. (2009). NK cells recognize and kill human glioblastoma cells with stem cell-like properties. *J. Immunol.* 182, 3530–3539. doi: 10.4049/jimmunol.0802845

Chan, L. C., Li, C. W., Xia, W., Hsu, J. M., Lee, H. H., Cha, J. H., et al. (2019). IL-6/JAK1 pathway drives PD-L1 Y112 phosphorylation to promote cancer immune evasion. *J. Clin. Invest.* 129, 3324–3338. doi: 10.1172/JCI126022

Chandra, D., Jahangir, A., Quispe-Tintaya, W., Einstein, M. H., and Gravekamp, C. (2013). Myeloid-derived suppressor cells have a central role in attenuated Listeria monocytogenes-based immunotherapy against metastatic breast cancer in young and old mice. *Br. J. Cancer* 108, 2281–2290. doi: 10.1038/bjc.2013.206

Cheever, M. A., and Higano, C. S. (2011). PROVENGE (Sipuleucel-T) in prostate cancer: the first FDA-approved therapeutic cancer vaccine. *Clin. Cancer Res.* 17, 3520–3526. doi: 10.1158/1078-0432.CCR-10-3126

Chen, X. H., Liu, Z. C., Zhang, G., Wei, W., Wang, X. X., Wang, H., et al. (2015). TGF-beta and EGF induced HLA-I downregulation is associated with epithelial-mesenchymal transition (EMT) through upregulation of snail in prostate cancer cells. *Mol. Immunol.* 65, 34–42. doi: 10.1016/j.molimm.2014.12.017

Chen, Y., Song, Y., Du, W., Gong, L., Chang, H., and Zou, Z. (2019). Tumor-associated macrophages: an accomplice in solid tumor progression. *J. Biomed. Sci.* 26:78. doi: 10.1186/s12929-019-0568-z

Cheung, L. S., Fu, J., Kumar, P., Kumar, A., Urbanowski, M. E., Ihms, E. A., et al. (2019). Second-generation IL-2 receptor-targeted diphtheria fusion toxin exhibits antitumor activity and synergy with anti-PD-1 in melanoma. *Proc. Natl. Acad. Sci. U.S.A.* 116, 3100–3105. doi: 10.1073/pnas.1815087116

Chiu, D. K., Tse, A. P., Xu, I. M., Di Cui, J., Lai, R. K., Li, L. L., et al. (2017). Hypoxia inducible factor HIF-1 promotes myeloid-derived suppressor cells accumulation through ENTPD2/CD39L1 in hepatocellular carcinoma. *Nat. Commun.* 8:517. doi: 10.1038/s41467-017-00530-7

Chockley, P. J., Chen, J., Chen, G., Beer, D. G., Standiford, T. J., and Keshamouni, V. G. (2018). Epithelial-mesenchymal transition leads to NK cell-mediated metastasis-specific immunosurveillance in lung cancer. *J. Clin. Invest.* 128, 1384–1396. doi: 10.1172/JCI97611

Choi, H. S., Kim, J. H., Kim, S. L., and Lee, D. S. (2019). Disruption of the NF-kappaB/IL-8 signaling axis by sulconazole inhibits human breast cancer stem cell formation. *Cells* 8:1007. doi: 10.3390/cells8091007

Chong, E. A., Melenhorst, J. J., Lacey, S. F., Ambrose, D. E., Gonzalez, V., Levine, B. L., et al. (2017). PD-1 blockade modulates chimeric antigen receptor (CAR)-modified T cells: refueling the CAR. *Blood* 129, 1039–1041. doi: 10.1182/blood-2016-09-738245

Cubillos-Ruiz, J. R., Martinez, D., Scarlett, U. K., Rutkowski, M. R., Nesbeth, Y. C., Camposeco-Jacobs, A. L., et al. (2010). CD277 is a negative co-stimulatory molecule universally expressed by ovarian cancer microenvironmental cells. *Oncotarget* 1, 329–338.

Cui, T. X., Kryczek, I., Zhao, L., Zhao, E., Kuick, R., Roh, M. H., et al. (2013). Myeloid-derived suppressor cells enhance stemness of cancer cells by inducing microRNA101 and suppressing the corepressor CtBP2. *Immunity* 39, 611–621. doi: 10.1016/j.immuni.2013.08.025

Di Ianni, M., Del Papa, B., De Ioanni, M., Moretti, L., Bonifacio, E., Cecchini, D., et al. (2008). Mesenchymal cells recruit and regulate T regulatory cells. *Exp. Hematol.* 36, 309–318. doi: 10.1016/j.exphem.2007.11.007

Dieci, M. V., Criscitiello, C., Goubar, A., Viale, G., Conte, P., Guarneri, V., et al. (2014). Prognostic value of tumor-infiltrating lymphocytes on residual disease after primary chemotherapy for triple-negative breast cancer: a retrospective multicenter study. *Ann. Oncol.* 25, 611–618. doi: 10.1093/annonc/mdt556

Facciabene, A., Peng, X., Hagemann, I. S., Balint, K., Barchetti, A., Wang, L. P., et al. (2011). Tumour hypoxia promotes tolerance and angiogenesis via CCL28 and T(reg) cells. *Nature* 475, 226–230. doi: 10.1038/nature10169

Fainaru, O., Shay, T., Hantisteanu, S., Goldenberg, D., Domany, E., and Groner, Y. (2007). TGFbeta-dependent gene expression profile during maturation of dendritic cells. *Genes Immun.* 8, 239–244. doi: 10.1038/sj.gene.6364380

Fang, W., Ye, L., Shen, L., Cai, J., Huang, F., Wei, Q., et al. (2014). Tumor-associated macrophages promote the metastatic potential of thyroid papillary cancer by releasing CXCL8. *Carcinogenesis* 35, 1780–1787. doi: 10.1093/carcin/bgu060

FDA (2017). *FDA Approval Brings First Gene Therapy to the United States [Online]*. Available online at: https://www.fda.gov/news-events/press-announcements/fda-approval-brings-first-gene-therapy-united-states (accessed August 04, 2021).

Finn, R. S., Qin, S., Ikeda, M., Galle, P. R., Ducreux, M., Kim, T. Y., et al. (2020). Atezolizumab plus bevacizumab in unresectable hepatocellular carcinoma. *N. Engl. J. Med.* 382, 1894–1905. doi: 10.1056/NEJMoa1915745

Foster, A. E., Mahendravada, A., Shinners, N. P., Chang, W. C., Crisostomo, J., Lu, A., et al. (2017). Regulated expansion and survival of chimeric antigen receptor-modified t cells using small molecule-dependent inducible MyD88/CD40. *Mol. Ther.* 25, 2176–2188. doi: 10.1016/j.ymthe.2017.06.014

Fourcade, J., Sun, Z., Benallaoua, M., Guillaume, P., Luescher, I. F., Sander, C., et al. (2010). Upregulation of Tim-3 and PD-1 expression is associated with tumor antigen-specific CD8+ T cell dysfunction in melanoma patients. *J. Exp. Med.* 207, 2175–2186. doi: 10.1084/jem.20100637

Fridman, W. H., Galon, J., Pages, F., Tartour, E., Sautes-Fridman, C., and Kroemer, G. (2011). Prognostic and predictive impact of intra- and peritumoral immune infiltrates. *Cancer Res.* 71, 5601–5605. doi: 10.1158/0008-5472.CAN-11-1316

Galland, S., Vuille, J., Martin, P., Letovanec, I., Caignard, A., Fregni, G., et al. (2017). Tumor-derived mesenchymal stem cells use distinct mechanisms to block the activity of natural killer cell subsets. *Cell Rep.* 20, 2891–2905. doi: 10.1016/j.celrep.2017.08.089

Gao, L., Yu, S., and Zhang, X. (2014). Hypothesis: Tim-3/galectin-9, a new pathway for leukemia stem cells survival by promoting expansion of myeloid-derived suppressor cells and differentiating into tumor-associated macrophages. *Cell Biochem. Biophys.* 70, 273–277. doi: 10.1007/s12013-014-9900-0

Gao, X., Zhu, Y., Li, G., Huang, H., Zhang, G., Wang, F., et al. (2012). TIM-3 expression characterizes regulatory T cells in tumor tissues and is associated with lung cancer progression. *PLoS One* 7:e30676. doi: 10.1371/journal.pone.0030676

Ginestier, C., Liu, S., Diebel, M. E., Korkaya, H., Luo, M., Brown, M., et al. (2010). CXCR1 blockade selectively targets human breast cancer stem cells in vitro and in xenografts. *J. Clin. Invest.* 120, 485–497. doi: 10.1172/JCI39397

Giuntoli, R. L., Lu, J., Kobayashi, H., Kennedy, R., and Celis, E. (2002). Direct costimulation of tumor-reactive CTL by helper T cells potentiate their proliferation, survival, and effector function. *Clin. Cancer Res.* 8, 922–931.

Goldstein, L. J., Perez, R. P., Yardley, D., Han, L. K., Reuben, J. M., Gao, H., et al. (2020). A window-of-opportunity trial of the CXCR1/2 inhibitor reparixin in operable HER-2-negative breast cancer. *Breast Cancer Res.* 22:4. doi: 10.1186/s13058-019-1243-8

Guo, L., Cheng, X., Chen, H., Chen, C., Xie, S., Zhao, M., et al. (2019). Induction of breast cancer stem cells by M1 macrophages through Lin-28B-let-7-HMGA2 axis. *Cancer Lett.* 452, 213–225. doi: 10.1016/j.canlet.2019.03.032

Guo, Y., Feng, K., Wang, Y., and Han, W. (2018). Targeting cancer stem cells by using chimeric antigen receptor-modified T cells: a potential and curable approach for cancer treatment. *Protein Cell* 9, 516–526. doi: 10.1007/s13238-017-0394-6

Heczey, A., Louis, C. U., Savoldo, B., Dakhova, O., Durett, A., Grilley, B., et al. (2017). CAR T cells administered in combination with lymphodepletion and PD-1 inhibition to patients with neuroblastoma. *Mol. Ther.* 25, 2214–2224. doi: 10.1016/j.ymthe.2017.05.012

Hsu, J. M., Xia, W., Hsu, Y. H., Chan, L. C., Yu, W. H., Cha, J. H., et al. (2018). STT3-dependent PD-L1 accumulation on cancer stem cells promotes immune evasion. *Nat. Commun.* 9:1908. doi: 10.1038/s41467-018-04313-6

Huang, B. Y., Zhan, Y. P., Zong, W. J., Yu, C. J., Li, J. F., Qu, Y. M., et al. (2015). The PD-1/B7-H1 pathway modulates the natural killer cells versus mouse glioma stem cells. *PLoS One* 10:e0134715. doi: 10.1371/journal.pone.0134715

Huergo-Zapico, L., Parodi, M., Cantoni, C., Lavarello, C., Fernandez-Martinez, J. L., Petretto, A., et al. (2018). NK-cell editing mediates epithelial-to-mesenchymal transition via phenotypic and proteomic changes in melanoma cell lines. *Cancer Res.* 78, 3913–3925. doi: 10.1158/0008-5472.CAN-17-1891

Idos, G. E., Kwok, J., Bonthala, N., Kysh, L., Gruber, S. B., and Qu, C. (2020). The prognostic implications of tumor infiltrating lymphocytes in colorectal cancer: a systematic review and meta-analysis. *Sci. Rep.* 10:3360. doi: 10.1038/s41598-020-60255-4

Iliopoulos, D., Hirsch, H. A., and Struhl, K. (2009). An epigenetic switch involving NF-kappaB, Lin28, Let-7 MicroRNA, and IL6 links inflammation to cell transformation. *Cell* 139, 693–706. doi: 10.1016/j.cell.2009.10.014

Imai, K., Matsuyama, S., Miyake, S., Suga, K., and Nakachi, K. (2000). Natural cytotoxic activity of peripheral-blood lymphocytes and cancer incidence: an 11-year follow-up study of a general population. *Lancet* 356, 1795–1799. doi: 10.1016/s0140-6736(00)03231-1

Jachetti, E., Caputo, S., Mazzoleni, S., Brambillasca, C. S., Parigi, S. M., Grioni, M., et al. (2015). Tenascin-C protects cancer stem-like cells from immune surveillance by arresting T-cell activation. *Cancer Res.* 75, 2095–2108. doi: 10.1158/0008-5472.CAN-14-2346

Jinushi, M., Chiba, S., Yoshiyama, H., Masutomi, K., Kinoshita, I., Dosaka-Akita, H., et al. (2011). Tumor-associated macrophages regulate tumorigenicity and anticancer drug responses of cancer stem/initiating cells. *Proc. Natl. Acad. Sci. U.S.A.* 108, 12425–12430. doi: 10.1073/pnas.1106645108

Katoh, M. (2017). Canonical and non-canonical WNT signaling in cancer stem cells and their niches: cellular heterogeneity, omics reprogramming, targeted therapy and tumor plasticity. *Int. J. Oncol.* 51, 1357–1369. doi: 10.3892/ijo.2017.4129

Kikushige, Y., Shima, T., Takayanagi, S., Urata, S., Miyamoto, T., Iwasaki, H., et al. (2010). TIM-3 is a promising target to selectively kill acute myeloid leukemia stem cells. *Cell Stem Cell* 7, 708–717. doi: 10.1016/j.stem.2010.11.014

Kloss, C. C., Lee, J., Zhang, A., Chen, F., Melenhorst, J. J., Lacey, S. F., et al. (2018). Dominant-negative TGF-beta receptor enhances PSMA-targeted human CAR T cell proliferation and augments prostate cancer eradication. *Mol. Ther.* 26, 1855–1866. doi: 10.1016/j.ymthe.2018.05.003

Knochelmann, H. M., Dwyer, C. J., Bailey, S. R., Amaya, S. M., Elston, D. M., Mazza-McCrann, J. M., et al. (2018). When worlds collide: Th17 and Treg cells in cancer and autoimmunity. *Cell Mol. Immunol.* 15, 458–469. doi: 10.1038/s41423-018-0004-4

Kobie, J., Wu, R., Kurt, R., Lou, S., Adelman, M., Whitesell, L., et al. (2003). Transforming growth factor β inhibits the antigen-presenting functions and antitumor activity of dendritic cell vaccines. *Cancer Res.* 63, 1860–1864.

Komura, N., Mabuchi, S., Shimura, K., Yokoi, E., Kozasa, K., Kuroda, H., et al. (2020). The role of myeloid-derived suppressor cells in increasing cancer stem-like cells and promoting PD-L1 expression in epithelial ovarian cancer. *Cancer Immunol. Immunother.* 69, 2477–2499. doi: 10.1007/s00262-020-02628-2

Koreth, J., Kim, H. T., Jones, K. T., Lange, P. B., Reynolds, C. G., Chammas, M. J., et al. (2016). Efficacy, durability, and response predictors of low-dose interleukin-2 therapy for chronic graft-versus-host disease. *Blood* 128, 130–137. doi: 10.1182/blood-2016-02-702852

Krempski, J., Karyampudi, L., Behrens, M. D., Erskine, C. L., Hartmann, L., Dong, H., et al. (2011). Tumor-infiltrating programmed death receptor-1+ dendritic cells mediate immune suppression in ovarian cancer. *J. Immunol.* 186, 6905–6913. doi: 10.4049/jimmunol.1100274

Kumar, S., Wilkes, D. W., Samuel, N., Blanco, M. A., Nayak, A., Alicea-Torres, K., et al. (2018). DeltaNp63-driven recruitment of myeloid-derived suppressor cells promotes metastasis in triple-negative breast cancer. *J. Clin. Invest.* 128, 5095–5109. doi: 10.1172/JCI99673

Kurebayashi, Y., Ojima, H., Tsujikawa, H., Kubota, N., Maehara, J., Abe, Y., et al. (2018). Landscape of immune microenvironment in hepatocellular carcinoma and its additional impact on histological and molecular classification. *Hepatology* 68, 1025–1041. doi: 10.1002/hep.29904

Kusmartsev, S., Nefedova, Y., Yoder, D., and Gabrilovich, D. I. (2004). Antigen-specific inhibition of CD8+ T cell response by immature myeloid cells in cancer is mediated by reactive oxygen species. *J. Immunol.* 172, 989–999. doi: 10.4049/jimmunol.172.2.989

Lee, T. K., Cheung, V. C., Lu, P., Lau, E. Y., Ma, S., Tang, K. H., et al. (2014). Blockade of CD47-mediated cathepsin S/protease-activated receptor 2 signaling provides a therapeutic target for hepatocellular carcinoma. *Hepatology* 60, 179–191. doi: 10.1002/hep.27070

Lewis, C. E., and Pollard, J. W. (2006). Distinct role of macrophages in different tumor microenvironments. *Cancer Res.* 66, 605–612. doi: 10.1158/0008-5472.CAN-05-4005

Li, Y., Wang, L., Pappan, L., Galliher-Beckley, A., and Shi, J. (2012). IL-1β promotes stemness and invasiveness of colon cancer cells through Zeb1 activation. *Mol. Cancer* 11:87. doi: 10.1186/1476-4598-11-87

Liu, F., Liu, Y., and Chen, Z. (2018). Tim-3 expression and its role in hepatocellular carcinoma. *J. Hematol. Oncol.* 11:126. doi: 10.1186/s13045-018-0667-4

Liu, S., Zhang, C., Wang, B., Zhang, H., Qin, G., Li, C., et al. (2021). Regulatory T cells promote glioma cell stemness through TGF-beta-NF-kappaB-IL6-STAT3 signaling. *Cancer Immunol. Immunother.* doi: 10.1007/s00262-021-02872-0 [Epub ahead of print].

Liu, X., Kwon, H., Li, Z., and Fu, Y. X. (2017). Is CD47 an innate immune checkpoint for tumor evasion? *J. Hematol. Oncol.* 10:12. doi: 10.1186/s13045-016-0381-z

Lopez-Soto, A., Huergo-Zapico, L., Galvan, J. A., Rodrigo, L., de Herreros, A. G., Astudillo, A., et al. (2013). Epithelial-mesenchymal transition induces an antitumor immune response mediated by NKG2D receptor. *J. Immunol.* 190, 4408–4419. doi: 10.4049/jimmunol.1202950

Lu, H., Clauser, K. R., Tam, W. L., Frose, J., Ye, X., Eaton, E. N., et al. (2014). A breast cancer stem cell niche supported by juxtacrine signalling from monocytes and macrophages. *Nat. Cell Biol.* 16, 1105–1117. doi: 10.1038/ncb3041

Luo, H., Zeng, C., Fang, C., Seeruttun, S. R., Lv, L., and Wang, W. (2014). A new strategy using ALDHhigh-CD8+T cells to inhibit tumorigenesis. *PLoS One* 9:e103193. doi: 10.1371/journal.pone.0103193

Ma, Y., Shurin, G. V., Peiyuan, Z., and Shurin, M. R. (2013). Dendritic cells in the cancer microenvironment. *J. Cancer* 4, 36–44. doi: 10.7150/jca.5046

Ma, Z., and Ji, J. (2020). N6-methyladenosine (m6A) RNA modification in cancer stem cells. *Stem Cells* 38, 1511–1519. doi: 10.1002/stem.3279

Malaer, J. D., and Mathew, P. A. (2020). Role of LLT1 and PCNA as natural killer cell immune evasion strategies of HCT 116 cells. *Anticancer Res.* 40, 6613–6621. doi: 10.21873/anticanres.14686

Malfitano, A. M., Pisanti, S., Napolitano, F., Di Somma, S., Martinelli, R., and Portella, G. (2020). Tumor-associated macrophage status in cancer treatment. *Cancers (Basel)* 12:1987. doi: 10.3390/cancers12071987

Maniati, E., Soper, R., and Hagemann, T. (2010). Up for Mischief? IL-17/Th17 in the tumour microenvironment. *Oncogene* 29, 5653–5662. doi: 10.1038/onc.2010.367

Mansour, F. A., Al-Mazrou, A., Al-Mohanna, F., Al-Alwan, M., and Ghebeh, H. (2020). PD-L1 is overexpressed on breast cancer stem cells through notch3/mTOR axis. *Oncoimmunology* 9:1729299. doi: 10.1080/2162402X.2020.1729299

Marshall, E. A., Ng, K. W., Kung, S. H., Conway, E. M., Martinez, V. D., Halvorsen, E. C., et al. (2016). Emerging roles of T helper 17 and regulatory T cells in lung cancer progression and metastasis. *Mol. Cancer* 15:67. doi: 10.1186/s12943-016-0551-1

Miao, Y., Yang, H., Levorse, J., Yuan, S., Polak, L., Sribour, M., et al. (2019). Adaptive immune resistance emerges from tumor-initiating stem cells. *Cell* 177, 1172–1186.e4. doi: 10.1016/j.cell.2019.03.025

Mima, K., Okabe, H., Ishimoto, T., Hayashi, H., Nakagawa, S., Kuroki, H., et al. (2012). CD44s regulates the TGF-beta-mediated mesenchymal phenotype and is associated with poor prognosis in patients with hepatocellular carcinoma. *Cancer Res.* 72, 3414–3423. doi: 10.1158/0008-5472.CAN-12-0299

Mitchem, J. B., Brennan, D. J., Knolhoff, B. L., Belt, B. A., Zhu, Y., Sanford, D. E., et al. (2013). Targeting tumor-infiltrating macrophages decreases tumor-initiating cells, relieves immunosuppression, and improves chemotherapeutic responses. *Cancer Res.* 73, 1128–1141. doi: 10.1158/0008-5472.CAN-12-2731

Mou, W., Xu, Y., Ye, Y., Chen, S., Li, X., Gong, K., et al. (2015). Expression of Sox2 in breast cancer cells promotes the recruitment of M2 macrophages to tumor microenvironment. *Cancer Lett.* 358, 115–123. doi: 10.1016/j.canlet.2014.11.004

Nagaraj, S., and Gabrilovich, D. (2010). Myeloid-Derived Suppressor Cells in Human Cancer. *Cancer J.* 16, 348–353. doi: 10.1097/PPO.0b013e3181eb3358

Napoletano, C., Bellati, F., Ruscito, I., Pernice, M., Zizzari, I. G., Caponnetto, S., et al. (2016). Immunological and clinical impact of cancer stem cells in vulvar cancer: role of CD133/CD24/ABCG2-expressing cells. *Anticancer Res.* 36, 5109–5116. doi: 10.21873/anticanres.11080

Nnv, R., and Kundu, G. C. (2018). Role of tumour associated macrophages (TAMs) in regulation of cancer stem cell (CSCs) enrichment in breast cancer. *ESMO Open* 3, A1–A463. doi: 10.1136/esmoopen-2018-EACR25.316

Ostrand-Rosenberg, S. (2010). Myeloid-derived suppressor cells: more mechanisms for inhibiting antitumor immunity. *Cancer Immunol. Immunother.* 59, 1593–1600. doi: 10.1007/s00262-010-0855-8

Ouzounova, M., Lee, E., Piranlioglu, R., El Andaloussi, A., Kolhe, R., Demirci, M. F., et al. (2017). Monocytic and granulocytic myeloid derived suppressor cells differentially regulate spatiotemporal tumour plasticity during metastatic cascade. *Nat. Commun.* 8:14979. doi: 10.1038/ncomms14979

Paluskievicz, C. M., Cao, X., Abdi, R., Zheng, P., Liu, Y., and Bromberg, J. S. (2019). T regulatory cells and priming the suppressive tumor microenvironment. *Front. Immunol.* 10:2453. doi: 10.3389/fimmu.2019.02453

Pan, Q., Li, Q., Liu, S., Ning, N., Zhang, X., Xu, Y., et al. (2015). Concise review: targeting cancer stem cells using immunologic approaches. *Stem Cells* 33, 2085–2092. doi: 10.1002/stem.2039

Pang, Y. B., He, J., Cui, B. Y., Xu, S., Li, X. L., Wu, M. Y., et al. (2019). A potential antitumor effect of dendritic cells fused with cancer stem cells in hepatocellular carcinoma. *Stem Cells Int.* 2019:5680327. doi: 10.1155/2019/5680327

Panni, R. Z., Sanford, D. E., Belt, B. A., Mitchem, J. B., Worley, L. A., Goetz, B. D., et al. (2014). Tumor-induced STAT3 activation in monocytic myeloid-derived suppressor cells enhances stemness and mesenchymal properties in human pancreatic cancer. *Cancer Immunol. Immunother.* 63, 513–528. doi: 10.1007/s00262-014-1527-x

Papaccio, F., Paino, F., Regad, T., Papaccio, G., Desiderio, V., and Tirino, V. (2017). Concise review: cancer cells, cancer stem cells, and mesenchymal stem cells: influence in cancer development. *Stem Cells Transl. Med.* 6, 2115–2125. doi: 10.1002/sctm.17-0138

Pardee, A. D., Shi, J., and Butterfield, L. H. (2014). Tumor-derived alpha-fetoprotein impairs the differentiation and T cell stimulatory activity of human dendritic cells. *J. Immunol.* 193, 5723–5732. doi: 10.4049/jimmunol.1400725

Peng, D., Tanikawa, T., Li, W., Zhao, L., Vatan, L., Szeliga, W., et al. (2016). Myeloid-derived suppressor cells endow stem-like qualities to breast cancer cells through IL6/STAT3 and NO/NOTCH cross-talk signaling. *Cancer Res.* 76, 3156–3165. doi: 10.1158/0008-5472.CAN-15-2528

Pietra, G., Manzini, C., Vitale, M., Balsamo, M., Ognio, E., Boitano, M., et al. (2009). Natural killer cells kill human melanoma cells with characteristics of cancer stem cells. *Int. Immunol.* 21, 793–801. doi: 10.1093/intimm/dxp047

Pittari, G., Filippini, P., Gentilcore, G., Grivel, J. C., and Rutella, S. (2015). Revving up natural killer cells and cytokine-induced killer cells against hematological malignancies. *Front. Immunol.* 6:230. doi: 10.3389/fimmu.2015.00230

Raggi, C., Mousa, H. S., Correnti, M., Sica, A., and Invernizzi, P. (2016). Cancer stem cells and tumor-associated macrophages: a roadmap for multitargeting strategies. *Oncogene* 35, 671–682. doi: 10.1038/onc.2015.132

Ravindran, S., Rasool, S., and Maccalli, C. (2019). The cross talk between cancer stem cells/cancer initiating cells and tumor microenvironment: the missing piece of the puzzle for the efficient targeting of these cells with immunotherapy. *Cancer Microenviron.* 12, 133–148. doi: 10.1007/s12307-019-00233-1

Rezalotfi, A., Ahmadian, E., Aazami, H., Solgi, G., and Ebrahimi, M. (2019). Gastric cancer stem cells effect on Th17/Treg balance; A bench to beside perspective. *Front. Oncol.* 9:226. doi: 10.3389/fonc.2019.00226

Rinkenbaugh, A. L., and Baldwin, A. S. (2016). The NF-kappaB pathway and cancer stem cells. *Cells* 5:16. doi: 10.3390/cells5020016

Ruffini, P. A. (2019). The CXCL8-CXCR1/2 axis as a therapeutic target in breast cancer stem-like cells. *Front. Oncol.* 9:40. doi: 10.3389/fonc.2019.00040

Ruiz de Galarreta, M., Bresnahan, E., Molina-Sanchez, P., Lindblad, K. E., Maier, B., Sia, D., et al. (2019). beta-catenin activation promotes immune escape and resistance to Anti-PD-1 therapy in hepatocellular carcinoma. *Cancer Discov.* 9, 1124–1141. doi: 10.1158/2159-8290.CD-19-0074

Sainz, B. Jr., Carron, E., Vallespinos, M., and Machado, H. L. (2016). Cancer stem cells and macrophages: implications in tumor biology and therapeutic strategies. *Mediators Inflamm.* 2016:9012369. doi: 10.1155/2016/9012369

Sakaguchi, S., Miyara, M., Costantino, C., and Hafler, D. (2010). FOXP3+ regulatory T cells in the human immune system. *Nat. Rev. Immunol.* 10, 490–500. doi: 10.1038/nri2785

Schatton, T., Schutte, U., Frank, N. Y., Zhan, Q., Hoerning, A., Robles, S. C., et al. (2010). Modulation of T-cell activation by malignant melanoma initiating cells. *Cancer Res.* 70, 697–708. doi: 10.1158/0008-5472.CAN-09-1592

Schott, A. F., Goldstein, L. J., Cristofanilli, M., Ruffini, P. A., McCanna, S., Reuben, J. M., et al. (2017). Phase Ib pilot study to evaluate reparixin in combination with weekly paclitaxel in patients with HER-2-Negative metastatic breast cancer. *Clin. Cancer Res.* 23, 5358–5365. doi: 10.1158/1078-0432.CCR-16-2748

She, M., Niu, X., Chen, X., Li, J., Zhou, M., He, Y., et al. (2012). Resistance of leukemic stem-like cells in AML cell line KG1a to natural killer cell-mediated cytotoxicity. *Cancer Lett.* 318, 173–179. doi: 10.1016/j.canlet.2011.12.017

Shi, T., Ma, Y., Yu, L., Jiang, J., Shen, S., Hou, Y., et al. (2018). Cancer immunotherapy: a focus on the regulation of immune checkpoints. *Int. J. Mol. Sci.* 19:1389. doi: 10.3390/ijms19051389

Shibue, T., and Weinberg, R. A. (2017). EMT, CSCs, and drug resistance: the mechanistic link and clinical implications. *Nat. Rev. Clin. Oncol.* 14, 611–629. doi: 10.1038/nrclinonc.2017.44

Shipitsin, M., Campbell, L. L., Argani, P., Weremowicz, S., Bloushtain-Qimron, N., Yao, J., et al. (2007). Molecular definition of breast tumor heterogeneity. *Cancer Cell* 11, 259–273. doi: 10.1016/j.ccr.2007.01.013

Solis-Castillo, L. A., Garcia-Romo, G. S., Diaz-Rodriguez, A., Reyes-Hernandez, D., Tellez-Rivera, E., Rosales-Garcia, V. H., et al. (2020). Tumor-infiltrating regulatory T cells, CD8/Treg ratio, and cancer stem cells are correlated with lymph node metastasis in patients with early breast cancer. *Breast Cancer* 27, 837–849. doi: 10.1007/s12282-020-01079-y

Spranger, S., Dai, D., Horton, B., and Gajewski, T. F. (2017). Tumor-residing Batf3 dendritic cells are required for effector T cell trafficking and adoptive T cell therapy. *Cancer Cell* 31, 711–723.e4. doi: 10.1016/j.ccell.2017.04.003

Stein, R. G., Ebert, S., Schlahsa, L., Scholz, C. J., Braun, M., Hauck, P., et al. (2019). Cognate nonlytic interactions between CD8(+) T cells and breast cancer cells induce cancer stem cell-like properties. *Cancer Res.* 79, 1507–1519. doi: 10.1158/0008-5472.CAN-18-0387

Su, R., Dong, L., Li, Y., Gao, M., Han, L., Wunderlich, M., et al. (2020). Targeting FTO suppresses cancer stem cell maintenance and Immune evasion. *Cancer Cell* 38, 79–96.e11. doi: 10.1016/j.ccell.2020.04.017

Sultan, M., Coyle, K. M., Vidovic, D., Thomas, M. L., Gujar, S., and Marcato, P. (2017). Hide-and-seek: the interplay between cancer stem cells and the immune system. *Carcinogenesis* 38, 107–118. doi: 10.1093/carcin/bgw115

Szarynska, M., Olejniczak, A., Kobiela, J., Laski, D., Sledzinski, Z., and Kmiec, Z. (2018). Cancer stem cells as targets for DC-based immunotherapy of colorectal cancer. *Sci. Rep*. 8:12042. doi: 10.1038/s41598-018-30525-3

Tallerico, R., Garofalo, C., and Carbone, E. (2016). A new biological feature of natural killer cells: the recognition of solid tumor-derived cancer stem cells. *Front. Immunol.* 7:179. doi: 10.3389/fimmu.2016.00179

Tallerico, R., Todaro, M., Di Franco, S., Maccalli, C., Garofalo, C., Sottile, R., et al. (2013). Human NK cells selective targeting of colon cancer-initiating cells: a role for natural cytotoxicity receptors and MHC class I molecules. *J. Immunol.* 190, 2381–2390. doi: 10.4049/jimmunol.1201542

Taniguchi, H., Suzuki, Y., and Natori, Y. (2019). The evolving landscape of cancer stem cells and ways to overcome cancer heterogeneity. *Cancers (Basel)* 11:532. doi: 10.3390/cancers11040532

Todaro, M., Alea, M. P., Di Stefano, A. B., Cammareri, P., Vermeulen, L., Iovino, F., et al. (2007). Colon cancer stem cells dictate tumor growth and resist cell death by production of interleukin-4. *Cell Stem Cell* 1, 389–402. doi: 10.1016/j.stem.2007.08.001

Treps, L., Perret, R., Edmond, S., Ricard, D., and Gavard, J. (2017). Glioblastoma stem-like cells secrete the pro-angiogenic VEGF-A factor in extracellular vesicles. *J. Extracell. Vesicles* 6:1359479. doi: 10.1080/20013078.2017.1359479

Tseng, H. C., Arasteh, A., Paranjpe, A., Teruel, A., Yang, W., Behel, A., et al. (2010). Increased lysis of stem cells but not their differentiated cells by natural killer cells; de-differentiation or reprogramming activates NK cells. *PLoS One* 5:e11590. doi: 10.1371/journal.pone.0011590

Tsuchiya, H., and Shiota, G. (2021). Immune evasion by cancer stem cells. *Regen. Ther.* 17, 20–33. doi: 10.1016/j.reth.2021.02.006

Visvader, J. E., and Lindeman, G. J. (2008). Cancer stem cells in solid tumours: accumulating evidence and unresolved questions. *Nat. Rev. Cancer* 8, 755–768. doi: 10.1038/nrc2499

Walker, J. D., Sehgal, I., and Kousoulas, K. G. (2011). Oncolytic herpes simplex virus 1 encoding 15-prostaglandin dehydrogenase mitigates immune suppression and reduces ectopic primary and metastatic breast cancer in mice. *J. Virol.* 85, 7363–7371. doi: 10.1128/JVI.00098-11

Wan, S., Zhao, E., Kryczek, I., Vatan, L., Sadovskaya, A., Ludema, G., et al. (2014). Tumor-associated macrophages produce interleukin 6 and signal via STAT3 to promote expansion of human hepatocellular carcinoma stem cells. *Gastroenterology* 147, 1393–1404. doi: 10.1053/j.gastro.2014.08.039

Wang, B., Wang, Q., Wang, Z., Jiang, J., Yu, S. C., Ping, Y. F., et al. (2014). Metastatic consequences of immune escape from NK cell cytotoxicity by human breast cancer stem cells. *Cancer Res.* 74, 5746–5757. doi: 10.1158/0008-5472.CAN-13-2563

Wang, D., Fu, L., Sun, H., Guo, L., and DuBois, R. N. (2015). Prostaglandin E2 promotes colorectal cancer stem cell expansion and metastasis in mice. *Gastroenterology* 149, 1884–1895.e4. doi: 10.1053/j.gastro.2015.07.064

Wang, D., Xu, J., Liu, B., He, X., Zhou, L., Hu, X., et al. (2018a). IL6 blockade potentiates the anti-tumor effects of gamma-secretase inhibitors in Notch3-expressing breast cancer. *Cell Death Differ.* 25, 330–339. doi: 10.1038/cdd.2017.162

Wang, F., Lau, J. K. C., and Yu, J. (2021). The role of natural killer cell in gastrointestinal cancer: killer or helper. *Oncogene* 40, 717–730. doi: 10.1038/s41388-020-01561-z

Wang, L., Liu, Y., Zhou, Y., Wang, J., Tu, L., Sun, Z., et al. (2019). Zoledronic acid inhibits the growth of cancer stem cell derived from cervical cancer cell by attenuating their stemness phenotype and inducing apoptosis and cell cycle arrest through the Erk1/2 and Akt pathways. *J. Exp. Clin. Cancer Res.* 38:93. doi: 10.1186/s13046-019-1109-z

Wang, Y., Chen, M., Wu, Z., Tong, C., Dai, H., Guo, Y., et al. (2018b). CD133-directed CAR T cells for advanced metastasis malignancies: a phase I trial. *Oncoimmunology* 7:e1440169. doi: 10.1080/2162402X.2018.1440169

Wei, F., Zhang, T., Deng, S. C., Wei, J. C., Yang, P., Wang, Q., et al. (2019). PD-L1 promotes colorectal cancer stem cell expansion by activating HMGA1-dependent signaling pathways. *Cancer Lett.* 450, 1–13. doi: 10.1016/j.canlet.2019.02.022

Wei, J., Barr, J., Kong, L. Y., Wang, Y., Wu, A., Sharma, A. K., et al. (2010). Glioma-associated cancer-initiating cells induce immunosuppression. *Clin. Cancer Res.* 16, 461–473. doi: 10.1158/1078-0432.CCR-09-1983

Wei, J., Wu, A., Kong, L. Y., Wang, Y., Fuller, G., Fokt, I., et al. (2011). Hypoxia potentiates glioma-mediated immunosuppression. *PLoS One* 6:e16195. doi: 10.1371/journal.pone.0016195

Wei, L., Laurence, A., and O'Shea, J. J. (2008). New insights into the roles of Stat5a/b and Stat3 in T cell development and differentiation. *Semin. Cell Dev. Biol.* 19, 394–400. doi: 10.1016/j.semcdb.2008.07.011

Wei, X., Yang, S., Pu, X., He, S., Yang, Z., Sheng, X., et al. (2019). Tumor-associated macrophages increase the proportion of cancer stem cells in lymphoma by secreting pleiotrophin. *Am. J. Transl. Res.* 11, 6393–6402.

Welte, T., Kim, I. S., Tian, L., Gao, X., Wang, H., Li, J., et al. (2016). Oncogenic mTOR signalling recruits myeloid-derived suppressor cells to promote tumour initiation. *Nat. Cell Biol.* 18, 632–644. doi: 10.1038/ncb3355

Werno, C., Menrad, H., Weigert, A., Dehne, N., Goerdt, S., Schledzewski, K., et al. (2010). Knockout of HIF-1alpha in tumor-associated macrophages enhances M2 polarization and attenuates their pro-angiogenic responses. *Carcinogenesis* 31, 1863–1872. doi: 10.1093/carcin/bgq088

Xiang, T., Long, H., He, L., Han, X., Lin, K., Liang, Z., et al. (2015). Interleukin-17 produced by tumor microenvironment promotes self-renewal of CD133+ cancer stem-like cells in ovarian cancer. *Oncogene* 34, 165–176. doi: 10.1038/onc.2013.537

Xiao, P., Long, X., Zhang, L., Ye, Y., Guo, J., Liu, P., et al. (2018). Neurotensin/IL-8 pathway orchestrates local inflammatory response and tumor invasion by inducing M2 polarization of Tumor-associated macrophages and epithelial-mesenchymal transition of hepatocellular carcinoma cells. *Oncoimmunology* 7:e1440166. doi: 10.1080/2162402X.2018.1440166

Xu, M., Zhao, Z., Song, J., Lan, X., Lu, S., Chen, M., et al. (2017). Interactions between interleukin-6 and myeloid-derived suppressor cells drive the chemoresistant phenotype of hepatocellular cancer. *Exp. Cell Res.* 351, 142–149. doi: 10.1016/j.yexcr.2017.01.008

Yamashita, T., Ji, J., Budhu, A., Forgues, M., Yang, W., Wang, H. Y., et al. (2009). EpCAM-positive hepatocellular carcinoma cells are tumor-initiating cells with stem/progenitor cell features. *Gastroenterology* 136, 1012–1024. doi: 10.1053/j.gastro.2008.12.004

Yang, J., Liao, D., Chen, C., Liu, Y., Chuang, T. H., Xiang, R., et al. (2013). Tumor-associated macrophages regulate murine breast cancer stem cells through a novel paracrine EGFR/Stat3/Sox-2 signaling pathway. *Stem Cells* 31, 248–258. doi: 10.1002/stem.1281

Yang, L., Dong, Y., Li, Y., Wang, D., Liu, S., Wang, D., et al. (2019). IL-10 derived from M2 macrophage promotes cancer stemness via JAK1/STAT1/NF-kappaB/Notch1 pathway in non-small cell lung cancer. *Int. J. Cancer* 145, 1099–1110. doi: 10.1002/ijc.32151

Yang, S., Wang, B., Guan, C., Wu, B., Cai, C., Wang, M., et al. (2011). Foxp3+IL-17+ T cells promote development of cancer-initiating cells in colorectal cancer. *J. Leukoc. Biol.* 89, 85–91. doi: 10.1189/jlb.0910506

Yang, X., Wang, D., Lin, J., Yang, X., and Zhao, H. (2020). Atezolizumab plus bevacizumab for unresectable hepatocellular carcinoma. *Lancet Oncol.* 21:e412. doi: 10.1016/S1470-2045(20)30430-7

Yi, H., Cho, H. J., Cho, S. M., Jo, K., Park, J. A., Kim, N. H., et al. (2012). Blockade of interleukin-6 receptor suppresses the proliferation of H460 lung cancer stem cells. *Int. J. Oncol.* 41, 310–316. doi: 10.3892/ijo.2012.1447

Yi, L., Xiao, H., Xu, M., Ye, X., Hu, J., Li, F., et al. (2011). Glioma-initiating cells: a predominant role in microglia/macrophages tropism to glioma. *J. Neuroimmunol.* 232, 75–82. doi: 10.1016/j.jneuroim.2010.10.011

Yin, T., Wang, G., He, S., Liu, Q., Sun, J., and Wang, Y. (2016). Human cancer cells with stem cell-like phenotype exhibit enhanced sensitivity to the cytotoxicity of IL-2 and IL-15 activated natural killer cells. *Cell Immunol.* 300, 41–45. doi: 10.1016/j.cellimm.2015.11.009

Yu, X., Li, H., and Ren, X. (2012). Interaction between regulatory T cells and cancer stem cells. *Int. J. Cancer* 131, 1491–1498. doi: 10.1002/ijc.27634

Zhang, B. L., Li, D., Gong, Y. L., Huang, Y., Qin, D. Y., Jiang, L., et al. (2019). Preclinical evaluation of chimeric antigen receptor-modified T cells specific to epithelial cell adhesion molecule for treating colorectal cancer. *Hum. Gene. Ther.* 30, 402–412. doi: 10.1089/hum.2018.229

Zhang, C., Hu, Y., and Shi, C. (2020a). Targeting natural killer cells for tumor immunotherapy. *Front. Immunol.* 11:60. doi: 10.3389/fimmu.2020.00060

Zhang, C., Wang, H., Wang, X., Zhao, C., and Wang, H. (2020b). CD44, a marker of cancer stem cells, is positively correlated with PD-L1 expression and immune cells infiltration in lung adenocarcinoma. *Cancer Cell Int.* 20:583. doi: 10.1186/s12935-020-01671-4

Zheng, F., Dang, J., Zhang, H., Xu, F., Ba, D., Zhang, B., et al. (2018). Cancer stem cell vaccination with PD-L1 and CTLA-4 blockades enhances the eradication of melanoma stem cells in a mouse tumor model. *J. Immunother.* 41, 361–368. doi: 10.1097/CJI.0000000000000242

Zhong, M., Zhong, C., Cui, W., Wang, G., Zheng, G., Li, L., et al. (2019). Induction of tolerogenic dendritic cells by activated TGF-beta/Akt/Smad2 signaling in RIG-I-deficient stemness-high human liver cancer cells. *BMC Cancer* 19:439. doi: 10.1186/s12885-019-5670-9

Zhou, W., Ke, S. Q., Huang, Z., Flavahan, W., Fang, X., Paul, J., et al. (2015). Periostin secreted by glioblastoma stem cells recruits M2 tumour-associated macrophages and promotes malignant growth. *Nat. Cell. Biol.* 17, 170–182. doi: 10.1038/ncb3090

Zhu, X., Prasad, S., Gaedicke, S., Hettich, M., Firat, E., and Niedermann, G. (2015). Patient-derived glioblastoma stem cells are killed by CD133- specific CAR T cells but induce the T cell aging marker CD57. *Oncotarget* 6, 171–184. doi: 10.18632/oncotarget.2767

Conflict of Interest: The authors declare that the research was conducted in the absence of any commercial or financial relationships that could be construed as a potential conflict of interest.

frontiers in Cell and Developmental Biology

ORIGINAL RESEARCH
published: 26 July 2021
doi: 10.3389/fcell.2021.646644

Niche Laminin and IGF-1 Additively Coordinate the Maintenance of Oct-4 Through CD49f/IGF-1R-Hif-2α Feedforward Loop in Mouse Germline Stem Cells

Heng-Kien Au[1,2,3,4,5†], Syue-Wei Peng[6,7†], Chin-Lin Guo[8†], Chien-Chia Lin[6,7], Yi-Lin Wang[6,7], Yung-Che Kuo[1,6], Tsz-Yau Law[6,7], Hong-Nerng Ho[1,2,9], Thai-Yen Ling[10] and Yen-Hua Huang[1,4,5,6,7,11,12]**

[1] Taipei Medical University (TMU) Research Center of Cell Therapy and Regeneration Medicine, Taipei Medical University, Taipei, Taiwan, [2] Department of Obstetrics and Gynecology, School of Medicine, College of Medicine, Taipei Medical University, Taipei, Taiwan, [3] Department of Obstetrics and Gynecology, Taipei Medical University Hospital, Taipei, Taiwan, [4] Center for Reproductive Medicine, Taipei Medical University Hospital, Taipei Medical University, Taipei, Taiwan, [5] International Ph.D. Program for Cell Therapy and Regeneration Medicine, College of Medicine, Taipei Medical University, Taipei, Taiwan, [6] Department of Biochemistry and Molecular Cell Biology, School of Medicine, College of Medicine, Taipei Medical University, Taipei, Taiwan, [7] Graduate Institute of Medical Sciences, College of Medicine, Taipei Medical University, Taipei, Taiwan, [8] Institute of Physics, Academia Sinica, Taipei, Taiwan, [9] Department of Obstetrics and Gynecology, Taipei Municipal Wanfang Hospital, Taipei, Taiwan, [10] Department and Graduate Institute of Pharmacology, College of Medicine, National Taiwan University, Taipei, Taiwan, [11] Comprehensive Cancer Center of Taipei Medical University, Taipei, Taiwan, [12] The Ph.D. Program for Translational Medicine, College of Medical Science and Technology, Taipei Medical University, Taipei, Taiwan

OPEN ACCESS

Edited by:
Francesca Diomede,
University of Studies G. d'Annunzio Chieti and Pescara, Italy

Reviewed by:
Lin Liu,
Nankai University, China
Briony Forbes,
Flinders University, Australia

***Correspondence:**
Thai-Yen Ling
tyling@ntu.edu.tw
Yen-Hua Huang
rita1204@tmu.edu.tw

[†] These authors have contributed equally to this work

Specialty section:
This article was submitted to Stem Cell Research, a section of the journal Frontiers in Cell and Developmental Biology

Received: 27 December 2020
Accepted: 03 June 2021
Published: 26 July 2021

Citation:
Au H-K, Peng S-W, Guo C-L, Lin C-C, Wang Y-L, Kuo Y-C, Law T-Y, Ho H-N, Ling T-Y and Huang Y-H (2021) Niche Laminin and IGF-1 Additively Coordinate the Maintenance of Oct-4 Through CD49f/IGF-1R-Hif-2α Feedforward Loop in Mouse Germline Stem Cells. Front. Cell Dev. Biol. 9:646644. doi: 10.3389/fcell.2021.646644

The mechanism on how extracellular matrix (ECM) cooperates with niche growth factors and oxygen tension to regulate the self-renewal of embryonic germline stem cells (GSCs) still remains unclear. Lacking of an appropriate *in vitro* cell model dramatically hinders the progress. Herein, using a serum-free culture system, we demonstrated that ECM laminin cooperated with hypoxia and insulin-like growth factor 1 receptor (IGF-1R) to additively maintain AP activity and Oct-4 expression of AP^{+}GSCs. We found the laminin receptor CD49f expression in d2 testicular GSCs that were surrounded by laminin. Laminin and hypoxia significantly increased the GSC stemness-related genes, including Hif-2α, Oct-4, IGF-1R, and CD49f. Cotreatment of IGF-1 and laminin additively increased the expression of IGF-IR, CD49f, Hif-2α, and Oct-4. Conversely, silencing IGF-1R and/or CD49f decreased the expression of Hif-2α and Oct-4. The underlying mechanism involved CD49f/IGF1R-(PI3K/AKT)-Hif-2α signaling loop, which in turn maintains Oct-4 expression, symmetric self-renewal, and cell migration. These findings reveal the additive niche laminin/IGF-IR network during early GSC development.

Keywords: germline stem cell, niche, extracellular matrix, hypoxia, laminin, IGF, self-renewal

Abbreviations: AP, alkaline phosphatase; GSCs, germline stem cells; Hif-2α, hypoxia-inducible factor 2 alpha; IGF-1, insulin-like growth factor 1; IGF-1R, insulin-like growth factor 1 receptor; PI3K, phosphatidylinositol 3-kinase; PGC, primordial germ cell.

INTRODUCTION

Germline stem cells (GSCs), including primordial germ cells (PGCs), postmigratory PGCs, and spermatogonial stem cells, are cells involving gamete production. During the embryogenesis, germ cells begin with early PGC specification through the expression of transcription factors, such as Fragilis, Stella, and Blimp1 to regulate PGC emergence (Saitou et al., 2002; Ohinata et al., 2005), and then followed by external BMP4 signaling that enables PGC competence (Lawson et al., 1999; Ying et al., 2000, 2001). In response to surrounding niche factors, competent PGCs can then either maintain self-renewal or migrate into the genital ridge, where they become mature germ cells. The robustness of these cellular behaviors requires the synergistic coordination of responses to niche factors, and defects in the self-renewal or maintenance of stemness during early germ cell development cause insufficient germ cell production in embryonic gonads, which can lead to infertility or formation of extragonadal germ cell tumors (Hoei-Hansen et al., 2006). Currently, the understanding of signaling and networking interactions among niche factors is still limited.

Niche factors have been referred to as secreted growth factors, cytokines, and morphogens. Recently, other factors, including oxygen level and extracellular matrix (ECM) composition, have been considered critical for maintaining the stemness of germ cells (Ginsburg et al., 1990; Lawson et al., 1999; Ying et al., 2000; Saitou et al., 2002; Ohinata et al., 2005). For example, a physiological hypoxic environment (with 1–5% O_2), which stabilizes hypoxia-inducible factor (HIF) by preventing its degradation (Ginouves et al., 2008), was reported to play a crucial role in embryogenesis and early germ cell survival (Scortegagna et al., 2005; Covello et al., 2006). Increasing Hif-2α expression by generating Hif-2α knockin mice was reported to enhance expression of the pluripotent transcription factor Oct-4 through direct promoter binding, whereas the loss of Hif-2α results in a severe deficiency of embryonic PGCs in the genital ridge (Covello et al., 2006) and subsequent azoospermia (Scortegagna et al., 2005).

In parallel, evidence has recently identified the association between ECM components and the regulation of stem cell fate (Mercier, 2016), where the signaling of ECM often acts through the cell surface receptor integrin, which is composed of various α and β subtypes specific to ECM components (Ying et al., 2001). Laminin is the major ECM component involved in stem cell self-renewal, migration, adhesion, and differentiation (Covello et al., 2006). It binds primarily to the heterodimeric integrins α3β1, α6β1, and α6β4 (Lawson et al., 1999). *In vitro* assay has shown that laminin maintains Oct-4/Sox2 expression and cell proliferation in embryonic stem cells (Ying et al., 2000; Ohinata et al., 2005). Overexpression of integrin α6, one of the integrin subunit specific to laminin, was found to enhance the proliferation, differentiation, and Oct-4/Sox2 expression in human mesenchymal stem cells *via* the PI3K/Akt/p53 pathway (Scortegagna et al., 2005).

Hypoxic response and ECM signaling might act along or coordinate with growth factor–mediated signaling to determine the fate of stem cells (Francis and Wei, 2010). Decoupling of the effects of these factors *in vivo* is unlikely because a single genetic deletion often causes embryonic fatality. Moreover, the use of conventional *in vitro* stem cell cultures is not possible because most of cell cultures use a serum-containing medium, which does not permit a distinction to be made between the effects of hypoxia and ECM and those mediated by growth factor signaling. To overcome this limitation, we previously developed a serum-free culture system to generate pluripotent GSCs by using wild-type neonatal mouse testes (Huang et al., 2009). These pluripotent GSCs, referred to as $CD49f^+AP^+$GSCs, display early germ cell characteristics, including high alkaline phosphatase (AP) activity, an abundance of cell surface proteins, such as the stage-specific embryonic antigen (SSEA)-1 and the laminin receptor integrin α6 (also referred to as CD49f), an ability to express PGC-related genes (e.g., *Oct-4*, *Nanog*, and *Blimp1*), and the capability to migrate and differentiate into multiple cell types *in vitro* as well as to form chimeras/teratomas *in vivo* (Huang et al., 2009). Using the $CD49f^+AP^+$GSCs as an *in vivo* model system, we demonstrated that the niche hypoxia-induced growth factor signaling, Hif-2α-IGF-1R, can maintain the expression of Oct-4 and the capacity of self-renewal in embryonic GSCs (Huang et al., 2009, 2014). However, whether laminin also plays a crucial role in maintaining GSC stemness and survival, and whether crosstalk occurs between laminin signaling and the signaling from other niche factors, such as hypoxia and growth factor IGF-1, remain unclear.

In the present study, we used the serum-free culture system to demonstrate the occurrence of additive crosstalk among the three niche factors that converges into a CD49f/IGF1R-(PI3K/Akt)-Hif-2α signaling loop, to maintain Oct-4 expression and increase cell migration in $CD49f^+AP^+$GSCs. These findings improve our understanding of the regulatory capacity of niche ECM and endocrinal signaling in the proliferation and maintenance of stemness in early embryonic GSCs, and may facilitate the development of potential strategies for engineering stem cell–based cell therapy in regenerative medicine.

RESULTS

Laminin Increases the Activity of AP and the Expression of Stemness-Related Genes in Mouse AP^+GSCs Under IGF-1 Free and Serum-Free Culture Conditions

Neonatal mouse testis (where GSCs reside) harvested on day 2 exhibited positive signals of stemness and hypoxia responses, as manifested in the immunohistochemical staining of Oct-4 and Hif-2α (**Figure 1A**). The abilities of self-renewal and differentiation of stem cells have been suggested to be associated with the presence of niche ECM factors, such as laminin (Covello et al., 2006). Consistently, we observed 7positive signals of immunostained CD49f in testicular GSCs harvested on day 2, which were surrounded by positive signals of laminin (**Figure 1B**). The effects of laminin on GSC stemness and hypoxia responses were confirmed by cultivating harvested AP^+GSCs on laminin-coated or non-coated substrates in serum-free medium

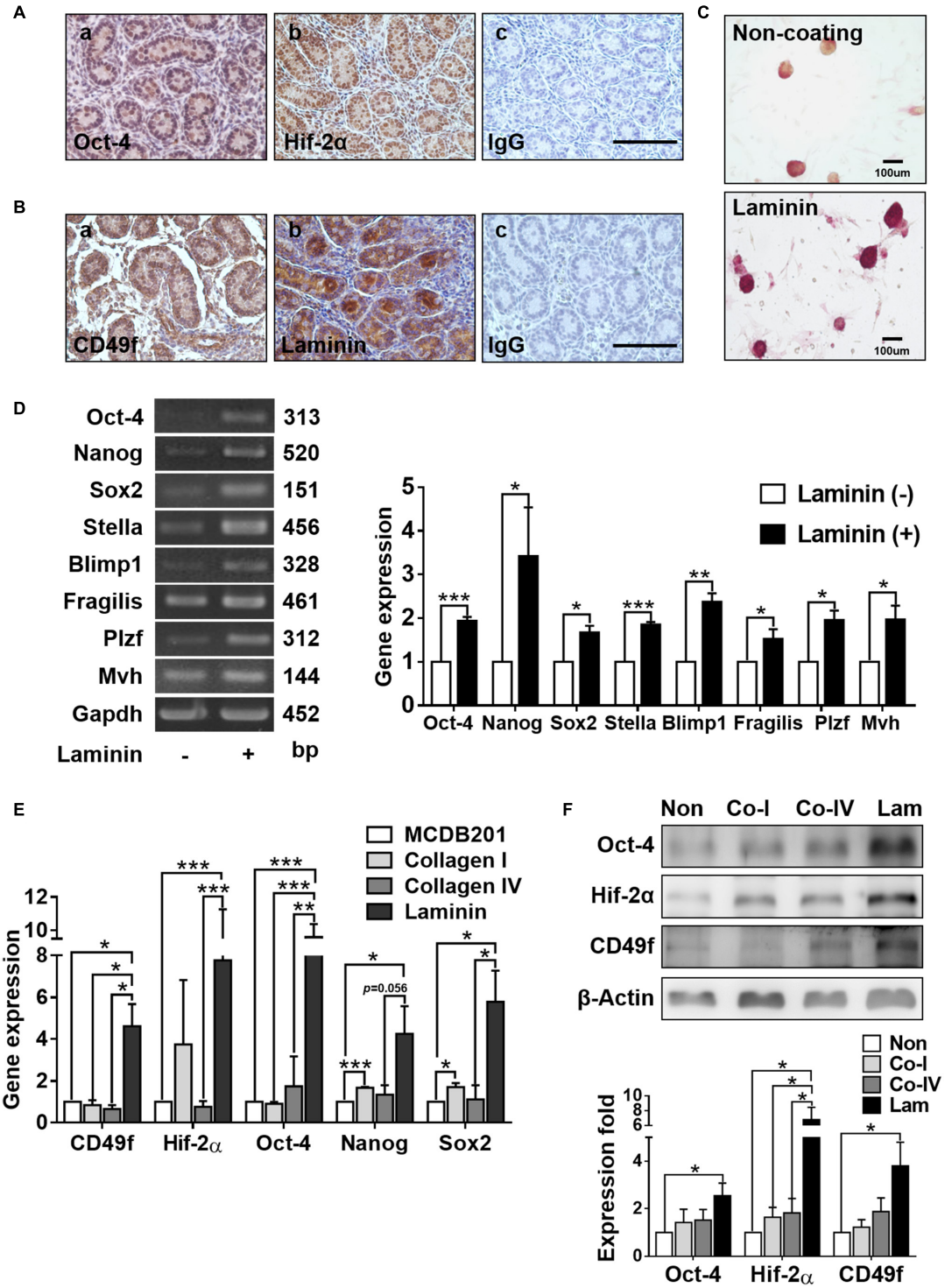

FIGURE 1 | Laminin increases alkaline phosphatase (AP) activity and stemness-related gene expression in mouse germline stem cells (GSCs) (AP^+GSCs). **(A,B)** Protein expression and localization of Oct-4 **(A-a)**, Hif-2α **(A-b)**, CD49f **(B-a)**, and laminin **(B-b)** in cells obtained from testes of 2 days postpartum mice. **(A-c,B-c)** Control. Bar = 100 μm. **(C)** Stained alkaline phosphatase (AP) activity in GSC colonies cultivated on laminin-coated or non-coated culture plates. Bar = 100 μm. **(D)** Gene expression in GSC colonies cultivated on laminin-coated or non-coated culture plates through reverse transcription polymerase chain reaction (RT-PCR) (left panel) and RT-qPCR (right panel) analyses. **(E)** Gene expression in magnetic-activated cell-sorting system (MACS)-purified $CD49f^+AP^+$GSCs cultivated on culture plates coated with different ECM components determined through RT-PCR analysis. **(F)** Protein expression in MACS-purified $CD49f^+AP^+$GSCs cultivated on culture plates coated with different ECM components through Western blot analysis. Lam: laminin. Co-I: type I collagen. Co-IV: type IV collagen. Statistical data are means ± SEM of at least three independent experiments for each condition. $^*p < 0.05$; $^{**}p < 0.01$; $^{***}p < 0.001$ (Student's *t*-test).

(Huang et al., 2014; Kuo et al., 2018). Compared with colony formation of AP^+GSCs in the absence of laminin, AP^+GSCs cultivated in the presence of laminin showed obviously a higher AP activity, more cell proliferation (**Figure 1C**), and significantly higher expressions of stemness-related genes, such as *Oct-4*, *Nanog*, *Sox2*, *Stella*, *Blimp1*, *Fragilis*, *Plzf*, and *Mvh* (**Figure 1D**).

To further identify the effect of laminin/CD49f signaling on GSC stemness and hypoxia responses, $CD49f^+AP^+$GSCs were isolated using the magnetic-activated cell sorting (MACS, Miltenyi Biotec), where the laminin receptor integrin α6, also known as CD49f, a cell surface marker of AP^+GSCs was used (Mercier, 2016). The cells were then cultured on substrates coated with various ECM components in serum-free medium. Previously, we found that these MACS-purified $CD49f^+$GSCs exhibited high AP activity and expressed pluripotency-related genes, such as *Oct-4*, *Nanog*, *Sox2*, and *Blimp1* (Huang et al., 2014). To mimic the physiological condition, type I collagen, which is enriched in the stroma, and type IV collagen and laminin, the two components enriched in the basement membrane surrounding GSCs *in vivo*, were used as coating materials. Compared with types I and IV collagen, laminin-coated substrates significantly enhanced the expression of CD49f and stemness/hypoxia-related genes at the mRNA (**Figure 1E**, *Oct-4*, *Nanog*, *Sox2*, and *Hif-2α*) or protein levels (**Figure 1F**, CD49f, Oct-4, and Hif-2α, the repeated data (n = 3) were provided in **Supplementary Figure 4**).

IGF-1 Increases the Expression of CD49f Involving IGF-1R-PI3K/Akt-mTOR/Hif-2α Signaling in $CD49f^+AP^+$GSCs

Previously, we showed that niche endocrinal IGF-1 signaling enhanced GSC stemness by upregulating the expression of Hif-2α, which in turn promoted not only Oct-4 expression through direct promoter binding (Huang et al., 2014; Kuo et al., 2018) but also IGF-1 and IGF-1R expression, which led to a self-perpetuating effect on IGF-1 signaling. We also found that the niche hypoxia can activate IGF-1R signaling and enable migration of AP^+GSCs through a Hif-2α-OCT-4/CXCR4 signaling loop (Huang et al., 2014; Kuo et al., 2018). Hypoxia, endocrinal IGF-1, and ECM laminin are all crucial niche factors for GSC self-renewal and development. Furthermore, both IGF-1 and laminin signaling utilizes the PI3K/Akt pathway (Nguyen et al., 2000; Akeno et al., 2002; Huang et al., 2009, 2014; Yu et al., 2012; Yazlovitskaya et al., 2019). Hence, we could hypothesize that crosstalk exists among signals from these factors.

To ascertain the possibility of crosstalk, we first examined whether hypoxia or IGF-1 signaling caused an amplification effect on laminin signaling by upregulating the expression of laminin receptor CD49f. We found that hypoxic culture conditions increased the expression of not only Hif-2α but also IGF-1R and CD49f in $CD49f^+AP^+$GSCs in the absence of IGF-1 and laminin (**Supplementary Figure 1**). We also found that in the absence of laminin, IGF-1 increased the expression of CD49f, along with IGF-1R, Hif-2α, and Oct-4, in $CD49f^+AP^+$GSCs in a dose-dependent manner; however, no such effect was observed when the cells were treated with epidermal growth factor (EGF) or transforming growth factor beta (TGF-β) (**Figure 2A**, the original data are provided in **Supplementary Figure 5**). The specificity of the involvement of IGF-1/IGF-1R signaling in the upregulation of CD49f expression was confirmed by genetic and pharmaceutical manipulation. First, two silencing RNA interference constructs that target endogenous IGF-1R (shIGF-1R) with different knockdown efficiencies were selected for IGF-1R knockdown experiments in $CD49f^+AP^+$GSCs (shIGF-1R#1 and shIGF-1R#2) (**Supplementary Figure 2**). We found that shIGF-1R#2 effectively suppressed not only the expression of IGF-1R but also the IGF-1-induced expression of CD49f, Oct-4, and Hif-2α in $CD49f^+AP^+$GSCs in the absence of laminin (**Figure 2B**, the repeated data (n = 3) are provided in **Supplementary Figure 6**). Second, pharmaceutical inhibitors that suppress IGF-1R/PI3K-Akt/mTOR signaling downstream to IGF-1 stimulation, such as cyclolignan picropodophyllin (PPP, a phospho-IGF-1R inhibitor), LY294002 (PI3K/Akt inhibitor), and rapamycin (mTOR inhibitor), were applied to IGF-1-treated $CD49f^+AP^+$GSCs in the absence of laminin. The aforementioned inhibitors also efficiently suppressed IGF-1-induced expression of CD49f, Oct-4, and Hif-2α in $CD49f^+AP^+$GSCs (**Figure 2C**, the repeated data (n = 3) are provided in **Supplementary Figure 7**).

Our previous study showed that IGF-1-mediated upregulation of IGF-1, IGF-1R, Oct-4, and Hif-2α all depended on the expression of Hif-2α (Huang et al., 2014; Kuo et al., 2018). To ascertain whether this was also applicable to IGF-1-induced CD49f upregulation, we performed genetic perturbation on Hif-2α expression. We used two RNA interference constructs that target endogenous Hif-2α (shHif-2α) with different knockdown efficiencies (#2 and #3). We found that knockdown of Hif-2α (particularly by shHif-2α #3) effectively suppressed not only the expression of Hif-2α but also the IGF-1-induced expression of Oct-4, IGF-1R, and CD49f (**Figure 2D**, the repeated data (n = 3) are provided in **Supplementary Figure 8**). These results suggest the crosstalk among laminin, hypoxia, and IGF-1 signaling and that PI3K/Akt-mTOR-Hif-2α signaling is involved in the IGF-1-mediated upregulation of CD49f expression in $CD49f^+AP^+$GSCs.

IGF-1 and Laminin Additively Increase the Expression of IGF-1R, CD49f, Hif-2α, and Oct-4 in $CD49f^+AP^+$GSCs

Robust control in GSC self-renewal and differentiation requires synergistic coordination in the responses to niche factors. Having shown that IGF-1 upregulated the expression of laminin receptor CD49f, we examined whether exposure to laminin reciprocally affected IGF-1 signaling. IGF-1 and laminin signaling have both been reported to activate the PI3K/Akt pathway (Nguyen et al., 2000; Akeno et al., 2002; Huang et al., 2009, 2014; Yu et al., 2012; Yazlovitskaya et al., 2019), indicating a potential synergy in their signaling. To examine this possibility, $CD49^+AP^+$GSCs were cultivated in serum-free culture medium in the presence or absence of laminin and with or without IGF-1 in the medium. **Figure 3A** shows that in the absence of IGF-1, laminin enhanced the expression

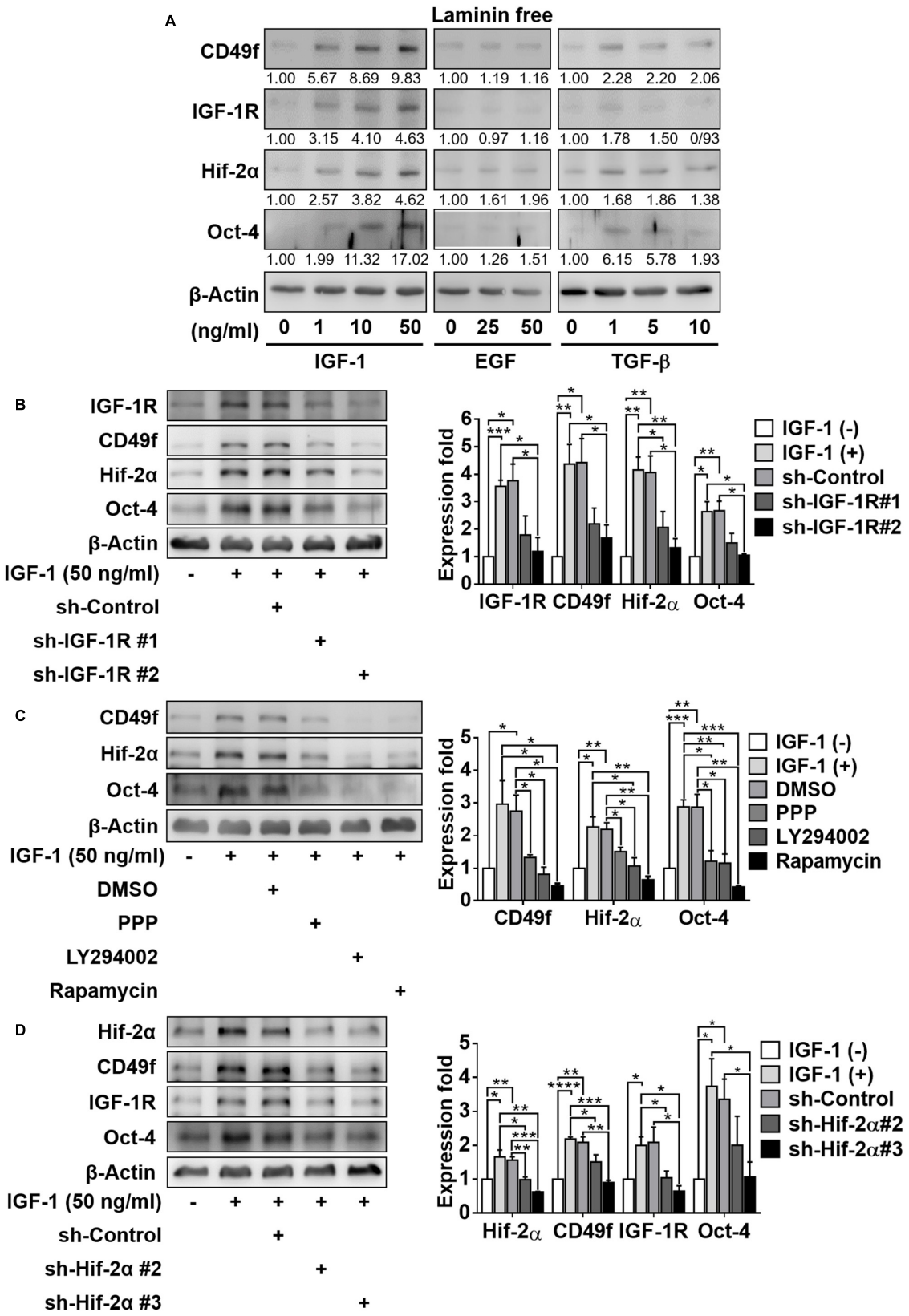

FIGURE 2 | Continued

FIGURE 2 | IGF-1 enhances the expression of CD49f, IGF1-R, and Oct-4 involving an IGF1R-PI3K/Akt-mTOR-Hif-2α signaling pathway in CD49f$^+$AP$^+$GSCs. **(A)** Effect of IGF-1 (0, 1, 10, and 50 ng/ml), EGF (0, 25, and 50 ng/ml), and TGF-β (0, 1, 5, and 10 ng/ml) on expression of CD49f, IGF-1R, Hif-2α, and Oct-4 in CD49f$^+$AP$^+$GSCs. The relative quantification was normalized to the corresponding β-Actin. **(B)** Protein expression of CD49f, Hif-2α, and Oct-4 in CD49f$^+$AP$^+$GSCs under IGF-1 treatment (50 ng/ml) with scramble shRNA or shIGF-1R in the absence of laminin. The knockdown efficiencies are given in **Supplementary Figure 2**. **(C)** Protein expression of CD49f, Hif-2α, and Oct-4 in CD49f$^+$AP$^+$GSCs under IGF-1 treatment (50 ng/ml) with or without PPP (1 μM), LY294002 (10 μM), or rapamycin (50 nM) in the absence of laminin. **(D)** Effect of shHif-2α on the expression of CD49f, IGF-1R, and Oct-4 in IGF-1-treated CD49f$^+$AP$^+$GSCs in the absence of laminin. Data are means ± SEM of at least three independent experiments. $^*p < 0.05$; $^{**}p < 0.01$; $^{***}p < 0.001$; $^{****}p < 0.0001$ (Student's *t*-test).

of not only CD49f but also that of IGF-1R, Oct-4, and Hif-2α in a dose-dependent manner and the repeated data (n = 3) are provided in **Supplementary Figure 9**. An additive enhancement of the expression of IGF-1R, CDC49f, Hif-2α, and Oct-4 in CD49f$^+$AP$^+$GSCs was observed when cells were cotreated with laminin (500 ng/cm^2) and IGF-1 (50 ng/ml). Cotreatment resulted in higher expression than did treating the cells with each of the factors alone, despite that the enhancement was weaker in Hif-2α and Oct-4 expressions (**Figures 3B,C**, the repeated data (n = 3) are provided in **Supplementary Figure 10**). In addition, the IGF-1-induced upregulation of Akt/mTOR activity and Oct-4/Hif-2α expression appeared in a dose-dependent manner in the presence of laminin (**Figure 3D**, the original data and repeated data are provided in **Supplementary Figure 11**). Likewise, the laminin-induced upregulation of expressions of IGF-1R, Oct-4, and Hif-2α exhibited a dose-dependent response to IGF-1 (**Figure 3E**, the original data were provided in **Supplementary Figure 12**). These data suggest that the effects of IGF-1 and laminin on the upregulation of IGF-1R, CD49f, Hif-2α, and Oct-4 expression are additive.

Both IGF-1R and CD49f Are Required for IGF-1/Laminin-Mediated Additive Upregulation of CD49f, IGF-1R, Oct-4, and Hif-2α Expression in CD49f$^+$AP$^+$GSCs

To confirm the specificity of the involvement of CD49f/IGF-1R in the laminin/IGF-1-mediated effect, constructs of silencing RNA interference that target endogenous CD49f (shCD49f) or IGF-1Rβ (shIGF-1R) were engineered and applied to CD49f$^+$AP$^+$GSCs cotreated with laminin (500°ng/cm^2) and IGF-1 (50°ng/ml). Five constructs for each target were engineered. Among them, we selected those with the highest knockdown efficiencies, shCD49f#5 for CD49f and shIGF-1R#2 for IGF-1Rβ (**Figure 4A**, the repeated data (n = 3) are provided in **Supplementary Figure 13**). Cotreatment with laminin and IGF-1 significantly increased the expression of CD49f, IGF-1R, Oct-4, and Hif-2α in CD49f$^+$AP$^+$GSCs compared with that in cells treated with laminin alone (**Figure 4B**, lane 2 vs. lane 1, and **Figure 4C**, bar 2 vs. bar 1); however, the addition of shCD49f#5 or shIGF-1R#2 effectively suppressed the effect of cotreatment on Hif-2α, Oct-4, CD49f, and IGF-1R expression (**Figure 4B**, lane 4–6 vs. lane 3, and **Figure 4C**, bar 4–6 vs. bar 3). **Figure 4D** shows the corresponding confocal images of Oct-4 and CD49f stained through immunocytochemistry. Given the activation of the PI3K-Akt pathway in laminin and IGF-1 signaling (Nguyen et al., 2000; Akeno et al., 2002; Huang et al., 2009, 2014; Yu et al., 2012; Yazlovitskaya et al., 2019) and the dependence of IGF-1 signaling on Hif-2α expression (Huang et al., 2014; Kuo et al., 2018), the results suggest the presence of additive crosstalk in IGF-1/laminin signaling that acts through a CD49f/IGF1R-(PI3K/Akt)-Hif-2α signaling loop, which in turn regulates the maintenance of Oct-4 expression of mouse CD49f$^+$AP$^+$GSCs.

Laminin Induces Cell Morphological Changes and Genetic Reprogramming

The development of germ cells begins with the specification of PGCs marked by the expression of transcription factors, such as Fragilis, Stella, and Blimp1 (Saitou et al., 2002; Ohinata et al., 2005), following which the cells acquire the ability to signal to external BMP4. BMP4 enables PGC competence (Lawson et al., 1999; Ying et al., 2000, 2001); this is the ability to facilitate niche development by secreting the basement membrane and paracrine components as well as the ability to migrate into the genital ridge where PGCs become mature germ cells. In the present work, we showed that laminin induced the upregulation of *Fragilis*, *Stella*, and *Blimp1* in CD49f$^+$AP$^+$GSCs (**Figure 1D**), as well as the upregulation of CD49f and IGF1-R (**Figure 3A**). To determine whether exposure to laminin enhanced the ability of CD49f$^+$AP$^+$GSCs to signal to BMP4, to participate in niche development, or to migrate, we performed RNA sequencing on CD49f$^+$AP$^+$GSCs cultivated in the presence or absence of laminin (500°ng/cm^2) in serum-free culture medium. Although our serum-free CD49f$^+$AP$^+$GSC model system served as a convenient platform to study the interplay of niche factor–mediated signaling *in vitro*, long-term cultivation on tissue-culture plates can problematically cause significant distortion of genotype and phenotype. Thus, we harvested the cells for RNA sequencing after 3 days of cultivation. The data were analyzed using fold change (i.e., $\log_2$) between the laminin-treated and untreated samples (**Figure 5A**). The results showed that exposure to laminin induced the maintenance of stemness, hypoxia response, and PI3K/Akt/mTOR signaling to some degree (**Figure 5A**, red, blue, and cyan, respectively). In addition, laminin increased the expression of receptor subunits for BMP4 signaling (**Figure 5A**, gray), the secretion of cytokines and basement membrane components (**Figure 5A**, green and pink), and the expression of molecules involved in cell migration (**Figure 5A**, orange). Upregulation of these genes were confirmed by RT-qPCR analysis (**Figure 5B**).

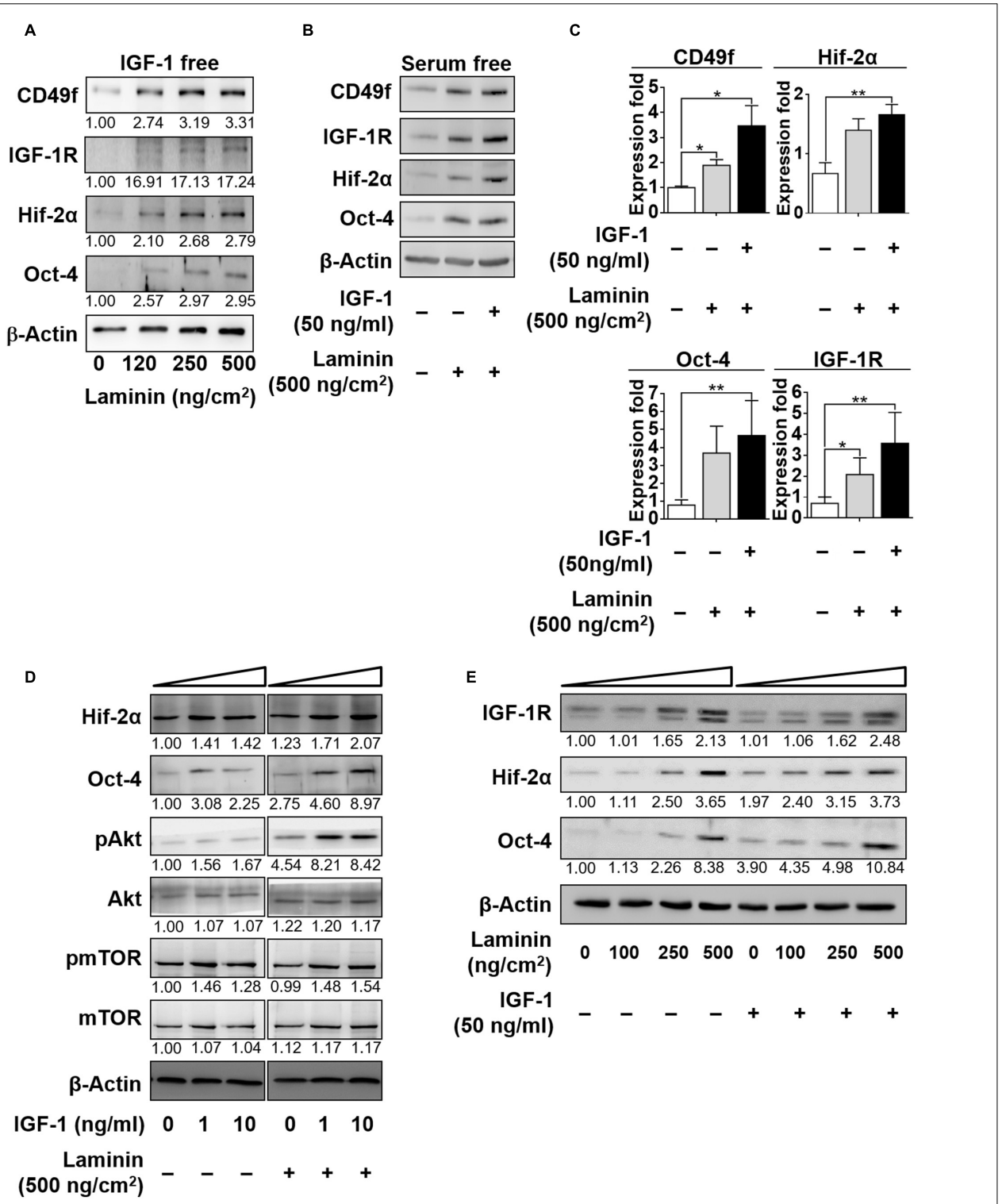

FIGURE 3 | IGF-1 and laminin act additively to increase the expression of CD49f, IGF-1R, Hif-2α, and Oct-4 in CD49f^{+}AP^{+}GSCs. **(A)** Dose-dependent effects of laminin (0, 120, 250, and 500 ng/cm^2) on the protein expression of CD49f, IGF-1R, Hif-2α and Oct-4 in CD49f^{+}AP^{+}GSCs in the absence of IGF-1. **(B)** Effects of laminin (500 ng/cm^2) with or without IGF-1 (50 ng/ml) treatment on the expressions of IGF-1R, CD49f, Hif-2α, and Oct-4. **(C)** Quantitative and statistical analysis of the effects on **(B)**. Data are means ± SEM of at least three independent experiments. *$p < 0.05$; **$p < 0.01$ (one-way ANOVA). **(D)** Dose-dependent effects of IGF-1 (0, 1, and 10 ng/ml) with or without laminin (500 ng/cm^2) treatment on the protein expression of Hif-2α, Oct-4, and on the Akt-mTOR signaling. **(E)** Dose-dependent effects of laminin (0, 100, 250, and 500 ng/cm^2) with or without IGF-1 (50 ng/ml) treatment on the expression of IGF-1R, Hif-2α, and Oct-4. The relative quantification was normalized to the corresponding β-actin.

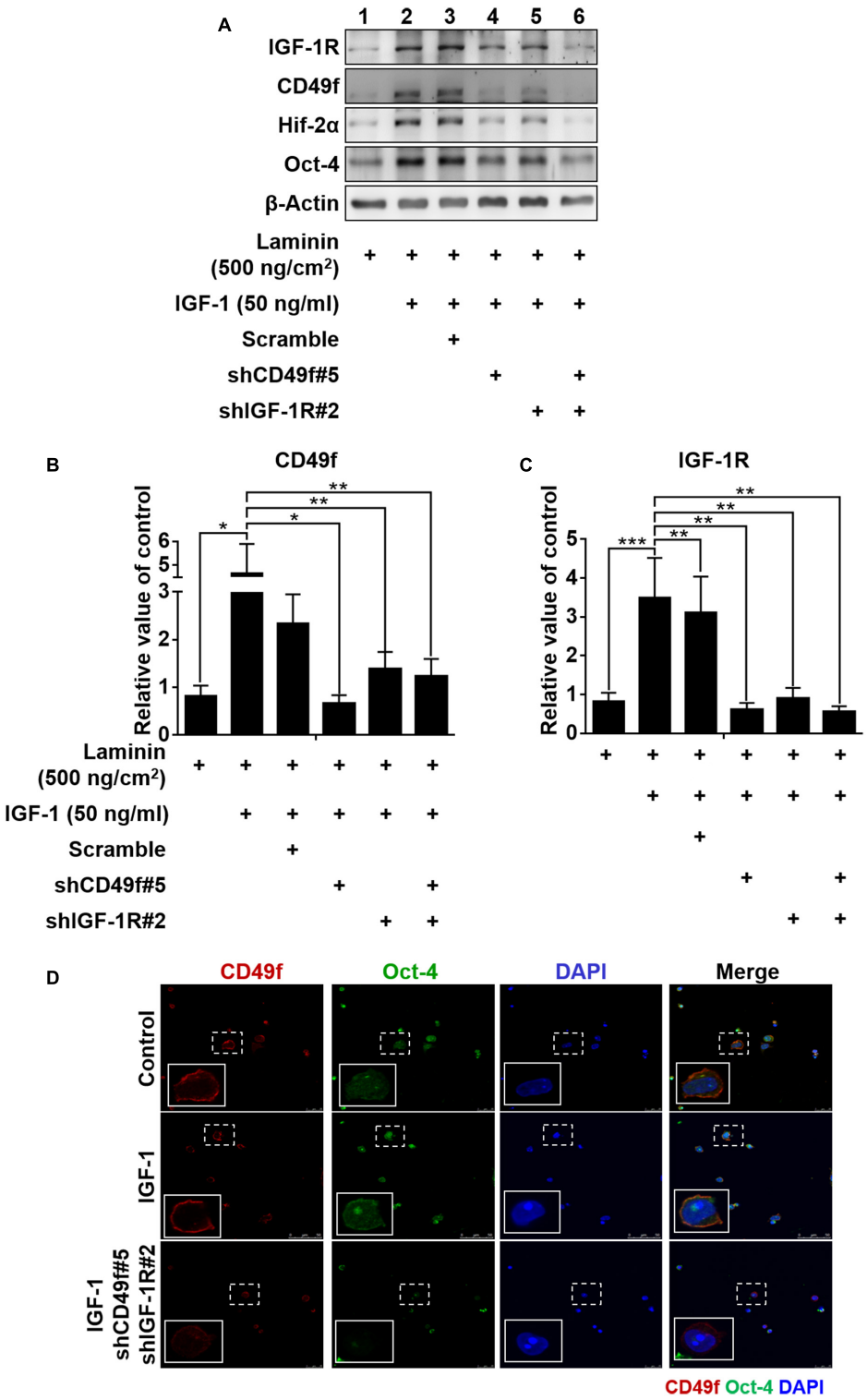

FIGURE 4 | Both IGF-1R and CD49f are required for IGF-1/laminin-mediated additive upregulation of CD49f, IGF-1R, Hif-2α, and Oct-4 expression in CD49f^{+}AP^{+}GSCs. **(A)** Suppression effects of shCD49f and/or shIGF-1R on the expression of Hif-2α, Oct-4, CD49f, and IGF-1R in CD49f^{+}AP^{+}GSCs treated with IGF-1 (50 ng/ml) on laminin-coated substrates (500 ng/cm^{2}). **(B,C)** The quantitative and statistical analyses of shCD49f- and/or shIGF-1R-mediated suppressing effects on the expression of **(B)** CD49f and **(C)** IGF-1R from **(A)**. Data are means ± SEM of at least three independent experiments. *$p < 0.05$; **$p < 0.01$, ***$p < 0.001$ (one-way ANOVA). **(D)** The suppressing effect of shCD49f and shIGF-1R on cellular localization of immunocytochemistry stained Hif-2α and Oct-4 in CD49f^{+}AP^{+}GSCs treated with IGF-1 (50 ng/ml) on laminin-coated culture plates (500 ng/cm^{2}).

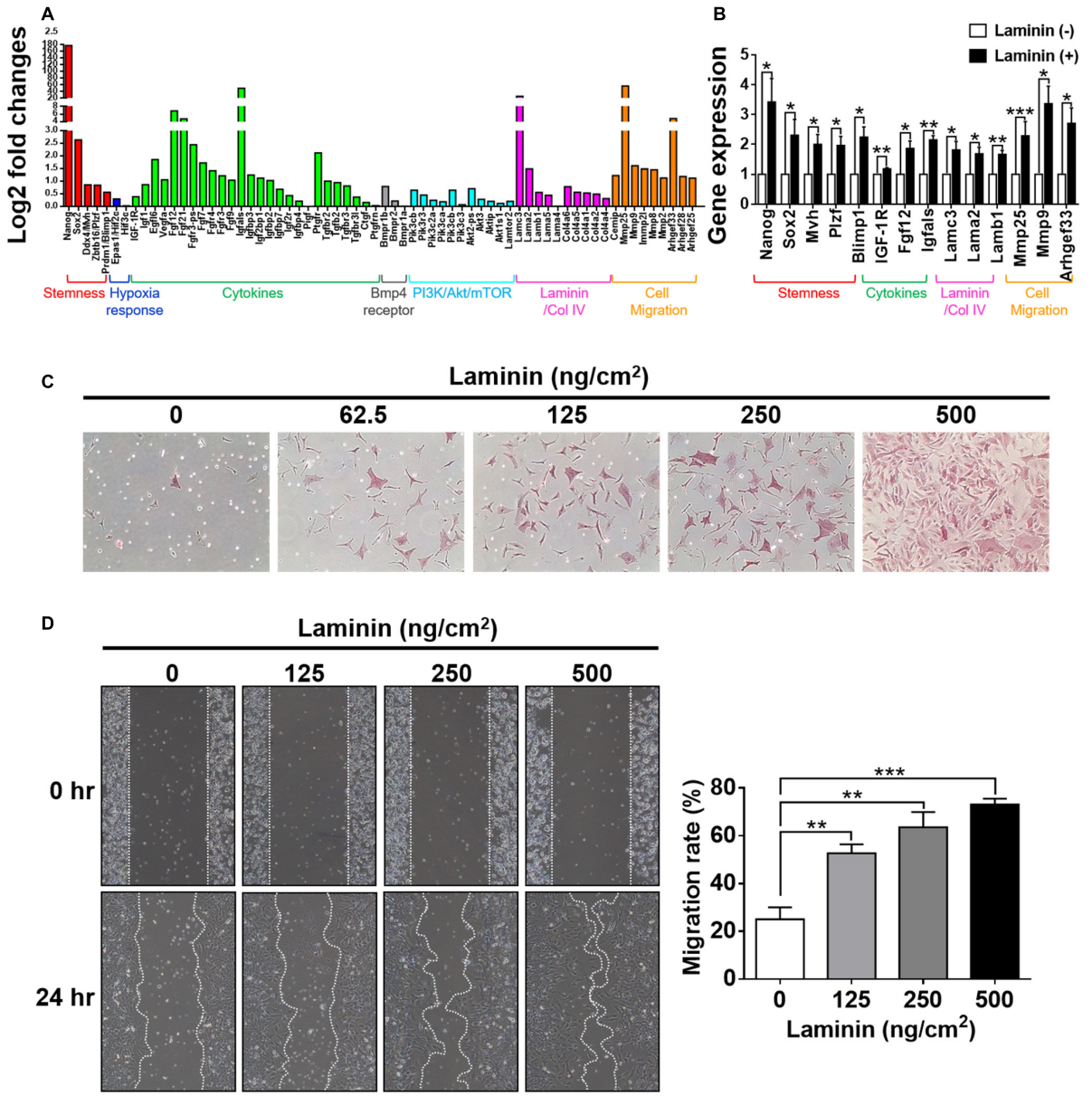

FIGURE 5 | Laminin induces morphological changes and genetic reprogramming. **(A)** Analyses of RNA-seq data collected from CD49f^{+}AP^{+}GSCs cultivated on laminin-coated and non-coated substrates. Genes were grouped into color categories. Red: stemness. Blue: hypoxia responses. Green: cytokines. Black: BMP4 receptors. Cyan: PI3K/Akt/mTOR pathway. Pink: basement membrane components. Orange: cell migration. **(B)** Validation of RNA-seq data in **(A)** by RT-qPCR. Data are means ± SEM of at least three independent experiments. *$p < 0.05$; **$p < 0.01$; ***$p < 0.001$ (Student's *t*-test). **(C)** Dose-dependent effects of laminin on cell morphology and alkaline phosphatase (AP) activity. The intensity of the red stain indicates AP activity. **(D)** Wound-healing assay showed that laminin coating enhanced cell migration in a dose-dependent manner. Data are means ± SEM of at least three independent experiments. **$p < 0.01$; ***$p < 0.001$ (one-way ANOVA).

To ascertain whether these laminin-induced genetic changes reprogrammed cell behavior, we performed cell-based phenotypic assays. First, we examined how cells changed their morphology in response to the exposure of laminin. By cultivating CD49f^{+}AP^{+}GSCs on substrates coated with various concentrations of laminin, we found that laminin enhanced cell spreading, protruding, and AP activity in a dose-dependent manner (**Figure 5C**). Next, we used wound-healing assay to examine how cells modulated their migration in response to laminin. The results showed that laminin enhanced cell migration in a dose-dependent manner (**Figure 5D**). Of note, none of these changes was related to cell proliferation as quantitative measurements on cell growth rates showed a laminin-independent trend (**Supplementary Figure 3**). Taken together, these results suggested that the exposure to laminin reprogrammed the ability of CD49f^{+}AP^{+}GSCs to migrate,

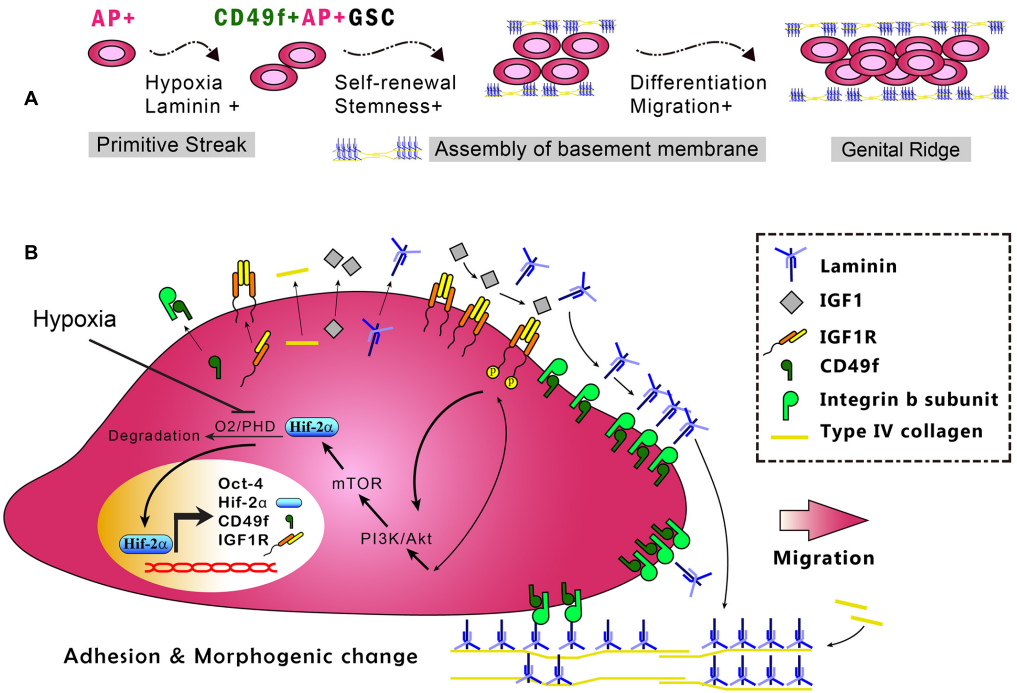

FIGURE 6 | *In vitro* model of the CD49f/IGF1R-Hif-2α regulatory circuit in CD49f$^+$AP$^+$GSCs. **(A)** Depiction of the stages in early germ cell development. **(B)** *In vitro* model of CD49f/IGF1R-Hif-2α signaling circuit in mouse CD49f$^+$AP$^+$GSCs under hypoxic conditions. AP, alkaline phosphatase; HIF, hypoxia-inducible protein; IGF-1, insulin-like growth factor-1; IGF-1R, insulin-like growth factor-1 receptor; PHD, prolyl hydroxylases. Notably, the laminin lattice network can be assembled on the cell surface through integrin and in turn be incorporated into the underlying type IV collagen network, thereby forming the basement membrane (Hohenester and Yurchenco, 2013; Yurchenco, 2015).

affected the assembly of the microenvironment, and maintained stemness, hypoxia response, and PI3K/Akt/mTOR signaling.

DISCUSSION

The fate of stem cells, including self-renewal and differentiation abilities, is regulated by the interplay of internal gene expression and external mechanochemical signals from the niche. In GSCs, development involves maintaining the ability of self-renewal and acquiring the ability to migrate into the genital ridge where the cells mature (**Figure 6A**). Examples of niche factors include oxygen tension, endocrinal factors, and ECM, all of which can signal to each other, resulting in a complex niche signaling network. For decades, the understanding of the niche signaling network has been hindered by the lack of proper *in vitro* cell model systems. This hindrance in GSC research has recently been resolved by our novel serum-free culture system. By using our serum-free culture system, we showed that niche hypoxia can activate the niche endocrinal IGF-1 signaling to maintain Oct-4 expression, promote symmetric self-renewal, and enable migration of AP$^+$GSCs through the Hif-2α-OCT-4/CXCR4 signaling loop (Huang et al., 2014; Kuo et al., 2018). That work highlighted the connection between two crucial niche factors, namely, hypoxia and endocrinal factors. However, the coordination of other critical niche factors, such as ECM, with hypoxia and endocrinal signals to maintain Oct-4 expression in AP$^+$GSCs remains unknown. Here, using CD49f$^+$AP$^+$GSCs as the model system, we advanced our previous findings by showing that niche hypoxia increases the expression of not only IGF-1R but also the laminin receptor CD49f. We also found an additive effect in CD49f/IGF1R-(PI3K/Akt)-Hif-2α signaling for the maintenance of Oct-4, and that exposure to niche ECM laminin results in genetic reprogramming of cell migration ability (**Figures 5B**, **6**). In the present study, we unveiled the niche-signaling network between ECM (laminin) and hypoxia–endocrinal signaling (IGF1-Hif-2α) in the embryonic development of CD49f$^+$AP$^+$GSCs.

Hypoxia (i.e., low oxygen tension) is a physiological condition that appears during early embryogenesis. It occurs predominately in tissues undergoing rapid growth and has been shown to promote the survival of stem cells, including human ES cells (Ezashi et al., 2005), PGCs (Scortegagna et al., 2005; Covello et al., 2006), induced pluripotent stem cells (iPSCs) (Yoshida et al., 2009), hematopoietic stem cells (Danet et al., 2003), and neural crest stem cells (Morrison et al., 2000; Studer et al., 2000). Hif-2α has been associated with early PGC development (Covello et al., 2006). When PGC cells migrate from the hindgut to the genital ridge, they maintain their Oct-4 levels and AP activity and increase their cell number from 50 (E8.5 embryos) to 20,000 (E12.5 genital ridges) (Covello et al., 2006). Experiments with transgenic mice have shown that the loss of Hif-2α (Hif-2α$^{-/-}$) severely reduced the number of PGCs from 20,000 to approximately 20 in E12.5 genital ridges (Covello et al., 2006)

and caused azoospermia (Scortegagna et al., 2005). As Hif-2α directly regulates Oct-4 (Covello et al., 2006) and c-Myc (Keith and Simon, 2007) expression, we can reasonably assume that regulating Hif-2α expression can affect Oct-4 expression and stem cell proliferation.

In support of the aforementioned assumption, we have previously shown that hypoxia elevates the expression of stemness-related genes (e.g., *Oct-4*, *Sox2*, *Nanog*, and *Klf-4*) in mouse AP^+GSCs. In particular, hypoxia can increase the expression of IGF-1/IGF-1R, which in turn stimulates the expression of Hif-2α (Huang et al., 2014) and leads to a feedforward loop between hypoxia and IGF-1 signaling. Herein, we additionally showed that Hif-2α knockdown suppressed IGF-1-induced IGF-1R/CD49f expression in $CD49f^+AP^+$GSCs (**Figure 2D**). Consistent with our results, IGF-1/IGF-1R signaling was reported to be associated with Hif-1α or Hif-2α expression in cancers and in cells of somatic lineage (Akeno et al., 2002; Carroll and Ashcroft, 2006; Catrina et al., 2006). Similarly, human cancer converged at the Hif-2α oncogenic axis has been suggested to require IGF-1R activation (Franovic et al., 2009). Thus, the crosstalk between hypoxia and IGF-1/IGF-1R signaling is manifested not only in the GSC development and maintenance but also in tumorigenesis (Lee et al., 2019). Identifying the molecular mechanisms underlying such crosstalk will not only benefit stem cell–based cell therapy for regenerative medicine but also provide insights into cancer biology and therapy.

ECM components (such as laminin) are the important niche factors in the microenvironment surrounding GSCs (**Figure 1B**). An increasing body of evidence has shown that niche laminin is highly associated with the development of embryonic germ cells and cancer. In stem cell development, for example, laminin was demonstrated to promote embryonic GSC migration—a significant amount of laminin receptor CD49f was found to be expressed in these cells (Hedger, 1997; Morita-Fujimura et al., 2009). Laminin/CD49f activation has also been shown to regulate Oct-4 expression through PI3K/Akt signaling in human mesenchymal stem cells (Yu et al., 2012). Consistently, laminin has been reported to be a potent substrate for large-scale expansion of induced pluripotent stem cells of humans (Paccola Mesquita et al., 2019). Remodeling of basal lamina at the niche of skeletal muscle stem cells was also found to mediate stem cell self-renewal, and genetic ablation of laminin-α1, disruption of integrin-α6 signaling, or the blockade of matrix metalloproteinase activity can impair satellite cell expansion and self-renewal (Rayagiri et al., 2018). In patients with somatic cancers, by contrast, cancer cells expressing a high level of laminin and CD49f are associated with poor prognosis, high recurrence rates, and high incidence rates of cancer stem cells (Chang et al., 2012; Vieira et al., 2014), and the blockade of a laminin-411–Notch axis was shown to inhibit glioblastoma growth through tumor–microenvironment crosstalk (Sun et al., 2019). Nevertheless, how laminin signaling is coupled with the signals from other niche factors, such as hypoxia and IGF-1, both of which play crucial roles in cancer and stem cell development, remains largely unknown.

Here, we showed that niche hypoxia upregulates the expression of not only IGF-1R but also the laminin receptor CD49f (**Supplementary Figure 1**) and that Hif-2α is involved in IGF-1-induced upregulation of CD49f (**Figure 2D**), while autocrine signals in IGF-1/IGF-1R and laminin/CD49f activation increased Hif-2α expression (**Figures 1–4**). These results provide evidence suggesting that the presence of crosstalk and a signaling network among the three niche factors, namely, hypoxia, endocrinal IGF-1, and ECM laminin, that can act additively through a CD49f/IGF1R-Hif-2α signaling loop to maintain Oct-4 expression in the embryonic $CD49f^+AP^+$GSCs.

In the present study, Oct-4 expression level was primarily used as the reporter to indicate the extent of stemness. Consistent with our results, the level of Oct-4 expression *in vivo* was closely associated with cell fate specification during embryogenesis (Sun et al., 2019). In male GSCs, for example, Oct-4 expression levels are different among PGCs, postmigratory PGCs (i.e., gonocytes), and spermatogonial stem cells (Pesce et al., 1998); furthermore, the importance of Oct-4 expression level in PGC cell fate specification has been documented using a conditional *Cre*/*loxP* gene-targeting strategy (Kehler et al., 2004). To regulate Oct-4 expression levels, several regulators have been identified, including Hif-2α (Covello et al., 2006), EpCAM (Huang et al., 2011), estrogen (Zhang et al., 2008; Jung et al., 2011), SUMO1/sentrin-specific peptidase proteins (Wu et al., 2012), and IGF-1/IGF-1R signaling (Bendall et al., 2007; Huang et al., 2009). Among these regulators, Hif-2α is well-documented because hypoxia is a common niche factor in embryonic stem cell development. One factor that has not been previously reported but was reported in the present study is laminin. In addition to laminin, IGF-1 signaling is of particular interest because its role in modulating the proliferation and pluripotency of stem cells has been extensively studied (Huang et al., 2009, 2014; Li and Geng, 2010). For example, studies have reported that IGF-1 cooperates with basic fibroblast growth factor to maintain self-renewal in human embryonic stem cells (Bendall et al., 2007; Huang et al., 2014). In parallel, the PI3K/Akt signaling axis, which is downstream to both IGF-1 and laminin signaling, has been reported to be involved in crosstalk with self-renewal mechanisms in embryonic stem cells (Watanabe et al., 2006; McLean et al., 2007). In the context of cancer, the activation of IGF-1R signaling has been demonstrated to initiate the expression of stemness in breast cancer (Motallebnezhad et al., 2016) and hepatocellular carcinomas (HCC) (Chang et al., 2015, 2016). Consistent with these reports, our previous data showed that the activation of the PI3K/Akt pathway can promote PGC proliferation and maintain Oct-4 expression in embryonic germ cells (Kimura et al., 2003; Moe-Behrens et al., 2003; Kuo et al., 2018) and that niche IL-6/IGF-IR signaling causes poor prognosis of hepatitis B virus (HBV)-related HCC because of Oct-4/Nanog expression (Chang et al., 2015).

In summary, this study used primary $CD49f^+AP^+$GSCs and serum-free culture medium and provided the first evidence demonstrating the enhanced expression of CD49f and IGF-1R because of hypoxia and the cooperation of niche laminin with the associated CD49f/IGF1R-(PI3K/Akt-mTOR)-Hif-2α signaling loop to maintain cell proliferation and Oct-4 expression in embryonic $CD49f^+AP^+$GSCs (**Figure 6**). Findings from this study provide important insights into the niche signaling

network among ECM laminin/CD49f signaling, endocrinal IGF-1/IGF-1R signaling, and hypoxia responses in early embryonic germ cell development. These insights have potential applications for future strategies to engineer cell therapy for regenerative medicine.

EXPERIMENTAL PROCEDURES

Electroporation of Short Hairpin RNA

The shControl (TRCN0000072246), shIGF-1R#1 (TRCN0000023489), shIGF-1R#2 (TRCN0000023491), shCD49f#3 (TRCN0000066150), and shCD49f#5 (TRCN0000066152) plasmids were purchased from National RNAi Core (Taiwan). Double-stranded hairpin oligonucleotides designed to target the mouse Hif-2α cDNA (NM_010137) at the sequence position 2052–2070 (5′-GATGAGGTCTGCAAAGGAC-3′, shRNA#2) and 87–105 (5′-GGAGACGGAGGTCTTCTAT-3′, shRNA#3) of the Hif-2α gene were cloned into the *Bam*HI/*Not*I site of the pGSH1-GFP vector to generate shHif-2α. Gene knocked-down GSCs were generated through electroporation with plasmids (15 μg). Electroporation was performed using an electroporator (BTX) at 250 V for three pulses, each pulse lasting 0.1 ms with an interval of 0.25 s.

RNA Isolation and Reverse-Transcription Polymerase Chain Reaction

The AP^+GSC colonies and the MACS-purified $CD49f^+$GSCs were collected, and the total RNA was extracted using an RNeasy Micro Kit (QIAGEN, Valencia, CA, United States) according to the manufacturer's instructions. Three micrograms of total RNA and a random primer (Invitrogen, Carlsbad, CA, United States) were used to synthesize complementary (c)DNA. The cDNA synthesis was performed at 42°C for 50 min in a final volume of 20 μl according to the manufacturer's instructions for Superscript III reverse transcriptase (Invitrogen). Polymerase chain reaction (PCR) was performed with PlatinumTaq polymerase (Invitrogen), and the real-time RT-qPCR amplicons were titrated within a linear range of amplification. The accession numbers, primer pair sequences, and annealing temperatures are listed in **Supplementary Table 1**. Beta-2 microglobin was used as an internal control. PCR products were separated through agarose gel electrophoresis, and the DNA bands were visualized using ethidium bromide under ultraviolet light. RT-qPCR analysis of at least three independent cultures was performed for all experiments.

Western Blotting Analysis

The MACS-purified $CD49f^+$GSCs were collected and lysed in reducing 2× Laemmli sample buffer, subjected to 10% SDS-PAGE, and then transferred to a polyvinylidene difluoride (PVDF) membrane for Western blot analysis. The primary antibodies used in the experiment are listed in **Supplementary Table 2**, and horseradish peroxidase (HRP)-conjugated anti-mouse/rabbit immunoglobulin G (IgG; 1:2,000) was used as the secondary antibody. The activity of HRP was detected using an enhanced chemiluminescence system according to the manufacturer's instructions (Amersham Pharmacia Biotech., Buckinghamshire, United Kingdom). Quantifications of the protein bands were performed using the SPOT DENSO software on an AlphaImager2200 instrument (Alpha Innotech Corporation, CA, United States).

RNA Sequencing Analysis

The MACS-purified $CD49f^+$GSCs cultivated on laminin-coated and non-coated substrates in the serum-free medium were harvested. RNA sequencing (RNA-seq) was performed by the Phalanx Biotech Group (Taipei, Taiwan). Briefly, RNA samples from the cell lysates were first enriched in mRNA by using oligo(dT) beads. Subsequently, double-stranded cDNA synthesis, end repair, the addition of the nucleotide "A" overhangs and adaptors, cDNA second-strand degradation, fragment selection, PCR amplification, library quality test, and illumine sequencing were performed. For sequencing, the amplified raw output was trimmed to a 150-bp fragment, and the cutoff was applied when the sliding window (four-base window) dropped below 15 or when the read was shorter than 35 base pair. This method yielded a total of 20 million reads. For sequence alignment, STAR was used to map preprocessed read data with the reference genome GRCm38.p6. After the reads were aligned to the genome, the package Cuffquant was used on the resulting alignment files to compute gene and transcript expression profiles. Cuffdiff, a module of the Cufflinks package, merged assemblies from two or more conditions to estimate the expression levels by calculating the number of RNA-seq fragments per kilobase of transcript per million (FPKM) fragments mapped. Cuffdiff was used to test the statistical significance of observed changes and identify genes that were regulated at the transcriptional or posttranscriptional level. Clustering analysis was performed to segregate upregulated and downregulated genes in the laminin-treated and non-laminin-treated samples. The differentially expressed genes in the laminin-treated and non-treated samples were then distributed according to fold change (i.e., $\log_2$) and significance (i.e., *p*- and *Q*-values).

Statistical Analysis

All experiments were repeated at least three times with individual samples. Data were expressed as the mean ± standard error of the mean (SEM). Differences in means were assessed using the *t*-test or one-way analysis of variance analysis (ANOVA) and *post-hoc* tests (GraphPad InStat 3.0, GraphPad Software, Inc., La Jolla, CA, United States). A p-value of < 0.05 was considered statistically significant.

DATA AVAILABILITY STATEMENT

The original contributions presented in the study are included in the article/**Supplementary Material**, further inquiries can be directed to the corresponding author/s.

ETHICS STATEMENT

The animal study protocol was approved by the Institutional Animal Care and Use Committee or Panel (IACUC/IACUP) at Taipei Medical University (Affidavit of Approval of Animal Use Protocol # LAC-2017-0532).

AUTHOR CONTRIBUTIONS

H-KA, S-WP, and C-CL: conception and design of the study, collection and organization of data, data analysis, and data interpretation. Y-CK, T-YLa, and Y-LW: collection and organization of data. H-NH: administrative and final approval of the manuscript. C-LG: RNA-seq data analysis, graphical summary, and manuscript writing. T-YLi and Y-HH: conception and design of the study, data analysis and interpretation, manuscript writing, and final approval of the manuscript. All authors contributed to the article and approved the submitted version.

FUNDING

This work was financially supported by research grants from the Ministry of Science and Technology, Taiwan (Grant numbers: MOST 105-2628-B-038-008-MY3, MOST 106-3114-B-038-001, MOST 107-2321-B-038-002, MOST 107-2314-B-038-057, MOST 107-2314-B-038-061, MOST 108-2320-B-038-033-MY3, MOST108-2314-B-038-006, MOST 108-2321-B-038-003, MOST109-2314-B-038-135, and MOST109-2321-B-038-003); Health and Welfare Surcharge of Tobacco Products (Grant numbers: MOHW 103-TD-B-111-01, MOHW 104-TDU-B-212-124-001, MOHW 105-TDU-B-212-134001, MOHW 106-TDU-B212-144001, MOHW 107-TDU-B-212-114014, and MOHW108-TDU-B-212-124014); Taipei Medical University (Grant numbers: TMU-T104-06, TMU-T105-06, TMU-T106-03, and 105TMUCIT-01-3); BioSeed International Co., Ltd. (A-108-093 and A-110-002) to Y-HH. Taipei Medical University Hospital (Grant numbers: 104TMU-TMUH-04 and 105TMU-TMUH-10) to H-KA. C-LG acknowledges financial support from MOST 104-2112-M-001-043-MY3, MOST 105-2627-M-001-006-, MOST 106-2627-M-001-005-, MOST 107-2627-M-001-001-, MOST 107-2119-M-001-039-, MOST 107-2112-M-001-040-MY3, and MOST 108-2119-M-001-018- as well as that from AS-105-TPA04 and AS-TP-109-M04.

SUPPLEMENTARY MATERIAL

The Supplementary Material for this article can be found online at: https://www.frontiersin.org/articles/10.3389/fcell.2021.646644/full#supplementary-material

REFERENCES

Akeno, N., Robins, J., Zhang, M., Czyzyk-Krzeska, M. F., and Clemens, T. L. (2002). Induction of vascular endothelial growth factor by Igf-I in osteoblast-like cells is mediated by the Pi3k signaling pathway through the hypoxia-inducible Factor-2alpha. *Endocrinology* 143, 420–425. doi: 10.1210/endo.143.2.8639

Bendall, S. C., Stewart, M. H., Menendez, P., George, D., Vijayaragavan, K., Werbowetski-Ogilvie, T., et al. (2007). Igf and Fgf cooperatively establish the regulatory stem cell niche of pluripotent human cells in vitro. *Nature* 448, 1015–1021. doi: 10.1038/nature06027

Carroll, V. A., and Ashcroft, M. (2006). Role of Hypoxia-Inducible Factor (Hif)-1alpha versus Hif-2alpha in the regulation of Hif target genes in response to hypoxia, insulin-like growth factor-I, or loss of von hippel-lindau function: implications for targeting the Hif pathway. *Cancer Res.* 66, 6264–6270. doi: 10.1158/0008-5472.CAN-05-2519

Catrina, S. B., Botusan, I. R., Rantanen, A., Catrina, A. I., Pyakurel, P., Savu, O., et al. (2006). Hypoxia-inducible factor-1alpha and hypoxia-inducible factor-2alpha are expressed in kaposi sarcoma and modulated by insulin-like growth factor-I. *Clin. Cancer Res.* 12, 4506–4514. doi: 10.1158/1078-0432.CCR-05-2473

Chang, C. I., Low, H. P., Qiu, L., Strohsnitter, W. C., and Hsieh, C. C. (2012). Prenatal modulation of breast density and breast stem cells by insulin-like growth factor-1. *Am. J. Stem Cells* 1, 239–252.

Chang, T. S., Chen, C. L., Wu, Y. C., Liu, J. J., Kuo, Y. C., Lee, K. F., et al. (2016). Inflammation promotes expression of stemness-related properties in Hbv-related Hepatocellular carcinoma. *PLoS One* 11:e0149897. doi: 10.1371/journal.pone.0149897

Chang, T. S., Wu, Y. C., Chi, C. C., Su, W. C., Chang, P. J., Lee, K. F., et al. (2015). Activation of Il6/Igfir confers poor prognosis of Hbv-related Hepatocellular carcinoma through induction of Oct-4/Nanog expression. *Clin. Cancer Res.* 21, 201–210. doi: 10.1158/1078-0432.CCR-13-3274

Covello, K. L., Kehler, J., Yu, H., Gordan, J. D., Arsham, A. M., Hu, C. J., et al. (2006). Hif-2alpha regulates Oct-4: effects of hypoxia on stem cell function, embryonic development, and tumor growth. *Genes Dev.* 20, 557–570. doi: 10.1101/gad.1399906

Danet, G. H., Pan, Y., Luongo, J. L., Bonnet, D. A., and Simon, M. C. (2003). Expansion of human scid-repopulating cells under hypoxic conditions. *J. Clin. Invest.* 112, 126–135. doi: 10.1172/JCI17669

Ezashi, T., Das, P., and Roberts, R. M. (2005). Low O2 tensions and the prevention of differentiation of Hes cells. *Proc. Natl. Acad. Sci. U.S.A.* 102, 4783–4788. doi: 10.1073/pnas.0501283102

Francis, K. R., and Wei, L. (2010). Human embryonic stem cell neural differentiation and enhanced cell survival promoted by hypoxic preconditioning. *Cell Death Dis.* 1:e22. doi: 10.1038/cddis.2009.22

Franovic, A., Holterman, C. E., Payette, J., and Lee, S. (2009). Human cancers converge at the Hif-2alpha oncogenic axis. *Proc. Natl. Acad. Sci. U.S.A.* 106, 21306–21311. doi: 10.1073/pnas.0906432106

Ginouves, A., Ilc, K., Macias, N., Pouyssegur, J., and Berra, E. (2008). Phds overactivation during chronic hypoxia "Desensitizes" hifalpha and protects cells from necrosis. *Proc. Natl. Acad. Sci. U.S.A.* 105, 4745–4750. doi: 10.1073/pnas.0705680105

Ginsburg, M., Snow, M. H., and McLaren, A. (1990). Primordial germ cells in the mouse embryo during gastrulation. *Development* 110, 521–528. doi: 10.1242/dev.110.2.521

Hedger, M. P. (1997). Testicular leukocytes: what are they doing? *Rev. Reprod.* 2, 38–47. doi: 10.1530/revreprod/2.1.38

Hoei-Hansen, C. E., Sehested, A., Juhler, M., Lau, Y. F., Skakkebaek, N. E., Laursen, H., et al. (2006). New evidence for the origin of intracranial germ cell tumours from primordial germ cells: expression of pluripotency and cell differentiation markers. *J. Pathol.* 209, 25–33. doi: 10.1002/path.1948

Hohenester, E., and Yurchenco, P. D. (2013). Laminins in basement membrane assembly. *Cell Adh. Migr.* 7, 56–63. doi: 10.4161/cam.2183121831

Huang, H. P., Chen, P. H., Yu, C. Y., Chuang, C. Y., Stone, L., Hsiao, W. C., et al. (2011). Epithelial cell adhesion molecule (Epcam) complex proteins promote transcription factor-mediated pluripotency reprogramming. *J. Biol. Chem.* 286, 33520–33532. doi: 10.1074/jbc.M111.256164

Huang, Y. H., Chin, C. C., Ho, H. N., Chou, C. K., Shen, C. N., Kuo, H. C., et al. (2009). Pluripotency of mouse spermatogonial stem cells maintained by Igf-1- dependent pathway. *FASEB J.* 23, 2076–2087. doi: 10.1096/fj.08-121939

Huang, Y. H., Lin, M. H., Wang, P. C., Wu, Y. C., Chiang, H. L., Wang, Y. L., et al. (2014). Hypoxia inducible factor 2alpha/insulin-like growth factor receptor signal loop supports the proliferation and Oct-4 maintenance of mouse germline stem cells. *Mol. Hum. Reprod.* 20, 526–537. doi: 10.1093/molehr/gau016

Jung, J. W., Park, S. B., Lee, S. J., Seo, M. S., Trosko, J. E., and Kang, K. S. (2011). Metformin represses self-renewal of the human breast carcinoma stem cells via inhibition of estrogen receptor-mediated Oct-4 expression. *PLoS One* 6:e28068. doi: 10.1371/journal.pone.0028068

Kehler, J., Tolkunova, E., Koschorz, B., Pesce, M., Gentile, L., Boiani, M., et al. (2004). Oct-4 Is Required for primordial germ cell survival. *EMBO Rep.* 5, 1078–1083. doi: 10.1038/sj.embor.7400279

Keith, B., and Simon, M. C. (2007). Hypoxia-inducible factors, stem cells, and cancer. *Cell* 129, 465–472. doi: 10.1016/j.cell.2007.04.019

Kimura, T., Suzuki, A., Fujita, Y., Yomogida, K., Lomeli, H., Asada, N., et al. (2003). Conditional loss of pten leads to testicular teratoma and enhances embryonic germ cell production. *Development* 130, 1691–1700. doi: 10.1242/dev.00392

Kuo, Y. C., Au, H. K., Hsu, J. L., Wang, H. F., Lee, C. J., Peng, S. W., et al. (2018). Igf-1r promotes symmetric self-renewal and migration of alkaline phosphatase(+) germ stem cells through Hif-2alpha-Oct-4/Cxcr4 loop under hypoxia. *Stem Cell Rep.* 10, 524–537. doi: 10.1016/j.stemcr.2017.12.003

Lawson, K. A., Dunn, N. R., Roelen, B. A., Zeinstra, L. M., Davis, A. M., Wright, C. V., et al. (1999). Bmp4 Is required for the generation of primordial germ cells in the mouse embryo. *Genes Dev.* 13, 424–436. doi: 10.1101/gad.13.4.424

Lee, K. L., Kuo, Y. C., Ho, Y. S., and Huang, Y. H. (2019). Triple-negative breast cancer: current understanding and future therapeutic breakthrough targeting cancer stemness. *Cancers* 11:1334. doi: 10.3390/cancers11091334

Li, Y., and Geng, Y. J. (2010). A potential role for insulin-like growth factor signaling in induction of pluripotent stem cell formation. *Growth Horm. IGF Res.* 20, 391–398. doi: 10.1016/j.ghir.2010.09.005

McLean, A. B., D'Amour, K. A., Jones, K. L., Krishnamoorthy, M., Kulik, M. J., Reynolds, D. M., et al. (2007). Activin a efficiently specifies definitive endoderm from human embryonic stem cells only when phosphatidylinositol 3-kinase signaling is suppressed. *Stem Cells* 25, 29–38. doi: 10.1634/stemcells.2006-0219

Mercier, F. (2016). Fractones: extracellular matrix niche controlling stem cell fate and growth factor activity in the brain in health and disease. *Cell Mol. Life. Sci.* 73, 4661–4674. doi: 10.1007/s00018-016-2314-y

Moe-Behrens, G. H., Klinger, F. G., Eskild, W., Grotmol, T., Haugen, T. B., and De Felici, M. (2003). Akt/Pten signaling mediates estrogen-dependent proliferation of primordial germ cells in vitro. *Mol. Endocrinol.* 17, 2630–2638. doi: 10.1210/me.2003-0006

Morita-Fujimura, Y., Tokitake, Y., and Matsui, Y. (2009). Heterogeneity of mouse primordial germ cells reflecting the distinct status of their differentiation, proliferation and apoptosis can be classified by the expression of cell surface proteins integrin Alpha6 and C-Kit. *Dev. Growth. Differ.* 51, 567–583. doi: 10.1111/j.1440-169X.2009.01119.x

Morrison, S. J., Csete, M., Groves, A. K., Melega, W., Wold, B., and Anderson, D. J. (2000). Culture in reduced levels of oxygen promotes clonogenic sympathoadrenal differentiation by isolated neural crest stem cells. *J. Neurosci.* 20, 7370–7376. doi: 10.1523/jneurosci.20-19-07370.2000

Motallebnezhad, M., Aghebati-Maleki, L., Jadidi-Niaragh, F., Nickho, H., Samadi-Kafil, H., Shamsasenjan, K., et al. (2016). The insulin-like growth factor-I receptor (Igf-Ir) in breast cancer: biology and treatment strategies. *Tumour Biol.* 37, 11711–11721. doi: 10.1007/s13277-016-5176-x

Nguyen, B. P., Gil, S. G., and Carter, W. G. (2000). Deposition of laminin 5 by keratinocytes regulates integrin adhesion and signaling. *J. Biol. Chem.* 275, 31896–31907. doi: 10.1074/jbc.M006379200

Ohinata, Y., Payer, B., O'Carroll, D., Ancelin, K., Ono, Y., Sano, M., et al. (2005). Blimp1 is a critical determinant of the germ cell lineage in mice. *Nature* 436, 207–213. doi: 10.1038/nature03813

Paccola Mesquita, F. C., Hochman-Mendez, C., Morrissey, J., Sampaio, L. C., and Taylor, D. A. (2019). Laminin as a potent substrate for large-scale expansion of human induced pluripotent stem cells in a closed cell expansion system. *Stem Cells Int.* 2019:9704945. doi: 10.1155/2019/9704945

Pesce, M., Gross, M. K., and Scholer, H. R. (1998). In line with our ancestors: Oct-4 and the mammalian germ. *Bioessays* 20, 722–732. doi: 10.1002/(sici)1521-1878(199809)20:9<722::aid-bies5>3.0.co;2-i

Rayagiri, S. S., Ranaldi, D., Raven, A., Mohamad Azhar, N. I. F., Lefebvre, O., Zammit, P. S., et al. (2018). Basal lamina remodeling at the skeletal muscle stem cell niche mediates stem cell self-renewal. *Nat. Commun.* 9:1075. doi: 10.1038/s41467-018-03425-3

Saitou, M., Barton, S. C., and Surani, M. A. (2002). A molecular programme for the specification of germ cell fate in mice. *Nature* 418, 293–300. doi: 10.1038/nature00927

Scortegagna, M., Ding, K., Zhang, Q., Oktay, Y., Bennett, M. J., Bennett, M., et al. (2005). Hif-2alpha regulates murine hematopoietic development in an erythropoietin-dependent manner. *Blood* 105, 3133–3140. doi: 10.1182/blood-2004-05-1695

Studer, L., Csete, M., Lee, S. H., Kabbani, N., Walikonis, J., Wold, B., et al. (2000). Enhanced proliferation, survival, and dopaminergic differentiation of Cns precursors in lowered oxygen. *J. Neurosci.* 20, 7377–7383. doi: 10.1523/jneurosci.20-19-07377.2000

Sun, T., Patil, R., Galstyan, A., Klymyshyn, D., Ding, H., Chesnokova, A., et al. (2019). Blockade of a laminin-411-notch axis with Crispr/Cas9 or a nanobioconjugate inhibits glioblastoma growth through tumor-microenvironment cross-talk. *Cancer Res.* 79, 1239–1251. doi: 10.1158/0008-5472.CAN-18-2725

Vieira, A. F., Ribeiro, A. S., Dionisio, M. R., Sousa, B., Nobre, A. R., Albergaria, A., et al. (2014). P-Cadherin signals through the laminin receptor Alpha6beta4 integrin to induce stem cell and invasive properties in basal-like breast cancer cells. *Oncotarget* 5, 679–692. doi: 10.18632/oncotarget.1459

Watanabe, S., Umehara, H., Murayama, K., Okabe, M., Kimura, T., and Nakano, T. (2006). Activation of Akt signaling is sufficient to maintain pluripotency in mouse and primate embryonic stem cells. *Oncogene* 25, 2697–2707. doi: 10.1038/sj.onc.1209307

Wu, Y. C., Ling, T. Y., Lu, S. H., Kuo, H. C., Ho, H. N., Yeh, S. D., et al. (2012). Chemotherapeutic sensitivity of testicular germ cell tumors under hypoxic conditions is negatively regulated by Senp1-controlled sumoylation of Oct-4. *Cancer Res.* 72, 4963–4973. doi: 10.1158/0008-5472.CAN-12-0673

Yazlovitskaya, E. M., Viquez, O. M., Tu, T., De Arcangelis, A., Georges-Labouesse, E., Sonnenberg, A., et al. (2019). The laminin binding Alpha3 and Alpha6 integrins cooperate to promote epithelial cell adhesion and growth. *Matrix Biol.* 77, 101–116. doi: 10.1016/j.matbio.2018.08.010

Ying, Y., Liu, X. M., Marble, A., Lawson, K. A., and Zhao, G. Q. (2000). Requirement of Bmp8b for the generation of primordial germ cells in the mouse. *Mol. Endocrinol.* 14, 1053–1063. doi: 10.1210/mend.14.7.0479

Ying, Y., Qi, X., and Zhao, G. Q. (2001). Induction of primordial germ cells from murine epiblasts by synergistic action of Bmp4 and Bmp8b signaling pathways. *Proc. Natl. Acad. Sci. U.S.A.* 98, 7858–7862. doi: 10.1073/pnas.151242798

Yoshida, Y., Takahashi, K., Okita, K., Ichisaka, T., and Yamanaka, S. (2009). Hypoxia enhances the generation of induced pluripotent stem cells. *Cell Stem Cell.* 5, 237–241. doi: 10.1016/j.stem.2009.08.001

Yu, K. R., Yang, S. R., Jung, J. W., Kim, H., Ko, K., Han, D. W., et al. (2012). Cd49f enhances multipotency and maintains stemness through the direct regulation of Oct-4 and Sox2. *Stem Cells* 30, 876–887. doi: 10.1002/stem.1052

Yurchenco, P. D. (2015). Integrating activities of laminins that drive basement membrane assembly and function. *Curr. Top. Membr.* 76, 1–30. doi: 10.1016/bs.ctm.2015.05.001S1063-5823(15)00055-1

Zhang, X., Zhang, J., Wang, T., Esteban, M. A., and Pei, D. (2008). Esrrb activates Oct-4 transcription and sustains self-renewal and pluripotency in embryonic stem cells. *J. Biol. Chem.* 283, 35825–35833. doi: 10.1074/jbc.M803481200

Conflict of Interest: The authors declare that the research was conducted in the absence of any commercial or financial relationships that could be construed as a potential conflict of interest.

Publisher's Note: All claims expressed in this article are solely those of the authors and do not necessarily represent those of their affiliated organizations, or those of the publisher, the editors and the reviewers. Any product that may be evaluated in this article, or claim that may be made by its manufacturer, is not guaranteed or endorsed by the publisher.

frontiers in Cell and Developmental Biology

ORIGINAL RESEARCH
published: 18 October 2021
doi: 10.3389/fcell.2021.725854

A Single-Cell Culture System for Dissecting Microenvironmental Signaling in Development and Disease of Cartilage Tissue

*Jade Tassey[1], Arijita Sarkar[1], Ben Van Handel[1], Jinxiu Lu[1], Siyoung Lee[1] and Denis Evseenko[1,2]**

[1] Department of Orthopaedic Surgery, Keck School of Medicine of USC, University of Southern California, Los Angeles, CA, United States, [2] Department of Stem Cell Research and Regenerative Medicine, University of Southern California, Los Angeles, CA, United States

Cartilage tissue is comprised of extracellular matrix and chondrocytes, a cell type with very low cellular turnover in adults, providing limited capacity for regeneration. However, in development a significant number of chondrocytes actively proliferate and remodel the surrounding matrix. Uncoupling the microenvironmental influences that determine the balance between clonogenic potential and terminal differentiation of these cells is essential for the development of novel approaches for cartilage regeneration. Unfortunately, most of the existing methods are not applicable for the analysis of functional properties of chondrocytes at a single cell resolution. Here we demonstrate that a novel 3D culture method provides a long-term and permissive *in vitro* niche that selects for highly clonogenic, colony-forming chondrocytes which maintain cartilage-specific matrix production, thus recapitulating the *in vivo* niche. As a proof of concept, clonogenicity of *Sox9*$^{IRES-EGFP}$ mouse chondrocytes is almost exclusively found in the highest GFP^{+} fraction known to be enriched for chondrocyte progenitor cells. Although clonogenic chondrocytes are very rare in adult cartilage, we have optimized this system to support large, single cell-derived chondrogenic organoids with complex zonal architecture and robust chondrogenic phenotype from adult pig and human articular chondrocytes. Moreover, we have demonstrated that growth trajectory and matrix biosynthesis in these organoids respond to a pro-inflammatory environment. This culture method offers a robust, defined and controllable system that can be further used to interrogate the effects of various microenvironmental signals on chondrocytes, providing a high throughput platform to assess genetic and environmental factors in development and disease.

Keywords: chondrogenic organoid, chondrosphere, single cell, clonogenicity, microenvironment, niche, arthritis

OPEN ACCESS

Edited by:
Stephanie Ma,
The University of Hong Kong,
Hong Kong, SAR China

Reviewed by:
Shih-Chieh Hung,
China Medical University, Taiwan
Wan-Ju Li,
University of Wisconsin–Madison,
United States

***Correspondence:**
Denis Evseenko
evseenko@usc.edu

Specialty section:
This article was submitted to Stem Cell Research, a section of the journal Frontiers in Cell and Developmental Biology

Received: *15 June 2021*
Accepted: *01 October 2021*
Published: *18 October 2021*

Citation:
Tassey J, Sarkar A, Van Handel B, Lu J, Lee S and Evseenko D (2021) A Single-Cell Culture System for Dissecting Microenvironmental Signaling in Development and Disease of Cartilage Tissue. Front. Cell Dev. Biol. 9:725854. doi: 10.3389/fcell.2021.725854

INTRODUCTION

Chondrocytes are specialized extracellular matrix-secreting cells that contribute to maintenance of healthy cartilage. Due to the avascular nature of cartilage, cellular maintenance and turnover is relatively low in adult and there is low regenerative potential upon injury or pathological microenvironments (Jayasuriya et al., 2016). The joint niche balances paracrine input from synovial

and immune cells and thus regulates chondrocyte response in both homeostasis and in diseased states, as seen in aberrant microenvironmental situations such as arthritis where the niche can drive loss of healthy matrix, chondrocyte hypertrophy and formation of fibrocartilage (Sokolove and Lepus, 2013; Shkhyan et al., 2018; Roseti et al., 2019). Although immature chondrocytes have some proliferative capacity (Yasuhara et al., 2011; Li et al., 2013), in pathological conditions such as osteoarthritis, this potential is insufficient to overcome degenerative signals in the microenvironment. Pro-degenerative factors, particularly interleukin 1 (IL-1β) and IL-6 family cytokines such as oncostatin M (OSM), overwhelm and suppress this regenerative potential, inevitably leading to cartilage degradation (Ni et al., 2015; Shkhyan et al., 2018).

The role of SRY-box transcription factor 9 (SOX9) in both homeostatic and arthritic chondrocytes have been well described (Haag et al., 2008; Zhang et al., 2015). Because SOX9 expression has been best described as a regulator of chondrogenesis, chondrocyte proliferation, and a marker for immature chondrocytes (Leung et al., 2011), it has the potential to be used for further assessment of their regenerative response to microenvironmental signaling. Increases in SOX9 activity have been correlated with stimulation by growth factors such as insulin-like growth factor-I (IGF-I) and fibroblast growth factor-2 (FGF-2) in articular chondrocytes (Shi et al., 2015), signifying its role in responding to the paracrine signals present in the niche. Other growth factors such as leukemia inhibitory factor (LIF), transforming growth factor-beta 1 (TGF-β1) and low levels of bone morphogenetic protein-4 (BMP-4) have been shown by our group to inhibit excessive chondrocyte maturation and hypertrophy (Wu et al., 2013), further suggesting that supplementation of growth factors can preserve SOX9-expressing chondrocytes in an immature state.

To model development and disease, multiple *in vitro* methods have been used to culture chondrocytes, however, chondrocytes grown in a 2-dimensional (2D) monolayer dedifferentiate into a fibroblast-like cell, losing expression of extracellular matrix molecules such as glycosaminoglycans (GAGs), collagen 2, and aggrecan (Caron et al., 2012; Wu et al., 2014; Matak et al., 2017). This loss of chondrogenic phenotype severely hinders the use of 2D *in vitro* experiments to accurately represent *in vivo* biology. To prevent this dedifferentiation of chondrocytes, many 3D culture systems of varying composition that attempt to mimic the chondrogenic niche have been developed, including agarose (Buschmann et al., 1992), fibrin glue (Perka et al., 2000), alginate (Almqvist et al., 2001), synthetic hydrogels (Ko et al., 2016) or aggregation into a pellet (Caron et al., 2012). Derivation of chondrocytes from mesenchymal stromal cells (MSCs) in a high-density pellet culture has also been utilized to assess chondrogenic capacity (Ullah et al., 2012). While these 3D methods are superior to traditional 2D culture of chondrocytes, there are no methods that offer single-cell resolution, which would provide a critical asset to interrogate the genetic and microenvironmental factors that influence the proliferative capacity of chondrocytes.

Here we present a novel 3D *in vitro* culture system using methylcellulose (MC), a culture method most commonly used for hematopoietic progenitor cell growth and differentiation (Li et al., 2013), for long-term culture of single chondrocytes. By supplementing MC with media previously established for the maintenance of human embryonic stem cell-derived chondrocyte progenitors, termed Maintenance Media (MM; Ferguson et al., 2018), we select for clonogenic colony-forming chondrocytes from developing tissue or adult articular cartilage by offering a microenvironment that best recapitulates the natural progenitor niche. In this method, chondrocytes from mouse, pig, and human form chondrospheres that retain their chondrogenic phenotype and resemble native cartilage, providing a more accurate surrogate for *in vivo* studies. These chondrogenic organoids can be maintained for at least 8–10 weeks, showing long-term stability of structure, viability and chondrogenic phenotype in a novel *in vitro* setting. This model enables the delineation of the impacts of pro-inflammatory stimuli on chondrocytes in a controllable setting that mimics microenvironmental signaling observed in arthritis, offering a novel and permissive system to model arthritis in a dish.

MATERIALS AND METHODS

Mouse Line and Breeding

Homozygous *Sox9*$^{IRES-EGFP}$ (shortened to *Sox9*^{GFP} henceforth; Strain 030137, Chan et al., 2011) and corresponding wildtype C57BL/6J (Strain 000664) mice were purchased from Jackson Laboratories and used for all subsequent *in vitro* studies. All procedures and breeding involving mice were approved by the Institutional Animal Care and Use Committee of USC and was compliant with all relevant ethical regulations regarding animal research.

Tissue Collection and Digestion

Mouse, human, and pig tissues were enzymatically digested for varying lengths of time at 37°C with mild agitation in digestion media consisting of DMEM/F12 (Corning) with 10% Fetal Bovine Serum (FBS; Corning), 1% penicillin/streptomycin/amphotericin B solution (P/S/A; Corning), 1 mg/mL dispase (Gibco), 1 mg/mL type 2 collagenase (Worthington), 10 μg/mL gentamycin (Teknova) and 100 μg/mL primocin (Invivogen). For mouse femoral heads, postnatal day 7 (P7) *Sox9*^{GFP} or C57BL/6J pups were sacrificed and both femoral heads were harvested. Each pup was harvested separately as a biological replicate. Femoral heads were lightly crushed with a mortar and pestle, then digested in digestion media for 4–6 h. For adult *Sox9*^{GFP} mouse knee joints, 4 months old or 1.5 years old knees were cut at the femur and the tibia and crushed lightly with a mortar and pestle. They were then placed in digestion media in an Erlenmeyer flask with a spin bar in 4°C overnight, then in 37°C for 4–6 h. For pig articular cartilage, 4–6 months old Yucatan minipig hind legs were purchased from Premier BioSource (formerly S&S Farms). The cartilage was shaved from the articular surface of the condyles, minced and digested in digestion media at 37°C for 16–24 h. For human samples, young adult human primary tissue samples aged 19–26 years and mature adult human primary tissue samples aged 57–60 years were obtained from National Disease Research Interchange (NDRI) and complied

with current IRB approval. All donated material was anonymous, carried no personal identifiers, and was obtained after informed consent. Human cartilage was digested in the same manner as pig cartilage. All cells were washed with DPBS (Corning) after digestion and strained through a 70 μm filter (Fisher) before use.

Methylcellulose and Liquid Culture Method of Chondrocytes

To culture isolated chondrocytes in a 3D environment, methylcellulose (H4100, StemCell Technologies) was resuspended in Maintenance Media (MM; Ferguson et al., 2018), which consists of DMEM/F12 (Corning) with 10% FBS (Corning) and 1% P/S/A (Corning) supplemented with fibroblast growth factor-2 (FGF2, 10 ng/mL), bone morphogenic protein-4 (BMP4, 1 ng/mL), insulin-like growth factor-1 (IGF1, 10 ng/mL), Leukemia Inhibitory Factor (LIF, 50 ng/L), Transforming Growth Factor-β1 (TGF-β1 10 ng/mL), and primocin (100 μg/mL). All supplemental growth factors were purchased from PeproTech Inc., and the final concentration of methylcellulose was 1%. Passage 0–1 chondrocytes were resuspended at low density (300–400 cells/mL) and plated in 6-well ultra-low attachment plates (Corning) for 3–4 weeks. *Sox9*^{GFP} femoral head cells were cultured in a hypoxic chamber with 5% O_2, whereas human and pig chondrocytes were cultured in normoxia. To ensure moisture and nutrients remained available to the cells, 120–160 μL of liquid MM was distributed twice weekly on the surface of the wells. After 3–4 weeks, colonies were counted for clonogenicity. Inclusion criteria consisted of clones larger than ∼40 μm in diameter or greater than 5 cell divisions as observed under a compound light microscope. All images of clones in methylcellulose were taken on an Echo Revolve Inverted microscope and scale bars were added using FIJI software (ImageJ). For individual clone culture in liquid media, colonies were plucked with a wide-bore pipette tip, washed in 10% FBS + 1% P/S/A + DMEM/F12 media, and transferred into a 96-well U-bottom ultra-low attachment plate (Corning) containing 200 μL of liquid MM. For arthritis in a dish experiments, addition of Oncostatin M (OSM; 10 ng/mL, PeproTech Inc.) to Maintenance Media was used. The remaining colonies were harvested for quantitative Real-Time PCR (qPCR) by washing the well with DPBS and further dilution of the methylcellulose by subsequent washing and centrifugation with DPBS in a 50 mL conical vial. To maintain the individual spheres in liquid, 100–120 μL of media was removed and added as necessary.

Flow Cytometry and FACS

All flow cytometry and FACS was performed on a BD FACSAria IIIu cell sorter. Mouse cells were washed twice in 1–2% FBS and stained with DAPI for viability. Populations of interest were sorted based on DAPI negativity, GFP expression, and lack of the following lineage markers: APC-Cy7: CD31 (endothelial cells), Ter119 (erythrocytes), and CD45 (leukocytes) at 1 μL antibody/10^6 cells (BioLegend). Cells were directly sorted into DMEM/F12 containing 10% FBS with 1% P/S/A. Flow cytometry data was analyzed using FlowJo software.

RNA Sequencing Library Preparation and Sequencing

Total RNA was isolated using QIAGEN RNeasy Mini kit and quantified using Qubit fluorometer (Thermo Fisher Scientific). Quality of the isolated RNA was checked using Agilent Bioanalyzer 2100. Universal Plus mRNA-Seq. Library with NuQuant (TECAN) was used to generate stranded RNA-seq libraries. Briefly, poly(A) RNA was selected followed by RNA fragmentation. Double stranded cDNA was generated thereafter using a mixture of random and oligo(dT) priming. The library was then constructed by end repairing the cDNA to generate blunt ends, ligation of Unique Dual Index (UDI) adaptors, strand selection and PCR amplification. Different adaptors were used for multiplexing samples in one lane. Quality of the library was checked using Agilent Bioanalyzer 2100. Sequencing was performed on Illumina HiSeq 3000 with single end 50 base pair reads.

RNA Sequencing Data Analysis

Raw fastq files were analyzed in Partek flow (version 10.0.21.0801). Reads were aligned to mouse GRCm38 (mm10) genome using Gencode Release M25 reference using STAR aligner (version 2.7.3a) (Dobin et al., 2013). Transcript levels were quantified to the reference using Partek E/M with default parameters. Normalization was done using counts per million (CPM) method. Genes were considered to be differentially expressed based on fold change >5 and FDR < 0.01. Heatmap for normalized gene expression was generated using Morpheus software[1]. Gene ontology enrichment analysis for the differentially expressed genes was performed using DAVID (Huang et al., 2009).

RNA Extraction and Quantitative Real-Time PCR

Total RNA was extracted using either the RNeasy Mini or Micro Kit (Qiagen) and cDNA was amplified using the Maxima First Strand cDNA Synthesis Kit (Thermo Fisher Scientific). Power SYBR Green (Applied Biosystems) RT-PCR amplification and detection was performed using an Applied Biosystems Step One Plus Real-Time PCR machine. The comparative Ct method for relative quantification (2-ΔΔCt) was used to quantitate gene expression, where results were normalized to ribosomal protein L7 (*RPL7*). Primer sequences used and corresponding GenBank Accession numbers are listed in **Supplementary Table 1**.

Histology, Immunohistochemistry, and Immunofluorescence

Tissues were fixed in either 10% formalin or 4% paraformaldehyde and sectioned at 5 μm. For DAB immunohistochemical (IHC) staining on pig slides, sections were deparaffinized using standard procedures and antigen retrieval was performed by incubating the slides in 1X citrate buffer pH 6.0 (Diagnostic Biosystems) at 60°C for 30 min followed by 15 min cooling at room temperature. For IHC on

[1]https://software.broadinstitute.org/morpheus

mouse slides, the above procedure was used with the addition of Proteinase K (Sigma) digestion at 37°C for 5 min after citrate buffer antigen retrieval. Endogenous peroxidase activity was quenched by treating samples with 3% H_2O_2 for 10 min at room temperature (RT). Sections were then blocked in 2.5% normal horse serum for 20 min, then incubated with primary antibodies diluted in PBS with 0.1–1% BSA (Sigma) overnight at 4°C. Sections were washed three times with TBS +0.05% Tween 20 (TBST, Sigma) before addition of HRP-conjugated secondary antibody for 30–120 min incubation at RT. Sections were washed three times with TBST after secondary incubation and DAB substrate (Vector Laboratories) was added until positive signal was observed. Sections were then immediately washed with tap water, counterstained in hematoxylin for 1 min and washed again with tap water before dehydration and mounting. Secondary antibody only (no primary antibody) controls were used for IHC, and a list of all antibodies and their concentrations used can be found in **Supplementary Table 2**. Toluidine Blue staining was performed on deparaffinized sections in accordance with standard laboratory techniques. For immunofluorescent visualization of apoptosis and proliferation, the TdT-mediated dUTP nick-end labeling (TUNEL; Promega Corp.) assay and the EdU Click-iT Assay Kit (Thermo Fisher Scientific) was performed as described in the manufacturer's protocols, respectively. For the EdU assay, 10 μM of EdU was added to liquid MM for 24 h prior to fixation. Fluorescent slides were counterstained with DAPI (10 μg/mL in DPBS) for 5 min. All slides were viewed using a ZEISS Axio Imager. A2 Microscope and images were taken using ZEN 2 software (Zeiss). Standard microscope camera settings were used and scale bars were added using FIJI software (ImageJ).

Statistical Analysis

The number of biological replicates and types of statistical analyses for each experiment are indicated in the figure legends. All statistical analyses were performed using Prism (version 9.0, GraphPad Software Inc.). All results are presented as mean ± SEM where $p < 0.05$ was considered statistically significant.

RESULTS

Murine *Sox9*^{GFPHi} Chondrocytes Are Clonogenic in a Novel 3D *in vitro* Culture System

The main purpose of this study was to derive an *in vitro* method that recapitulated the 3D microenvironment to promote long-term retention of a chondrogenic phenotype at a single-cell level. To achieve this, chondrocytes were seeded at low density in methylcellulose (MC) reconstituted with Maintenance Media (MM) and cultured for 3–4 weeks (**Figure 1**). Once single cell-derived chondrogenic organoids, or chondrospheres, were established in MC, we transitioned the chondrospheres into liquid Maintenance Media to advance maturation for further assessment.

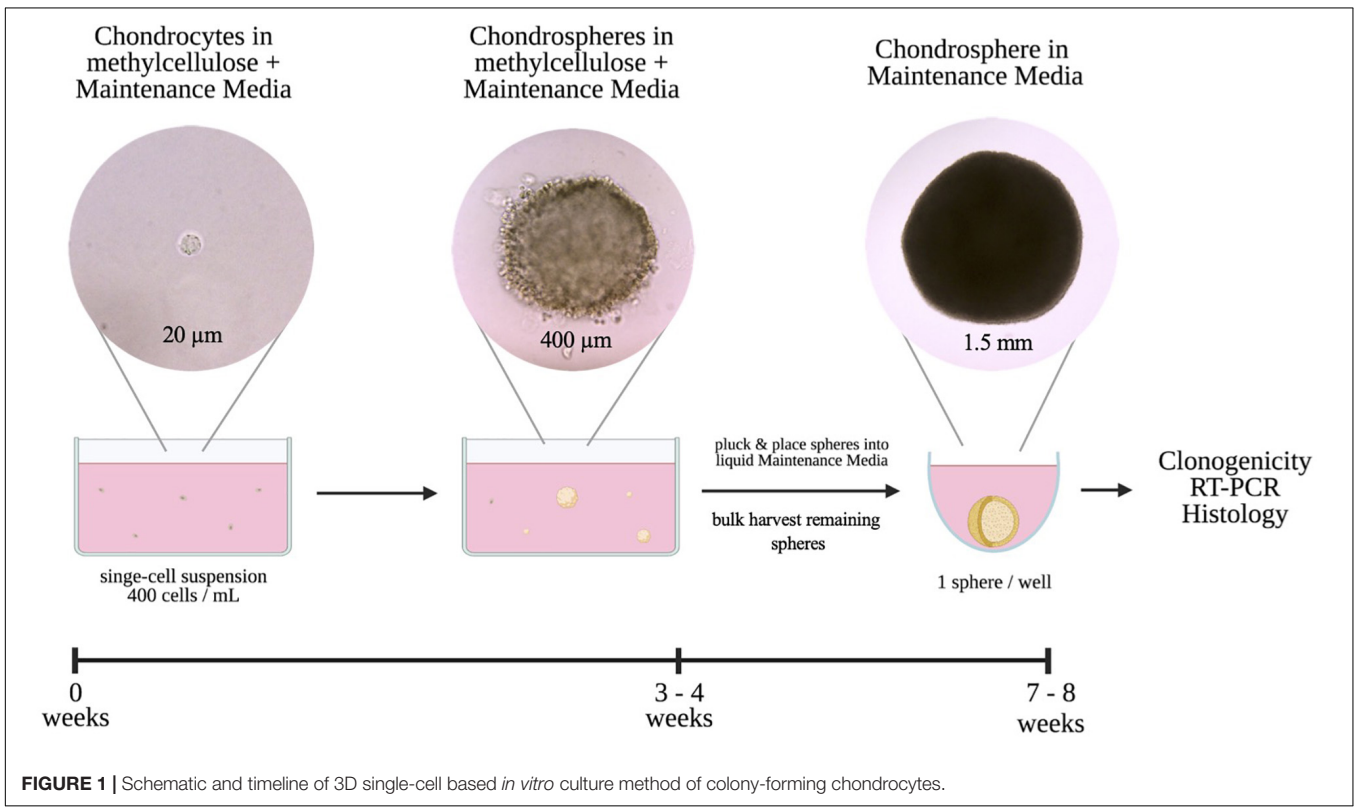

FIGURE 1 | Schematic and timeline of 3D single-cell based *in vitro* culture method of colony-forming chondrocytes.

As a proof of concept, we wanted to address which cells contribute to colony formation by utilizing the *Sox9*^{GFP} reporter mouse (**Figure 2**). Due to an abundance of chondrocytes within the femoral heads of postnatal day 7 (P7) pups (Blumer et al., 2007), we isolated and digested the femoral heads and plated the cells in MC to see if *Sox9* expression was retained. These cells formed large chondrospheres that maintained high levels of GFP expression after 4 and 8 weeks in culture

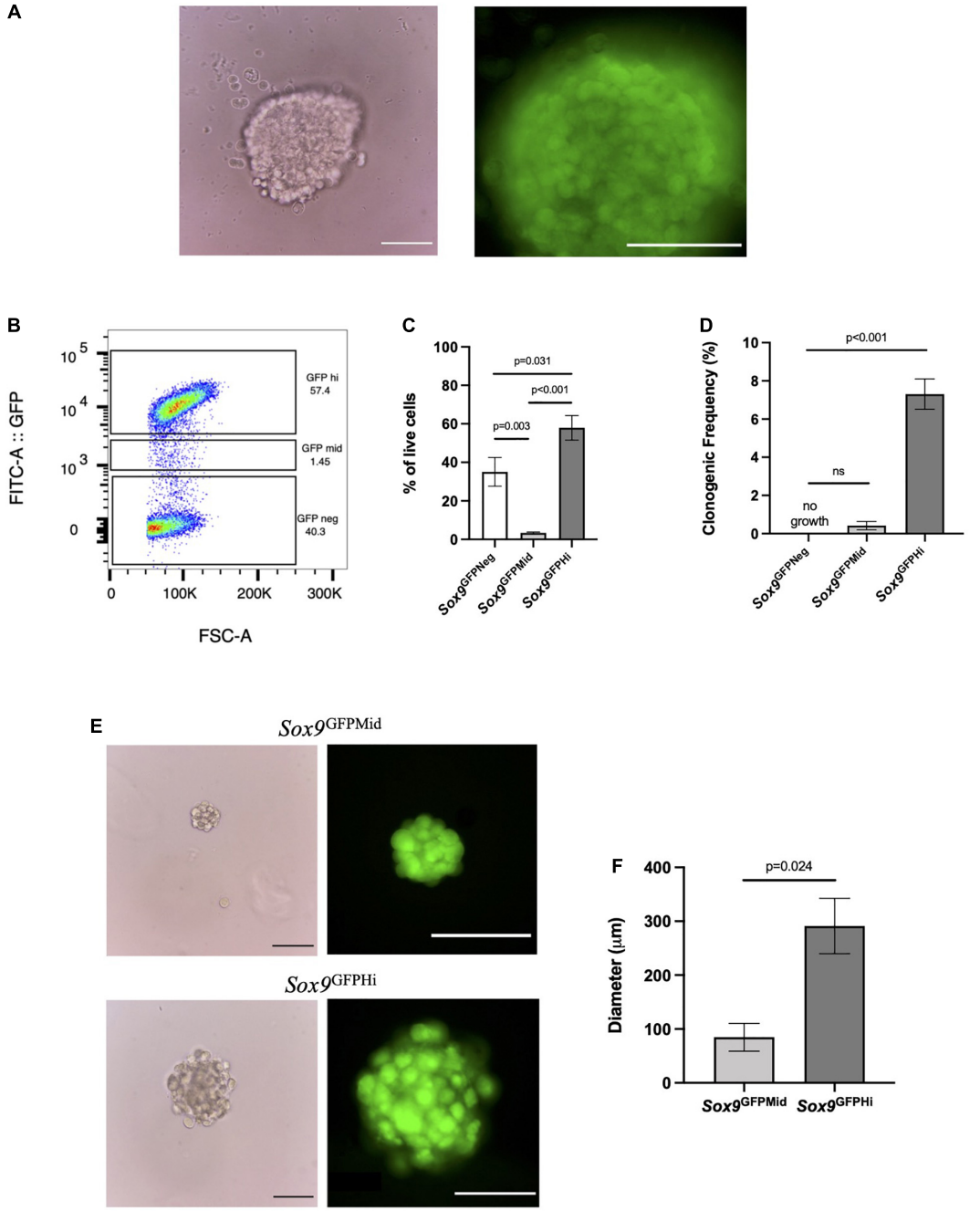

FIGURE 2 | *Sox9*^{GFPHi} chondrocytes demonstrate increased clonogenic and proliferative capacity. **(A)** Unsorted P7 *Sox9*^{GFP} femoral chondrocytes after 3 weeks in methylcellulose (MC), Scale bar = 100 μm. **(B)** Representative FACS gating strategy and **(C)** frequency of live cells in *Sox9*^{GFP} fractions; $n = 6$ biological replicates and p-values calculated using one-way ANOVA with Tukey's correction for multiple comparisons. **(D)** Clonogenicity of *Sox9*^{GFP} fractions in MC; $n = 3$ biological replicates and p-values calculated using One-Way ANOVA with Tukey's correction for multiple comparisons. **(E)** Representative images of mid (upper row) and high (lower row) *Sox9*^{GFP} chondrospheres in MC after 4 weeks, scale bar = 100 μm. **(F)** Average diameter of chondrospheres in MC, $n = 2$ biological replicates, p-value calculated with unpaired t-test. All error bars represent mean ± SEM.

(**Figure 2A** and **Supplementary Figure 1A**, respectively). To interrogate if there were specific populations of *Sox9*-expressing cells generating the chondrogenic organoids, we fractionated cells via FACS based on level of *Sox9* expression into negative, mid or high GFP expression (**Figure 2B**) using wildtype P7 femoral head cells as a control (**Supplementary Figure 1B**). The negative and high fractions of *Sox9*^{GFP} cells represented about 40 and 57% the of the population, respectively, whereas the mid fraction represented less than 10% of live cells (**Figure 2C**), indicating an enrichment of *Sox9*^{GFPHi} cells endogenously found within the femoral heads. We plated the fractionated groups in MC, and after 4 weeks in MC, clonogenic frequency was assessed. A significant trend between increased clonogenicity and high *Sox9* expression was observed (**Figure 2D**), whereas cells in the *Sox9*^{GFPNeg} did not form any colonies. Furthermore, *Sox9* expression was detected in both the *Sox9*^{GFPMid} and *Sox9*^{GFPHi} fractions after culture in MC (**Figure 2E**), but the average diameter of the *Sox9*^{GFPHi} chondrospheres was about three-fold higher than the *Sox9*^{GFPMid} chondrospheres (**Figure 2F**), suggesting increased proliferative and/or matrix deposition capacity associated with *Sox9* expression, a trend also seen in the proliferating chondrocytes of the growth plate (Dy et al., 2012).

To better understand the differentiation pathways of the *Sox9*^{GFPHi} chondrospheres, transcriptomic analyses were performed. We used RNA-sequencing to compare the *Sox9*^{GFPHi} chondrospheres with previously published datasets using murine synovial fibroblasts to represent dedifferentiated chondrocytes commonly seen in long-term 2D culture (Saeki and Imai, 2020), and murine chondrocytes cultured in a 3D pellet assay designed for hypertrophic differentiation to represent terminally differentiated chondrocytes (Singh et al., 2021). The heat map for gene expression of selected chondrogenic genes indicated a clear enrichment in the *Sox9*^{GFPHi} chondrospheres after long-term *in vitro* culture when compared to fibroblasts or hypertrophic, pelleted chondrocytes (**Figure 3A**). Furthermore, Gene Ontology (GO) analyses of the genes significantly enriched (>5 fold-change, FDR < 0.01) in *Sox9*^{GFPHi} chondrospheres versus fibroblasts yielded categories related to cartilage and chondrocyte development, as well as extracellular matrix organization (**Figure 3B**). Conversely, when observing the genes significantly enriched in the hypertrophic pellet versus the *Sox9*^{GFPHi} chondrospheres, categories such as chondrocyte differentiation, ossification, and apoptotic process were upregulated (**Figure 3C**).

We then wanted to further validate the trends seen in the transcriptomic analyses via quantitative PCR performed on freshly isolated and cultured fractions of *Sox9*^{GFP} femoral chondrocytes (**Figure 3D**). Genes such as *Col2a1* and *Acan* in the freshly isolated *Sox9*^{GFPHi} fraction showed increased trends compared to freshly isolated *Sox9*^{GFPNeg} fraction and was maintained in the cultured *Sox9*^{GFPMid} and *Sox9*^{GFPHi} fractions. No cell growth was seen in the plated *Sox9*^{GFPNeg} fraction. *Col1a1* expression was relatively unchanged in the cultured chondrocytes, whereas *Col10a1* was enriched in both the freshly isolated and cultured *Sox9*^{GFPHi} cells (**Figure 3D**), suggesting that this culture system allows for natural differentiation of chondrocytes that are found in the femoral head. Of note, *Sox9* gene expression of freshly isolated *Sox9*^{GFPMid} chondrocytes was more akin to the *Sox9*^{GFPNeg} fraction, however, after 4 weeks in MC, cultured *Sox9*^{GFPMid} chondrocyte gene expression was more similar to the plated *Sox9*^{GFPHi} fraction, despite their differences in clonogenicity and size (**Figures 2D,F**).

To assess the quality of matrix formed and organizational structure within the *in vitro* mouse chondrogenic organoids, we histologically compared *Sox9*^{GFP} chondrospheres grown for 8 weeks total to P7 femoral heads. Interestingly, the chondrospheres stained for GAGs comparably to femoral heads (**Figure 4A**) and collagen II was detected throughout the spheres (**Figure 4B**, upper right panels), but largely localized to the periphery as seen in the femoral head. Sox9 expression was also detected in the chondrospheres, as well as collagen X expression similar to the femoral head (**Figure 4B**, lower row). Both the mouse chondrospheres and the femoral head strongly stained for aggrecan (**Figure 4B**). When assessing apoptosis within the chondrospheres, TUNEL staining was sparse and randomly patterned, dissimilar to the centralized cell death observed in conventional aggregate pellet cultures (**Figure 4C**, left and middle; Weissenberger et al., 2020). Cell proliferation was observed at the periphery of the spheres (**Figure 4C**, right). Taken together, these results show that chondrocytes can form large and zonally structured multicellular organoids from a single cell *in vitro* and that the *Sox9*^{GFPHi} fraction exhibits the highest clonogenicity and chondrogenic capacity. Previously published literature states that colony-forming units in hematopoietic and mesenchymal systems are only typical for progenitor cells (Friedenstein et al., 1974; Sacchetti et al., 2007; Frisch and Calvi, 2014), suggesting that this system is preferentially selecting, based on their *in vivo* function, for the most immature chondrocytes with colony-initiating potential.

Because proliferative capacity of chondrocytes declines with age, we assessed levels of *Sox9*^{GFPHi} cells in the mouse knee joints at different stage of ontogeny. We digested knee joints of young adult mice (4 months old) and mature adult mice (1.5 years old) and assessed GFP levels in the lineage negative fraction ($CD45^-/CD31^-/Ter119^-$; **Figure 5**). Interestingly, *Sox9* expression shifted to favor the *Sox9*^{GFPMid} fraction in young adult mouse knee joints, and the *Sox9*^{GFPHi} fraction in knee joint was almost non-existent in mature adult mouse knee joints (**Figures 5A–D**). Furthermore, qPCR showed that the *Sox9*^{GFPHi} fraction isolated from young adult knees had the most chondrogenic gene expression except for *Prg4* (**Figure 5E**). When assessing gene expression in *Sox9*^{GFPNeg} and *Sox9*^{GFPMid} fractions of mature adult mouse knee joints, most chondrogenic genes were not detectable or not statistically significantly different from the *Sox9*^{GFPNeg} fraction (**Supplementary Figure 1C**). Altogether, this decrease in *Sox9* expression could indicate that a significant fraction of *Sox9*-expressing cells in the knee joint is lost with age.

Human Articular Chondrocytes of All Ages Have Clonogenic Capacity

Given that genetic reporters are not available for clinically relevant chondrocytes, we wanted to assess whether this *in vitro* culture system could be used to select for human colony-forming chondrocytes. Articular chondrocytes isolated from

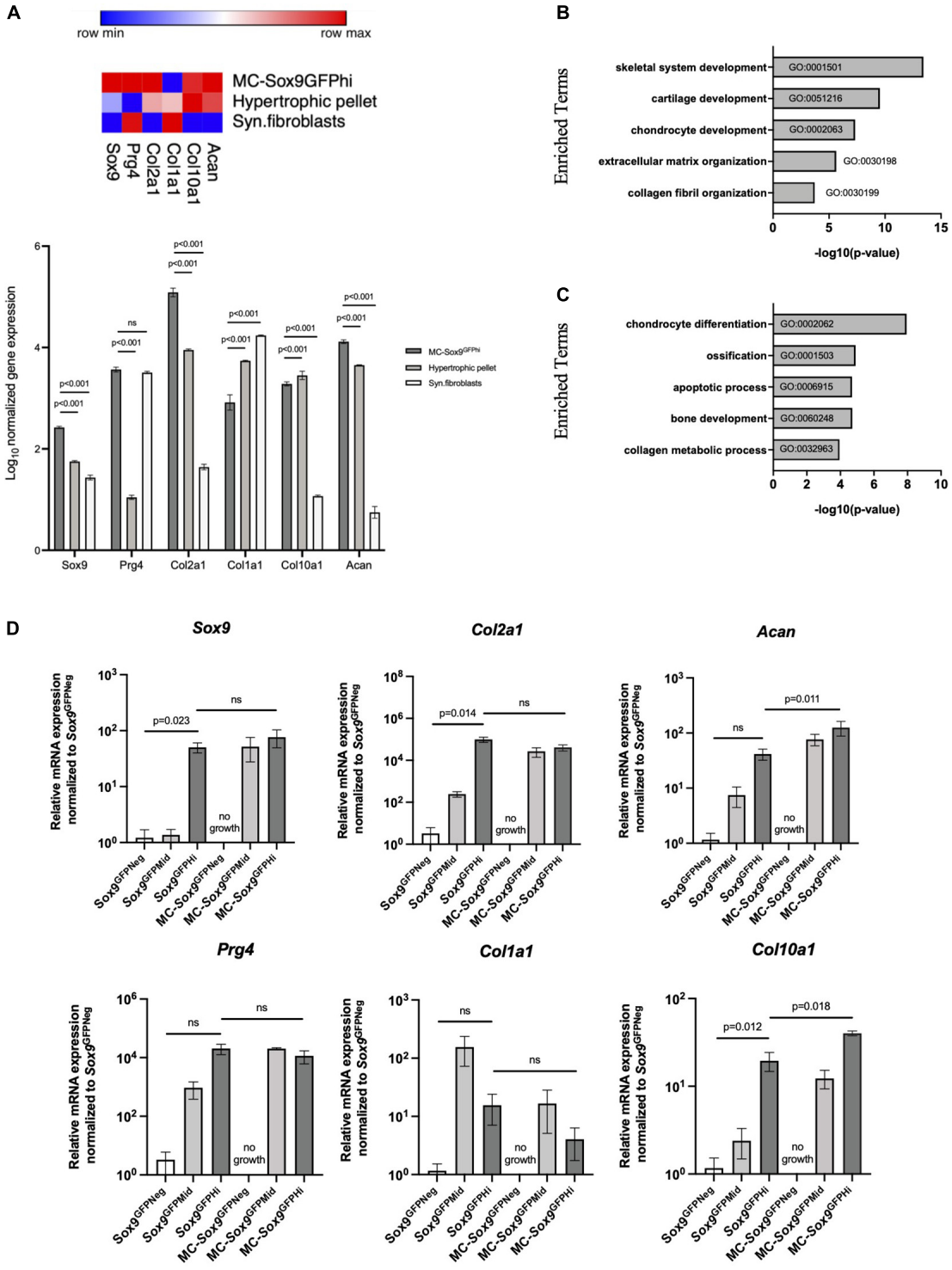

FIGURE 3 | *Sox9*^{GFP} chondrocytes cultured in 3D culture maintain chondrogenic gene expression. **(A)** Heatmap and quantification showing the normalized bulk-sequencing gene expression profile for selected chondrogenic genes in *Sox9*^{GFPHi} chondrospheres, hypertrophic pellet, and synovial fibroblasts (Saeki and Imai, 2020 and Singh et al., 2021, respectively). Color scale denotes the minimum (blue) and maximum (red) expression value across each row. *P*-values were calculated with two-way ANOVA with Tukey's correction for multiple comparisons. **(B)** Gene Ontology analysis showing enriched terms of *Sox9*^{GFPHi} chondrospheres versus synovial fibroblasts ($n = 2$ and 3, respectively). **(C)** Gene Ontology analysis showing enriched terms of hypertrophic pellets versus *Sox9*^{GFPHi} chondrospheres ($n = 3$ and 2, respectively). **(D)** Quantitative PCR analyses of chondrocyte-specific genes after normalizing expression to freshly isolated *Sox9*^{GFPNeg} chondrocytes; $n = 4$ biological replicates for freshly isolated *Sox9*^{GFP} fractions, $n = 2$ biological replicates for MC – *Sox9*^{GFP} fractions. *P*-values were calculated with one-way ANOVA with Tukey's correction for multiple comparisons; all error bars represent mean ± SEM.

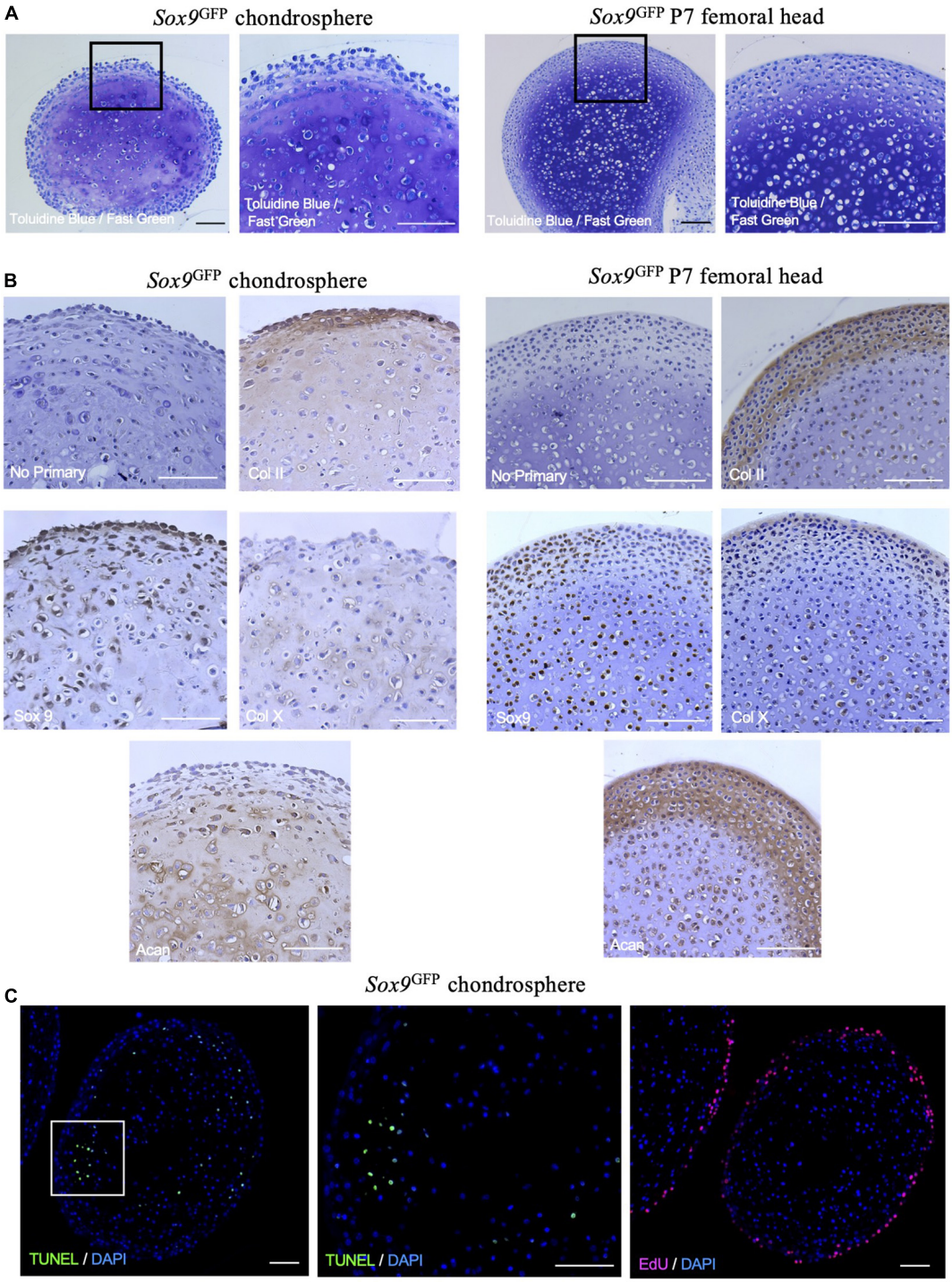

FIGURE 4 | *Sox9*^{GFP} chondrospheres self-organize and form extracellular matrix similar to native femoral head after 8 weeks in culture. **(A)** Toluidine Blue/Fast Green staining for GAGs in *Sox9*^{GFP} chondrospheres (left) and P7 femoral head (right). **(B)** Immunohistochemistry of collagen II, Sox9, collagen X, and aggrecan in *Sox9*^{GFP} chondrospheres (left) and P7 femoral head (right). No primary antibody staining is provided as a negative control. **(C)** TUNEL staining to detect apoptosis (left, middle) and EdU staining to detect proliferation (right) in *Sox9*^{GFP} chondrospheres. Scale bar = 100 μm.

human young adult and mature adult were plated in our method (**Figure 6**). Intriguingly, we found that both age groups had cells capable of forming clones (**Figure 6A**). The young and mature adult chondrocytes had similar clonogenic frequency (**Figure 6B**), and for all tested donors only a very small percentage (around 5% or less) of articular chondrocytes

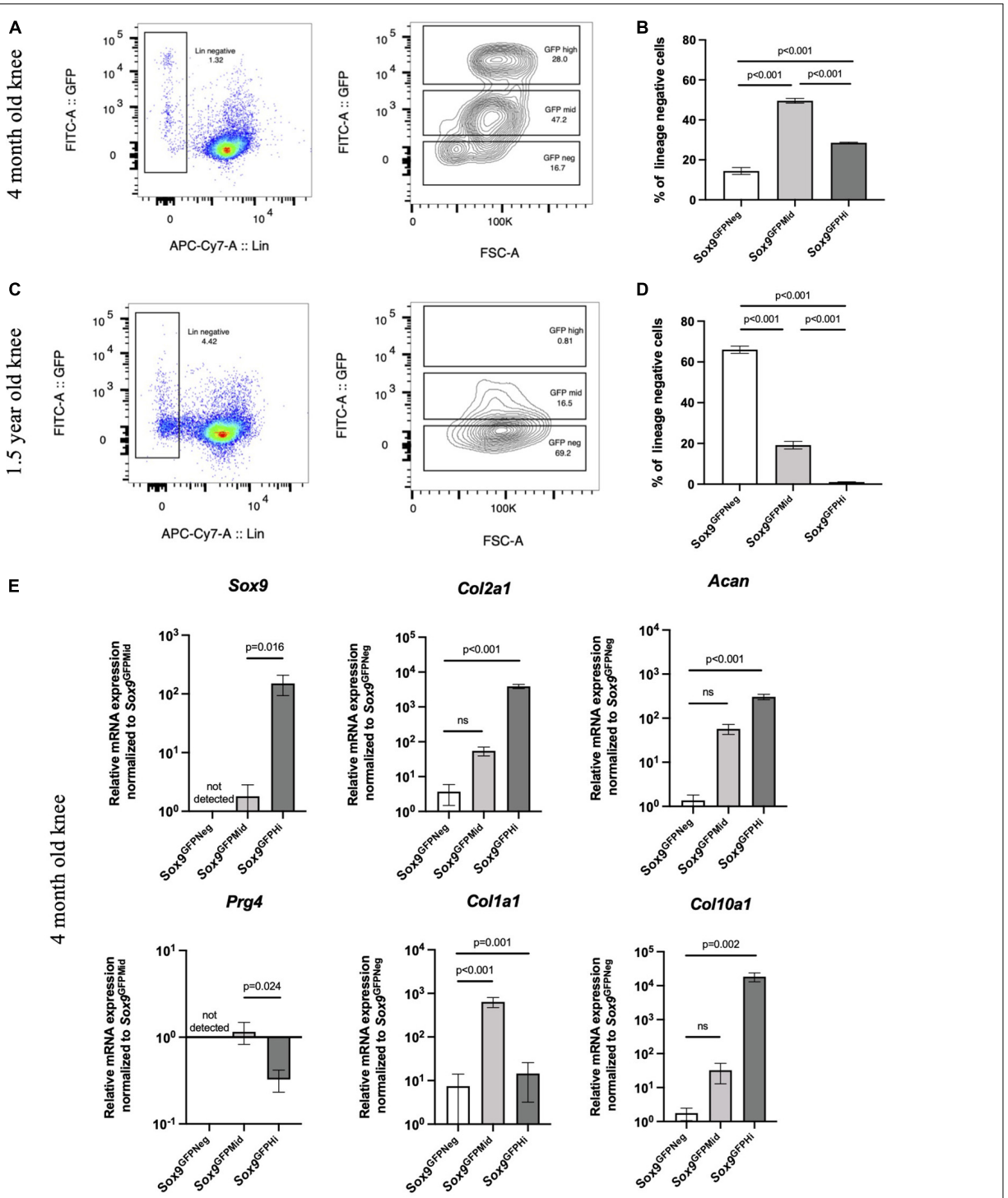

FIGURE 5 | *Sox9*^{GFPHi} cells in the knee joint show highest chondrogenic gene expression but diminish with age. Representative FACS plot **(A)** and quantification **(B)** of *Sox9*^{GFP} levels in 4 months old *Sox9*^{GFP} knee joint; $n = 3$ biological replicates. Representative FACS plot **(C)** and quantification **(D)** of GFP levels in 1.5 years old *Sox9*^{GFP} knee joint; $n = 3$ biological replicates. **(E)** qPCR of chondrogenic genes in 4 months old *Sox9*^{GFP} cells in the knee joint, $n = 6$ biological replicates. Data represented as mean ± SEM and all *p*-values calculated using one-way ANOVA with Tukey's correction for multiple comparisons.

formed multicellular organoids. Young adult chondrocytes formed significantly larger chondrospheres than mature adult chondrocytes (**Figure 6C**), and further analysis via qPCR showed that chondrogenic genes *SOX9*, *COL2A1*, and *ACAN* were maintained compared to freshly isolated cells (**Figures 6D,E**). However, while *COL1A1* and *COL10A1* showed upward trends in

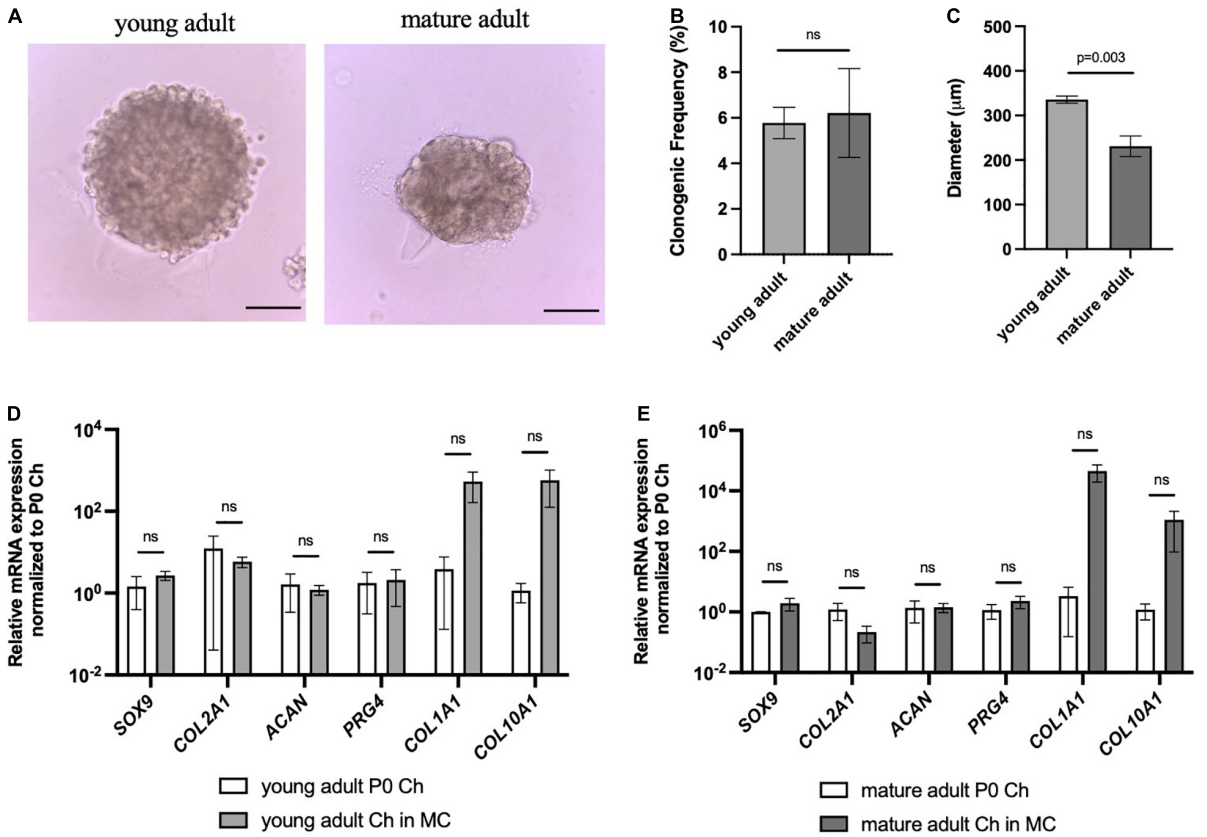

FIGURE 6 | Human articular chondrocytes of different ages demonstrate clonality and retention of chondrogenic genes in 3D culture. **(A)** Representative images of young and mature adult chondrospheres in MC after 4 weeks, scale bar = 100 μm. **(B)** Clonogenic frequency of chondrocytes in MC, $n = 2$ biological replicates. **(C)** Diameter of chondrospheres of young and mature adult chondrospheres in MC, $n = 2$ biological replicates. qPCR of chondrogenic genes in young adult **(D)**, and mature adult **(E)** chondrospheres cultured in MC after normalizing expression to freshly isolated chondrocytes of respective samples, $n = 2$ biological replicates. Data represented as mean ± SEM and *p*-values calculated using an unpaired *t*-test.

culture, these results were not statistically significant. These data indicate that while key chondrogenic genes are not lost, further optimization is needed to ensure that human chondrospheres do not transition into a fibrocartilage or hypertrophic phenotype.

Porcine Articular Chondrocytes Maintain Chondrogenic and Clonogenic Capacity

Next, we wanted to assess whether articular chondrocytes from a large animal used to model cartilage repair and arthritis can respond to the microenvironment of our 3D culture system. Chondrocytes isolated from porcine articular cartilage were cultured in MC for 3 weeks, where sizable chondrogenic organoids were formed (**Figure 7A**, left). Clonogenic frequency was similar to the *Sox9*^{GFPHi} fraction in mouse at 8–10% (**Figure 7B**). These porcine chondrospheres further grew in liquid Maintenance Media, reaching up to 1–1.5 mm in diameter (**Figure 7A**, right; **Figure 7C**), and compared to freshly isolated articular chondrocytes, chondrogenic gene expression was maintained even after long-term culture in our system (**Figure 7D**). *PRG4* expression decreased with culture in MC, however, began to increase back to native levels in the liquid phase of culture, suggesting reactivation of articular surface-specific markers.

To further confirm that porcine articular chondrocytes retained their chondrogenic features after culture, we histologically assessed chondrospheres generated after 7- and 10-weeks (**Figure 8**). Similar to the P7 mouse chondrocytes, articular chondrocytes stained strongly for GAGs at both 7 and 10 weeks of culture (**Figure 8A**). Of note, immunohistochemical staining indicated that collagen II expression was present on the majority of chondrocytes, whereas SOX9 expression was enriched after 7 weeks but diminished at 10 weeks (**Figure 8B**), potentially reflecting the maturation process. Collagen I was also detected at minimal levels in pockets (**Figure 8B**), suggesting little to no fibrocartilage formation. TUNEL staining showed minimal and sparse pockets of apoptotic cells at both 7 and 10 weeks in culture (**Figure 8C**), suggesting retention of viability in the center of the sphere where hypoxia and lack of nutrients are often observed in larger aggregates (Ware et al., 2016). Proliferating chondrocytes at the periphery of the chondrogenic organoids were still detected after 10 weeks of culture in our system (**Figure 8D**). Altogether, these data reveal that this culture system can mimic a native niche to support clonogenic,

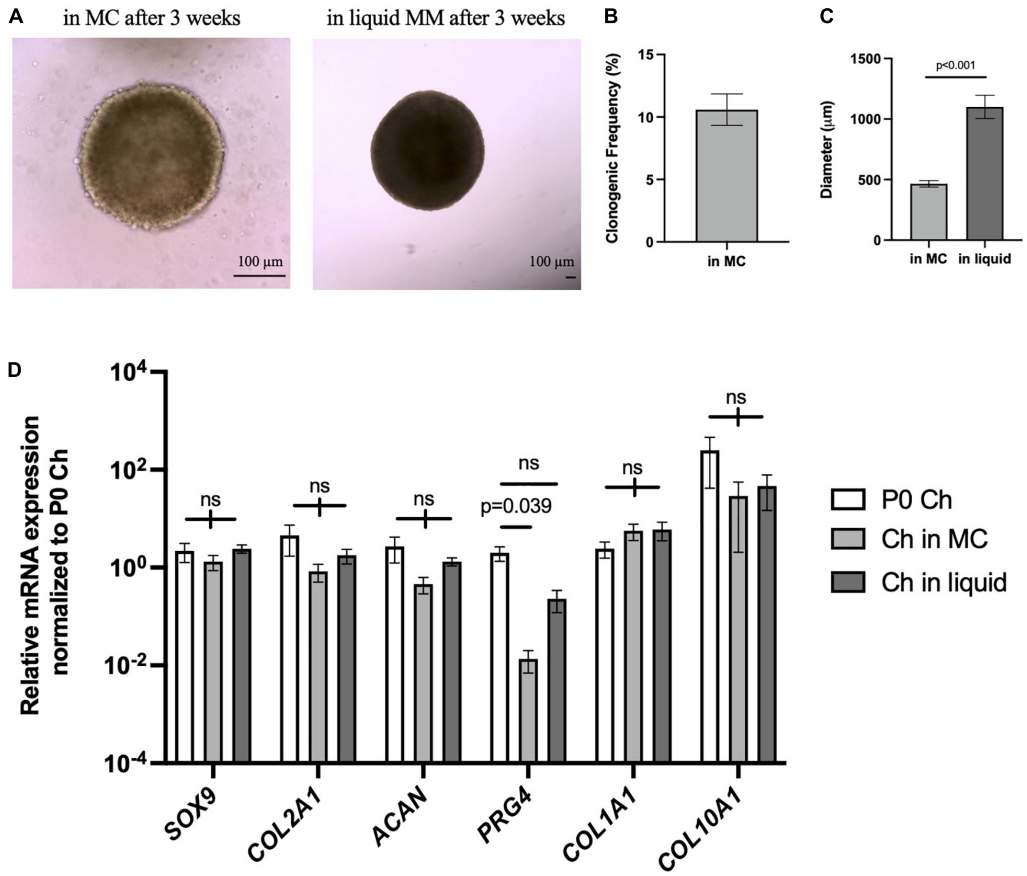

FIGURE 7 | Porcine articular chondrocytes proliferate and maintain chondrogenic identity in 3D culture. **(A)** Representative images of pig chondrospheres in MC after 3 weeks (left) and after transition into liquid media for an additional 3 weeks (right); scale bar = 100 µm. **(B)** Clonogenic frequency of chondrospheres in MC, $n = 9$ biological replicates. **(C)** Average diameter of chondrospheres in MC versus liquid; $n = 9$ biological replicates, p-value calculated using an unpaired t-test. **(D)** qPCR of chondrogenic genes after normalizing expression to freshly isolated P0 chondrocytes; $n = 9$ biological replicates and p-value calculated by two-way ANOVA with Tukey's correction for multiple comparisons. All data represented as mean ± SEM.

colony-forming chondrocytes from a large animal, offering a customizable system that can be further used to interrogate pathophysiological environments.

Arthritis in a Dish: Microenvironmental Cues Can Be Modified to Mimic Pro-degenerative Stimuli

After demonstrating that articular chondrocytes can form cartilage-like structures in our *in vitro* system, we then started manipulating microenvironmental factors to mimic a pro-inflammatory environment observed in arthritic joints. Porcine articular chondrocytes were cultured for 3 weeks in MC and transferred into liquid Maintenance Media for 1 week before the addition of the pro-inflammatory cytokine OSM for an additional 3 weeks (**Figure 9A**). Compared to chondrogenic organoids maintained in MM alone, chondrospheres exposed to pro-inflammatory cytokine OSM showed decreased density and size (**Figures 9B,C**). In response to OSM exposure, qPCR demonstrated that the spheres significantly downregulated chondrogenic genes *ACAN* and *COL2A1* but only marginally decreased *SOX9* expression (**Figure 9D**), an observation consistent with the early stages of osteoarthritic cartilage degeneration (Zhang et al., 2015). Although *COL1A1* was unchanged upon OSM treatment, significant *ADAMTS5* and *MMP13* upregulation indicated activation of catabolic pathways seen in degenerating cartilage (**Figure 9E**; Chan et al., 2017). The *COL2A1/ COL1A1* ratio also showed a significant decrease in collagen II expression upon OSM exposure (**Figure 9F**), demonstrating a shift in the overall matrix composition. These results highlight the responsiveness of articular chondrocytes to pro-inflammatory stimuli most commonly found in diseased settings, showing a proof of concept for creating a dynamic and customizable *in vitro* readout for manipulating the joint niche. This will allow for assessment of genetic and microenvironmental factors that promote arthritic phenotypes in chondrocytes.

DISCUSSION

In this study, we have shown that chondrocytes can be cultured at a single-cell level in a 3D environment that recapitulates the *in*

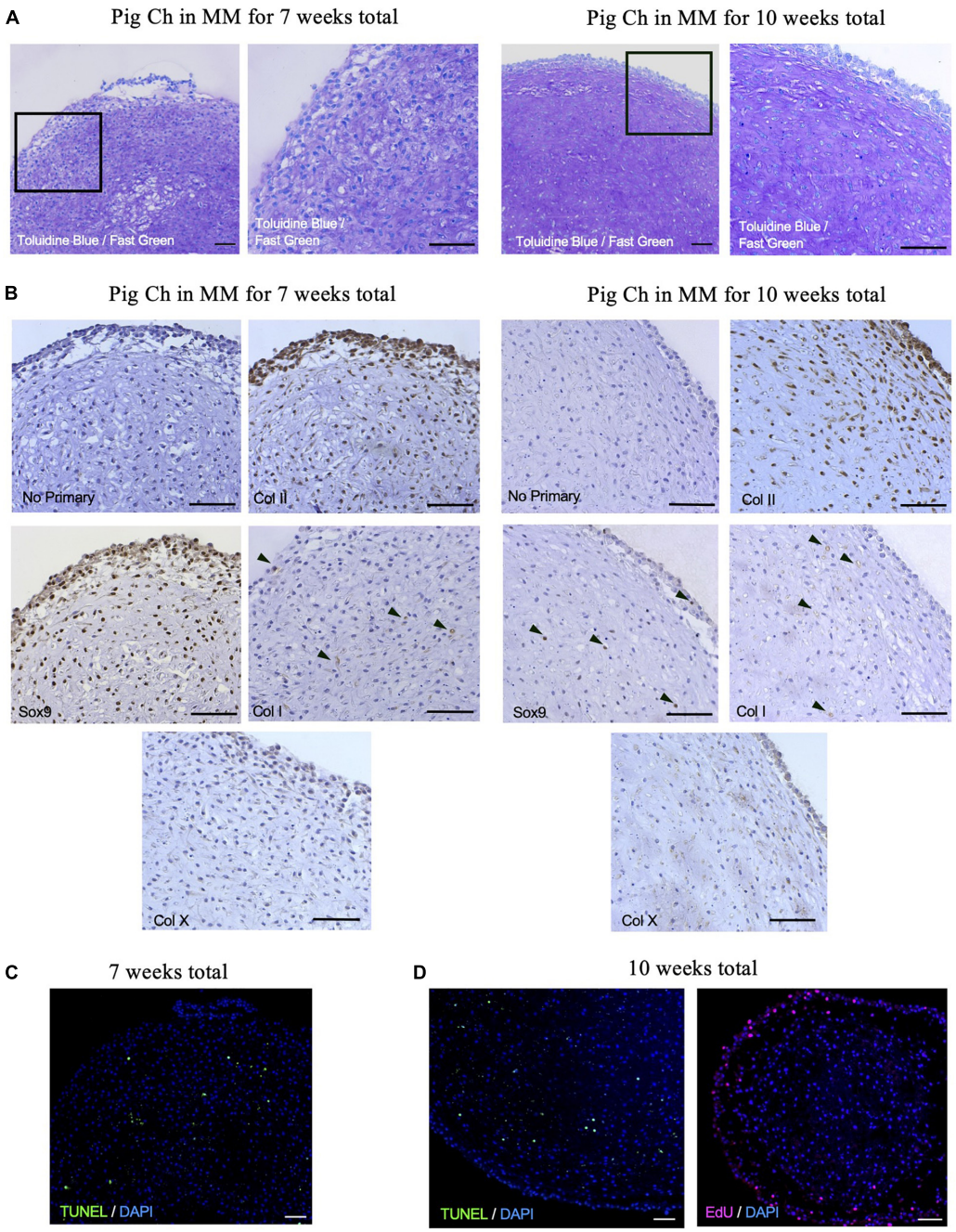

FIGURE 8 | Porcine articular chondrospheres self-organize and deposit extracellular matrix. **(A)** Toluidine Blue/Fast Green staining for GAGs in pig articular chondrospheres cultured for 7 weeks (left) or 10 weeks total (right). **(B)** Immunohistochemistry of collagen II, Sox9, collagen I, and collagen X in pig articular chondrospheres cultured for 7 weeks (left) or 10 weeks total (right). Black arrows demarcate positive staining, no primary antibody staining is provided as a negative control. **(C)** TUNEL staining to detect apoptosis shown in chondrospheres cultured for 7 weeks. **(D)** TUNEL staining (left) and EdU staining to detect proliferation (right) shown in chondrospheres cultured for 10 weeks. Scale bar = 100 μm.

vivo niche, permitting them to retain their chondrogenic identity *in vitro*. We have demonstrated that three different species representing both small and large animals, as well as clinically relevant cells from human, show retention of the chondrogenic phenotype which allow for assessment of cells that can be genetically modified to interrogate molecular mechanisms of cellular regeneration and response to pro-inflammatory stimuli. While the use of methylcellulose culture has been described for assessing clonogenicity in hematopoietic cells (Matsui et al., 2004; Li et al., 2013), here it is used in conjunction with Maintenance Media, which provides chondrogenic factors and other factors preventing chondrocyte maturation (LIF) produced by synovial cells of both young and adult joints (Wu et al., 2013). Our *in vitro* model contributes to the maintenance of clonogenic

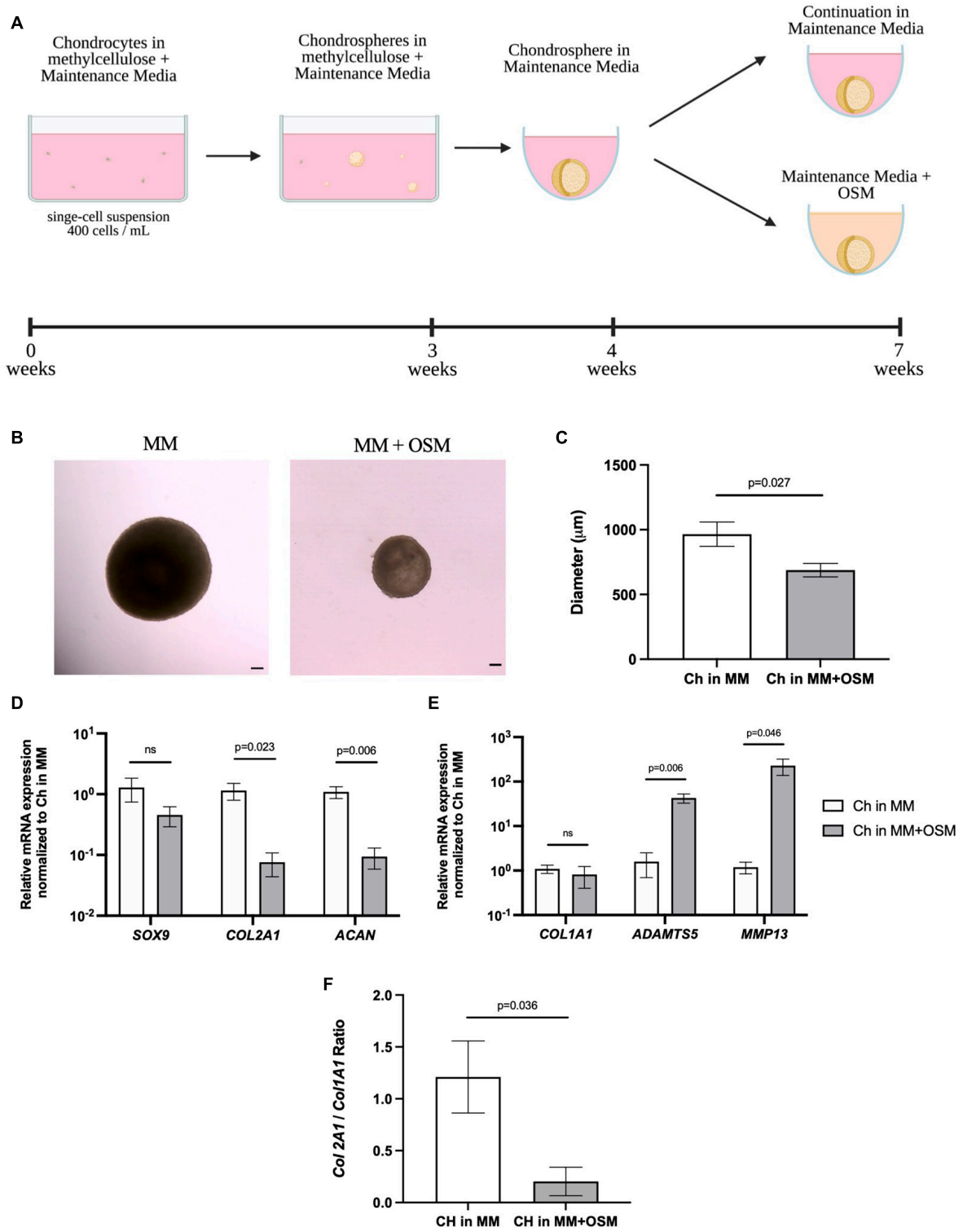

FIGURE 9 | Porcine articular chondrospheres degrade and upregulate catabolic genes in response to pro-inflammatory stimuli. **(A)** Schematic and timeline of MC with MM culture method and introduction of pro-inflammatory cytokine OSM at 4 weeks. **(B)** Representative images of a pig articular chondrospheres in liquid MM alone (left) or liquid MM + OSM (right) after 3 weeks exposure, scale bar = 100 μm. **(C)** Average diameter of chondrospheres cultured in liquid MM or MM + OSM. **(D)** qPCR of anabolic genes after normalizing expression to chondrospheres cultured in MM alone, $n = 4$ biological replicates. **(E)** qPCR of catabolic genes after normalizing expression to chondrospheres cultured in MM alone, $n = 4$ biological replicates. **(F)** Collagen II/Collagen I ratio for chondrospheres in MM alone versus MM + OSM, $n = 4$ biological replicates. All data are represented as mean ±SEM and p-value calculated using an unpaired t-test.

colony-forming chondrocytes found in articular cartilage without promoting a fibrotic or hypertrophic phenotype, thus providing a more favorable physiological niche than traditional 2D culture systems allow. *In vivo* assays to assess feasibility and integration of chondrospheres into cartilage defects would be valuable and is our future direction, where improved production of large chondrospheres from patient autologous bio-specimens generated in this method has the potential to be therapeutically relevant for articular cartilage repair.

Based on the retention and selectivity of high *Sox9*^{GFP} expression in juvenile mouse femoral cells cultured in this method, it is likely that this culture system is only permissive for cells of chondrogenic lineage that are immature in nature. Deletion of *Sox9* in aggrecan-expressing cells inhibits chondrogenesis and chondrocyte proliferation (Akiyama et al., 2002; Dy et al., 2012), whereas a decrease in *Sox9* at different stages of development is essential for progression to a terminally differentiated, hypertrophic state (Leung et al., 2011). Because *Sox9* expression is retained even after 4 weeks in our culture system, it is feasible that this retention correlates to selection of an immature chondrocyte with minimal hypertrophy, our system recapitulating a progenitor niche, or a combination of both. Additionally, *Sox9*^{GFPHi} cells are minimally present in the articular cartilage of aged 1.5 years old mice. This finding is consistent with our previous studies in humans, showing that the percentage of SOX9 cells declines with age, and cells with high levels of SOX9 expression also express other progenitor markers such as GLI1, BMPR1B, and Integrin alpha 4, as well as activated STAT3 signaling (Ferguson et al., 2018).

Due to the natural development of the juvenile femoral head, there will be *Sox9*-expressing pre-hypertrophic cells, osteochondral precursor cells, and mesenchymal stromal cells that may co-express GAGs and collagen X where the secondary ossification center will form (Blumer et al., 2007; Madsen et al., 2011; Yen et al., 2021), which could explain the high gene expression levels of *Col10a1* seen by qPCR and RNA sequencing in both the freshly isolated and cultured *Sox9*^{GFPHi} fraction, respectively. Indeed, we observed the most differentiated, pre-hypertrophic/hypertrophic-like cells localized to the middle of the chondrogenic organoid. The immature and actively proliferating cells were found in the peripheral zone, concurrent with rare progenitor cells found on the superficial articular surface (Shwartz et al., 2016; Li et al., 2017), further suggesting self-organization of the cells *in vitro*. The increased expression levels of *Col1a1* within the *Sox9*^{GFP} mid fraction assessed by qPCR could also be due to a contamination of the *ligamentum teres femoris* when processing the femoral heads. Because this culture system is likely not permissive for cell types outside of the chondrocyte lineage, *Col1a1* expression in the *Sox9*^{GFPMid} or *Sox9*^{GFPHi} fraction is not maintained after culture. Overall, our data shows that *Sox9* expression correlates with the highest clonal and chondrogenic capacity and these cells are exclusively selected for in this system, allowing for future assessment of subpopulations found in immature clonogenic chondrocytes to advance our understanding of what drives regenerative potential.

Interestingly, human articular chondrocytes from young and mature adults demonstrate clonality in this culture system, but the percentage of cells with colony forming potential was relatively low in all tested specimens. Moreover, cultured cells showed an upward trend in *COL1A1* and *COL10A1* gene expression compared to freshly isolated cells, but neither the young or mature groups were statistically significant. Adult human cells did not show the same level of proliferation as the chondrocytes isolated from mice or pigs. Despite the multi-cellular appearance, no human chondrospheres of the age groups were large enough to move into the liquid phase of culture. This indicates the necessity of further optimization of culture conditions such as additional proliferation-inducing factors, or a hypoxic environment, which has also been shown to increase matrix accumulation specifically for human cell culture (Markway et al., 2013). Continual studies to further advance this culture technique for human cells are ongoing. Nevertheless, chondrogenic genes specific for hyaline-like cartilage were maintained, indicating some retention of a healthy chondrogenic phenotype.

It was interesting that porcine articular chondrocytes, considered a cell with limited self-renewal capacity, proliferated to such great extent that we observed. While it should be noted that porcine articular cartilage has been shown to spontaneously heal partial-thickness cartilage defects without bone marrow stimulation (Fisher et al., 2015), the level of growth observed in porcine articular chondrocytes was impressive. Diameters of up to 1–1.5 mm were reached with maintenance of chondrogenic genes expression, signifying highly anabolically active chondrocytes even after 6 weeks of total culture time. *COL10A1* expression was endogenously high in freshly isolated porcine articular chondrocytes, which have been previously described (Rucklidge et al., 1996), but could also be attributed to our chondrocyte harvest method including some hypertrophic chondrocytes found just above the subchondral bone. We did not detect hallmark fibrocartilage features as seen with minimal collagen I staining and *COL1A1* expression, supporting the superiority of our long-term culture method compared to 2D culture where cells rapidly de-differentiate and loose heir chondrogenic identity. Although there was a decrease in Sox9 detected via IHC by 10 weeks culture time, proliferative cells were still detected at the periphery of the chondrosphere as well as heavy GAG staining, validating our culture system's ability to recreate a niche that supports progenitor cells long-term.

When looking at functional outcomes of porcine chondrospheres assessed in the arthritis in a dish model, exposure to the pro-inflammatory cytokine OSM significantly decreased the density and size of the spheres and upregulated catabolic genes most associated with ECM degradation and osteoarthritis (Heinegård and Saxne, 2011). This switch from anabolic to catabolic mechanisms of the chondrospheres due to OSM exposure supports previous data that show a decrease in aggrecan and TGF-β1 in chondrocytes cultured in 3D with OSM (Sanchez et al., 2004). This demonstrates the *in vitro* system's capability of customization and multiplexing pro-inflammatory stimuli to assess potential anti-inflammatory or protective signaling in clinically relevant cells. Small molecule screening or cellular pathway inhibition are our future directions in further developing this readout for modulating outcomes of chondrospheres exposed to pro-inflammatory stimuli.

Altogether, this novel *in vitro* culture system offers a robust and controllable system that can provide essential niche signaling to support and maintain colony forming chondrocytes at a single-cell level. Continual optimization will allow us to further perturbate responses of different chondrocyte subsets to extracellular stimuli in an *in vitro* model, which will be of great value for future genetic modifications to define genes required for regeneration in chondrocytes or development of new treatments specifically designed to enhances endogenous regenerative potential of articular cartilage tissue in diseases such as osteoarthritis.

DATA AVAILABILITY STATEMENT

The datasets presented in this study can be found in online repositories. The names of the repository/repositories and accession number(s) can be found below: https://www.ncbi.nlm.nih.gov/geo/, GSE184561.

ETHICS STATEMENT

The animal study was reviewed and approved by the Institutional Animal Care and Use Committee of USC.

AUTHOR CONTRIBUTIONS

JT, BV, and DE conceptualized the study and interpreted the data. JT, AS, JL, and SL performed the experiments. JT wrote the manuscript. BV and DE revised and approved the manuscript. All authors contributed to the article and approved the submitted version.

FUNDING

Research reported in this publication was supported by the following funding sources: National Institutes of Health grant R01AR071734 (DE), National Institutes of Health grant R01AG058624 (DE), Department of Defense grant W81XWH-13-1-0465 (DE), and California Institute for Regenerative Medicine grant TRAN1-09288 (DE).

ACKNOWLEDGMENTS

All schematics were created with Biorender.com. We thank the USC Stem Cell Flow Cytometry Core for their assistance and support.

SUPPLEMENTARY MATERIAL

The Supplementary Material for this article can be found online at: https://www.frontiersin.org/articles/10.3389/fcell.2021.725854/full#supplementary-material

Supplementary Figure 1 | Supplemental characterization of Sox9GFP chondrospheres, femoral head, and knee joints. **(A)** Representative FACS analysis of dissociated Sox9GFP spheres after 8 weeks total culture. **(B)** Representative FACS plot of GFP expression in wild-type P7 femoral head cells (left) and quantification (right) as percentage of live cells; $n = 4$ biological replicates, p-values calculated using one-way ANOVA with Tukey's correction for multiple comparisons. **(C)** qPCR of chondrogenic genes in 1.5-year-old Sox9GFP cells in the knee joint, $n = 3$ biological replicates. Data are represented as mean ±SEM and p-values calculated using an unpaired t-test.

Supplementary Table 1 | qPCR primer sequences.

Supplementary Table 2 | Antibodies used for IHC.

REFERENCES

Akiyama, H., Chaboissier, M. C., Martin, J. F., Schedl, A., and de Crombrugghe, B. (2002). The transcription factor Sox9 has essential roles in successive steps of the chondrocyte differentiation pathway and is required for expression of Sox5 and Sox6. *Genes Dev.* 16, 2813–2828. doi: 10.1101/gad.1017802

Almqvist, K. F., Wang, L., Wang, J., Baeten, D., Cornelissen, M., Verdonk, R., et al. (2001). Culture of chondrocytes in alginate surrounded by fibrin gel: characteristics of the cells over a period of eight weeks. *Ann. Rheum. Dis.* 60, 781–790. doi: 10.1136/ard.60.8.781

Blumer, M. J., Longato, S., Schwarzer, C., and Fritsch, H. (2007). Bone development in the femoral epiphysis of mice: the role of cartilage canals and the fate of resting chondrocytes. *Dev. Dyn.* 236, 2077–2088. doi: 10.1002/dvdy.21228

Buschmann, M. D., Gluzband, Y. A., Grodzinsky, A. J., Kimura, J. H., and Hunziker, E. B. (1992). Chondrocytes in agarose culture synthesize a mechanically functional extracellular matrix. *J. Orthop. Res.* 10, 745–758. doi: 10.1002/jor.1100100602

Caron, M. M., Emans, P. J., Coolsen, M. M., Voss, L., Surtel, D. A., Cremers, A., et al. (2012). Redifferentiation of dedifferentiated human articular chondrocytes: comparison of 2D and 3D cultures. *Osteoarthritis Cartilage* 20, 1170–1178. doi: 10.1016/j.joca.2012.06.016

Chan, C. M., Macdonald, C. D., Litherland, G. J., Wilkinson, D. J., Skelton, A., Europe-Finner, G. N., et al. (2017). Cytokine-induced MMP13 expression in human chondrocytes is dependent on activating transcription factor 3 (ATF3) regulation. *J. Biol. Chem.* 292, 1625–1636. doi: 10.1074/jbc.m116.756601

Chan, H. Y., Sivakamasundari, S., Xing, X., Kraus, P., Yap, S. P., Ng, P., et al. (2011). Comparison of IRES and F2A-based locus-specific multicistronic expression in stable mouse lines. *PLoS One* 6:e28885. doi: 10.1371/journal.pone.0028885

Dobin, A., Davis, C. A., Schlesinger, F., Drenkow, J., Zaleski, C., Jha, S., et al. (2013). STAR: ultrafast universal RNA-seq aligner. *Bioinformatics* 29, 15–21. doi: 10.1093/bioinformatics/bts635

Dy, P., Wang, W., Bhattaram, P., Wang, Q., Wang, L., Ballock, R. T., et al. (2012). Sox9 directs hypertrophic maturation and blocks osteoblast differentiation of growth plate chondrocytes. *Dev. Cell* 22, 597–609. doi: 10.1016/j.devcel.2011.12.024

Ferguson, G. B., Van Handel, B., Bay, M., Fiziev, P., Org, T., Lee, S., et al. (2018). Mapping molecular landmarks of human skeletal ontogeny and pluripotent stem cell-derived articular chondrocytes. *Nat. Commun.* 9:3634. doi: 10.1038/s41467-018-05573-y

Fisher, M. B., Belkin, N. S., Milby, A. H., Henning, E. A., Bostrom, M., Kim, M., et al. (2015). Cartilage repair and subchondral bone remodeling in response to focal lesions in a mini-pig model: implications for tissue engineering. *Tissue Eng. Part A* 21, 850–860. doi: 10.1089/ten.tea.2014.0384

Friedenstein, A. J., Deriglasova, U. F., Kulagina, N. N., Panasuk, A. F., Rudakowa, S. F., Luriá, E. A., et al. (1974). Precursors for fibroblasts in different populations of hematopoietic cells as detected by the in vitro colony assay method. *Exp. Hematol.* 2, 83–92.

Frisch, B. J., and Calvi, L. M. (2014). Hematopoietic stem cell cultures and assays. *Methods Mol. Biol.* 1130, 315–324. doi: 10.1007/978-1-62703-989-5_24

Haag, J., Gebhard, P. M., and Aigner, T. (2008). SOX gene expression in human osteoarthritic cartilage. *Pathobiology* 75, 195–199. doi: 10.1159/000124980

Heinegård, D., and Saxne, T. (2011). The role of the cartilage matrix in osteoarthritis. *Nat. Rev. Rheumatol.* 7, 50–56. doi: 10.1038/nrrheum.2010.198

Huang, Dw, Sherman, B. T., and Lempicki, R. A. (2009). Systematic and integrative analysis of large gene lists using DAVID bioinformatics resources. *Nat. Protoc.* 4, 44–57. doi: 10.1038/nprot.2008.211

Jayasuriya, C. T., Chen, Y., Liu, W., and Chen, Q. (2016). The influence of tissue microenvironment on stem cell-based cartilage repair. *Ann. N. Y. Acad. Sci.* 1383, 21–33. doi: 10.1111/nyas.13170

Ko, C. Y., Ku, K. L., Yang, S. R., Lin, T. Y., Peng, S., Peng, Y. S., et al. (2016). In vitro and in vivo co-culture of chondrocytes and bone marrow stem cells in photocrosslinked PCL-PEG-PCL hydrogels enhances cartilage formation. *J. Tissue Eng. Regen. Med.* 10, E485–E496. doi: 10.1002/term.1846

Leung, V. Y., Gao, B., Leung, K. K., Melhado, I. G., Wynn, S. L., Au, T. Y., et al. (2011). SOX9 governs differentiation stage-specific gene expression in growth plate chondrocytes via direct concomitant transactivation and repression. *PLoS Genet.* 7:e1002356. doi: 10.1371/journal.pgen.1002356

Li, L., Newton, P. T., Bouderlique, T., Sejnohova, M., Zikmund, T., Kozhemyakina, E., et al. (2017). Superficial cells are self-renewing chondrocyte progenitors, which form the articular cartilage in juvenile mice. *FASEB J.* 31, 1067–1084. doi: 10.1096/fj.201600918r

Li, Q., Bohin, N., Wen, T., Ng, V., Magee, J., Chen, S. C., et al. (2013). Oncogenic Nras has bimodal effects on stem cells that sustainably increase competitiveness. *Nature* 504, 143–147. doi: 10.1038/nature12830

Madsen, S. H., Goettrup, A. S., Thomsen, G., Christensen, S. T., Schultz, N., Henriksen, K., et al. (2011). Characterization of an ex vivo femoral head model assessed by markers of bone and cartilage turnover. *Cartilage* 2, 265–278. doi: 10.1177/1947603510383855

Markway, B. D., Cho, H., and Johnstone, B. (2013). Hypoxia promotes redifferentiation and suppresses markers of hypertrophy and degeneration in both healthy and osteoarthritic chondrocytes. *Arthritis Res. Ther.* 15:R92. doi: 10.1186/ar4272

Matak, D., Brodaczewska, K. K., Lipiec, M., Szymanski, Ł, Szczylik, C., and Czarnecka, A. M. (2017). Colony, hanging drop, and methylcellulose three dimensional hypoxic growth optimization of renal cell carcinoma cell lines. *Cytotechnology* 69, 565–578. doi: 10.1007/s10616-016-0063-2

Matsui, W., Huff, C. A., Wang, Q., Malehorn, M. T., Barber, J., Tanhehco, Y., et al. (2004). Characterization of clonogenic multiple myeloma cells. *Blood* 103, 2332–2336. doi: 10.1182/blood-2003-09-3064

Ni, J., Yuan, X. M., Yao, Q., and Peng, L. B. (2015). OSM is overexpressed in knee osteoarthritis and Notch signaling is involved in the effects of OSM on MC3T3-E1 cell proliferation and differentiation. *Int. J. Mol. Med.* 35, 1755–1760. doi: 10.3892/ijmm.2015.2168

Perka, C., Spitzer, R. S., Lindenhayn, K., Sittinger, M., and Schultz, O. (2000). Matrix-mixed culture: new methodology for chondrocyte culture and preparation of cartilage transplants. *J. Biomed. Mater. Res.* 49, 305–311. doi: 10.1002/(SICI)1097-4636(20000305)49:3<305::AID-JBM2>3.0.CO;2-9

Roseti, L., Desando, G., Cavallo, C., Petretta, M., and Grigolo, B. (2019). Articular cartilage regeneration in osteoarthritis. *Cells* 8:1305. doi: 10.3390/cells8111305

Rucklidge, G. J., Milne, G., and Robins, S. P. (1996). Collagen type X: a component of the surface of normal human, pig, and rat articular cartilage. *Biochem. Biophys. Res. Commun.* 224, 297–302. doi: 10.1006/bbrc.1996.1024

Sacchetti, B., Funari, A., Michienzi, S., Di Cesare, S., Piersanti, S., Saggio, I., et al. (2007). Self-renewing osteoprogenitors in bone marrow sinusoids can organize a hematopoietic microenvironment. *Cell* 131, 324–336. doi: 10.1016/j.cell.2007.08.025

Saeki, N., and Imai, Y. (2020). Reprogramming of synovial macrophage metabolism by synovial fibroblasts under inflammatory conditions. *Cell Commun. Signal.* 18:188. doi: 10.1186/s12964-020-00678-8

Sanchez, C., Deberg, M. A., Burton, S., Devel, P., Reginster, J. Y., and Henrotin, Y. E. (2004). Differential regulation of chondrocyte metabolism by oncostatin M and interleukin-6. *Osteoarthritis Cartilage* 12, 801–810. doi: 10.1016/j.joca.2004.06.011

Shi, S., Wang, C., Acton, A. J., Eckert, G. J., and Trippel, S. B. (2015). Role of sox9 in growth factor regulation of articular chondrocytes. *J. Cell. Biochem.* 116, 1391–1400. doi: 10.1002/jcb.25099

Shkhyan, R., Van Handel, B., Bogdanov, J., Lee, S., Yu, Y., Scheinberg, M., et al. (2018). Drug-induced modulation of gp130 signalling prevents articular cartilage degeneration and promotes repair. *Ann. Rheum. Dis.* 77, 760–769. doi: 10.1136/annrheumdis-2017-212037

Shwartz, Y., Viukov, S., Krief, S., and Zelzer, E. (2016). Joint development involves a continuous influx of Gdf5-positive cells. *Cell Rep.* 15, 2577–2587. doi: 10.1016/j.celrep.2016.05.055

Singh, P., Lessard, S. G., Mukherjee, P., Rourke, B., and Otero, M. (2021). Changes in DNA methylation accompany changes in gene expression during chondrocyte hypertrophic differentiation in vitro. *Ann. N. Y. Acad. Sci.* 1490, 42–56. doi: 10.1111/nyas.14494

Sokolove, J., and Lepus, C. M. (2013). Role of inflammation in the pathogenesis of osteoarthritis: latest findings and interpretations. *Ther. Adv. Musculoskelet. Dis.* 5, 77–94. doi: 10.1177/1759720X12467868

Ullah, M., Hamouda, H., Stich, S., Sittinger, M., and Ringe, J. (2012). A reliable protocol for the isolation of viable, chondrogenically differentiated human mesenchymal stem cells from high-density pellet cultures. *Biores. Open Access* 1, 297–305. doi: 10.1089/biores.2012.0279

Ware, M. J., Colbert, K., Keshishian, V., Ho, J., Corr, S. J., Curley, S. A., et al. (2016). Generation of homogenous three-dimensional pancreatic cancer cell spheroids using an improved hanging drop technique. *Tissue Eng. Part C Methods* 22, 312–321. doi: 10.1089/ten.tec.2015.0280

Weissenberger, M., Weissenberger, M. H., Gilbert, F., Groll, J., Evans, C. H., and Steinert, A. F. (2020). Reduced hypertrophy in vitro after chondrogenic differentiation of adult human mesenchymal stem cells following adenoviral SOX9 gene delivery. *BMC Musculoskelet. Disord.* 21:109. doi: 10.1186/s12891-020-3137-4

Wu, L., Bluguermann, C., Kyupelyan, L., Latour, B., Gonzalez, S., Shah, S., et al. (2013). Human developmental chondrogenesis as a basis for engineering chondrocytes from pluripotent stem cells. *Stem Cell Reports* 1, 575–589. doi: 10.1016/j.stemcr.2013.10.012

Wu, L., Gonzalez, S., Shah, S., Kyupelyan, L., Petrigliano, F. A., McAllister, D. R., et al. (2014). Extracellular matrix domain formation as an indicator of chondrocyte dedifferentiation and hypertrophy. *Tissue Eng. Part C Methods* 20, 160–168. doi: 10.1089/ten.tec.2013.0056

Yasuhara, R., Ohta, Y., Yuasa, T., Kondo, N., Hoang, T., Addya, S., et al. (2011). Roles of β-catenin signaling in phenotypic expression and proliferation of articular cartilage superficial zone cells. *Lab. Invest.* 91, 1739–1752. doi: 10.1038/labinvest.2011.144

Yen, Y., Chien, M., Wu, P., and Hung, S. (2021). PP2A in LepR+ mesenchymal stem cells contributes to embryonic and postnatal endochondral ossification through Runx2 dephosphorylation. *Commun. Biol.* 4:658. doi: 10.1038/s42003-021-02175-1

Zhang, Q., Ji, Q., Wang, X., Kang, L., Fu, Y., Yin, Y., et al. (2015). SOX9 is a regulator of ADAMTSs-induced cartilage degeneration at the early stage of human osteoarthritis. *Osteoarthritis Cartilage* 23, 2259–2268. doi: 10.1016/j.joca.2015.06.014

Conflict of Interest: The authors declare that the research was conducted in the absence of any commercial or financial relationships that could be construed as a potential conflict of interest.

Publisher's Note: All claims expressed in this article are solely those of the authors and do not necessarily represent those of their affiliated organizations, or those of the publisher, the editors and the reviewers. Any product that may be evaluated in this article, or claim that may be made by its manufacturer, is not guaranteed or endorsed by the publisher.

frontiers in Cell and Developmental Biology

MINI REVIEW
published: 25 October 2021
doi: 10.3389/fcell.2021.727640

The Role of Cancer-Associated Fibroblast as a Dynamic Player in Mediating Cancer Stemness in the Tumor Microenvironment

Jia Jian Loh[1] *and Stephanie Ma*[1,2]*

[1] School of Biomedical Sciences, Li Ka Shing Faculty of Medicine, The University of Hong Kong, Hong Kong, Hong Kong,
[2] State Key Laboratory of Liver Research, The University of Hong Kong, Pokfulam, Hong Kong, SAR China

OPEN ACCESS

Edited by:
Takahiko Hara,
Tokyo Metropolitan Institute of Medical Science, Japan

Reviewed by:
Borhane Guezguez,
German Cancer Research Center (DKFZ), Germany
Linli Zhou,
University of Cincinnati, United States
Yuhang Zhang,
University of Cincinnati, United States

***Correspondence:**
Stephanie Ma
stefma@hku.hk

Specialty section:
This article was submitted to Stem Cell Research, a section of the journal Frontiers in Cell and Developmental Biology

Received: 19 June 2021
Accepted: 24 September 2021
Published: 25 October 2021

Citation:
Loh JJ and Ma S (2021) The Role of Cancer-Associated Fibroblast as a Dynamic Player in Mediating Cancer Stemness in the Tumor Microenvironment. Front. Cell Dev. Biol. 9:727640. doi: 10.3389/fcell.2021.727640

The enrichment of cancer-associated fibroblast (CAFs) in a tumor microenvironment (TME) cultivates a pro-tumorigenic niche *via* aberrant paracrine signaling and matrix remodeling. A favorable niche is critical to the maintenance of cancer stem cells (CSCs), a population of cells that are characterized by their enhanced ability to self-renew, metastasis, and develop therapy resistance. Mounting evidence illustrates the interplay between CAF and cancer cells expedites malignant progression. Therefore, targeting the key cellular components and factors in the niche may promote a more efficacious treatment. In this study, we discuss how CAF orchestrates a niche that enhances CSC features and the potential therapeutic implication.

Keywords: inflammation, targeted therapy, tumor microenvironment, cancer associated fibroblast, cancer stem cell, cancer stemness

INTRODUCTION

Tumors are illustrated as "wounds that do not heal" due to the enrichment of fibroblasts and immune cells at the tumor site, which highly mimics that of an inflammatory response of a non-neoplastic tissue (Dvorak, 1986). Indeed, cancer-associated fibroblast (CAF) constitutes the bulk of the stromal component in solid tumors. Cancer cells hijack the normal physiological function of activated fibroblast functions during wound recovery to fuel malignant development. Given cancer stemness accelerates disease progression and impinges therapy, understanding how CAFs cultivate a niche that bestows cancer stem cell (CSC) features in cancer cells may facilitate novel therapeutic intervention.

CANCER-ASSOCIATED FIBROBLAST AS A DYNAMIC PLAYER IN PROMOTING CANCER STEMNESS

Cancer-associated fibroblast, also known as tumor-associated fibroblast, is generally regarded as fibroblasts that exist within or enveloping the tumor (Öhlund et al., 2014). The presence of

CAFs throughout tumor development, from the incipient stage to advanced stages, alludes to CAF participation in tumor initiation and progression (Erez et al., 2010). Compared with non-tumor fibroblast (NF) or peri-tumor fibroblast, CAFs are located more proximal to the neoplastic region and exhibit a greater activation marker, namely actin smooth muscle (αSMA) and fibroblast activation protein (FAP) (Qin et al., 2016, 2019). However, compiling studies indicate CAF displays vast heterogeneity within a tumor with distinct functions, underscoring the importance of identifying the function of how each subtype contributes to malignancy (Öhlund et al., 2017; Costa et al., 2018; Lambrechts et al., 2018). A myriad of elements may affect CAF subtypes, for instance, proximity to the tumor. CAF subsets were distinguished based on their expression of α*SMA* and *IL6* with high-α*SMA* localized nearer to the tumor and high-*IL6* further, indicating juxtacrine and paracrine interaction between cancer cells and fibroblast may stimulate the CAF to differentiate to subtypes with distinct functions (Öhlund et al., 2017). Aside from molecular markers, the secretome of CAF and NF can be discerned as the former secretes a greater abundance of ligands that promote stemness properties of HCC (Jiang et al., 2017; Álvarez-Teijeiro et al., 2018). CAF plays an extensive role in shaping the extracellular matrix (ECM) of the tissues, allowing it to exert its oncogenic influence by modulating the physical properties of the TME. In addition to promoting cancer progression, fibroblasts are shown to be educated by neoplastic cells to their benefits, depicting the dynamic cellular network in the TME (**Figure 1**).

Cancer stem cells are generally deemed as a rare population of cancer cells that share similar features to normal stem cells, including the ability to self-renew and differentiate into lineages that comprise the tumor bulk, thus regarded as tumorigenic, as opposed to non-CSC cancer cells (Reya et al., 2001; Clarke et al., 2006). Common CSC markers include surface markers, such as CD24, CD44, CD90, CD133, EpCAM, LGR5, and aldehyde dehydrogenase (ALDH) ALDH activity (summarized in Walcher et al., 2020). Moreover, expressions of stemness genes, such as *OCT4*, *SOX2*, and *NANOG*, are often deployed to measure cancer stemness. Functional surrogate to assess cancer stemness properties includes *in vitro* sphere formation and *in vivo* limiting dilution in which cancer cells are injected at low doses into animal models. Cancer cells with greater stemness are generally considered to have augmented metastasis ability due to their enhanced ability to reconstitute a tumor at the secondary site, and the acquisition of EMT is coupled with elevated stem cell properties, including stem cell markers and tumorigenicity, signifying EMT mimics features of CSC (Mani et al., 2008; Baccelli and Trumpp, 2012; Oskarsson et al., 2014). Emerging evidence illustrates that stemness properties of cancer cells are dependent on their niche (Plaks et al., 2015; Batlle and Clevers, 2017). Factors derived from niche may promote plasticity of non-CSC cancer cells into CSC, whereas depletion of factors may reduce the CSC population, thereby implicating niche factors as potential therapeutic targets (Batlle and Clevers, 2017). Given the CAF fosters the niche by enriching pro-tumor factors and remodeling the matrix of the TME, understanding how a niche facilitates cancer initiation and progression will allow us to contrive therapy targeting the key cellular components and factors sustaining cancer stemness.

Cancer Cells Educate Cancer-Associated Fibroblast to Adopt a Pro-tumor Phenotype

Accumulating research illuminates the cancer cells instigate pro-tumor CAF to foster a pro-favorable niche. Transforming growth factor-β3 (TGF-β3) derived from HNSCC cells can activate CAF to secrete POSTN, leading to greater metastasis ability of the neoplastic cells (Qin et al., 2016). Prostate cancer cells can recruit marrow-derived mesenchymal stem cells (MSCs) and activate them into CAF by TGF-β1 (Barcellos-de-Souza et al., 2016). Of significance, MSC-derived CAF can recruit and induce monocytes into M2 macrophages, illustrating the CAF capacity to govern the TME. Cardiotrophin-like cytokine factor (CLCF1) derived from CAF stimulates the production of C-X-C motif ligand 6 (CXCL6) and TGF-β, which not only escalate stemness properties of cancer cells but also stimulate CLCF1 expression in the CAF, thereby fostering a positive feedback loop that expedites malignancy (Song et al., 2021). Furthermore, CXCL6 and TGF-β can enhance infiltration and development of pro-tumor N2-neutrophils (Song et al., 2021), corroborating CAF capacity to foster an immunosuppressive TME. Sonic hedgehog (SHH) ligand derived from $CD24^{+}CD49f^{hi}$breast CSCs constructs a pro-tumorigenic TME by activating CAF (Valenti et al., 2017). Cancer cells-derived hedgehog (Hh) instigates the production of pro-tumor paracrine factors and ECM constituents in CAF (Cazet et al., 2018). Autocrine and colorectal cancer cells-derived paracrine signaling of IL34 facilitate the conversion of normal fibroblast into CAF that adopts a pro-tumor secretome that includes stemness-promoting factors, such as Netrin-1 and FGF2 protein (Giulianelli et al., 2019; Sung et al., 2019). The coculture of HNSCC cells and CAF stimulate CAF to generate WNT3A, leading to increased cancer stemness (Le et al., 2019).

Exosomal miRNAs are gaining interest as a mediator between cancer cell-fibroblast crosstalk. Activation of focal adhesion kinase (FAK) signaling by cancer cell-derived miRNA stimulates the production of CAF-derived exosomes that facilitate the spheroid formation and metastasis (Wu et al., 2020). Tumor-derived exosomal miR-1247-3p triggers the activation of fibroblast by fueling NF-κB signaling consequently stimulates the CAF to secrete a greater abundance of IL6 and IL8, instigating the cancer cells to an EMT phenotype with enhanced lung metastases (Fang et al., 2018). Exosomal miR-9-5p elevates IL6 production in CAF, leading to enhanced spheroid-forming ability (Zhang et al., 2020). In summary, targeting the aforementioned factors or exosomes may disrupt the ability of cancer cells to assemble a pro-tumor niche.

Cancer Cell-Educated Cancer-Associated Fibroblast Cultivates a Supportive Secondary Site for Colonization

The TGF-β family is shown to play pivotal roles in allowing cancer cells to colonize secondary sites. TGF-β3 rooted from

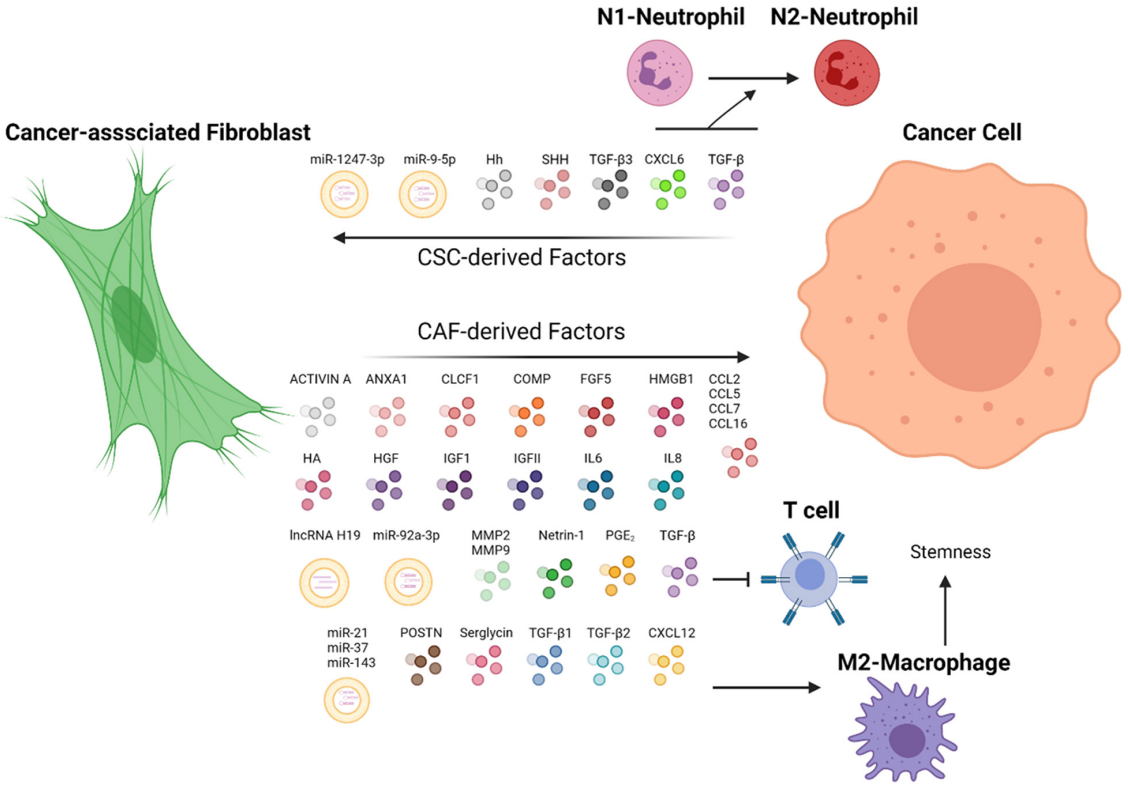

FIGURE 1 | CAF and cancer cells in a dynamic TME. CAF secretes chemokines that can potentiate stemness and metastasis properties of cancer cells *via* distinct pathways. In turn, cancer cells have demonstrated the capacity to direct CAF to fuel their malignant properties. Immune cells, such as T cells, macrophages, and neutrophils, are orchestrated by CAF-cancer cell interaction to promote tumor progression. ANXA1, Annexin A1; CLCF1, cardiotrophin-like cytokine factor 1; COMP, cartilage oligomeric matrix protein; CXCL6, C-X-C motif chemokine ligand 6; CXCL12, C-X-C motif chemokine ligand 12; CCL2, CC-chemokine ligand 2; CCL5, CC-chemokine ligand 5; CCL7, CC-chemokine ligand 7; CCL16, CC-chemokine ligand 16; FGF5, fibroblast growth factor 5; HA, hyaluronan; Hh, hedgehog ligand; HMGB1, high-mobility group box protein 1; HGF, hepatocyte growth factor; IGFI, insulin-like growth factor 1; IGFII, insulin-like growth factor 2; IL6, interleukin 6; IL8, interleukin 8; MMP2; matrix metalloproteinase-2; MMP9, matrix metalloproteinase-9; POSTN, periostin; PGE_2, prostaglandin E_2; SHH, sonic hedgehog ligand; TGF-β, transforming growth factor-β; TGF-β1, transforming growth factor-β 1; TGF-β2, transforming growth factor-β 2; TGF-β3, transforming growth factor-β 3; WNT3a, Wnt Family Member 3A. The figure is created with BioRender.com.

cancer cells fortifies a favorable niche to colonize a foreign site by stimulating fibroblast-derived POSTN, which is crucial for initiating breast cancer cell colonization at the lung by maintaining CSC properties *via* the Wnt signaling (Malanchi et al., 2011). In accordance, HNSCC cancer cells secrete TGF-β3 that enhances POSTN secretion from CAF, resulting in the augmented migratory phenotype of cancer cells (Qin et al., 2016). Upon stimulation by TGF-β, CAF confers colorectal cancer cells-enhanced tumor-initiating capacity and reduced tumor latency (Calon et al., 2015). Tumor organoids with elevated TGF-β profoundly enhanced ability to form liver metastases by orchestrating a pro-tumor stroma niche (Calon et al., 2015). Colorectal cancer (CRC) fueled by driver mutations in the *Lgr5* + stem cells is accompanied by enrichment of CAF-derived TGF-β that suppresses the tumor-killing T cell populations, thus leading to greater metastases to the liver (Tauriello et al., 2018), highlighting the interplay between CAF, immune cells, and cancer cells. Conversely, the TGF-β-signaling inhibitor significantly dampened the tumor volume and liver metastases of the colon.

Paracrine Signaling of Cancer-Associated Fibroblast Enhances Cancer Stem Cell Features

In a tumor, fibroblast-secreted factors and cytokines, which serve for tissue recovery, are seized by cancer cells. Compiling studies have depicted the critical roles of CAF-derived factors in maintaining the CSC features of cancer cells by promoting stemness pathways (**Table 1**). HGF is reported to enhance cancer stemness by potentiating the frequency of $CD44^+$, $CD47^+$, and $CD90^+$ HCC CSC and spheroid formation, stemness and EMT gene expressions (Lau et al., 2016; Ding et al., 2018; Yan et al., 2018). Mechanistically, HGF exerts its oncogenic influence *via* distinct mechanisms in a tissue-dependent manner. HGF augments ERK/FRA1/HEY1, STAT3/TWIST1, and YAP/HIF-1α in HCC, gastric cancer, and pancreatic cancer, respectively (Lau et al., 2016; Ding et al., 2018; Yan et al., 2018). CAF-derived IL6 is demonstrated to fuel stemness as evident in increased spheroid formation, stemness genes markers *via* STAT3 signaling (Xiong et al., 2018; Zhang et al., 2020). CAF paracrine signaling regulates

the AKT pathway *via* insulin-like growth factor 2 (IGFII), thereby promoting *NANOG* expression, enhanced tumorigenicity *in vivo,* and ALDH activity (Chen et al., 2014). The AKT signaling is also mediated by cartilage oligomeric matrix protein (COMP) to fuel EMT and spheroid formation (Li et al., 2018). CC-chemokine ligand 2, 5, 7, and 16 (CCL2, CCL5, CCL7, and CXCL16) potentiate EMT *via* the Hh and TGF-β signaling (Liu et al., 2016). Serglycin (SRGN), a proteoglycan secreted from cancer cells and CAFs, renders chemoresistance and EMT features *via* a CD44-dependent NF-κB activation (Guo et al., 2017). The binding of CAF-derived periostin (POSTN) to protein tyrosine kinase 7 (PTK7) drives the β-catenin signaling, leading to increased expression of CSC markers and stemness genes (Yu et al., 2018). Annexin A1 (AnxA1) secreted from CAF potentiates stemness and EMT genes expressions, and spheroid formation (Geary et al., 2014). Prostaglandin E_2 (PGE_2) produced from fibroblasts drives the expansion of tumor-initiating cells by inducing YAP signaling (Roulis et al., 2020). The cellular crosstalk within the TME was displayed as CAFs recruit tumor-associated macrophages (TAMs) *via* CXCL12 secretion and induces the M2-phenotype TAMs, subsequently promotes stemness and EMT signature genes (Li et al., 2019). Alteration in specific genes may dictate the impact of CAF on cancer cells. Androgen receptor (AR)-depleted CAF enhances the production of IFN-γ and M-CSF, leading to increased cancer stemness (Liao et al., 2017). Notch1-depleted CAFs augment $CD271^+$ melanoma CSC frequency (Du et al., 2019) and metastasis to the lung (Shao et al., 2016). Together, blocking CAF-derived factors or a downstream signaling cascade may be a therapeutic revenue to diminish cancer stemness.

Cancer-Associated Fibroblast Mediates Cancer Stemness via Extracellular Matrix Remodeling

A fundamental function of activated fibroblast is its participation in ECM homeostasis by synthesizing ECM constituents, including collagen and fibronectin, and producing ECM-degrading proteases to aid communication and trafficking of inflammatory cells (Kalluri, 2016). While the impact of matrix stiffness remains controversial as studies indicate both softer matrix (Tan et al., 2014; Ng et al., 2021) and stiffer matrix (Pang et al., 2016; Tao et al., 2021) can instigate cancer stemness, the role of CAF in mediating the stiffness of the ECM illustrates its ability to affect stemness. Indeed, collagen deposited by CAF functions as a mechano signal to escalate stem cell markers and spheroid formation ability (Cazet et al., 2018). Additionally, hyaluronan (HA), a major constituent of the ECM that boosts CSC self-renewal and EMT (summarized in Chanmee et al., 2015), is shown to be highly produced by CAF (Affo et al., 2021). Given CAFs are a source of ECM-degrading proteases, namely matrix metalloproteinases (MMPs), they can affect CSC properties by remodeling the ECM. Studies demonstrated IL6 derived from prostate cancer cells elicits pro-tumor FAP^+CAF (Giannoni et al., 2010). Consequently, these FAP^+ CAF secretes MMP2 and MMP9 to potentiate EMT and stemness genes. MMP3 that is predominantly produced by fibroblast (Witty et al., 1995) is demonstrated to promote stem cell population by enhancing canonical Wnt signaling, potentially leading to hyperplastic growth of normal tissues (Kessenbrock et al., 2013), depicting fibroblast can contribute to tumor initiation *via* ECM remodeling. Future research can focus on ablating the effect of CAF on the ECM, either by targeting ECM constitutes or MMPs, to attenuate the CAF-mediated oncogenic effect.

Cancer-Associated Fibroblast Role in Endowing Drug Resistance

The augmented cancer stemness conferred by CAF may endow cancer resistance to conventional therapy. Patients with breast cancer, who are resistant to chemotherapy, show a greater abundance of CAF marked with a cluster of differentiation 10 (CD10) and G protein-coupled receptor 77 (GRP77) cell surface proteins (Su et al., 2018). $CD10^+GRP77^+$ CAFs promote sphere formation, the proportion of $ALDH^+$ and $CD44^+CD24^-$ breast CSCs, and chemoresistance properties of cancer cells by secreting IL6 and IL8. A similar phenomenon was observed in HNSCC as CAFs undergoing autophagy secrete greater levels of IL6 and IL8 to confer chemoresistance (New et al., 2017). Increased *NANOG* and *SOX2* stemness gene expression in cancer cells treated with CAF-conditioned media may lead to greater cisplatin resistance (Peltanova et al., 2021). CAF-derived TGF-β1 drives self-renewal and gemcitabine resistance by upregulation of activating transcription factor 4 (ATF4) *via* the SMAD2/3 pathway (Wei et al., 2021). SRGN facilitates cisplatin resistance *via* inducing NANOG (Guo et al., 2017). In line, CAF-rooted TGF-β2 can elicit stemness and chemoresistance by enhancing GLI Family Zinc Finger 2 (GLI2) (Tang et al., 2018). CAF-derived exosomes enhance the stemness properties of $CD133^+$ colorectal CSCs, leading to greater chemoresistance to fluorouracil and oxaliplatin (Hu et al., 2015). Additionally, exosomal miR-92a-3p derived from colorectal CAF targets anti-tumor F-box/WD repeat-containing protein 7 (FBXW7) and a modulator of apoptosis 1 (MOAP1), thereby endowing chemoresistance to cancer cells (Hu et al., 2019). In line, exosomal miRNA was demonstrated to confer chemoresistance in prostate cancer (Shan et al., 2020) and head and neck cancer (Qin et al., 2019). CAF-derived exosomal long non-coding RNA (lncRNA) H19 was exhibited to enable stemness expression by sponging miR-141 that targets β-catenin (Ren et al., 2018).

Another mechanism that CAF mediates chemoresistance resides in its ability to remodel the ECM. Studies have demonstrated HA upregulates NANOG/STAT signaling, leading to increased expression of multidrug transporter (MDR1) that contributes to chemoresistance (Bourguignon et al., 2008). In accordance, HA-CD44 interaction mediates stemness signaling that governs miRNA regulation of genes involved in chemoresistance in breast cancer cells (Bourguignon et al., 2009) and HNSCC cells (Bourguignon et al., 2012a,b). HA mediates $CD44v3^{high}ALDH1^{high}$HNSCC CSC *via* an epigenetic alteration to promote cisplatin chemoresistance (Bourguignon et al., 2016). The ability of CAF to mediate matrix stiffness *via* MMPs may be an area of interest. Given matrix stiffness

TABLE 1 | Cancer-associated fibroblast (CAF)-derived factors on cancer stemness.

Factors	Disease	Mechanism	References
ACTIVIN A and IGF1	Breast cancer	CSC secretes SHH to cultivate pro-tumor CAF which then generates ACTIVIN A and IGF1 to promote stemness*	Valenti et al., 2017
ANXA1	Prostate cancer	Induces EMT and stemness markers	Geary et al., 2014
CCL2, CCL5, CCL7, and CXCL16	Hepatocellular carcinoma	Promotes Hh and TGF-β signaling in HCC cells	Liu et al., 2016
CLCF1	Hepatocellular carcinoma	Promotes AKT/ERK/STAT3 signaling. STAT3 target genes, CXCL6, and TGF-β induce CAF's CLCF1 secretion, thus forming CAF-cancer cell positive feedback*	Song et al., 2021
COMP	Hepatocellular carcinoma	Promotes ERK and AKT signaling in HCC cells	Li et al., 2018; Sun et al., 2019
CXCL12	Oral squamous cell carcinoma	Induces M2-phenotype of TAMs that promote EMT and stemness in cancer	Li et al., 2019
FGF5	Triple-negative breast cancer	Cancer cell-derived HH induces FGF5 production from CAF; FGF5 elevates stemness genes expression in cancer cells*	Cazet et al., 2018
HGF	Hepatocellular carcinoma	Promotes c-MET/ERK/FRA1/HEY1 axis in HCC cells*	Lau et al., 2016
	Gastric cancer	Promotes c-Met/STAT3/twist1 signaling and EMT signaling	Ding et al., 2018
	Pancreatic Cancer	Promotes c-MET/YAP/HIF-1α signaling	Yan et al., 2018
	Intrahepatic cholangiocarcinoma	Promotes AKT/ERK signaling	Affo et al., 2021
HMGB1	Luminal breast cancer	Promotes stemness markers and ALDH1+ population upon binding to TLR4	Zhao et al., 2017
IGFII	Lung cancer	Promotes IGII/IGF1R/AKT/NANOG signaling	Chen et al., 2014
IL6	Hepatocellular carcinoma	Promotes STAT3/NOTCH1/NICD/HES1 signaling	Xiong et al., 2018
	Intrahepatic cholangiocarcinoma	Promotes STAT3/EZH2 cascade. Neoplastic cell-secreted exosomal miR-9-5p upregulates IL6 production*	Zhang et al., 2020
IL6 and IL8	Head and Neck cancer	Promote chemoresistance	New et al., 2017
	Hepatocellular carcinoma	HCC cell-derived mi-1247-3p stimulate CAF to produce IL6 and IL8, which promotes stemness and EMT*	Fang et al., 2018
	Breast cancer	$CD10^{+}GRP77^{+}$ CAF-derived IL6 and IL8 stemness	Su et al., 2018
Netrin-1	Non-small cell lung cancer and colon cancer	Promote stemness marker and ALDH1A expression	Sung et al., 2019
Netrin-1 and FGF2	Colorectal cancer	IL34-acitvated CAF increases Netrin-1 and FGF2 expression	Franze et al., 2020
MMP2 and MMP9	Prostate carcinoma	Cancer cell-derived IL6 activate CAF to produce MMP2 and MMP9, in turn, promote EMT and stemness*	Giannoni et al., 2010
PGE_2	Intestinal cancer	Promotes pro-oncogenic PTGER4/YAP	Roulis et al., 2020
POSTN	Breast cancer	Activates Wnt signaling	Malanchi et al., 2011
	Head and neck cancer	TGF-β3 activated CAF to secrete POSTN	Qin et al., 2016
	Human head and neck squamous cell carcinoma	Promotes PTK7/GSKβ/β-catenin signaling	Yu et al., 2018
TGF-β	Colorectal cancer	CSC modulates CAF-derived TGF-β to suppress the tumor-killing T cell populations*	Tauriello et al., 2018
TGF-β1	Pancreatic Cancer	Promotes the upregulation of ATF via the SMAD2/3 pathway	Wei et al., 2021
TGF-β2	Colorectal cancer	Upregulates GLI2 expression	Tang et al., 2018
SRGN	Non-small cell lung cancer	Promote stemness gene markers in CD44-dependent manner	Guo et al., 2017
WNT3A	Human head and neck squamous cell carcinoma	Neoplastic cells activate WNT3A production in CAF*	Le et al., 2019
Exosomal miR-21, miR-143, and miR-378	Breast cancer	Enhances stemness and EMT	Donnarumma et al., 2017
Exosomal lncRNA H19	Colorectal cancer	Sponges miR-141 that target β-catenin	Ren et al., 2018
Exosomal miR-92a-3p	Colorectal cancer	Targets FBXW7 to enhance β-catenin activity and MOAP1 to enhance chemoresistance properties	Hu et al., 2019
Exosomal miR-196a	Head and Neck cancer	Targets CDKN1B and ING5, to promote cisplatin resistance	Qin et al., 2019
Exosomal miR-423-5p	Prostate cancer	Promotes chemoresistance by targeting GREM2, leading to TGF-β pathway activity	Shan et al., 2020

**Denotes a cancer cell-to-CAF dialog.*

regulates stemness and chemoresistance (Ng et al., 2021); how a CAF-mediated ECM fosters a niche that endows chemoresistance warrants further investigations.

Single-Cell RNA Sequencing Identified Cancer-Associated Fibroblast Subsets With Distinct Functions on Cancer Stemness

State-of-the-art single-cell transcriptomic profiling of intrahepatic cholangiocarcinoma (ICC) revealed six distinct fibroblast populations (Zhang et al., 2020). Vascular CAFs (vCAF), the most abundant population, were found to secrete IL6 to promote self-renewal of cancer cells. Of note, the characterization of the function of other CAF subtypes identified such as matrix CAFs, which expressed high ECM signature genes, would be an interesting area of research. Lineage tracing coupled with single-cell RNA sequencing (scRNA-seq) in sophisticated animal models categorized CAF into myofibroblast (myCAF) and inflammatory and growth factor-enriched CAF (iCAF) populations that modulate tumor cell proliferation *via* distinct mechanisms; the former has a high level of hyaluronan synthase 2 (*Has2*) that can enhance pro-tumor HA; the latter secretes HGF (Affo et al., 2021). scRNA-seq identified prostaglandin-endoperoxide synthase 2 (Ptgs2)-expressing fibroblasts that expand tumor-initiating stem cells *via* YAP signaling, whereas ablation of Ptgs2 diminished the occurrence of the small intestine and colon cancers (Roulis et al., 2020). Capturing cellular diversity at single-cell resolution ignites exciting research questions as follows: how cellular and non-cellular components of the TME govern CAF identity? How each subtype contributes to disease progression? How CAFs differentiate or undifferentiate into different subtypes?

POTENTIAL THERAPEUTIC STRATEGY AND CHALLENGES

Targeting Multiple Cancer-Associated Fibroblast-Derived Factors to Circumvent Stemness

As aforementioned (**Table 1**), cancer-promoting bioactive molecules derived from stromal cells may be targeted using specific neutralizing antibodies, particularly in combination with chemotherapy. However, the promising preclinical results have yet to yield optimistic results in clinical settings. A Phase 2 trial (NCT00433446) examining siltuximab (CNTO328), an anti-IL6 antibody, showed siltuximab did not have clinical benefit for patients with advanced prostate cancer (Dorff et al., 2010). Similarly, the addition of siltuximab (CNTO328) to mitoxantrone/prednisone regimen did not yield improved clinical (NCT00385827) outcomes compared to mitoxantrone/prednisone alone in treating advanced prostate cancer (Fizazi et al., 2012). The Phase 2, single-arm, clinical trial (NCT00992186) explored the efficacy of carlumab (CNTO 888), antibody targeting (CCL2), in patients with metastatic castration-resistant prostate cancer (CRPC), who had undergone docetaxel treatment (Pienta et al., 2013). However, none of the patients treated with carlumab showed partial or complete remission. One key possibility is that, while the CCL2 level was depleted upon carlumab administration, the level rebounded rapidly within a week, thus suggesting carlumab cannot suppress CCL2 for the clinically meaningful duration (Pienta et al., 2013). Nonetheless, the addition of siltuximab to bortezomib-melphalan-prednisone (VMP) demonstrated marginal clinical benefits in multiple myeloma by statistically improving partial response rate (San-Miguel et al., 2014). Together, these imply more precise stratification of patients and usage of biomarkers may result in better clinical outcomes. Of note, several clinical trials are exploring the clinical utility of neutralizing antibodies that target HGF (NCT04368507), MET (NCT04077099), and IL6R (NCT03999749). Aside from neutralizing antibodies, a combination of inhibitors-targeting receptors, including Osimertinib (an EGFR inhibitor) and Savolitinib (MET inhibitors), are being tested in clinical trials (NCT03778229). Notably, MP0250, a drug candidate targeting HGF and VEGF, which have met the safety requirement and demonstrated clinical efficacy, is being tested in combination with existing drugs to treat multiple myeloma (NCT03136653). Given the TME is often accompanied by an upsurge of cytokines and chemokines, targeting multiple factors may promote treatment efficacy.

Depleting Pro-tumor Cancer-Associated Fibroblast

The ability of CAF to endow stemness of cancer cells makes it an intriguing therapy. CAF is shown to be more positively correlated with gene sets associated with poor prognosis compared with epithelial cancer cells, immune cells, and endothelial cells (Calon et al., 2015), substantiating targeting CAF as a potential therapeutic avenue. Studies have demonstrated that α*SMA* expression represents a marker for worse prognosis in colorectal cancer, indicating myofibroblast abundance is crucial to disease prediction (Tsujino et al., 2007). In accordance, studies conducted in tongue cancer and oral cancer depicted similar results (Vered et al., 2010; Marsh et al., 2011).

However, the heterogeneity of CAF necessitates precise identification of more specific markers as tumor-restraining CAF exists. Genetic deletion of α*SMA* in mouse models enhances the progression of pancreatic ductal adenocarcinoma (PDAC) as evidenced by a lower survival rate in α*SMA*-depleted mice (Ozdemir et al., 2014). Interestingly, the myofibroblast-depleted tumor demonstrated enhanced spheroid-forming ability, indicating a greater proportion of CSC. Indeed, identification of CAF subtypes shows they promote or suppress tumor progression in a tissue-dependent manner (Galbo et al., 2021), corroborating the need for further investigation into more CAF-specific markers. Recent work has illuminated the potential therapeutic benefit of targeting tumor-promoting fibroblasts. Administration of GRP77 neutralizing antibody-targeting CAF depletes CAF-secreted IL6 and IL8, thereby abolishing a stem cell-supporting niche and sensitizing breast cancer cells to doxycycline, leading to significant shrinkage of the tumor

volume (Su et al., 2018), highlighting the therapeutic potential of targeting precise tumor-promoting CAF.

Rewire Pro-tumor Cancer-Associated Fibroblast Into Quiescent or Anti-tumor Fibroblast

Reeducating pro-tumor CAF into a quiescent state or even anti-tumor CAF is a tempting strategy. Vitamin D metabolite 1α, 25-dihydroxyvitamin D3 [1,25(OH)2D3] is shown to deplete the oncogenic influence of stromal fibroblast to the cancer cells, while 1,25(OH)2D3-treated stromal fibroblast displayed a gene signature that favors a clinical outcome (Ferrer-Mayorga et al., 2017). VDR activation of the stromal fibroblast using calcipotriol, a vitamin D analog, diminished expression of genes involved in growth factors and cytokines, for instance, the *IL6* and *POSTN*, thereby suppressing a tumor-promoting secretome (Sherman et al., 2014). Additionally, the combination treatment of calcipotriol and gemcitabine markedly prolonged survival in preclinical models. Moreover, high vitamin D receptor (VDR) expression in stromal cells predicts favorable survival (Ferrer-Mayorga et al., 2017). All-trans retinoic acid (ATRA), also known as tretinoin, a vitamin A metabolite, renders pancreatic stellate cells into a quiescent state, which, in turn, secreted a greater level of secreted frizzled-related protein 4 (sFRP4) that negatively modulates Wnt signaling of cancer cells in a paracrine manner (Froeling et al., 2011). Indeed, ATRA has passed the safety in Phase I clinical trial (NCT03307148) and will proceed to Phase II (NCT04241276) as encouraging therapeutic responses were observed (Kocher et al., 2020). Given vitamins are essential for healthy tissue and their toxicity is relatively lower compared to chemotherapy, repurposing vitamin analogs to rewire activated fibroblast into a quiescent state may present a viable therapeutic strategy that can be translated into the clinical settings.

Another strategy to rewire the population of fibroblasts is by reprogramming the fibroblast using growth factors as exemplified in the plasticity of CAF found in PDAC. While IL1 induces fibroblast into having an inflammatory phenotype categorized by an elevated cytokines production, TGF-β antagonizes an IL1-induced phenotype and stimulates the fibroblast to adopt a myofibroblastic phenotype with less tumorigenesis, particularly reduced expression of factors promoting cancer stemness such as *Il6* and *Cxcl12* (Biffi et al., 2019). Together, this rationalizes the option to rewire tumor-promoting into tumor-restraining fibroblast. To account for the ability of the cancer cell to instigate tumor-promoting CAFs, inhibitors may be deployed to circumvent cancer cell-mediated activation of CAF. Breast cancer cells activate CAF *via* the hedgehog signaling to cultivate a stem cell niche by ECM remodeling and FGF5 secretion that promote docetaxel chemoresistance (Cazet et al., 2018). As such, targeting the crosstalk *via* smoothened inhibitors (SMOi), a hedgehog-signaling inhibitor, sensitizes triple-negative breast cancer (TNBC) to docetaxel. Concomitantly, inhibition of hedgehogs abrogates the activated stromal cells, thereby augmenting the efficacy of chemotherapy in treating pancreatic cancer (Olive et al., 2009). However, either genetic depletion or pharmacological inhibition of SHH, a ligand that activates pancreatic CAFs, resulted in less stromal composition but also a more aggressive tumor (Rhim et al., 2014), suggesting treatment should be tailored based on tissue and treatment.

FUTURE PERSPECTIVES

Advances in single-cell RNA sequencing may not only aid the characterization of cell types based on their molecular profiles and, subsequently, functions but also have the potential to be used to identify new biomarkers for patient stratification and tailor-personalized medicine (Dominguez et al., 2020). Harnessing single-cell RNA-sequencing to profile CAF at the molecular level, future studies can address outstanding questions, including the origin and development of specific CAF subtypes, identification of biomarkers corresponding to each subtype, how each CAF subtype interacts with its niche, and amenable therapeutic opportunities to tackle tumor-promoting CAF. A more holistic approach investigating the CAF molecular profile, for instance, epitranscriptomic and epigenetics (Delaunay and Frye, 2019; Song et al., 2020), may unravel novel insights into how CAF shuttles between cell types. Recent studies have unmasked that the altered epigenetics profile between CAF and NF allows the former to generate greater levels of WNT5A that confers malignancy to the neoplastic cells (Maeda et al., 2020). A critical unmet knowledge gap in our understanding of CAF function is if juxtracrine signaling between CAF and cancer cells affects cancer stemness.

Given the TME is a dynamic region with various cell types actively contributing to tumor progression, merely focusing on targeting a single aspect seems unlikely to yield any long-term therapeutic benefit. For example, targeting niche factors alone may not be sufficient to eradicate the tumor due to the inclination of cancer cells to evolve into a niche-independent malignancy as the disease progresses (Fujii et al., 2016). Therefore, comprehensive characterization of cell types and their respective functions in the TME may pave the way for a multimodal approach to improve cancer treatment.

AUTHOR CONTRIBUTIONS

JL wrote the review article. SM edited the review article and provided funding support. Both authors contributed to the article and approved the submitted version.

FUNDING

This project was supported in part by grants from the Research Grants Council of Hong Kong—Theme-Based Research Scheme (T12-704/16-R), Collaborative Research Fund (C7026-18G), and the Health and Medical Research Fund from Food and Health Bureau of the Hong Kong Government (06172546).

REFERENCES

Affo, S., Nair, A., Brundu, F., Ravichandra, A., Bhattacharjee, S., Matsuda, M., et al. (2021). Promotion of cholangiocarcinoma growth by diverse cancer-associated fibroblast subpopulations. *Cancer Cell* 39, 866–882.e11. doi: 10.1016/j.ccell.2021.03.012

Álvarez-Teijeiro, S., Garcia-Inclan, C., Villaronga, M. A., Casado, P., Hermida-Prado, F., Granda-Diaz, R., et al. (2018). Factors secreted by cancer-associated fibroblasts that sustain cancer stem properties in head and neck squamous carcinoma cells as potential therapeutic targets. *Cancers* 10:334. doi: 10.3390/cancers10090334

Baccelli, I., and Trumpp, A. (2012). The evolving concept of cancer and metastasis stem cells. *J. Cell Biol.* 198, 281–293. doi: 10.1083/jcb.201202014

Barcellos-de-Souza, P., Comito, G., Pons-Segura, C., Taddei, M. L., Gori, V., Becherucci, V., et al. (2016). Mesenchymal stem cells are recruited and activated into carcinoma-associated fibroblasts by prostate cancer microenvironment-derived TGF-beta1. *Stem Cells* 34, 2536–2547. doi: 10.1002/stem.2412

Batlle, E., and Clevers, H. (2017). Cancer stem cells revisited. *Nat. Med.* 23, 1124–1134. doi: 10.1038/nm.4409

Biffi, G., Oni, T. E., Spielman, B., Hao, Y., Elyada, E., Park, Y., et al. (2019). IL1-induced JAK/STAT signaling Is antagonized by TGFbeta to shape CAF heterogeneity in pancreatic ductal adenocarcinoma. *Cancer Discov.* 9, 282–301. doi: 10.1158/2159-8290.CD-18-0710

Bourguignon, L. Y., Peyrollier, K., Xia, W., and Gilad, E. (2008). Hyaluronan-CD44 interaction activates stem cell marker Nanog, Stat-3-mediated MDR1 gene expression, and ankyrin-regulated multidrug efflux in breast and ovarian tumor cells. *J. Biol. Chem.* 283, 17635–17651. doi: 10.1074/jbc.M800109200

Bourguignon, L. Y., Spevak, C. C., Wong, G., Xia, W., and Gilad, E. (2009). Hyaluronan-CD44 interaction with protein kinase C(epsilon) promotes oncogenic signaling by the stem cell marker Nanog and the Production of microRNA-21, leading to down-regulation of the tumor suppressor protein PDCD4, anti-apoptosis, and chemotherapy resistance in breast tumor cells. *J. Biol. Chem.* 284, 26533–26546. doi: 10.1074/jbc.M109.027466

Bourguignon, L. Y., Earle, C., Wong, G., Spevak, C. C., and Krueger, K. (2012a). Stem cell marker (Nanog) and Stat-3 signaling promote MicroRNA-21 expression and chemoresistance in hyaluronan/CD44-activated head and neck squamous cell carcinoma cells. *Oncogene* 31, 149–160. doi: 10.1038/onc.2011.222

Bourguignon, L. Y., Wong, G., Earle, C., and Chen, L. (2012b). Hyaluronan-CD44v3 interaction with Oct4-Sox2-Nanog promotes miR-302 expression leading to self-renewal, clonal formation, and cisplatin resistance in cancer stem cells from head and neck squamous cell carcinoma. *J. Biol. Chem.* 287, 32800–32824. doi: 10.1074/jbc.M111.308528

Bourguignon, L. Y., Wong, G., and Shiina, M. (2016). Up-regulation of histone methyltransferase, DOT1L, by matrix hyaluronan promotes microRNA-10 expression leading to tumor cell invasion and chemoresistance in cancer stem cells from head and neck squamous cell carcinoma. *J. Biol. Chem.* 291, 10571–10585. doi: 10.1074/jbc.M115.700021

Calon, A., Lonardo, E., Berenguer-Llergo, A., Espinet, E., Hernando-Momblona, X., Iglesias, M., et al. (2015). Stromal gene expression defines poor-prognosis subtypes in colorectal cancer. *Nat. Genet.* 47, 320–329. doi: 10.1038/ng.3225

Cazet, A. S., Hui, M. N., Elsworth, B. L., Wu, S. Z., Roden, D., Chan, C. L., et al. (2018). Targeting stromal remodeling and cancer stem cell plasticity overcomes chemoresistance in triple negative breast cancer. *Nat. Commun.* 9:2897. doi: 10.1038/s41467-018-05220-6

Chanmee, T., Ontong, P., Kimata, K., and Itano, N. (2015). Key roles of hyaluronan and its CD44 receptor in the stemness and survival of cancer stem cells. *Front. Oncol.* 5:180. doi: 10.3389/fonc.2015.00180

Chen, W. J., Ho, C. C., Chang, Y. L., Chen, H. Y., Lin, C. A., Ling, T. Y., et al. (2014). Cancer-associated fibroblasts regulate the plasticity of lung cancer stemness via paracrine signalling. *Nat. Commun.* 5:3472. doi: 10.1038/ncomms4472

Clarke, M. F., Dick, J. E., Dirks, P. B., Eaves, C. J., Jamieson, C. H., Jones, D. L., et al. (2006). Cancer stem cells - perspectives on current status and future directions: AACR workshop on cancer stem cells. *Cancer Res.* 66, 9339–9344. doi: 10.1158/0008-5472.CAN-06-3126

Costa, A., Kieffer, Y., Scholer-Dahirel, A., Pelon, F., Bourachot, B., Cardon, M., et al. (2018). Fibroblast heterogeneity and immunosuppressive environment in human breast cancer. *Cancer Cell* 33, 463–479.e10. doi: 10.1016/j.ccell.2018.01.011

Delaunay, S., and Frye, M. (2019). RNA modifications regulating cell fate in cancer. *Nat. Cell Biol.* 21, 552–559. doi: 10.1038/s41556-019-0319-0

Ding, X., Ji, J., Jiang, J., Cai, Q., Wang, C., Shi, M., et al. (2018). HGF-mediated crosstalk between cancer-associated fibroblasts and MET-unamplified gastric cancer cells activates coordinated tumorigenesis and metastasis. *Cell Death Dis.* 9:867. doi: 10.1038/s41419-018-0922-1

Dominguez, C. X., Muller, S., Keerthivasan, S., Koeppen, H., Hung, J., Gierke, S., et al. (2020). Single-cell RNA sequencing reveals stromal evolution into LRRC15(+) myofibroblasts as a determinant of patient response to cancer immunotherapy. *Cancer Discov.* 10, 232–253. doi: 10.1158/2159-8290.CD-19-0644

Donnarumma, E., Fiore, D., Nappa, M., Roscigno, G., Adamo, A., Iaboni, M., et al. (2017). Cancer-associated fibroblasts release exosomal microRNAs that dictate an aggressive phenotype in breast cancer. *Oncotarget* 8, 19592–19608. doi: 10.18632/oncotarget.14752

Dorff, T. B., Goldman, B., Pinski, J. K., Mack, P. C., Lara, P. N. Jr., Van Veldhuizen, P. J. Jr., et al. (2010). Clinical and correlative results of SWOG S0354: a phase II trial of CNTO328 (siltuximab), a monoclonal antibody against interleukin-6, in chemotherapy-pretreated patients with castration-resistant prostate cancer. *Clin. Cancer Res.* 16, 3028–3034. doi: 10.1158/1078-0432.CCR-09-3122

Du, Y., Shao, H., Moller, M., Prokupets, R., Tse, Y. T., and Liu, Z. J. (2019). Intracellular Notch1 signaling in cancer-associated fibroblasts dictates the plasticity and stemness of melanoma stem/initiating cells. *Stem Cells* 37, 865–875. doi: 10.1002/stem.3013

Dvorak, H. F. (1986). Tumors: wounds that do not heal. Similarities between tumor stroma generation and wound healing. *N. Engl. J. Med.* 315, 1650–1659. doi: 10.1056/NEJM198612253152606

Erez, N., Truitt, M., Olson, P., Arron, S. T., and Hanahan, D. (2010). Cancer-associated fibroblasts are activated in incipient neoplasia to orchestrate tumor-promoting inflammation in an NF-kappaB-dependent manner. *Cancer Cell* 17, 135–147. doi: 10.1016/j.ccr.2009.12.041

Fang, T., Lv, H., Lv, G., Li, T., Wang, C., Han, Q., et al. (2018). Tumor-derived exosomal miR-1247-3p induces cancer-associated fibroblast activation to foster lung metastasis of liver cancer. *Nat. Commun.* 9:191. doi: 10.1038/s41467-017-02583-0

Ferrer-Mayorga, G., Gomez-Lopez, G., Barbachano, A., Fernandez-Barral, A., Pena, C., Pisano, D. G., et al. (2017). Vitamin D receptor expression and associated gene signature in tumour stromal fibroblasts predict clinical outcome in colorectal cancer. *Gut* 66, 1449–1462. doi: 10.1136/gutjnl-2015-310977

Fizazi, K., De Bono, J. S., Flechon, A., Heidenreich, A., Voog, E., Davis, N. B., et al. (2012). Randomised phase II study of siltuximab (CNTO 328), an anti-IL6 monoclonal antibody, in combination with mitoxantrone/prednisone versus mitoxantrone/prednisone alone in metastatic castration-resistant prostate cancer. *Eur. J. Cancer* 48, 85–93. doi: 10.1016/j.ejca.2011.10.014

Franze, E., Di Grazia, A., Sica, G. S., Biancone, L., Laudisi, F., and Monteleone, G. (2020). Interleukin-34 enhances the tumor promoting function of colorectal cancer-associated fibroblasts. *Cancers* 12:3537. doi: 10.3390/cancers12123537

Froeling, F. E., Feig, C., Chelala, C., Dobson, R., Mein, C. E., Tuveson, D. A., et al. (2011). Retinoic acid-induced pancreatic stellate cell quiescence reduces paracrine Wnt-beta-catenin signaling to slow tumor progression. *Gastroenterology* 141, 1486–1497. doi: 10.1053/j.gastro.2011.06.047

Fujii, M., Shimokawa, M., Date, S., Takano, A., Matano, M., Nanki, K., et al. (2016). A colorectal tumor organoid library demonstrates progressive loss of niche factor requirements during tumorigenesis. *Cell Stem Cell* 18, 827–838. doi: 10.1016/j.stem.2016.04.003

Galbo et al., P. M. Jr., Zang, X., and Zheng, D. (2021). Molecular features of cancer-associated fibroblast subtypes and their implication on cancer pathogenesis, prognosis, and immunotherapy resistance. *Clin. Cancer Res.* 1, 2636–2647. doi: 10.1158/1078-0432.CCR-20-4226

Geary, L. A., Nash, K. A., Adisetiyo, H., Liang, M., Liao, C. P., Jeong, J. H., et al. (2014). CAF-secreted annexin A1 induces prostate cancer cells to gain stem cell-like features. *Mol. Cancer Res.* 12, 607–621. doi: 10.1158/1541-7786.MCR-13-0469

Giannoni, E., Bianchini, F., Masieri, L., Serni, S., Torre, E., Calorini, L., et al. (2010). Reciprocal activation of prostate cancer cells and cancer-associated fibroblasts

stimulates epithelial-mesenchymal transition and cancer stemness. *Cancer Res.* 70, 6945–6956. doi: 10.1158/0008-5472.CAN-10-0785

Giulianelli, S., Riggio, M., Guillardoy, T., Perez Pinero, C., Gorostiaga, M. A., Sequeira, G., et al. (2019). FGF2 induces breast cancer growth through ligand-independent activation and recruitment of ERalpha and PRBDelta4 isoform to MYC regulatory sequences. *Int. J. Cancer* 145, 1874–1888. doi: 10.1002/ijc.32252

Guo, J. Y., Hsu, H. S., Tyan, S. W., Li, F. Y., Shew, J. Y., Lee, W. H., et al. (2017). Serglycin in tumor microenvironment promotes non-small cell lung cancer aggressiveness in a CD44-dependent manner. *Oncogene* 36, 2457–2471. doi: 10.1038/onc.2016.404

Hu, J. L., Wang, W., Lan, X. L., Zeng, Z. C., Liang, Y. S., Yan, Y. R., et al. (2019). CAFs secreted exosomes promote metastasis and chemotherapy resistance by enhancing cell stemness and epithelial-mesenchymal transition in colorectal cancer. *Mol. Cancer* 18:91. doi: 10.1186/s12943-019-1019-x

Hu, Y., Yan, C., Mu, L., Huang, K., Li, X., Tao, D., et al. (2015). Fibroblast-derived exosomes contribute to chemoresistance through priming cancer stem cells in colorectal cancer. *PLoS One* 10:e0125625. doi: 10.1371/journal.pone.0125625

Jiang, J., Ye, F., Yang, X., Zong, C., Gao, L., Yang, Y., et al. (2017). Peri-tumor associated fibroblasts promote intrahepatic metastasis of hepatocellular carcinoma by recruiting cancer stem cells. *Cancer Lett.* 404, 19–28. doi: 10.1016/j.canlet.2017.07.006

Kalluri, R. (2016). The biology and function of fibroblasts in cancer. *Nat. Rev. Cancer* 16, 582–598. doi: 10.1038/nrc.2016.73

Kessenbrock, K., Dijkgraaf, G. J., Lawson, D. A., Littlepage, L. E., Shahi, P., Pieper, U., et al. (2013). A role for matrix metalloproteinases in regulating mammary stem cell function via the Wnt signaling pathway. *Cell Stem Cell* 13, 300–313. doi: 10.1016/j.stem.2013.06.005

Kocher, H. M., Basu, B., Froeling, F. E. M., Sarker, D., Slater, S., Carlin, D., et al. (2020). Phase I clinical trial repurposing all-trans retinoic acid as a stromal targeting agent for pancreatic cancer. *Nat. Commun.* 11:4841. doi: 10.1038/s41467-020-18636-w

Lambrechts, D., Wauters, E., Boeckx, B., Aibar, S., Nittner, D., Burton, O., et al. (2018). Phenotype molding of stromal cells in the lung tumor microenvironment. *Nat. Med.* 24, 1277–1289. doi: 10.1038/s41591-018-0096-5

Lau, E. Y., Lo, J., Cheng, B. Y., Ma, M. K., Lee, J. M., Ng, J. K., et al. (2016). Cancer-associated fibroblasts regulate tumor-initiating cell plasticity in hepatocellular carcinoma through c-Met/FRA1/HEY1 signaling. *Cell Rep.* 15, 1175–1189. doi: 10.1016/j.celrep.2016.04.019

Le, P. N., Keysar, S. B., Miller, B., Eagles, J. R., Chimed, T. S., Reisinger, J., et al. (2019). Wnt signaling dynamics in head and neck squamous cell cancer tumor-stroma interactions. *Mol. Carcinog.* 58, 398–410. doi: 10.1002/mc.22937

Li, Q., Wang, C., Wang, Y., Sun, L., Liu, Z., Wang, L., et al. (2018). HSCs-derived COMP drives hepatocellular carcinoma progression by activating MEK/ERK and PI3K/AKT signaling pathways. *J. Exp. Clin. Cancer Res.* 37:231. doi: 10.1186/s13046-018-0908-y

Li, X., Bu, W., Meng, L., Liu, X., Wang, S., Jiang, L., et al. (2019). CXCL12/CXCR4 pathway orchestrates CSC-like properties by CAF recruited tumor associated macrophage in OSCC. *Exp. Cell Res.* 378, 131–138. doi: 10.1016/j.yexcr.2019.03.013

Liao, C. P., Chen, L. Y., Luethy, A., Kim, Y., Kani, K., MacLeod, A. R., et al. (2017). Androgen receptor in cancer-associated fibroblasts influences stemness in cancer cells. *Endocr. Relat. Cancer* 24, 157–170. doi: 10.1530/ERC-16-0138

Liu, J., Chen, S., Wang, W., Ning, B. F., Chen, F., Shen, W., et al. (2016). Cancer-associated fibroblasts promote hepatocellular carcinoma metastasis through chemokine-activated hedgehog and TGF-beta pathways. *Cancer Lett.* 379, 49–59. doi: 10.1016/j.canlet.2016.05.022

Maeda, M., Takeshima, H., Iida, N., Hattori, N., Yamashita, S., Moro, H., et al. (2020). Cancer cell niche factors secreted from cancer-associated fibroblast by loss of H3K27me3. *Gut* 69, 243–251. doi: 10.1136/gutjnl-2018-317645

Malanchi, I., Santamaria-Martinez, A., Susanto, E., Peng, H., Lehr, H. A., Delaloye, J. F., et al. (2011). Interactions between cancer stem cells and their niche govern metastatic colonization. *Nature* 481, 85–89. doi: 10.1038/nature10694

Mani, S. A., Guo, W., Liao, M. J., Eaton, E. N., Ayyanan, A., Zhou, A. Y., et al. (2008). The epithelial-mesenchymal transition generates cells with properties of stem cells. *Cell* 133, 704–715. doi: 10.1016/j.cell.2008.03.027

Marsh, D., Suchak, K., Moutasim, K. A., Vallath, S., Hopper, C., Jerjes, W., et al. (2011). Stromal features are predictive of disease mortality in oral cancer patients. *J. Pathol.* 223, 470–481. doi: 10.1002/path.2830

New, J., Arnold, L., Ananth, M., Alvi, S., Thornton, M., Werner, L., et al. (2017). Secretory autophagy in cancer-associated fibroblasts promotes head and neck cancer progression and offers a novel therapeutic target. *Cancer Res.* 77, 6679–6691. doi: 10.1158/0008-5472.CAN-17-1077

Ng, K. Y., Shea, Q. T., Wong, T. L., Luk, S. T., Tong, M., Lo, C. M., et al. (2021). Chemotherapy-enriched THBS2-deficient cancer stem cells drive hepatocarcinogenesis through matrix softness induced histone H3 modifications. *Adv. Sci.* 8:2002483. doi: 10.1002/advs.202002483

Öhlund, D., Elyada, E., and Tuveson, D. (2014). Fibroblast heterogeneity in the cancer wound. *J. Exp. Med.* 211, 1503–1523. doi: 10.1084/jem.20140692

Öhlund, D., Handly-Santana, A., Biffi, G., Elyada, E., Almeida, A. S., Ponz-Sarvise, M., et al. (2017). Distinct populations of inflammatory fibroblasts and myofibroblasts in pancreatic cancer. *J. Exp. Med.* 214, 579–596. doi: 10.1084/jem.20162024

Olive, K. P., Jacobetz, M. A., Davidson, C. J., Gopinathan, A., McIntyre, D., Honess, D., et al. (2009). Inhibition of Hedgehog signaling enhances delivery of chemotherapy in a mouse model of pancreatic cancer. *Science* 324, 1457–1461. doi: 10.1126/science.1171362

Oskarsson, T., Batlle, E., and Massague, J. (2014). Metastatic stem cells: sources, niches, and vital pathways. *Cell Stem Cell* 14, 306–321. doi: 10.1016/j.stem.2014.02.002

Ozdemir, B. C., Pentcheva-Hoang, T., Carstens, J. L., Zheng, X., Wu, C. C., Simpson, T. R., et al. (2014). Depletion of carcinoma-associated fibroblasts and fibrosis induces immunosuppression and accelerates pancreas cancer with reduced survival. *Cancer Cell* 25, 719–734. doi: 10.1016/j.ccr.2014.04.005

Pang, M. F., Siedlik, M. J., Han, S., Stallings-Mann, M., Radisky, D. C., and Nelson, C. M. (2016). Tissue stiffness and hypoxia modulate the integrin-linked kinase ILK to control breast cancer stem-like cells. *Cancer Res.* 76, 5277–5287. doi: 10.1158/0008-5472.CAN-16-0579

Peltanova, B., Liskova, M., Gumulec, J., Raudenska, M., Polanska, H. H., Vaculovic, T., et al. (2021). Sensitivity to cisplatin in head and neck cancer cells is significantly affected by patient-derived cancer-associated fibroblasts. *Int. J. Mol. Sci.* 22:1912. doi: 10.3390/ijms22041912

Pienta, K. J., Machiels, J. P., Schrijvers, D., Alekseev, B., Shkolnik, M., Crabb, S. J., et al. (2013). Phase 2 study of carlumab (CNTO 888), a human monoclonal antibody against CC-chemokine ligand 2 (CCL2), in metastatic castration-resistant prostate cancer. *Invest. New Drugs* 31, 760–768. doi: 10.1007/s10637-012-9869-8

Plaks, V., Kong, N., and Werb, Z. (2015). The cancer stem cell niche: how essential is the niche in regulating stemness of tumor cells? *Cell Stem Cell* 16, 225–238. doi: 10.1016/j.stem.2015.02.015

Qin, X., Guo, H., Wang, X., Zhu, X., Yan, M., Wang, X., et al. (2019). Exosomal miR-196a derived from cancer-associated fibroblasts confers cisplatin resistance in head and neck cancer through targeting CDKN1B and ING5. *Genome Biol.* 20:12. doi: 10.1186/s13059-018-1604-0

Qin, X., Yan, M., Zhang, J., Wang, X., Shen, Z., Lv, Z., et al. (2016). TGFbeta3-mediated induction of Periostin facilitates head and neck cancer growth and is associated with metastasis. *Sci. Rep.* 6:20587. doi: 10.1038/srep20587

Ren, J., Ding, L., Zhang, D., Shi, G., Xu, Q., Shen, S., et al. (2018). Carcinoma-associated fibroblasts promote the stemness and chemoresistance of colorectal cancer by transferring exosomal lncRNA H19. *Theranostics* 8, 3932–3948. doi: 10.7150/thno.25541

Reya, T., Morrison, S. J., Clarke, M. F., and Weissman, I. L. (2001). Stem cells, cancer, and cancer stem cells. *Nature* 414, 105–111. doi: 10.1038/35102167

Rhim, A. D., Oberstein, P. E., Thomas, D. H., Mirek, E. T., Palermo, C. F., Sastra, S. A., et al. (2014). Stromal elements act to restrain, rather than support, pancreatic ductal adenocarcinoma. *Cancer Cell* 25, 735–747. doi: 10.1016/j.ccr.2014.04.021

Roulis, M., Kaklamanos, A., Schernthanner, M., Bielecki, P., Zhao, J., Kaffe, E., et al. (2020). Paracrine orchestration of intestinal tumorigenesis by a mesenchymal niche. *Nature* 580, 524–529. doi: 10.1038/s41586-020-2166-3

San-Miguel, J., Blade, J., Shpilberg, O., Grosicki, S., Maloisel, F., Min, C. K., et al. (2014). Phase 2 randomized study of bortezomib-melphalan-prednisone with or without siltuximab (anti-IL6) in multiple myeloma. *Blood* 123, 4136–4142. doi: 10.1182/blood-2013-12-546374

Shan, G., Gu, J., Zhou, D., Li, L., Cheng, W., Wang, Y., et al. (2020). Cancer-associated fibroblast-secreted exosomal miR-423-5p promotes chemotherapy resistance in prostate cancer by targeting GREM2 through the TGF-beta signaling pathway. *Exp. Mol. Med.* 52, 1809–1822. doi: 10.1038/s12276-020-0431-z

Shao, H., Cai, L., Moller, M., Issac, B., Zhang, L., Owyong, M., et al. (2016). Notch1-WISP-1 axis determines the regulatory role of mesenchymal stem cell-derived stromal fibroblasts in melanoma metastasis. *Oncotarget* 7, 79262–79273. doi: 10.18632/oncotarget.13021

Sherman, M. H., Yu, R. T., Engle, D. D., Ding, N., Atkins, A. R., Tiriac, H., et al. (2014). Vitamin D receptor-mediated stromal reprogramming suppresses pancreatitis and enhances pancreatic cancer therapy. *Cell* 159, 80–93. doi: 10.1016/j.cell.2014.08.007

Song, H., Liu, D., Dong, S., Zeng, L., Wu, Z., Zhao, P., et al. (2020). Epitranscriptomics and epiproteomics in cancer drug resistance: therapeutic implications. *Signal Transduct. Target. Ther.* 5:193. doi: 10.1038/s41392-020-00300-w

Song, M., He, J., Pan, Q. Z., Yang, J., Zhao, J., Zhang, Y. J., et al. (2021). Cancer-associated fibroblast-mediated cellular crosstalk supports hepatocellular carcinoma progression. *Hepatology* 73, 1717–1735. doi: 10.1002/hep.31792

Su, S., Chen, J., Yao, H., Liu, J., Yu, S., Lao, L., et al. (2018). CD10(+)GPR77(+) cancer-associated fibroblasts promote cancer formation and chemoresistance by sustaining cancer stemness. *Cell* 172, 841–856.e16. doi: 10.1016/j.cell.2018.01.009

Sun, L., Wang, Y., Wang, L., Yao, B., Chen, T., Li, Q., et al. (2019). Resolvin D1 prevents epithelial-mesenchymal transition and reduces the stemness features of hepatocellular carcinoma by inhibiting paracrine of cancer-associated fibroblast-derived COMP. *J. Exp. Clin. Cancer Res.* 38, 170. doi: 10.1186/s13046-019-1163-6

Sung, P. J., Rama, N., Imbach, J., Fiore, S., Ducarouge, B., Neves, D., et al. (2019). Cancer-associated fibroblasts produce netrin-1 to control cancer cell plasticity. *Cancer Res.* 79, 3651–3661. doi: 10.1158/0008-5472.CAN-18-2952

Tan, Y., Tajik, A., Chen, J., Jia, Q., Chowdhury, F., Wang, L., et al. (2014). Matrix softness regulates plasticity of tumour-repopulating cells via H3K9 demethylation and Sox2 expression. *Nat. Commun.* 5:4619. doi: 10.1038/ncomms5619

Tang, Y. A., Chen, Y. F., Bao, Y., Mahara, S., Yatim, S., Oguz, G., et al. (2018). Hypoxic tumor microenvironment activates GLI2 via HIF-1alpha and TGF-beta2 to promote chemoresistance in colorectal cancer. *Proc. Natl. Acad. Sci. U. S. A.* 115, E5990–E5999. doi: 10.1073/pnas.1801348115

Tao, B., Song, Y., Wu, Y., Yang, X., Peng, T., Peng, L., et al. (2021). Matrix stiffness promotes glioma cell stemness by activating BCL9L/Wnt/beta-catenin signaling. *Aging* 13, 5284–5296. doi: 10.18632/aging.202449

Tauriello, D. V. F., Palomo-Ponce, S., Stork, D., Berenguer-Llergo, A., Badia-Ramentol, J., Iglesias, M., et al. (2018). TGFbeta drives immune evasion in genetically reconstituted colon cancer metastasis. *Nature* 554, 538–543. doi: 10.1038/nature25492

Tsujino, T., Seshimo, I., Yamamoto, H., Ngan, C. Y., Ezumi, K., Takemasa, I., et al. (2007). Stromal myofibroblasts predict disease recurrence for colorectal cancer. *Clin. Cancer Res.* 13, 2082–2090. doi: 10.1158/1078-0432.CCR-06-2191

Valenti, G., Quinn, H. M., Heynen, G., Lan, L., Holland, J. D., Vogel, R., et al. (2017). Cancer stem cells regulate cancer-associated fibroblasts via activation of hedgehog signaling in mammary gland tumors. *Cancer Res.* 77, 2134–2147. doi: 10.1158/0008-5472.CAN-15-3490

Vered, M., Dobriyan, A., Dayan, D., Yahalom, R., Talmi, Y. P., Bedrin, L., et al. (2010). Tumor-host histopathologic variables, stromal myofibroblasts and risk score, are significantly associated with recurrent disease in tongue cancer. *Cancer Sci.* 101, 274–280. doi: 10.1111/j.1349-7006.2009.01357.x

Walcher, L., Kistenmacher, A. K., Suo, H., Kitte, R., Dluczek, S., Strauss, A., et al. (2020). Cancer stem cells- origins and biomarkers: perspectives for targeted personalized therapies. *Front. Immunol.* 11:1280. doi: 10.3389/fimmu.2020.01280

Wei, L., Lin, Q., Lu, Y., Li, G., Huang, L., Fu, Z., et al. (2021). Cancer-associated fibroblasts-mediated ATF4 expression promotes malignancy and gemcitabine resistance in pancreatic cancer via the TGF-beta1/SMAD2/3 pathway and ABCC1 transactivation. *Cell Death Dis.* 12:334. doi: 10.1038/s41419-021-03574-2

Witty, J. P., Wright, J. H., and Matrisian, L. M. (1995). Matrix metalloproteinases are expressed during ductal and alveolar mammary morphogenesis, and misregulation of stromelysin-1 in transgenic mice induces unscheduled alveolar development. *Mol. Biol. Cell* 6, 1287–1303. doi: 10.1091/mbc.6.10.1287

Wu, H. J., Hao, M., Yeo, S. K., and Guan, J. L. (2020). FAK signaling in cancer-associated fibroblasts promotes breast cancer cell migration and metastasis by exosomal miRNAs-mediated intercellular communication. *Oncogene* 39, 2539–2549. doi: 10.1038/s41388-020-1162-2

Xiong, S., Wang, R., Chen, Q., Luo, J., Wang, J., Zhao, Z., et al. (2018). Cancer-associated fibroblasts promote stem cell-like properties of hepatocellular carcinoma cells through IL6/STAT3/Notch signaling. *Am. J. Cancer Res.* 8, 302–316.

Yan, B., Jiang, Z., Cheng, L., Chen, K., Zhou, C., Sun, L., et al. (2018). Paracrine HGF/c-MET enhances the stem cell-like potential and glycolysis of pancreatic cancer cells via activation of YAP/HIF-1alpha. *Exp. Cell Res.* 371, 63–71. doi: 10.1016/j.yexcr.2018.07.041

Yu, B., Wu, K., Wang, X., Zhang, J., Wang, L., Jiang, Y., et al. (2018). Periostin secreted by cancer-associated fibroblasts promotes cancer stemness in head and neck cancer by activating protein tyrosine kinase 7. *Cell Death Dis.* 9:1082. doi: 10.1038/s41419-018-1116-6

Zhang, M., Yang, H., Wan, L., Wang, Z., Wang, H., Ge, C., et al. (2020). Single-cell transcriptomic architecture and intercellular crosstalk of human intrahepatic cholangiocarcinoma. *J. Hepatol.* 73, 1118–1130. doi: 10.1016/j.jhep.2020.05.039

Zhao, X. L., Lin, Y., Jiang, J., Tang, Z., Yang, S., Lu, L., et al. (2017). High-mobility group box 1 released by autophagic cancer-associated fibroblasts maintains the stemness of luminal breast cancer cells. *J. Pathol.* 243, 376–389. doi: 10.1002/path.4958

Conflict of Interest: The authors declare that the research was conducted in the absence of any commercial or financial relationships that could be construed as a potential conflict of interest.

Publisher's Note: All claims expressed in this article are solely those of the authors and do not necessarily represent those of their affiliated organizations, or those of the publisher, the editors and the reviewers. Any product that may be evaluated in this article, or claim that may be made by its manufacturer, is not guaranteed or endorsed by the publisher.

frontiers in Cell and Developmental Biology

ORIGINAL RESEARCH
published: 01 November 2021
doi: 10.3389/fcell.2021.725630

Dephosphorylation of Caveolin-1 Controls C-X-C Motif Chemokine Ligand 10 Secretion in Mesenchymal Stem Cells to Regulate the Process of Wound Healing

*Panpan Wang[1], Yingji Zhao[1], Juan Wang[1], Zhiying Wu[2], Bingdong Sui[1,2], Xueli Mao[1,3], Songtao Shi[1,3] and Xiaoxing Kou[1,3]**

[1] South China Center of Craniofacial Stem Cell Research, Hospital of Stomatology, Sun Yat-sen University, Guangdong Provincial Key Laboratory of Stomatology, Guangzhou, China, [2] Department of Microbiology, Zhongshan School of Medicine, Key Laboratory for Tropical Diseases Control of the Ministry of Education, Sun Yat-sen University, Guangzhou, China, [3] Key Laboratory for Stem Cells and Tissue Engineering, Sun Yat-sen University, Ministry of Education, Guangzhou, China

OPEN ACCESS

Edited by:
Cheng Ming Chuong, University of Southern California, United States

Reviewed by:
Gloria Bonuccelli, University of Salford, United Kingdom
Chao-Kai Hsu, National Cheng Kung University, Taiwan

***Correspondence:**
Xiaoxing Kou
kouxiaoxing@mail.sysu.edu.cn

Specialty section:
This article was submitted to Stem Cell Research, a section of the journal Frontiers in Cell and Developmental Biology

Received: *15 June 2021*
Accepted: *11 October 2021*
Published: *01 November 2021*

Citation:
Wang P, Zhao Y, Wang J, Wu Z, Sui B, Mao X, Shi S and Kou X (2021) Dephosphorylation of Caveolin-1 Controls C-X-C Motif Chemokine Ligand 10 Secretion in Mesenchymal Stem Cells to Regulate the Process of Wound Healing. Front. Cell Dev. Biol. 9:725630. doi: 10.3389/fcell.2021.725630

Mesenchymal stem cells (MSCs) secrete cytokines in a paracrine or autocrine manner to regulate immune response and tissue regeneration. Our previous research revealed that MSCs use the complex of Fas/Fas-associated phosphatase-1 (Fap-1)/caveolin-1 (Cav-1) mediated exocytotic process to regulate cytokine and small extracellular vesicles (EVs) secretion, which contributes to accelerated wound healing. However, the detailed underlying mechanism of cytokine secretion controlled by Cav-1 remains to be explored. We show that Gingiva-derived MSCs (GMSCs) could secrete more C-X-C motif chemokine ligand 10 (CXCL10) but showed lower phospho-Cav-1 (p-Cav-1) expression than skin-derived MSCs (SMSCs). Moreover, dephosphorylation of Cav-1 by a Src kinase inhibitor PP2 significantly enhances CXCL10 secretion, while activating phosphorylation of Cav-1 by H_2O_2 restraints CXCL10 secretion in GMSCs. We also found that Fas and Fap-1 contribute to the dephosphorylation of Cav-1 to elevate CXCL10 secretion. Tumor necrosis factor-α serves as an activator to up-regulate Fas, Fap-1, and down-regulate p-Cav-1 expression to promote CXCL10 release. Furthermore, local applying p-Cav-1 inhibitor PP2 could accelerate wound healing, reduce the expression of α-smooth muscle actin and increase cleaved-caspase 3 expression. These results indicated that dephosphorylation of Cav-1 could inhibit fibrosis during wound healing. The present study establishes a previously unknown role of p-Cav-1 in controlling cytokine release of MSC and may present a potential therapeutic approach for promoting scarless wound healing.

Keywords: phospho-caveolin-1, CXCL10, mesenchymal stem cells, wound healing, secretion

INTRODUCTION

Wound healing is a complex process involving increased proliferation, adhesion, and migration of cells from connective tissue and epithelium, inflammatory reactions, and extracellular matrix remodeling. Oral gingival and mucosal wounds heal faster with minimal scar formation than cutaneous wounds (Hu et al., 2014). Mesenchymal stem cells (MSCs), capable of self-renewal and differentiation into mesenchymal and non-mesenchymal lineages (Abe et al., 2012), are essential players in maintaining tissue homeostasis (Gronthos et al., 2006). As resident cells, MSCs from the gingival or skin play an important role during the wound healing process (Li et al., 2018). However, the detailed mechanism by which MSCs contribute to wound healing is still not fully understood.

Numerous secreted factors, including cytokines, growth factors, chemokines, contribute to the remolding process of cutaneous wound healing (Forbes and Rosenthal, 2014; Rani et al., 2015). MSCs secrete cytokines in a paracrine or autocrine manner to regulate immune response and tissue regeneration. Gingiva-derived MSCs (GMSCs) have a distinct neural crest origin and show characteristics of self-renewal, multipotent differentiation, and immunomodulatory capacities both *in vitro* and *in vivo* (Zhang et al., 2009; Xu et al., 2013). Our previous study showed that GMSCs displayed different secretion profiles compared with skin-derived MSCs (SMSCs) and produce a higher amount of interleukin-1 receptor antagonist (IL-1RA) to accelerate gingival and cutaneous wound healing in mice (Kou et al., 2018). However, the critical role of other cytokines secreted by MSCs in wound healing has not been elucidated except IL-1RA.

Previously, we found that MSCs use Fas/Fas-associated phosphatase-1 (Fap-1) complex combined with the caveolin-1 (Cav-1) to activate the exocytotic process, secrete cytokines, and small EVs (Kou et al., 2018). However, the detailed underlying mechanism of cytokine secretion controlled by Cav-1 remains obscure. Cav-1 is a scaffold protein and the main protein component of caveolae. It participates in various cellular functions, including transcytosis, potocytosis, signal transduction endocytosis, proliferation, and differentiation (Predescu et al., 1997; Zhang et al., 2021). Cav-1 tyrosine 14 (Y14) is the primary phosphorylation site targeted by Src (Huang and He, 2017). The increase of phospho-Cav-1 (p-Cav-1) versus total Cav-1 is related to the reducing plasma membrane-attached caveolae and a simultaneous increase of cytoplasmic vesicles (Zimnicka et al., 2016). Studies suggest that phosphorylation of Cav-1 is associated with the formation and internalization of caveolae. Previous research also revealed that Y14 phosphorylation regulates divergent actions on stem cells, such as migration, proliferation, and survival (Park and Han, 2009). We thus hypothesized that phosphorylation of Cav-1 might regulate the secretion process of MSCs. In the current study, we show that dephosphorylation of Cav-1 controls the cytokine secretion capacity of MSCs to secrete a higher amount of C-X-C motif chemokine ligand 10 (CXCL10) and may serve as a potential therapeutic approach for promoting scarless wound healing.

MATERIALS AND METHODS

Animals

Female C57BL/6J, B6.MRL-Fas^{lpr}/J (MRL/*lpr*, Fas-deficient), and B6.Cg-Cav1^{TM1Mls}/J (Cav-1 knockout) mice were purchased from the Jackson Laboratory (Bar Harbor, ME, United States) and Laboratory Animal Center of Sun Yat-sen University. Age-matched 8–10-week female mice from the same background were used in all experiments. All the animals were fed under specific pathogen-free conditions with an ambient temperature of 24°C, 55–65% relative humidity, and a 12:12 h light:dark cycle. Animal experiments were performed under protocols institutionally approved by Animal Care and Use Committee of Sun Yat-sen University (SYSU-IACUC-2021-000118).

Reagents and Chemicals

Src kinase inhibitor 4-amino-5-(4-chlorophenyl)-7-(t-butyl) pyrazolo[3,4-d]pyrimidine (PP2) was purchased from Sigma-Aldrich (St. Louis, MO, United States). Recombinant mice tumor necrosis factor-α (TNF-α) (315-01A), interferon-γ (IFN-γ) (500-P119) was purchased from PeproTech (Rocky Hill, NJ, United States). *Fas* (sc-2931) and *Fap-1* (sc-145067) small interfering RNA (siRNA) was purchased from Santa Cruz Biotechnology (Santa Cruz, CA, United States). Lipofectamine^{TM} RNAiMAX transfection reagent (#13778030) was purchased from Thermo Fisher Scientific (Waltham, MA, United States). Mouse Cytokine Array Panel A (ARY006) was obtained from R&D system (Minneapolis, MN, United States). Mouse CXCL10 enzyme-linked immunosorbent assay (ELISA) Kit (ab214563) was purchased from Abcam (Cambridge, MA, United States). DeadEnd^{TM} Fluorometric TUNEL System (G3250) was purchased from Promega (Madison, WI, United States).

Antibodies

Anti-Fas antibody (05-351) was purchased from Millipore (Burlington, MA, United States). Anti-Fap-1 (MBS242520) were purchased from MyBioSource (MyBioSource, CA, United States). Anti-CXCL10 (sc-374092), Cav-1 (7C8) antibodies were purchased from Santa Cruz Biotechnology (Santa Cruz, CA, United States). Anti-Caspase-3 (5A1E), Cleaved Caspase-3 (Asp175), Anti-p-Cav-1 (3251), proliferating cell nuclear antigen (PCNA) (2586s) were purchased from Cell Signaling Technology (Danvers, MA, United States). Anti-α-smooth muscle actin (α-SMA) antibody was purchased from eBioscience (14-9760-82). Anti-actin (A2066) antibody was purchased from Sigma-Aldrich (St. Louis, MO, United States). Collagen I (bs-10423R) and Collagen III (bs-0549R) were purchased from Bioss (Cambridge, MA, United States). Alexa Fluor 488, Alexa Fluor 568, and Alexa Fluor 647 secondary antibodies were purchased from Invitrogen (Carlsbad, CA, United States).

Isolation of Mouse and Human Gingival, and Skin Mesenchymal Stem Cells

Murine GMSCs and SMSCs were isolated and cultured as reported by our previous study (Zhang et al., 2009; Xu et al., 2013; Kou et al., 2018). To put it simply, gingival tissue around the

molars and dorsal skin tissues of mice were separated and minced. Then tissues were incubated in 2 mg/ml collagenase type I (Worthington Biochemical) and 4 mg/ml dispase II (Roche Diagnostics) in phosphate-buffered saline (PBS) for 1 h at 37°C. Single cell suspension was obtained by filtering through a 70 μm cell strainer (BD Biosciences). And then, cells were seeded in 10 cm diameter culture dish (Corning, NY, United States) in complete media containing alpha minimum essential medium (α-MEM, Invitrogen) supplemented with 20% fetal bovine serum (FBS), 2 mM L-glutamine, 55 mM 2-mercaptoethanol, 100 U/ml penicillin, and 100 μg/ml streptomycin (Invitrogen) at 37°C in 5% CO_2. After an initial incubation for 48 h, the cultures were washed with PBS to eliminate the non-adherent cells. Colony-forming attached cells were cultured for another 7 days and then passaged with TrypLE^{TM} Express Enzyme (Thermo Fisher Scientific) once for further experimental use.

Human gingiva and skin were obtained as remnant or discarded tissues following routine procedures at Guanghua School and Hospital of Stomatology, Sun Yat-sen University, under the protocol approved by the Medical Ethics Committee of Hospital of Stomatology, Sun Yat-sen University (KQEC-2021-23-01). Tissues were minced aseptically and digested as previously mentioned. Cell suspension was filtered through a 70 μm cell strainer; plated in 100-mm culture dishes with α-MEM containing 15% FBS, 2 mM L-glutamine, 100 U/ml penicillin, and 100 μg/ml streptomycin, 10 mM L-ascorbic acid phosphate and cultured at 37°C in a humidified culture incubator with 5% CO_2. The plastic-adherent cells were passaged and maintained in the complete growth medium. Cells from second to sixth passages were used in the experiments.

Transfection of Small Interfering RNA in GMSCs

GMSCs were passaged on a culture plate and were 50–70% confluent at the time of transfection. *Fas*, *Fap-1*, and *Cav-1* siRNA (Santa Cruz Biotechnology) were used to treat the GMSCs according to the manufacturer's instructions. Non-targeting control siRNA (Santa Cruz Biotechnology) was used as negative controls. Transfected GMSCs were incubated at 37°C for 48 h before further assay. The efficiency of siRNA knockdown was confirmed by western blotting analysis. Transfected cells were then treated with different concentrations of IFN-γ or TNF-α for 24 h, cells were used for protein extraction for western blotting, and the culture supernatants were used for ELISA.

Cytokine Array and Enzyme-Linked Immunosorbent Assay Analysis

Total 0.4×10^6 cells were seeded in 6-well plate, after the cell were attached, cells were serum deprived for 12 h and then treated with different stimuli for 48 h. Cell supernatant were collected and centrifuged at 2000 *g* for 10 min. And then supernatant were analyzed using a Mouse Cytokine Array Panel A Array Kit (R&D Systems) according to the manufacturer's instructions. The results were scanned and analyzed using ImageJ software. CXCL10 levels of the cell culture supernatant were measured by ELISA kit according to the manufacturer's protocol.

Western Blotting

Total protein from cells and tissues were extracted using M-PER mammalian protein extraction reagent (Thermo Fisher Scientific, United States) with protease and phosphatase inhibitors cocktail (Thermo Fisher Scientific, United States). According to the manufacturer's instructions, proteins from cytoplasmic and membrane fractions were extracted using Mem-PER Plus Membrane Protein Extraction Kit (Thermo Fisher Scientific). Briefly, adherent cells were lysed with a permeabilization buffer and centrifuged at 16,000 *g* for 15 min to separate the cytosolic and membrane proteins. Then, the cytosolic proteins were extracted from the supernatant, and the pellet was lysed again in a solubilization buffer to collect the membrane-associated proteins. Proteins were quantified using the BCA protein assay kit (Thermo Scientific, United States) following the manufacturer's instructions. Then, 20 μg of proteins was separated by electrophoresis with 12% SDS-PAGE gel, and transferred onto a polyvinylidene difluoride membrane (Millipore, United States). Membranes were blocked with 5% BSA and 0.1% Tween 20 for 1 h, followed by overnight incubation with the primary antibodies at 4°C. The membranes were then incubated under room temperature for 1 h in species-related horseradish peroxidase-conjugated secondary antibody (Santa Cruz Biotechnology) and detected using SuperSignal West Pico Chemiluminescent Substrate (Thermo Fisher Scientific) and Biomax film (Bio-Rad); the sensitivity of this substrate was chosen to detect low-picogram amounts of protein in polyvinylidene difluoride membrane. β-actin was used as the internal loading control.

Wound Healing in Mice

A 1.5 cm × 1.5 cm full-thickness wounds were created in the dorsal skin of the mice. Seven days after surgery, wounds were topically submucosally injected with 100 μl placebo (PBS) or 100 μl PP2 (50 mg/kg body weight) in PBS every other day. Digital photographs of the cutaneous wounds were taken, including a ruler for scale. The percentage of wound closure (expressed as a percentage of the initial wound area) was quantified on photographs using ImageJ public domain software (NIH, Bethesda, MD, United States). Mice were sacrificed and tissues around the wound were harvested 14 days later.

Histology

For histological analyses, the excised skin from wound sites was fixed in 4% formalin overnight, dehydrated with a graded-alcohol series, embedded in paraffin, and sectioned perpendicularly to the wound surface into 5-μm-thick sections. Hematoxylin and eosin (H&E) staining was used for histological observations. Masson's trichrome staining (Trichrome Stain LG Solution, Sigma-Aldrich) was applied to determine the degree of collagen maturity according to the manufactures' instructions. For immunofluorescent staining, wound tissue was fixed in 4% paraformaldehyde overnight, dehydrated in 30% sucrose solution, embedded in OCT, and sectioned perpendicularly to the wound surface into 5-μm-thick sections.

Immunofluorescence Study

Cells growing on coverslips were fixed in 4% paraformaldehyde, permeabilized with 0.2% Triton-X, blocked with blocking buffer (5% BSA, 0.3% Triton-100 in 1× PBS) for 1 h at RT. Subsequently, coverslips were incubated with the primary antibodies overnight and then stained with secondary antibodies in the dark at room temperature for 1 h. Then, slides were mounted with Vectashield mounting medium containing 4',6-diamidino-2-phenylindole (DAPI) (Vector Laboratories Burlingame, United States). Isotype-matched control antibodies (Invitrogen) were used as negative controls. Images were acquired using a Carl Zeiss Airscan LSM-900 confocal microscope or Zeiss Elyra 7 with Lattice SIM and analyzed using the Zen 2.3 SP1 software, Blue Edition. Three-dimensional reconstruction of 2D *Z*-stack data from SIM-microscope was performed using IMARIS software (Oxford).

TUNEL Assay

Excised skin slices were obtained and incubated with permeabilization solution (PBS; 0.1% Triton X-100; 0.1% sodium citrate) for 2 min on ice and then the slices were incubated with a TUNEL reaction mix for 30 min at 37°C, two additional washing steps were performed, and the cells were then stained with DAPI for a further 7 min. The number of TUNEL-positive stained cells was divided by the number of DAPI-stained nuclei. The stained cells were analyzed using Zeiss LSM 900 confocal microscope with a 63× oil immersion objective.

Statistical Analysis

All data are shown as mean ± SD. Statistical analysis was performed by GraphPad Prism 8 (GraphPad Software, San Diego, CA, United States). Comparisons between two groups were analyzed using independent unpaired two-tailed Student's *t*-tests. Differences between more than two groups were assessed by one-way analysis of variance (ANOVA) with Tukey's *post hoc* test. P-values < 0.05 were considered statistically significant.

RESULTS

GMSCs Produce and Secrete Higher Amounts of C-X-C Motif Chemokine Ligand 10 Than SMSCs

In order to confirm the different secretion profiles between GMSCs and SMSCs, we compared the cytokine secretion pattern in the culture supernatant of murine GMSCs and SMSCs using the Proteome Profiler Cytokine Array. We found that in addition to previously reported IL-1RA (Kou et al., 2018), GMSCs also secreted a higher amount of CXCL10, a potent chemokine for activated T lymphocytes, compared to SMSCs (**Figure 1A**). ELISA analysis further confirmed that GMSCs secreted a higher level of CXCL10 (**Figure 1B**). In addition, western blotting analysis showed that both human and mouse GMSCs expressed elevated CXCL10 than SMSCs (**Figure 1C** and **Supplementary Figure 1A**). Next, we showed that CXCL10 was co-expressed with MSC markers CD73 in both GMSCs and SMSCs (**Figure 1D**).

GMSCs Displayed Lower Caveolin-1 Phosphorylation Than SMSCs

Our previous research revealed that GMSCs use the Fas/Fap-1/Cav-1 cascade to regulate cytokine and EV secretion (Kou et al., 2018). Previous research revealed that phosphorylation of Cav-1 is associated with the formation and internalization of caveolae and is involved in lots of cellular functions (Han et al., 2021). Tyrosine residue Y14 located at the NH2-terminus of Cav-1 protein, is the premier phosphorylation site (Shi et al., 2021). We thus speculated that change of Cav-1 Y14 phosphorylation status might contribute to Fas/Fap-1/Cav-1 cascade-controlled cytokine secretion of MSCs. Western blotting analysis revealed that Cav-1 Y14 phosphorylation in human and mouse GMSCs was lower than in SMSCs, while this trend was not observed in Cav-1 expression (**Figure 2A** and **Supplementary Figure 1A**). Semi-quantification analysis confirmed the significant difference of p-Cav-1 between GMSCs and SMSCs (**Supplementary Figure 2**). To further confirm the difference of Cav-1 phosphorylation between GMSCs and SMSCs, we performed immunofluorescent staining and used super-resolution structured illumination microscopy (SIM) to show that despite similar membrane located p-Cav-1 signal in both GMSCs and SMSCs, cytoplasmic p-Cav-1 was weaker in human and mouse GMSCs than SMSCs (**Figure 2B** and **Supplementary Figures 1B, 3**). On the other hand, although Cav-1 signal intensity did not show a significant difference between GMSCs and SMSCs, Cav-1 signal was nearly completely absent from p-Cav-1 in GMSCs, and lots of Cav-1 signals were colocalized with p-Cav-1 (indicated by merged yellow signal) in SMSCs (**Figure 2B**). In many cell types, caveolae are usually single or in chains or grape-like clusters (Stan, 2005). The three-dimensional reconstruction of SIM (3D-SIM) images further showed that the patterns of p-Cav-1 on the cell membrane of the two kinds of MSCs were different. Specifically, p-Cav-1 caveolae clusters on the GMSCs cell membrane were larger and plump, while the p-Cav-1 structure on SMSCs cell membrane was smaller and slender. 3D-SIM images further revealed that even the membrane p-Cav-1 has a different pattern.

Next, we confirmed that p-Cav-1 and Cav-1 signal was co-expressed with MSC marker CD73 (**Figure 2C**). Phosphorylation of Cav-1 is associated with the formation of caveolae, and we found most of the p-Cav-1 signal located on the cell edge. We, therefore, investigated the dynamic change of Cav-1 phosphorylation during the cell attachment process of suspended GMSCs. In the suspended GMSCs (1 h group), p-Cav-1 was dispersed throughout the intracellular compartment, where it was almost wholly co-localized with Cav-1. When the cells were attached, p-Cav-1 showed time-dependent translocation from the intracellular compartment to the plasma membrane, leading to increased p-Cav-1-labeled cell region of the GMSCs (**Figure 2D**).

Dephosphorylation of Caveolin-1 Controlled C-X-C Motif Chemokine Ligand 10 Secretion in GMSCs

GMSCs secreted a higher amount of CXCL10 and expressed decreased p-Cav in contrast to SMSCs (**Figures 1**, **2**). Our

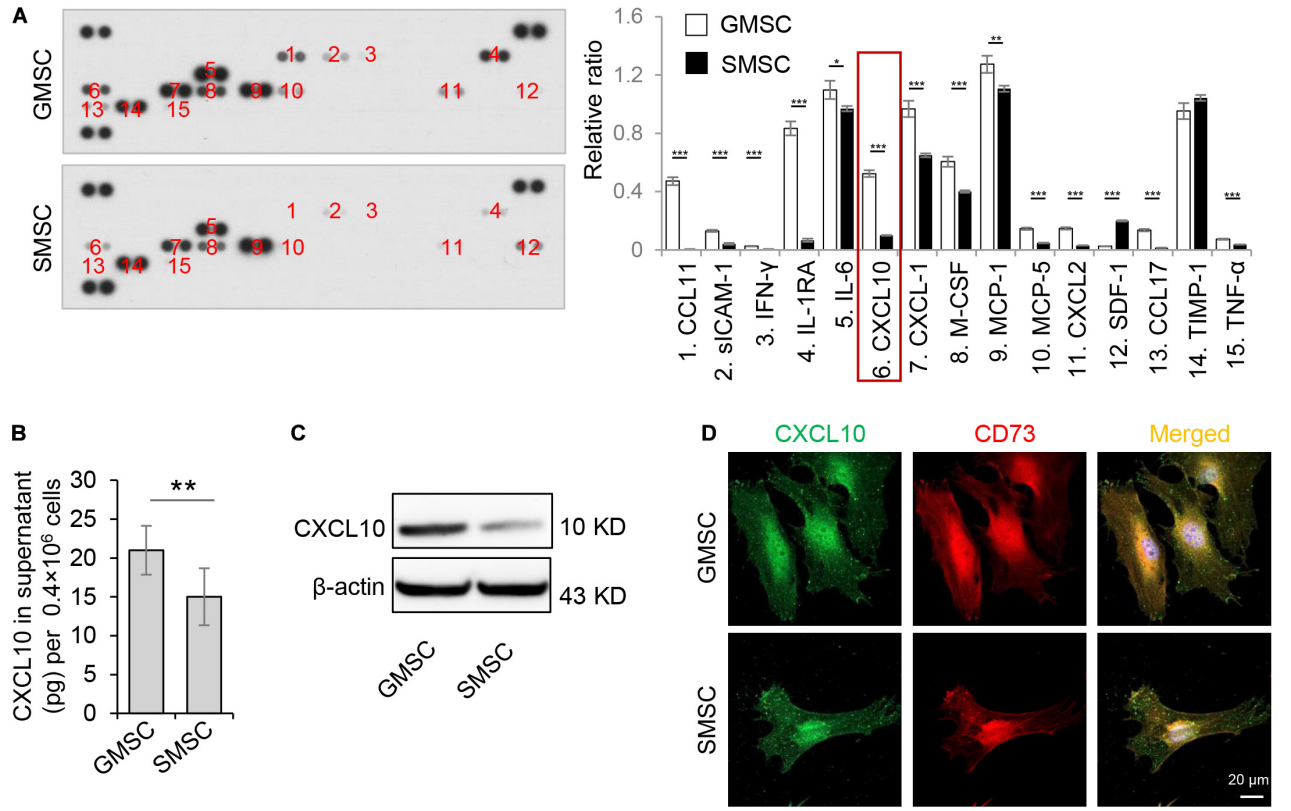

FIGURE 1 | Murine GMSCs produce and secrete higher amounts of CXCL10 than SMSCs. **(A)** Cytokine array analysis of cytokines in cell culture supernatant from mouse GMSCs and SMSCs. Equal volume of cell culture supernatant were taken from 48 h incubation of 0.4 × 10^6 cells. **(B)** ELISA analysis of CXCL10 in the culture supernatant of GMSCs and SMSCs. **(C)** Western blotting analysis showed that the protein expression of CXCL10 was higher in GMSCs than SMSCs. β-Actin was used as a protein loading control. **(D)** CXCL10 (green) co-expressed with the MSC marker CD73 (red) in GMSCs and SMSCs as analyzed by immunocytofluorescence staining. Scale bar, 20 μm. All results are representative of data obtained from at least three independent experiments. *$P < 0.05$, **$P < 0.01$, ***$P < 0.001$. Error bars are means ± SD. Data were analyzed using independent unpaired two-tailed Student's *t*-tests.

previous study revealed that the complex of Fas/Fap-1/Cav-1 controlled EV/cytokine release (Kou et al., 2018). Here, we hypothesized that dephosphorylation of Cav-1 might control the secretion of CXCL10 in MSCs. Src kinase inhibitor 4-amino-5-(4-chlorophenyl)-7-(t-butyl) pyrazolo[3,4-d] pyrimidine (PP2) is an efficient Cav-1 phosphorylation inhibitor (Zimnicka et al., 2016). After PP2 treatment, GMSCs showed dose-dependent Cav-1 dephosphorylation on Y14, along with an increased accumulation of intercellular CXCL10 (**Figure 3A**). Meanwhile, CXCL10 secretion into the culture supernatant was elevated in a PP2 dose-dependent manner (**Figure 3B**). Acute H_2O_2 exposure can serve as a Cav-1 Y14 phosphorylation activator (Chen et al., 2005). After H_2O_2 treatment, GMSC showed a dose-dependent increase of Cav-1 phosphorylation on Y14, along with a decreased accumulation of intercellular CXCL10 (**Figure 3C**). Meanwhile, CXCL10 secretion into the culture supernatant was decreased in a H_2O_2 dose-dependent manner (**Figure 3D**). These data suggested that dephosphorylation of Cav-1 contributes to CXCL10 secretion in GMSCs.

To further confirm this phenomenon, GMSCs from *Cav-1*$^{-/-}$ mice were used. Accompany with the absence of p-Cav-1, *Cav-1*$^{-/-}$ GMSCs showed decreased intercellular accumulation of CXCL10, but secreted a higher amount of CXCL10 in the culture supernatant compared to WT control GMSCs (**Figures 3E,F**). Next, we used siRNA to knock down *Cav-1* and repress the phosphorylation of Cav-1 in GMSCs. We found that cytoplasmic CXCL10 expression was decreased, but CXCL10 secretion into the culture supernatant was elevated (**Figures 3G,H**). These data suggest that dephosphorylation of Cav-1 may control CXCL10 secretion in GMSCs.

Fas Controlled Dephosphorylation of Caveolin-1 and C-X-C Motif Chemokine Ligand 10 Secretion

Previously study showed that Fas and Fap-1 complex bind to Cav-1 to control sEV/cytokine release (Kou et al., 2018). We thus speculated whether Fas and Fap-1 control dephosphorylation of Cav-1 and CXCL10 secretion. Western blotting showed that GMSCs from *Fas*-deficient MRL/*lpr* mice showed an elevated level of p-Cav-1 and decreased expression of CXCL10, along with the diminished secretion of CXCL10 to the culture supernatant (**Figures 4A,B**). When *Fas* expression was knocked down in GMSCs by siRNA, p-Cav-1 level in GMSCs was elevated

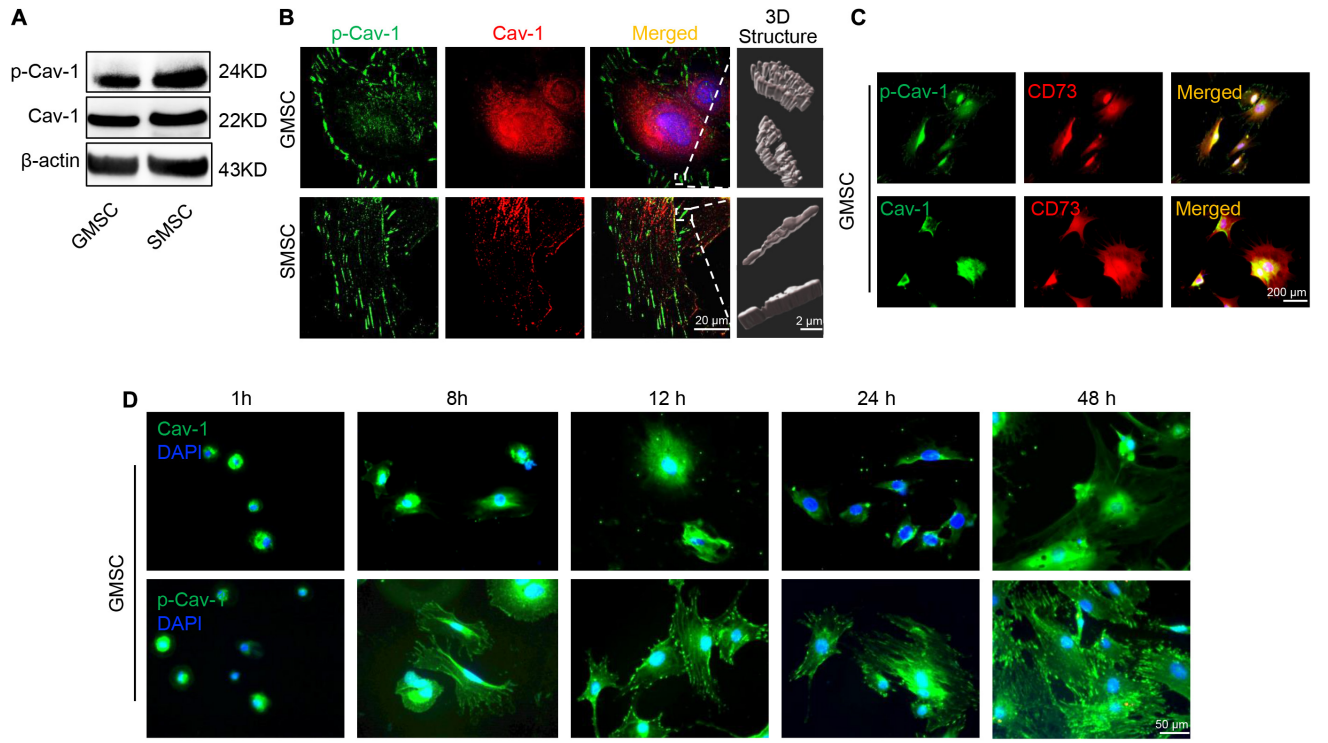

FIGURE 2 | Murine GMSCs displayed lower Cav-1 phosphorylation than SMSCs. **(A)** Western blotting analysis showed the expression of p-Cav-1 and Cav-1 in GMSCs and SMSCs. **(B)** Higher resolution images of Cav-1 (red) and p-Cav-1 (green) in MSCs captured by SIM microscopy. Scale bar, 20 μm. Right panel, 3D reconstruction of 2D *Z*-stack data showed the different steric structures of p-Cav-1 in GMSCs and SMSCs. Scale bar, 2 μm. **(C)** Immunofluorescence analysis showed that p-Cav-1 or Cav-1 (green) co-localized with the MSC marker CD73 (red) in GMSCs. Scale bar, 200 μm. **(D)** Representative immunofluorescence staining images of p-Cav-1 and Cav-1 (green) in GMSCs at indicated time point after seeding to the culture plate. Time dependent p-Cav-1 translocation could be observed. Scale bar, 50 μm.

along with repressive capacity of CXCL10 secretion into the culture supernatant (**Figures 4C,D**). These data suggested Fas controlled dephosphorylation of Cav-1 and secretion of CXCL10. Interestingly, we found that CXCL10 expression was declined in both *Fas*-deficient MRL/*lpr* GMSCs and *Fas* siRNA-treated GMSCs (**Figures 4A,C**), which suggested Fas may also control the expression of CXCL10.

To further confirm the Fas-controlled dephosphorylation of Cav-1, we performed immunofluorescent staining and used SIM microscopy to show that cytoplasmic p-Cav-1 signal was weaker in WT GMSCs than in *Fas*-deficient MRL/*lpr* GMSCs (**Figure 4E**). Although Cav-1 signal intensity did not show a significant difference between WT GMSCs and Fas-deficient MRL/*lpr* GMSCs, the Cav-1 signal showed marked clustering in the cytoplasm of Fas-deficient MRL/*lpr* GMSCs (**Figure 4E**). On the other hand, the Cav-1 signal was nearly completely absent from p-Cav-1 in WT GMSC, and most of Cav-1 signal was co-localized with p-Cav-1 (indicated by merged yellow signal) in *Fas*-deficient MRL/*lpr* GMSCs (**Figure 4E**). The 3D-SIM images further showed that p-Cav-1 structure on *Fas*-deficient MRL/*lpr* GMSCs membrane was smaller and slender than in the WT GMSCS (**Figure 4E**). The phenomenon was also observed in SMSCs (**Figure 2B**).

Next, we performed immunocytofluorescence staining to show the interaction of Fas with p-Cav-1 or Cav-1 in WT GMSCs. We found that the distribution patterns of Fas and p-Cav-1 were different in the cytoplasm and membrane of GMSCs (**Figure 4F**). Whereas Fas and Cav-1 signals showed similar distribution, and co-localization of Fas and Cav-1 was detected in the cytoplasm and membrane of GMSCs (**Figure 4F**). These data indicated Fas contribute to the dephosphorylation of Cav-1 and may bind to dephosphorylated Cav-1 to control CXCL10 secretion in MSCs (**Figure 4F**).

Fas-Associated Phosphatase-1 Controlled Dephosphorylation of Caveolin-1 and C-X-C Motif Chemokine Ligand 10 Secretion

Fas-associated phosphatase-1 is a protein tyrosine phosphatase and can binding to the cytosolic domain of Fas. It is also a critical component of the Fas/Fap-1/Cav-1 complex (Sato et al., 1995; Kou et al., 2018). To assess the functional role of Fap-1 in dephosphorylation of Cav-1 and CXCL10 release, we used siRNA to knock down *Fap-1* expression (**Figure 5A**). We found that *Fap-1* knockdown leads to increase of Cav-1 phosphorylation

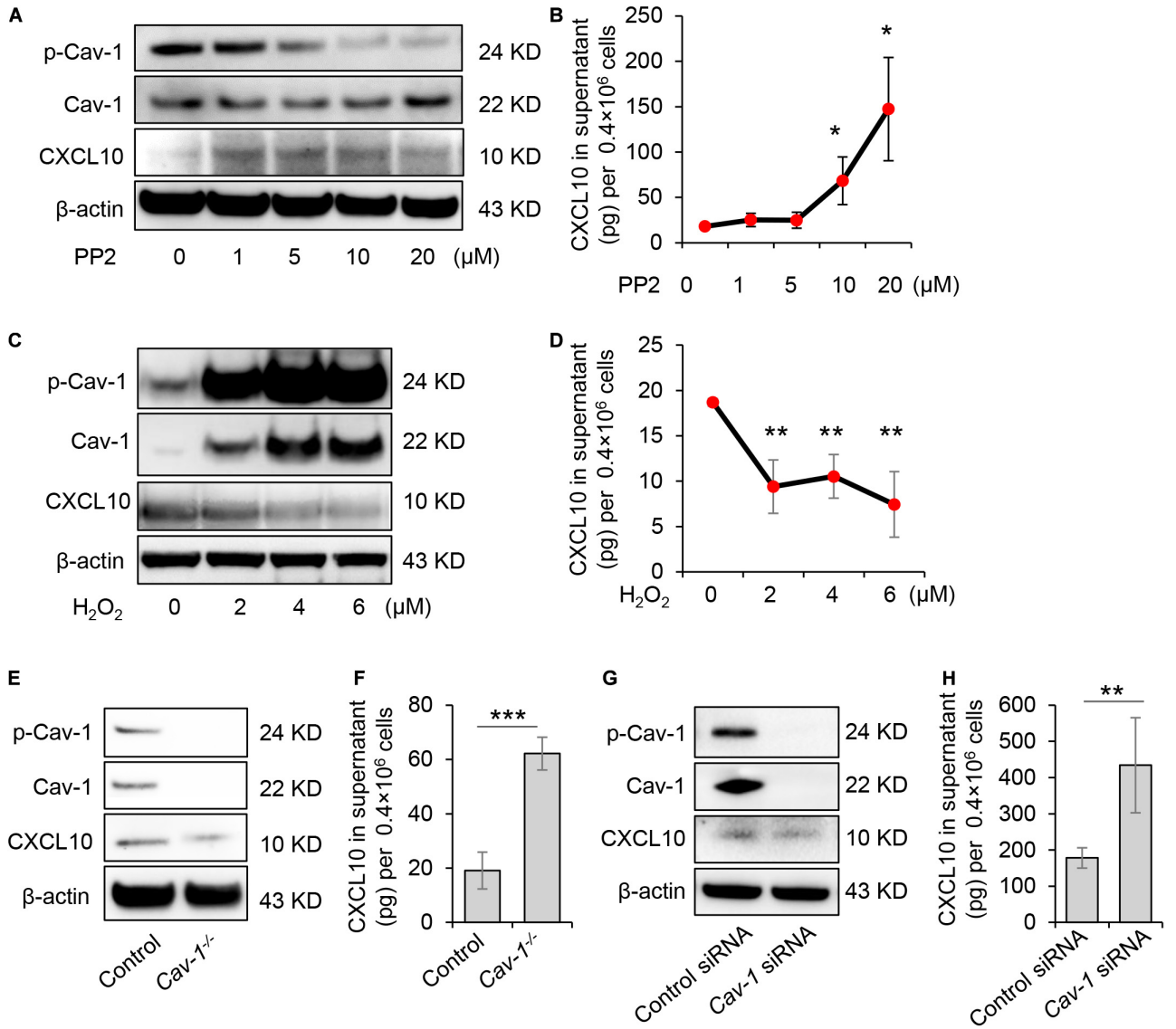

FIGURE 3 | Dephosphorylation of Cav-1 controlled CXCL10 secretion in murine GMSCs. **(A)** Western blotting analysis showed cytoplasmic protein expression of p-Cav-1, Cav-1, and CXCL10 of GMSCs treated with different dose of PP2 for 2 h. **(B)** ELISA analysis of CXCL10 secretion in the culture supernatant from GMSCs treated with different dose of PP2 for 24 h. $^{*}P < 0.05$ compared with control group. **(C)** Western blotting analysis showed cytoplasmic protein expression of p-Cav-1, Cav-1, and CXCL10 of GMSCs treated with different dose of H_2O_2 for 0.5 h. **(D)** ELISA analysis of CXCL10 secretion in the culture supernatant from GMSCs treated with different dose of H_2O_2 for 24 h. $^{**}P < 0.01$ compared with control group. **(E)** Western blotting analysis showed absent expression of Cav-1 and p-Cav-1 and decreased cytoplasmic CXCL10 in *Cav-1*$^{-/-}$ GMSCs. **(F)** Knocking out of *Cav-1* elevated CXCL10 secretion into the culture supernatant of GMSCs as analyzed by ELISA. $^{***}P < 0.001$ compared with WT GMSCs control. **(G)** Western blotting analysis confirmed the efficiency of *Cav-1* siRNA, and showed that knocking down of *Cav-1* decreased cytoplasmic CXCL10 in GMSCs. **(H)** Knocking down of *Cav-1* elevated CXCL10 secretion in the culture supernatant of GMSCs as analyzed by ELISA. $^{**}P < 0.01$ compared with GMSCs treated with control siRNA. All results are representative of data generated in at least three independent experiments. Error bars are means ± SD. Data were analyzed using independent unpaired two-tailed Student's *t*-tests or one-way ANOVA.

and reduced intercellular CXCL10 accumulation, along with a decrease of CXCL10 secretion into the culture supernatant (**Figure 5B**). In addition, *Fap-1* knockdown did not affect the expression of Fas and Cav-1 (**Figure 5A**). Immunofluorescence staining further confirmed that *Fap-1* knockdown lead to the increase of cytoplasmic p-Cav-1 (**Figure 5C**). In addition, Cav-1 signal showed marked clustering in the cytoplasm in Fap-1 knockdown GMSCs (**Figure 5D**).

Tumor Necrosis Factor-α Up-Regulates Fas and Fas-Associated Phosphatase-1 to Dephosphorylate Caveolin-1 to Activate C-X-C Motif Chemokine Ligand 10 Secretion

Mesenchymal stem cells function can be elicited by inflammatory cytokines such as TNF-α and IFN-γ. We, therefore, speculated

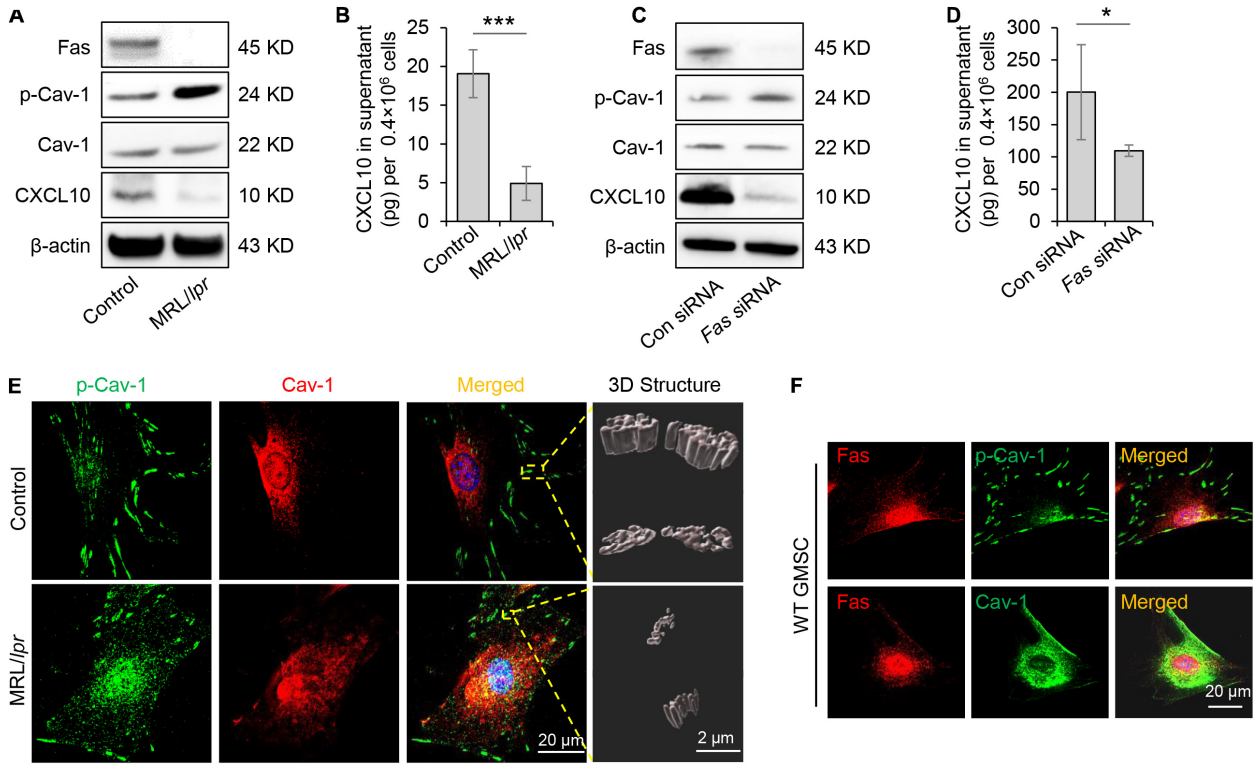

FIGURE 4 | Fas controlled dephosphorylation of Cav-1 and CXCL10 release in murine GMSCs. **(A)** Western blotting analysis of p-Cav-1, Cav-1, and CXCL10 in GMSCs from *Fas*-deficient MRL/*lpr* mice. **(B)** Knocking out of *Fas* down-regulated CXCL10 secretion in GMSCs culture supernatant as analyzed by ELISA. ***$P < 0.001$ compared with WT GMSCs control. **(C)** Western blotting analysis confirmed the efficiency of *Fas* siRNA, and showed that knocking down of *Fas* up-regulated p-Cav-1 expression and reduced cytoplasmic CXCL10 in GMSCs. **(D)** Knocking down of *Fas* decreased CXCL10 secretion in the culture supernatant of GMSCs as analyzed by ELISA. *$P < 0.05$ compared with GMSCs treated with control siRNA. **(E)** Higher resolution images of Cav-1 (red) and p-Cav-1 (green) in MSCs captured by SIM microscopy. Scale bar, 20 μm. Right panel, 3D reconstruction of 2D *Z*-stack data showed the different steric structures of p-Cav-1 in GMSCs and MRL/*Lpr* GMSCs. Scale bar, 2 μm. **(F)** Immunocytofluorescence staining images of p-Cav-1, Cav-1, (green) and Fas (red) in GMSCs. Scale bar, 20 μm. All results are representative of data generated in at least three independent experiments. Error bars are means ± SD. Data were analyzed using independent unpaired two-tailed Student's *t*-tests.

whether TNF-α and IFN-γ could promote the secretion of CXCL10 by MSCs. We found that both TNF-α and IFN-γ significantly enhanced the secretion of CXCL10 in the culture supernatant in a dose-dependent manner (**Figure 6A**). Furthermore, TNF-α was more efficient to induce the secretion of CXCL10 than IFN-γ, so we used TNF-α in the following experiments. To test whether TNF-α affects Fas/Fap-1 controlled Cav-1 dephosphorylation and Cav-1 dephosphorylation-related CXCL10 secretion, we showed that TNF-α treatment up-regulated the expression of Fas or Fap-1 but not Cav-1 in WT GMSC, MRL/*lpr* GMSCs, and *Fap-1* siRNA-treated GMSCs (**Figures 6B,C**), which was consistent with our previous study (Kou et al., 2018). In addition, TNF-α treatment induced a marked decrease of Cav-1 phosphorylation in WT GMSC but only slightly reduced p-Cav-1 level in MRL/*lpr* GMSCs and *Fap-1* siRNA-treated GMSCs (**Figure 6B**). Moreover, TNF-α treatment induced elevated intracellular accumulation of CXCL10 in MRL/*lpr* GMSCs and *Fap-1* siRNA-treated GMSCs, along with the attenuated secretion of CXCL10 into the culture supernatant when compared to WT control GMSCs (**Figures 6D,E**). These data suggested that TNF-α may serve as an activator to enhance CXCL10 release through dephosphorylation of Cav-1 and up-regulation of Fas and Fap-1.

Next, we used immunofluorescent staining to show that Cav-1 translocated to the cell membrane region at 15–45 min after TNF-α treatment. Simultaneously, p-Cav-1 signal was disappeared from the membrane and was dispersed throughout the cytoplasm after TNF-α treatment (**Figure 6F**). Western blotting further confirmed that TNF-α treatment decreased p-Cav-1 and increased Cav-1 expression in the cell membrane, but increased Cav-1 phosphorylation in the cytoplasm (**Figure 6G**). These data indicated that TNF-α treatment induces dephosphorylation of membrane p-Cav-1 to control Fas/Fap-1-mediated CXCL10 release.

Dephosphorylation of Caveolin-1 Control Wound Healing Process

Oral gingival/mucosal wounds heal faster than cutaneous wounds and exhibit minimal scar formation (Hakkinen et al., 2000). We found that GMSCs showed lower expression of p-Cav-1 (**Figure 2A**) and higher production of CXCL10 than

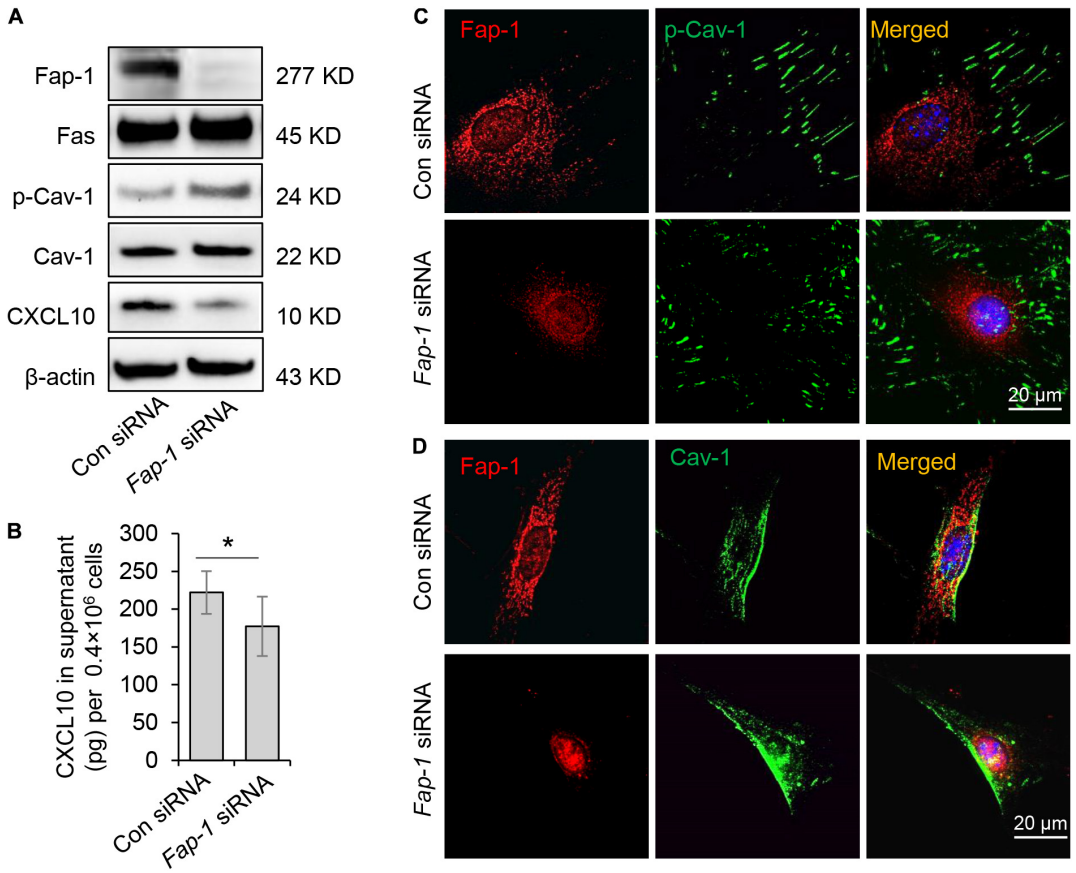

FIGURE 5 | Fas-associated phosphatase-1 controlled dephosphorylation of Cav-1 and CXCL10 release in murine GMSCs. **(A)** Western blotting analysis was used to confirm the efficiency of *Fap-1* siRNA, and knocking down of *Fap-1* up-regulated p-Cav-1 expression but reduced cytoplasmic CXCL10. **(B)** ELISA analysis showed that knocking down of *Fap-1* decreased CXCL10 secretion in the culture supernatant of GMSCs. *$P < 0.05$. **(C)** Immunocytofluorescence staining images of p-Cav-1 (green) and Fap-1 (red) in WT control and *Fap-1* deficient GMSCs. Scale bar, 20 μm. **(D)** Immunocytofluorescence staining images of Cav-1 (green) and Fap-1 (red) in WT control and *Fap-1* deficient GMSCs. Scale bar, 20 μm. All results are representative of data generated in at least three independent experiments. Error bars are means ± SD. Data were analyzed using independent unpaired two-tailed Student's *t*-tests.

SMSCs (**Figure 1C**). CXCL10 is capable of inhibiting the migration of dermal fibroblasts by blocking their release from the substratum. We thus hypothesized whether dephosphorylation of Cav-1 and CXCL10 production could promote cutaneous wound healing. Src kinase inhibitor PP2 was locally injected around the wound sites every 2 days, 7 days after wounding. We found that PP2 injection decreased Cav-1 phosphorylation and promoted CXCL10 production around the cutaneous wound area (**Figures 7A,B**). More importantly, mice treated with PP2 showed accelerated wound closure at 9 and 11 days post-wounding compared to control mice (**Figures 7C,D**). H&E and Masson's trichrome staining showed that almost whole epithelialization and excessive collagen formation were detected 14 days post-wounding, while PP2 injection reduced massive collagen deposition to a normal level (**Figures 7E,F** and **Supplementary Figure 4**). Immunofluorescent staining of Collagen I and Collagen III confirmed that PP2 treatment diminished collagen deposition at the wound areas (**Figure 7G**).

Since α-SMA is considered as a marker of scaring (Shinde et al., 2017). We used immunofluorescent staining to show that PP2 treatment leads to reduced expression of α-SMA and PCNA at the wound areas (**Figure 7H**), contributing to the down-regulation of hyperproliferative fibrosis during wound healing. Fibroblasts exhibit apoptotic phenotypes during wound heals but remained active in hypertrophic scars. Promoting the apoptosis of hyperproliferative scar fibroblasts contributes to the therapeutic effect of anti-scar drugs (Shao et al., 2020). Using TUNEL staining, we show that PP2 also increased cell apoptosis during wound healing (**Figure 7I**). Western blotting analysis confirmed that PP2 injection reduced the expression of α-SMA and PCNA, and increased the expression of apoptotic marker cleaved-caspase 3 in wound tissue (**Figure 7J**).

DISCUSSION

Adult cutaneous wound healing often ends up with cutaneous scarring, compromising the functional mobility and cosmetic outcomes (Zhang et al., 2016). However, like fetal wounds, oral gingival/mucosal wounds healing are characterized by

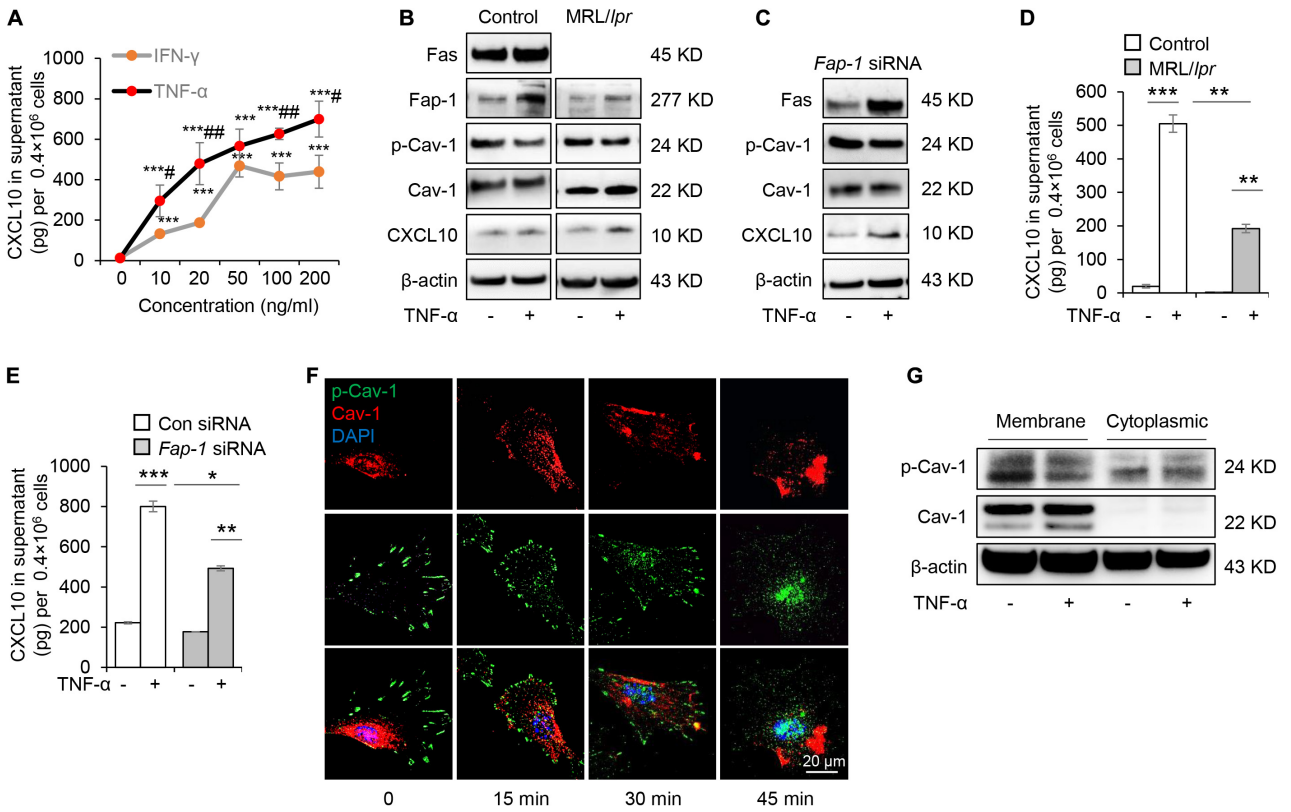

FIGURE 6 | Tumor necrosis factor-αTNF-α up-regulates Fas and Fap-1 to dephosphorylate Cav-1 to activate CXCL10 secretion in murine GMSCs. **(A)** ELISA analysis of CXCL10 secretion in the culture supernatant from WT GMSCs treated with indicated dose of TNF-α or IFN-γ. $^{***}P < 0.001$, TNF-α or IFN-γ treated GMSCs versus control; $^{\#}P < 0.05$, $^{\#\#}P < 0.01$, TNF-α treated GMSCs versus IFN-γ treated GMSCs. **(B)** Western blotting analysis of Fap-1, Fas, p-Cav-1, Cav-1, CXCL10 protein expression of WT GMSCs and MRL/*Lpr* GMSCs with or without TNF-α (20 ng/ml) treatment. **(C)** Western blotting analysis of Fap-1, Fas, p-Cav-1, Cav-1, CXCL10 expression of control and *Fap-1* siRNA-treated GMSCs with or without TNF-α (20 ng/ml) treatment. **(D)** ELISA analysis of CXCL10 secretion in the culture supernatant from WT GMSCs, MRL/*lpr* GMSCs with or without TNF-α (20 ng/ml) treatment for 48 h. $^{**}P < 0.01$, $^{***}P < 0.001$. **(E)** ELISA analysis of CXCL10 secretion in the culture supernatant from control and *Fap-1* siRNA-treated GMSCs with or without TNF-α (20 ng/ml) treatment for 48 h. $^{*}P < 0.05$*, $^{**}P < 0.01$, $^{***}P < 0.001$. **(F)** Immunocytofluorescence staining of GMSCs at various time points after TNF-α (20 ng/ml) treatment. p-Cav-1 (green) translocation from the cell membrane to the cytoplasm was indicated. Scale bar, 20 μm. **(G)** Western blotting analysis of protein expression of p-Cav-1, Cav-1 in cell membrane and cytoplasm. The results confirmed the translocation of p-Cav-1 from the cell membrane to cytoplasm upon TNF-α treatment. All results are representative of data generated in at least three independent experiments. Error bars are means ± SD. Data were analyzed using independent unpaired two-tailed Student's *t*-tests.

markedly reduced inflammation, rapid re-epithelialization, and minimal scar formation (Hakkinen et al., 2000). Previous studies contribute this phenomenon to oral microbiota stimulating wound healing, the moist environment, and growth factors present in saliva etc. (Larjava et al., 2011). The present study unrevealed the function of Y14 phosphorylated Cav-1, which acts as a switch to regulate CXCL10 secretion in MSCs and mediate the fibrosis process of wound healing.

Mesenchymal stem cells isolated from different tissues exhibit different properties. They exert immunomodulatory effects by both cell-to-cell contacts and secreting biologically active substances, growth factors, cytokines, chemokines, and exosomes (Rani et al., 2015). The cytokine secretion profile of MSCs was found to be depend on the cell origin but not on the individuality of the donors (Park et al., 2009). The multitude of cytokines and growth factors secreted from MSCs are known to confer multifunctional functionality (Ivanova-Todorova et al., 2009). Gingiva is a unique oral tissue attached to the alveolar bone of tooth sockets, recognized as a biological mucosal barrier and a distinct component of oral mucosal immunity (Mao et al., 2017). Besides several unique stem cell-like properties, 90% GMSCs were derived from cranial neural crest cells and showed a superior capacity to differentiate into neural cells and chondrocytes and induce activated T-cell apoptosis (Zhang et al., 2009; Xu et al., 2013). Our previous study reported that GMSCs secrete higher amounts of sEVs and IL-1RA (Kou et al., 2018). The present study focus on Cav-1 dephosphorylation controlled MSCs secretion and found that besides IL-1RA, GMSCs also secreted a higher amount of CXCL10.

C-X-C motif chemokine ligand 10, also named IP-10, is a potent chemokine for activated T lymphocytes and regulates cell proliferation, apoptosis, and angiogenesis in infectious and inflammatory diseases and cancer (Liu et al., 2011). It is produced in the late stage of wound healing, becoming evident 4 days after wounding (Engelhardt et al., 1998). This pleiotropic molecule exerting potent biological functions during the whole process

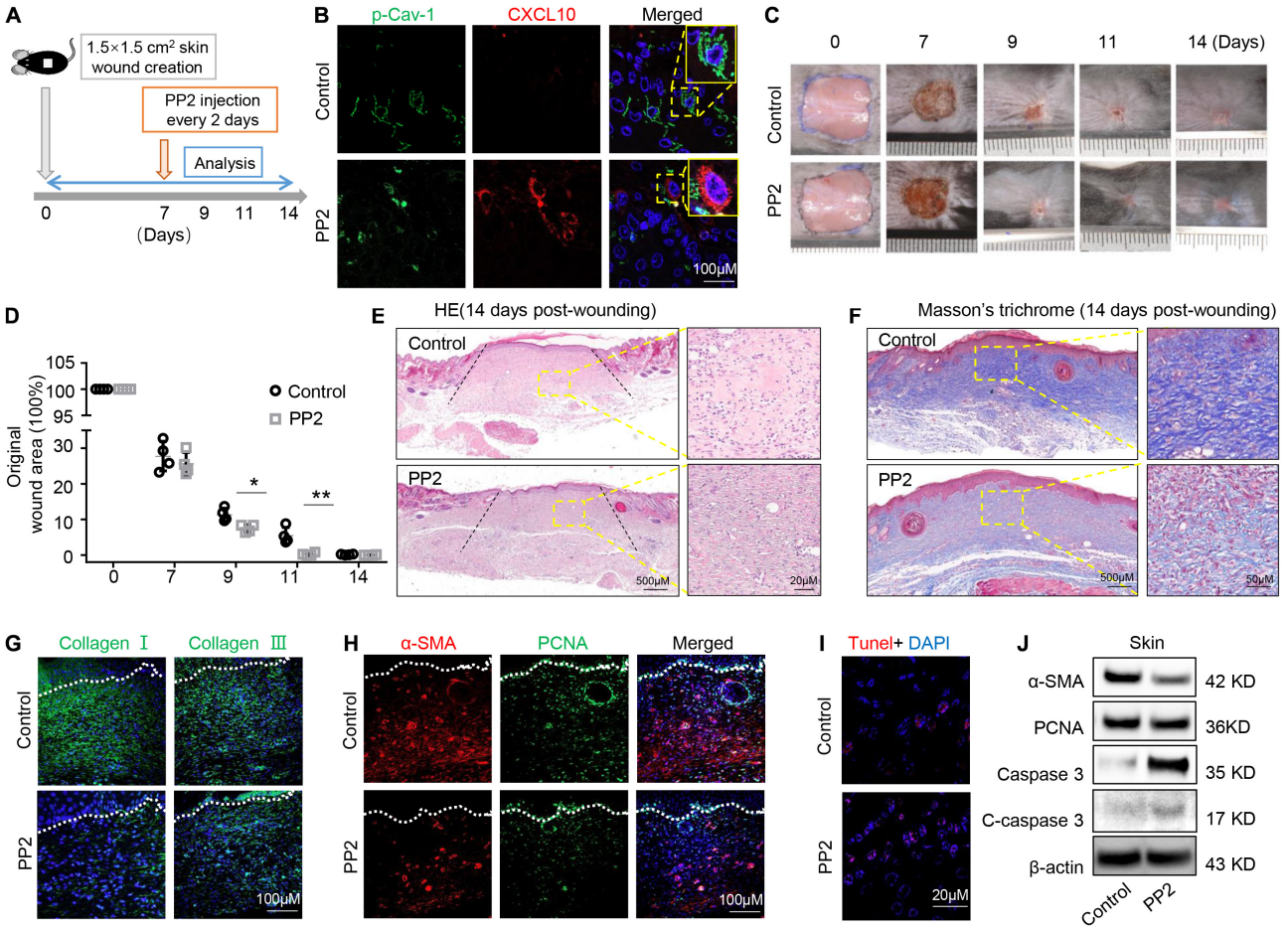

FIGURE 7 | Dephosphorylation of caveolin-1 controls wound healing process in mice. **(A)** Scheme diagram illustrating the cutaneous wound procedure in C57BL/6 mice and treatment with PP2 or PBS. **(B)** Immunocytofluorescence staining of p-Cav-1 (green) and CXCL10 (red) in the wound area in control and PP2 treated group. Scale bar, 100 μm. Magnified images of the boxed region are showed in the upper right boxes. **(C)** Representative macroscopic images of cutaneous wound area in mice after treatment with and without PP2. **(D)** Quantification of wound area in mice over time. PP2 treatment could accelerate wound healing process on 9 and 11 days post-wounding compared to WT control mice. $^{*}P < 0.05$, $^{**}P < 0.01$. **(E)** Representative H&E image from cutaneous wounds in control and PP2 treated mice 14 days post-wounding. Scale bar, 500 μm. The black dash lines indicate the margin the unhealed wound area. The right box is a higher magnification of the boxed region in the image. Scale bar, 20 μm. **(F)** Evaluation of collagen maturity by Masson's trichrome staining of wounds following treatment with PBS or PP2 at 14 days post-wounding. Scale bar, 500 μm. The right box is a higher magnification of the boxed region in the image. Scale bar, 50 μm. Note the bulky collagen fibers in control group. **(G)** Immunofluorescence analysis showed the expression of Collagen I and Collagen III (green) in the wound area in control and PP2 treated group. Scale bar, 100 μm. **(H)** Immunofluorescence analysis showed the staining of α-SMA (red) and PCNA (green) in the wound area in control and PP2 treated group. Scale bar, 100 μm. **(I)** TUNEL-positive apoptotic cells (red) in the wound area of PP2 treated group was significantly higher than in the control group. Scale bar, 20 μm. **(J)** Western blotting analysis of protein expression of α-SMA, PCNA, caspase 3, and cleaved-caspase 3 in wound area.

of wound healing: prolongs the granulation phase (Shiraha et al., 1999), and inhibits angiogenesis (Bodnar et al., 2009). These studies suggest that CXCL10 production represses cell proliferation and vessel formation. On the other hand, during the proliferation and remodeling phase of wound healing, excessive angiogenesis and over-proliferation, and migration of fibroblasts lead to scar formation (Rees et al., 2015). Here, we found that GMSCs secreted more CXCL10 into the cell culture supernatant, which may contribute to the scarless wound healing in gingiva. Furthermore, we showed that injection of Cav-1 phosphorylation inhibitor at the late stage of wounding promotes CXCL10 production at the wound area and accelerated cutaneous wound healing, repressed massive collagen formation and angiogenesis. Our finding was consistent with previous studies that CXCL10 inhibits the formation of fibrosis in healing infarct tissues (Saxena et al., 2014). To sum up, control the production of CXCL10 at the late stage of wound healing could be an attractive approach for limiting scar formation.

Along with the difference in CXCL10 secretion, we also found that more Cav-1 was dephosphorylated in GMSCs compared with SMSCs. Cav-1 drives the formation of flask-shaped membrane invaginations known as caveolae that participate in signaling, clathrin-independent endocytosis, and mechanotransduction (Tiwari et al., 2016). Cav-1 phosphorylation has been associated with cellular processes such as focal adhesion dynamics, cell migration and invasion,

cancer cell metabolism, and response to mechanical, oxidative stress (Wong et al., 2020). Adhesion-dependent caveolar endocytosis is genuinely dependent on Cav-1 phosphorylation. However, controversial results could be found whether adhesion could regulate p-Cav-1 levels (del Pozo et al., 2005; Buwa et al., 2021). Here we found that p-Cav-1 showed time-dependent translocation from the intracellular compartment to the plasma membrane during cell attachment, which suggested that the adhesion process could regulate p-Cav-1 translocation. Several studies have confirmed the primary function of Cav-1 phosphorylation on Y14-mediated endocytosis, such as albumin, insulin (Sverdlov et al., 2007; Zimnicka et al., 2016). However, the relationship of Cav-1 phosphorylation on cell secretion is still unknown. Previous studies demonstrated that p-Cav-1 is involved in the process of insulin secretion by interacting with cell division cycle in pancreatic β-cells, which comprise an integral part of the insulin secretion vesicles (Haddad et al., 2020). Our previous study showed that MSCs secrete cytokines and EVs *via* the Fas/Fap-1/Cav-1 complex (Kou et al., 2018). The present study went further to reveal that dephosphorylation of Cav-1 acts as a switch in controlling cytokine CXCL10 secretion in MSCs.

Dynamic changes in wound healing are paralleled by changes in abundance cytokines and growth factors. MSCs can function as immunomodulatory and anti-inflammatory component resources, and the inflammatory microenvironment, *vice versa*, may stimulate paracrine factor production to promote MSC-mediated tissue homeostasis (Zhang et al., 2009). Several soluble factors have been attributed to the cross-talk with MSCs and immune cells, such as interleukin-10, prostaglandin E2, NO, and indoleamine 2,3-dioxygenase (Spaggiari et al., 2008). TNF-α and IFN-γ, two important pro-inflammatory cytokines secreted by activated T cells, serve as critical feedback signal molecules in the cross-talk between immune cells and MSCs (Bernardo and Fibbe, 2013). In this study, we found that both IFN-γ and TNF-α dose-dependently activate CXCL10 secretion in GMSCs. In addition, we found that TNF-α serves as an activator to enhance CXCL10 release through dephosphorylation of Cav-1 and up-regulation of Fas and Fap-1. TNF-α may take effect by translocating Cav-1 and p-Cav-1 from the cell membrane region to the nuclear region. These results extended our knowledge about the interaction between MSCs and the immune microenvironment.

Oral gingival/mucosal wounds heal faster than cutaneous ones, with minimal scar formation (Hakkinen et al., 2000). Here we show that dephosphorylation of Cav-1 mediated CXCL10 release could regulate fibrosis of wound healing and may contribute to the minimal scar formation in gingival wound healing. Normal wound healing starts with hemostasis and inflammation, granulation and proliferation, and finally ends with wound remodeling (Perry et al., 2010). The fibrosis wound also undergoes physical contraction throughout the entire wound-healing process, which is believed to be mediated by contractile fibroblasts (myofibroblasts) that appear in the wound (Guo and Dipietro, 2010). Myofibroblasts are activated fibroblasts marked by α-SMA expression and stress fiber formation. In this study, α-SMA expression was reduced by PP2 treatment. In addition, we also found that PCNA was down-regulated, and the expression of cleaved caspase-3 was up-regulated. The primary manifestation of hypertrophic scar is fibroblasts remain hyperactive and proliferate continuously, resulting in excessive collagen synthesis and deposition (Shao et al., 2020). Here, PP2 injection repressed Cav-1 phosphorylation and promoted apoptosis in wound tissue, suggesting that the compound reduces the population of hypertrophic scar fibroblasts not only by inhibiting cell proliferation but also by inducing cell apoptosis. PP2 induced apoptosis was also consistent with previous studies that p-Cav-1 and Cav-1 regulate the process of apoptosis (Han et al., 2015). CXCL10 was used to alleviate fibrosis disease, such as bleomycin-induced pulmonary bleomycin-induced pulmonary fibrosis (Tager et al., 2004), and p-Cav-1 was also reported to be key player in the process of fibrosis (Shihata et al., 2017). Our results were consistent with previous studies and raise the possibility of new approaches to alleviate scar formation during wound healing.

The results of the present study for the first time showed that dephosphorylation of Cav-1 controls secretion of CXCL10 in MSCs. TNF-α serves as an activator to up-regulate Fas, Fap-1, and down-regulate p-Cav-1 to promote CXCL10 secretion. In addition, we found that dephosphorylation of Cav-1 may regulate the skin wound healing process by relieving collagen deposition. Although detail study is still needed to explore the molecular mechanisms of p-Cav-1 mediated MSCs secretion, our evidence suggests that the blockade of Cav-1 phosphorylation at Y14 in MSCs accelerates CXCL10 secretion and would be beneficial in scarless wound healing.

DATA AVAILABILITY STATEMENT

The raw data supporting the conclusions of this article will be made available by the authors, without undue reservation.

ETHICS STATEMENT

The studies involving human participants were reviewed and approved by the Guanghua School and Hospital of Stomatology, Sun Yat-sen University. The patients/participants provided their written informed consent to participate in this study. The animal study was reviewed and approved by the Sun Yat-sen University Animal Care and Use Committee.

AUTHOR CONTRIBUTIONS

PW contributed to designing study plan, performing experimental procedures, and drafting and final approval of the manuscript. YZ, JW, and ZW contributed to cell and animal experiments, immunofluorescence stain, data acquisition, and manuscript writing. BS and XM contributed to performing experiments, data acquisition, and analysis and interpretation. SS and XK contributed to the project conception, experimental design, writing manuscript, and supervision. All authors approved the final version of the manuscript.

FUNDING

This work was supported by grants from the Guangdong Financial Fund for High-Caliber Hospital Construction (174-2018-XMZC-0001-03-0125, D-07 to SS, D-11 to XK), the Pearl River Talent Recruitment Program (2019ZT08Y485, 2019QN01Y138, and 2019JC01Y182), the National Science and Technology Major Project of the Ministry of Science and Technology of China (2018ZX10302207-001002), the Sun Yat-sen University Young Teacher Key Cultivation Project (18ykzd05 to XK), the National Natural Science Foundation of China (82170924 to XK, 81500871 to PW, and 81800969 to JW), and Natural Science Foundation of Guangdong Province China (2016A030310214 to PW, 2016A030313262 to XM, and 2017A030310508 to JW).

SUPPLEMENTARY MATERIAL

The Supplementary Material for this article can be found online at: https://www.frontiersin.org/articles/10.3389/fcell.2021.725630/full#supplementary-material

REFERENCES

Abe, Y., Murano, M., Murano, N., Morita, E., Inoue, T., Kawakami, K., et al. (2012). Simvastatin attenuates intestinal fibrosis independent of the anti-inflammatory effect by promoting fibroblast/myofibroblast apoptosis in the regeneration/healing process from TNBS-induced colitis. *Dig. Dis. Sci.* 57, 335–344. doi: 10.1007/s10620-011-1879-4

Bernardo, M. E., and Fibbe, W. E. (2013). Mesenchymal stromal cells: sensors and switchers of inflammation. *Cell Stem Cell* 13, 392–402. doi: 10.1016/j.stem.2013.09.006

Bodnar, R. J., Yates, C. C., Rodgers, M. E., Du, X., and Wells, A. (2009). IP-10 induces dissociation of newly formed blood vessels. *J. Cell Sci.* 122(Pt 12), 2064–2077. doi: 10.1242/jcs.048793

Buwa, N., Kannan, N., Kanade, S., and Balasubramanian, N. (2021). Adhesion-dependent Caveolin-1 tyrosine-14 phosphorylation is regulated by FAK in response to changing matrix stiffness. *FEBS Lett.* 595, 532–547. doi: 10.1002/1873-3468.14025

Chen, D. B., Li, S. M., Qian, X. X., Moon, C., and Zheng, J. (2005). Tyrosine phosphorylation of caveolin 1 by oxidative stress is reversible and dependent on the c-src tyrosine kinase but not mitogen-activated protein kinase pathways in placental artery endothelial cells. *Biol. Reprod.* 73, 761–772. doi: 10.1095/biolreprod.105.040881

del Pozo, M. A., Balasubramanian, N., Alderson, N. B., Kiosses, W. B., Grande-García, A., Anderson, R. G., et al. (2005). Phospho-caveolin-1 mediates integrin-regulated membrane domain internalization. *Nat. Cell Biol.* 7, 901–908. doi: 10.1038/ncb1293

Engelhardt, E., Toksoy, A., Goebeler, M., Debus, S., Bröcker, E. B., and Gillitzer, R. (1998). Chemokines IL-8, GROalpha, MCP-1, IP-10, and Mig are sequentially and differentially expressed during phase-specific infiltration of leukocyte subsets in human wound healing. *Am. J. Pathol.* 153, 1849–1860. doi: 10.1016/s0002-9440(10)65699-4

Forbes, S. J., and Rosenthal, N. (2014). Preparing the ground for tissue regeneration: from mechanism to therapy. *Nat. Med.* 20, 857–869. doi: 10.1038/nm.3653

Gronthos, S., Akintoye, S. O., Wang, C. Y., and Shi, S. (2006). Bone marrow stromal stem cells for tissue engineering. *Periodontol.* 2000, 188–195. doi: 10.1111/j.1600-0757.2006.00154.x

Guo, S., and Dipietro, L. A. (2010). Factors affecting wound healing. *J. Dent. Res.* 89, 219–229. doi: 10.1177/0022034509359125

Haddad, D., Al Madhoun, A., Nizam, R., and Al-Mulla, F. (2020). Role of caveolin-1 in diabetes and its complications. *Oxid. Med. Cell Longev.* 2020:9761539. doi: 10.1155/2020/9761539

Hakkinen, L., Uitto, V.-J., and Larjava, H. (2000). Cell biology of gingival wound healing. *Periodontol. 2000* 24, 127–152. doi: 10.1034/j.1600-0757.2000.2240107.x

Han, C., Wang, Y. J., Wang, Y. C., Guan, X., Wang, L., Shen, L. M., et al. (2021). Caveolin-1 downregulation promotes the dopaminergic neuron-like differentiation of human adipose-derived mesenchymal stem cells. *Neural Regen. Res.* 16, 714–720. doi: 10.4103/1673-5374.295342

Han, F., Zhang, L., Zhou, Y., and Yi, X. (2015). Caveolin-1 regulates cell apoptosis and invasion ability in paclitaxel-induced multidrug-resistant A549 lung cancer cells. *Int. J. Clin. Exp. Pathol.* 8, 8937–8947.

Hu, M. S., Maan, Z. N., Wu, J. C., Rennert, R. C., Hong, W. X., Lai, T. S., et al. (2014). Tissue engineering and regenerative repair in wound healing. *Ann. Biomed. Eng.* 42, 1494–1507. doi: 10.1007/s10439-014-1010-z

Huang, Y., and He, Q. (2017). Inhibition of c-Src protects paraquat induced microvascular endothelial injury by modulating caveolin-1 phosphorylation and caveolae mediated transcellular permeability. *Environ. Toxicol. Pharmacol.* 52, 62–68. doi: 10.1016/j.etap.2017.01.023

Ivanova-Todorova, E., Bochev, I., Mourdjeva, M., Dimitrov, R., Bukarev, D., Kyurkchiev, S., et al. (2009). Adipose tissue-derived mesenchymal stem cells are more potent suppressors of dendritic cells differentiation compared to bone marrow-derived mesenchymal stem cells. *Immunol. Lett.* 126, 37–42. doi: 10.1016/j.imlet.2009.07.010

Kou, X., Xu, X., Chen, C., Sanmillan, M. L., Cai, T., Zhou, Y., et al. (2018). The Fas/Fap-1/Cav-1 complex regulates IL-1RA secretion in mesenchymal stem cells to accelerate wound healing. *Sci. Transl. Med.* 10:eaai8524. doi: 10.1126/scitranslmed.aai8524

Larjava, H., Wiebe, C., Gallant-Behm, C., Hart, D. A., Heino, J., and Haekkinen, L. (2011). Exploring scarless healing of oral soft tissues. *J. Can. Dent. Assoc.* 77:b18.

Li, X., Guo, L., Liu, Y., Su, Y., Xie, Y., Du, J., et al. (2018). MicroRNA-21 promotes wound healing via the Smad7-Smad2/3-Elastin pathway. *Exp. Cell Res.* 362, 245–251. doi: 10.1016/j.yexcr.2017.11.019

Liu, M., Guo, S., Hibbert, J. M., Jain, V., Singh, N., Wilson, N. O., et al. (2011). CXCL10/IP-10 in infectious diseases pathogenesis and potential therapeutic implications. *Cytokine Growth Factor Rev.* 22, 121–130. doi: 10.1016/j.cytogfr.2011.06.001

Mao, X., Liu, Y., Chen, C., and Shi, S. (2017). Mesenchymal stem cells and their role in dental medicine. *Dent. Clin. North Am.* 61, 161–172. doi: 10.1016/j.cden.2016.08.006

Park, C. W., Kim, K. S., Bae, S., Son, H. K., Myung, P. K., Hong, H. J., et al. (2009). Cytokine secretion profiling of human mesenchymal stem cells by antibody array. *Int. J. Stem Cells* 2, 59–68. doi: 10.15283/ijsc.2009.2.1.59

Park, J. H., and Han, H. J. (2009). Caveolin-1 plays important role in EGF-induced migration and proliferation of mouse embryonic stem cells: involvement of PI3K/Akt and ERK. *Am. J. Physiol. Cell Physiol.* 297, C935–C944. doi: 10.1152/ajpcell.00121.2009

Perry, D. M., McGrouther, D. A., and Bayat, A. (2010). Current tools for noninvasive objective assessment of skin scars. *Plast. Reconstr. Surg.* 126, 912–923. doi: 10.1097/PRS.0b013e3181e6046b

Predescu, S. A., Predescu, D. N., and Palade, G. E. (1997). Plasmalemmal vesicles function as transcytotic carriers for small proteins in the continuous endothelium. *Am. J. Physiol.* 272(2 Pt 2), H937–H949. doi: 10.1152/ajpheart.1997.272.2.H937

Rani, S., Ryan, A. E., Griffin, M. D., and Ritter, T. (2015). Mesenchymal stem cell-derived extracellular vesicles: toward cell-free therapeutic applications. *Mol. Ther.* 23, 812–823. doi: 10.1038/mt.2015.44

Rees, P. A., Greaves, N. S., Baguneid, M., and Bayat, A. (2015). Chemokines in wound healing and as potential therapeutic targets for reducing cutaneous scarring. *Adv. Wound Care* 4, 687–703. doi: 10.1089/wound.2014.0568

Sato, T., Irie, S., Kitada, S., and Reed, J. C. (1995). FAP-1: a protein tyrosine phosphatase that associates with Fas. *Science* 268, 411–415. doi: 10.1126/science.7536343

Saxena, A., Bujak, M., Frunza, O., Dobaczewski, M., Gonzalez-Quesada, C., Lu, B., et al. (2014). CXCR3-independent actions of the CXC chemokine CXCL10 in the infarcted myocardium and in isolated cardiac fibroblasts are mediated through proteoglycans. *Cardiovasc. Res.* 103, 217–227. doi: 10.1093/cvr/cvu138

Shao, T., Tang, W., Li, Y., Gao, D., Lv, K., He, P., et al. (2020). Research on function and mechanisms of a novel small molecule WG449E for hypertrophic scar. *J. Eur. Acad. Dermatol. Venereol.* 34, 608–618. doi: 10.1111/jdv.16028

Shi, X., Wen, Z., Wang, Y., Liu, Y. J., Shi, K., and Jiu, Y. (2021). Feedback-driven mechanisms between phosphorylated caveolin-1 and contractile actin assemblies instruct persistent cell migration. *Front. Cell Dev. Biol.* 9:665919. doi: 10.3389/fcell.2021.665919

Shihata, W. A., Putra, M. R. A., and Chin-Dusting, J. P. F. (2017). Is there a potential therapeutic role for caveolin-1 in fibrosis? *Front. Pharmacol.* 8:567. doi: 10.3389/fphar.2017.00567

Shinde, A. V., Humeres, C., and Frangogiannis, N. G. (2017). The role of α-smooth muscle actin in fibroblast-mediated matrix contraction and remodeling. *Biochim. Biophys. Acta Mol. Basis Dis.* 1863, 298–309. doi: 10.1016/j.bbadis.2016.11.006

Shiraha, H., Glading, A., Gupta, K., and Wells, A. (1999). IP-10 inhibits epidermal growth factor-induced motility by decreasing epidermal growth factor receptor-mediated calpain activity. *J. Cell Biol.* 146, 243–254. doi: 10.1083/jcb.146.1.243

Spaggiari, G. M., Capobianco, A., Abdelrazik, H., Becchetti, F., Mingari, M. C., and Moretta, L. (2008). Mesenchymal stem cells inhibit natural killer-cell proliferation, cytotoxicity, and cytokine production: role of indoleamine 2,3-dioxygenase and prostaglandin E2. *Blood* 111, 1327–1333. doi: 10.1182/blood-2007-02-074997

Stan, R. V. (2005). Structure of caveolae. *Biochim. Biophys. Acta* 1746, 334–348. doi: 10.1016/j.bbamcr.2005.08.008

Sverdlov, M., Shajahan, A. N., and Minshall, R. D. (2007). Tyrosine phosphorylation-dependence of caveolae-mediated endocytosis. *J. Cell. Mol. Med.* 11, 1239–1250. doi: 10.1111/j.1582-4934.2007.00127.x

Tager, A. M., Kradin, R. L., LaCamera, P., Bercury, S. D., Campanella, G. S., Leary, C. P., et al. (2004). Inhibition of pulmonary fibrosis by the chemokine IP-10/CXCL10. *Am. J. Respir. Cell Mol. Biol.* 31, 395–404. doi: 10.1165/rcmb.2004-0175OC

Tiwari, A., Copeland, C. A., Han, B., Hanson, C. A., Raghunathan, K., and Kenworthy, A. K. (2016). Caveolin-1 is an aggresome-inducing protein. *Sci. Rep.* 6:38681. doi: 10.1038/srep38681

Wong, T. H., Dickson, F. H., Timmins, L. R., and Nabi, I. R. (2020). Tyrosine phosphorylation of tumor cell caveolin-1: impact on cancer progression. *Cancer Metastasis Rev.* 39, 455–469. doi: 10.1007/s10555-020-09892-9

Xu, X., Chen, C., Akiyama, K., Chai, Y., Le, A. D., Wang, Z., et al. (2013). Gingivae contain Neural-crest- and mesoderm-derived mesenchymal stem cells. *J. Dent. Res.* 92, 825–832. doi: 10.1177/0022034513497961

Zhang, Q., Shi, S., Liu, Y., Uyanne, J., Shi, Y., Shi, S., et al. (2009). Mesenchymal stem cells derived from human gingiva are capable of immunomodulatory functions and ameliorate inflammation-related tissue destruction in experimental colitis. *J. Immunol.* 183, 7787–7798. doi: 10.4049/jimmunol.0902318

Zhang, W., Wang, H., Yuan, Z., Chu, G., Sun, H., Yu, Z., et al. (2021). Moderate mechanical stimulation rescues degenerative annulus fibrosus by suppressing caveolin-1 mediated pro-inflammatory signaling pathway. *Int. J. Biol. Sci.* 17, 1395–1412. doi: 10.7150/ijbs.57774

Zhang, Y. F., Zhou, S. Z., Cheng, X. Y., Yi, B., Shan, S. Z., Wang, J., et al. (2016). Baicalein attenuates hypertrophic scar formation via inhibition of the transforming growth factor-beta/Smad2/3 signalling pathway. *Br. J. Dermatol.* 174, 120–130. doi: 10.1111/bjd.14108

Zimnicka, A. M., Husain, Y. S., Shajahan, A. N., Sverdlov, M., Chaga, O., Chen, Z., et al. (2016). Src-dependent phosphorylation of caveolin-1 Tyr-14 promotes swelling and release of caveolae. *Mol. Biol. Cell* 27, 2090–2106. doi: 10.1091/mbc.E15-11-0756

Conflict of Interest: The authors declare that the research was conducted in the absence of any commercial or financial relationships that could be construed as a potential conflict of interest.

Publisher's Note: All claims expressed in this article are solely those of the authors and do not necessarily represent those of their affiliated organizations, or those of the publisher, the editors and the reviewers. Any product that may be evaluated in this article, or claim that may be made by its manufacturer, is not guaranteed or endorsed by the publisher.

frontiers in Cell and Developmental Biology

ORIGINAL RESEARCH
published: 16 November 2021
doi: 10.3389/fcell.2021.771773

Colloidal Self-Assembled Patterns Maintain the Pluripotency and Promote the Hemopoietic Potential of Human Embryonic Stem Cells

Jiao Lin[1†], Jiahui Zeng[2†], Wencui Sun[2†], Kun Liu[1], Myagmartsend Enkhbat[1], Danying Yi[2], Javad Harati[1], Jiaxin Liu[2], Peter Kingshott[3], Bo Chen[2], Feng Ma[2*] and Peng-Yuan Wang[1,3*]*

[1]Shenzhen Key Laboratory of Biomimetic Materials and Cellular Immunomodulation, Shenzhen Institute of Advanced Technology, Chinese Academy of Sciences, Shenzhen, China, [2]Stem Cell Center, Institute of Blood Transfusion, Chinese Academy of Medical Sciences and Peking Union Medical College (CAMS and PUMC), Chengdu, China, [3]Department of Chemistry and Biotechnology, Swinburne University of Technology, Hawthorn, VIC, Australia

OPEN ACCESS

Edited by:
Rita Yen-Hua Huang,
Taipei Medical University, Taiwan

Reviewed by:
Feng-Huei Lin,
National Taiwan University, Taiwan
Wen-Ping Chen,
National Taiwan University, Taiwan

***Correspondence:**
Bo Chen
bo_chen@ibt.pumc.edu.cn
Feng Ma
mafeng@ibt.pumc.edu.cn
Peng-Yuan Wang
pywang0624@gmail.com

[†]These authors have contributed equally to this work and share first authorship

Specialty section:
This article was submitted to Stem Cell Research, a section of the journal Frontiers in Cell and Developmental Biology

Received: 07 September 2021
Accepted: 26 October 2021
Published: 16 November 2021

Citation:
Lin J, Zeng J, Sun W, Liu K, Enkhbat M, Yi D, Harati J, Liu J, Kingshott P, Chen B, Ma F and Wang P-Y (2021) Colloidal Self-Assembled Patterns Maintain the Pluripotency and Promote the Hemopoietic Potential of Human Embryonic Stem Cells. Front. Cell Dev. Biol. 9:771773. doi: 10.3389/fcell.2021.771773

The generation of blood cells in a significant amount for clinical uses is still challenging. Human pluripotent stem cells-derived hemopoietic cells (hPSC-HCs) are a promising cell source to generate blood cells. Previously, it has been shown that the attached substrates are crucial in the maintenance or differentiation of hPSCs. In this study, a new family of artificial extracellular matrix (ECM) called colloidal self-assembled patterns (cSAPs: #1–#5) was used for the expansion of mouse and human PSCs. The optimized cSAP (i.e., #4 and #5) was selected for subsequent hemopoietic differentiation of human embryonic stem cells (hESCs). Results showed that the hematopoietic potential of hESCs was enhanced approx 3–4 folds on cSAP #5 compared to the flat control. The cell population of hematopoietic progenitors (i.e., $CD34^+CD43^+$ cells) and erythroid progenitors (i.e., CD71+GPA+ cells) were enhanced 4 folds at day 8 and 3 folds at day 14. RNA sequencing analysis of cSAP-derived hESCs showed that there were 300 genes up-regulated and 627 genes down-regulated compared to the flat control. The enriched signaling pathways, including up-regulation (i.e., Toll-like receptor, HIF-1a, and Notch) or down-regulation (i.e., FAs, MAPK, JAK/STAT, and TGF-β) were classic in the maintenance of hESC phenotype Real time PCR confirmed that the expression of focal adhesion (PTK2, VCL, and CXCL14) and MAPK signaling (CAV1) related genes was down-regulated 2-3 folds compared to the flat control. Altogether, cSAP enhances the pluripotency and the hematopoietic potential of hESCs that subsequently generates more blood-like cells. This study reveals the potential of cSAPs on the expansion and early-stage blood cell lineage differentiation of hPSCs.

Keywords: colloidal self-assembly, artificial ECM, pluripotent stem cells, hematopoiesis, blood cells, focal adhesion

1 INTRODUCTION

Substrate for anchor-dependent cells is crucial for self-renew and lineage commitment, including human embryonic stem cells (hESCs) (Murphy et al., 2014). In the last decades, substrates with different nanostructures such as nanogrooves and nanopillars have been applied to manipulate cell fate. Nanostructured surfaces can be further modified chemically using coatings or grafting technology to enhance bio-functionality. However, these surfaces are still far from an extracellular matrix (ECM) like substrate. ECM mimetic surface presenting hierarchical structures and multiple chemistries are rare to be found (Wang et al., 2016a).

Recently, a new family of substrates composed of various colloidal particles with different sizes and materials named self-assembled patterns (cSAPs) was developed in our group (Wang et al., 2015a). The particles can be pre- or post-modified, ultimately providing a complex surface of the cSAPs (Diba et al., 2019). Surface topography, roughness, hydrophilicity, chemistry, and even stiffness can be fine-tuned. The behaviors of human stem cells and adult cells have been investigated on the cSAPs (Wang et al., 2016b; Cui et al., 2019). Cell reprogramming of human fibroblasts into human induced pluripotent stem cells (hiPSCs) has also been studied on these new substrates (Wang et al., 2016c). cSAPs have shown the potential to control cell adhesion and subsequently the fate decision of cells.

Generation of blood cells *in vitro* with a significant amount for clinical uses is still challenging. Human pluripotent stem cells (hPSCs), including hESCs and hiPSCs, are promising sources to generate blood-like cells. The hematopoietic potential of hPSCs has a significant application in the cure of blood-related diseases such as Thalassemia (Papapetrou, 2017) or hemophilia (Wang et al., 2013). Several co-culture differentiation systems, such as the OP9 stromal cells and the aorta–gonad–mesonephros-derived stromal cells (AGM-S3) (Ledran et al., 2008), have been established for blood-like cell generation. These systems use a nature-inspired microenvironment to stimulate definitive hematopoiesis *in vitro*. These systems are useful to identify the function of critical genes in normal or abnormal hematopoiesis. For example, the AGM-S3 co-culture system could be used to check the detailed cellular and molecular mechanism of hematopoiesis influenced by the critical gene (Chen et al., 2017; Zeng et al., 2020). It also has potential utility in screening for compounds that promote human hematopoiesis, which is possible to set up a high throughput screening system for compound function screening using the AGM-S3 co-culture system (Chang et al., 2019). However, the current approach *in vitro* blood cell generation is far from satisfying clinical needs in terms of quality and number (Moreno-Gimeno et al., 2010). Therefore, the improvement of the efficiency of hematopoietic differentiation of hPSC-HCs is essential.

In this proof-of-concept study, human and mouse PSCs' morphology and growth were screened on five cSAPs. The selected cSAPs were used to expand and stimulate hESCs used for the downstream hematopoietic differentiation into HCs and blood-like cells. The outcomes imply that the expansion of hESCs

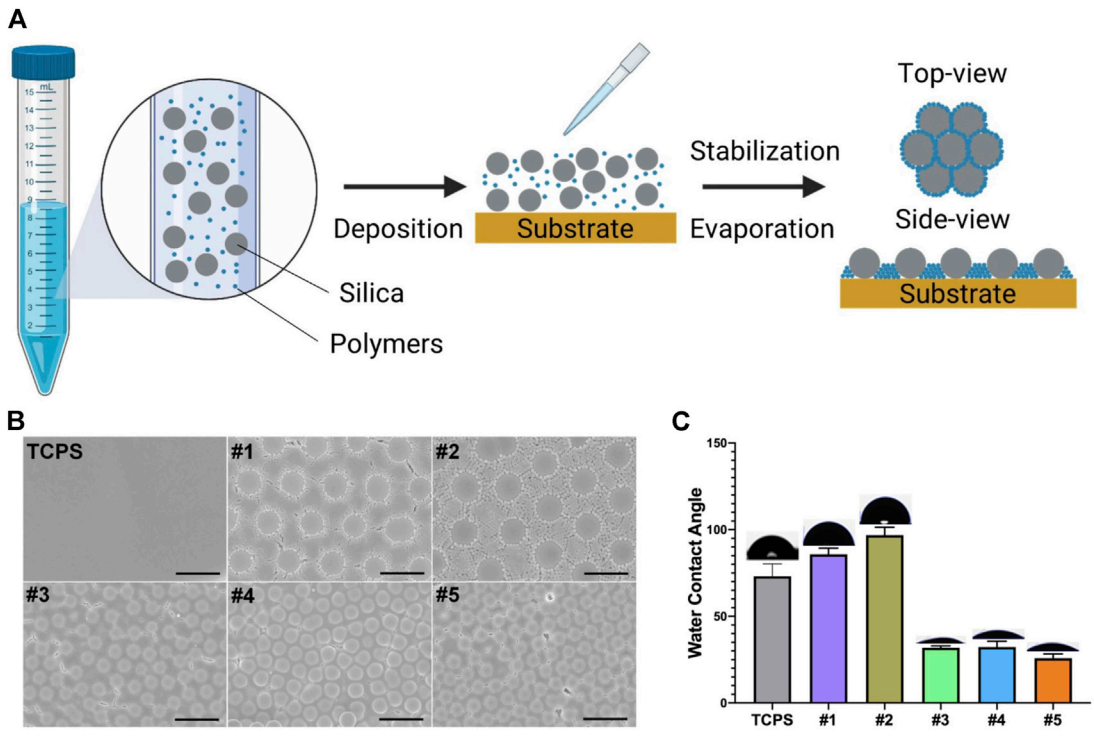

FIGURE 1 | Fabrication and characterization of cSAPSs. **(A)** Scheme of cSAPs preparation. **(B)** SEM of TCPS and five selected cSAPs. Scale bar represents 5 μm. **(C)** Surface wettability of the substrates was analyzed using water contact angle test (degrees). Five spots on each surface were analyzed (n = 5). Error bar = STDEV.

is a crucial step prior to the hematopoietic differentiation using the stromal cell co-culture system, and the cSAP is a valuable tool for *in vitro* blood cell production.

2 MATERIALS AND METHODS

2.1 Colloidal Self-Assembled Patterns

Five substrates were selected from our library and fabricated according to our previous protocol (Wang et al., 2016b) (**Figure 1A**). Briefly, cSAPs #1 and #2 was composed of SiO_2 with 5 μm diameter and polystyrene (PS) with 200 or 400 nm diameter, #3, #4, and #5 was composed of SiO_2 with 2 μm diameter and PS with 65 nm diameter, carboxy-PS (PSC) with 50 or 100 nm diameter, and the cSAPs were fabricated within the 24-well tissue culture plates (TCPS, Falcon). TCPS was the flat control group in this study.

Scanning electron microscopy (SEM, ZEISS SUPRA ® 55, Carl Zeiss, Germany) and water contact angle (WCA) was used to characterize the surface structures and wettability of these cSAPs using an automated contact angle measurement device (PT-705B, Precise Test, China) at room temperature. Other detailed characterizations have been done previously (Wang et al., 2016b).

2.2 Cell Culture

H1 hESCs and human induced pluripotent stem cells (hiPSCs) were routinely cultured in Matrigel (BD, United State) coated 60 mm Petri dishes with mTeSR1 medium (Stem Cells, United State), and passaged using ReleSR (Stem Cells, United State) with a ratio of 1:3 every other day. E14 mESCs and mouse induced pluripotent stem cells (miPSCs) were routinely maintained on gelatin (Yeasen, China) coated 6-well tissue culture plates in mouse ESC medium (DMEM-knockout, GIBCO, United State) containing 20% FBS, 1% NEAA, 1% L-Glutamine, 1% penicillin, and streptomycin (P/S, GIBCO, United State), 0.15 mM 1-thioglycerol (Sigma, United State), 1000 U/mL leukemia inhibitory factor (Millipore), and two chemical inhibitors (2i), 3 μM CHIR99021 and 1 μM PD0325901 (Stemgent, United State). mESCs and miPSCs were passaged using trypsin-EDTA (Invitrogen, United State) with a ratio of 1:6 every other day. All the medium was changed daily.

All cells used in this study were passaged three times on cSAPs prepared in 24-well tissue culture plate or control surfaces coated by Matrigel or Gelatin for further research. The experimental group was named cSAP #X (X = 1, 2, 3, 4, 5) and TCPS (as a flat control). Cell inoculatiion density of mESCs and miPSCs in experimental group was 2×10^4 cells/cm^2. Cell density of hESCs and hiPSCs was adjusted according to the colony quantity. Cell culture in experimental group was same to the routinely cultured cells, mESCs and miPSCs was passaged at a ratio of 1:6, hESCs and hiPSCs was passaged at a ratio of 1:3. Medium was changed every day. Cell morphology was captured every day by an inverted microscope (Olympus-IX71).

2.3 Real-Time qPCR

Total RNA was extracted from cells with the MiniBEST universal RAN extraction Kit (Takara, Japan). cDNA was made with 1 mg of total RNA based on the manufacturer's protocol using the PrimeScript^{TM} RT Master Mix (Takara, Japan), and subsequent real-time qPCR was carried out in triplicates, using the 2 × RealStar Green Mixture (GENE STAR, China) on Light Cycler 96 System cording to manufacturer's instructions (Roche, United State). Amplifications were performed using the following conditions: 95°Cfor 2 min, followed by 40 cycles of 95°C for 15 s, 60°C for 15 s, and 72°C for 30 s. Gene expression was normalized to *Gapdh*, and then the TCPS control. The sequences of all primers used were listed in **Supplementary Table S1**.

2.4 Hemopoietic Differentiation of Human Embryonic Stem Cells

hESCs were co-cultured with mouse stromal cell line AGM-S3 to induce their differentiation into hematopoietic cells, as reported before (Chen et al., 2017). hESCs were cut into small squares of 1.5×10^3 cells, and then plated onto the irradiated AGM-S3 cells and cultured in the hPSC maintenance medium [high glucose Dulbecco's modified Eagle's medium, DMEM, F-12 nutrient mixture, 20% knockout serum replacement (KSR), 1% L-glutamine, 1% non-essential amino acid solution (NEAA; Gibco), and 5 ng/ml basic FGF (b-FGF; Wako)] for 3 days (Chen et al., 2017). The medium was changed to the hematopoiesis-inducing medium (Iscove's Modified Dulbecco's Medium (IMDM) containing 10% fetal bovine serum (FBS; Hyclone), 1% NEAA (Gibco), 60 ng/ml ascorbic acid (Sigma), and 20 ng/ml vascular endothelial growth factor (VEGF; Wako)), referred as day 0 (D0) (Chen et al., 2017; Zhou et al., 2019). The culture medium was replaced every day. The co-cultures were dissociated by 0.05–0.25% trypsin-EDTA (Invitrogen) at D8 or D14 for further analysis. This experiment was run at least three times in parallel.

2.5 Flow Cytometry

Flow cytometry experiments were performed according to a previous report (Chen et al., 2017). Briefly, the co-cultured cells at D8 or D14 were dissociated with 0.25% trypsin-EDTA solution. The cell suspension was obtained by filtration through a 70-μm nylon mesh. Before immunostaining, cells were blocked by rabbit serum at 4°C for 30 min. Cells were stained with the anti-CD34/CD43 antibodies (at D8 and D14), and anti-CD34/CD45 or anti-GPA/CD71 antibodies (at D14) at 4°C for 30 min (**Supplementary Table S2**). Flow cytometric analysis was performed using the FACS Canto II system (BD Biosciences). All FACS data were analyzed using FlowJo 10 software.

2.6 Hematopoietic Colony-forming Assay

According to the previous studies, the hematopoietic colony-forming assay of co-cultured cells was performed (Chen et al., 2017; Sun et al., 2020). Briefly, co-cultured cells were dissociated by 0.25% trypsin/EDTA into single cells at day 14.5×10^4 cells were suspended in 80% MethoCult H4230 (Stem cells) containing 100 ng/ml stem cell factor (SCF), 100 ng/ml interleukin-6 (IL-6), 10 ng/ml interleukin-3 (IL-3), 10 ng/ml Fms-related tyrosine kinase three ligand (FL), 10 ng/ml thrombopoietin (TPO),

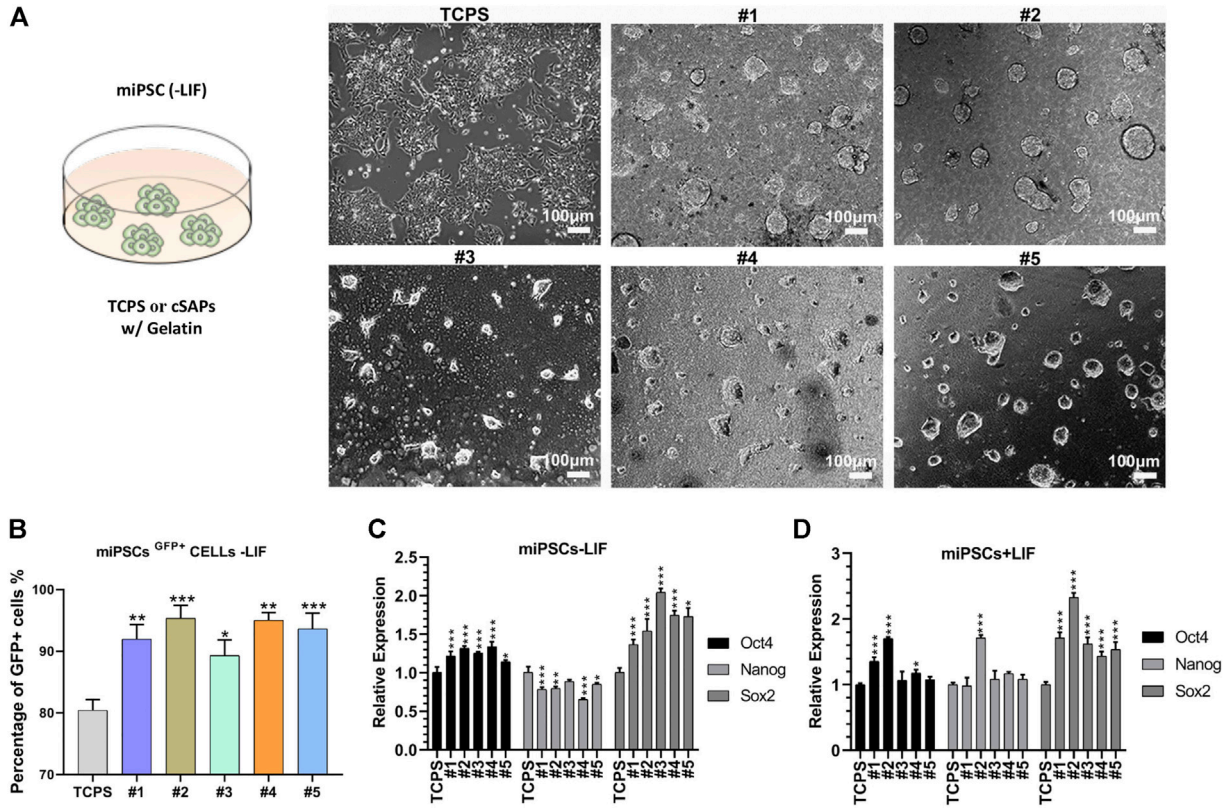

FIGURE 2 | Pluripotency of miPSCs on different substrates coated with gelatin. **(A)** Colony morphology of miPSCs cultured on different surfaces after day 3. Scale bar = 100 μm. **(B)** FACS analysis of the Oct4+ cells without LIF. qPCR analysis of pluripotent markers, *Oct4, Nanog, and Sox2* **(C)** without and **(D)** with LIF. Samples were triplicates (n = 3). Error bar = STDEV.

10 ng/ml granulocyte-macrophage colony-stimulating factor (GM-CSF), and 4 units/ml erythropoietin (EPO), and then incubated in 5% CO_2 at 37°C for another 14 days. The number of colony-forming unit erythroid (CFU-E) colonies was counted at 7–10 days, while the number of burst-forming unit-erythroid (BFU-E), colony-forming unit-mixed (CFU-Mix), and colony-forming unit-granulocyte/macrophage (CFU-GM) colonies were counted at 12–14 days. This experiment was run at least three times in parallel.

2.7 RNA Sequencing

H1 hESCs cultured on cSAPs and flat control (TCPS) for two passages (4 days/passage) were dissociated with 0.5 mM EDTA for RNAseq. Total RNA of each 1×10^6 cells was extracted by 1 ml TRIzol (Life Technologies) and purified according to the standard instruction. RNA Sequence analysis was performed by BGI Tech (Shenzhen, China). The analysis of gene function was performed with the multi-group data mining system of Dr. Tom (http://report.bgi.com). Gene changes on cSAP #5 compare to TCPS over 2-fold were defined as significant.

2.8 Immunofluorescence Staining

Cells were cultured in multi-well plates were fixed with 4% paraformaldehyde (PFA) for 30 min at 4°C, and washed three times with wash buffer (5% FBS in PBS). They were then incubated with membrane permeation reagent (PBS containing 0.3% Triton-100 and 5% FBS) at 4°C for 30 min, stained overnight at 4°C with anti-OCT4/SOX2/SSEA4 antibodies (mouse anti-human), washed three times with PBS containing 5% skim milk, and then incubated for 30 min at room temperature with secondary antibodies (FITC-conjugated secondary Ab, goat anti-mouse) (**Supplementary Table S2**). Nuclei were labeled with DAPI. After washing three times with PBS, the sample was imaged under a fluorescence microscope.

2.9 Statistical Analysis

All data are presented as means ± SD; statistical analyses were performed by GraphPad Prism 8 using the Student's t-test, one-way ANOVA with Dunnett post hoc test, and two-way ANOVA with Tukey's post hoc test. $p < 0.05$ was considered significant.

3 RESULTS

3.1 Colloidal Self-Assembled Patterns Characterization

cSAPs were fabricated by mixing different particles together and depositing them on the tissue culture plates (TCPS); after

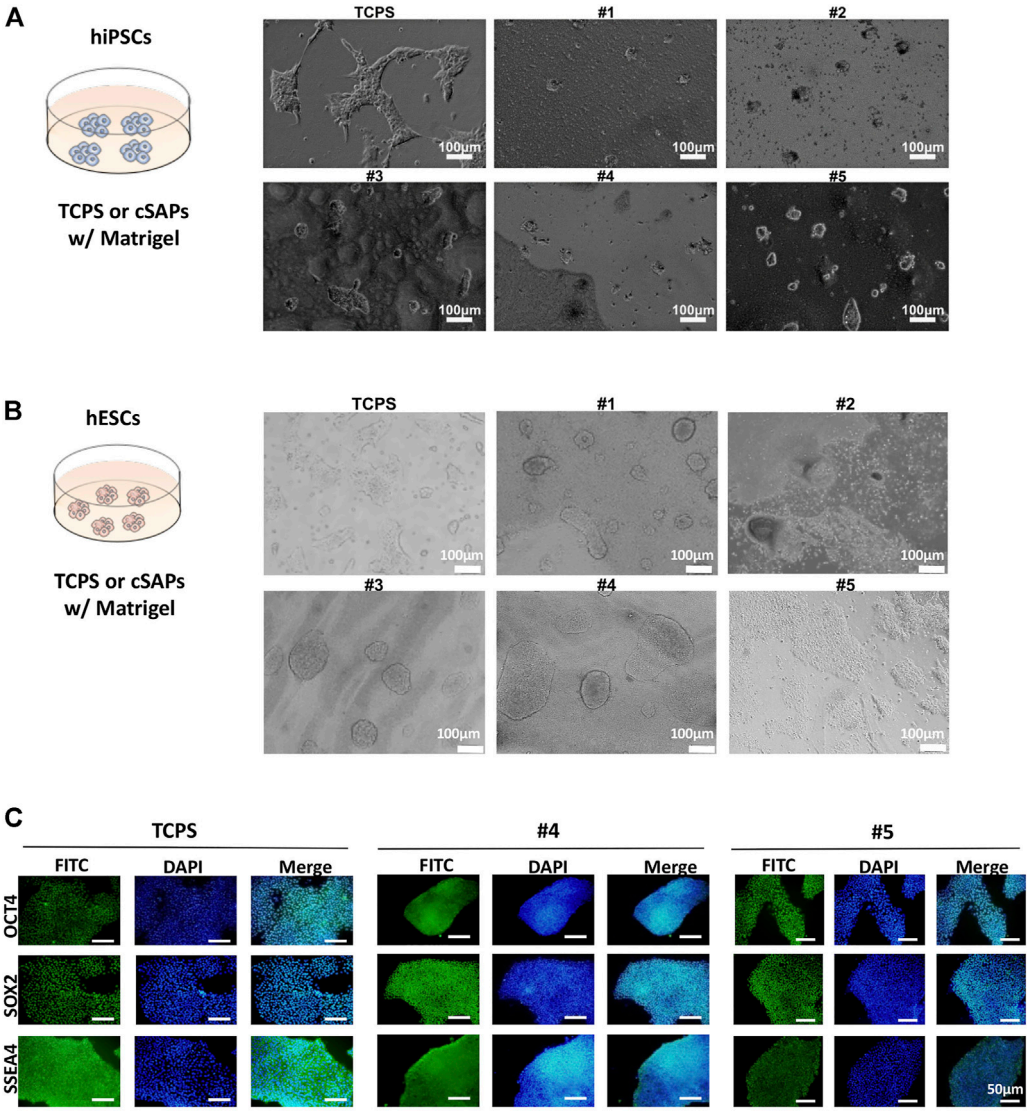

FIGURE 3 | Pluripotency of hiPSCs and hESCs on different substrates coated with Matrigel. Colony morphology of **(A)** hiPSCs after 3 days and **(B)** hESCs after three passages cultured on different surfaces. Scale bar = 100 μm. **(C)** Immunostaining of pluripotent markers (OCT4, SOX2, and SSEA4) of hESCs after three passages' culture on cSAPs and TCPS, Scale bars = 50 μm.

evaporation, particles were distributed on the surface according to the principle of self-assembly (**Figure 1A**). The surface topography of cSAPs was measured by SEM and showed that the large particles and small particles were orderly distributed on the surfaces (**Figure 1B**). Due to the differences of the surface on chemestry and topography, surface wettability showed that water contact angle (WCA) of cSAP #1 and #2 (SiO_2 = 5 μm; PS = 200 and 400 nm) was more hydrophobic (85.8 ± 3.5 and 96.8 ± 4.6 degree), than the cSAP #3, #4, and #5 (SiO2 = 2 μm; PS = 65 nm, PSC = 50 and 100 nm), and the WCA of cSAP #3, #4, and #5 was 31.8 ± 1.1, 32.3 ± 3.2, and 25.8 ± 2.4 degree, respectively (**Figure 1C**).

3.2 Colloidal Self-Assembled Patterns Maintain Pluripotency of miPSCs, hiPSCs, and hESCs

The colony morphology of miPSCs on cSAPs was significantly different from that on the TCPS control (**Figure 2A**). miPSCs colonies on cSAPs were more 3D-like, especially on the cSAP #1 and #2. The PSC colonies were dome-like morphology on the cSAP #4 and #5, neither 3D spheroids nor 2D-like colonies. miPSCs cultured on cSAPs without LIF (Leukemia Inhibitory Factor) had a higher percentage of *Oct4*-GFP positive cells after 7 days than TCPS without and even with LIF, indicating that cSAPs could maintain the pluripotency of PSCs

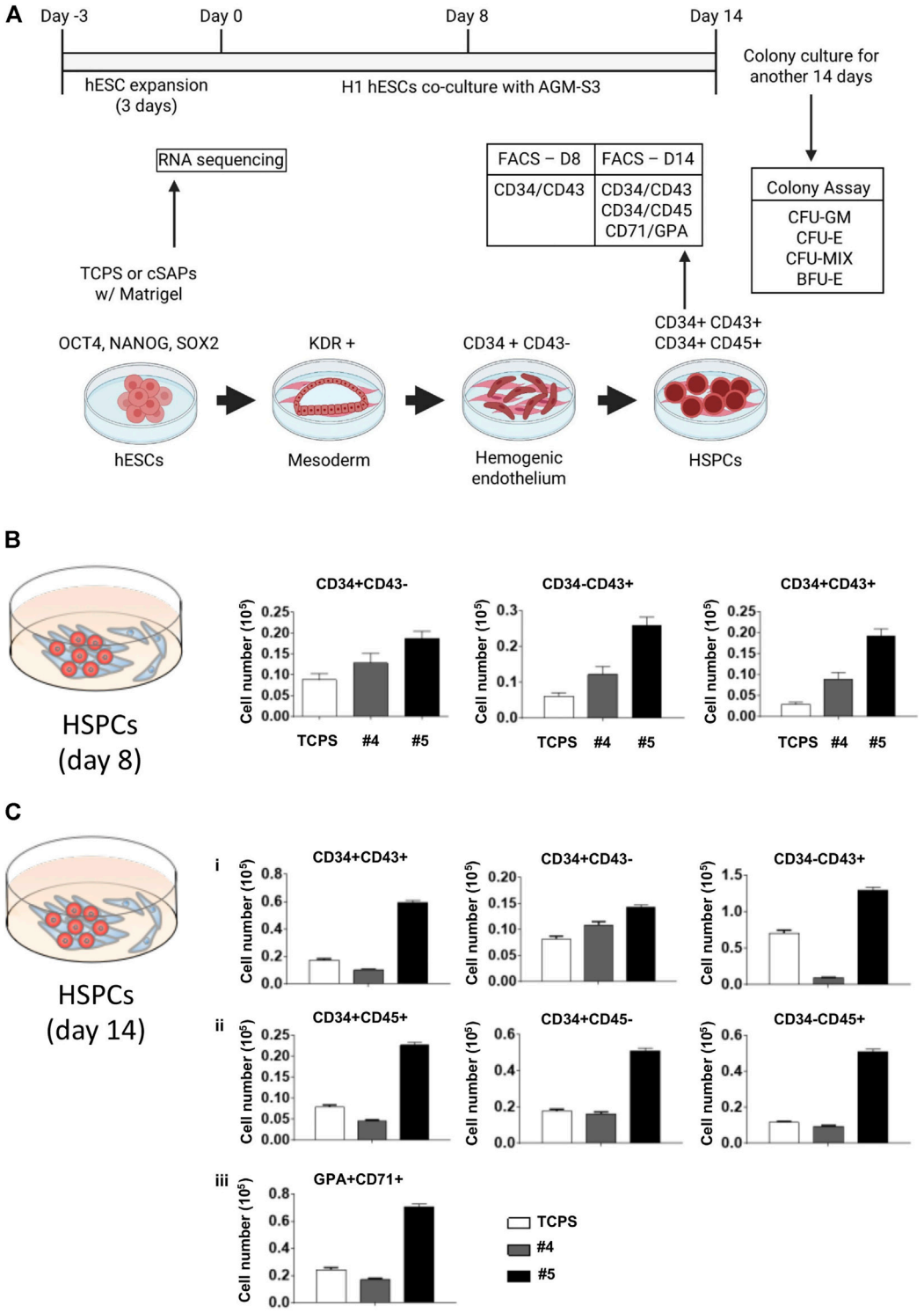

FIGURE 4 | Hemopoietic differentiation of cSAP-cultured hESCs. **(A)** Scheme of the H1 hESC expansion and hemopoietic differentiation. FACS analysis of the hemopoietic efficiency of cSAP-cultured hESCs after **(B)** 8 days and **(C)** 14 days. Error bar = SEM.

(**Figure 2B** and **Supplementary Figure S1A**). Percentage of *Oct4*-GFP positive cells was more than 90% on cSAPs, except the cSAP #3, which was similar to the cells cultured within LIF (i.e., ~80%).

Gene expression analysis showed that pluripotent markers (i.e., *Oct4, Nanog,* and *Sox2*) of miPSCs were similar (i.e., *Oct4* and *Nanog,* fold changes < 1.5) or higher (i.e., *Sox2,* fold changes > 1.5) on

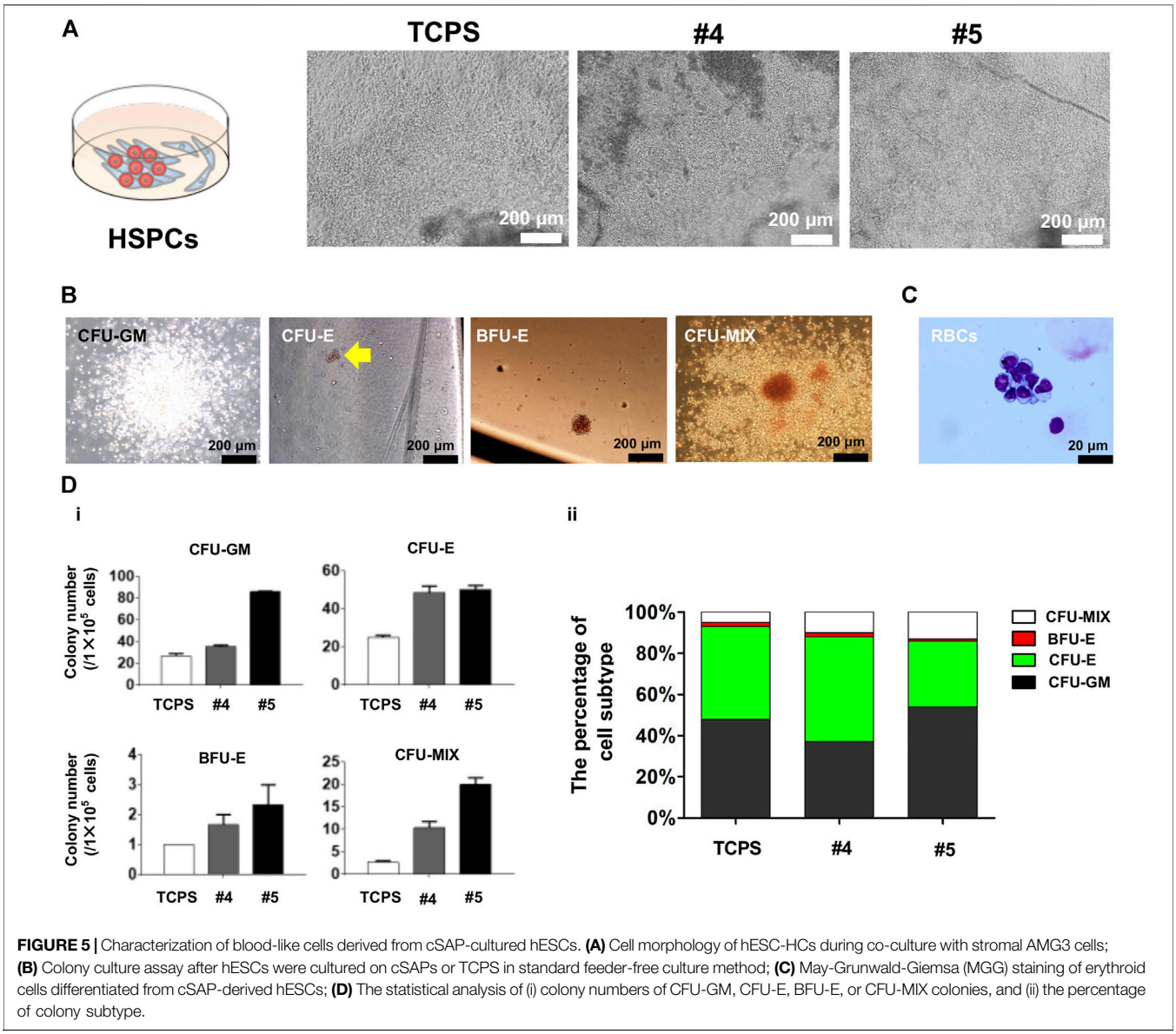

FIGURE 5 | Characterization of blood-like cells derived from cSAP-cultured hESCs. **(A)** Cell morphology of hESC-HCs during co-culture with stromal AMG3 cells; **(B)** Colony culture assay after hESCs were cultured on cSAPs or TCPS in standard feeder-free culture method; **(C)** May-Grunwald-Giemsa (MGG) staining of erythroid cells differentiated from cSAP-derived hESCs; **(D)** The statistical analysis of (i) colony numbers of CFU-GM, CFU-E, BFU-E, or CFU-MIX colonies, and (ii) the percentage of colony subtype.

the cSAPs compared to the TCPS control without LIF (**Figure 2C**). Gene expression of miPSCs was also analyzed under LIF conditions. The results showed that *Sox2* expression was significantly higher on cSAPs than TCPS, while *Oct4* and *Nanog* were similar between surfaces (**Figure 2D**). The high expression of Sox2 may indicate neural stem and progenitor cells in some cSAPs groups (Ellis et al., 2004). The effects of cSAPs on miPSCs and mESCs were different because three genes of mESCs expressed similarity between surfaces (fold changes < 1.5, **Figure 2C** and **Supplementary Figure S1B**).

Gene expression of mesoderm markers of miPSCs was higher on cSAPs than the TCPS control without LIF (**Supplementary Figure S1C**). On average, the expression of *mT*, *mSnail2*, and m*Foxa2* on cSAPs, except cSAP #5, was significantly higher than the TCPS control (fold changes > 2, **Supplementary Figure S1C**).

hiPSCs and hESCs also showed different colony morphology compared with TCPS and slight differences between cSAPs, similar to miPSCs on cSAPs showing a more 3D-like colony morphology (**Figures 3A,B**). For hESCs can not grow well without Matrigel, all surfaces used in culturing hESCs were precoated with Matrigel. FACS analysis (**Figure 4** and **Supplementary Figure S2**) and the hematopoietic colony form assay (**Figure 5**) showed that only H1 hESCs cultured on cSAP#4 and #5 had better hematopoietic differentiation efficiency than the TCPS control when co-cultured with AGM-S3, so only #4 and #5 were chosen for further analysis of hESCs pluripothency. Besides, immunostaining of pluripotent markers, i.e., *OCT4, SOX2,* and *SSEA4,* showed that passaged hESCs were in high pluripotency on cSAPs, i.e., cSAP #4 and cSAP #5, and TCPS (**Figure 3C**).

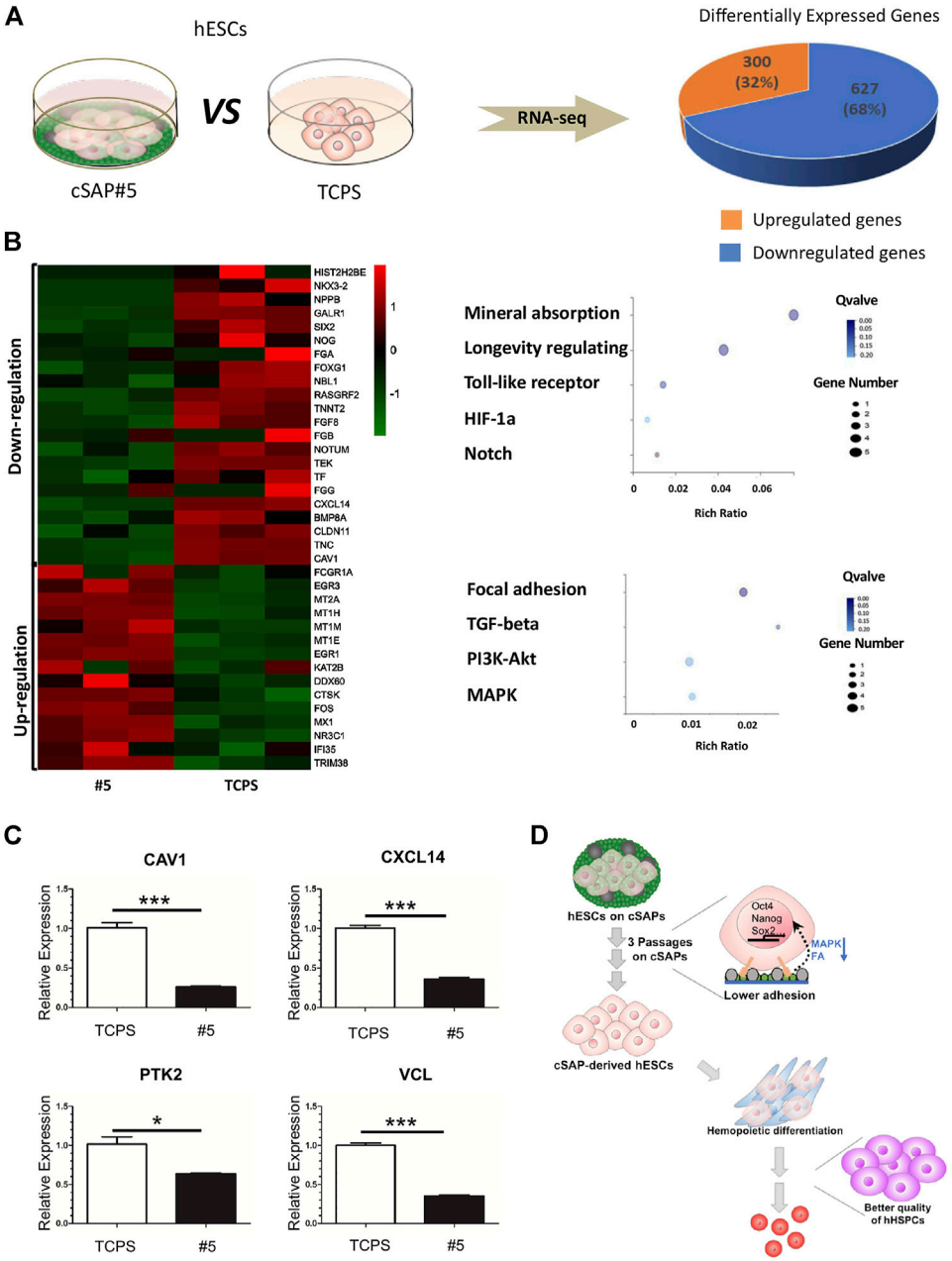

FIGURE 6 | The transcriptional profile and qPCR analysis of cSAP-derived hESCs. **(A)** RNA-seq analysis of transcriptional profiling of cSAP #5-derived and TCPS-derived hESCs; **(B)** The differential expression genes (DEG) analysis. The selected genes were presented by heatmap, and the selected enriched pathways were shown by dot-plot. **(C)** qPCR results of CAV1, CXCL14, PTK2, and VCL expression after three passages' culture (n = 4). **(D)** Schematic illustration of the role of cSAP in the maintenance of pluripotency and the improvement of the hemopoietic potential of hPSCs.

3.3 Colloidal Self-Assembled Patterns Promote the Hematopoietic Potential of Human Embryonic Stem Cells

Cell number of hESC-HCs from cSAP-derived hESCs was higher than the TCPS control after 8 and 14 days (**Figure 4** and **Supplementary Figure S2**). cSAPs, especially cSAP #5, strongly increased the cell populations of $CD34^+CD43^-$ (~2-folds), $CD34^-CD43^+$ (~4-folds), and $CD34^+CD43^+$ cells (~5-folds; hematopoietic progenitors) at D8 (**Figure 4B** and **Supplementary Figure S2A**). Also, cell populations of $CD34^+CD43^-$ (~1.5-folds), $CD34^-CD43^+$ (~1.5-folds), and $CD34^+CD43^+$ (~3-folds), $CD34^+CD45^-$ (~2-folds), $CD34^-CD45^+$ (~5-folds on cSAP #5), $CD34^+CD45^+$ (~3-folds), and CD71 + GPA + cells (~3-folds; erythroid progenitors) at D14 (**Figure 4C** and **Supplementary Figure S2B**).

The morphology of hESC-HCs on cSAPs was better compared to the TCPS control (**Figure 5A**). The colony assay proved that the hematopoiesis potentials of hESCs were significantly enhanced on cSAPs, especially #5. The numbers of CFU-GM, CFU-E, BFU-E, and CFU-MIX generated from cSAP-derived hESC-HCs were approx. 3-fold, 2-fold, 2-fold, and 7.5-fold higher than the TCPS control. Colony number represents the hematopoiesis potentials of H1 hESCs derived from different culture conditions to produce granulocyte/macrophage progenitors (CFU-GM), erythroid progenitors (CFU-E and BFU-E), and hematopoietic progenitors (CFU-MIX) after D14 of co-cultures (**Figure 5B**). The erythroid cells were confirmed by May-Grunwald-Giemsa (MGG) staining (**Figure 5C**). After co-culture differentiation and hematopoietic colony form culture, the absolute numbers of four kinds of colonies generated by H1 hESCs cultured on cSAPs#4 and #5 increased significantly compared with TCPS, especially cSAPs#5. Percentage of cell subtypes showed that H1 hESCs cultured on cSAPs# 5 were prone to generate the erythro-myeloid progenitor (EMP) in hematopoietic differentiation. Therefore, the cSAP #5-derived hESCs had significantly higher hematopoietic potentials to produce hematopoietic progenitors (i.e., $CD34^{+}CD45^{+}$ cells) and erythroid progenitors (i.e., GPA + $CD71^{+}$ cells) compared to the TCPS control (**Figure 5D**).

3.4 Colloidal Self-Assembled Patterns Alter the Transcriptome Profile of Cultured Human Embryonic Stem Cells

RNA-seq was used to analyze the change of cellular transcriptional profiling of hESCs after culturing on cSAP #5 (**Figure 4A**). Results showed that 300 genes (e.g., *EGR3, MT1M, EGR1, DDX60, FOS,* and *MX1*) were up-regulated significantly (32% of total differential expression genes), while the 627 genes (e.g., *NPPB, GALR1, SIX2, FOXG1, NBL1, RASGRF2, TNNT2, FGF8, NOTUM, TEK, TF, CXCL14, TNC,* and *CAV1*) were down-regulated significantly (68% of total differential expression genes) on cSAP #5 compared to the TCPS control (**Figures 6A,B**).

According to RNAseq analysis, the genes regulated on cSAPs were enriched in mineral absorption, longevity regulating, Toll-like receptor signaling, HIF-1a signaling, Notch signaling that were up-regulated, and the focal adhesion, TGF-β signaling, PI3K-Akt signaling, and MAPK signaling that were down-regulated (**Figure 6B**). According to the RNA-seq results we found that expression of CAV1 and CXCL14 was down-regulated (**Figure 6B**), and was consistent with qPCR verification (**Figure 6C**). CXCL14 is found concentrated in the focal adhesions, the down-regulated expression of CXCL14 (~2.79 fold) on cSAP #5 resulted in lower expression of PTK2 (~1.61 fold) and VCL (~2.83 fold) (**Figure 6C**). The dot-plot also showed focal adhesion was enriched in down-regulated DEGs (**Figure 6B**). CAV1 can function as a scaffolding protein contribute to the activation of the MAP kinase pathway (Mineo et al., 1996; Engelman et al., 1998). In this study, the down-regulated MAPK pathway in **Figure 6B** may be the result of lower CAV1 (~3.90 fold) expression on cSAP #5 (**Figure 6C**). Lower expression of CAV1 can promote hematopoietic differentiation of hESCs when co-cultured with stromal cells under hematopoietic induction condition (Choi et al., 2012). Therefore, cSAP-cultured hESCs having higher blood cell differentiation ability could be a consequence of down-regulation of focal adhesion and MAPK signaling (**Figure 6D**).

4 DISCUSSION

Pluripotent stem cells (PSCs) can self-renew unlimitedly and differentiate into three germ layers *in vitro*. For example, under specific induction conditions, hPSCs can be differentiated sequentially to mesodermal cells, hematopoietic progenitor cells, and mature hematopoietic cells (Lim et al., 2013). *In vitro* hematopoietic differentiation facilitates a better understanding of hematopoiesis and embryonic development. Besides, the production of blood-like cells is significant in regenerative medicine.

Nowadays, three major *in vitro* differentiation systems have been established for the generation of hESC-derived HCs, including embryoid body (EB) culture, co-culture with feeder cells, and culture with extracellular matrix (ECM) protein-coated surfaces (Chen et al., 2014). Among these methods, the microenvironments for hESC expansion are critical to determining the subsequent HSC generation (Ma et al., 2008; Slukvin, 2013). ECM protein-coated surfaces, such as fibronectin, collagen IV, laminin, collagen I, entactin, and heparin-sulfate proteoglycan, have been developed to induce differentiation of mesodermal and hematopoietic lineages under more chemical defined conditions (Chen et al., 2011; Nakamura-Ishizu et al., 2012). However, few studies manipulated the adhesion status of hESCs prior to hematopoietic differentiation. Furthermore, previous studies heavily relied on biological modulators such as paracrine molecules and medium molecules, while the effects of biophysical stimulations during the process were rarely explored.

It has been demonstrated that the surface coating of cell culture substrate was able to modulate the fate of cells, including directional differentiation of mesenchymal and pluripotent stem cells (Wang et al., 2016a). Surface decoration with nanostructures and bioactive signals can reconstruct the stem cell niche's microenvironments, which provide biophysical cues to the attached cells (Dalby et al., 2007). A previous study demonstrated that reduction of focal adhesions of mESCs was able to be maintained the cells in an undifferentiated and pluripotent state, while stronger cell adhesion resulted in stem cell differentiation (Taleahmad et al., 2017). The current study employed that colony morphology and adhesive force of PSCs varied on different cSAPs and the TCPS control. Further analysis demonstrated that PSCs' pluripotent state was adhesion- and morphology-dependent, where more 3D-like colonies on cSAPs have higher pluripotency than the 2D culture. cSAPs can affect adhesion molecules and regulate the pluripotency of PSCs. This

phenomenon is consistent with previous studies using different materials (Zujur et al., 2017).

Previous studies did show that physical cues on the substrate facilitate the generation of hESC-HCs. For example, graphene oxide (GO) had been reported to promote Endothelial-to-Hematopoietic Transition (EHT) and then the hESC-HC generation (Garcia-Alegria et al., 2016). In the current study, cSAPs don't have superior conductivity or biofunctionality but hierarchical micro- and nanostructure and dual chemistries. It has been demonstrated that these properties will alter protein adsorption from the medium, cell adhesion, cell migration, and ECM synthesis of adhered cells (Wang et al., 2011; Wang et al., 2012; Wang et al., 2015b). cSAPs can maintain the pluripotent status of PSCs and stimulate mesodermal commitment. The chemical and physical properties of different cSAPs can maintain the pluripotency of PSCs to a different extent. According to a previous report, PSCs in a naïve state have more robust self-renew capability and limited potential toward lineage differentiation (Lee et al., 2017). Besides, the naïve PSCs need capacitation for triggering multi-lineage differentiation (Rostovskaya et al., 2019). According to the colony morphology, cSAPs may reverse the cells back into a naïve-like state (e.g., cSAP #2) or a state of capacitation (e.g., cSAP #5). The result implies that cSAP-derived hESCs have a better hematopoietic potential due to optimal cell adhesion and colony formation.

Controlling the cellular status of hESCs during expansion can enhance the hemopoietic potential in the AGM-S3 co-culture system. cSAPs coating with Matrigel or proteins can be seen as an artificial ECM that modulates the adhesion of hESCs during expansion. cSAP derived hESCs can generate 2–4 folds of HCs compared to the TCPS control. According to RNAseq data, a flock of genes related to mineral absorption, such metallothionein 1 (MT1) family, MX1, and NR3C1, and the signaling pathways of Toll-like receptor, HIF-1a, Notch were up-regulated. The genes related to cell adhesion and signaling pathways of MAPK, Jak-STAT, and TGF-β were down-regulated.

The changes of these genes and pathways play vital roles in hematopoiesis. For example, Notch signaling controls the hematopoiesis and inflammation process (Šućur et al., 2020). Toll-like receptors and HIF-1a signaling can influence the generation of hematopoietic stem and progenitor cells (Capitano, 2019; Wielockx et al., 2019). The JAK/STAT signaling pathway controls about 50 cytokine signals to orchestrate hematopoiesis (Staerk and Constantinescu, 2012; Morris et al., 2018). MAPK signaling is involved in the generation of hematopoietic stem and progenitor cells (HSPC), erythropoiesis, mylogenesis (Geest and Coffer, 2009). TGF-β signaling can influence the generation of HSCs (Blank and Karlsson, 2015). Some of these genes were not directly relevant to hematopoiesis, which mechanisms need further research to discover. For example, many transcript factors, such as *FOS, EGR1, FOXG1, TF*, and other types of genes, such as MT1 family (Metallothionein), *DDX60* (Probable ATP-Dependent RNA Helicase), *MX1*(Interferon related GTPase), indicated a close couple to the promotion effects caused by culturing hESCs with cSAP. However, the mechanism of cSAP induced biological changes is unclear. The relationship between changing transcriptional profiles and promoting hematopoiesis needs to be elucidated using further analysis such as gene sequence and proteomics at a single cell level.

5 CONCLUSION

The hemopoietic potential of hESCs is critical in blood generation and related regenerative medicine. This study demonstrates that the adhesion and pluripotency of hESCs are crucial in subsequent hemopoietic differentiation. cSAP can be a new family of artificial ECMs (protein- or peptide-modified cSAPs) where the surface presents complex physical and chemical cues. cSAP modulate hESC adhesion and the ability to conduct hemopoietic differentiation. By merely manipulating hESCs using cSAPs, the number of hematopoietic progenitors and erythroid progenitors can be enhanced 3–4 folds. Altogether, cSAP could be the next-generation tool for hESC expansion and blood cell generation.

DATA AVAILABILITY STATEMENT

The RNAseq data presented in the study are deposited in the Array Express repository, accession number E-MTAB-11123.

AUTHOR CONTRIBUTIONS

P-YW and BC conceived and supervised this study. JLn, KL, and ME conducted material fabrication and characterization. JZ, WS, and DY conducted cell culture and data analysis. JH helped processing and uploading the RNAseq data. JLu, FM, and PK provided useful comments. JLn, BC, and P-YW wrote and revised the manuscript. All authors have approved the final version of the manuscript.

ACKNOWLEDGMENTS

P-YW thanks the support from the Ministry of Science and Technology of China (2019YFE0113000); The National Natural and Science Foundation of China (The General Program: 31870988); The CAS-CSIRO cooperative project (172644KYSB20200048); The Department of Science and Technology of Guangdong Province (International Collaborative Project: 2021A0505030055); The Science, Technology, and Innovation Commission of Shenzhen Municipality (the International Innovation and Collaboration Program, 20180928115804736 and the Shenzhen Key Laboratory, ZDSYS20190902093409851). Authors also thanks the support from the CAMS Initiatives for Innovative Medicine (2016-I2M-1-018 to

FM and 2017-I2M-3-021 to JLu); Sichuan Provincial Science and Technology Department Key R&D projects (020YFSY0023 to BC); Chengdu Science and Technology Project-Technology Innovation R&D (2018-YF05-01341-SN to BC).

REFERENCES

Blank, U., and Karlsson, S. (2015). TGF-β Signaling in the Control of Hematopoietic Stem Cells. *Blood* 125, 3542–3550. doi:10.1182/blood-2014-12-618090

Capitano, M. L. (2019). Toll-like Receptor Signaling in Hematopoietic Stem and Progenitor Cells. *Curr. Opin. Hematol.* 26, 207–213. doi:10.1097/moh.0000000000000511

Chang, J., Sun, W., Zeng, J., Xue, Y., Zhang, Y., Pan, X., et al. (2019). Establishment of an *In Vitro* System Based on AGM-S3 Co-culture for Screening Traditional Herbal Medicines that Stimulate Hematopoiesis. *J. Ethnopharmacol.* 240, 111938. doi:10.1016/j.jep.2019.111938

Chen, G., Gulbranson, D. R., Hou, Z., Bolin, J. M., Ruotti, V., Probasco, M. D., et al. (2011). Chemically Defined Conditions for Human iPSC Derivation and Culture. *Nat. Methods* 8, 424–429. doi:10.1038/nmeth.1593

Chen, B., Mao, B., Huang, S., Zhou, Y., Tsuji, K., and Ma, F. (2014). Human Embryonic Stem Cell-Derived Primitive and Definitive Hematopoiesis. *Intech, Pluripotent Stem Cell Biology - Advances in Mechanisms, Methods and Models*, 87–113. doi:10.5772/58628

Chen, B., Teng, J., Liu, H., Pan, X., Zhou, Y., Huang, S., et al. (2017). Inducible Overexpression of RUNX1b/c in Human Embryonic Stem Cells Blocks Early Hematopoiesis from Mesoderm. *J. Mol. Cel Biol.* 9, 262–273. doi:10.1093/jmcb/mjx032

Choi, K.-D., Vodyanik, M. A., Togarrati, P. P., Suknuntha, K., Kumar, A., Samarjeet, F., et al. (2012). Identification of the Hemogenic Endothelial Progenitor and its Direct Precursor in Human Pluripotent Stem Cell Differentiation Cultures. *Cel Rep.* 2, 553–567. doi:10.1016/j.celrep.2012.08.002

Cui, C., Wang, J., Qian, D., Huang, J., Lin, J., Kingshott, P., et al. (2019). Binary Colloidal Crystals Drive Spheroid Formation and Accelerate Maturation of Human-Induced Pluripotent Stem Cell-Derived Cardiomyocytes. *ACS Appl. Mater. Inter.* 11, 3679–3689. doi:10.1021/acsami.8b17090

Dalby, M. J., Gadegaard, N., Tare, R., Andar, A., Riehle, M. O., Herzyk, P., et al. (2007). The Control of Human Mesenchymal Cell Differentiation Using Nanoscale Symmetry and Disorder. *Nat. Mater* 6, 997–1003. doi:10.1038/nmat2013

Diba, F. S., Reynolds, N., Thissen, H., Wang, P. Y., and Kingshott, P. (2019). Tunable Chemical and Topographic Patterns Based on Binary Colloidal Crystals (BCCs) to Modulate MG63 Cell Growth. *Adv. Funct. Mater.* 29, 1904262. doi:10.1002/adfm.201904262

Ellis, P., Fagan, B. M., Magness, S. T., Hutton, S., Taranova, O., Hayashi, S., et al. (2004). SOX2, a Persistent Marker for Multipotential Neural Stem Cells Derived from Embryonic Stem Cells, the Embryo or the Adult. *Dev. Neurosci.* 26, 148–165. doi:10.1159/000082134

Engelman, J. A., Chu, C., Lin, A., Jo, H., Ikezu, T., Okamoto, T., et al. (1998). Caveolin-mediated Regulation of Signaling along the P42/44 MAP Kinase cascade *In Vivo*. *FEBS Lett.* 428, 205–211. doi:10.1016/s0014-5793(98)00470-0

Garcia-Alegria, E., Iliut, M., Stefanska, M., Silva, C., Heeg, S., Kimber, S. J., et al. (2016). Graphene Oxide Promotes Embryonic Stem Cell Differentiation to Haematopoietic Lineage. *Sci. Rep.* 6, 25917. doi:10.1038/srep25917

Geest, C. R., and Coffer, P. J. (2009). MAPK Signaling Pathways in the Regulation of Hematopoiesis. *J. Leukoc. Biol.* 86, 237–250. doi:10.1189/jlb.0209097

Ledran, M. H., Krassowska, A., Armstrong, L., Dimmick, I., Renström, J., Lang, R., et al. (2008). Efficient Hematopoietic Differentiation of Human Embryonic Stem Cells on Stromal Cells Derived from Hematopoietic Niches. *Cell Stem Cell* 3, 85–98. doi:10.1016/j.stem.2008.06.001

Lee, J.-H., Laronde, S., Collins, T. J., Shapovalova, Z., Tanasijevic, B., McNicol, J. D., et al. (2017). Lineage-Specific Differentiation Is Influenced by State of Human Pluripotency. *Cel Rep.* 19, 20–35. doi:10.1016/j.celrep.2017.03.036

Lim, W. F., Inoue-Yokoo, T., Tan, K. S., Lai, M. I., and Sugiyama, D. (2013). Hematopoietic Cell Differentiation from Embryonic and Induced Pluripotent Stem Cells. *Stem Cel Res. Ther.* 4, 71. doi:10.1186/scrt222

Ma, F., Ebihara, Y., Umeda, K., Sakai, H., Hanada, S., Zhang, H., et al. (2008). Generation of Functional Erythrocytes from Human Embryonic Stem Cell-Derived Definitive Hematopoiesis. *Proc. Natl. Acad. Sci.* 105, 13087–13092. doi:10.1073/pnas.0802220105

Mineo, C., James, G. L., Smart, E. J., and Anderson, R. G. W. (1996). Localization of Epidermal Growth Factor-Stimulated Ras/Raf-1 Interaction to Caveolae Membrane. *J. Biol. Chem.* 271, 11930–11935. doi:10.1074/jbc.271.20.11930

Moreno-Gimeno, I., Ledran, M. H., and Lako, M. (2010). Hematopoietic Differentiation from Human ESCs as a Model for Developmental Studies and Future Clinical Translations. Invited Review Following the FEBS Anniversary Prize Received on 5 July 2009 at the 34th FEBS Congress in Prague. *FEBS J.* 277, 5014–5025. doi:10.1111/j.1742-4658.2010.07926.x

Morris, R., Kershaw, N. J., and Babon, J. J. (2018). The Molecular Details of Cytokine Signaling via the JAK/STAT Pathway. *Protein Sci.* 27, 1984–2009. doi:10.1002/pro.3519

Murphy, W. L., McDevitt, T. C., and Engler, A. J. (2014). Materials as Stem Cell Regulators. *Nat. Mater* 13, 547–557. doi:10.1038/nmat3937

Nakamura-Ishizu, A., Okuno, Y., Omatsu, Y., Okabe, K., Morimoto, J., Uede, T., et al. (2012). Extracellular Matrix Protein Tenascin-C Is Required in the Bone Marrow Microenvironment Primed for Hematopoietic Regeneration. *Blood* 119, 5429–5437. doi:10.1182/blood-2011-11-393645

Papapetrou, E. P. (2017). Gene and Cell Therapy for β-Thalassemia and Sickle Cell Disease with Induced Pluripotent Stem Cells (iPSCs): The Next Frontier. *Adv. Exp. Med. Biol.* 1013, 219–240. doi:10.1007/978-1-4939-7299-9_9

Rostovskaya, M., Stirparo, G. G., and Smith, A. (2019). *Development*. England: Cambridge, 146.

Slukvin, I. I. (2013). Deciphering the Hierarchy of Angiohematopoietic Progenitors from Human Pluripotent Stem Cells. *Cell Cycle* 12, 720–727. doi:10.4161/cc.23823

Staerk, J., and Constantinescu, S. N. (2012). The JAK-STAT Pathway and Hematopoietic Stem Cells from the JAK2 V617F Perspective. *Jak-Stat* 1, 184–190. doi:10.4161/jkst.22071

Šućur, A., Filipović, M., Flegar, D., Kelava, T., Šisl, D., Lukač, N., et al. (2020). Notch Receptors and Ligands in Inflammatory Arthritis – a Systematic Review. *Immunol. Lett.* 223, 106–114. doi:10.1016/j.imlet.2020.04.010

Sun, W., Zeng, J., Chang, J., Xue, Y., Zhang, Y., Pan, X., et al. (2020). RUNX1-205, a Novel Splice Variant of the Human RUNX1 Gene, Has Blockage Effect on Mesoderm-Hemogenesis Transition and Promotion Effect during the Late Stage of Hematopoiesis. *J. Mol. Cel Biol.* 12, 386–396. doi:10.1093/jmcb/mjaa019

Taleahmad, S., Mirzaei, M., Samadian, A., Hassani, S.-N., Haynes, P. A., Salekdeh, G. H., et al. (2017). Low Focal Adhesion Signaling Promotes Ground State Pluripotency of Mouse Embryonic Stem Cells. *J. Proteome Res.* 16, 3585–3595. doi:10.1021/acs.jproteome.7b00322

Wang, P.-Y., Yu, J., Lin, J.-H., and Tsai, W.-B. (2011). Modulation of Alignment, Elongation and Contraction of Cardiomyocytes through a Combination of Nanotopography and Rigidity of Substrates. *Acta Biomater.* 7, 3285–3293. doi:10.1016/j.actbio.2011.05.021

Wang, P.-Y., Clements, L. R., Thissen, H., Jane, A., Tsai, W.-B., and Voelcker, N. H. (2012). Screening Mesenchymal Stem Cell Attachment and Differentiation on Porous Silicon Gradients. *Adv. Funct. Mater.* 22, 3414–3423. doi:10.1002/adfm.201200447

Wang, J. J., Kuang, Y., Zhang, L. L., Shen, C. L., Wang, L., Lu, S. Y., et al. (2013). Phenotypic Correction and Stable Expression of Factor VIII in Hemophilia A Mice by Embryonic Stem Cell Therapy. *Genet. Mol. Res.* 12, 1511–1521. doi:10.4238/2013.may.13.4

SUPPLEMENTARY MATERIAL

The Supplementary Material for this article can be found online at: https://www.frontiersin.org/articles/10.3389/fcell.2021.771773/full#supplementary-material

Wang, P.-Y., Pingle, H., Koegler, P., Thissen, H., and Kingshott, P. (2015). Self-assembled Binary Colloidal crystal Monolayers as Cell Culture Substrates. *J. Mater. Chem. B* 3, 2545–2552. doi:10.1039/c4tb02006e

Wang, P.-Y., Bennetsen, D. T., Foss, M., Ameringer, T., Thissen, H., and Kingshott, P. (2015). Modulation of Human Mesenchymal Stem Cell Behavior on Ordered Tantalum Nanotopographies Fabricated Using Colloidal Lithography and Glancing Angle Deposition. *ACS Appl. Mater. Inter.* 7, 4979–4989. doi:10.1021/acsami.5b00107

Wang, P.-Y., Thissen, H., and Kingshott, P. (2016). Modulation of Human Multipotent and Pluripotent Stem Cells Using Surface Nanotopographies and Surface-Immobilised Bioactive Signals: A Review. *Acta Biomater.* 45, 31–59. doi:10.1016/j.actbio.2016.08.054

Wang, P.-Y., Thissen, H., and Kingshott, P. (2016). Stimulation of Early Osteochondral Differentiation of Human Mesenchymal Stem Cells Using Binary Colloidal Crystals (BCCs). *ACS Appl. Mater. Inter.* 8, 4477–4488. doi:10.1021/acsami.5b12660

Wang, P.-Y., Hung, S. S.-C., Thissen, H., Kingshott, P., and Wong, R. C.-B. (2016). Binary Colloidal Crystals (BCCs) as a Feeder-free System to Generate Human Induced Pluripotent Stem Cells (hiPSCs). *Sci. Rep.* 6, 36845. doi:10.1038/srep36845

Wielockx, B., Grinenko, T., Mirtschink, P., and Chavakis, T. (2019). Hypoxia Pathway Proteins in Normal and Malignant Hematopoiesis. *Cells* 8, 155. doi:10.3390/cells8020155

Zeng, J., Zhang, H., Liu, Y., Sun, W., Yi, D., Zhu, L., et al. (2020). Overexpression of P21 Has Inhibitory Effect on Human Hematopoiesis by Blocking Generation of CD43 + Cells via Cell-Cycle Regulation. *IJSC* 13, 202–211. doi:10.15283/ijsc20033

Zhou, Y., Zhang, Y., Chen, B., Dong, Y., Zhang, Y., Mao, B., et al. (2019). Overexpression of GATA2 Enhances Development and Maintenance of Human Embryonic Stem Cell-Derived Hematopoietic Stem Cell-like Progenitors. *Stem Cel. Rep.* 13, 31–47. doi:10.1016/j.stemcr.2019.05.007

Zujur, D., Kanke, K., Lichtler, A. C., Hojo, H., Chung, U. I., and Ohba, S. (2017). Three-dimensional System Enabling the Maintenance and Directed Differentiation of Pluripotent Stem Cells under Defined Conditions. *Sci. Adv.* 3, e1602875. doi:10.1126/sciadv.1602875

Conflict of Interest: The authors declare that the research was conducted in the absence of any commercial or financial relationships that could be construed as a potential conflict of interest.

Publisher's Note: All claims expressed in this article are solely those of the authors and do not necessarily represent those of their affiliated organizations, or those of the publisher, the editors and the reviewers. Any product that may be evaluated in this article, or claim that may be made by its manufacturer, is not guaranteed or endorsed by the publisher.

frontiers in Cell and Developmental Biology

REVIEW
published: 02 February 2022
doi: 10.3389/fcell.2022.803280

Nutritional Regulation of Mammary Tumor Microenvironment

Nikita Thakkar[1,2], *Ye Bin Shin*[1] *and Hoon-Ki Sung*[1,2]*

[1]*Translational Medicine Program, The Hospital for Sick Children, Toronto, ON, Canada,* [2]*Department of Laboratory Medicine and Pathobiology, University of Toronto, Toronto, ON, Canada*

The mammary gland is a heterogeneous organ comprising of immune cells, surrounding adipose stromal cells, vascular cells, mammary epithelial, and cancer stem cells. In response to nutritional stimuli, dynamic interactions amongst these cell populations can be modulated, consequently leading to an alteration of the glandular function, physiology, and ultimately disease pathogenesis. For example, obesity, a chronic over-nutritional condition, is known to disrupt homeostasis within the mammary gland and increase risk of breast cancer development. In contrast, emerging evidence has demonstrated that fasting or caloric restriction can negatively impact mammary tumorigenesis. However, how fasting induces phenotypic and functional population differences in the mammary microenvironment is not well understood. In this review, we will provide a detailed overview on the effect of nutritional conditions (i.e., overnutrition or fasting) on the mammary gland microenvironment and its impact on mammary tumor progression.

Keywords: mammary gland, breast cancer, obesity, white adipose tissue, fasting, tumor microenvironment

OPEN ACCESS

Edited by:
Rita Yen-Hua Huang,
Taipei Medical University, Taiwan

Reviewed by:
Raghu P Kataru,
Memorial Sloan Kettering Cancer Center, United States
Yung-Che Kuo,
Taipei Medical University, Taiwan

***Correspondence:**
Hoon-Ki Sung
hoon-ki.sung@sickkids.ca

Specialty section:
This article was submitted to Stem Cell Research, a section of the journal Frontiers in Cell and Developmental Biology

Received: *27 October 2021*
Accepted: *12 January 2022*
Published: *02 February 2022*

Citation:
Thakkar N, Shin YB and Sung H-K (2022) Nutritional Regulation of Mammary Tumor Microenvironment. Front. Cell Dev. Biol. 10:803280. doi: 10.3389/fcell.2022.803280

INTRODUCTION

The relationship between nutrition and cancer has been well established with obesity increasing the risk and progression of breast cancer by 20–40% in post-menopausal women (Munsell et al., 2014). As the mammary gland is a heterogeneous organ constituted of white adipose tissue (WAT), nutritional excess conditions can drive interactions between several populations within the WAT, altering mammary gland integrity and function. In particular, obesity-driven WAT remodeling is known to alter secretory immune and fibrotic profiles (Revelo et al., 2014; Ruiz-Ojeda et al., 2019). Due to obesity, adipocyte size increases beyond the physiological range. This induces cellular stress and apoptosis of adipocytes. As a result, pro-inflammatory macrophages infiltrate to surround these apoptotic adipocytes while extracellular matrix (ECM) is deposited, resulting in a constitutive state of fibro-inflammation within the tissue (Castoldi et al., 2015; Verma et al., 2020). Intriguingly, fibro-inflammation is a hallmark of dysfunctional WAT and is associated with increased cancer incidence (Divella et al., 2016). Obesity-induced mammary WAT fibro-inflammation and interactions of various cell populations provide a microenvironment that contributes to the survival of cancerous cells (Quail and Dannenberg, 2019). Consequently, chronic overnutrition conditions can promote tumor initiation, progression, and metastasis (Park et al., 2000; Ramamonjisoa and Ackerstaff, 2017; Quail and Dannenberg, 2019). Thus, modulation of the mammary WAT microenvironment through nutritional alterations could be an innovative intervention for the prevention and treatment of breast cancer.

Over the past few years, fasting regimens have emerged as effective nutritional interventions to aid with weight loss and improve whole-body metabolism (Varady et al., 2008). While caloric restriction

(CR) refers to a restriction in caloric intake, intermittent fasting (IF) is characterized by periodic cycles of fasting followed by free eating which can encompass various nutritional regimes and eating strategies (Klempel et al., 2013; Catterson et al., 2018; Kim et al., 2019). For example, time-restricted feeding (TRF) refers to the restriction of energy intake during specific time frames throughout the day (e.g., 16:8 TRF—16-h of fasting with an 8-h of eating window) (Moro et al., 2016). Other forms of IF include fasting days throughout the week (e.g., 2:1 IF—2 days of normal eating followed by 1 day of fasting) (Kim et al., 2017; Kim et al., 2019; Lee et al., 2020). Fasting regimens protect hematopoietic stem cells from chemotherapy-induced immunosuppression (Cheng et al., 2014), restore healthier cardiometabolic profiles (Almeneessier et al., 2018), improve glucose homeostasis and insulin intolerance (Cho et al., 2019), and initiate an anti-inflammatory response (Kim et al., 2017). Interestingly, emerging evidence has demonstrated that fasting can also negatively impact tumorigenesis (Nencioni et al., 2018).

A longer nighttime fast is associated with improved glycemic control (Lee et al., 2020), decreased breast cancer biomarkers such as leptin and insulin-like growth factor 1 (IGF-1) (Marinac et al., 2015a; Marinac et al., 2015b), and overall reduced breast cancer recurrence (Marinac et al., 2016). In one study, mice were subjected to TRF using high-fat diet (HFD) to induce obesity. These obese mice treated with TRF displayed delayed mammary tumor onset, reduced tumor growth, and total tumor weight (Sundaram and Yan, 2018). In addition to the impact fasting has on breast cancer biomarkers and tumor progression, recent literature has highlighted the therapeutic potential of fasting (Buono and Longo, 2018; Nencioni et al., 2018; Zhao et al., 2021). Fasting prior to administration of chemotherapy (Lee et al., 2012), immune checkpoint blockade therapy (Ajona et al., 2020), and radiotherapy (De La Cruz Bonilla et al., 2019) has shown to decrease tumor growth and improve overall survival, indicating that fasting can improve therapeutic effectiveness in various cancer treatments. As such, fasting regimes are emerging as a promising therapy for cancer patients. However, how fasting modulates the tumor microenvironment to improve cancer outcome is not well understood.

As the mammary gland is composed of WAT, WAT contributes many populations that form the tumor microenvironment. WAT is a heterogeneous tissue composed of adipose stromal cells (ASC), various immune cells, vascular cells, and mammary epithelial cells (Verma et al., 2020). Nutritional excess conditions can alter these microenvironmental populations to favor mammary tumor growth. Alterations in ASC regulate adipocyte expansion, inflammation, and ECM formation (Zhang et al., 2019; Verma et al., 2020). Thereby, ASC play a critical role in maintaining tissue integrity (Hillers et al., 2018). Modulation of immune cells can alter their ability to target abnormal cell growth and control immunosuppression (Cheng et al., 2014). On the other hand, vascular cells regulate nutrient and oxygen supply, which are needed for cancer growth (Yang et al., 2018). Together, these populations have the potential to create a pro-tumor microenvironment which enhances cancer stem cell activity and transforms mammary epithelial cells to promote cancer cell growth (Chamberlin et al., 2017). Hence, as WAT dynamically remodels in response to excess nutrition, these microenvironment populations also remodel to form the tumor microenvironment in breast tissue. As such, investigating the impact of fasting on the mammary tumor microenvironment has been of key interest. In this review, we will summarize the impact of obesity and fasting in the mammary WAT microenvironment cell populations including ASCs, immune cells, vascular cells, mammary epithelial and cancer stem cells, with an emphasis on their contributions to tumorigenesis. For the purposes of this review, studies discussed regarding mammary gland in preclinical models are from inguinal WAT.

ADIPOSE STROMAL CELLS AND CANCER ASSOCIATED FIBROBLASTS

Nutritional excess conditions (e.g., obesity) can disrupt the homeostasis of the mammary gland. Pathological obesity is characterized by the expansion of adipocytes through hyperplastic (increase in number) and hypertrophic (increase in size) growth. ASC largely regulate adipocyte expansion. Also known as mesenchymal stem cells or adipocyte precursor cells, ASC are immunomodulatory bipotential stem cells that have the ability to differentiate into adipocytes or fibroblasts (Casteilla et al., 2011). Their adipogenic differentiation and determination is heavily dependent on PPARγ and C/EBPα, two major early key regulators of adipogenesis (Lechner et al., 2013). However, nutritional conditions can impact their differentiation potential. Obese conditions create a chronic-low grade inflammatory state due to the upregulation of pro-inflammatory mediators such as TNFα (Tzanavari et al., 2010). Upregulation of pro-inflammatory TNFα mediates the inhibition and reversal of adipocyte differentiation by suppressing the expression of adipogenic marker PPARγ, resulting in reduced *de novo* adipogenesis (Karagiannides et al., 2006; Tchkonia et al., 2007). As such, the body stores excess energy through adipocyte hypertrophy. These larger adipocytes exhibit necrotic-like abnormalities and inflammation, contributing to unfavorable fat expansion and insulin resistance (Shao et al., 2018). Furthermore, activation of receptors responsible for immune cytokine signaling such as toll-like receptor 4 exhibit increased ECM deposition and fibrosis (Vila et al., 2014), in part by downregulation of adipogenic marker PPARγ (Wei et al., 2010). Hence, coupled with adipocyte expansion, the microenvironment of obese WAT experiences hypoxia, adipocyte death, dysregulated angiogenesis, ECM deposition, and immune cell infiltration (Verma et al., 2020), overall creating an unhealthy microenvironment. Consequently, this unhealthy microenvironment can inhibit ductal growth, impair mammary gland function, and foster tumor growth (Lin and Li, 2007; Ullah et al., 2017). Thus, healthy WAT expansion is of vast interest to prevent the formation of a pro-tumor microenvironment.

Over recent years, fasting has been shown to be effective against obesity largely due to its effect on the adipocyte

population. Obese mice subjected to 16 weeks of an IF regimen consisting of 2 feeding days followed by 1 fasting day exhibited decreased WAT weight as well as adipocyte size, without major alterations in whole-body lean mass (Kim et al., 2017). Tang et al. illustrated that adipogenesis is enhanced in mice subjected to 24-h refeeding after a 72-h fast through an upregulation of differentiation transcription factors promoting adipogenesis such as PPARγ and C/EBPα (Tang et al., 2017). In addition, a hallmark of fasting-induced WAT changes includes *beiging* or *browning*, a phenomenon describing adipocytes that acquire brown adipocyte-like characteristics. Subjecting mice to 40% CR, 40% of normal caloric intake, diet for 5 weeks resulted in greater hyperplastic growth, reduced hypertrophy, and multilocular lipids, indicative of WAT *browning* (Fabbiano et al., 2016). Furthermore, inguinal mammary WAT exhibited increased expression of *browning* markers such as *UCP1, Cidea, PPARγ*, and adipose-fatty acid binding protein 4 (*Fabp4*) (Fabbiano et al., 2016). Similarly, alternate-day fasting for 15 cycles resulted in increased expression of thermogenic *browning* markers and multilocular lipid accumulation of inguinal WAT. This WAT *browning* was demonstrated in part due to elevated levels of acetate and lactate (Li et al., 2017). Since WAT *browning* promotes healthy storage of fat through hyperplastic growth (Fabbiano et al., 2016), IF-induced *browning* serves as a potential therapy to promote healthy adipogenesis, maintain tissue integrity, and combat the growing obesity epidemic.

While WAT *browning* has been established as an essential component mediating fasting-induced metabolic benefits, recent evidence has highlighted novel interactions for resident beige adipocytes in mammary tumors. To investigate the influence of UCP1+ beige adipocytes on tumor growth, Singh et al. sorted UCP1+ and UCP1- fractions from xenografted breast cancer tumors. Subcutaneously injecting mammary tumor fraction depleted for UCP1+ adipocytes into nude mice significantly reduced tumor growth, suggesting that beige adipocytes may contribute to breast cancer development (Singh et al., 2016). Additionally, membrane-bound extracellular vesicle exosome interactions between adipocytes and tumor cells have emerged as a potential mechanism to induce WAT *browning* and lipolysis in the mammary tumor (Zhao et al., 2018; Wu et al., 2019). Co-culturing breast cancer cells and mature adipocytes decreases lipid droplet size, number, triglyceride content, and adipogenic marker *PPARγ,* while increasing *UCP-1* levels and lipolytic activity. Subjecting cancer cells to cultured medium from mature adipocytes increases invasion and downregulation of epithelial marker E-cadherin (Wu et al., 2019), indicating increased aggressiveness. These studies suggest that tumor cells can take advantage of surrounding adipocytes (cancer-associated adipocytes) to induce thermogenesis and lipolysis to amplify their nutrient supply. Often upregulated by lipolysis and obesity is *Fabp4*. Genetic deletion of *Fabp4* eradicated obesity-associated mammary tumor growth and development (Hao et al., 2018), highlighting a potential biomarker to predict obesity-induced aggressiveness. As fasting has been shown to induce WAT *browning* (Kim et al., 2017), the impact fasting has on preventing or exacerbating cancer-associated adipocytes in the mammary tumor is inconclusive. Since adipocytes within the mammary gland supply lipids to neighboring cells for nutritional functions (Zwick et al., 2018), it is essential to understand whether fasting-induced lipolytic activity could increase energy supply for cancer cells and potentially aggravate progression of mammary tumors.

As adipocytes surrounding the tumor lose lipids, these cells can acquire fibroblast-like features. Thereby, cancer-associated adipocytes can represent an intermediate population with fibroblast features including increased fibronectin, collagen 1, fibroblast-stromal protein (FSP) (Bochet et al., 2013), alpha-smooth actin (αSMA) (Inoue et al., 2016), fibroblast activation protein (FAP) (Kahounova et al., 2018), and vimentin expression (Hsia et al., 2016). Although the origin is unknown, one attractive theory is that mature adipocytes can transform into cancer-associated adipocytes and acquire fibroblast features to become fibroblast-like cells (Bochet et al., 2013). These fibroblast-like ASCs are known as cancer associated fibroblasts (CAF). Activated CAFs can impact tumor microenvironment and modulate cancer metastasis through ECM remodeling, angiogenesis, and growth factor secretion (Sahai et al., 2020). Isolating circulating ASCs from obese donors and subjecting them to breast cancer MCF-7 cells *in vitro* demonstrated decreased adipogenic differentiation potential and increased expression of fibrotic markers such as αSMA, FAP, and FSP (Strong et al., 2017). Furthermore, examination of ASC isolated from diet-induced obese mice mammary gland WAT revealed decreased differentiation and upregulation of activated fibroblasts marker, αSMA. Co-inoculating obese mice ASCs and mammary tumor cells into lean mice resulted in larger tumor growth, enhanced proliferation, and increased invasion (Hillers et al., 2018). In addition, an independent study demonstrated that in lung cancer, CAFs promote epithelial-to-mesenchymal transition and enhance the metastatic potential of cancer cells through an IL-6 mediated pathway. Administering IL-6 neutralizing antibody abolished the effects of CAF-induced cell migration, possibly leading to reduced metastasis (Wang et al., 2017). These findings suggest that HFD-induced obesity can reduce adipogenic differentiation of ASCs while augmenting ASC conversion to CAF (Hillers et al., 2018).

A study by Wu et al. demonstrated that mature adipocytes expressing programmed death-ligand 1 (PD-L1) inhibit activation of anti-tumor CD8+ T cells when administered anti-PD-L1 antibody *in vitro*. While depletion of PD-L1 expression on mature adipocytes promotes CD8+ T cell activation, ASC specific PD-L1 expression inactivates cytotoxicity of CD8+ T cell, suggesting context dependent immune modulatory function of PD-L1. Pharmacologic inhibition of adipogenesis in mammary tumors reduces PD-L1 expression and enhances anti-tumor efficacy, highlighting a potential role of the ASC population to modulate therapeutic effectiveness by controlling adipogenesis (Wu et al., 2018). Currently, there are no published studies showing the direct impact fasting has on the ASC or CAF population in breast cancer. As fasting is known to decrease IL-6 (Speaker et al., 2016) and is thought to modulate the ASC population to promote healthy adipocyte expansion, understanding how the ASC and CAF populations are modulated in response to fasting is critical

to expand our knowledge into fasting-induced microenvironmental changes.

IMMUNE CELLS—MYELOID CELLS

Obesity induces mammary WAT expansion and is coupled with an accumulation of immune cells, specifically macrophages (Kolb and Zhang, 2020; Colleluori et al., 2021). WAT-resident macrophages proliferate while newly recruited monocyte-derived macrophages accumulate. These macrophages can assist with regulating physiological processes and maintaining metabolic function of WAT. In particular, these infiltrated pro-inflammatory adipose-tissue macrophage (ATM) surround necrotic cells to reabsorb lipids forming crown-like structures (CLS). As a highly abundant population, CLS macrophages secrete several pro-inflammatory mediators including TNFα, IL-6, CRP, and MCP-1 (Lumeng et al., 2007; Coats et al., 2017) into the microenvironment, resulting in chronic low-grade inflammation. Since WAT constitutes a major component of the breast tissue microenvironment, this chronic low-grade inflammation is associated with increased breast cancer risk, reduced overall survival, and recurrence-free survival (Pajares et al., 2013; Ecker et al., 2019).

Historically in WAT tissue biology, there are two distinct macrophage population. M1-like CD11c + pro-inflammatory macrophages are induced by pro-inflammatory factors such as interferon gamma (IFN γ), IL-6, IL-1β, and predominantly contribute to the formation of CLS. In comparison, classical CD206+ M2-like macrophages are anti-inflammatory, contributing to tissue repair and production of anti-inflammatory cytokines such as IL-4 and IL-13 (Novak and Koh, 2013). In general, to maintain tissue integrity and homeostasis of WAT, a balance between pro-inflammatory and anti-inflammatory macrophages is required (Lumeng et al., 2007). Intriguingly, as obesity disturbs this balance by favoring M1-like macrophages, IF has been shown to restore balance with M2-like polarization (Zhao et al., 2018). Kim et al. demonstrated that induction of VEGF through a 2:1 feeding-to fasting-regimen of IF induces alternative activation of M2-like macrophages, promoting visceral WAT *browning* and thermogenesis (Kim et al., 2017). Similarly, 40% CR stimulates *browning* of mammary inguinal WAT through increased eosinophil infiltration, type 2 cytokine signaling and M2-like macrophage polarization. Suppression of type 2 signaling prevented *browning* and mammary inguinal WAT loss with CR, highlighting the importance of immune signaling and macrophage polarization for CR benefits (Fabbiano et al., 2016). Since chronic low-grade inflammation and presence of M1-like CLS are associated with increased risk of tumor onset (Carter et al., 2018; Faria et al., 2020), the polarization of M2-like macrophages through IF or CR could contribute to restoring a balance between M1-like and M2-like macrophages in the mammary microenvironment. This subsequently could decrease mammary WAT inflammation and potentially suppress the initiation of mammary tumor formation.

The stage at which IF induces M2-like macrophage polarization and accumulation could alter the benefits of IF on mammary tumorigenesis. Whereas M2-like macrophage accumulation prior to tumor onset can decrease inflammation and thereby suppress tumor onset, accumulation of M2-like macrophages during tumor progression may worsen prognosis. Jeong et al. established an association between M1-like macrophages and higher overall and disease-free survival in tissue microarrays of human invasive breast cancer, suggesting M2-like macrophages accelerate tumor progression (Jeong et al., 2019). Thus, further research is necessary to understand the impact IF-induced M2-like polarization could have during different stages of tumor development. As extremely plastic cells, increasing literature indeed highlights many other macrophage subcategories (Chavez-Galan et al., 2015). In the tumor context, using classical M1-like and M2-like macrophages is insufficient to characterize the tumor-associated macrophage population. Understanding the various roles different tumor-associated macrophage populations play in mammary tumor development and how these populations are altered by IF, could provide novel insight into the shaping of the tumor microenvironment (Narita et al., 2018; Mao et al., 2021).

Though macrophages are the most abundant leukocytes, eosinophils and myeloid derived suppressor cells (MDSC) also exist in the mammary gland. As shown by Fabbino et al., CR stimulates *browning* of mammary WAT through increased eosinophil infiltration (Fabbiano et al., 2016). Increased serum eosinophils counts are associated with better breast cancer prognosis, response to therapy, and long-term survival (Martens et al., 2016). Notably, a positive association between eosinophilia and disease outcome has been detected widely in metastatic melanoma (Simon et al., 2020) and recently in breast cancer (Onesti et al., 2020). In fact, Zheng et al. demonstrated that immune checkpoint blockade administration of anti-CTLA-4 treatment in MMTV-Polyomavirus Middle T-antigen (MMTV-PyMT) model increased eosinophil infiltration. Pharmacological depletion of eosinophils decreased the anti-tumor effect of CTLA-4, thereby promoting tumor growth (Zheng et al., 2020). As eosinophils counts are predictive for cancer prognosis (Martens et al., 2016) and play at least a partial role in mediating immune checkpoint blockade antibody response in mammary tumors (Zheng et al., 2020), IF-mediated upregulation in eosinophils may contribute to enhancing therapeutic efficacy and consequently improving breast cancer prognosis.

On the other hand, little is known about the direct impact of fasting on the MDSC population in the mammary gland and tumor microenvironment. Under HFD conditions, mammary tumors isolated from obese mice displayed increased tumor progression and enhancement of the MDSC population. Depleting MDSC in obese mice protected against diet-induced metabolic dysfunction and inflammation, which was sufficient to decrease tumor volume, liver metastasis, and improve overall survival. They discovered that HFD induces MDSC′ PD-L1 expression, thereby inactivating CD8+ T cell cytotoxic activity (Clements et al., 2018) and enhancing immunosuppression. However, the direct

interaction of fasting on the immunophenotype of MDSC has not been clearly documented.

Intriguingly, metformin, an AMP-activated protein kinase (AMPK) activator, has become an emerging therapy in breast cancer (Goodman et al., 2014). Preclinical AMPK activator, OSU-53, suppresses breast cancer (MDA-MB-231 xenograft) growth by 47–49% (Lee et al., 2011). Importantly, AMPK and its downstream pathways have been shown to be activated by IF or fasting (Kajita et al., 2008; Viscarra et al., 2011). Since obesity-induced chronic low-grade inflammation is known to increase tumor-associated MDSCs, anti-obesity interventions such as IF could modulate the MDSC population (Salminen et al., 2019). In a study by Turbitt et al., mice were subjected to one of three possible treatments including 10%kcal HFD feeding, 60%kcal HFD feeding, or 30%kcal CR feeding for 16 weeks. These dietary regimens produced overweight, obese, and lean mice respectively which were subsequently injected with pancreatic tumor cells. A linear association between greater adiposity and tumor growth was observed, with obese animals bearing the largest tumors. Additionally, overweight/obese tumors contained a lower CD8: MDSC ratio, with an overall greater proportion of MDSC's and a lower proportion of CD8+ T cell (Turbitt et al., 2019). Though this study was conducted in pancreatic cancer, systemic activation of AMPK through CR could have important implications in modulating the MDSC population in breast cancer.

IMMUNE CELLS—LYMPHOID CELLS

While myeloid populations like tumor-associated macrophages, eosinophils, and MDSCs are predominantly involved in immunosuppression, lymphoid populations inherently aid with alleviating this immunosuppression and participating in tumor-killing cytotoxic activity. In particular, CD8+ T cells play a critical role in modulating the mammary WAT microenvironment in response to obesity and tumorigenesis. MMTV-PyMT mice fed 60% HFD for 14–20 weeks promoted tumor initiation and progression via modulation of CD8+ T cell population (Kado et al., 2019). Obesity induced a phenotypic switch in tumor CD8+ T cells to promote early exhaustion as cells acquire exhaustive immune checkpoint receptor PD-1 (Kado et al., 2019). Consequently, the increase in PD-1+ CD8+ cells by diet-induced obesity resulted in reduced expression of cytotoxic genes such as IFN γ and granzyme B (GzB) (Kado et al., 2019), suggesting that obesity decreases anti-tumor cytotoxic activity by induction of T cell exhaustion. Along with decreased proliferative capacity and activity of CD8+ T cells, an independent study discovered HFD initiates metabolic reprogramming of cancer cell to increase lipid uptake, while starving CD8+ T cells (Ringel et al., 2020). Prolyl-hydroxylase 3 (PHD3) is a protein in normal cells that has been shown to inhibit excessive lipid metabolism. Overexpression of PHD3 in tumor cells enhanced anti-tumor activity by blocking cancer cell metabolic reprogramming, resulting in slower tumor growth (Ringel et al., 2020). As similar metabolic reprogramming was observed in human cancers, this study provided a novel insight into changes in cellular components of the tumor microenvironment in response to diet-induced obesity. Taken together, these studies highlight the immunosuppressive nature of diet-induced obesity on tumor-associated CD8+ T cells.

Intriguingly, Biase et al. revealed a fasting-mimicking diet (FMD), a high-fat and low-carb CR diet, to enhance CD8+ tumor-infiltrating lymphocytes (TIL) in breast cancer (Di Biase et al., 2016). Triple negative breast cancer 4T1 tumor-bearing female mice subjected to 4 days of FMD sensitized tumors to chemotherapeutic doxorubicin and cyclophosphamide treatment as tumor volume was significantly decreased by 3-fold. The combination of FMD and chemotherapy (doxorubicin) significantly increased CD8+ TILs and their cytotoxic enzyme (e.g., GzB) and enhanced tumor cell apoptosis (Di Biase et al., 2016). Conversely, depleting CD8+ TIL's by neutralizing antibody increases regulatory T cells (Tregs). Subjecting Balb/C nude mice lacking T-lymphocytes to FMD was not effective at reducing tumor size, increasing GzB, or cleaved-caspase-3 levels, highlighting the critical role that TIL play in mediating FMD effects (Di Biase et al., 2016). This study uncovered Heme-Oxygenase 1 downregulation to be essential for FMD-induced increase in CD8+ TIL cytotoxicity. Overall, this study suggests that FMD increases CD8+ TIL cytotoxicity by reducing Heme-Oxygenase 1 expression with associated Treg downregulation (Di Biase et al., 2016). Since HFD was shown to change metabolic programming of cancer cells in the tumor microenvironment and IF is known to decrease several metabolic parameters such as insulin and glucose, future studies should investigate how IF can impact tumor microenvironment metabolic programming. In particular, it would be interesting to see the impact of IF on PHD3. This could provide promising novel targets and IF mimetics that could improve anti-tumor activity and enhance current therapeutics.

Another key lymphoid population that plays an important role in anti-tumor properties is Natural Killer cells (NK). Though an important population in the tumor context, NK cells have not been thoroughly examined for their role in obesity in the mammary gland (Ohmura et al., 2010). Under obese conditions, alterations in resident NK cells have been observed in epididymal fat but not subcutaneous fat (Lee et al., 2016). A subpopulation of NK cells resembling T cells exists and are referred to as NKT cells. With just 4 days of HFD, NKT cells are activated and promote M2-like macrophage polarization in the depot. NKT-deficient CD1d −/− mice subjected to HFD challenge showed impaired metabolic parameters, without polarization of M2-like macrophages (Ji et al., 2012). This suggests that NKT cells play a WAT depot specific role in contributing to obesity-induced WAT remodeling. Additionally, compared to lean counterparts, obese mammary tumor-bearing mice demonstrated decreased ligand NKp46 expression on circulating NK cells and increased activating NK receptor NKG2D ligand MULT1 expression in visceral WAT (Spielmann et al., 2020). As such, this paper alluded that NK cells may be occupied in managing inflamed visceral WAT microenvironments during obese conditions and therefore are unable to kill mammary tumor cells, leading to accelerated tumor growth. Future research into the effect of prolonged HFD feeding on NK/NKT receptor and ligand activity in the mammary

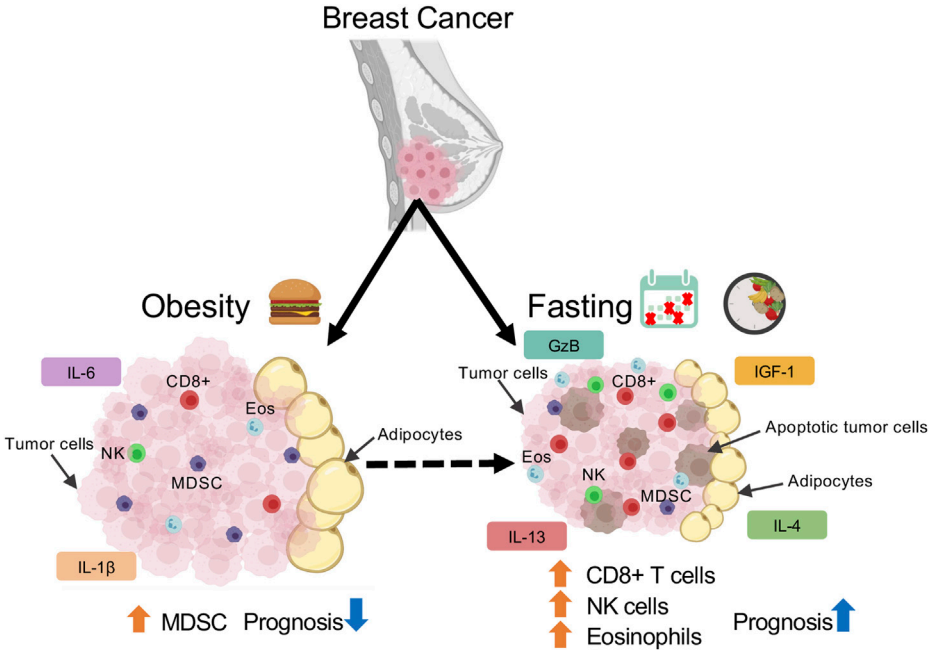

FIGURE 1 | Schematic depicting immune population changes in mammary tumor microenvironment in response to obesity and fasting conditions.

gland could provide insight into whether there is a differential role for NK cells in mammary WAT.

In an independent liver study, mice subjected to a 3 days fast increased tumor-necrosis factor-related apoptosis inducing ligand and CD69+ NK cells, without major alterations in resident NK cell number. These NK cells displayed enhanced antitumor function in comparison to the fed group (Dang et al., 2014). Though this study was conducted in the liver, such an effect in a mammary tumor could be instrumental in targeting tumors. As one of the key populations responsible for cytotoxic activity in tumors, understanding how NK cells change under obese conditions in the mammary gland could shed light into on their potential contribution to anti-tumor activity by fasting regimens.

Collectively, fasting regimens can alleviate immunosuppression by potentially increasing eosinophil, CD8+ T cells, and NK cells while decreasing MDSC cells (**Figure 1**). However, as fasting is a systemic response, it may alter immune populations not only in the mammary gland or tumor, but in circulation as well. Several studies have alluded to variations in cell number, immune cell production, and T cell priming in lymphoid organs upon fasting (Strissel et al., 2010; Shushimita et al., 2014; Buono and Longo, 2019; Nagai et al., 2019; Rangan et al., 2019). Upon 50% CR, CD8+, CD4+ T cells, Tregs, NK, and mature B cells decreased in WAT and spleen, yet CD8+ and CD4+ T cells were increased in bone marrow (Collins et al., 2019). This allows cells to preserve a state of energy conservation and allow for T cell priming by CXCR4-CXCL12 activity on CD4+ memory T cells. As the major function of $CD4^+$ memory T cells is immunosurveillance, memory T cell homing was associated with enhanced protection against infections and tumors (Collins et al., 2019). Similarly, another study revealed prolonged fasting (48-h) significantly deceased white blood cell and hemopoietic stem cell numbers. Refeeding after fasting increased the number and activity of hematopoietic progenitor populations, suggesting that refeeding can rejuvenate immune cells to weaken immunosuppression caused by chemotoxicity in a cancer context (Cheng et al., 2014). In a randomized study of 129 patients, subjecting HER2-negative early breast cancer patients to FMD and chemotherapy reduced disease progression and DNA damage in plasma T-lymphocytes (De Groot et al., 2020), thereby reducing hematological toxicity (De Groot et al., 2015). Altogether, these studies imply that fasting accelerates recovery after chemotoxicity in breast cancer through T cell priming and functioning of the bone marrow. Future research investigating changes in lymphoid populations within lymphoid organs, tumor, and in circulation upon fasting and refeeding could provide insight into how fasting changes the lymphoid immune response.

VASCULAR CELLS

With obesity, several pro-angiogenic factors are secreted from the microenvironment to induce a transient switch to activate angiogenesis. Activation of angiogenesis is critical to ensure a sufficient supply of nutrients and oxygen to cells for healthy expansion. However, a balance between pro-angiogenic and anti-angiogenic factors is necessary to prevent endothelial cell dysfunction (Herold and Kalucka, 2020). Obesity-related expansion of WAT is accompanied by endothelial dysfunction as there is an increase in the pro-angiogenic and pro-inflammatory stimulus. Maintaining an adequate supply while sustaining proper endothelial function is essential to prevent WAT inflammation,

fibrosis, and pockets of hypoxia, all of which contribute to unhealthy WAT and are hallmarks for mammary tumorigenesis.

A key pro-angiogenic molecule implicated in mammary gland expansion and tumorigenesis is Vascular Endothelial Growth Factor (VEGF). VEGF is known to regulate vascular permeability, angiogenesis, and the expansion of lymphatic vessels through lymphangiogenesis (Kim et al., 2017). Under basal conditions, overexpression of adipose-specific VEGF triggers angiogenesis and *browning* of inguinal mammary WAT (Elias et al., 2012; Sun et al., 2012; Sung et al., 2013). Intriguingly, transplanting this overexpressing adipose-VEGF tissue into diet-induced obese mice improved systemic metabolic benefits and reduced inflammation (Park et al., 2017). Notably, 24-h fasting significantly increases inguinal WAT-VEGF expression in overall tissue and adipocytes (Hua et al., 2021). In fact, metabolic benefits of IF such as WAT *browning,* and M2-like macrophage polarization have been shown to be mediated by adipose-VEGF expression. Whereas adipose-VEGF knockout mice are unable to gain metabolic benefits of IF, periodic expression of adipose-VEGF (i.e., IF-mimicking effect) is sufficient to induce IF metabolic improvements in non-fasted animals (Kim et al., 2017), highlighting the important role VEGF plays in promoting the healthy remodeling of obese WAT.

As upregulation of VEGF promotes healthy expansion of WAT, this same mechanism can promote growth and dissemination of solid tumors such as breast cancer. Unlike the formation of mature vessels under normal and obese conditions, intratumor vessels are irregular, disorganized, and leaky, leading to hypoxia and inefficient delivery of antitumor agents into tumor microenvironment (Yang et al., 2018). In contrast to obese conditions where it is beneficial to upregulate VEGF, in the tumor context VEGF is thought to aid in the proliferation and expansion of tumor. Silencing VEGF expression via small interfering RNA significantly reduced tumor growth and angiogenesis in breast cancer MCF-7 xenografted mice (Chen et al., 2017). As such, combining traditional chemotherapies with anti-VEGF therapies has been extensively investigated in many cancers. However, anti-VEGF therapy such as bevacizumab has largely failed to improve survival in breast cancer patients. In particular, obese breast cancer patients respond poorly to anti-VEGF therapy due to decreased sensitivity in the tumor (Incio et al., 2018). HFD feeding in breast cancer cell E0771 inoculated mice decreased anti-VEGF therapy efficacy from 50 to 28%. These obese tumors experienced hypovascularity, hypoxia, and increased abundance of cancer-associated adipocytes (Incio et al., 2018). Treatment of anti-VEGF therapy-induced cancer cell necrosis in adipocyte-poor regions while adipocyte-rich regions remained viable, attributed to increased pro-inflammatory molecule IL-6. Inhibiting IL-6 and VEGF increased functional vascular density, reduced hypoxia, attenuated infiltration of Tregs, decreased mammary tumor growth, and metastasis (Incio et al., 2018). Furthermore, combining anti-VEGF blockade with inhibition of IL-6 plus chemotherapeutic agent doxorubicin in obese mice delayed tumor progression similar to lean mice on VEGF blockade and doxorubicin. Inhibition of IL-6 did not further delay progression in lean animals, thereby suggesting that obesity promotes resistance to anti-VEGF therapy in breast cancer specifically by IL-6 (Incio et al., 2018). As subcutaneous IL-6 is known to decrease with fasting (Speaker et al., 2016), combining IF with anti-VEGF therapy could have a beneficial impact on tumor growth. Research examining the impact of IF could prove to be a powerful tool for anti-VEGF therapy effectiveness. As anti-VEGF therapy has shown poor clinical results in mitigating breast cancer, this insight is essential to understand the translatability of IF into a clinical setting.

In addition to VEGF, angiopoietin-like 4 (ANGPTL4) has been investigated in implanted E0071 mammary tumors. Knocking out or neutralizing ANGPTL4 in mice decreased obesity-induced angiogenesis and tumor growth (Kolb et al., 2019). As 24-h fasting in humans has been shown to increase mRNA and protein ANGPTL4 in mammary WAT (Ruppert et al., 2020), fasting may accelerate obesity-induced tumor angiogenesis. As a result, this could contribute to cancer cell survival through an ample supply of oxygen and nutrients. However, De Lorenzo et al. investigated the impact of 4T1 cell implantation into the mammary gland of BALB/c mice after 5 weeks of 40% CR. Along with CR decreasing tumor weight, metastasis, cell proliferation, and increasing apoptosis, CR mice also displayed significantly lower intratumor microvessel density than control counterparts. This significant decrease was attributed to decreased total vessel length and circulating serum VEGF levels, suggesting CR decreases tumor angiogenesis (De Lorenzo et al., 2011). Collectively, there is a lack of studies investigating the impact of IF in the tumor microenvironment on pro-angiogenic, anti-angiogenic factors, and overall vascular cells. As lymphangiogenesis is an integral process through which cancer cells metastasize, understanding the impact IF has on the vascular microenvironment will provide insight into cancer cell dissemination into local and distant organs. In-depth analysis of vascular markers and collective population will provide a better understanding of IF's potential to modulate the breast cancer vascular microenvironment.

MAMMARY EPITHELIAL CELLS AND CANCER STEM CELLS

A predominant population of the mammary gland are mammary epithelial cells. Remodeling of these cells initiates processes that are characteristic to the mammary gland during lactation and puberty (Olson et al., 2010). During these processes, mammary epithelial cells interact closely with neighboring adipocytes (Colleluori et al., 2021). As such, the mammary epithelial population is sensitive to nutritional conditions. Subjecting C57BL/6–60% HFD decreased basal/myoepithelial specific markers while increasing mammary epithelial progenitor activity and estrogen receptor expression, specifically in luminal cells. Interestingly, switching mice fed HFD for 15 weeks to control diet for a further 5 weeks, mimicking a weight loss regimen, reversed the observed epithelial cell changes. These results were recapitulated in human mammary tissue,

indicating that obesity can directly alter stem/progenitor epithelial populations (Chamberlin et al., 2017).

To investigate mammary epithelial gland structure alterations in response to obesity, Mustafi et al. subjected 4-week-old spontaneous tumor developing simian virus 40 large T antigen (SV40taG) mice to 60% HFD for 8 weeks. In addition to enhanced tumor progression, *ex vivo* MRI and histology demonstrated denser parenchyma, irregularly enlarged ducts, dilated blood vessels, increased WAT, and increased tumor invasion (Mustafi et al., 2017), showcasing HFD-induced mammary epithelial dysregulation. Indeed, dissociation of obese mammary tumor into single cells grown *in vitro* revealed increased proliferation rates and self-renewal capacity in an independent study. Growing these cancer stem cell-enriched populations on collagen-coated migration chambers showed increased invasiveness, increased expression of the mesenchymal marker N-cadherin, and higher cancer stem cell-associated genes *Sox2* and *Notch Receptor 2* (Hillers-Ziemer et al., 2020). Collectively, these studies suggest amplification of cancer stem cell activity, proliferation, and aggressiveness in response to obesity.

While obese conditions enhance mesenchymal marker expression, CR has importantly been shown to affect epithelial-to-mesenchymal transition in the mammary tumor. As a critical pathway involved in tumor invasion, growth, and metastasis, Dunlap et al. investigated the impact of CR focusing on two characterized cell types in the mammary tumor of transgenic MMTV-WNT-1 mice. Compared to epithelial cells (CD44 high/CD24 high), mesenchymal cells from MMTV-WNT-1(CD44 high/CD24 low) mice were tumor-initiating cells with greater tumorsphere-forming and migration abilities. Obese tumors from mice fed with 60% HFD prior to and after tumor implantation experienced upregulated mesenchymal cells and overall enhanced epithelial-to-mesenchymal transition characterized by markers such as *N-cadherin*, *Fibronectin*, transforming growth factor-β (*TGFβ*), *Snail,* and *Oct4.* On the other hand, 30% CR suppressed tumor progression, inhibited epithelial-to-mesenchymal transition and intratumoral adipocyte accumulation, implying that dietary interventions such as CR can modulate epithelial-mesenchymal-transition thereby affecting the progression of mammary tumors (Dunlap et al., 2012).

In addition to the influence nutritional conditions can have on epithelial cells, adipokines regulated by nutritional conditions such as leptin can impact the mammary gland and tumor microenvironment. Increased under obese conditions, leptin is associated with increased breast cancer risk and thereby serves as a potential biomarker for post-menopausal overweight/obese patients (Pan et al., 2018). Upregulation of leptin disrupts epithelial polarity and sensitizes non-cancer cells to proliferative stimuli to expand the stem cell/progenitor population, subsequently initiating early stages of malignancy (Tenvooren et al., 2019). Additionally, leptin promotes expression of epithelial-to-mesenchymal transcription factors, cancer stem cell activity, expression of metastatic *TGFβ1* pathway (Mishra et al., 2017; Olea-Flores et al., 2019), in part by activation of inflammasomes (Raut et al., 2019). As leptin is secreted by adipocytes within the breast tissue, leptin can alter the tumor microenvironment. Increased leptin due to obesity explains the increased risk of invasive/metastatic tumors and overall poor survival in obese breast cancer patients. Intriguingly, numerous studies have shown fasting significantly decreases leptin (Trepanowski et al., 2018; Al-Rawi et al., 2020) and increases adiponectin (Varady et al., 2010; Kim et al., 2017). Adipose-secreted cytokine adiponectin decreases breast cancer growth by the accumulation and activation of autophagosomes resulting in autophagic cell death in the mammary tumor (Chung et al., 2017). Currently, there lacks research examining the effect of fasting-related decreases in leptin and increases in adiponectin on mammary epithelial polarization, cancer stem cell activity, autophagy, invasion, and metastasis. This could enhance our knowledge and provide a potential explanation for the delayed onset observed in mammary tumor fasting studies.

DISCUSSION

In this review, we provided a detailed overview on of the effect of nutritional conditions such as obesity and fasting on ASCs, CAFs, immune cells, vascular cells, mammary epithelial, and cancer stem cells, all of which play an important role in the tumor microenvironment (**Figure 2**).

Studies have highlighted potential mechanisms responsible for modulating the tumor microenvironment in response to fasting. As immune surveillance is a critical component to killing cancer cells, most studies have examined the mechanism through which immune cell activity is modulated to enhance cytotoxicity. Ajona et al. demonstrated that the enhanced anti-tumor activity in response to fasting in combination with immune checkpoint blockade is attributed to decreased IGF-1 and IGF-1R in tumor cells. Subjecting mammary tumor-bearing mice to IGF-1R inhibitor and immune checkpoint blockade was sufficient to mimic the anti-tumor effect of fasting in lung cancer (Ajona et al., 2020). Furthermore, abolishing IGF-1 adequately mimicked prolonged fasting (48-h) and accelerated hematopoietic stem-cell protection and renewal following chemotherapy, thereby relieving immunosuppression (Cheng et al., 2014).

Although a reduction in IGF-1 is thought to be a leading candidate explaining fasting-induced tumor immunogenicity and improved therapeutic response, there are other possible mechanisms. Reduction in stress oxygenase enzyme Heme Oxygenase-1 by FMD increased immunogenicity via cytotoxic CD8+ T cells infiltration in mammary tumors and overall improved response to chemotherapy (Di Biase et al., 2016). On the other hand, FMD or fasting in HER2-negative breast cancer patients resulted in better mitigation of DNA damage in T-lymphocytes (De Groot et al., 2020). As immune cells are a key population responsible for anti-tumor activity, further research examining the mechanism behind fasting-induced immune cell changes are warranted.

Cancer cells and normal cells undergo differential stress resistance responses, and cancer cells are generally more sensitive to nutrient deprivation than normal cells (Raffaghello et al., 2008). Typically tumor cell survival is dependent on initiation of the "Warburg effect," a phenomenon where the

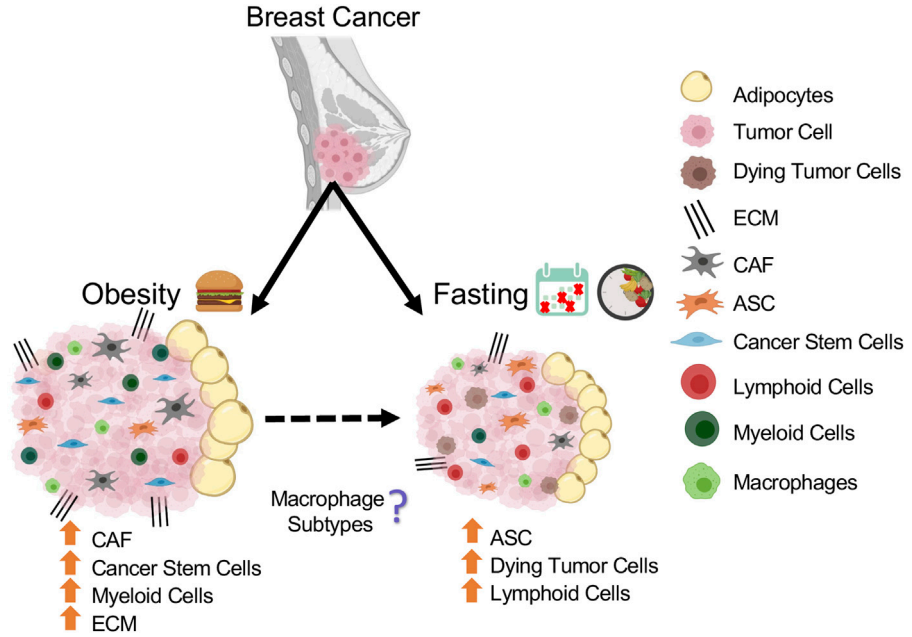

FIGURE 2 | Schematic summarizing the population changes in mammary tumor microenvironment in response to obesity and fasting conditions.

tumor cells experience high glucose uptake with lactate production under hypoxic conditions (Vander Heiden et al., 2009). This promotes ATP production through oxygen-independent pathways with reduced ROS-related DNA damage, contributing to chemoresistance (Zhou et al., 2010; Zhao et al., 2013). Bianchi et al. demonstrated that 48-h fasting promotes an anti-Warburg effect in colon cancer which drives glycolysis and oxidative phosphorylation to generate ROS and subsequent cancer cell apoptosis (Bianchi et al., 2015). This could explain the reported fasting-induced enhanced cancer cell sensitivity to chemotherapy and immunotherapy, which results in improved treatment response.

While the fasting effect has been investigated in the tumor immune cells, the impact fasting has on other cell populations in tumor is unknown. As discussed in this review, there are several potential mechanisms such as fasting-associated VEGF induction (Chen et al., 2017; Kim et al., 2017; Yang et al., 2018), AMPK activation (Kajita et al., 2008; Viscarra et al., 2011; Salminen et al., 2019), and downregulation of adipose-secreted leptin (Weigle et al., 1997; Pan et al., 2018) that can impact these individual populations. Since the tumor microenvironment is quite heterogeneous with various cell types, each population in the breast tissue plays an important role to contribute to disease pathogenesis. It is likely that a single mechanism is not responsible for modulating various cell populations in tumor microenvironment in response to fasting. Therefore, deepening our knowledge about how obesity and fasting can alter ASCs, CAFs, vascular cells, mammary epithelial, and cancer stem cells is essential to not only understand the microenvironmental transformation that undergoes with breast cancer, but also how to prevent it. Furthermore, expanding our understanding of possible mechanisms altering these populations could highlight novel targets that could be explored for cancer treatments.

Though not discussed in this review, a common effect that accompanies cancer progression is cancer cachexia. This occurs when cancer cells secrete factors that induce a hypermetabolic phenotype in adipose tissue and muscle tissue (Vazeille et al., 2017). As cancer patients commonly lose appetite, the hypermetabolic phenotype is often accompanied by inadequate caloric intake. This leads to drastic reductions in both lean and fat mass (Porporato, 2016). In fact, metastatic cancer patients with hypermetabolism associated with cancer cachexia exhibit reduced therapeutic response and survival (Vazeille et al., 2017; Baracos et al., 2018). As IF is known to increase resting energy expenditure and metabolic rate under non-tumorigenic conditions (Liu et al., 2019), it is possible that IF could have further adverse effects in metastatic cancer patients exhibiting cancer cachexia. Hence, studies in the future must closely examine the effect of IF on cancer cachexia.

Over recent years, new technologies have emerged to help provide a comprehensive detailed overview of tumor microenvironment interactions. Single-cell analyses such as high dimensional mass cytometry, known as CyTOF, utilize 40+ cell surface and intracellular markers to phenotypically and functionally characterize populations (Gadalla et al., 2019). Similarly, single-cell RNA or nuclei sequencing provides insight into the transcriptomic changes within each population in the microenvironment (Seow et al., 2020), also highlighting metabolic alterations (Xiao et al., 2019). Most recently, Jackson et al. revealed novel subgroups of breast cancer and associated cellular populations using single-cell analyses, highlighting the

TABLE 1 | Summary of the outcomes and limitations of all clinical trials discussed in this review examining the effect of fasting on cancer.

Study	Sample population	Tumor model	Fasting schedule	Outcome	Limitations
Marinac et al. (2016)	- 2,413 breast cancer patients - Age: 27–70 years - No diabetes mellitus	- Breast cancer	- Time Restricted Feeding - nightly fasting (~12.5 h/night)	- ↓ hemoglobin A_{1c} level - ↑ nightly fasting <13 h was associated with reduced breast cancer recurrence - ↑ sleep duration	- *ERBB2* status was not available for a large portion of sample population - Analyzed multiple primary endpoints for prognosis but did not control for multiple comparisons
De Groot et al. (2020)	- 129 patients with HER2-negative stage II/III breast cancer - No diabetes mellitus	- Breast Cancer	- FMD - 4-days of plant-based low amino-acid substitution diet followed by 3 days of ad libitum feeding	- ↓ DNA damage post chemotherapy - ↑ sensitization to chemotherapy (increase in % tumor cell loss) - ↑ response to radiological therapy	- ↓ compliance with each cycle of FMD - Participants in the control group fasted some days impacting FMD analysis
De Groot et al. (2015)	- 13 patients with HER2-negative stage II/III breast cancer - No diabetes mellitus - Age ≥18 years - Adequate bone marrow, renal, cardiac, and liver function	- Breast Cancer	- Short-term fasting - 6 cycles of fasting 24 h prior and after start of chemotherapy (only allowed water, tea or coffee with no sugar)	- ↑ recovery of chemotherapy-induced DNA damage and toxicity in healthy cells - Evidence of STF providing protection against chemotherapy-associated hematological toxicity - ↓ in plasma IGF-1 which mediates protective effects for healthy cells	- Small sample size (2 participants withdrew after 3 cycles of FMD) - High dose of dexamethasone was given during FMD cycles which can counteract the therapeutic effects of STF
Safdie et al. (2009)	- 10 patient case study (7 female, 3 male) - Median age: 61 years	- Breast (4), Prostate (2), Ovarian (1), Non-small cell carcinoma of the lung (1), Esophageal adenocarcinoma (1)	- Short-term fasting - varying hours between 40–140 h in total prior chemotherapy and 5–56 h post chemotherapy compared to patients who did not fast	- ↓ reports of nausea, vomiting, diarrhea, abdominal cramps, and mucositis compared to control group fed *ad libitum*	- Inconsistent fasting periods - Medical reports between participants were reviewed retrospectively (eg. demographic information, diagnosis, treatment, imaging and laboratory analysis)
Bauersfeld et al. (2018)	- 34 patients -Age ≥ 18 years -No diabetes mellitus -Anticipated life expectancy >3 months	-Gynecological cancer (breast or ovarian cancer)	- Short-term fasting - 36 h prior to chemotherapy and 24 h post treatment (total 60 fasting hours)	- ↑ Quality of life (QoL) for fasted patients compared to control and reduce fatigue during chemotherapy	- Small sample size - Cross-over study design may produce carry-over effects and bias - Study was conducted in Germany where there is a positive notion with the idea of fasting so participants may be biased to state that QoL has improved
Dorff et al. (2016)	- 20 patients - Median age: 61 years - 85% women	- Urothelial (bladder), ovarian or breast cancer	- Short-term fasting - 2 fasting cycles of each 24-h, 48-h and 72 h fasts consecutively compared to baseline measurements of participants	- ↑ hematopoietic protection with prolonged fasting periods - ↓ myelosuppression with fewer occurrences of neutropenia	- Confounding variables as not all participants are diagnosed with similar stage of cancer progression - Incomplete compliance of fast since they were allowed "rescue food" of 200 kcal per day

STF, Short-Term Fasting; FMD, Fasting-Mimicking Diet.

potential to use such techniques for targeted patient diagnosis and treatment (Jackson et al., 2020). These techniques have been used to investigate immune checkpoint blockade receptor expression on TIL (Beyrend et al., 2019), as well as to characterize and compare stromal cell heterogeneity between cancers (Qian et al., 2020). Future research utilizing these techniques will provide a unique opportunity to explore the tumor microenvironment in response to nutritional conditions such as obesity and fasting in an efficient and comprehensive manner (Jackson et al., 2020), with potential insight into each population.

Although many clinical studies have investigated the effect of fasting regimens in healthy, obese, and diabetic humans (Heilbronn et al., 2005; Harvie et al., 2011; Varady et al., 2013; Dorff et al., 2016; Gabel et al., 2018; Sutton et al., 2018; Hutchison et al., 2019; Lee et al., 2020; Wilkinson et al., 2020), there are few studies that have investigated the impact of fasting in cancer conditions. A 10-case series report examined the feasibility of fasting prior (48–140 h) and/or following chemotherapy (5–56 h) in cancer patients. Aside from hunger and light-headedness, no major side effects were reported. In fact, 6 patients reported a reduction in fatigue, weakness, and gastrointestinal side effects (Safdie et al., 2009). To further evaluate the quality of life in a randomized control study, Bauersfeld et al. conducted a trial where 34 ovarian and breast cancer patients were randomized to either a 60-h fasting duration (maximum 350 kcal), 36-h prior to chemotherapy and 24-h after chemotherapy, or control diet for the first 3 cycles of chemotherapy or second 3 cycles of chemotherapy. In addition to self-reported improved quality of life, decreased fatigue, and no major changes in weight, a greater benefit was observed with individuals subjected to fasting prior to chemotherapy in the first 3 cycles rather than later 3 cycles (Bauersfeld et al., 2018). Taken together, these studies suggest positive adherence and feasibility to fasting regimens in cancer patients.

In addition to the quality of life, a study of HER2-negative breast cancer patients with stage 2/3 breast cancer were randomized to 48-h fasting (24-h prior to and 24-h after chemotherapy) to evaluate chemotherapy-induced toxicity. Interestingly, erythrocyte and thrombocyte counts 1 week after chemotherapy were significantly greater in the fasted group, indicating reduced hematological toxicity and faster recovery of DNA damage (De Groot et al., 2015). Similarly, in an independent study, 48-h fasting prior to platinum-based chemotherapy or 72-h fasting (48-h prior to and 24-h after chemotherapy) resulted in decreased leukocyte DNA damage and a non-significant trend towards reduced neutropenia (Dorff et al., 2016). These studies are summarized in **Table 1**. Collectively, these studies suggest that fasting regimens in combination with current therapies are feasible and demonstrate positive benefits with mitigating toxicity.

Currently, there are many clinical trials undergoing to further examine the adherence, feasibility, and effectiveness of fasting in various cancers (Nencioni et al., 2018; U.S. National Library of Medicine, 2021). This research will shed light on whether fasting-associated benefits observed in preclinical models are translated into clinical settings, as well as the potential of fasting as a therapy. As the obesity epidemic increases worldwide, the global cancer burden is also expected to increase (Sung et al., 2021). Since fasting is a tangible, zero-cost, non-toxic, and easily applicable regimen, investigating the potential of fasting in the cancer setting is of significant value as current therapies are insufficient. Overall, this review provided a comprehensive overview of the current literature exploring obesity as well as fasting, with an emphasis on the mammary gland tissue and the development of breast cancer. As breast cancer is the most commonly diagnosed cancer (Sung et al., 2021), understanding how fasting regimens influence the mammary tumor microenvironment will provide insight into the mechanisms behind fasting-induced tumor benefits and can provide novel fasting-mimetics that can be easily translated in clinical settings.

AUTHOR CONTRIBUTIONS

NT, YS, and H-KS conceived and designed the research. All authors agreed to the final version of the manuscript.

FUNDING

This research was funded by the Canadian Institute of Health Research (CIHR, PJT-162083) of Canada, Natural Sciences and Engineering Research Council (NSERC, RGPIN-2016-06610) of Canada, Sun Life Financial New Investigator Award and Reuben and Helene Dennis Scholar Award of Banting and Best Diabetic Centre (BBDC), University of Toronto. NT is supported by SickKids Restracomp Scholarship.

REFERENCES

Ajona, D., Ortiz-Espinosa, S., Lozano, T., Exposito, F., Calvo, A., Valencia, K., et al. (2020). Short-term Starvation Reduces IGF-1 Levels to Sensitize Lung Tumors to PD-1 Immune Checkpoint Blockade. *Nat. Cancer* 1, 75–85. doi:10.1038/s43018-019-0007-9

Al-Rawi, N., Madkour, M., Jahrami, H., Salahat, D., Alhasan, F., Bahammam, A., et al. (2020). Effect of Diurnal Intermittent Fasting during Ramadan on Ghrelin, Leptin, Melatonin, and Cortisol Levels Among Overweight and Obese Subjects: A Prospective Observational Study. *PLoS One* 15, e0237922. doi:10.1371/journal.pone.0237922

Almeneessier, A. S., Pandi-Perumal, S. R., and Bahammam, A. S. (2018). Intermittent Fasting, Insufficient Sleep, and Circadian Rhythm: Interaction and Effects on the Cardiometabolic System. *Curr. Sleep Med. Rep* 4, 179–195. doi:10.1007/s40675-018-0124-5

Baracos, V. E., Martin, L., Korc, M., Guttridge, D. C., and Fearon, K. C. H. (2018). Cancer-associated Cachexia. *Nat. Rev. Dis. Primers* 4, 17105. doi:10.1038/nrdp.2017.105

Bauersfeld, S. P., Kessler, C. S., Wischnewsky, M., Jaensch, A., Steckhan, N., Stange, R., et al. (2018). The Effects of Short-Term Fasting on Quality of Life and Tolerance to Chemotherapy in Patients with Breast and Ovarian Cancer: a Randomized Cross-Over Pilot Study. *BMC Cancer* 18, 476. doi:10.1186/s12885-018-4353-2

Beyrend, G., Van Der Gracht, E., Yilmaz, A., Van Duikeren, S., Camps, M., Höllt, T., et al. (2019). PD-L1 Blockade Engages Tumor-Infiltrating Lymphocytes to Co-express Targetable Activating and Inhibitory Receptors. *J. Immunotherapy Cancer* 7, 217. doi:10.1186/s40425-019-0700-3

Bianchi, G., Martella, R., Ravera, S., Marini, C., Capitanio, S., Orengo, A., et al. (2015). Fasting Induces Anti-warburg Effect that Increases Respiration but Reduces ATP-Synthesis to Promote Apoptosis in colon Cancer Models. *Oncotarget* 6, 11806–11819. doi:10.18632/oncotarget.3688

Bochet, L., Lehuédé, C., Dauvillier, S., Wang, Y. Y., Dirat, B., Laurent, V., et al. (2013). Adipocyte-derived Fibroblasts Promote Tumor Progression and Contribute to the Desmoplastic Reaction in Breast Cancer. *Cancer Res.* 73, 5657–5668. doi:10.1158/0008-5472.CAN-13-0530

Buono, R., and Longo, V. D. (2018). Starvation, Stress Resistance, and Cancer. *Trends Endocrinol. Metab.* 29, 271–280. doi:10.1016/j.tem.2018.01.008

Buono, R., and Longo, V. D. (2019). When Fasting Gets Tough, the Tough Immune Cells Get Going-Or Die. *Cell* 178, 1038–1040. doi:10.1016/j.cell.2019.07.052

Carter, J. M., Hoskin, T. L., Pena, M. A., Brahmbhatt, R., Winham, S. J., Frost, M. H., et al. (2018). Macrophagic "Crown-like Structures" Are Associated with an Increased Risk of Breast Cancer in Benign Breast Disease. *Cancer Prev. Res.* 11, 113–119. doi:10.1158/1940-6207.CAPR-17-0245

Casteilla, L., Planat-Benard, V., Laharrague, P., and Cousin, B. (2011). Adipose-derived Stromal Cells: Their Identity and Uses in Clinical Trials, an Update. *Wjsc* 3, 25–33. doi:10.4252/wjsc.v3.i4.25

Castoldi, A., Naffah De Souza, C., Câmara, N. O. S., and Moraes-Vieira, P. M. (2015). The Macrophage Switch in Obesity Development. *Front. Immunol.* 6, 637. doi:10.3389/fimmu.2015.00637

Catterson, J. H., Khericha, M., Dyson, M. C., Vincent, A. J., Callard, R., Haveron, S. M., et al. (2018). Short-Term, Intermittent Fasting Induces Long-Lasting Gut Health and TOR-independent Lifespan Extension. *Curr. Biol.* 28, 1714–1724. e1714. doi:10.1016/j.cub.2018.04.015

Chamberlin, T., D'Amato, J. V., and Arendt, L. M. (2017). Obesity Reversibly Depletes the Basal Cell Population and Enhances Mammary Epithelial Cell Estrogen Receptor Alpha Expression and Progenitor Activity. *Breast Cancer Res.* 19, 128. doi:10.1186/s13058-017-0921-7

ChÃ¡vez-GalÃ¡n, L., Olleros, M. L., Vesin, D., and Garcia, I. (2015). Much More Than M1 and M2 Macrophages, There Are Also CD169+ and TCR+ Macrophages. *Front. Immunol.* 6, 263. doi:10.3389/fimmu.2015.00263

Chen, J., Sun, X., Shao, R., Xu, Y., Gao, J.-q., and Liang, W.-q. (2017). VEGF siRNA Delivered by Polycation Liposome-Encapsulated Calcium Phosphate Nanoparticles for Tumor Angiogenesis Inhibition in Breast Cancer. *Ijn* 12, 6075–6088. doi:10.2147/IJN.S142739

Cheng, C.-W., Adams, G. B., Perin, L., Wei, M., Zhou, X., Lam, B. S., et al. (2014). Prolonged Fasting Reduces IGF-1/PKA to Promote Hematopoietic-Stem-Cell-Based Regeneration and Reverse Immunosuppression. *Cell Stem Cell* 14, 810–823. doi:10.1016/j.stem.2014.04.014

Cho, Y., Hong, N., Kim, K.-w., Cho, S., Lee, M., Lee, Y.-h., et al. (2019). The Effectiveness of Intermittent Fasting to Reduce Body Mass Index and Glucose Metabolism: A Systematic Review and Meta-Analysis. *Jcm* 8, 1645. doi:10.3390/jcm8101645

Chung, S. J., Nagaraju, G. P., Nagalingam, A., Muniraj, N., Kuppusamy, P., Walker, A., et al. (2017). ADIPOQ/adiponectin Induces Cytotoxic Autophagy in Breast Cancer Cells through STK11/LKB1-Mediated Activation of the AMPK-ULK1 axis. *Autophagy* 13, 1386–1403. doi:10.1080/15548627.2017.1332565

Clements, V. K., Long, T., Long, R., Figley, C., Smith, D. M. C., and Ostrand-Rosenberg, S. (2018). Frontline Science: High Fat Diet and Leptin Promote Tumor Progression by Inducing Myeloid-Derived Suppressor Cells. *J. Leukoc. Biol.* 103, 395–407. doi:10.1002/JLB.4HI0517-210R

Coats, B. R., Schoenfelt, K. Q., Barbosa-Lorenzi, V. C., Peris, E., Cui, C., Hoffman, A., et al. (2017). Metabolically Activated Adipose Tissue Macrophages Perform Detrimental and Beneficial Functions during Diet-Induced Obesity. *Cel Rep.* 20, 3149–3161. doi:10.1016/j.celrep.2017.08.096

Colleluori, G., Perugini, J., Barbatelli, G., and Cinti, S. (2021). Mammary Gland Adipocytes in Lactation Cycle, Obesity and Breast Cancer. *Rev. Endocr. Metab. Disord.* 22, 241–255. doi:10.1007/s11154-021-09633-5

Collins, N., Han, S.-J., Enamorado, M., Link, V. M., Huang, B., Moseman, E. A., et al. (2019). The Bone Marrow Protects and Optimizes Immunological Memory during Dietary Restriction. *Cell* 178, 1088–1101. e1015. doi:10.1016/j.cell.2019.07.049

Dang, V. T. A., Tanabe, K., Tanaka, Y., Tokumoto, N., Misumi, T., Saeki, Y., et al. (2014). Fasting Enhances TRAIL-Mediated Liver Natural Killer Cell Activity via HSP70 Upregulation. *PLoS One* 9, e110748. doi:10.1371/journal.pone.0110748

De Groot, S., Lugtenberg, R. T., Cohen, D., Welters, M. J. P., Ehsan, I., Vreeswijk, M. P. G., et al. (2020). Fasting Mimicking Diet as an Adjunct to Neoadjuvant Chemotherapy for Breast Cancer in the Multicentre Randomized Phase 2 DIRECT Trial. *Nat. Commun.* 11, 3083. doi:10.1038/s41467-020-16138-3

De Groot, S., Vreeswijk, M. P., Welters, M. J., Gravesteijn, G., Boei, J. J., Jochems, A., et al. (2015). The Effects of Short-Term Fasting on Tolerance to (Neo) Adjuvant Chemotherapy in HER2-Negative Breast Cancer Patients: a Randomized Pilot Study. *BMC Cancer* 15, 652. doi:10.1186/s12885-015-1663-5

De La Cruz Bonilla, M., Stemler, K. M., Jeter-Jones, S., Fujimoto, T. N., Molkentine, J., Asencio Torres, G. M., et al. (2019). Fasting Reduces Intestinal Radiotoxicity, Enabling Dose-Escalated Radiation Therapy for Pancreatic Cancer. *Int. J. Radiat. Oncology*Biology*Physics* 105, 537–547. doi:10.1016/j.ijrobp.2019.06.2533

De Lorenzo, M. S., Baljinnyam, E., Vatner, D. E., Abarzua, P., Vatner, S. F., and Rabson, A. B. (2011). Caloric Restriction Reduces Growth of Mammary Tumors and Metastases. *Carcinogenesis* 32, 1381–1387. doi:10.1093/carcin/bgr107

Divella, R., De Luca, R., Abbate, I., Naglieri, E., and Daniele, A. (2016). Obesity and Cancer: the Role of Adipose Tissue and Adipo-Cytokines-Induced Chronic Inflammation. *J. Cancer* 7, 2346–2359. doi:10.7150/jca.16884

Di Biase, S., Lee, C., Brandhorst, S., Manes, B., Buono, R., Cheng, C.-W., et al. (2016). Fasting-Mimicking Diet Reduces HO-1 to Promote T Cell-Mediated Tumor Cytotoxicity. *Cancer Cell* 30, 136–146. doi:10.1016/j.ccell.2016.06.005

Dorff, T. B., Groshen, S., Garcia, A., Shah, M., Tsao-Wei, D., Pham, H., et al. (2016). Safety and Feasibility of Fasting in Combination with Platinum-Based Chemotherapy. *BMC Cancer* 16, 360. doi:10.1186/s12885-016-2370-6

Dunlap, S. M., Chiao, L. J., Nogueira, L., Usary, J., Perou, C. M., Varticovski, L., et al. (2012). Dietary Energy Balance Modulates Epithelial-To-Mesenchymal Transition and Tumor Progression in Murine Claudin-Low and Basal-like Mammary Tumor Models. *Cancer Prev. Res.* 5, 930–942. doi:10.1158/1940-6207.CAPR-12-0034

Ecker, B. L., Lee, J. Y., Sterner, C. J., Solomon, A. C., Pant, D. K., Shen, F., et al. (2019). Impact of Obesity on Breast Cancer Recurrence and Minimal Residual Disease. *Breast Cancer Res.* 21, 41. doi:10.1186/s13058-018-1087-7

Elias, I., Franckhauser, S., Ferré, T., Vilà, L., Tafuro, S., Muñoz, S., et al. (2012). Adipose Tissue Overexpression of Vascular Endothelial Growth Factor Protects against Diet-Induced Obesity and Insulin Resistance. *Diabetes* 61, 1801–1813. doi:10.2337/db11-0832

Fabbiano, S., Suárez-Zamorano, N., Rigo, D., Veyrat-Durebex, C., Stevanovic Dokic, A., Colin, D. J., et al. (2016). Caloric Restriction Leads to Browning of White Adipose Tissue through Type 2 Immune Signaling. *Cel Metab.* 24, 434–446. doi:10.1016/j.cmet.2016.07.023

Faria, S. S., Corrêa, L. H., Heyn, G. S., De Sant'ana, L. P., Almeida, R. d. N., and Magalhães, K. G. (2020). Obesity and Breast Cancer: The Role of Crown-Like Structures in Breast Adipose Tissue in Tumor Progression, Prognosis, and Therapy. *J. Breast Cancer* 23, 233–245. doi:10.4048/jbc.2020.23.e35

Gabel, K., Hoddy, K. K., Haggerty, N., Song, J., Kroeger, C. M., Trepanowski, J. F., et al. (2018). Effects of 8-hour Time Restricted Feeding on Body Weight and Metabolic Disease Risk Factors in Obese Adults: A Pilot Study. *Nha* 4, 345–353. doi:10.3233/NHA-170036

Gadalla, R., Noamani, B., Macleod, B. L., Dickson, R. J., Guo, M., Xu, W., et al. (2019). Validation of CyTOF against Flow Cytometry for Immunological Studies and Monitoring of Human Cancer Clinical Trials. *Front. Oncol.* 9, 415. doi:10.3389/fonc.2019.00415

Goodman, M., Liu, Z., Zhu, P., and Li, J. (2014). AMPK Activators as a Drug for Diabetes, Cancer and Cardiovascular Disease. *Pharmaceut Reg. Aff.* 03. doi:10.4172/2167-7689.1000118

Hao, J., Zhang, Y., Yan, X., Yan, F., Sun, Y., Zeng, J., et al. (2018). Circulating Adipose Fatty Acid Binding Protein Is a New Link Underlying Obesity-Associated Breast/Mammary Tumor Development. *Cel Metab.* 28, 689–705. doi:10.1016/j.cmet.2018.07.006

Harvie, M. N., Pegington, M., Mattson, M. P., Frystyk, J., Dillon, B., Evans, G., et al. (2011). The Effects of Intermittent or Continuous Energy Restriction on Weight Loss and Metabolic Disease Risk Markers: a Randomized Trial in Young Overweight Women. *Int. J. Obes.* 35, 714–727. doi:10.1038/ijo.2010.171

Heilbronn, L. K., Smith, S. R., Martin, C. K., Anton, S. D., and Ravussin, E. (2005). Alternate-day Fasting in Nonobese Subjects: Effects on Body Weight, Body Composition, and Energy Metabolism. *Am. J. Clin. Nutr.* 81, 69–73. doi:10.1093/ajcn/81.1.69

Herold, J., and Kalucka, J. (2020). Angiogenesis in Adipose Tissue: The Interplay between Adipose and Endothelial Cells. *Front. Physiol.* 11, 624903. doi:10.3389/fphys.2020.624903

Hillers, L. E., D'amato, J. V., Chamberlin, T., Paderta, G., and Arendt, L. M. (2018). Obesity-Activated Adipose-Derived Stromal Cells Promote Breast Cancer Growth and Invasion. *Neoplasia* 20, 1161–1174. doi:10.1016/j.neo.2018.09.004

Hillers-Ziemer, L. E., Mcmahon, R. Q., Hietpas, M., Paderta, G., Lebeau, J., Mccready, J., et al. (2020). Obesity Promotes Cooperation of Cancer Stem-like Cells and Macrophages to Enhance Mammary Tumor Angiogenesis. *Cancers* 12, 502. doi:10.3390/cancers12020502

Hsia, L.-t., Ashley, N., Ouaret, D., Wang, L. M., Wilding, J., and Bodmer, W. F. (2016). Myofibroblasts Are Distinguished from Activated Skin Fibroblasts by the Expression of AOC3 and Other Associated Markers. *Proc. Natl. Acad. Sci. USA* 113, E2162–E2171. doi:10.1073/pnas.1603534113

Hua, L., Li, J., Feng, B., Jiang, D., Jiang, X., Luo, T., et al. (2021). Dietary Intake Regulates White Adipose Tissues Angiogenesis via Liver Fibroblast Growth Factor 21 in Male Mice. *Endocrinology* 162, bqaa244. doi:10.1210/endocr/bqaa244

Hutchison, A. T., Regmi, P., Manoogian, E. N. C., Fleischer, J. G., Wittert, G. A., Panda, S., et al. (2019). Time-Restricted Feeding Improves Glucose Tolerance in Men at Risk for Type 2 Diabetes: A Randomized Crossover Trial. *Obesity* 27, 724–732. doi:10.1002/oby.22449

Incio, J., Ligibel, J. A., Mcmanus, D. T., Suboj, P., Jung, K., Kawaguchi, K., et al. (2018). Obesity Promotes Resistance to Anti-VEGF Therapy in Breast Cancer by Up-Regulating IL-6 and Potentially FGF-2. *Sci. Transl. Med.* 10, eaag0945. doi:10.1126/scitranslmed.aag0945

Inoue, S.-i., Takahashi, K., Okumura-Noda, H., and Kinoshita, T. (2016). Auxin Influx Carrier AUX1 Confers Acid Resistance for Arabidopsis Root Elongation through the Regulation of Plasma Membrane H+-ATPase. *Plant Cel Physiol* 57, 2194–2201. doi:10.1093/pcp/pcw136

Jackson, H. W., Fischer, J. R., Zanotelli, V. R. T., Ali, H. R., Mechera, R., Soysal, S. D., et al. (2020). The Single-Cell Pathology Landscape of Breast Cancer. *Nature* 578, 615–620. doi:10.1038/s41586-019-1876-x

Jeong, H., Hwang, I., Kang, S. H., Shin, H. C., and Kwon, S. Y. (2019). Tumor-Associated Macrophages as Potential Prognostic Biomarkers of Invasive Breast Cancer. *J. Breast Cancer* 22, 38–51. doi:10.4048/jbc.2019.22.e5

Ji, Y., Sun, S., Xia, S., Yang, L., Li, X., and Qi, L. (2012). Short Term High Fat Diet challenge Promotes Alternative Macrophage Polarization in Adipose Tissue via Natural Killer T Cells and Interleukin-4. *J. Biol. Chem.* 287, 24378–24386. doi:10.1074/jbc.M112.371807

Kado, T., Nawaz, A., Takikawa, A., Usui, I., and Tobe, K. (2019). Linkage of CD8+ T Cell Exhaustion with High-Fat Diet-Induced Tumourigenesis. *Sci. Rep.* 9, 12284. doi:10.1038/s41598-019-48678-0

Kahounová, Z., Kurfürstová, D., Bouchal, J., Kharaishvili, G., Navrátil, J., Remšík, J., et al. (2018). The Fibroblast Surface Markers FAP, Anti-fibroblast, and FSP Are Expressed by Cells of Epithelial Origin and May Be Altered during Epithelial-To-Mesenchymal Transition. *Cytometry* 93, 941–951. doi:10.1002/cyto.a.23101

Kajita, K., Mune, T., Ikeda, T., Matsumoto, M., Uno, Y., Sugiyama, C., et al. (2008). Effect of Fasting on PPARγ and AMPK Activity in Adipocytes. *Diabetes Res. Clin. Pract.* 81, 144–149. doi:10.1016/j.diabres.2008.05.003

Karagiannides, I., Thomou, T., Tchkonia, T., Pirtskhalava, T., Kypreos, K. E., Cartwright, A., et al. (2006). Increased CUG Triplet Repeat-Binding Protein-1 Predisposes to Impaired Adipogenesis with Aging. *J. Biol. Chem.* 281, 23025–23033. doi:10.1074/jbc.M513187200

Kim, K.-H., Kim, Y. H., Son, J. E., Lee, J. H., Kim, S., Choe, M. S., et al. (2017). Intermittent Fasting Promotes Adipose Thermogenesis and Metabolic Homeostasis via VEGF-Mediated Alternative Activation of Macrophage. *Cell Res* 27, 1309–1326. doi:10.1038/cr.2017.126

Kim, Y. H., Lee, J. H., Yeung, J. L.-H., Das, E., Kim, R. Y., Jiang, Y., et al. (2019). Thermogenesis-independent Metabolic Benefits Conferred by Isocaloric Intermittent Fasting in Ob/ob Mice. *Sci. Rep.* 9, 2479. doi:10.1038/s41598-019-39380-2

Klempel, M. C., Kroeger, C. M., and Varady, K. A. (2013). Alternate Day Fasting (ADF) with a High-Fat Diet Produces Similar Weight Loss and Cardio-protection as ADF with a Low-Fat Diet. *Metabolism* 62, 137–143. doi:10.1016/j.metabol.2012.07.002

Kolb, R., Kluz, P., Tan, Z. W., Borcherding, N., Bormann, N., Vishwakarma, A., et al. (2019). Obesity-associated Inflammation Promotes Angiogenesis and Breast Cancer via Angiopoietin-like 4. *Oncogene* 38, 2351–2363. doi:10.1038/s41388-018-0592-6

Kolb, R., and Zhang, W. (2020). Obesity and Breast Cancer: A Case of Inflamed Adipose Tissue. *Cancers* 12, 1686. doi:10.3390/cancers12061686

Lechner, S., Mitterberger, M. C., Mattesich, M., and Zwerschke, W. (2013). Role of C/EBPβ-LAP and C/EBPβ-LIP in Early Adipogenic Differentiation of Human white Adipose-Derived Progenitors and at Later Stages in Immature Adipocytes. *Differentiation* 85, 20–31. doi:10.1016/j.diff.2012.11.001

Lee, B.-C., Kim, M.-S., Pae, M., Yamamoto, Y., Eberlé, D., Shimada, T., et al. (2016). Adipose Natural Killer Cells Regulate Adipose Tissue Macrophages to Promote Insulin Resistance in Obesity. *Cel Metab.* 23, 685–698. doi:10.1016/j.cmet.2016.03.002

Lee, C., Raffaghello, L., Brandhorst, S., Safdie, F. M., Bianchi, G., Martin-Montalvo, A., et al. (2012). Fasting Cycles Retard Growth of Tumors and Sensitize a Range of Cancer Cell Types to Chemotherapy. *Sci. Transl. Med.* 4, 124ra127. doi:10.1126/scitranslmed.3003293

Lee, J. H., Verma, N., Thakkar, N., Yeung, C., and Sung, H.-K. (2020). Intermittent Fasting: Physiological Implications on Outcomes in Mice and Men. *Physiology* 35, 185–195. doi:10.1152/physiol.00030.2019

Lee, K.-H., Hsu, E.-C., Guh, J.-H., Yang, H.-C., Wang, D., Kulp, S. K., et al. (2011). Targeting Energy Metabolic and Oncogenic Signaling Pathways in Triple-Negative Breast Cancer by a Novel Adenosine Monophosphate-Activated Protein Kinase (AMPK) Activator. *J. Biol. Chem.* 286, 39247–39258. doi:10.1074/jbc.M111.264598

Li, G., Xie, C., Lu, S., Nichols, R. G., Tian, Y., Li, L., et al. (2017). Intermittent Fasting Promotes White Adipose Browning and Decreases Obesity by Shaping the Gut Microbiota. *Cel Metab.* 26, 672–685. doi:10.1016/j.cmet.2017.08.019

Lin, Y., and Li, Q. (2007). Expression and Function of Leptin and its Receptor in Mouse Mammary Gland. *Sci. China Ser. C* 50, 669–675. doi:10.1007/s11427-007-0077-2

Liu, B., Page, A. J., Hutchison, A. T., Wittert, G. A., and Heilbronn, L. K. (2019). Intermittent Fasting Increases Energy Expenditure and Promotes Adipose Tissue browning in Mice. *Nutrition* 66, 38–43. doi:10.1016/j.nut.2019.03.015

Lumeng, C. N., Bodzin, J. L., and Saltiel, A. R. (2007). Obesity Induces a Phenotypic Switch in Adipose Tissue Macrophage Polarization. *J. Clin. Invest.* 117, 175–184. doi:10.1172/JCI29881

Mao, T., Wei, Q., Zhao, F., and Zhang, C. (2021). Short-term Fasting Reshapes Fat Tissue. *Endocr. J.* 68, 387–398. doi:10.1507/endocrj.EJ20-0405

Marinac, C. R., Natarajan, L., Sears, D. D., Gallo, L. C., Hartman, S. J., Arredondo, E., et al. (2015a). Prolonged Nightly Fasting and Breast Cancer Risk: Findings from NHANES (2009-2010). *Cancer Epidemiol. Biomarkers Prev.* 24, 783–789. doi:10.1158/1055-9965.EPI-14-1292

Marinac, C. R., Nelson, S. H., Breen, C. I., Hartman, S. J., Natarajan, L., Pierce, J. P., et al. (2016). Prolonged Nightly Fasting and Breast Cancer Prognosis. *JAMA Oncol.* 2, 1049–1055. doi:10.1001/jamaoncol.2016.0164

Marinac, C. R., Sears, D. D., Natarajan, L., Gallo, L. C., Breen, C. I., and Patterson, R. E. (2015b). Frequency and Circadian Timing of Eating May Influence Biomarkers of Inflammation and Insulin Resistance Associated with Breast Cancer Risk. *PLoS One* 10, e0136240. doi:10.1371/journal.pone.0136240

Martens, A., Wistuba-Hamprecht, K., Foppen, M. G., Yuan, J., Postow, M. A., Wong, P., et al. (2016). Baseline Peripheral Blood Biomarkers Associated with Clinical Outcome of Advanced Melanoma Patients Treated with Ipilimumab. *Clin. Cancer Res.* 22, 2908–2918. doi:10.1158/1078-0432.CCR-15-2412

Mishra, A. K., Parish, C. R., Wong, M.-L., Licinio, J., and Blackburn, A. C. (2017). Leptin Signals via TGFB1 to Promote Metastatic Potential and Stemness in Breast Cancer. *PLoS One* 12, e0178454. doi:10.1371/journal.pone.0178454

Moro, T., Tinsley, G., Bianco, A., Marcolin, G., Pacelli, Q. F., Battaglia, G., et al. (2016). Effects of Eight Weeks of Time-Restricted Feeding (16/8) on Basal Metabolism, Maximal Strength, Body Composition, Inflammation, and Cardiovascular Risk Factors in Resistance-Trained Males. *J. Transl Med.* 14, 290. doi:10.1186/s12967-016-1044-0

Munsell, M. F., Sprague, B. L., Berry, D. A., Chisholm, G., and Trentham-Dietz, A. (2014). Body Mass index and Breast Cancer Risk According to Postmenopausal Estrogen-Progestin Use and Hormone Receptor Status. *Epidemiol. Rev.* 36, 114–136. doi:10.1093/epirev/mxt010

Mustafi, D., Fernandez, S., Markiewicz, E., Fan, X., Zamora, M., Mueller, J., et al. (2017). MRI Reveals Increased Tumorigenesis Following High Fat Feeding in a Mouse Model of Triple-Negative Breast Cancer. *NMR Biomed.* 30, e3758. doi:10.1002/nbm.3758

Nagai, M., Noguchi, R., Takahashi, D., Morikawa, T., Koshida, K., Komiyama, S., et al. (2019). Fasting-Refeeding Impacts Immune Cell Dynamics and Mucosal Immune Responses. *Cell* 178, 1072–1087. e1014. doi:10.1016/j.cell.2019.07.047

Narita, T., Kobayashi, M., Itakura, K., Itagawa, R., Kabaya, R., Sudo, Y., et al. (2018). Differential Response to Caloric Restriction of Retroperitoneal, Epididymal, and Subcutaneous Adipose Tissue Depots in Rats. *Exp. Gerontol.* 104, 127–137. doi:10.1016/j.exger.2018.01.016

Nencioni, A., Caffa, I., Cortellino, S., and Longo, V. D. (2018). Fasting and Cancer: Molecular Mechanisms and Clinical Application. *Nat. Rev. Cancer* 18, 707–719. doi:10.1038/s41568-018-0061-0

Novak, M. L., and Koh, T. J. (2013). Macrophage Phenotypes during Tissue Repair. *J. Leukoc. Biol.* 93, 875–881. doi:10.1189/jlb.1012512

Ohmura, K., Ishimori, N., Ohmura, Y., Tokuhara, S., Nozawa, A., Horii, S., et al. (2010). Natural Killer T Cells Are Involved in Adipose Tissues Inflammation and Glucose Intolerance in Diet-Induced Obese Mice. *Atvb* 30, 193–199. doi:10.1161/ATVBAHA.109.198614

Olea-Flores, M., Zuñiga-Eulogio, M., Tacuba-Saavedra, A., Bueno-Salgado, M., Sánchez-Carvajal, A., Vargas-Santiago, Y., et al. (2019). Leptin Promotes Expression of EMT-Related Transcription Factors and Invasion in a Src and FAK-dependent Pathway in MCF10A Mammary Epithelial Cells. *Cells* 8, 1133. doi:10.3390/cells8101133

Olson, L. K., Tan, Y., Zhao, Y., Aupperlee, M. D., and Haslam, S. Z. (2010). Pubertal Exposure to High Fat Diet Causes Mouse Strain-dependent Alterations in Mammary Gland Development and Estrogen Responsiveness. *Int. J. Obes.* 34, 1415–1426. doi:10.1038/ijo.2010.51

Onesti, C. E., Josse, C., Boulet, D., Thiry, J., Beaumecker, B., Bours, V., et al. (2020). The Relative Eosinophil Count in Breast Cancer as an Emerging Prognostic Biomarker. *Eur. J. Cancer* 138, 1761176. doi:10.1016/S0959-8049(20)30766-8

Pajares, B., Pollán, M., Martín, M., Mackey, J. R., Lluch, A., Gavila, J., et al. (2013). Obesity and Survival in Operable Breast Cancer Patients Treated with Adjuvant Anthracyclines and Taxanes According to Pathological Subtypes: a Pooled Analysis. *Breast Cancer Res.* 15, R105. doi:10.1186/bcr3572

Pan, H., Deng, L.-L., Cui, J.-Q., Shi, L., Yang, Y.-C., Luo, J.-H., et al. (2018). Association between Serum Leptin Levels and Breast Cancer Risk. *Medicine (Baltimore)* 97, e11345. doi:10.1097/MD.0000000000011345

Park, C. C., Bissell, M. J., and Barcellos-Hoff, M. H. (2000). The Influence of the Microenvironment on the Malignant Phenotype. *Mol. Med. Today* 6, 324–329. doi:10.1016/s1357-4310(00)01756-1

Park, J., Kim, M., Sun, K., An, Y. A., Gu, X., and Scherer, P. E. (2017). VEGF-A-Expressing Adipose Tissue Shows Rapid Beiging and Enhanced Survival after Transplantation and Confers IL-4-Independent Metabolic Improvements. *Diabetes* 66, 1479–1490. doi:10.2337/db16-1081

Porporato, P. E. (2016). Understanding Cachexia as a Cancer Metabolism Syndrome. *Oncogenesis* 5, e200. doi:10.1038/oncsis.2016.3

Qian, J., Olbrecht, S., Boeckx, B., Vos, H., Laoui, D., Etlioglu, E., et al. (2020). A Pan-Cancer Blueprint of the Heterogeneous Tumor Microenvironment Revealed by Single-Cell Profiling. *Cel Res* 30, 745–762. doi:10.1038/s41422-020-0355-0

Quail, D. F., and Dannenberg, A. J. (2019). The Obese Adipose Tissue Microenvironment in Cancer Development and Progression. *Nat. Rev. Endocrinol.* 15, 139–154. doi:10.1038/s41574-018-0126-x

Raffaghello, L., Lee, C., Safdie, F. M., Wei, M., Madia, F., Bianchi, G., et al. (2008). Starvation-dependent Differential Stress Resistance Protects normal but Not Cancer Cells against High-Dose Chemotherapy. *Proc. Natl. Acad. Sci.* 105, 8215–8220. doi:10.1073/pnas.0708100105

Ramamonjisoa, N., and Ackerstaff, E. (2017). Characterization of the Tumor Microenvironment and Tumor-Stroma Interaction by Non-invasive Preclinical Imaging. *Front. Oncol.* 7, 3. doi:10.3389/fonc.2017.00003

Rangan, P., Choi, I., Wei, M., Navarrete, G., Guen, E., Brandhorst, S., et al. (2019). Fasting-Mimicking Diet Modulates Microbiota and Promotes Intestinal Regeneration to Reduce Inflammatory Bowel Disease Pathology. *Cel Rep.* 26, 2704–2719. e2706. doi:10.1016/j.celrep.2019.02.019

Raut, P. K., Kim, S.-H., Choi, D. Y., Jeong, G.-S., and Park, P.-H. (2019). Growth of Breast Cancer Cells by Leptin Is Mediated via Activation of the Inflammasome: Critical Roles of Estrogen Receptor Signaling and Reactive Oxygen Species Production. *Biochem. Pharmacol.* 161, 73–88. doi:10.1016/j.bcp.2019.01.006

Revelo, X. S., Luck, H., Winer, S., and Winer, D. A. (2014). Morphological and Inflammatory Changes in Visceral Adipose Tissue during Obesity. *Endocr. Pathol.* 25, 93–101. doi:10.1007/s12022-013-9288-1

Ringel, A. E., Drijvers, J. M., Baker, G. J., Catozzi, A., García-Cañaveras, J. C., Gassaway, B. M., et al. (2020). Obesity Shapes Metabolism in the Tumor Microenvironment to Suppress Anti-tumor Immunity. *Cell* 183, 1848–1866. doi:10.1016/j.cell.2020.11.009

Ruiz-Ojeda, F. J., Méndez-Gutiérrez, A., Aguilera, C. M., and Plaza-Díaz, J. (2019). Extracellular Matrix Remodeling of Adipose Tissue in Obesity and Metabolic Diseases. *Ijms* 20, 4888. doi:10.3390/ijms20194888

Ruppert, P. M. M., Michielsen, C. C. J. R., Hazebroek, E. J., Pirayesh, A., Olivecrona, G., Afman, L. A., et al. (2020). Fasting Induces ANGPTL4 and Reduces LPL Activity in Human Adipose Tissue. *Mol. Metab.* 40, 101033. doi:10.1016/j.molmet.2020.101033

Safdie, F. M., Dorff, T., Quinn, D., Fontana, L., Wei, M., Lee, C., et al. (2009). Fasting and Cancer Treatment in Humans: A Case Series Report. *Aging* 1, 988–1007. doi:10.18632/aging.100114

Sahai, E., Astsaturov, I., Cukierman, E., Denardo, D. G., Egeblad, M., Evans, R. M., et al. (2020). A Framework for Advancing Our Understanding of Cancer-Associated Fibroblasts. *Nat. Rev. Cancer* 20, 174–186. doi:10.1038/s41568-019-0238-1

Salminen, A., Kauppinen, A., and Kaarniranta, K. (2019). AMPK Activation Inhibits the Functions of Myeloid-Derived Suppressor Cells (MDSC): Impact on Cancer and Aging. *J. Mol. Med.* 97, 1049–1064. doi:10.1007/s00109-019-01795-9

Seow, J. J. W., Wong, R. M. M., Pai, R., and Sharma, A. (2020). Single-Cell RNA Sequencing for Precision Oncology: Current State-Of-Art. *J. Indian Inst. Sci.* 100, 579–588. doi:10.1007/s41745-020-00178-1

Shao, M., Vishvanath, L., Busbuso, N. C., Hepler, C., Shan, B., Sharma, A. X., et al. (2018). De Novo adipocyte Differentiation from Pdgfrβ+ Preadipocytes Protects against Pathologic Visceral Adipose Expansion in Obesity. *Nat. Commun.* 9, 890. doi:10.1038/s41467-018-03196-x

Shushimita, S., De Bruijn, M. J. W., De Bruin, R. W. F., IJzermans, J. N. M., Hendriks, R. W., and Dor, F. J. M. F. (2014). Dietary Restriction and Fasting Arrest B and T Cell Development and Increase Mature B and T Cell Numbers in Bone Marrow. *PLoS One* 9, e87772. doi:10.1371/journal.pone.0087772

Simon, S. C. S., Hu, X., Panten, J., Grees, M., Renders, S., Thomas, D., et al. (2020). Eosinophil Accumulation Predicts Response to Melanoma Treatment with Immune Checkpoint Inhibitors. *Oncoimmunology* 9, 1727116. doi:10.1080/2162402X.2020.1727116

Singh, R., Parveen, M., Basgen, J. M., Fazel, S., Meshesha, M. F., Thames, E. C., et al. (2016). Increased Expression of Beige/Brown Adipose Markers from Host and Breast Cancer Cells Influence Xenograft Formation in Mice. *Mol. Cancer Res.* 14, 78–92. doi:10.1158/1541-7786.MCR-15-0151

Speaker, K. J., Paton, M. M., Cox, S. S., and Fleshner, M. (2016). A Single Bout of Fasting (24 H) Reduces Basal Cytokine Expression and Minimally Impacts the

Sterile Inflammatory Response in the White Adipose Tissue of Normal Weight F344 Rats. *Mediators Inflamm.* 2016, 1–13. doi:10.1155/2016/1698071

Spielmann, J., Mattheis, L., Jung, J.-S., Rausse, H., Glass, M., Bähr, I., et al. (2020). Effects of Obesity on NK Cells in a Mouse Model of Postmenopausal Breast Cancer. *Sci. Rep.* 10, 20606. doi:10.1038/s41598-020-76906-5

Strissel, K. J., Defuria, J., Shaul, M. E., Bennett, G., Greenberg, A. S., and Obin, M. S. (2010). T-cell Recruitment and Th1 Polarization in Adipose Tissue during Diet-Induced Obesity in C57BL/6 Mice. *Obesity (Silver Spring)* 18, 1918–1925. doi:10.1038/oby.2010.1

Strong, A. L., Pei, D. T., Hurst, C. G., Gimble, J. M., Burow, M. E., and Bunnell, B. A. (2017). Obesity Enhances the Conversion of Adipose-Derived Stromal/Stem Cells into Carcinoma-Associated Fibroblast Leading to Cancer Cell Proliferation and Progression to an Invasive Phenotype. *Stem Cell Int.* 2017, 1–11. doi:10.1155/2017/9216502

Sun, K., Asterholm, I. W., Kusminski, C. M., Bueno, A. C., Wang, Z. V., Pollard, J. W., et al. (2012). Dichotomous Effects of VEGF-A on Adipose Tissue Dysfunction. *Proc. Natl. Acad. Sci.* 109, 5874–5879. doi:10.1073/pnas.1200447109

Sundaram, S., and Yan, L. (2018). Time-restricted Feeding Mitigates High-Fat Diet-Enhanced Mammary Tumorigenesis in MMTV-PyMT Mice. *Nutr. Res.* 59, 72–79. doi:10.1016/j.nutres.2018.07.014

Sung, H.-K., Doh, K.-O., Son, J. E., Park, J. G., Bae, Y., Choi, S., et al. (2013). Adipose Vascular Endothelial Growth Factor Regulates Metabolic Homeostasis through Angiogenesis. *Cel Metab.* 17, 61–72. doi:10.1016/j.cmet.2012.12.010

Sung, H., Ferlay, J., Siegel, R. L., Laversanne, M., Soerjomataram, I., Jemal, A., et al. (2021). Global Cancer Statistics 2020: GLOBOCAN Estimates of Incidence and Mortality Worldwide for 36 Cancers in 185 Countries. *CA A. Cancer J. Clin.* 71, 209–249. doi:10.3322/caac.21660

Sutton, E. F., Beyl, R., Early, K. S., Cefalu, W. T., Ravussin, E., and Peterson, C. M. (2018). Early Time-Restricted Feeding Improves Insulin Sensitivity, Blood Pressure, and Oxidative Stress Even without Weight Loss in Men with Prediabetes. *Cel Metab.* 27, 1212–1221. e1213. doi:10.1016/j.cmet.2018.04.010

Tang, H.-N., Tang, C.-Y., Man, X.-F., Tan, S.-W., Guo, Y., Tang, J., et al. (2017). Plasticity of Adipose Tissue in Response to Fasting and Refeeding in Male Mice. *Nutr. Metab. (Lond)* 14, 3. doi:10.1186/s12986-016-0159-x

Tchkonia, T., Pirtskhalava, T., Thomou, T., Cartwright, M. J., Wise, B., Karagiannides, I., et al. (2007). Increased TNFα and CCAAT/enhancer-binding Protein Homologous Protein with Aging Predispose Preadipocytes to Resist Adipogenesis. *Am. J. Physiology-Endocrinology Metab.* 293, E1810–E1819. doi:10.1152/ajpendo.00295.2007

Tenvooren, I., Jenks, M. Z., Rashid, H., Cook, K. L., Muhlemann, J. K., Sistrunk, C., et al. (2019). Elevated Leptin Disrupts Epithelial Polarity and Promotes Premalignant Alterations in the Mammary Gland. *Oncogene* 38, 3855–3870. doi:10.1038/s41388-019-0687-8

Trepanowski, J. F., Kroeger, C. M., Barnosky, A., Klempel, M., Bhutani, S., Hoddy, K. K., et al. (2018). Effects of Alternate-Day Fasting or Daily Calorie Restriction on Body Composition, Fat Distribution, and Circulating Adipokines: Secondary Analysis of a Randomized Controlled Trial. *Clin. Nutr.* 37, 1871–1878. doi:10.1016/j.clnu.2017.11.018

Turbitt, W. J., Collins, S. D., Meng, H., and Rogers, C. J. (2019). Increased Adiposity Enhances the Accumulation of MDSCs in the Tumor Microenvironment and Adipose Tissue of Pancreatic Tumor-Bearing Mice and in Immune Organs of Tumor-free Hosts. *Nutrients* 11, 3012. doi:10.3390/nu11123012

Tzanavari, T., Giannogonas, P., and Karalis, K. P. (2010). TNF-α and Obesity. *Curr. Dir. Autoimmun.* 11, 145–156. doi:10.1159/000289203

Ullah, R., Su, Y., Shen, Y., Li, C., Xu, X., Zhang, J., et al. (2017). Postnatal Feeding with High-Fat Diet Induces Obesity and Precocious Puberty in C57BL/6J Mouse Pups: a Novel Model of Obesity and Puberty. *Front. Med.* 11, 266–276. doi:10.1007/s11684-017-0530-y

U.S. National Library of Medicine (2021). *Search of: Fasting, Cancer - List Results - ClinicalTrials.Gov [Online]*. ClinicalTrials.gov: NIH: U.S. National Library of Medicine. Available: https://clinicaltrials.gov/ct2/results?cond=fasting+and+cancer&term=&cntry=&state=&city=&dist= (Accessed August 20, 2021).

Vander Heiden, M. G., Cantley, L. C., and Thompson, C. B. (2009). Understanding the Warburg Effect: the Metabolic Requirements of Cell Proliferation. *Science* 324, 1029–1033. doi:10.1126/science.1160809

Varady, K. A., Allister, C. A., Roohk, D. J., and Hellerstein, M. K. (2010). Improvements in Body Fat Distribution and Circulating Adiponectin by Alternate-Day Fasting versus Calorie Restriction☆. *J. Nutr. Biochem.* 21, 188–195. doi:10.1016/j.jnutbio.2008.11.001

Varady, K. A., Bhutani, S., Klempel, M. C., Kroeger, C. M., Trepanowski, J. F., Haus, J. M., et al. (2013). Alternate Day Fasting for Weight Loss in normal Weight and Overweight Subjects: a Randomized Controlled Trial. *Nutr. J.* 12, 146. doi:10.1186/1475-2891-12-146

Varady, K. A., Roohk, D. J., McEvoy-Hein, B. K., Gaylinn, B. D., Thorner, M. O., and Hellerstein, M. K. (2008). Modified Alternate-day Fasting Regimens Reduce Cell Proliferation Rates to a Similar Extent as Daily Calorie Restriction in Mice. *FASEB j.* 22, 2090–2096. doi:10.1096/fj.07-098178

Vazeille, C., Jouinot, A., Durand, J.-P., Neveux, N., Boudou-Rouquette, P., Huillard, O., et al. (2017). Relation between Hypermetabolism, Cachexia, and Survival in Cancer Patients: a Prospective Study in 390 Cancer Patients before Initiation of Anticancer Therapy. *Am. J. Clin. Nutr.* 105, 1139–1147. doi:10.3945/ajcn.116.140434

Verma, N., Thakkar, N., Phillips, J., Ealey, K., and Sung, H.-K. (2020). Dynamic Remodeling of white Adipose Tissue by Intermittent Fasting. *Curr. Opin. Food Sci.* 34, 21–29. doi:10.1016/j.cofs.2020.10.023

Vila, I. K., Badin, P.-M., Marques, M.-A., Monbrun, L., Lefort, C., Mir, L., et al. (2014). Immune Cell Toll-like Receptor 4 Mediates the Development of Obesity- and Endotoxemia-Associated Adipose Tissue Fibrosis. *Cel Rep.* 7, 1116–1129. doi:10.1016/j.celrep.2014.03.062

Viscarra, J. A., Champagne, C. D., Crocker, D. E., and Ortiz, R. M. (2011). 5′AMP-activated Protein Kinase Activity Is Increased in Adipose Tissue of Northern Elephant Seal Pups during Prolonged Fasting-Induced Insulin Resistance. *J. Endocrinol.* 209, 317–325. doi:10.1530/JOE-11-0017

Wang, L., Cao, L., Wang, H., Liu, B., Zhang, Q., Meng, Z., et al. (2017). Cancer-associated Fibroblasts Enhance Metastatic Potential of Lung Cancer Cells through IL-6/STAT3 Signaling Pathway. *Oncotarget* 8, 76116–76128. doi:10.18632/oncotarget.18814

Wei, J., Ghosh, A. K., Sargent, J. L., Komura, K., Wu, M., Huang, Q.-Q., et al. (2010). PPARγ Downregulation by TGFß in Fibroblast and Impaired Expression and Function in Systemic Sclerosis: A Novel Mechanism for Progressive Fibrogenesis. *PLoS One* 5, e13778. doi:10.1371/journal.pone.0013778

Weigle, D. S., Duell, P. B., Connor, W. E., Steiner, R. A., Soules, M. R., and Kuijper, J. L. (1997). Effect of Fasting, Refeeding, and Dietary Fat Restriction on Plasma Leptin Levels1. *J. Clin. Endocrinol. Metab.* 82, 561–565. doi:10.1210/jcem.82.2.3757

Wilkinson, M. J., Manoogian, E. N. C., Zadourian, A., Lo, H., Fakhouri, S., Shoghi, A., et al. (2020). Ten-Hour Time-Restricted Eating Reduces Weight, Blood Pressure, and Atherogenic Lipids in Patients with Metabolic Syndrome. *Cel Metab.* 31, 92–104. e105. doi:10.1016/j.cmet.2019.11.004

Wu, B., Sun, X., Gupta, H. B., Yuan, B., Li, J., Ge, F., et al. (2018). Adipose PD-L1 Modulates PD-1/pd-L1 Checkpoint Blockade Immunotherapy Efficacy in Breast Cancer. *Oncoimmunology* 7, e1500107. doi:10.1080/2162402X.2018.1500107

Wu, Q., Li, J., Li, Z., Sun, S., Zhu, S., Wang, L., et al. (2019). Exosomes from the Tumour-Adipocyte Interplay Stimulate Beige/brown Differentiation and Reprogram Metabolism in Stromal Adipocytes to Promote Tumour Progression. *J. Exp. Clin. Cancer Res.* 38, 223. doi:10.1186/s13046-019-1210-3

Xiao, Z., Dai, Z., and Locasale, J. W. (2019). Metabolic Landscape of the Tumor Microenvironment at Single Cell Resolution. *Nat. Commun.* 10, 3763. doi:10.1038/s41467-019-11738-0

Yang, J., Yan, J., and Liu, B. (2018). Targeting VEGF/VEGFR to Modulate Antitumor Immunity. *Front. Immunol.* 9, 978. doi:10.3389/fimmu.2018.00978

Zhang, W.-C., Qin, F., Wang, X.-J., Liu, Z.-F., Zhu, L., Zeng, A., et al. (2019). Adipose-Derived Stromal Cells Attenuate Adipose Inflammation in Obesity through Adipocyte Browning and Polarization of M2 Macrophages. *Mediators Inflamm.* 2019, 1–10. doi:10.1155/2019/1731540

Zhao, H., Shang, Q., Pan, Z., Bai, Y., Li, Z., Zhang, H., et al. (2018). Exosomes from Adipose-Derived Stem Cells Attenuate Adipose Inflammation and Obesity through Polarizing M2 Macrophages and Beiging in White Adipose Tissue. *Diabetes* 67, 235–247. doi:10.2337/db17-0356

Zhao, X., Yang, J., Huang, R., Guo, M., Zhou, Y., and Xu, L. (2021). The Role and its Mechanism of Intermittent Fasting in Tumors: Friend or Foe? *Cancer Biol. Med.* 18, 63–73. doi:10.20892/j.issn.2095-3941.2020.0250

Zhao, Y., Butler, E. B., and Tan, M. (2013). Targeting Cellular Metabolism to Improve Cancer Therapeutics. *Cell Death Dis* 4, e532. doi:10.1038/cddis.2013.60

Zheng, X., Zhang, N., Qian, L., Wang, X., Fan, P., Kuai, J., et al. (2020). CTLA4 Blockade Promotes Vessel Normalization in Breast Tumors via the Accumulation of Eosinophils. *Int. J. Cancer* 146, 1730–1740. doi:10.1002/ijc.32829

Zhou, M., Zhao, Y., Ding, Y., Liu, H., Liu, Z., Fodstad, O., et al. (2010). Warburg Effect in Chemosensitivity: Targeting Lactate Dehydrogenase-A Re-sensitizes Taxol-Resistant Cancer Cells to Taxol. *Mol. Cancer* 9, 33. doi:10.1186/1476-4598-9-33

Zwick, R. K., Guerrero-Juarez, C. F., Horsley, V., and Plikus, M. V. (2018). Anatomical, Physiological, and Functional Diversity of Adipose Tissue. *Cel Metab.* 27, 68–83. doi:10.1016/j.cmet.2017.12.002

Conflict of Interest: The authors declare that the research was conducted in the absence of any commercial or financial relationships that could be construed as a potential conflict of interest.

frontiers in Cell and Developmental Biology

REVIEW
published: 11 March 2022
doi: 10.3389/fcell.2022.752326

Uncovering Pharmacological Opportunities for Cancer Stem Cells—A Systems Biology View

*Cristina Correia[1], Taylor M Weiskittel[1], Choong Yong Ung[1], Jose C Villasboas Bisneto[2], Daniel D Billadeau[3,4], Scott H Kaufmann[1,2,4] and Hu Li[1]**

[1]Department of Molecular Pharmacology and Experimental Therapeutics, Mayo Clinic, Rochester, MN, United States, [2]Division of Hematology, Department of Medicine, Mayo Clinic, Rochester, MN, United States, [3]Department of Immunology, Mayo Clinic, Rochester, MN, United States, [4]Division of Oncology Research, Mayo Clinic, Rochester, MN, United States*

Cancer stem cells (CSCs) represent a small fraction of the total cancer cell population, yet they are thought to drive disease propagation, therapy resistance and relapse. Like healthy stem cells, CSCs possess the ability to self-renew and differentiate. These stemness phenotypes of CSCs rely on multiple molecular cues, including signaling pathways (for example, WNT, Notch and Hedgehog), cell surface molecules that interact with cellular niche components, and microenvironmental interactions with immune cells. Despite the importance of understanding CSC biology, our knowledge of how neighboring immune and tumor cell populations collectively shape CSC stemness is incomplete. Here, we provide a systems biology perspective on the crucial roles of cellular population identification and dissection of cell regulatory states. By reviewing state-of-the-art single-cell technologies, we show how innovative systems-based analysis enables a deeper understanding of the stemness of the tumor niche and the influence of intratumoral cancer cell and immune cell compositions. We also summarize strategies for refining CSC systems biology, and the potential role of this approach in the development of improved anticancer treatments. Because CSCs are amenable to cellular transitions, we envision how systems pharmacology can become a major engine for discovery of novel targets and drug candidates that can modulate state transitions for tumor cell reprogramming. Our aim is to provide deeper insights into cancer stemness from a systems perspective. We believe this approach has great potential to guide the development of more effective personalized cancer therapies that can prevent CSC-mediated relapse.

Keywords: cancer stem cells, cellular niche, tumor microenvironment, systems biology, immunotherapy, drug resistance

OPEN ACCESS

Edited by:
Stephanie Ma,
The University of Hong Kong, Hong Kong SAR, China

Reviewed by:
YM Tsui,
The University of Hong Kong, Hong Kong SAR, China
Susan Mertins,
Leidos Biomedical Research, Inc., United States

****Correspondence:***
Hu Li
li.hu@mayo.edu

Specialty section:
This article was submitted to Stem Cell Research, a section of the journal Frontiers in Cell and Developmental Biology

Received: *02 August 2021*
Accepted: *10 February 2022*
Published: *11 March 2022*

Citation:
Correia C, Weiskittel TM, Ung CY, Villasboas Bisneto JC, Billadeau DD, Kaufmann SH and Li H (2022) Uncovering Pharmacological Opportunities for Cancer Stem Cells—A Systems Biology View. Front. Cell Dev. Biol. 10:752326. doi: 10.3389/fcell.2022.752326

INTRODUCTION

In cancer, a gain of stemness can have profound implications on tumor aggressiveness, drug response and clinical outcome (**Figure 1A**). Here, we provide a systems biology overview of how the immune cell niche, cellular contexts, and molecular or genetic perturbations contribute to stem cell-like properties of malignant cells. We start by describing the sources of tumor heterogeneity and defining the cellular niche as a dynamic spatial domain harboring cancer stem cells (CSCs). We then elaborate on how this cellular niche is critical for communication between cell populations and move through

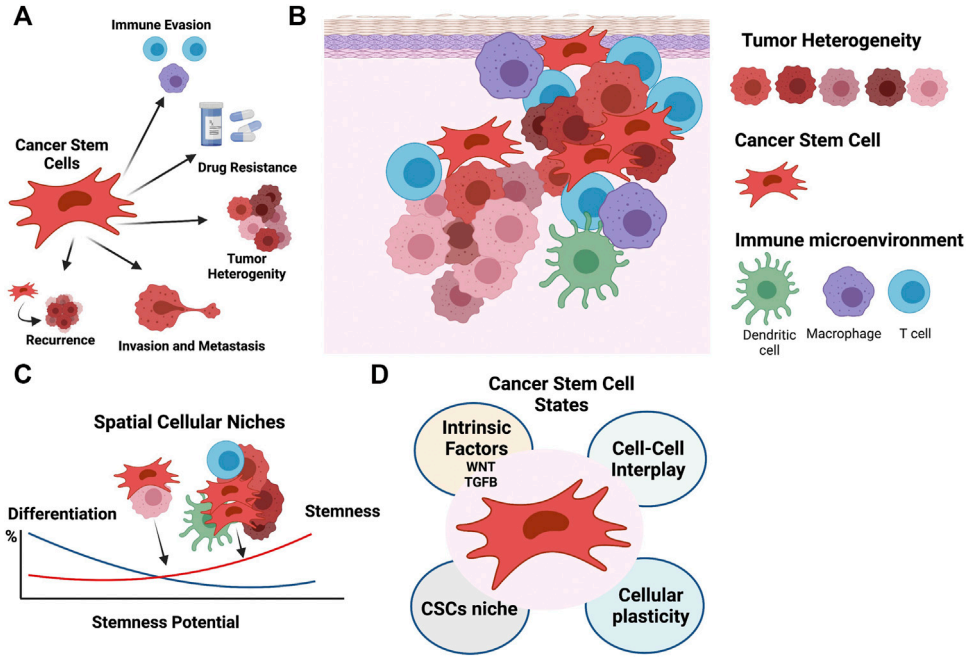

FIGURE 1 | The cellular niche sustains the phenotypically diversity of cancer stem cells. **(A)** CSCs play fundamental roles in cancer, including contributing to tumor heterogeneity, and immune evasion, promoting migration and recurrence, and driving chemoresistance. **(B)** The CSC niche is supported by the tumor components, stroma, immune infiltrate, and tumor microenvironment. **(C)** Cell-cell interactions define spatial cancer niches and contribute to the phenotypically diversity of CSCs and cellular heterogeneity. **(D)** CSC phenotypic states are modulated by an array of factors, including intrinsic factors like WNT and TGFB pathway activation, cell-cell interactions, cellular plasticity, and the cellular niche. Figure created with BioRender.com.

the biological pathways endowing these stemness properties. We outline how systems biology approaches present an important strategy for identifying the crosstalk between immune cells, the bulk cancer, and CSCs. Finally, we discuss how these systems biology approaches open new avenues to dissect and manipulate cellular states and niches to impact cancer progression.

SOURCES OF TUMOR HETEROGENEITY

Tumor complexity not only arises from the intrinsic diversity of the tumor cells themselves, but also from their interactions with other non-tumor cell types. The intratumoral heterogeneity of the cancer cells arises through mechanisms such as genomic instability, clonal evolution, cellular differentiation, and reversible plasticity. These contributions have been well studied, but most analyses fail to systematically characterize the contributions of other cells to cancer cell heterogeneity. Immune cells, which are also part of the tumor niche, present over 350 CD (cluster of differentiation) antigens, secrete close to 100 cytokines and chemokines, and belong to subtypes that express thousands of unique gene signatures (Davis et al., 2017). These immune cells, as well as other non-malignant stromal cells, co-exist with cancer cells, thus creating complex biological entities. Moreover, these stromal cells interact with and shape the evolution of the cancer cell populations (**Figure 1B**).

From a systems biology perspective, the contribution of each source of heterogeneity can be understood by dissecting cell populations, cellular niches, niche dynamics and the crosstalk between them. This will ultimately help devise disease spatial resolution maps that shed light on mechanisms of cancer progression and drug resistance. Such complex systems exhibit emergent properties that are not just the aggregation of unconnected individual behaviors, but are instead unique phenomena that reflect synergy in interactions between cells. The scientific discipline of systems biology aims to provide a quantitative and dynamic framework that leverages mathematical and computational techniques to unravel the complexity of cellular processes. This approach is applied with the view that a holistic view of systems will not only inform how a gene connects to a protein and an activity, but also help elucidate how a cellular phenotype is contingent on the biological context (where and when) (Kirschner, 2005). As such, systems biology approaches have the power to dissect the interplay between tumor and immune cells to characterize higher order properties and systems interconnectivity. For example, interrelationships between ligands and receptors have been an active area of research where a variety of system methodologies have been applied to define ligand/receptor co-expression, formation of multimeric complexes and cellular activity (see section entitled Probing the cellular niche: Technological advances). The large breadth of 'omics data now available is enabling systems approaches to give new insights. Here, we will highlight the potential of systems biology to dissect the determinants of cancer stemness present in the cellular niche.

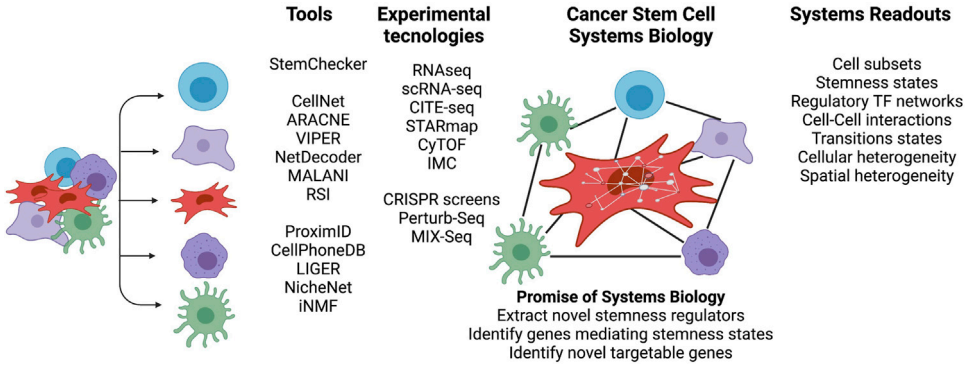

FIGURE 2 | Cancer stem cell systems biology—Novel insights gained by integrated analyses. Overview of breadth of high-throughput technologies and tools to characterize the cross talk between CSCs, immune and tumor cells in a cellular niche. The niche cell subsets can be probed, for example, using bulk and single cell RNA-seq or cytometry by time-of-flight (CyTOF). CITE-Seq, STARmap and IMC (imaging cytometry) can spatially probe the cellular niche. A variety of systems tools provide a framework to interrogate signaling pathways, derive regulatory TF networks and understand the diversity of CSC phenotypes and their niches. Figure created with BioRender.com.

STEMNESS OF CANCER CELLS

Stemness, defined as the potential for self-renewal and differentiation from the cell of origin, was originally attributed to normal embryonic stem cells that give rise to all cells in adult organisms. However, it has long been known that cancer cells show markers and properties of embryonic stem cells (Friedmann-Morvinski and Verma, 2014). Cancer progression often involves the gradual loss of a differentiated phenotype and acquisition of progenitor or stem cell-like features. Undifferentiated primary tumors are more likely to result in metastasis to distant organs, causing disease progression and poor prognosis, as well as resistance to available therapies. Within a tumor, phenotypic diversity and spatial cellular variation may also impact expression of key embryonic stem cell regulators, resulting in distinct paths to cancer stemness (**Figure 1C**).

SYSTEMS BIOLOGY AND CANCER STEM CELL STATES

Dedifferentiation of Cancer Cells

Although CSCs exhibit the stem cell-like properties of self-renewal and differentiation, they do not necessarily originate from the transformation of normal tissue adult stem cells (Friedmann-Morvinski and Verma, 2014). Oncogenic hits initiating malignant transformation may over time lead to a more dedifferentiated state and contribute to tumor cell heterogeneity. For instance, reverse engineered gene regulatory networks (GRNs) reconstructed by methods such as mode-of-action by network identification (MNI) approach, were used in our earlier studies and allowed the identification of HOXA1 as a key modulator capable of reversal phenotypes in breast cancer (Brock et al., 2014). Such inducibility of tumor plasticity suggests that CSCs do not necessarily originate from normal stem cells. Instead, under certain circumstances, cancer cells can dedifferentiate and acquire cancer stem cell (CSC)-like properties (Lyssiotis and Kimmelman, 2017). Here, the microenvironment of a tumor provides ample molecular cues and opportunities for cell-to-cell signaling to modulate the epigenome and phenotypic stem cell-like programs in cancer cells, frequently independent of their genetic backgrounds (**Figures 1C,D**) (Gingold et al., 2016). A variety of systems biology approaches, which are able to dissect transcriptional programs in various cellular states (Huggins et al., 2017; Luke et al., 2019), can also be used to understand CSCs (**Figure 2**). For instance, CellNet (Cahan et al., 2014) can reverse engineer GRNs to find transcription factors that are crucial in cell state maintenance. Others, like ARACNe (Basso et al., 2005) and VIPER (Alvarez et al., 2016), utilize GRN reverse engineering approaches to enrich for cellular regulons and identify regulatory genes that determine specific biological conditions. As an example, a set of systems biology tools developed in our lab have the potential to provide deeper look into CSC biology. For example, NetDecoder (da Rocha et al., 2016) builds a context specific network based on prior biological knowledge and enables genome-wide modeling of signal flows to extract genes that are critical under a specific biological context. Alternatively, Machine Learning Assisted Network Inference (MALANI) (Ghanat Bari et al., 2017), a machine learning-based method, creates *de novo* biological networks and has the ability to extract "dark genes" that are neither differentially expressed nor mutated but can play important roles in CSCs' stemness. Moreover, Regulostat Inferelator (RSI) (Ung et al., 2019) searches for gene pairs that act like biological rheostats and can modulate phenotypic transitions in cancer cells, for example, the acquisition of stemness properties.

WNT-β-Catenin Signaling and Stem Cell-like Phenotype in CSCs

Canonical WNT is a major pathway that regulates CSCs and induces stemness in several cancers (Vermeulen et al., 2010; Nguyen et al., 2019). The hallmark of this pathway is the activation of β-catenin-mediated transcriptional activity. WNT canonical pathway signaling

is initiated by the binding of a WNT family protein to cell surface receptors to activate signal transduction (Kalbasi and Ribas, 2020; Yang et al., 2016). In the presence of WNT ligand, β-catenin evades proteasomal degradation, translocates to nuclei and activates transcription. This has several consequences for the CSC niche: 1) Increased phenotypic heterogeneity, 2) spatial diversity, and 3) impact on *de novo* immune response (Holtzhausen et al., 2015; Spranger et al., 2015; Luke et al., 2019) [for review see (Galluzzi et al., 2019)]. In particular, heterogenous activity of WNT has been observed in colon cancer, with high activity seen in regions close to stromal components (Vermeulen et al., 2010) (**Figure 1D**). Moreover, WNT-β-catenin pathway activation has been associated with immune exclusion of dendritic cells (DC) and T-cells from melanomas (Spranger et al., 2015; Spranger and Gajewski, 2015) and other cancers (Luke et al., 2019). With a reduction of CXCL9/10, CCL4 and other chemokines, recruitment of DCs and cross-priming of effector T cells in tumors is limited (Spranger et al., 2017). Further, DCs are re-wired to a regulatory state that is immune tolerant (Hall et al., 2011).

While WNT signaling in tumor cells is associated with a worse outcome, WNT signaling in the lymphoid compartment appears to modulate anti-tumor responses. In particular the WNT-β-catenin pathway regulates TCF1, a transcriptional factor that plays a critical role in T cell differentiation. TCF1 acts by biasing the differentiation of naïve T cell to $CD4^+$ T helper subsets (Th1, Th2, and Th17). Moreover, WNT-β-catenin signaling promotes the generation of memory T cells, whereas the expansion of naïve $CD8^+$ T cells and differentiation of effector T cells are inhibited (van de Wetering et al., 1991; Bienz and Clevers, 2003; Luke et al., 2019) [See review (Wang B et al., 2018) for in depth description]. This and additional observations support the pursuit of WNT inhibitors and combinatorial targeting of the WNT-β-catenin pathway to improve clinical outcomes of patients to overcome primary, adaptive, and acquired resistance to immunotherapy (Wang B et al., 2018; Zhang et al., 2020). However, as suggested by Wang B et al. (2018), it remains to be determined whether this strategy can be translated into the clinical practice to ultimately help devise better individualized immunotherapy treatments for cancer patients.

Systems biology approaches are also used to interrogate signaling and phenotypical programs that sustain cancer stemness (**Figure 2**). For instance, Pinto et al. (2015) collected 132 stemness signatures using publicly available gene expression datasets, RNAi screen results, and Transcription Factor (TF) binding site data to generate an interactive web-based server (StemChecker) that reports the overlap of input genes with stem cell signatures and the targets of transcription factors. Conversely, Malta *el al.* used a variety of normal stem cells with one-class regression machine learning to extract stem signatures, which they then used to infer a stemness score in many cancers (Malta et al., 2018). These studies showed that WNT and TGFB signaling pathways act in a different range in CSCs compared to non-neoplastic stem cells.

In poorly differentiated tumors, overexpression of key embryonic stem cell regulators (e.g., NANOG, OCT4, SOX2, c-MYC) (Malta et al., 2018) was observed to correlate with poorer outcomes. Further analysis also indicated that dedifferentiation features are associated with 1) mutations in genes that encode oncogenes and epigenetic modifiers, 2) perturbations in specific mRNA/miRNA transcriptional networks, and 3) deregulation of signaling pathways (Malta et al., 2018). Overall, these observations highlight the need to consider the CSC niche as distinct from normal stem cell niches. For this reason, future analysis must take into account the co-existence of diverse cell states and embrace dedifferentiation as a path to cancer stemness.

PROMISE OF PROBING THE CELLULAR NICHE

Tumor Microenvironment

The tumor microenvironment is the ecosystem that surrounds tumor cells inside the body. It includes a variety of cell types, including immune cells, stromal cells, adipocytes, fibroblasts, and vascular cells, as well as extracellular vesicles (EVs), extracellular matrix and molecules produced and released by all of these cell types. These TME components are not just bystanders in the tumorigenic process, but instead play a decisive role in tumor differentiation, epigenetics, dissemination, immune evasion, and drug resistance (Labani-Motlagh et al., 2020). In particular, the cross-talk between tumor cells and cells in the TME fuels and shapes tumor progression, giving rise to dynamic and complex ecosystems in both primary and metastatic sites.

Because most cancer deaths result from the development of distant metastasis, it is important to decode the dynamic interactions between cancer cells and the TME in individual sites during tumor development, progression, and response to therapy. For example, metastatic cells can differ from neoplastic cells at the primary site in key ways as they adapt to the unique metabolic conditions in the metastatic site (e.g., Ferraro et al., 2021), acquire mutations, evolve independently, and persist despite exposure to therapy. However, our ability to infer the cell-cell communications and investigate cellular plasticity in metastases is limited by the often simplistic models or is built on knowledge gained from the primary tumor. Therefore, developing models that focus on investigating the immune and transcriptional landscapes as well as cellular cross-talk by screening distant metastasis will help to better characterize dormant micro-metastases and identify new therapies to target metastatic tumors.

In current studies designed to understand the role of TME in the transition of ductal carcinoma *in situ* (DCIS) to invasive breast cancer (IBC) and progressive disease, Risom et al. used a multicompartmental analysis to compare functional biological states during tumor progression. Tumor invasiveness was correlated with a higher number of cancer associated fibroblasts (CAFs) and density of fibrillar collagen, a shift from monocytes to antigen presenting cells (APCs) and intraductal macrophages, and increased density of T and B cells in stromal compartments. These findings highlight a model in breast cancer (BC) where invasiveness occurs through the dynamic interactions with surrounding stroma and immune cells with the epithelial compartment of the tumor (Risom et al., 2022). Further, in a recent clinical trial (Hurvitz et al., 2020), BC patients were randomized to receive

three distinct anti-HER2 treatments (trastuzumab, lapatinib, trastuzumab + lapatinib) followed by six cycles of standard combination chemotherapy along with the same anti-HER2 therapy. Serial analysis of the pre- and post- treatment demonstrated an increase of immune and stromal signatures after HER2 targeted-therapy alone but decreasing strengths of these signatures after addition of chemotherapy to the HER2 targeted-therapy. In particular, there was a reduction of M1 macrophages and increase in $CD8^+$ T cells (Hurvitz et al., 2020). Collectively, these findings support the view that the TME changes over time, highlighting the possibility that factors converge to select the most adaptable tumorigenic cells and ecological environments for the tumor to thrive and reach its metastatic potential.

As a result of metabolic differences from site to site (Ferraro et al., 2021), as well as likely differences in cell types and cellular products, the TME is increasingly viewed as a highly heterogenous milieu that varies across tumor sites or so-called niches (spatial heterogeneity). This complexity needs to be considered at a systems level to design better therapeutic options for cancer patients. For example, the identification of the tumor dominant immune evasion mechanism within the TME can inform on the best patient therapeutic approach (Sanmamed and Chen, 2018). On the other hand, tumor stiffness can dictate a drug's ability to reach the tumor (Olive et al., 2009). Clinically, a major challenge to understanding the TME is the limited ability to capture sequential tissue samples from cancer patients. However, recent advances in three-dimensional (3D) platforms like organ on a chip and microfluidic devices, as well as the development of humanized mouse models or explant 3D cultures model (patient- or mouse-derived tumor spheroids) (Sanmamed and Chen, 2014; Zitvogel et al., 2016; Jenkins et al., 2018; Vunjak-Novakovic et al., 2021), can provide an excellent opportunity to bridge this gap. Collectively, these tools have been developed with the view that a better understanding of the interplay of bi-directional communication between the tumor and TME, and CSCs will help identify improved cancer therapies.

The Cellular Niche and Tumor Microenvironment

The term "niche" is commonly used to describe an anatomically distinct regions within a tissue (or tumor). This description, however, fails to capture the interactions with surrounding cell populations and microenvironmental cues. Instead, a niche might be more properly viewed as a spatiotemporal dynamic state that is modulated by external perturbations to induce a permissive tumorigenic environment. Because tumor cells, stroma and immune cells are crucial determinants of malignant growth (Visvader, 2011; Plaks et al., 2015), understanding how a cellular niche responds to each cell type in the TME is crucial for successful therapeutic targeting. In particular, cell-cell communication mediated by surface receptor-ligand interactions is an attractive process for pharmacological intervention. Accordingly, more needs to be known about this cell-cell communication. Moreover, immune cells are known to rewire in response to external stimuli arising from physical interactions with neighboring cells and secreted ligands. The resulting communication between tumor and immune cells impacts tissue homeostasis and disease progression. For example, in high-grade serous ovarian cancer (HGSOC), cancer cell progenitors have been found to migrate from the fallopian tube to more distal locations where the cellular niche allows for phenotypic shifting and propagation (Ng and Barker, 2015). In this way the cellular niche is intimately tied to cancer stemness and *vice versa* (**Figure 1B–D**).

Highly Dynamic Cellular States and CSCs

During tumor evolution, it appears that tumor cell-extrinsic factors (the TME) as well as tumor cell-intrinsic factors (e.g., epigenomic changes) influence cellular states. Recently, Marjanovic et al. (2020) and LaFave et al. (2020) showed that a diverse and continuous range of states exist in a model of lung cancer progression. These co-existing states, which captured lineage infidelity and cellular plasticity, exhibited features of drastically different cell types, suggesting the ability of cancers to explore a broad phenotypic space. Although some of the cells in these lung cancers resemble stem cells and CSCs in their ability for robust growth and differentiation potential, their phenotypic programs are distinct (LaFave et al., 2020). Thus, a key step to better understanding CSCs is to thoroughly characterize their transcriptional states and ability to switch between CSC and non-CSC states.

PROBING THE CELLULAR NICHE: TECHNOLOGICAL ADVANCES

A challenge with CSCs is that only a small number of stem cell markers have been identified. This limited set of markers reflects the small proportion of CSCs generally present in tumors and the poor conservation of CSC surface markers across cancers. Therefore, from a systems perspective, an *ab initio* approach is best for the identification of CSCs.

A diverse array of high-throughput technologies has been used to zoom in on CSCs and their niches within cancer patients. The oldest and most common modality is RNAseq. A limitation of traditional bulk RNAseq, however, is that it averages expression across thousands of cells within a sample. Because of this limitation, understanding and constructing regulatory networks for distinct types such as CSCs has been difficult with bulk RNAseq alone.

There is, however, precedent for studying distinct tumor components using bulk RNAseq. CIBERSORT (Newman et al., 2015) has been used extensively to computationally dissect immune cell populations from these bulk samples; and several methods exist for constructing tissue level networks. CIBERSORT uses a knowledge-based signature matrix that encapsulates major 22 functionally defined human hematopoietic subsets to deconvolute and infer cell composition from gene expression profile data, utilizing support vector machine (SVM) regression methods. This approach has played a key role in decoding immune cell

population, particularly in bulk solid tumors where tissue dissociation protocols and cellular enrichment techniques limit the efficacy of single-cell methods and provide only a partial view of the wider cell heterogeneity. Extending this approach in a new direction, a groundbreaking study by Thorsson *et al.* used TCGA RNAseq data across 33 cancer types and more then 10,000 patients to identify signatures for six TME subtypes and demonstrate that these TME subtypes can be associated with prognosis as well as genetic and immune modulatory alterations (Thorsson et al., 2018). Reflecting the importance of the TME to tumor behavior, the TME subtypes identified by Thorsson *et al.* were reportedly able to predict disease outcomes and help guide novel treatments. More recently, Bagaev *et al.* derived 29 expression signatures to establish four TME subtypes (immune enriched fibrotic, immune enriched non-fibrotic, fibrotic and depleted) that correlate with immunotherapy efficacy in melanoma (Bagaev et al., 2021). As demonstrated by these studies, it is possible to use RNAseq to study a subpopulation of cells (e.g., immune cells or stromal cells) if the transcriptional profile is detectable and distinctive. However, given the rarity of CSCs, it has been difficult to study CSCs themselves using bulk RNAseq. Moreover, while publicly available multi-omics signatures from non-neoplastic stem cells were previously used to derive a stemness score in tumors (Malta et al., 2018) that can then be applied using deconvolutional methodologies to identify CSCs in bulk RNAseq, a key caveat is that CSCs do not necessarily share the same transcriptional programs as normal stem cells counterparts. Taking a different approach, Aran *et al.* probed the normal tissue adjacent to the tumor (NAT), which is morphologically similar but phenotypically different from the tumor and focused on stromal pathways to query the interaction between adjacent tissues (Aran et al., 2017). These authors uncovered NAT-specific characteristics, namely activation of pro-inflammatory immediate-early response genes concordant with endothelial cell stimulation. Furthermore, previous studies on breast NAT suggested that the microenvironment surrounding the tumor, not the epithelial cells, is essential for understanding disease recurrence and developing surgical strategies (Graham et al., 2011). These studies have shown that by zooming into the tumor niche and its adjacent boundaries we can acquire deeper understanding of cell-cell interplay and dissect the phenotypic states that sustain stemness.

With the advent of single-cell RNAseq (scRNA-seq), new avenues to investigate and quantify molecular features at single-cell resolution have emerged. Single-cell technologies have the ability to directly evaluate cell states, heterogeneity, and lineages (Saelens et al., 2019). However, more effort is required to provide understanding of cell-cell interactions as well as their co-evolution and adaptation to perturbations in the cellular milieu, which is needed for the construction of a comprehensive cellular interaction map (Elmentaite et al., 2019). Current efforts to build a human body atlas (Regev et al., 2017) will provide important information on the baseline stromal, tumor and immune tissue heterogeneity. Tissue specificity is particularly important in immune cells because they both circulate and remain tissue resident; profiling of both populations can enhance understanding of which cells are recruited to become part of the TME. Despite the promise of scRNA-seq, it also has a key limitation: Enrichment and dissociation strategies that are used to separate single cells for profiling and capture cells of interest disrupt tissue organization and result in loss of spatial information (Elmentaite et al., 2019).

Single-cell computational frameworks have thus far focused in dissecting the ligand-receptor interactome based on expression of ligands and receptors across cell populations. The various computational frameworks take different approaches (Zhou et al., 2017; Cohen et al., 2018; Kumar et al., 2018). CellPhoneDB (Efremova et al., 2020) uses scRNA-seq to decode intercellular communication networks by inferring multimeric ligand-receptor interactions between cell states based on expression of a receptor by one cell state and a ligand by another cell state. By assessing which structural complexes are ubiquitously expressed in a tissue and not varied between cellular states, ligand-receptor cell specificity is assured. Because multi-subunit heteromeric complexes often swap subunits to ensure ligand specificity, expression of all subunits of a functional complex is required for downstream signaling. Vento-Tormo first applied CellPhoneDB to the study of early human pregnancy and interaction between fetal and maternal cells with a focus on trophoblast-decidua interactions that underlie common diseases of pregnancy such as pre-eclampsia and still births (Vento-Tormo et al., 2018). The authors uncovered receptor-ligand complexes that can modulate trophoblast differentiation. Moreover, they identified an association between three major decidual natural killer (NK) cell populations, their cell markers, and their expression of cytokines, chemokines and receptors, with different reproductive outcomes, providing a cell atlas to understand normal and pathological pregnancies (Vento-Tormo et al., 2018). In the context of CSCs, such a strategy could potentially be applied to dissect receptor-ligand interactions that help sustain stemness if achievable scRNA-seq resolution allows for the reliable identification of CSCs.

Using RNA velocity measurements that predict the fate of cell populations (splicing and non-splicing ratio) and provide a measure of stemness, we can potentially identify CSCs in a non-biased manner. Such strategy is particularly attractive when we consider the potential heterogeneity of the CSC compartment. This strategy was employed by Gautam et al. (2021) to generate a multispecies cell roadmap for human and porcupine ocular compartments. The ability to use organoids and enrich for stem cell like progenitors offers new possibilities to further decode CSCs.

Boisset *et al.* have manually microdissected 727 mouse interacting cellular structures and used scRNA-seq to create an interacting cellular network (Boisset et al., 2018). Using permutations, they have created a null distribution of random interactions between cell populations that permits identification of enriched or depleted interactions as compared to the background model. More recently, the authors of NicheNet have assembled prior knowledge on ligand-receptors and their signaling pathways using public resources and used expression datasets to generate weighted networks with regulatory scores that infer activity (Browaeys et al., 2020). Overall, these studies

provide immense insight into the cell-cell interactome, but these studies all make several key assumptions: 1) That transcripts encoding receptors are translated into proteins that are translocated to the membrane, 2) that ligands are successfully transported out of the cells, and 3) that cells are in proximity with interacting partners in tissue space (Elmentaite et al., 2019). These approaches are now starting to be applied to extremely rare populations such as CSCs and yield great promise to depict their secretome.

Mass cytometry (cytometry by time-of-flight, CyTOF) has revolutionized human immune cell profiling by allowing the simultaneous measurement of >40 surface markers on a single-cell basis (Bracci et al., 2020). CyTOF is particularly valuable when analyzing samples with a limited number of cells such as tumor biopsies, longitudinal studies or response to therapy, e.g., in clinical trials (Gadalla et al., 2019). The high degree of multiplexing in the CyTOF is possible because antibodies are coupled to rare metal isotopes that provide a unique mass tag to each marker to overcome spectral overlap commonly observed in multiparameter flow cytometry. Recently, Gallad *et al.* validated CyTOF panel data against flow cytometry and demonstrated equivalent ability to identify cell subsets or perform phenotyping, but with smaller cell numbers (Gadalla et al., 2019). CyTOF barcoding strategies enable the marking cells from separate samples, which allows for the simultaneous measurement of multiple samples, thus eliminating multiple sources of sample-to-sample variability (Behbehani et al., 2014). CyTOF has been applied to characterize CSCs specifically in leukemias and lymphomas; however, this requires *a priori* knowledge of the proteins at the cell surface and available antibodies amenable to conjugation. More recent studies have used CyTOF in combination with CITE-Seq (cellular indexing of transcriptomes and epitopes by sequencing), thus creating a multimodal approach with simultaneous quantification of single-cell transcriptomes and surface proteins. For example, Yao *et al.* have demonstrated that B cell, monocyte/macrophage, and plasmacytoid dendritic cell abundance across three methods (scRNA-seq, CyTOF and CITE-Seq) is consistent, but T cell measurements have greater variability. Additionally, this trimodal analysis indicates that there is a good correlation across scRNA-seq and protein expression for highly expressed cell type markers (Yao et al., 2020). Because these three single-cell approaches enable the simultaneous identification of cell types, cell states and characterization of cellular heterogeneity at transcriptomic and/or protein levels, understanding the concordance of the measurements among these three modalities is of great interest. Collectively, these observations suggest that the of use multimodal omic datasets can open new avenues to dissect CSC-immune cell interactions.

A major limitation of these single-cell techniques is the lack of spatial transcriptomic information that is key for understanding the CSC niche. 3D intact-tissue RNA sequencing methods exemplified by STARmap allow for mapping of more than 1,000 genes in sections of mouse brain to define cell types and establish a roadmap for cell organization principles (Wang X et al., 2018). Alternatively, imaging cytometry (IMC) is emerging as a transformative technique that allows for multiparametric analysis of >40 protein markers in frozen and FFPE (formalin-fixed, paraffin-embedded) tissue samples (Chang et al., 2017; Bouzekri et al., 2019). IMC provides a unique window into structural features of the tissue under investigation, validates spatial ligand-receptor interactions and identifies the distribution of cell types within the tissue to build a spatial map (Bodenmiller, 2016). In breast cancer, for example, clear differences have been noted in markers like cytokeratin, HER2, E-cadherin and c-MYC within single tumors, highlighting the intra- and interpatient heterogeneity that can be captured with IMC (Giesen et al., 2014; Wagner et al., 2019). As a result, IMC has the ability identify each cell type in its environmental cellular context, thereby providing a unique spatially resolved view of the tissue and allowing more accurate inference of cellular functional states. The downside is that this approach is not yet suitable for high-throughput screening of ligand-receptor interactions due the limited scanned tissue area (1 μm), high sample cost, and paucity of computational platforms available for data analyses. Bodenmiller *et al.* have developed multivariate computational tools to visualize and analyze multiplexed images of human tissue sections generated by IMC (Schapiro et al., 2017). Another platform recently proposed by Greenald *et al.* utilizes a library containing a large collection of manually curated cells, TissueNet (one million cells from six organs and different imaging platforms) and a deep learning model to achieve human-like cell and nuclear segmentation (Greenwald et al., 2021).

Future IMC studies focusing on a well-defined tissue sections that can be layered with 'omic information will be of great interest for dissecting the interplay of between cell populations (Bodenmiller, 2016). Whether IMC layered with 'omic data can also inform studies of rare cells such as CSCs remains to be seen.

FUTURE DIRECTIONS IN MANIPULATING THE CANCER STEM CELL NICHE

Biological Perturbations to Modulate the Cellular Niche

A systems biology strategy to decode mechanisms underlying CSC cell fate decisions involves challenging stemness regulatory networks with external experimental perturbations. Upon acquisition of unimodal and bimodal single cell omics or matched multi-omics, cell fate control decisions can be inspected to define robust cell states and novel regulators that control stemness transitions. Experimentally, this can be achieved using RNAi knockdown and CRISPR-based knockout experiments. High throughput methods that generate large perturbation datasets like the Connectivity Map (CMAP) are limited in their biological contexts (Lamb et al., 2006; Bush et al., 2017; Ye et al., 2018). Conversely, Perturb-Seq combines pooled perturbation screens with scRNA-seq and cellular readouts to assay many cells within a mixed culture (Dixit et al., 2016). MIX-Seq, a more recent approach, provides the ability to pool hundreds of cancer cell lines and co-treat them with one or more perturbations, simultaneously profile the cells' readout using scRNAseq, and resolve the identity of each cell based on single-nucleotide polymorphism (SNP) profiles (McFarland et al., 2020). Application of these exciting new approaches will undoubtedly expand current understanding of how genetic and phenotypic perturbations impact cells in different contexts, providing new tools that can potentially be applied to CSCs and their cellular niche.

SYSTEMS 'OMICS INTEGRATION

With the sea of available 'omic data, there is an urgent need for multi-omic data integration to provide systems-level information. Clustering of multi-omics has been implemented at various steps in the data analysis pipeline (e.g., early *vs.* late integration) [see reviews (Ramazzotti et al., 2018; Rappoport and Shamir, 2018)]. A drawback to all these strategies is that all data are treated equally, which may not reflect the biology of a disease (Ramazzotti et al., 2018). Recently, Stuart *el al.* suggested harmonizing single cell data across distinct modalities by selecting anchors (a common set of features) between datasets to recover matching cell states (Stuart et al., 2019; Stuart and Satija, 2019). A second key challenge is that some methods implicitly assume that data heterogeneity arises mostly from technical variation and is of no biological importance. To overcome this limitation, LIGER (linked inference of genomic experimental relationships) uses integrative non-negative matrix factorization (iNMF) for data reduction combined with joint clustering to define a cell label and assemble a neighborhood graph (Welch et al., 2019). Gao *et al.* have subsequently expanded LIGER capabilities to iteratively incorporate multiple data modalities and massive datasets (Gao et al., 2021). Overall, these strategies recover cell states but do not zoom in deep enough to capture the interplay between cells or levels of 'omic data.

To dissect the cellular niches, future strategies will need to integrate 'omic data in a way that achieves a better understanding of cellular states and their contributions to the diversity of CSC phenotypes. Such innovations will be key if we are to design novel therapeutic strategies that can disrupt key cell-cell communications and lead to the demise of CSC populations.

POPULATION DYNAMICS

Single cell experiments allow the study of tumors and their heterogenous cell populations that often coexist in an evolutionary continuum. Pseudotime trajectory methods (also known as trajectory inference methods) (Trapnell et al., 2014; Haghverdi et al., 2016; Setty et al., 2016; Saelens et al., 2019; Wolf et al., 2019) allow for the placement of cell populations within a trajectory based on their expression profiles. Because most single cell datasets are static and represent a unique snapshot in time, these cellular trajectories represent more a cellular states axis rather than real time, while encapsulating information from past and present. A challenge with the current pseudotime methodologies is that multiple dynamics can lead to the same cellular "state." For example, cellular fate decisions such as cell death, proliferation, or differentiation can result from multiple causes. In order to understand the origin of these fates, we need to know the directionality of the biological process. Our ability to merge several biological snapshots in time, for example, from time series data, can help to decode the range of "real" existing states. Otherwise, the exploration of cellular states is currently being addressed in the field using dynamic inference methods. For example, Weinreb *et al.* used a dynamic inference framework named population balance analysis (Weinreb et al., 2018) that aims to limit the state search space by introducing biophysical constrains (cell density) to define cellular states. Conversely, Fischer et al. (2019) used RNA velocity information (spliced to unspliced ratio) as a mean to provide directionality to cellular trajectories. RNA velocity provides a measure of a cell's internal compass (La Manno et al., 2018; Bergen et al., 2021) by quantifying nascent and mature messenger RNA. Here, we can also use matched multi-omic data integration (scRNA-seq and scATAC-seq) to identify key biological entities in each cell population and constrain the range of truly available cellular states to infer cell population dynamics. Future integration of multi-modal omics with spatial information derived from IMC will help to increase our spaciotemporal resolution, infer more accurate cell relatedness measures, and tackle key questions such as the extent of diversity of the CSC niche and which candidate targets are promising to reduce or re-wire CSC populations.

CANCER STEM CELL SYSTEMS BIOLOGY—EMERGING INSIGHTS INTO CSC STEMNESS

Figure 2 summarizes representative systems biology approaches that can decipher stemness of CSCs. Current and new technological advances are essential to probe different layers of CSC regulation. Moreover, there is an urgent need for deep cell phenotyping using insights gained from integration of available systems approaches. Cell subsets can be investigated for *in silico* isolation of CSCs and used to explore the degrees of stemness defined by the combined actions of signaling pathway activities, cell-cell interactions, and TF regulatory networks to formulate phenotypic recipes that drive cellular states. To mirror the fact that CSCs are exposed to a myriad of cellular environmental stimuli, perturbation experiments open the possibly to study the impact of genetic changes, zoom into cellular rewiring, and identify cellular vulnerabilities. A combination of these approaches may overcome current limitations in targeting CSCs and allow the identification of novel targetable genes.

FUTURE IMPACT ON INDIVIDUALIZED MEDICINE

In summary, CSCs reside in tumor ecosystems composed of a plethora of cell types communicating in ways that drive cellular phenotypes. Therapeutics that target cell-cell interactions have become a useful tool in clinical practice and can be considered for CSC targeting (He and Xu, 2020). Key examples include ipilimumab, which targets the CD28/cytotoxic T lymphocyte antigen 4 (CTLA4) interaction, as well as pembrolizumab and nivolumab, which both target the programmed cell death 1 (PD1)/PD1 ligand 1 (PD-L1) interaction (Topalian et al., 2012). In addition to these FDA-approved immune checkpoint inhibitors, other inhibitory immunoreceptors that are being evaluated as potential targets for clinical intervention include LAG3, TIM3, TIGIT, B7H3, CD93, CD73, adenosine A2A receptor and BTLA (He and Xu, 2020). Despite the clear success of immune checkpoint inhibitors in several tumor types, response rates are limited (10–30%), especially in solid

tumors (Hamanishi et al., 2015; Sarkar et al., 2016; Dempke et al., 2017; Disis et al., 2019; Palaia et al., 2020). The limited response rates seen with these agents are likely due to the complex network of interactions involving multiple cell types present in the TME, including CSCs, which leads to phenotypic heterogeneity we do not yet adequately understand (Sarkar et al., 2016). CSCs themselves exhibit immunosuppressive properties such as expression of inhibitory checkpoint ligands, low expression of MHC-I molecules and natural killer cell (NK cell) receptors, and low or absent expression of innate immune receptors, which renders the CSCs resistant to killing by a variety of immune cells (Bayik and Lathia, 2021). Inhibitory activity of immune checkpoints are determined by the cell surface levels of inhibitory receptors, ligand interactions with those receptors, turnover processes, and posttranslational modifications that regulate signal transduction (He and Xu, 2020). Therefore, most recently, CSC targeting has been carried out with combinations of dendritic cell-based vaccines, oncolytic viruses, and immune checkpoint blockades (for review see (Badrinath and Yoo, 2019)). Better understanding of potentially targetable ligand-receptor interactions involving CSCs has the potential to tailor these strategies. Furthermore, such understanding has the potential to expand the targetable interactions beyond tumor-immune cell interactions to include tumor-nonimmune stroma interactions as well.

Successful application of singe cell technologies and the integration of different modalities are paramount for better understanding of the factors that determine whether CSCs will respond to various therapies or not. Improved ability to quantify ligand-receptor interactions, dissect their spatial relationship (co-localization) and assess their association with outcome appear to be needed if we are to devise individualized CSC targeting. Indeed, current analyses suggest that for tumor-immune targeting there may not be a single predictor of clinical response. Instead, it is possible that the strengths of multiple ligand-receptor interactions will need to be assessed in addition to immune checkpoint components in order to predict response to immune checkpoint blockade (Ribas and Wolchok, 2018). Systems biology techniques are capable of extracting this biological information from 'omic data and helping derive a systems view.

In contrast to CSC cell surface markers that are expressed on stem cells, intracellular stem cell markers such as aldehyde dehydrogenase (ALDH) enzymes are an intracellular target amenable of intervention that can also enable some level of treatment individualization. ALDH activity identifies CSCs in numerous cancers (Deng et al., 2010; Landen et al., 2010; Silva et al., 2011). Recently, Raghavan et al. demonstrated that ovarian cancer spheroids derived from cells that survived chemotherapy (cisplatin) displayed lower ALDH expression, complete loss of CD133 expression, and resistance to cisplatin/ALDH inhibitor combination treatment while spheroids that were resistant to cisplatin/JAK2 inhibitor combinations contained an increased number of $ALDH^+$ cells (Raghavan et al., 2017; Chefetz et al., 2019). Thus, stratification of patients according to their CSC type (i.e., CSC markers and expression levels) pre- and post-therapy can potentially lead to more personalized treatment approaches (Patsalias and Kozovska, 2021). Ultimately this approach will not only allow us to better stratify patients for targeted and combinatorial therapies, but also potentially identify novel targets in CSCs.

CONCLUSION

Targeting CSCs, as well as the phenotypic and functional heterogeneity of the bulk tumor cells derived from them, remains an unsolved clinical challenge. Phenotypic plasticity of CSCs fuels adaptive phenotypes that contribute to tumor chemoresistance and poor clinical outcomes. A second layer of complexity arises from spatially distinct CSC niches. In this review we focused on interrogating the tumor niche to zoom in on the resident CSCs and provide insights on potential pharmacological approaches. To date no scholarly review covers this specific topic under a unified systems biology framework and new insights on targeting CSCs and strategies to engineer TME are still limited. The use of 'omics technologies as well as systems biology and computational methodologies has the potential to revolutionize the process of identifying and studying the CSC niche. While a wide array of methods have been developed to interrogate tumor heterogeneity, available methods still do not fully characterize the phenotypic states of CSCs or asses their plasticity and its impact on drug sensitivity. Therefore, there is an urgent need to develop tools that better integrate multimodal datasets to capture these cellular complexities. A crucial next step in the study of CSCs is to characterize their contributions to intratumoral heterogeneity, at various regulatory levels, from genotype to phenotype. If we are successful, the development of models to spatially localize CSC populations within tumors and dissect their contributions to tumor initiation, progression, and drug resistance will ultimately allow us to devise innovative strategies that target CSCs and improve cancer therapy.

AUTHOR CONTRIBUTIONS

CC, TMW, CYU, JCVB, DDB, SHK, and HL drafted and edited the manuscript.

FUNDING

This work was supported by grants from National Institutes of Health (NIH) (R01 CA208517, R01 AG056318, R01 AG61796, P50 CA136393, R01 CA240323); the Glenn Foundation for Medical Research, the Mayo Clinic Center for Biomedical Discovery, the Mayo Clinic Center for Individualized Medicine, Mayo Clinic Cancer Center, and the David F. and Margaret T. Grohne Cancer Immunology and Immunotherapy Program.

REFERENCES

Alvarez, M. J., Shen, Y., Giorgi, F. M., Lachmann, A., Ding, B. B., Ye, B. H., et al. (2016). Functional Characterization of Somatic Mutations in Cancer Using Network-Based Inference of Protein Activity. *Nat. Genet.* 48 (8), 838–847. doi:10.1038/ng.3593

Aran, D., Camarda, R., Odegaard, J., Paik, H., Oskotsky, B., Krings, G., et al. (2017). Comprehensive Analysis of normal Adjacent to Tumor Transcriptomes. *Nat. Commun.* 8 (1), 1077. doi:10.1038/s41467-017-01027-z

Badrinath, N., and Yoo, S. Y. (2019). Recent Advances in Cancer Stem Cell-Targeted Immunotherapy. *Cancers (Basel)* 11 (3), E310. doi:10.3390/cancers11030310

Bagaev, A., Kotlov, N., Nomie, K., Svekolkin, V., Gafurov, A., Isaeva, O., et al. (2021). Conserved Pan-Cancer Microenvironment Subtypes Predict Response to Immunotherapy. *Cancer Cell* 39 (6), 845–865. doi:10.1016/j.ccell.2021.04.014

Basso, K., Margolin, A. A., Stolovitzky, G., Klein, U., Dalla-Favera, R., and Califano, A. (2005). Reverse Engineering of Regulatory Networks in Human B Cells. *Nat. Genet.* 37 (4), 382–390. doi:10.1038/ng1532

Bayik, D., and Lathia, J. D. (2021). Cancer Stem Cell-Immune Cell Crosstalk in Tumour Progression. *Nat. Rev. Cancer* 21, 526. doi:10.1038/s41568-021-00366-w

Behbehani, G. K., Thom, C., Zunder, E. R., Finck, R., Gaudilliere, B., Fragiadakis, G. K., et al. (2014). Transient Partial Permeabilization with Saponin Enables Cellular Barcoding Prior to Surface Marker Staining. *Cytometry* 85 (12), 1011–1019. doi:10.1002/cyto.a.22573

Bergen, V., Soldatov, R. A., Kharchenko, P. V., and Theis, F. J. (2021). RNA Velocity-Current Challenges and Future Perspectives. *Mol. Syst. Biol.* 17 (8), e10282. doi:10.15252/msb.202110282

Bienz, M., and Clevers, H. (2003). Armadillo/β-catenin Signals in the Nucleus - Proof beyond a Reasonable Doubt? *Nat. Cel Biol.* 5 (3), 179–182. doi:10.1038/ncb0303-179

Bodenmiller, B. (2016). Multiplexed Epitope-Based Tissue Imaging for Discovery and Healthcare Applications. *Cel Syst.* 2 (4), 225–238. doi:10.1016/j.cels.2016.03.008

Boisset, J.-C., Vivié, J., Grün, D., Muraro, M. J., Lyubimova, A., and van Oudenaarden, A. (2018). Mapping the Physical Network of Cellular Interactions. *Nat. Methods* 15 (7), 547–553. doi:10.1038/s41592-018-0009-z

Bouzekri, A., Esch, A., and Ornatsky, O. (2019). Multidimensional Profiling of Drug-treated Cells by Imaging Mass Cytometry. *FEBS Open Bio* 9 (9), 1652–1669. doi:10.1002/2211-5463.12692

Bracci, L., Fragale, A., Gabriele, L., and Moschella, F. (2020). Towards a Systems Immunology Approach to Unravel Responses to Cancer Immunotherapy. *Front. Immunol.* 11, 582744. doi:10.3389/fimmu.2020.582744

Brock, A., Krause, S., Li, H., Kowalski, M., Goldberg, M. S., Collins, J. J., et al. (2014). Silencing HoxA1 by Intraductal Injection of siRNA Lipidoid Nanoparticles Prevents Mammary Tumor Progression in Mice. *Sci. Transl. Med.* 6 (217), 217ra2. doi:10.1126/scitranslmed.3007048

Browaeys, R., Saelens, W., and Saeys, Y. (2020). NicheNet: Modeling Intercellular Communication by Linking Ligands to Target Genes. *Nat. Methods* 17 (2), 159–162. doi:10.1038/s41592-019-0667-5

Bush, E. C., Ray, F., Alvarez, M. J., Realubit, R., Li, H., Karan, C., et al. (2017). PLATE-Seq for Genome-wide Regulatory Network Analysis of High-Throughput Screens. *Nat. Commun.* 8 (1), 105. doi:10.1038/s41467-017-00136-z

Cahan, P., Li, H., Morris, S. A., Lummertz da Rocha, E., Daley, G. Q., and Collins, J. J. (2014). CellNet: Network Biology Applied to Stem Cell Engineering. *Cell* 158 (4), 903–915. doi:10.1016/j.cell.2014.07.020

Chang, Q., Ornatsky, O. I., Siddiqui, I., Loboda, A., Baranov, V. I., and Hedley, D. W. (2017). Imaging Mass Cytometry. *Cytometry* 91 (2), 160–169. doi:10.1002/cyto.a.23053

Chefetz, I., Grimley, E., Yang, K., Hong, L., Vinogradova, E. V., Suciu, R., et al. (2019). A Pan-ALDH1A Inhibitor Induces Necroptosis in Ovarian Cancer Stem-like Cells. *Cel Rep.* 26 (11), 3061–3075. doi:10.1016/j.celrep.2019.02.032

Cohen, M., Giladi, A., Gorki, A.-D., Solodkin, D. G., Zada, M., Hladik, A., et al. (2018). Lung Single-Cell Signaling Interaction Map Reveals Basophil Role in Macrophage Imprinting. *Cell* 175 (4), 1031–1044. doi:10.1016/j.cell.2018.09.009

da Rocha, E. L., Ung, C. Y., McGehee, C. D., Correia, C., and Li, H. (2016). NetDecoder: a Network Biology Platform that Decodes Context-specific Biological Networks and Gene Activities. *Nucleic Acids Res.* 44 (10), e100. doi:10.1093/nar/gkw166

Davis, M. M., Tato, C. M., and Furman, D. (2017). Systems Immunology: Just Getting Started. *Nat. Immunol.* 18 (7), 725–732. doi:10.1038/ni.3768

Dempke, W. C. M., Fenchel, K., Uciechowski, P., and Dale, S. P. (2017). Second- and Third-Generation Drugs for Immuno-Oncology Treatment-The More the Better? *Eur. J. Cancer* 74, 55–72. doi:10.1016/j.ejca.2017.01.001

Deng, S., Yang, X., Lassus, H., Liang, S., Kaur, S., Ye, Q., et al. (2010). Distinct Expression Levels and Patterns of Stem Cell Marker, Aldehyde Dehydrogenase Isoform 1 (ALDH1), in Human Epithelial Cancers. *PLoS One* 5 (4), e10277. doi:10.1371/journal.pone.0010277

Disis, M. L., Taylor, M. H., Kelly, K., Beck, J. T., Gordon, M., Moore, K. M., et al. (2019). Efficacy and Safety of Avelumab for Patients with Recurrent or Refractory Ovarian Cancer. *JAMA Oncol.* 5 (3), 393–401. doi:10.1001/jamaoncol.2018.6258

Dixit, A., Parnas, O., Li, B., Chen, J., Fulco, C. P., Jerby-Arnon, L., et al. (2016). Perturb-Seq: Dissecting Molecular Circuits with Scalable Single-Cell RNA Profiling of Pooled Genetic Screens. *Cell* 167 (7), 1853–1866. doi:10.1016/j.cell.2016.11.038

Efremova, M., Vento-Tormo, M., Teichmann, S. A., and Vento-Tormo, R. (2020). CellPhoneDB: Inferring Cell-Cell Communication from Combined Expression of Multi-Subunit Ligand-Receptor Complexes. *Nat. Protoc.* 15 (4), 1484–1506. doi:10.1038/s41596-020-0292-x

Elmentaite, R., Teichmann, S. A., and Madissoon, E. (2019). Studying Immune to Non-immune Cell Cross-Talk Using Single-Cell Technologies. *Curr. Opin. Syst. Biol.* 18, 87–94. doi:10.1016/j.coisb.2019.10.005

Ferraro, G. B., Ali, A., Luengo, A., Kodack, D. P., Deik, A., Abbott, K. L., et al. (2021). Fatty Acid Synthesis Is Required for Breast Cancer Brain Metastasis. *Nat. Cancer* 2 (4), 414–428. doi:10.1038/s43018-021-00183-y

Fischer, D. S., Fiedler, A. K., Kernfeld, E. M., Genga, R. M. J., Bastidas-Ponce, A., Bakhti, M., et al. (2019). Inferring Population Dynamics from Single-Cell RNA-Sequencing Time Series Data. *Nat. Biotechnol.* 37 (4), 461–468. doi:10.1038/s41587-019-0088-0

Friedmann-Morvinski, D., and Verma, I. M. (2014). Dedifferentiation and Reprogramming: Origins of Cancer Stem Cells. *EMBO Rep.* 15 (3), 244–253. doi:10.1002/embr.201338254

Gadalla, R., Noamani, B., MacLeod, B. L., Dickson, R. J., Guo, M., Xu, W., et al. (2019). Validation of CyTOF against Flow Cytometry for Immunological Studies and Monitoring of Human Cancer Clinical Trials. *Front. Oncol.* 9, 415. doi:10.3389/fonc.2019.00415

Galluzzi, L., Spranger, S., Fuchs, E., and López-Soto, A. (2019). WNT Signaling in Cancer Immunosurveillance. *Trends Cel Biol.* 29 (1), 44–65. doi:10.1016/j.tcb.2018.08.005

Gao, C., Liu, J., Kriebel, A. R., Preissl, S., Luo, C., Castanon, R., et al. (2021). Iterative Single-Cell Multi-Omic Integration Using Online Learning. *Nat. Biotechnol.* 39, 1000. doi:10.1038/s41587-021-00867-x

Gautam, P., Hamashima, K., Chen, Y., Zeng, Y., Makovoz, B., Parikh, B. H., et al. (2021). Multi-species Single-Cell Transcriptomic Analysis of Ocular Compartment Regulons. *Nat. Commun.* 12 (1), 5675. doi:10.1038/s41467-021-25968-8

Ghanat Bari, M., Ung, C. Y., Zhang, C., Zhu, S., and Li, H. (2017). Machine Learning-Assisted Network Inference Approach to Identify a New Class of Genes that Coordinate the Functionality of Cancer Networks. *Sci. Rep.* 7 (1), 6993. doi:10.1038/s41598-017-07481-5

Giesen, C., Wang, H. A. O., Schapiro, D., Zivanovic, N., Jacobs, A., Hattendorf, B., et al. (2014). Highly Multiplexed Imaging of Tumor Tissues with Subcellular Resolution by Mass Cytometry. *Nat. Methods* 11 (4), 417–422. doi:10.1038/nmeth.2869

Gingold, J., Zhou, R., Lemischka, I. R., and Lee, D.-F. (2016). Modeling Cancer with Pluripotent Stem Cells. *Trends Cancer* 2 (9), 485–494. doi:10.1016/j.trecan.2016.07.007

Graham, K., Ge, X., de las Morenas, A., Tripathi, A., and Rosenberg, C. L. (2011). Gene Expression Profiles of Estrogen Receptor-Positive and Estrogen Receptor-Negative Breast Cancers Are Detectable in Histologically normal Breast Epithelium. *Clin. Cancer Res.* 17 (2), 236–246. doi:10.1158/1078-0432.ccr-10-1369

Greenwald, N. F., Miller, G., Moen, E., Kong, A., Kagel, A., Dougherty, T., et al. (2021). Whole-cell Segmentation of Tissue Images with Human-Level Performance Using Large-Scale Data Annotation and Deep Learning. *Nat. Biotechnol* 1–11. doi:10.1038/s41587-021-01094-0

Haghverdi, L., Büttner, M., Wolf, F. A., Buettner, F., and Theis, F. J. (2016). Diffusion Pseudotime Robustly Reconstructs Lineage Branching. *Nat. Methods* 13 (10), 845–848. doi:10.1038/nmeth.3971

Hall, J. A., Grainger, J. R., Spencer, S. P., and Belkaid, Y. (2011). The Role of Retinoic Acid in Tolerance and Immunity. *Immunity* 35 (1), 13–22. doi:10.1016/j.immuni.2011.07.002

Hamanishi, J., Mandai, M., Ikeda, T., Minami, M., Kawaguchi, A., Murayama, T., et al. (2015). Safety and Antitumor Activity of Anti-PD-1 Antibody, Nivolumab, in Patients with Platinum-Resistant Ovarian Cancer. *J. Clin. Oncol.* 33 (34), 4015–4022. doi:10.1200/jco.2015.62.3397

He, X., and Xu, C. (2020). Immune Checkpoint Signaling and Cancer Immunotherapy. *Cell Res.* 30 (8), 660–669. doi:10.1038/s41422-020-0343-4

Holtzhausen, A., Zhao, F., Evans, K. S., Tsutsui, M., Orabona, C., Tyler, D. S., et al. (2015). Melanoma-Derived Wnt5a Promotes Local Dendritic-Cell Expression of IDO and Immunotolerance: Opportunities for Pharmacologic Enhancement of Immunotherapy. *Cancer Immunol. Res.* 3 (9), 1082–1095. doi:10.1158/2326-6066.cir-14-0167

Huggins, I. J., Bos, T., Gaylord, O., Jessen, C., Lonquich, B., Puranen, A., et al. (2017). The WNT Target SP5 Negatively Regulates WNT Transcriptional Programs in Human Pluripotent Stem Cells. *Nat. Commun.* 8 (1), 1034. doi:10.1038/s41467-017-01203-1

Hurvitz, S. A., Caswell-Jin, J. L., McNamara, K. L., Zoeller, J. J., Bean, G. R., Dichmann, R., et al. (2020). Pathologic and Molecular Responses to Neoadjuvant Trastuzumab And/or Lapatinib from a Phase II Randomized Trial in HER2-Positive Breast Cancer (TRIO-US B07). *Nat. Commun.* 11 (1), 5824. doi:10.1038/s41467-020-19494-2

Jenkins, R. W., Aref, A. R., Lizotte, P. H., Ivanova, E., Stinson, S., Zhou, C. W., et al. (2018). *Ex Vivo* Profiling of PD-1 Blockade Using Organotypic Tumor Spheroids. *Cancer Discov.* 8 (2), 196–215. doi:10.1158/2159-8290.CD-17-0833

Kalbasi, A., and Ribas, A. (2020). Tumour-intrinsic Resistance to Immune Checkpoint Blockade. *Nat. Rev. Immunol.* 20 (1), 25–39. doi:10.1038/s41577-019-0218-4

Kirschner, M. W. (2005). The Meaning of Systems Biology. *Cell* 121 (4), 503–504. doi:10.1016/j.cell.2005.05.005

Kumar, M. P., Du, J., Lagoudas, G., Jiao, Y., Sawyer, A., Drummond, D. C., et al. (2018). Analysis of Single-Cell RNA-Seq Identifies Cell-Cell Communication Associated with Tumor Characteristics. *Cel Rep.* 25 (6), 1458–1468. doi:10.1016/j.celrep.2018.10.047

La Manno, G., Soldatov, R., Zeisel, A., Braun, E., Hochgerner, H., Petukhov, V., et al. (2018). RNA Velocity of Single Cells. *Nature* 560 (7719), 494–498. doi:10.1038/s41586-018-0414-6

Labani-Motlagh, A., Ashja-Mahdavi, M., and Loskog, A. (2020). The Tumor Microenvironment: A Milieu Hindering and Obstructing Antitumor Immune Responses. *Front. Immunol.* 11, 940. doi:10.3389/fimmu.2020.00940

LaFave, L. M., Kartha, V. K., Ma, S., Meli, K., Del Priore, I., Lareau, C., et al. (2020). Epigenomic State Transitions Characterize Tumor Progression in Mouse Lung Adenocarcinoma. *Cancer Cell* 38 (2), 212–228. doi:10.1016/j.ccell.2020.06.006

Lamb, J., Crawford, E. D., Peck, D., Modell, J. W., Blat, I. C., Wrobel, M. J., et al. (2006). The Connectivity Map: Using Gene-Expression Signatures to Connect Small Molecules, Genes, and Disease. *Science* 313 (5795), 1929–1935. doi:10.1126/science.1132939

Landen, C. N., Jr., Goodman, B., Katre, A. A., Steg, A. D., Nick, A. M., Stone, R. L., et al. (2010). Targeting Aldehyde Dehydrogenase Cancer Stem Cells in Ovarian Cancer. *Mol. Cancer Ther.* 9 (12), 3186–3199. doi:10.1158/1535-7163.mct-10-0563

Luke, J. J., Bao, R., Sweis, R. F., Spranger, S., and Gajewski, T. F. (2019). WNT/β-catenin Pathway Activation Correlates with Immune Exclusion across Human Cancers. *Clin. Cancer Res.* 25 (10), 3074–3083. doi:10.1158/1078-0432.ccr-18-1942

Lyssiotis, C. A., and Kimmelman, A. C. (2017). Metabolic Interactions in the Tumor Microenvironment. *Trends Cel Biol.* 27 (11), 863–875. doi:10.1016/j.tcb.2017.06.003

Malta, T. M., Sokolov, A., Gentles, A. J., Burzykowski, T., Poisson, L., Weinstein, J. N., et al. (2018). Machine Learning Identifies Stemness Features Associated with Oncogenic Dedifferentiation. *Cell* 173 (2), 338–e15. doi:10.1016/j.cell.2018.03.034

Marjanovic, N. D., Hofree, M., Chan, J. E., Canner, D., Wu, K., Trakala, M., et al. (2020). Emergence of a High-Plasticity Cell State during Lung Cancer Evolution. *Cancer Cell* 38 (2), 229–246. doi:10.1016/j.ccell.2020.06.012

McFarland, J. M., Paolella, B. R., Warren, A., Geiger-Schuller, K., Shibue, T., Rothberg, M., et al. (2020). Multiplexed Single-Cell Transcriptional Response Profiling to Define Cancer Vulnerabilities and Therapeutic Mechanism of Action. *Nat. Commun.* 11 (1), 4296. doi:10.1038/s41467-020-17440-w

Newman, A. M., Liu, C. L., Green, M. R., Gentles, A. J., Feng, W., Xu, Y., et al. (2015). Robust Enumeration of Cell Subsets from Tissue Expression Profiles. *Nat. Methods* 12 (5), 453–457. doi:10.1038/nmeth.3337

Ng, A., and Barker, N. (2015). Ovary and Fimbrial Stem Cells: Biology, Niche and Cancer Origins. *Nat. Rev. Mol. Cel Biol.* 16 (10), 625–638. doi:10.1038/nrm4056

Nguyen, V. H. L., Hough, R., Bernaudo, S., and Peng, C. (2019). Wnt/β-catenin Signalling in Ovarian Cancer: Insights into its Hyperactivation and Function in Tumorigenesis. *J. Ovarian Res.* 12 (1), 122. doi:10.1186/s13048-019-0596-z

Olive, K. P., Jacobetz, M. A., Davidson, C. J., Gopinathan, A., McIntyre, D., Honess, D., et al. (2009). Inhibition of Hedgehog Signaling Enhances Delivery of Chemotherapy in a Mouse Model of Pancreatic Cancer. *Science* 324 (5933), 1457–1461. doi:10.1126/science.1171362

Palaia, I., Tomao, F., Sassu, C. M., Musacchio, L., and Benedetti Panici, P. (2020). Immunotherapy for Ovarian Cancer: Recent Advances and Combination Therapeutic Approaches. *Onco Targets Ther.* 13, 6109–6129. doi:10.2147/ott.s205950

Patsalias, A., and Kozovska, Z. (2021). Personalized Medicine: Stem Cells in Colorectal Cancer Treatment. *Biomed. Pharmacother.* 141, 111821. doi:10.1016/j.biopha.2021.111821

Pinto, J. P., Kalathur, R. K., Oliveira, D. V., Barata, T., Machado, R. S. R., Machado, S., et al. (2015). StemChecker: a Web-Based Tool to Discover and Explore Stemness Signatures in Gene Sets. *Nucleic Acids Res.* 43 (W1), W72–W77. doi:10.1093/nar/gkv529

Plaks, V., Kong, N., and Werb, Z. (2015). The Cancer Stem Cell Niche: How Essential Is the Niche in Regulating Stemness of Tumor Cells? *Cell Stem Cell* 16 (3), 225–238. doi:10.1016/j.stem.2015.02.015

Raghavan, S., Mehta, P., Ward, M. R., Bregenzer, M. E., Fleck, E. M. A., Tan, L., et al. (2017). Personalized Medicine-Based Approach to Model Patterns of Chemoresistance and Tumor Recurrence Using Ovarian Cancer Stem Cell Spheroids. *Clin. Cancer Res.* 23 (22), 6934–6945. doi:10.1158/1078-0432.ccr-17-0133

Ramazzotti, D., Lal, A., Wang, B., Batzoglou, S., and Sidow, A. (2018). Multi-omic Tumor Data Reveal Diversity of Molecular Mechanisms that Correlate with Survival. *Nat. Commun.* 9 (1), 4453. doi:10.1038/s41467-018-06921-8

Rappoport, N., and Shamir, R. (2018). Multi-omic and Multi-View Clustering Algorithms: Review and Cancer Benchmark. *Nucleic Acids Res.* 46 (20), 10546–10562. doi:10.1093/nar/gky889

Regev, A., Teichmann, S. A., Lander, E. S., Amit, I., Benoist, C., Birney, E., et al. (2017). The Human Cell Atlas. *Elife* 6, e27041. doi:10.7554/eLife.27041

Ribas, A., and Wolchok, J. D. (2018). Cancer Immunotherapy Using Checkpoint Blockade. *Science* 359 (6382), 1350–1355. doi:10.1126/science.aar4060

Risom, T., Glass, D. R., Liu, C. C., Rivero-Gutiérrez, B., Baranski, A., McCaffrey, E. F., et al. (2022). Transition to Invasive Breast Cancer Is Associated with Progressive Changes in the Structure and Composition of Tumor Stroma. *Cell* 185 (2), 299–310.e18. doi:10.1016/j.cell.2021.12.023

Saelens, W., Cannoodt, R., Todorov, H., and Saeys, Y. (2019). A Comparison of Single-Cell Trajectory Inference Methods. *Nat. Biotechnol.* 37 (5), 547–554. doi:10.1038/s41587-019-0071-9

Sanmamed, M. F., and Chen, L. (2014). Inducible Expression of B7-H1 (PD-L1) and its Selective Role in Tumor Site Immune Modulation. *Cancer J.* 20 (4), 256–261. doi:10.1097/ppo.0000000000000061

Sanmamed, M. F., and Chen, L. (2018). A Paradigm Shift in Cancer Immunotherapy: From Enhancement to Normalization. *Cell* 175 (2), 313–326. doi:10.1016/j.cell.2018.09.035

Sarkar, S., Sabhachandani, P., Stroopinsky, D., Palmer, K., Cohen, N., Rosenblatt, J., et al. (2016). Dynamic Analysis of Immune and Cancer Cell Interactions at Single Cell Level in Microfluidic Droplets. *Biomicrofluidics* 10 (5), 054115. doi:10.1063/1.4964716

Schapiro, D., Jackson, H. W., Raghuraman, S., Fischer, J. R., Zanotelli, V. R. T., Schulz, D., et al. (2017). histoCAT: Analysis of Cell Phenotypes and Interactions in Multiplex Image Cytometry Data. *Nat. Methods* 14 (9), 873–876. doi:10.1038/nmeth.4391

Setty, M., Tadmor, M. D., Reich-Zeliger, S., Angel, O., Salame, T. M., Kathail, P., et al. (2016). Wishbone Identifies Bifurcating Developmental Trajectories from Single-Cell Data. *Nat. Biotechnol.* 34 (6), 637–645. doi:10.1038/nbt.3569

Silva, I. A., Bai, S., McLean, K., Yang, K., Griffith, K., Thomas, D., et al. (2011). Aldehyde Dehydrogenase in Combination with CD133 Defines Angiogenic Ovarian Cancer Stem Cells that Portend Poor Patient Survival. *Cancer Res.* 71 (11), 3991–4001. doi:10.1158/0008-5472.can-10-3175

Spranger, S., and Gajewski, T. F. (2015). A New Paradigm for Tumor Immune Escape: β-catenin-driven Immune Exclusion. *J. Immunotherapy Cancer* 3, 43. doi:10.1186/s40425-015-0089-6

Spranger, S., Bao, R., and Gajewski, T. F. (2015). Melanoma-intrinsic β-catenin Signalling Prevents Anti-tumour Immunity. *Nature* 523 (7559), 231–235. doi:10.1038/nature14404

Spranger, S., Dai, D., Horton, B., and Gajewski, T. F. (2017). Tumor-Residing Batf3 Dendritic Cells Are Required for Effector T Cell Trafficking and Adoptive T Cell Therapy. *Cancer Cell* 31 (5), 711–723. doi:10.1016/j.ccell.2017.04.003

Stuart, T., and Satija, R. (2019). Integrative Single-Cell Analysis. *Nat. Rev. Genet.* 20 (5), 257–272. doi:10.1038/s41576-019-0093-7

Stuart, T., Butler, A., Hoffman, P., Hafemeister, C., Papalexi, E., Mauck, W. M., et al. (2019). Comprehensive Integration of Single-Cell Data. *Cell* 177 (7), 1888–1902. doi:10.1016/j.cell.2019.05.031

Thorsson, V., Gibbs, D. L., Brown, S. D., Wolf, D., Bortone, D. S., Ou Yang, T. H., et al. (2018). The Immune Landscape of Cancer. *Immunity* 48 (4), 812. doi:10.1016/j.immuni.2018.03.023

Topalian, S. L., Drake, C. G., and Pardoll, D. M. (2012). Targeting the PD-1/B7-H1(PD-L1) Pathway to Activate Anti-tumor Immunity. *Curr. Opin. Immunol.* 24 (2), 207–212. doi:10.1016/j.coi.2011.12.009

Trapnell, C., Cacchiarelli, D., Grimsby, J., Pokharel, P., Li, S., Morse, M., et al. (2014). The Dynamics and Regulators of Cell Fate Decisions Are Revealed by Pseudotemporal Ordering of Single Cells. *Nat. Biotechnol.* 32 (4), 381–386. doi:10.1038/nbt.2859

Ung, C. Y., Ghanat Bari, M., Zhang, C., Liang, J., Correia, C., and Li, H. (2019). Regulostat Inferelator: a Novel Network Biology Platform to Uncover Molecular Devices that Predetermine Cellular Response Phenotypes. *Nucleic Acids Res.* 47 (14), e82. doi:10.1093/nar/gkz417

van de Wetering, M., Oosterwegel, M., Dooijes, D., and Clevers, H. (1991). Identification and Cloning of TCF-1, a T Lymphocyte-specific Transcription Factor Containing a Sequence-specific HMG Box. *EMBO J.* 10 (1), 123–132. doi:10.1002/j.1460-2075.1991.tb07928.x

Vento-Tormo, R., Efremova, M., Botting, R. A., Turco, M. Y., Vento-Tormo, M., Meyer, K. B., et al. (2018). Single-cell Reconstruction of the Early Maternal-Fetal Interface in Humans. *Nature* 563 (7731), 347–353. doi:10.1038/s41586-018-0698-6

Vermeulen, L., De Sousa E Melo, F., van der Heijden, M., Cameron, K., de Jong, J. H., Borovski, T., et al. (2010). Wnt Activity Defines colon Cancer Stem Cells and Is Regulated by the Microenvironment. *Nat. Cel Biol.* 12 (5), 468–476. doi:10.1038/ncb2048

Visvader, J. E. (2011). Cells of Origin in Cancer. *Nature* 469 (7330), 314–322. doi:10.1038/nature09781

Vunjak-Novakovic, G., Ronaldson-Bouchard, K., and Radisic, M. (2021). Organs-on-a-chip Models for Biological Research. *Cell* 184 (18), 4597–4611. doi:10.1016/j.cell.2021.08.005

Wagner, J., Rapsomaniki, M. A., Chevrier, S., Anzeneder, T., Langwieder, C., Dykgers, A., et al. (2019). A Single-Cell Atlas of the Tumor and Immune Ecosystem of Human Breast Cancer. *Cell* 177 (5), 1330–1345. doi:10.1016/j.cell.2019.03.005

Wang B, B., Tian, T., Kalland, K.-H., Ke, X., and Qu, Y. (2018). Targeting Wnt/β-Catenin Signaling for Cancer Immunotherapy. *Trends Pharmacol. Sci.* 39 (7), 648–658. doi:10.1016/j.tips.2018.03.008

Wang X, X., Allen, W. E., Wright, M. A., Sylwestrak, E. L., Samusik, N., Vesuna, S., et al. (2018). Three-dimensional Intact-Tissue Sequencing of Single-Cell Transcriptional States. *Science* 361 (6400), eaat5691. doi:10.1126/science.aat5691

Weinreb, C., Wolock, S., Tusi, B. K., Socolovsky, M., and Klein, A. M. (2018). Fundamental Limits on Dynamic Inference from Single-Cell Snapshots. *Proc. Natl. Acad. Sci. USA* 115 (10), E2467–E2476. doi:10.1073/pnas.1714723115

Welch, J. D., Kozareva, V., Ferreira, A., Vanderburg, C., Martin, C., and Macosko, E. Z. (2019). Single-Cell Multi-Omic Integration Compares and Contrasts Features of Brain Cell Identity. *Cell* 177 (7), 1873–1887. doi:10.1016/j.cell.2019.05.006

Wolf, F. A., Hamey, F. K., Plass, M., Solana, J., Dahlin, J. S., Göttgens, B., et al. (2019). PAGA: Graph Abstraction Reconciles Clustering with Trajectory Inference through a Topology Preserving Map of Single Cells. *Genome Biol.* 20 (1), 59. doi:10.1186/s13059-019-1663-x

Yang, K., Wang, X., Zhang, H., Wang, Z., Nan, G., Li, Y., et al. (2016). The Evolving Roles of Canonical WNT Signaling in Stem Cells and Tumorigenesis: Implications in Targeted Cancer Therapies. *Lab. Invest.* 96 (2), 116–136. doi:10.1038/labinvest.2015.144

Yao, L., Jayasinghe, R. G., Thomas, B. E., Bhasin, S. S., Fernandez, N., Kourelis, T., et al. (2020). Integrated Cytof, Scrna-Seq and Cite-Seq Analysis of Bone Marrow Immune Microenvironment in the Mmrf Commpass Study. *Blood* 136, 28–29. doi:10.1182/blood-2020-142534

Ye, C., Ho, D. J., Neri, M., Yang, C., Kulkarni, T., Randhawa, R., et al. (2018). DRUG-seq for Miniaturized High-Throughput Transcriptome Profiling in Drug Discovery. *Nat. Commun.* 9 (1), 4307. doi:10.1038/s41467-018-06500-x

Zhang, X., Wang, L., and Qu, Y. (2020). Targeting the β-catenin Signaling for Cancer Therapy. *Pharmacol. Res.* 160, 104794. doi:10.1016/j.phrs.2020.104794

Zhou, J. X., Taramelli, R., Pedrini, E., Knijnenburg, T., and Huang, S. (2017). Extracting Intercellular Signaling Network of Cancer Tissues Using Ligand-Receptor Expression Patterns from Whole-Tumor and Single-Cell Transcriptomes. *Sci. Rep.* 7 (1), 8815. doi:10.1038/s41598-017-09307-w

Zitvogel, L., Pitt, J. M., Daillère, R., Smyth, M. J., and Kroemer, G. (2016). Mouse Models in Oncoimmunology. *Nat. Rev. Cancer* 16 (12), 759–773. doi:10.1038/nrc.2016.91

Conflict of Interest: The authors declare that the research was conducted in the absence of any commercial or financial relationships that could be construed as a potential conflict of interest.

Publisher's Note: All claims expressed in this article are solely those of the authors and do not necessarily represent those of their affiliated organizations, or those of the publisher, the editors and the reviewers. Any product that may be evaluated in this article, or claim that may be made by its manufacturer, is not guaranteed or endorsed by the publisher.

frontiers | Frontiers in Cell and Developmental Biology

REVIEW
published: 14 June 2022
doi: 10.3389/fcell.2022.862791

Self-Sustained Regulation or Self-Perpetuating Dysregulation: ROS-dependent HIF-YAP-Notch Signaling as a Double-Edged Sword on Stem Cell Physiology and Tumorigenesis

*Chin-Lin Guo**

Institute of Physics, Academia Sinica, Taipei, Taiwan

Organ development, homeostasis, and repair often rely on bidirectional, self-organized cell-niche interactions, through which cells select cell fate, such as stem cell self-renewal and differentiation. The niche contains multiplexed chemical and mechanical factors. How cells interpret niche structural information such as the 3D topology of organs and integrate with multiplexed mechano-chemical signals is an open and active research field. Among all the niche factors, reactive oxygen species (ROS) have recently gained growing interest. Once considered harmful, ROS are now recognized as an important niche factor in the regulation of tissue mechanics and topology through, for example, the HIF-YAP-Notch signaling pathways. These pathways are not only involved in the regulation of stem cell physiology but also associated with inflammation, neurological disorder, aging, tumorigenesis, and the regulation of the immune checkpoint molecule PD-L1. Positive feedback circuits have been identified in the interplay of ROS and HIF-YAP-Notch signaling, leading to the possibility that under aberrant conditions, self-organized, ROS-dependent physiological regulations can be switched to self-perpetuating dysregulation, making ROS a double-edged sword at the interface of stem cell physiology and tumorigenesis. In this review, we discuss the recent findings on how ROS and tissue mechanics affect YAP-HIF-Notch-PD-L1 signaling, hoping that the knowledge can be used to design strategies for stem cell-based and ROS-targeting therapy and tissue engineering.

Keywords: ROS, HIF, YAP, notch, tissue mechanics

OPEN ACCESS

Edited by:
Cheng Ming Chuong, University of Southern California, United States

Reviewed by:
*Sayan Chakraborty, Institute of Molecular and Cell Biology (A*STAR), Singapore*
Che-Chang Chang, Taipei Medical University, Taiwan

***Correspondence:**
Chin-Lin Guo
guochin@phys.sinica.edu.tw

Specialty section:
This article was submitted to Stem Cell Research, a section of the journal Frontiers in Cell and Developmental Biology

Received: *26 January 2022*
Accepted: *29 April 2022*
Published: *14 June 2022*

Citation:
Guo C-L (2022) Self-Sustained Regulation or Self-Perpetuating Dysregulation: ROS-dependent HIF-YAP-Notch Signaling as a Double-Edged Sword on Stem Cell Physiology and Tumorigenesis. Front. Cell Dev. Biol. 10:862791. doi: 10.3389/fcell.2022.862791

INTRODUCTION

The ability to self-renew and the potential to differentiate, at least, into one type of mature cell have made stem cells an essential element at various stages of development and a promising tool for regenerative medicine. In general, the selection of stem cell fate depends on the interplay of intracellular signaling and extracellular niche factors. These niche factors can be specified into two groups: chemical molecular factors and physical-mechanical factors. The chemical factors include molecular oxygen (O_2), reactive oxygen species (ROS), cell metabolites, morphogens, cytokines,

growth factors, and extracellular matrix (ECM) molecules. The physical factors contain passive elements (e.g., stiffness, plasticity, viscoelasticity, and 3D topology) and active mechanical forces (created by the cells and the surrounding environment, e.g., compression, stretching, hydrodynamic flow, hydrostatic pressure, and gravity). The responses to these mechano-chemical factors, such as hypoxic responses, cell mechanotransduction, and ROS signaling, have gained growing interest, as accumulating lines of evidence indicated that their interplay is involved in the regulation of stem cell homeostasis and development. Furthermore, the interplay of these responses can lead to tumorigenesis in the presence of genomic instability and aberrant cell signaling. In particular, ROS, the byproduct of energy production that has once been considered harmful due to their ability to damage DNA and proteins, are now recognized as an important signaling factor for the regulation of pathways involved in stem cell physiology and tumor progression.

ROS can spontaneously be created in the natural environment. For living systems, ROS are mainly produced by the mitochondria (Murphy, 2009; Juan et al., 2021) and the membrane-bound NADPH oxidases (NOX) (Bedard and Krause, 2007; Ushio-Fukai, 2009). The production of ROS is primarily controlled by cell metabolism, O_2, ROS themselves, and several signaling events of niche factors. Examples of these signaling events include the signaling for transforming growth factor-β (TGF-β) (Hiraga et al., 2013; Yan et al., 2014; Watson et al., 2016; Yazaki et al., 2021), epidermal growth factor (EGF) (Azimi et al., 2017; Dustin et al., 2020), insulin (Besse-Patin and Estall, 2014), insulin-like growth factor-1 (IGF-1) (Kang et al., 2016), inflammatory and immune-regulatory cytokines such as angiotensin II and tumor necrosis factor-alpha (TNF-α) (Anilkumar et al., 2008), calcium (Gorlach et al., 2015; Feno et al., 2019), mechanotransduction (Sauer et al., 2008; Brandes et al., 2014a), integrin-ECM interactions (de Rezende et al., 2012; Eble and de Rezende, 2014), and cell–cell adhesions (Lim et al., 2008). Conversely, ROS modulate the activities of several cell fate-decision factors. These factors include the oxygen sensor hypoxia-inducible factor (HIF) (Gerald et al., 2004; Saito et al., 2015; Kobayashi et al., 2021), the mechano-transducer Yes-associated protein (YAP) (Cho et al., 2020), the transducer for the cell differentiation transcription factor Notch, Notch intracellular domain (NICD) (Cai W.-X. et al., 2014; Caliceti et al., 2014; Yan et al., 2014; Sprouse et al., 2019; Yazaki et al., 2021), and the immune suppressor programmed death ligand-1 (PD-L1) (Bailly, 2020). Herein, HIF, YAP, and NICD act as a triad in stem cell physiology and tumorigenesis, as they can physically associate to influence each other (Qiang et al., 2012; Hu et al., 2014; Manderfield et al., 2015; Totaro et al., 2018a; Zhang X. et al., 2018; Engel-Pizcueta and Pujades, 2021). These associations include the coupling between the α subunits of HIF (i.e., HIF-1α/HIF-2α) and YAP (Xiang et al., 2015; Ma et al., 2017; Zhao et al., 2020) and the coupling between YAP and Notch (Totaro et al., 2018a). As for PD-L1, it is the ligand for the immune checkpoint receptors, programmed death-1 (PD-1) (Noman et al., 2014; Janse van Rensburg et al., 2018; Mansour et al., 2020). Recent studies indicate that the expression of PD-L1 is coupled with YAP, Notch, and HIF-1alpha signaling to potentiate the immune suppression and evasion in the progression of tumors (Barsoum et al., 2014; Noman et al., 2014; Lee et al., 2017; Miao et al., 2017; Kim M. H. et al., 2018; Zhou et al., 2019; Wen et al., 2020). Through these couplings, negative and positive feedback regulations can likely be established in the ROS-dependent YAP-HIF-Notch-(PD-L1) signaling axis, leading to a differential or switch-like behavior in the decision of cell fate. Thus, the interplay of hypoxic responses, ROS signaling, and cell mechanotransduction acts as a double-edged sword at the interface of organ development, tissue homeostasis, and cancer progression.

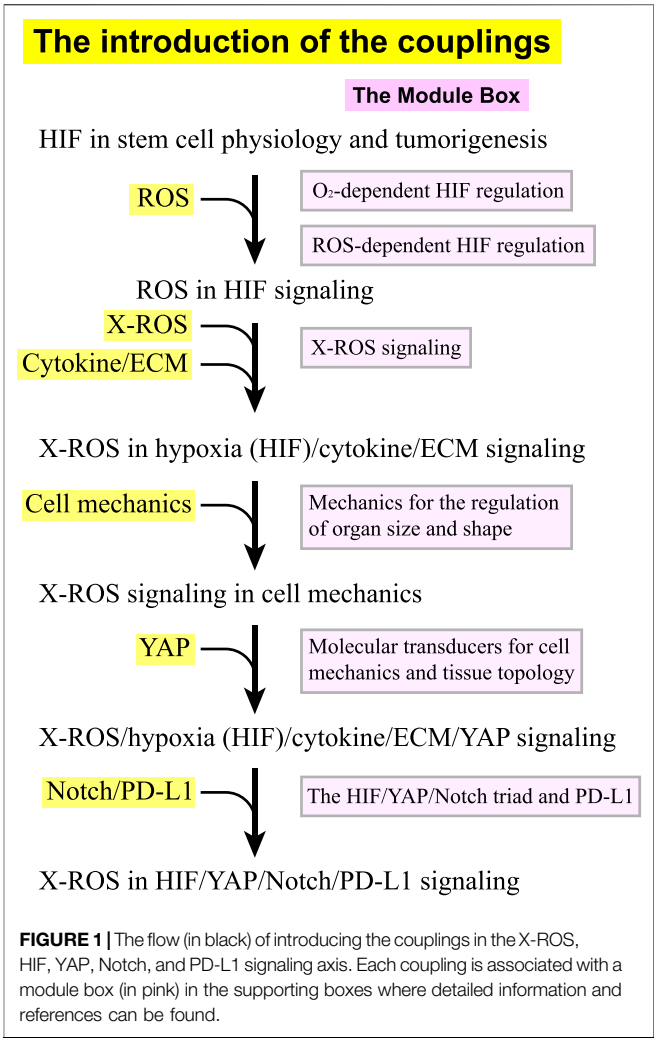

FIGURE 1 | The flow (in black) of introducing the couplings in the X-ROS, HIF, YAP, Notch, and PD-L1 signaling axis. Each coupling is associated with a module box (in pink) in the supporting boxes where detailed information and references can be found.

This review discusses how ROS are involved in the HIF, YAP, and Notch signaling pathways and how their coupling leads to positive or negative feedback for stem cell physiology and tumorigenesis. Given the complexity and the abundant molecular information in the coupling of ROS, HIF, YAP, Notch, PD-L1, and cell–ECM signaling, we organize this review in the following way. We define the signaling in ROS, HIF, YAP, Notch, PD-L1, cell–ECM, and cell mechanics as separated "modules" and introduce/add their coupling one

after another. Along with the introduction of the couplings, we provide "module boxes" for each component as the supporting boxes, where detailed molecular–cellular information and references can be found. **Figure 1** shows that we start with a brief discussion on HIF signaling in stem cell biology and tumors (**Section I**), followed by a section on the roles of ROS in HIF signaling (**Section II**). We then add the coupling of NOX-derived ROS (X-ROS) with the hypoxia (HIF)/cytokine/ECM signaling (**Section III**), followed by a section on the coupling of X-ROS with cell mechanics (**Section IV**), where we introduce the functional significance of cell mechanics and mechanotransduction. We then add the coupling of X-ROS/hypoxia (HIF)/cytokine/ECM signaling with YAP signaling (**Section V**), followed by the final section where we discuss the integrated roles of X-ROS in the HIF/YAP/Notch/PD-L1 signaling (**Section VI**). In the module boxes, we discuss how molecular oxygen O_2 regulates HIF stability (Module Box I), how ROS regulate HIF stability (Module Box II), and the X-ROS signaling (Module Box III). A modeling section is provided to discuss the phase diagram of ROS production quantitatively (Math Box I). How cell mechanics regulate organ size and shape (Module Box IV), the molecular transducers for cell mechanics and tissue topology (Module Box V), and the coupling of HIF/YAP/Notch triad with PD-L1 (Module Box VI) are also addressed.

MAIN TEXT

The Roles of HIF in Stem Cell Physiology and Tumorigenesis

For stem cell applications, one important issue is to maintain the full pluripotency of stem cells, which often requires hypoxia conditions. The major cellular responses to hypoxia are primarily mediated by hypoxia-inducible factors (HIFs) which act as transcription factors (Ezashi et al., 2005). HIFs consist of one α subunit and one β subunit. While the β subunit is expressed constitutively, the α subunit is regulated in an O_2- and ROS-dependent manner (Module Boxes I and II). Under normoxia, the α subunits are continuously ubiquitinated and targeted to degradation. Under hypoxia, the α subunit is stabilized to form a dimer with the β subunit. By translocating to the nucleus, the dimer regulates downstream gene expression through binding to the hypoxia-responsive element (HRE) (Harris, 2002). Three forms of α subunits, HIF-1α, HIF-2α, and HIF-3α, have been identified (Wang et al., 1995; Tian et al., 1997; Xu and Li, 2021). While HIF-1α and HIF-2α are structurally similar and share functions to a certain extent, HIF-3α contains several splice variants, some of which act as dominant-negative inhibitors of HIF-1α or HIF-2α (Majmundar et al., 2010; Xu and Li, 2021). Under hypoxia, HIF-1α induces transcription of more than 60 genes to regulate responses such as erythropoiesis, angiogenesis, cell proliferation, cell survival, and glucose and iron metabolism. By doing so, HIF-1α promotes oxygen delivery to the hypoxic region (Semenza, 2003) and switches cells to glycolytic metabolism in response to hypoxia (Lee J.-W. et al., 2004). HIF-1α also induces the expression of genes responsible for collagen deposition and stiffening (Gilkes et al., 2013), one of which is the gene for lysyl oxidase (LOX), the enzyme crosslinking ECM (Ji et al., 2013). In addition, through the altered metabolic flux that promotes the hydroxylation of collagen, HIF-1α renders the collagen matrix more resistant to degradation (Stegen et al., 2019). ECM stiffening, in turn, further promotes metabolic reprogramming (Ge et al., 2021). It has been shown that the altered cell metabolism can potentially activate HIF-1 (Halligan et al., 2016), leading to a positive feedback cycle. Consequently, niche stiffening and niche hypoxia can act synergistically through HIF-alpha to promote a bifurcated selection of cancer cell fate between the apoptotic and the aggressive phenotypes (Lv et al., 2017). In comparison, HIF-2α primarily regulates the expression of a panel of embryonic transcription factors and stemness-related genes such as OCT4, NANOG, and SOX2 (Covello et al., 2006; Gordan et al., 2007; Hu et al., 2014; Petruzzelli et al., 2014). Nevertheless, there are lines of evidence showing that HIF-2α also participates in ECM remodeling. For example, HIF-2α induces the expression of LOX to accelerate ECM deposition and crosslinking in thyroid-associated orbitopathy (Hikage et al., 2019) and the expression of laminin receptor CD49f to facilitate stem cell development in germline stem cells (GSCs), where the expression of CD49f further enhances the expression of HIF-2α, thereby forming a positive feedback loop (Au et al., 2021) (**Figure 2A**).

The segregation of biological functions in HIF-1α and HIF-2α signaling makes it plausible that these two factors are stabilized under different hypoxia conditions (Hu et al., 2014). HIF-1α is stabilized under severe hypoxia (niche oxygen concentrations <2%, i.e., $[O_2] < 20$ μM) (Hu et al., 2014). In comparison, HIF-2α is stabilized in a wider range of oxygen concentrations: from physiological oxygen concentrations (~7%, i.e., $[O_2]$ ~70 μM) to severely low oxygen concentrations (<2%) (Hu et al., 2014). The restricted requirement for HIF-1α stabilization indicates that the upregulation of glycolysis only occurs if the niche oxygen concentration is extremely low. As a result, the cells primarily use oxidative phosphorylation as the major energy production process. In contrast, the fact that HIF-2α is stabilized in a wide range of oxygen concentrations indicates that the cells can robustly maintain certain behavior such as stemness over the fluctuation of niche oxygen, a requisite to sustain cell fate in a fluctuating microenvironment. Note that the restricted conditions for the stabilization of HIF-1α might no longer exist in tumors, allowing tumor cells to use anaerobic metabolism and elicit angiogenesis even with abundant O_2 in the niche (Semenza, 2003; Masoud and Li, 2015). In fact, both HIF-1α and HIF-2α play important roles in tumor angiogenesis (Krock et al., 2011), survival (Chen and Sang, 2016), proliferation (Hubbi and Semenza, 2015), immune evasion (Barsoum et al., 2014), plasticity (Terry et al., 2017), invasion and metastasis (Zhong et al., 1999), chemo- and radio-therapy resistance (Moeller et al., 2004; Rohwer and Cramer, 2011), pH regulation, and metabolism (Hulikova et al., 2013). These two factors also help the emergence and the maintenance of cancer stem cells

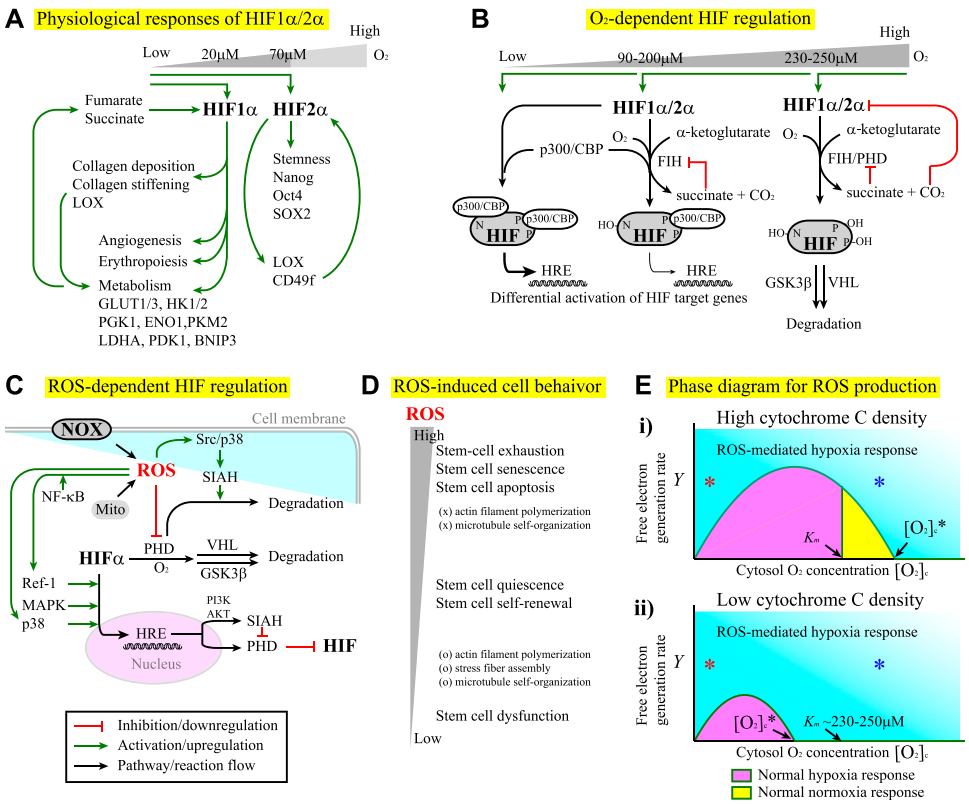

FIGURE 2 | (A) The differential responses of HIF-1α and HIF-2α to hypoxia conditions. See the main text for details. For all the figures hereafter, red lines indicate inhibition or downregulation, green lines indicate activation or upregulation, blue lines indicate physical association or recruitment, and black lines indicate the flow of the pathways, cascades, or reaction. **(B)** The factor inhibiting HIF (FIH) and prolyl hydroxylase domain-containing proteins (PHD) regulate HIF-1α and HIF-2α stability and transcriptional activity in an O_2 concentration-dependent manner. See Module Box II for details. **(C)** ROS produced by the NOX and/or the mitochondria (Mito) exhibit both positive and negative effects on the regulation of HIF-α subunits. See Module Box III for details. **(D)** Stem cells exhibit differential phenotypical behavior and cytoskeletal dynamics in response to the changes in ROS concentrations. **(E)** The phase diagrams for the separation of ROS-mediated hypoxia responses (cyan) from normal hypoxia (pink) and/or normoxia (yellow) responses at **(i)** high and **(ii)** low cytochrome C densities corresponding to the high and low critical oxygen concentrations ($[O_2]_c$*) for the onset of ROS-mediated hypoxia responses, respectively. See Math Box I for details. K_m is the K_m value of PHD for $[O_2]$ association (~230–250 μM (Fong and Takeda, 2008)). The *x*-axis indicates the cytoplasmic oxygen concentrations (in arbitrary units). The *y*-axis indicates the free-electron generation rate in the electron transfer chain (in arbitrary units). Red * and blue * indicate that ROS-mediated hypoxia responses can occur at low and high (even above K_m) oxygen concentrations, respectively, as long as the free electron generation rate *y* is sufficiently high.

(CSCs). The detailed review can be found elsewhere (Heddleston et al., 2010; Schoning et al., 2017; Tong et al., 2018).

The Roles of ROS in HIF Signaling

In vivo, the stability of HIF-α subunits is primarily regulated by molecular oxygen (Module Box I and **Figure 2B**) and ROS (Module Box II and **Figure 2C**). Once stabilized, HIF-1α induces the transcription of multiple genes to boost glucose and energy metabolism (**Figure 2A**). Examples include genes for glucose transporters (e.g., GLUT1 and GLUT3), hexokinase (e.g., HK1 and HK2), pyruvate conversion [e.g., lactate dehydrogenase A (LDHA), pyruvate dehydrogenase kinase (PDK), pyruvate kinase M2 (PKM2), enolase 1 (ENO1)], and mitochondrial autophagy [e.g., BCL2/adenovirus E1B 19 kDa protein-interacting protein 3 (BNIP3)], the detailed review of which can be found elsewhere (Semenza, 2010). The boost of glucose metabolism leads to the accumulation of intermediate-state metabolites, among which α-ketoglutarate (Duran et al., 2013), fumarate (Yang et al., 2012), and succinate (Tannahill et al., 2013), the by-products in the Krebs cycle, can regulate the stability of HIF through the positive or negative modulation on the activity of prolyl hydroxylase domain-containing proteins (PHD), the primary enzyme to destabilize HIF-α subunits (Module Box I and **Figure 2B**). Consequently, positive and/or negative feedback might exist in the interdependent regulation of HIF-1 activity and metabolic reprogramming. Metabolic reprogramming also occurs in response to ECM stiffening (Ge et al., 2021) through a YAP/TAZ-mediate upregulation of GLUT1/GLUT3 (Cosset et al., 2017; Liu et al., 2020b). The resultant stabilization of HIF-1α can further stiffen ECM (Gilkes et al., 2013), leading to positive feedback in the coupling of hypoxia responses and ECM remodeling (**Figure 2A**). Moreover, the activity of HIF-1α is sensitive to stressful conditions such as hypercapnia (Selfridge et al., 2016), in which the HIF-1α activity is suppressed, and the host is at the risk of opportunistic infections (Cummins et al., 2014). In fact, tissue

hypoxia has a significant impact on inflammatory signaling pathways (Cummins et al., 2016), a part of which depends on ROS (Kohchi et al., 2009; Chen et al., 2016). The term "immunometabolism" for the interdependence of HIF activity and immunity has thus been proposed (Halligan et al., 2016). Besides, ROS is an essential factor for cell functioning and a deleterious factor for mutations, tumorigenesis, and cell apoptosis (Skonieczna et al., 2017). Such a dual role of ROS has been found in the selection of stem cell fate. For example, while ROS at moderately low levels are required to maintain stem cell quiescence and self-renewal, ROS at moderately high levels lead to stem cell proliferation and differentiation (Valle-Prieto and Conget, 2010; Burtenshaw et al., 2017). Consequently, over-suppressing ROS levels impairs stem-cell functioning, and over-elevating ROS levels leads to stem-cell exhaustion, premature aging (senescence), and apoptosis (Schieber and Chandel, 2014) (**Figure 2D**).

ROS are primarily produced in mitochondria (Murphy, 2009; Juan et al., 2021), where free electrons in the electron transport chain (ETC) are leaked to bind to O_2 and form superoxide $O_2\bullet$ (or O_2^-) instead of the water molecule. In general, the yield of ROS depends on the generation rate of free electrons (set as Y) and the intracellular oxygen concentration (set as $[O_2]_c$). To see how a free electron selects to become O_2^- rather than a water molecule, we set up a simple mathematical analysis (Math Box I) and obtained a critical cytoplasmic oxygen concentration $[O_2]_c^*$. For $[O_2]_c$ above $[O_2]_c^*$, the free electrons predominantly select to become ROS. We also obtained the critical electron generation rate $\boldsymbol{Y}^*$. For $\boldsymbol{Y}$ above $\boldsymbol{Y}^*$, over 50% of the free electrons select to become ROS (**Figure 2E**). In the absence of any feedback or transcriptional regulation, the phase diagram in **Figure 2C** suggests three scenarios. The first occurs when the critical oxygen concentration $[O_2]_c^*$ (depends on the density of cytochrome c) is above the K_m of value of PHD for $[O_2]$c association (**Figure 2E(i)**), where PHD is the primary enzyme to destabilize HIF alpha subunits (Module Box I and **Figure 2B**). For this case, there is a region, $K_m \le [O_2]_c \le [O_2]_c^*$, in which PHD promotes the degradation of HIF-α subunits through the association with O_2 and below which (i.e., $[O_2]_c < K_m$) HIF-α subunits are stabilized. When $[O_2]_c > [O_2]_c^*$, PHD is deactivated by ROS through, for example, cysteine oxidation (Module Box II and **Figure 2C**), and hence, HIF-α subunits are stabilized. Such a scenario leads to a "pathological" hypoxia response under hyperoxia conditions; in other words, the oxygen concentration is above normoxia, but HIF signaling is activated. The second scenario occurs when $[O_2]_c^*$ is less than K_m (**Figure 2E**(ii)). In this case, PHD is always deactivated by ROS even for $[O_2]_c > K_m$, the region where PHD is supposed to promote the degradation of HIF-α subunits. This scenario allows cells to maintain HIF signaling over a wide range of niche oxygen concentrations, which might be used for robust control of stem cell fate or for aberrant cellular behavior (such as tumorigenesis and cancer stemness). The third is that ROS-mediated hypoxia response can always occur at extremely low and high oxygen concentrations (**Figure 2E**, red * and blue *, respectively), as long as the yield of free electrons by cell metabolism is sufficiently high (as in the case of tumor or inflammation). This scenario might contribute to the pathological hypoxia responses under normoxia or hyperoxia conditions.

The fact that not only O_2, but also ROS serve as a HIF regulator might be rationalized by the observation that hypoxia responses, such as those mediated by HIF-2α, are often required for the maintenance of stemness in stem cells (Ezashi et al., 2005; Covello et al., 2006; Keith and Simon, 2007; Mazumdar et al., 2009; Pervaiz et al., 2009; Heddleston et al., 2010; Abdollahi et al., 2011; Hu et al., 2014; Petruzzelli et al., 2014). Having ROS as an additional regulator might help cells to maintain a robust control on stemness against the niche oxygen fluctuation. The ability to use ROS as an additional regulator allows cells to maintain a robust control on stemness against the niche oxygen fluctuation. Regarding the interplay of ROS and hypoxia responses, we should point out that there are both positive and negative feedback regulations. To maximize the usage of O_2 as the major energy resources, the yield of free electrons from cell metabolism must fit the availability of O_2 in the niche. A high yield of free electrons demands more O_2 from the niche. Using the leakage of electrons into ROS as a signal, this demand evokes hypoxia responses, as one consequence of HIF-1α signaling is to induce angiogenesis (Krock et al., 2011) which can enhance O_2 delivery to the niche. Enhanced delivery of O_2, however, might not cope with the demand of removing abundant free electrons but instead produce more ROS. In addition, hypoxia responses include upregulating the expression of oxygen carriers and glycolytic enzymes (Hu et al., 2014). Such effects lead to higher intracellular oxygen concentrations (by the abundance of carriers) and larger free-electron generation rates (by excessive glycolysis), hence creating a positive feedback loop to couple sustained ROS production and hypoxia responses into a vicious cycle. Fortunately, prolonged HIF-1α signaling increases the expression of ROS scavengers, prolyl hydroxylase domain-containing protein 2 (PHD2), and the factor inhibiting HIF 1 (FIH-1), which promote HIF-1α degradation (Kobayashi et al., 2021) and cease HIF signaling as negative feedback control.

The existence of positive and negative feedback provides a possibility of bifurcation and suggests that ROS signaling can be a double-edged sword (Saito et al., 2015; Di Meo et al., 2016). Under normal conditions, cells use the multiplex versatility of ROS-mediated hypoxia responses to adapt to or cope with niche fluctuations (Pervaiz et al., 2009; Valle-Prieto and Conget, 2010), thereby maintaining stem cell physiology and cell fate in a robust manner. In the abnormal situations such as tumorigenesis, tumor cells take advantage of ROS-mediated hypoxia responses to promote cancer stemness, invasiveness, drug resistance, and immune evasion (Keith and Simon, 2007; Mazumdar et al., 2009; Heddleston et al., 2010; Barsoum et al., 2014; Peng and Liu, 2015; Aponte and Caicedo, 2017; Schoning et al., 2017; Yeo et al., 2017; Tong et al., 2018). ROS can also cause stem cell exhaustion and premature aging (Turrens, 2003; Schieber and Chandel, 2014; De Gaetano et al., 2021) (**Figure 2D**). The onset of these physiological and pathological processes is certainly cell- and tissue-context dependent and could be differential or switch-like. In fact, switch-like behavior with a multi-stability has been reported in the ROS regulation of human cells (Huang JH. et al., 2021). Elucidating how these

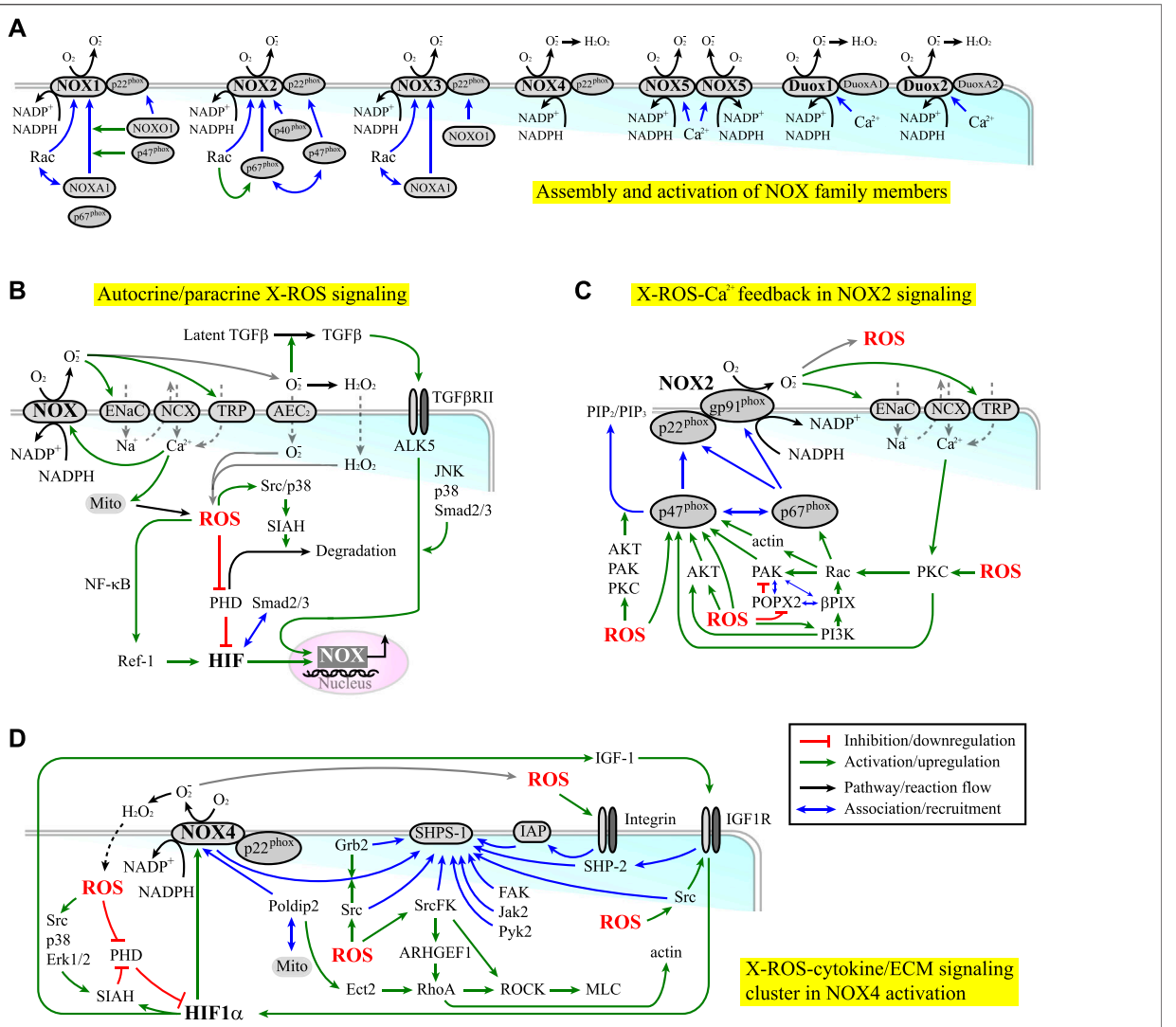

FIGURE 3 | (A) The assembly (blue lines) and activation (green lines) of NOX family members. **(B)** NOX-derived ROS (X-ROS) signaling can elicit both autocrine and paracrine effects. Red lines indicate inhibition or downregulation. Green lines indicate activation or upregulation. Blue lines indicate physical association or recruitment. Black lines indicate the flow of the pathways or a reaction. **(C)** NOX2 signaling is coupled with cytoskeleton dynamics and kinase/phosphatase activities through an X-ROS-Ca^{2+} feedback loop. **(D)** NOX4 signaling is associated with the clustering of signaling molecules involved in the cytokine/integrin-ECM signaling.

processes occur requires a molecular–cellular understanding of the interplay between ROS and other signaling pathways.

The Coupling of NOX-Derived ROS (X-ROS) With Hypoxia/Cytokine/ECM Signaling

Apparently, molecular oxygen is not the only niche factor regulating stem cell physiology. Other factors include ECM molecules and cytokines such as TGFβ1, bone morphogenic protein (BMP), angiotensin II (Ang II), platelet-derived growth factor (PDGF), EGF, and IGF-1. Similarly, mitochondria are the only source of producing ROS. Other sources include membrane-bound NADPH oxidases (NOX) (Bedard and Krause, 2007), cytochrome p450 (Veith and Moorthy, 2018), xanthine oxidase (XO) (Battelli et al., 2016b; a), and nitric oxide synthase (NOS) (Wilkinson-Berka et al., 2013; Di Meo et al., 2016). Among them, NOX are known to regulate the differentiation and self-renewal of stem cells and potentiate the self-renewal, metastasis, and drug resistance of CSCs through, for example, Notch, mitogen-activated protein kinases (MAPKs, including Erk1/2, Jun N-terminal kinase (JNK), and p38 kinase), and phosphatidyl-inositol-3-kinase- (PI3K-) AKT signaling (Skonieczna et al., 2017). Crosstalk between NOX and the signaling of TGFβ1 (Ning et al., 2002), BMP (Sanchez-De-Diego et al., 2019), Ang II (Nguyen Dinh Cat et al., 2013), PDGF (Al-Eisa and Dhaunsi, 2017), EGF (Weng et al., 2018), and IGF-1 (Xi et al., 2013; Kang et al., 2016) has also been reported and/or reviewed. Moreover, NOX potentiate the interaction between ECM and cell surface receptors such as integrin β1 (Heo and Lee, 2011), thereby facilitating cell adhesion and migration, particularly in the presence of niche cytokine factors such as IGF-1 (Chiarugi et al., 2003; Meng et al., 2008; Heo and Lee, 2011; Xi et al., 2013).

NOX can produce ROS in the extracellular space (e.g., the niche) and inside the cells. Seven members of NOX have been identified, including NOX1-5 and dual oxidase 1-2 (Duox1-2), each of which has its own NOX gp91^{phox} homolog (Brown and Griendling, 2009; Brandes et al., 2014a; b; Fukai and Ushio-Fukai, 2020) (Module Box III and **Figure 3A**). The ROS produced by NOX in the extracellular space can enter or regulate nearby cells as a paracrine signal through ion exchangers and ion channels, such as anion exchange protein 2 (AEC2) (Ghio et al., 2003) and epithelial sodium channels (ENaC) (Helms et al., 2008; Liu et al., 2016b) (**Figures 3B,C**). Alternatively, they can liberate latent cytokines stored in the ECM reservoirs, such as TGF-β1 (Watson et al., 2016), leading to a systemic niche remodeling. On the contrary, the ROS produced in the cell can serve as an autonomous signal to induce oxidative stress (Schieber and Chandel, 2014) or hypoxia responses (e.g., through inactivating PHD to elicit HIF-1α/HIF-2α signaling (**Figure 2C**)). In turn, hypoxia responses mediated by HIF-1α signaling can upregulate the expression of NOX (e.g., NOX4 (Diebold et al., 2010)) and PHD (Kobayashi et al., 2021) (**Figure 3B**). These lines of evidence suggest that both positive and negative feedback regulations exist in the axis of NOX-ROS-HIF signaling and that NOX act both upstream and downstream of the HIF signaling.

Beyond the HIF-mediated regulation on the expression level, the activities of NOX are modulated by the assembly and the post-translational modifications (PTMs) of their cytoplasmic and membrane subunits. In fact, almost all NOX subunits are subject to functional-relevant PTMs. Such regulation is under the crosstalk with cytokine signaling (e.g., IGF-1, TGF-β1, EGF, and PDGF signaling) and integrin/ECM signaling (including those involved in cell mechanotransduction (Brandes et al., 2014a), cell adhesion (Schroder, 2014), and cell migration (Brown and Griendling, 2009)). Further, these signaling activities are reciprocally modulated by ROS (Ning et al., 2002; Chiarugi et al., 2003; Ali et al., 2006; Block et al., 2008; Meng et al., 2008; Heo and Lee, 2011; Touyz and Briones, 2011; Xi et al., 2013; Brandes et al., 2014a; Jiang et al., 2014; Yan et al., 2014; Gau and Roy, 2018; Pietruczuk et al., 2019; Fukai and Ushio-Fukai, 2020). In the presence of cooperative or synergistic coupling in the NOX/cytokine/ECM signaling, a bistable or multi-stable switch might be established to potentiate the selection of cell fate, as observed in the regulation of ROS (Huang JH. et al., 2021). This scenario is likely to occur in the processes involving NOX1-2 and NOX4, in that NOX2 and NOX4 are reported to involve in stem cell differentiation and self-renewal, and NOX1-2 and NOX4 are found to potentiate CSC growth, survival, and drug resistance (Brandes et al., 2014b; Skonieczna et al., 2017). The regulations of these NOX mainly occur through serine/threonine phosphorylation (NOX1-3) and tyrosine phosphorylation (NOX4) (Rastogi et al., 2016; Skonieczna et al., 2017). In comparison, the regulation of NOX5 and Duox1-2 primarily depends on calcium. This difference is correlated with the fact that most cancers have dysregulated kinase/phosphatase activities. Other than cancers, NOX-derived ROS correlate with diseases such as cardiomyopathies (Prosser et al., 2011; Kerr et al., 2015). The term "X-ROS" has thus been invented to describe the rapid and localized mechano-chemical signaling elicited by "NOX-derived ROS" (Prosser et al., 2011). A brief review of the regulation of NOX 1-4 and a short discussion on how they are coupled with cytokine and ECM signaling can be found in Module Box III.

One example of positive coupling in X-ROS/cytokine/ECM signaling is the potential feedback amplification along the NOX2-ROS-Ca^{2+}-protein kinase C (PKC) signaling axis (Module Box III and **Figure 3C**). Another is the NOX4-ROS-HIF-IGF-1 signaling, which occurs through the clustering of NOX4, steroid receptor coactivator (Src) kinase, Src homology 2- (SH2-) domain-containing protein tyrosine phosphatase (SHP) substrate-1 (SHPS-1), growth factor receptor-bound protein 2 (Grb2), integrin-associated protein (IAP), and growth factor receptors such as IGF-1 receptor (IGF-1R) (Module Box III and **Figure 3D**). Among them, IAP is a transmembrane protein associated with several integrins. The association of IGF-1R with IAP thus enables the crosstalk between IGF-1R and ECM/integrin signaling, thereby coupling ROS signaling and growth factor stimulation with cell–ECM adhesion and cell migration (Maile et al., 2003). To add more systemic niche effects, NOX4-derived ROS can induce HIF-1α signaling (e.g., through downregulating the PHD activity (Xu and Li, 2021), which in turn upregulates the expressions of NOX4 (Diebold et al., 2010) and IGF-1 (Poon et al., 2009; Prabhakar and Semenza, 2012; Huang et al., 2017), leading to autonomous (through NOX and IGF-1) and non-autonomous effects (through IGF-1 acting on neighboring cells) in X-ROS-HIF-IGF-1 signaling (**Figure 3D**).

The association of NOX4 and Src kinase within the SHPS-1 scaffold allows Src kinase to phosphorylate NOX4 and enhance ROS production (Xi et al., 2013). Reciprocally, ROS target and oxidize the cysteine residues at the catalytic domain of Src kinase, thereby activating the kinase (Giannoni et al., 2010; Ray et al., 2012; Xu et al., 2017; Heppner et al., 2018; Dustin et al., 2020; Heppner, 2021). Such mutual interplay leads to localized feedback amplification in IGF-1 and integrin/ECM signaling. A detailed review of redox regulation on, for example, IGF-1 signaling can be found elsewhere (Lennicke and Cocheme, 2021a; Lennicke and Cocheme, 2021b). Clearly, with the abundance of cysteine residues in most signaling molecules, Src kinase is not the only substrate sensitive to ROS. The MAPKs (including JNK (Santabarbara-Ruiz et al., 2015), Erk (Aikawa et al., 1997), p38 kinase (Kulisz et al., 2002; Emerling et al., 2005; Lee et al., 2012; Santabarbara-Ruiz et al., 2015), and big MAP kinase (BMK1/Erk5) (Abe et al., 1996), the Ca^{2+}/calmodulin-dependent kinase 2 (CaMK2) (Basu et al., 2019), the cGMP-dependent protein kinase or protein kinase G (PKG), the PI3K/AKT (Ray et al., 2012; Koundouros and Poulogiannis, 2018), the PKC (Gong et al., 2015; Steinberg, 2015), the cAMP-dependent protein kinase (PKA (Andre et al., 2013)), and the focal adhesion kinase (FAK) (Ben Mahdi et al., 2000) are redox sensitive and subject to activation by ROS. In parallel, protein serine/threonine phosphatases (PPP, including PP1 (Kim et al., 2015), PP2A (Low et al., 2014; Raman and Pervaiz, 2019), and PP2C-like partner of PIX 2 (POPX2 (Kim P. R. et al., 2020))), and protein tyrosine phosphatases (PTP), including PTP1B, the low

molecular weight PTP (LMW-PTP, the major PTP for FAK) (Chiarugi et al., 2003), PTEN (Ray et al., 2012), SHP-2 (Chattopadhyay et al., 2017), and cdc25C (Rudolph, 2005; Seth and Rudolph, 2006; Han et al., 2018)) are also redox-sensitive and can be inhibited by oxidation. Through the ROS-mediated modulation of the kinase and phosphatase activity and the reciprocal phosphorylation-dependent ROS production, it is possible to have positive or negative feedback loops in the ROS-dependent cytokine/ECM signaling. Moreover, the feedback regulation on the expression levels has been reported. For example, ROS-activated p38 kinase and Erk1/2, two key kinases involved in cytokine signaling, can enhance the expressions of NOX (e.g., NOX4 (Diebold et al., 2010)) and the nuclear translocation of HIF-1α (Richard et al., 1999; Sodhi et al., 2000; Flugel et al., 2007). Nuclear HIF-1α, in turn, promotes the expression of seven in absentia homolog 2 (SIAH2), one of the enzymes targeting PHDs for ubiquitin-mediated proteasome degradation (Xu and Li, 2021), in a PI3K/AKT-dependent manner (Koundouros and Poulogiannis, 2018; Perillo et al., 2020). Src and p38 kinases can further phosphorylate and activate SIAH2 (Khurana et al., 2006; Sarkar et al., 2012), thereby forming the positive feedback amplification in HIF-1 signaling (**Figures 2B**, **3C**). In addition, HIF-1α can induce the deposition and stiffening of collagen (Gilkes et al., 2013), and ROS can upregulate the expression of integrins and ECM molecules such as laminin (Liu J. et al., 2016) and fibronectin (Lee H. B. et al., 2004). These effects reinforce the ligand-receptor interactions in the ROS-modulated cytokine and ECM signaling (Lamari et al., 2007; Liu J. et al., 2016).

The preferential coupling of NOX4 with protein tyrosine kinases (PTKs) raises an important issue in stem cell biology. From an evolutionary point of view, PTKs have a specific relation with ROS. PTKS were primarily present in multicellular organisms during the episodes of increasing atmospheric O_2 concentrations, which drove the use of O_2 as the major energy resource in multicellular organisms (Dustin et al., 2020). The emergence of NOX in multicellular organisms had evolved at the same time (Kawahara et al., 2007; Holmstrom and Finkel, 2014). Thus, it is reasonable that PTKs are related to cell differentiation and functionalization in multicellular organisms (thus linked to stem cell homeostasis) (Dustin et al., 2020) and that NOX are coupled with RTKs in oxidative phosphorylation, metabolism, and tissue remodeling, as in the case of NOX4 (e.g., through Poldip2, TGFβ, and IGF-1/insulin signaling). In fact, PTKs have been recognized as a major target for clinical treatments (i.e., through tyrosine kinase inhibitors (TKI)) of cancers (Zhang et al., 2009; Dustin et al., 2020). Likewise, NOX have been used as a target for the treatments of, for example, thrombosis, osteoarthritis, diabetes-related complications, stroke, cancers, and pulmonary fibrosis (Bonner and Arbiser, 2012; Hecker et al., 2012; Violi and Pignatelli, 2014; Morel et al., 2015; Zhang et al., 2016; Peng et al., 2019). A HIF-1α/NOX4 signal pathway has been identified to induce drug and radiation resistance in ovarian cancer (Liu W. J. et al., 2021). It would be interesting to investigate whether a combinatory target therapy on NOX and PTKs provides additive or synergistic benefits on diseases such as cancer and systemic diseases.

The Coupling of X-ROS Signaling With Cell Mechanics

Besides cytokine/ECM signaling, other feedback amplifications in ROS responses include the mitochondria-dependent, ROS-induced ROS release, and the mitochondria-mediated crosstalk between ROS and the calcium flux, a detailed review of which can be found elsewhere (Zorov et al., 2014; Gorlach et al., 2015; Javadov, 2015; Feno et al., 2019). Herein, we focus on the coupling of NOX with cell mechanics and mechanotransduction, an emerging issue in the fields of stem cell research, cell therapy, wound healing, and cancer (Paszek et al., 2005; Kono et al., 2012; Liu et al., 2020a; Wilkinson and Hardman, 2020; Bergert et al., 2021; Hayward et al., 2021). In fact, a great deal of interest has recently been raised in the roles of cell mechanics in the key cellular processes, such as proliferation, cell death, cell differentiation, and cell migration (Chen et al., 1997; Horowitz et al., 1999; Lecuit and Lenne, 2007; Settleman and Baum, 2008; Grosberg et al., 2011), and the maintenance of stem cell pluripotency (Discher et al., 2009; Jaalouk and Lammerding, 2009; Mammoto and Ingber, 2009; Wozniak and Chen, 2009). These key processes often involve molecular–cellular interactions at the boundaries, ranging from the membrane of a single cell to the interfaces between cells and between cells and ECM. Examples include epithelial–mesenchymal interaction (EMI) in the hair follicle (Sick et al., 2006) and tooth (Mammoto et al., 2011) formation, EMI in wound healing (Chong et al., 2009; Seltana et al., 2010), endothelial cell–pericyte interaction in angiogenesis (Gerhardt and Betsholtz, 2003), and endothelial cell–hepatocyte interaction in liver development and regeneration (Inamori et al., 2009). In these examples, the importance of cell mechanics is manifested in the ability of cells to control their size and shape (i.e., 3D topology and geometry) at the interacting boundaries, which in turn profoundly influence the binary decision of cells, for example, to proliferate or differentiate (Folkman and Moscona, 1978; Spiegelman and Ginty, 1983; Piccolo et al., 2014). In line, recent experiments have shown that the fate of stem cells (e.g., self-renewal and differentiation) and the development of organs (such as branching morphogenesis in tubular organs) can be controlled by engineered geometries on the cell–cell and cell–ECM interacting boundaries (Chen et al., 1997; Nelson et al., 2006; Gomez et al., 2010; Silver et al., 2020). Conversely, abnormality or failure in the control of cell size and shape at the interacting boundaries is often found in diseases such as organ malformation, atherosclerosis, cancer, and tumor invasion (Chen et al., 1997; Paszek et al., 2005; Nelson et al., 2006), and cancer-associated fibroblast- (CAF-) aided initiation and maintenance of cancer stemness (Chen et al., 2014). A conceptual discussion on how mechanics contribute to the regulation of cell/organ size and shape can be found in Module Box IV. Reviews on the details of mechano-sensing can also be found elsewhere (Cai et al., 2021).

From the molecular signaling perspective, X-ROS and cell mechanics act both upstream and downstream of each other. This reciprocal coupling occurs through the cytoskeletal dynamics. On the one hand, X-ROS can activate Ras-related C3 botulinum toxin substrate 1 (Rac1) through, for example, the X-ROS-Ca^{2+}-PKC

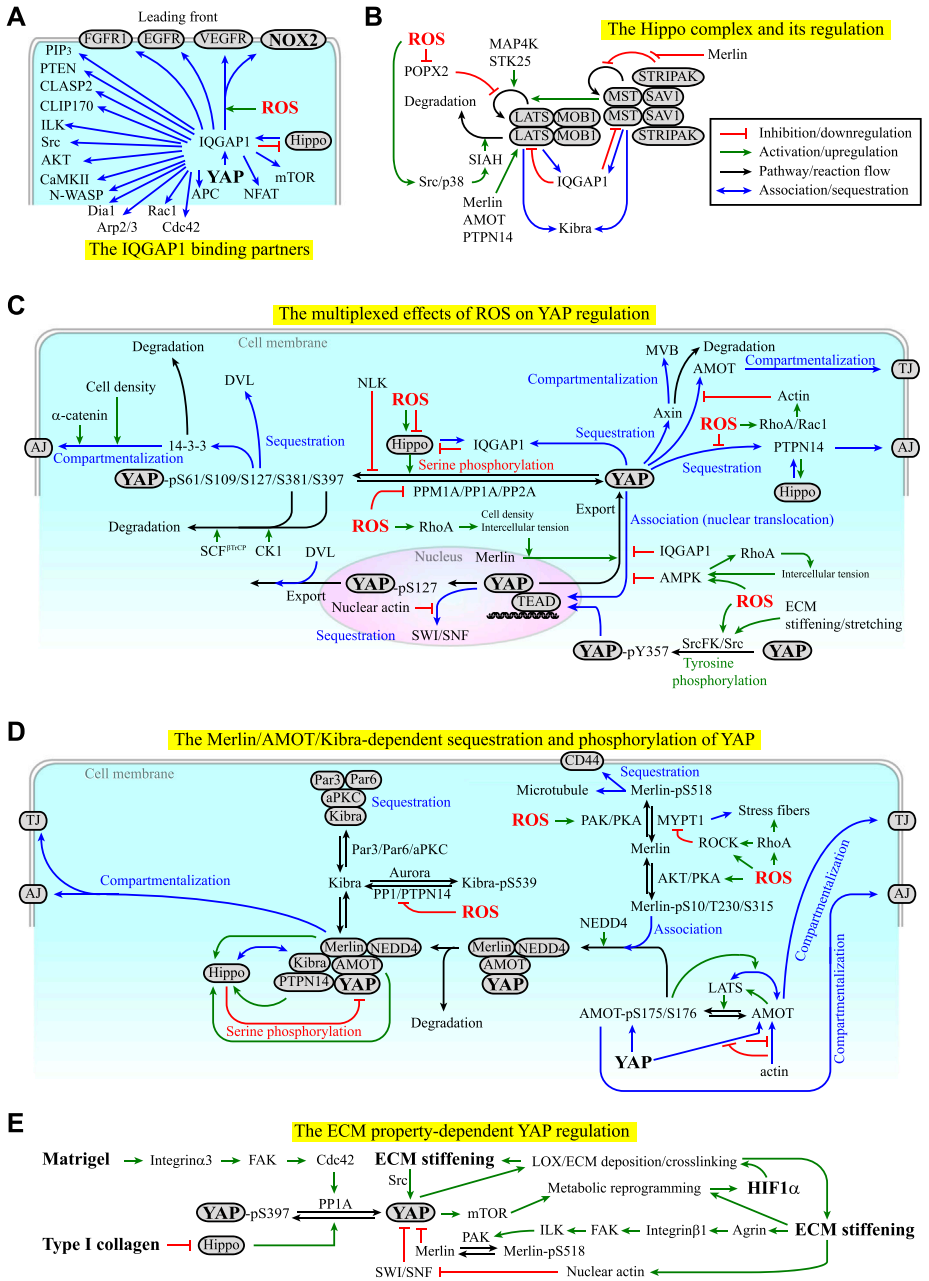

FIGURE 4 | (A) Examples of the binding partners of IQ motif-containing GTPase activating protein 1 (IQGAP1). Red lines indicate inhibition or downregulation. Green lines indicate activation or upregulation. Blue lines indicate physical association or recruitment. See Module Boxes IV and V for details. **(B)** The Hippo complex is regulated by itself and several kinases, phosphatases, and molecular scaffolds in a ROS-dependent manner. See Module Box V for details. Black lines indicate the flow of the pathways, cascades, or a reaction. **(C)** ROS exhibit both positive and negative effects on the regulation of YAP signaling manifested in the phosphorylation, dephosphorylation, sequestration, degradation, and compartmentalization of YAP. Red texts indicate inhibition. Blue texts indicate sequestration, association, or compartmentalization. Green texts indicate activation. **(D)** Merlin, angiomotin (AMOT), kidney and brain expressed protein (KIBRA), and protein tyrosine phosphatase non-receptor type 14 (PTPN14) act with the Hippo complex and cytoskeletons to regulate the phosphorylation, sequestration, compartmentalization, and degradation of YAP in a ROS-dependent manner. See Module Box V for details. **(E)** The ECM components and mechanical properties can regulate YAP signaling in a self-perpetuating manner. See Main Text and Module Box V for details.

coupling (Module Box IV and **Figure 3C**), and Ras homolog family member A (RhoA), through, for example, cysteine oxidization on the Rho GEF ARHGEF1 (MacKay et al., 2017) (Module Box IV and **Figure 3D**), by which they promote actin filament polymerization and actomyosin contractility. X-ROS-mediated cysteine oxidization also enables the association of Ras GTPase-activating-like protein or IQ motif-containing GTPase activating protein 1 (IQGAP1) with NOX2 and cytokine

receptors such as VEGF receptor (VEGFR) at the lamellipodial leading front of migrating cells (Ikeda et al., 2005; Kaplan et al., 2011) (**Figure 4A**). IQGAP1 is a scaffold protein that binds to microtubule plus-end binding proteins such as cytoplasmic linker associated protein 2 (CLASP2), YAP, and the regulators of YAP in the Hippo pathway, MST2, and LATS1 (Watanabe et al., 2009; Sayedyahossein et al., 2016; Quinn et al., 2021) (Module Box IV and **Figure 4A**). As a result, X-ROS signaling influences cell mechanics by modulating cytoskeletal dynamics and the distribution of mechano-transducers such as YAP. On the other hand, actin enhances NOX-mediated ROS production, and an actin-binding site has been identified on the subunit of NOX2, $p47^{phox}$ (Tamura et al., 2006) (Module Box III). $p47^{phox}$ is redox-sensitive, and sequential phosphorylation and S-glutathionylation of $p47^{phox}$ leads to sustained O_2^- production (Nagarkoti et al., 2018). These lines of evidence suggest a self-perpetuating amplification of the ROS-dependent cytokine/ECM signaling and cytoskeletal dynamics.

The effect of ROS on cytoskeletal dynamics appears to depend on the ROS levels. It has been shown that ROS at low (physiologically relevant) levels promote actin filament polymerization, stress fiber assembly, and microtubule self-organization, yet ROS at high levels compromise these processes (Khairallah et al., 2012; Xu et al., 2017; Loehr et al., 2018) (**Figure 2D**). The explicit mechanisms remain elusive (Wilson and Gonzalez-Billault, 2015). To date, the most well-studied example of the coupling of NOX-ROS and cell mechanics is the microtubule-dependent X-ROS signaling in cardiomyocytes and skeletal muscle cells (Prosser et al., 2011; Prosser et al., 2013; Kerr et al., 2015; Limbu et al., 2015; Robison et al., 2016; Caporizzo et al., 2018; Chen et al., 2018; Caporizzo et al., 2019; Scarborough et al., 2021; Uchida et al., 2021) (Module Box IV). With the interdependence between cytoskeletal dynamics and X-ROS signaling, it is plausible that X-ROS signaling is sensitive to the mechanical modulation in cell morphogenesis and acts in part as a mechano-transducer. The integration of these effects can lead to a self-perpetuated amplification of the cellular mechanical responses, which might serve as a switch for the selection of stem cell fate (see examples in Module Box IV).

The Coupling of X-ROS-Hypoxia/Cytokine/ECM Signaling With YAP Signaling

One goal of cell/tissue mechanics is to shape organs and tissues into the proper form. In this process, what is needed is the control over the proliferation and differentiation of stem cells and tissue-specific progenitor cells. The fundamental question is how these cells know when and where to stop growing after the organ reaches a certain size and topology. In principle, the growth control should arise from a proper balance of three cellular processes, namely, cell division, cell differentiation, and programmed cell death (apoptosis), in a time- and space-dependent manner. The classical "chemical-driven" view on the control of organ size and topology was started by Alan Turing's famous work on the dynamic instability of interacting morphogens (Turing, 1952) and is amplified by the focus of molecular biology and genetics on regulatory mechanisms implemented by diffusive molecules. However, attempts to create organ-scale tissues by diffusive morphogens have limited success. Indeed, if organ pattern formation relies on chemical gradients only, it would be impossible to explain several remarkable examples of ordered proliferation, differentiation, and self-organization of the entire organ spontaneously emerging *in vitro* from naive cells cultured in media saturated with mitogens and growth factors (Sasai, 2013). Using soluble factors alone also makes it difficult to realize how fluctuating microenvironments can robustly template cell behavior in time and space with micrometer accuracy (Huang and Ingber, 1999; Discher et al., 2009). It appears that a "mechanics-driven," non-autonomous effect must exist; in other words, the tissue is endowed with a capacity to inform individual cells with certain "structure-code messengers" about its size and entire topology (Nelson et al., 2006; Piccolo et al., 2014), by which a long-range regulation can be imposed on individual cells (Guo et al., 2012), guiding them to shape the tissue in synchrony with other cells.

The transcriptional coactivators, YAP/TAZ, which boost organ growth and are suppressed by the Hippo complex (Module Box V and **Figure 4B**), are likely to be the "structure-code messengers" in organ development, homeostasis, repair, and tumorigenesis (Wang et al., 2009; Li et al., 2010; Lian et al., 2010; Zhao et al., 2010a; Dupont et al., 2011; Yu et al., 2015; Panciera et al., 2017). The activity of YAP/TAZ is mainly regulated through PTMs (e.g., serine/threonine and tyrosine phosphorylation and dephosphorylation, and ubiquitination), sequestration, and compartmentalization (**Figure 4C**). The effectors modulating the PTMs of YAP include the Hippo pathway components such as MST1/2, SAV1, LATS1/2, MOB1, MAP4Ks, and STK25, tyrosine kinases such as Src kinase, the E3 ubiquitin ligase $SCF^{\beta\text{-}TrCP}$, protein phosphatase (PP), and protein tyrosine phosphatase (PTP) (Module Box V). We should point out that the consequences of serine/threonine phosphorylation and tyrosine phosphorylation of YAP are different. While the serine/threonine phosphorylation of YAP promotes YAP sequestration, compartmentalization, or ubiquitination, the tyrosine phosphorylation of YAP promotes YAP nuclear translocation and signaling (Rosenbluh et al., 2012; Smoot et al., 2018; Sugihara et al., 2018) (**Figure 4C**). For the sequestration of YAP, the major adaptors and scaffold molecules include 14-3-3, α-catenin, Dishevelled (DVL), angiomotin (AMOT), IQGAP1, kidney and brain expressed protein (KIBRA), Merlin, Expanded (Ex), protein tyrosine phosphatase non-receptor type 14 (PTPN14), and Switch/Sucrose non-fermentable (SWI/SNF) (Module Box V and **Figures 4C,D**). Among them, the association of YAP with AMOT in the cytoplasm is under competition with actin filaments, hence linking cytoskeletal dynamics to YAP regulation (Mana-Capelli et al., 2014) (Module Box V and **Figures 4C,D**). Likewise, in the nucleus, polymerized nuclear actin filaments (induced by, e.g., the exposure of cells to stiff ECM) bind to SWI/SNF and relieve its sequestration of YAP (Chang et al., 2018). Cell mechanics are also linked to the Merlin-dependent YAP regulation. Merlin phosphorylation at S518, for

example, is counteracted by myosin phosphatase target subunit 1-(MYPT1-) regulated PP1c, the phosphatase for myosin light chain (MLC) (Jin et al., 2006; Kiss et al., 2019; Alvarez-Santos et al., 2020). When RhoA, Rho-associated kinase (ROCK), or both are activated (e.g., by integrin–ECM interactions), MYPT1 can be inhibited by ROCK (Kawano et al., 1999) and/or sequestered to stress fibers (Joo and Yamada, 2014), thereby maintaining Merlin at the inactive, S518-phosphorylated state (Module Box V and **Figure 4D**). The compartmentalization of YAP mainly occurs at adherens junctions (AJs, by, e.g., PTPN14, 14-3-3, and Merlin), tight junctions (TJs, by, e.g., AMOT and Merlin), and multi-vesicular body (MVB, by, e.g., axin) (Module Box V and **Figures 4C,D**).

Several mechanisms have been identified to activate YAP signaling in an X-ROS- and/or cell mechanics-dependent manner. These mechanisms are to change the PTMs, the sequestration, and/or the compartmentalization states of YAP. Examples of the processes include 1) enhancing the degradation or dephosphorylation of LATS (Kim P. R. et al., 2020; Zhao et al., 2020) (**Figure 4B**), *2*) reducing YAP S127/S397 phosphorylation (e.g., by PP1A, PP2A, PPM1A (Schlegelmilch et al., 2011; Li et al., 2016; Hu et al., 2017; Zhou et al., 2021), or Nemo-like kinase (NLK) (Moon et al., 2017)) (**Figure 4C**), *3*) reducing YAP-Merlin association (by, e.g., enhancing Merlin S518 phosphorylation (Morrison et al., 2001; Sherman and Gutmann, 2001)) (**Figure 4D**), and *4*) attenuating YAP-AMOT association (by, e.g., promoting actin filament polymerization to compete for binding to AMOT (Mana-Capelli et al., 2014)) (**Figures 4C,D**). A mechanism similar to example 4 is to reduce YAP-SWI/SNF association by nuclear actin filament polymerization (Chang et al., 2018) (**Figure 4C**). The effects of X-ROS in these processes are complex, as they can be additive, synergistic, or contradicting. To demonstrate such complexity, we use ROS-mediated LATS degradation and dephosphorylation as an example.

The degradation of LATS is primarily mediated by the E3 ubiquitin ligase, SIAH2 (Ma et al., 2015; Zhao et al., 2020) (**Figure 4B**), the enzyme targeting PHDs for degradation (Nakayama and Ronai, 2004; Qi et al., 2013) (**Figure 2C**), thus connecting the regulation of hypoxia responses with YAP signaling. SIAH2 can be upregulated by p38 kinase and Src kinase (Khurana et al., 2006; Sarkar et al., 2012), which are redox-sensitive and can be activated by X-ROS (Abe et al., 1996; Aikawa et al., 1997; Kulisz et al., 2002; Emerling et al., 2005; Ray et al., 2012; Xu et al., 2017; Koundouros and Poulogiannis, 2018; Basu et al., 2019; Perillo et al., 2020). This effect places X-ROS upstream of YAP activation (**Figure 4B**). On the contrary, the dephosphorylation of LATS is primarily mediated by POPX2, which is also redox-sensitive and can be inhibited by ROS through cysteine oxidation (Kim P. R. et al., 2020). This effect places ROS upstream of YAP suppression (**Figure 4B**). Thus, X-ROS exhibit contradicting effects on YAP regulation (**Figure 4C**).

Contradicting effects, in fact, appear in many aspects of the ROS-dependent YAP regulation. For example, ROS can activate not only Src and p38 kinases (which activates SIAH), but also Src family kinase (SrcFK) (Tominaga et al., 2000; MacKay et al., 2017) and PKC (Xu et al., 2017) through cysteine oxidation or ROS-Ca^{2+} coupling (Shirai and Saito, 2002) (**Figures 3B,C**). PKC and SrcFK, in turn, activate Rac1 (Cathcart, 2004; Brown and Griendling, 2009; Gorlach et al., 2015) and Rho guanine nucleotide exchange factor 1 (ARHGEF1) (MacKay et al., 2017) to promote p21-activated protein kinase (PAK) activation and RhoA activation, respectively. The resulting effects include actin filament polymerization (by Rac1 and RhoA), MLC phosphorylation and stress fiber formations (by RhoA) (Tominaga et al., 2000), and MYPT1 inhibition (Kawano et al., 1999) or sequestration to the phosphorylated MLC (by RhoA) (Joo and Yamada, 2014). Among them, actin filaments compete with YAP for the binding of AMOT, thus releasing YAP from the AMOT-mediated sequestration (**Figure 4C**). PAK catalyzes Merlin S518 phosphorylation (Shaw et al., 2001) to prevent Merlin from binding to YAP (**Figure 4D**). RhoA-mediated inhibition and sequestration of MYPT1 prevent MYPT1 from dephosphorylating $Merlin^{pS518}$ (**Figure 4D**). These effects act additively or synergistically to promote YAP signaling. At the same time, RhoA-mediated ROCK activation at the epithelial circumferential actin belt increases intercellular tension and promotes the release of Merlin from AJs to enable Merlin-mediated YAP nuclear export (Furukawa et al., 2017), thereby suppressing YAP signaling (**Figure 4C**). If not exported, the nuclear YAP requires the binding of TEAD for signaling, which can be disrupted by 5′ AMP-activated protein kinase-(AMPK-) mediated YAP phosphorylation at S94 (Mo et al., 2015), and elevated ROS levels were found to increase the AMPK activity (Irrcher et al., 2009) (**Figure 4C**). In addition, ROS can suppress not only POPX2 (which dephosphorylates LATS), but also PP1 (Santos et al., 2016) and PP2A (Rao and Clayton, 2002; Raman and Pervaiz, 2019), both of which can dephosphorylate YAP to promote YAP signaling (Schlegelmilch et al., 2011; Li et al., 2016) (**Figure 4C**). These inhibitory effects place ROS upstream of YAP suppression and certainly contradict the aforementioned ROS-mediated YAP activation. Moreover, ROS can activate not only Src, p38, PKC, and SrcFK, but also PKA and AKT, yet the effects of the two kinases on Merlin-YAP association are different or even conflicting (Module Box V and **Figure 4D**). It is thus likely that the effect of X-ROS on YAP signaling is multiplexed and dependent on the context of the niche and the cellular status.

One consistent influence of X-ROS on YAP signaling is to promote the association of YAP with IQGAP1 (**Figure 4C**), which brings YAP to the cell leading front (**Figure 4A**). Another consistency is the effect of intercellular tension on the regulation of YAP signaling. In epithelial organs, the intercellular tension is primarily determined by the contractility at the circumferential actin belt around the AJs. RhoA/ROCK-mediated enhancement of tension at the circumferential actin belt has been shown to promote the release of Merlin from AJs, thereby facilitating Merlin-mediated YAP nuclear export (Furukawa et al., 2017). Consistently applying forces at E-cadherin to mimic the high intercellular tension state has been shown to activate AMPK (Bays et al., 2017), which disrupts the YAP-TEAD association and suppresses the nuclear signaling of YAP (Mo et al., 2015). Moreover, the

activated AMPK reinforces the RhoA/ROCK/MLC-mediated contractility to keep the cells at a high-tension state, thereby forming a positive feedback loop for the maintenance of the epithelial barrier (Bays et al., 2017) and the suppression of YAP signaling (**Figure 4C**). The third consistency is the ROS-mediated activation of tyrosine kinases and suppression of tyrosine phosphates. Unlike the negative regulation of serine phosphorylation of YAP by LATS and other kinases such as AKT and JNK (Basu et al., 2003; Danovi et al., 2008), tyrosine phosphorylation of YAP (at, e.g., Y357) by the redox-sensitive Src kinase or SrcFK promotes the nuclear translocation and signaling of YAP (Rosenbluh et al., 2012; Smoot et al., 2018; Sugihara et al., 2018) (**Figure 4C**). ROS-activated Src kinase can also suppress LATS by upregulating SIAH2 (**Figure 4B**), and ROS can inhibit tyrosine phosphates (Hecht and Zick, 1992; Lewis and Aitken, 2001; Chao et al., 2011) such as PTPN14, the inhibition of which abolishes the PTPN14-mediated sequestration of YAP (Liu et al., 2013) (**Figure 4C**). As a result, the regulations of ROS on tyrosine kinases and phosphatases lead to a synergistic or additive effect on YAP signaling.

X-ROS can be generated in integrin-ECM signaling and cell migration (Module Box III and **Figures 3B–D**). In these processes, integrin-ECM signaling can promote the dephosphorylation of YAP^{pS397}, likely through an integrin α3-FAK-Cdc42-PP1A cascade, leading to the YAP nuclear translocation and potentiating mTOR signaling in stem cell-based tissue renewal (Hu et al., 2017) (**Figure 4E**). Stiffening and stretching of ECM also leads to Src kinase activation (Koudelkova et al., 2021), which in turn promotes tyrosine phosphorylation and nuclear translocation of YAP (**Figures 4D,E**). In fact, the mechano-chemical properties of ECM, such as ECM stiffness and ECM components, exhibit a profound impact on YAP signaling. The type I collagen, for example, can stimulate YAP nuclear translocation to suppress adipogenic differentiation in preadipocytes, likely through downregulating the expressions of Hippo pathway kinases (Liu X. et al., 2020). The crosslinking of collagen by, for example, LOX and LOX-like (LOXL) enzymes (Levental et al., 2009) increases ECM stiffness to promote YAP nuclear translocation (Dupont et al., 2011; Noguchi et al., 2018) and metabolic reprogramming (Ge et al., 2021) which can potentially activate HIF-1 signaling (Halligan et al., 2016). HIF-1α signaling and YAP signaling, in turn, can induce the expression of genes responsible for collagen deposition and stiffening directly (Gilkes et al., 2013; Ji et al., 2013) and indirectly (Liu et al., 2015; Noguchi et al., 2017), leading to a self-perpetuating vicious cycle in tissue fibrosis (Noguchi et al., 2018). Another example of the influence of ECM on YAP signaling is Agrin, an ECM proteoglycan that transduces ECM stiffness and cell rigidity to YAP signaling. Agrin activates p21-activated protein kinase- (PAK-) 1 through the integrinβ1-FAK-integrin-linked kinase (ILK) signaling axis, which subsequently phosphorylates Merlin at S518 (Chakraborty et al., 2017) and reduces YAP-Merlin association (Module Box V and **Figures 4D,E**). Reciprocally, the effect of YAP on ECM remodeling often requires the presence of other niche factors such as TGFβ (Fujii et al., 2012; Noguchi et al., 2018). TGFβ also enhances the association of SIAH2 with LATS2 (Ma et al., 2016) for degradation. These lines of evidence place X-ROS-coupled cytokine/ECM signaling and cell mechanics upstream of YAP signaling. Nevertheless, we should point out that ROS are generally considered an inducer of premature senescence and aging (Kodama et al., 2013; Davalli et al., 2016; Marazita et al., 2016), and YAP signaling can prevent premature senescence yet often lead to tumorigenesis (Xie et al., 2013; Xu X. et al., 2021). How to optimize their interplay to boost longevity while minimizing the risk of tumorigenesis will be an interesting subject to investigate.

YAP signaling dictates the selection of cell fate, and it is likely that YAP signaling follows switch-like behavior. For the therapeutic purpose, it will be convenient if ROS-mediated effects also act as a switch at different stages of stem cell development and tumor progression, whereby pharmaceutical interventions can be explicitly applied to turn "on" or "off" specific or unwanted effects (Kim P. R. et al., 2020). In fact, switch-like enhancement of YAP-mediated epithelial-mesenchymal transition (EMT) has been proposed in cell migration on substrates engineered with nano-scale topographic cues (Park et al., 2019). The potential coexistence of the compatible and conflicting ROS-mediated effects on YAP signaling suggests that X-ROS and cell mechanics regulate YAP activity in a multiplex, niche factor context-dependent manner and can lead to a differential rather than switch-like response. Whether there is segregation between differential and switch-like YAP responses in the variation of niche factors and how such segregation depends on the physiological or pathological niche conditions remain to be resolved.

The Coupling of X-ROS With HIF/YAP/Notch Triad and PD-L1 Signaling

The involvement of SIAH2 in X-ROS-HIF-1α and X-ROS-YAP signaling suggests that HIF and YAP might be interdependent or connected in the regulation of cell fate and tissue responses. In fact, YAP forms complexes with HIF-1α and acts as the transcription activator of HIF-1α (Xiang et al., 2015; Zhao et al., 2020), and HIF-1α was found to promote YAP activation (Li H. et al., 2018). Positive feedback thus appears in the HIF/SIAH/YAP axis, which might play an important role not only in stem cell physiology but also in tumorigenesis (Module Box VI and **Figure 5A**). The tumor microenvironment (TME) is often characterized by an abundance of ROS and the stiffening of ECM. From the discussion in the previous sections, we note that both HIF-1α and YAP are sensitive to the ECM stiffness and ROS and that the yield of ROS depends on the O_2 concentration and the metabolic activities in the TME. An intriguing question is then how the YAP target genes are differentially regulated by ROS-independent and ROS-dependent HIF signaling in response to the change of ECM stiffness and niche O_2 concentrations. Unfortunately, no quantitative data on this perspective are available to date, and studies are thus warranted.

The complexity in HIF-YAP coupling increases when Notch signaling is considered. In contrast to the regulation of organ size by the Hippo pathway (Yu et al., 2015), Notch signaling regulates

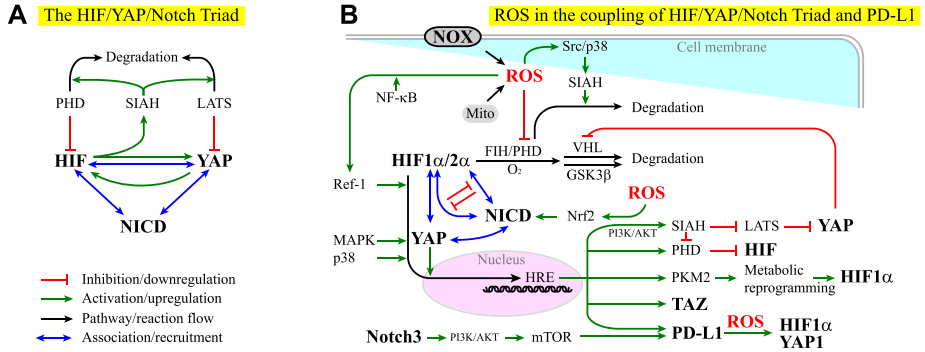

FIGURE 5 | (A) HIF, YAP, and Notch act as a triad in that their effectors can associate to influence each other. See Module Box VI for details. NICD stands for the notch intracellular domain. Red lines indicate inhibition or downregulation. Green lines indicate activation or upregulation. Blue lines indicate physical association or recruitment. Black lines indicate the flow of the pathways or a reaction. **(B)** ROS exhibit both positive and negative effects on the coupling of the HIF/YAP/Notch triad and PD-L1 signaling. See the main text and Module Box VI for details.

the exquisite timing and spatial programming in the organ plan, including the spatiotemporal specification of cell fate and cell differentiation, tissue patterning, and the maintenance of stem cells (Artavanis-Tsakonas et al., 1999; Lasky and Wu, 2005; Sirin and Susztak, 2012; Kessler et al., 2015; Teo et al., 2019). Notch signaling is also associated with a neurological disorder, inflammation, senescence, aging, tumorigenicity, cancer drug resistance, cancer metastasis, cancer stemness, and cancer immune evasion (Sharma et al., 2011; Liu et al., 2012; Wang et al., 2014c; Balistreri et al., 2016; Hoare and Narita, 2018; Wu et al., 2018; Liu et al., 2021a; Xiu et al., 2021). YAP/TAZ forms a complex with the Notch effector, Notch intracellular domain (NICD), to promote the transcription of Notch target genes (Manderfield et al., 2012). Recent studies suggest a coupling of YAP/TAZ and Notch signaling pathways. This coupling can be positive or negative, with YAP/TAZ acting upstream of, downstream of, or in parallel with Notch signaling (Module Box VI). Moreover, YAP/TAZ, HIF-1α, and HIF-2α can bind to NICD to promote the transcriptional activity in a mutually exclusive manner (Hu et al., 2014) (Module Box VI and **Figure 5A**). Such HIF-Notch coupling can be found in, for example, neurological disorder and degeneration, brain function and angiogenesis, and the maintenance of glioblastoma stem cells (Gustafsson et al., 2005; Chen et al., 2010; Qiang et al., 2012; Hu et al., 2014; Li Y. et al., 2018; Kim S. et al., 2020). Conversely, Notch signaling is required for HIF to preserve the full pluripotency of stem cells under hypoxia (Gustafsson et al., 2005), the condition wherein stem cells maintain their stemness (Ezashi et al., 2005). These lines of evidence suggest that HIF, YAP, and Notch act as a triad in the regulation of stem cell physiology and the dysregulation of cell behavior in tumorigenesis.

In addition to YAP and HIF, recent studies have shown that Notch is associated with various subtypes of X-ROS signaling and involved in oxidative stress (Zhang H.-M. et al., 2018). For example, reciprocal ROS-Notch signaling has been identified in the clusters of circulating tumor cells (CTCs) and myeloid-derived suppressor cells (MDSCs), where CTCs have been considered as the *bona fide* precursors for metastatic tumors and MDSCs, a group of undifferentiated, bone marrow-derived heterogeneous cells with enhanced ability of immune suppression (Gabrilovich and Nagaraj, 2009; Wen et al., 2020), are known to promote neoplastic growth by inhibiting the tumoricidal activity of T cells (Aceto et al., 2014; Boral et al., 2017; Sprouse et al., 2019). Several mechanisms have been identified in X-ROS/cytokine/ECM signaling-coupled Notch signaling. The first is to act through the coupling of TGFβ1 and NOX4-derived ROS in epithelial cells, where niche factor TGFβ1 induces NOX4 expression (through p38 kinase (Ning et al., 2002)), ROS-dependent Nrf2 activation and expression, NOX4-derived ROS production, and Nrf2-dependent Notch signaling (Yazaki et al., 2021), which in turn induces EMT (Matsuno et al., 2012). Herein, Nrf2 stands for nuclear factor erythroid-derived 2-related factor 2, a leucine-zipper transcription factor (Moi et al., 1994). Nrf2 and its repressor Kelch-like ECH-associated protein 1 (Keap1) act as the major regulators for cell redox levels (Sporn and Liby, 2012). It has been shown that elevated ROS levels alone are sufficient to trigger Notch signaling for the homeostasis of airway basal stem cells in an Nrf2-dependent manner (Paul et al., 2014) (**Figure 5B**). The second is to act through the combination of the GSK3β-mediated crosstalk between Notch and Wnt/β-catenin signaling pathways (Force and Woodgett, 2009; Caliceti et al., 2014), the X-ROS-mediated activation of GSK3β (Wang C.-Y. et al., 2014), and the downregulation of β-catenin by a redox-sensitive negative regulator of Wnt signaling pathway, nucleoredoxin (NRX) (Shin et al., 2004; Funato and Miki, 2010; Funato et al., 2010). Note that GSK3β is also involved in the HIF-α subunit regulation (Flugel et al., 2007) (Module Box I and **Figures 2B,C**) and the axin-dependent YAP degradation and compartmentalization (Azzolin et al., 2014) (Module Box V and **Figure 4C**). The third is to act through niche mechanics- and ROS-interdependent integrin signaling (Werner and Werb, 2002; Gregg et al., 2004; Buricchi et al., 2007; Taddei et al., 2007; Zeller et al., 2013; Xu Z. et al., 2021), where the activation of ILK potentiates Notch signaling (Maydan et al., 2010) and regulates GSK3β activity (Maydan et al., 2010).

YAP signaling can upregulate PD-L1, the ligand for the cell surface glycoprotein PD-1 that suppresses immune responses in chronic inflammation and in the tumor microenvironment (TME) (Greenwald et al., 2005; Janse van Rensburg et al., 2018), particularly in cancer cells (Lee et al., 2017; Miao et al., 2017). However, YAP is not alone. Recent studies have identified a Notch signaling pathway through the Notch3-PI3K-AKT-mTOR axis to be responsible for the overexpression of PD-L1 in breast cancer stem cell-like (CSC-like) cells (Mansour et al., 2020) (**Figure 5B**). Under hypoxia, the common niche condition in the TME, HIF-1α but not HIF-2α, has been found to bind to an HRE in the PD-L1 promoter region to overexpress PD-L1 in myeloid-derived suppressor cells (MDSCs) (Noman et al., 2014), by which HCCs evade immune systems (Wen et al., 2020). A concomitant elevation of cell surface PD-L1 and intracellular HIF-2α expression has also been observed in solid tumors (Chang et al., 2016; Tawadros and Khalafalla, 2018; Guo et al., 2019; Zhou et al., 2019), where enhanced activities in ERK, AKT, IκBα (nuclear factor of kappa light polypeptide gene enhancer in B-cells inhibitor, alpha), and NF-κB were found to be involved in PD-L1 overexpression (Guo et al., 2019). Conversely, PD-L1 overexpression can promote the expression of HIF-1α and YAP-1 in a ROS-dependent manner (Tung et al., 2018), perhaps through the interaction of PD-L1 with vimentin, a major cytoskeletal element contributing to cell stiffness and EMT (Ancel et al., 2019), or through the nuclear translocation of PD-L1 and subsequent operation on a panel of immune regulation-related genes (Gao et al., 2020; Jaccard and Ho, 2020) (**Figure 5B**).

The coupling of PD-L1 and HIF/YAP/Notch signaling has led to a proposed idea that the targeting therapy on HIF/YAP/Notch signaling pathways, along with the conventional chemotherapy and immune therapy, might serve as a potential surrogate for cancer treatment (Janghorban et al., 2018) (Module Box VI). Given the coupling of X-ROS in HIF/YAP/Notch signaling, it is legitimate to ask whether niche ROS affect PD-L1 expression and/or signaling. **Figure 2E** shows that when the yield of free electrons from the respiratory chain (i.e., ETC) exceeds a certain level with respect to the niche oxygen concentration, ROS can be created and leak to the cytoplasm. This situation is likely to occur at the TME, where tumor cells often carry enhanced glycolysis. In addition, the TME contains inflammatory cells that produce a significant amount of ROS through, for example, NOX, and modify the oxidative stress of the TME, which in turn can influence the antitumor effect of immune responses. It is, therefore, important to evaluate the impact of ROS on PD-L1 expression and functions (Bailly, 2020). This impact is complex and bi-directional. For example, X-ROS and cell mechanics can upregulate HIF and YAP signaling activities and expression levels (Abe et al., 1996; Aikawa et al., 1997; Kulisz et al., 2002; Emerling et al., 2005; Ray et al., 2012; Hu et al., 2017; Xu et al., 2017; Koundouros and Poulogiannis, 2018; Basu et al., 2019; Perillo et al., 2020), which in turn promote PD-L1 expression (Noman et al., 2014; Janse van Rensburg et al., 2018). Conversely, PD-L1 can induce HIF-1α expression in a ROS-dependent manner and, in turn, upregulate YAP1 expression (Tung et al., 2018) (**Figure 5B**). These lines of evidence suggest a potential self-perpetuating amplification in the ROS-HIF/YAP-PD-L1 axis. As a result, enhancing ROS production might promote the PD-L1 expression, and scavenging ROS can repress the PD-L1 expression. Nevertheless, there are contradicting examples in cancer cell lines, where applying ROS-generation drugs leads to PD-L1 downregulation and applying ROS scavengers promotes PD-L1 expression (Bailly, 2020). More studies on the interplay of ROS and PD-L1 are thus warranted.

CONCLUSION REMARKS

Except for the anti-pathogen capacity, ROS have long been considered harmful due to the ability to damage DNA and proteins but is now recognized as an important element in regulating stem cell physiology. Exploding evidence over the past decade further indicates that ROS are intensively coupled with tissue mechanics and HIF-YAP-Notch signaling. Such coupling is manifested in organ development, homeostasis, and repair, and when things go wrong, the coupling can lead to tumorigenesis. This review discusses the interplay of ROS (particularly NOX-derived ROS (i.e., X-ROS)) and the HIF-YAP-Notch signaling. The potentiation of PD-L1 expression in response to ROS-HIF-YAP-Notch signaling is also addressed. Most importantly, we point out the existence of multiplexed positive and negative feedback couplings that occur at different times (i.e., transient or prolonged) and spatial (i.e., autonomous (within the cell) or non-autonomous (within the niche)) scales. Understanding under what niche conditions these couplings can lead to differential or switch-like tissue responses and/or change self-sustained regulation in stem cell physiology to self-perpetuating dysregulation in cancer progression will help us move into the clinical realm to design strategies for stem cell-based and X-ROS-targeting therapy.

SUPPORTING BOXES

Math Box I: The Estimated Phase Diagram of ROS Production

ROS are mainly produced by mitochondria (Murphy, 2009; Juan et al., 2021). In the regular energy production process, the decomposition of carbon hydrates yields CO_2 and H_2, the latter of which forms the high-energy electron donors: nicotinamide adenine dinucleotide phosphate- (NADP-) H, and flavin adenine dinucleotide- (FAD-) H_2. These donors bring electrons to the mitochondria's inner membrane electron transport chain (ETC), through which the electrons are delivered to the molecular oxygen O_2 in exchange for a buildup of pH gradient and an electrochemical potential across the membrane. When the proton flows back through the membrane, it drives the rotation of the membrane-bound ATP synthase and phosphorylates ADP into ATP. This process is called "chemiosmosis," a process by which oxidative phosphorylation generates ATP (Anraku, 1988; Kracke et al., 2015). Eukaryote ETC consists of NADH-coenzyme Q oxidoreductase (Complex I), succinate-Q oxidoreductase (Complex II), electron transfer flavoprotein-Q oxidoreductase, Q-cytochrome c oxidoreductase (Complex III), and cytochrome c oxidase (Complex IV) (Kracke

et al., 2015). Among them, Complexes I, III, and IV are transmembrane proteins coupling the transfer of electrons with the transport of protons. Q stands for ubiquinone, a lipid-soluble electron carrier, and cytochrome c is a water-soluble electron carrier. For an effective electron transfer, the electron donated from NADPH and $FADH_2$ should be transported between the lipid-soluble and water-soluble carriers along the membrane to reach the final target Complex IV, where it binds to O_2 to form H_2O. In reality, however, the anionic nature of the free electron allows it to escape through the transmembrane complexes to both sides of the inner mitochondrial membrane (Murphy, 2009), where it binds to O_2 delivered by cytoplasmic oxygen carriers such as cytoglobin (Novianti et al., 2020). This "leakage" primarily occurs at Complexes I/III and, in turn, forms superoxide, $O_2\bullet$ (or O_2^-), a major form of ROS (Murphy, 2009; Bleier and Drose, 2013).

The theoretical value for the reduction of O_2 to O_2^- in mitochondria was estimated as −68 to −230 mV/mole (Murphy, 2009) and thus is thermodynamically favorable (Andreyev et al., 2005). To see how the free electron selects the "leakage" over the regular path to reach O_2, we considered the internal electron transfer in the catalytic cycle of Complex IV, which has been documented as the rate-limiting step (Sarti et al., 1988). Complex IV contains four electron carriers, including two heme groups, heme "a" and heme "a3," each of which contains an iron ion, and two Cu groups, the first of which contains two copper ions and is referred to as CuA/CuA and the second is formed by a single copper ion and referred to as CuB (Voet and Voet, 2011). Complex IV receives free electrons from the water-soluble carrier, cytochrome c, and passes the electrons internally through CuA/CuA to "a," "a3," and finally CuB. While the function of CuA/CuA and "a" is primarily for electron transfer, "a3" and CuB form a binuclear center not only for electron transfer but also for O_2 association and reduction. Adjacent to the binuclear center is a tyrosine group (Tyr244-OH) which also participates in the process of O_2 reduction. To proceed, we hereafter used the label "$\boldsymbol{X}$" to represent the binuclear center, a3(Fe)-(CuB)-(Tyr244-OH). Likewise, we used "$\boldsymbol{c}$" to denote cytochrome c. In terms of the redox state, we used "$\boldsymbol{c}^0$" and "$\boldsymbol{c}^-$" to indicate the reference state and the reduced state (i.e., carrying one free electron) of cytochrome c, respectively. As for $\boldsymbol{X}$, its catalytic cycle starts from the reference state, a3($Fe^{3+}OH^-$)-(CuB^{2+})-(Tyr244-O^-) (referred to as $\boldsymbol{X}^0$). In each cycle, four electrons from four reduced cytochrome c molecules are used, along with the consumption of four protons from the mitochondrial matrix (equivalent to pumping four protons to the intermembrane space). The first electron and proton reduce the copper ion and restore the tyrosine group of $\boldsymbol{X}$ into a3($Fe^{3+}OH^-$)-(CuB^+)-(Tyr244-OH) (referred to as $\boldsymbol{X}^-$). The second electron and proton reduce the Fe^{3+} of $\boldsymbol{X}$ into a3(Fe^{2+})-(CuB^+)-(Tyr244-OH) (referred to as $\boldsymbol{X}^{2-}$), during which the hydroxide ligand, OH^-, at "a3" is protonated and lost as water, creating a void for O_2 association. Upon association, the oxygen is rapidly reduced by two electrons from a3(Fe^{2+}), one electron from (CuB^+), and one electron and a proton from (Tyr244-OH). The reduction of O_2, in turn, transforms $\boldsymbol{X}$ into the fully oxidized state, a3($Fe^{4+}O^{2-}$)-($CuB^{2+}OH^-$)-(Tyr244-O*) (referred to as $\boldsymbol{X}^{2+}$), where Tyr244-O* indicates a neutral tyrosine radical. Following O_2 reduction is the addition of the third electron and proton that reduces tyrosine radical and converts $\boldsymbol{X}$ to a partially oxidized state, a3($Fe^{4+}O^{2-}$)-(CuB^{2+})-(Tyr244-O^-) (referred to as $\boldsymbol{X}^+$), with the yield of one water molecule. The fourth electron reduces the iron ion, and with the oxygen atom picking up a proton from the matrix, converts $\boldsymbol{X}$ back to a3($Fe^{3+}OH^-$)-(CuB^{2+})-(Tyr244-O^-), that is, the $\boldsymbol{X}^0$ state (Voet and Voet, 2011; Wikstrom and Springett, 2020) (**Figure 1B**).

In the absence of protein degradation and synthesis, we set $(\boldsymbol{c}^0 + \boldsymbol{c}^-) = \rho_c$ and $(\boldsymbol{X}^0 + \boldsymbol{X}^- + \boldsymbol{X}^{2-} + \boldsymbol{X}^+ + \boldsymbol{X}^{2+}) = \rho_{IV}$, with ρ_c and ρ_{IV} as the densities of cytochrome c and Complex IV on the mitochondrial inner membrane, respectively. Ignoring the spatial inhomogeneity and fluctuation of free electrons and O_2, we used the following equations to address the dynamics of X and c:

$$\frac{dX^0}{dt} = k_{IET}c^-[\mathrm{H}^+]X^+ - k_{IET}c^-[\mathrm{H}^+]X^0, \tag{1}$$

$$\frac{dX^-}{dt} = k_{IET}c^-[\mathrm{H}^+]X^0 - k_{IET}c^-[\mathrm{H}^+]X^-, \tag{2}$$

$$\frac{dX^{2-}}{dt} = k_{IET}c^-[\mathrm{H}^+]X^- - k_{O2}[\mathrm{O}_2]_m X^{2-}, \tag{3}$$

$$\frac{dX^{2+}}{dt} = k_{O2}[\mathrm{O}_2]_m X^{2-} - k_{IET}c^-[\mathrm{H}^+]X^{2+}, \tag{4}$$

$$\frac{dX^+}{dt} = k_{IET}c^-[\mathrm{H}^+]X^{2+} - k_{IET}c^-[\mathrm{H}^+]X^+, \tag{5}$$

$$\frac{dc^-}{dt} = k_{ETC}[e^-]c^0 - k_{IET}[\mathrm{H}^+]\left(X^+ + X^0 + X^{2+} + X^-\right)c^-, \tag{6}$$

$$\frac{d[e^-]}{dt} = Y - \left(k_{leak}[\mathrm{O}_2]_c + k_{ETC}c^0\right)[e^-]. \tag{7}$$

k_{IET} was referred to as the internal electron transfer rate from cytochrome c to the binuclear center of Complex IV (for simplicity, we used a single entity to represent all the transfer events). $[H^+]$ was the proton concentration in the mitochondrial matrix. $[O_2]_m$ indicated the mitochondrial molecular oxygen concentration, and k_{O2} was the association rate with Complex IV. $[e^-]$ stood for the density of free electron that was generated at a rate $\boldsymbol{Y}$ and transferred through ETC to the cytochrome c at a rate k_{ETC}, or leaked at a rate k_{leak} to cytoplasmic O_2, the concentration of which was set as $[O_2]_c$. These parameters and variables were tissue context- and physiology-dependent, and estimates had been made in = previous studies (Murphy, 2009; Wikstrom and Springett, 2020). In principle, $[O_2]_m$ could be related to $[O_2]_c$. Using an estimate of $[O_2]_c$ as 120 μM (Wikstrom and Springett, 2020) and $[O_2]_m$ as 25 μM (Murphy, 2009), we could set them at a ratio of ~0.2.

At the steady state, all of the "X" states in **Eqs 1–5** could be solved in terms of $\boldsymbol{X}^0$ and used to express the steady-state solutions of c^- and e^- in **Eqs 6**, **7**:

$$X^0 = \rho_{IV} \Big/ \left(4 + \frac{k_{IET}[\mathrm{H}^+]c^-}{k_{O2}[\mathrm{O}_2]_m}\right), \tag{8}$$

$$c^- = \rho_C k_{ETC}[e^-]/\left(4k_{IET}[\mathrm{H}^+]X^0 + k_{ETC}[e^-]\right), \quad (9)$$

$$[e^-] = Y/\left(k_{leak}[\mathrm{O}_2]_c + k_{ETC}\left(\rho_C - c^-\right)\right), \quad (10)$$

$$z \equiv \frac{c^-}{\rho_C} = \frac{1}{1 + \frac{4\frac{\rho_{IV}}{Y}k_{IET}[\mathrm{H}^+]\left(\frac{k_{leak}[\mathrm{O}_2]_c}{k_{ETC}} + \rho_C(1-z)\right)}{4 + \frac{k_{IET}[\mathrm{H}^+]\rho_C}{k_{\mathrm{O}2}[\mathrm{O}_2]_m} \times z}}, \quad (11)$$

$$w \equiv \frac{k_{ETC}\left(\rho_C - c^-\right)}{k_{leak}[\mathrm{O}_2]_c} = \frac{k_{ETC}\rho_C(1-z)}{k_{leak}[\mathrm{O}_2]_c}. \quad (12)$$

Combining **Eqs 8–10**, we had **Eq. 11**, which defined the fraction of reduced cytochrome c with respect to all the cytochrome c on the membrane as z ($0 \le z \le 1$). Examining the left-hand and the right-hand sides of **Eq. 11**, we found that there was always a solution of z between zero and one. In **Eq. 12**, we defined the ratio of electrons selecting the regular path over the leakage to reach O_2. When w was less than one, most electrons selected the leakage. The critical z^* at $w = 1$ was found in **Eq. 12**:

$$z^* = 1 - \frac{k_{leak}[\mathrm{O}_2]_c}{k_{ETC}\rho_C}. \quad (13)$$

From **Eq. 13**, the maximal $[O_2]_c*$ for $w \ge 1$ read as follows:

$$[\mathrm{O}_2]_c^* = \frac{k_{ETC}\rho_C}{k_{leak}}. \quad (14)$$

Eq. 14 suggests a critical cytoplasmic oxygen concentration $[O_2]_c^*$, which increases with the density of available cytochrome c on the mitochondrial membrane, ρ_C. For cytoplasmic oxygen concentration above $[O_2]_c^*$, electrons generated in ETC predominantly leaked and formed ROS. Using Eqs. **11–14**, for a given $[O_2]_c$, we obtained the critical electron generation rate Y^* in the ETC, and for $Y > Y^*$, the generated electrons predominantly selected the leakage over the regular path to reach O_2:

$$\begin{aligned} Y^* &= \frac{8\rho_{IV}k_{IET}[\mathrm{H}^+]\rho_C\left(1 - \frac{k_{leak}[\mathrm{O}_2]_c}{k_{ETC}\rho_C}\right)}{4 + \frac{k_{IET}[\mathrm{H}^+]\rho_C}{k_{\mathrm{O}2}[\mathrm{O}_2]_m}\left(1 - \frac{k_{leak}[\mathrm{O}_2]_c}{k_{ETC}\rho_C}\right)} \\ &= \frac{\frac{8\rho_{IV}k_{IET}k_{leak}[\mathrm{H}^+]}{k_{ETC}}[\mathrm{O}_2]_c^*\left(1 - \frac{[\mathrm{O}_2]_c}{[\mathrm{O}_2]_c^*}\right)}{4 + \frac{k_{IET}k_{leak}[\mathrm{H}^+]}{k_{O2}k_{ETC}\frac{[\mathrm{O}_2]_m}{[\mathrm{O}_2]_c}} \times \frac{[\mathrm{O}_2]_c^*}{[\mathrm{O}_2]_c}\left(1 - \frac{[\mathrm{O}_2]_c}{[\mathrm{O}_2]_c^*}\right)} \text{ for } [\mathrm{O2]c} \le [\mathrm{O2]*} \\ &= kETC\rho C/kleak, Y^* = 0. \end{aligned} \quad (15)$$

Using the estimate that $[O_2]_m/[O_2]_c \sim 0.2$, we obtained the maximal electron generation rate on the variation of cytoplasmic oxygen concentrations (**Figure 2E**). Below this rate, over 50% of electrons would be used for oxidative phosphorylation.

Module Box I: O_2-Dependent Regulation of HIF-α Stability

The cells use the oxygen-sensing regulations to regulate the stability of HIF-α subunits in response to niche oxygen. For HIF-1α, these regulations occur at its functional motifs: proline 402 and 564 at its N-terminal activation domain (NAD) and asparagine 803 at its C-terminal transactivation domain (CTAD). Both NAD and CTAD can recruit E1A binding protein p300 (p300)/cyclic adenosine monophosphate response element-binding protein-binding protein (CREB-binding protein, CREBBP, or CBP) co-activators to enhance the transcriptional activity of HIF. The HIF prolyl hydroxylase domain-containing proteins (PHD or HIF prolyl hydroxylases (HPH)) 1-3 (Fong and Takeda, 2008) and the factor inhibiting HIF (FIH) (Lando et al., 2002; Sim et al., 2018) are the main enzymes responsible for the oxygen-sensing post-translational modifications (PTMs) of HIF-α subunits (**Figure 2B**). PHD is a Fe^{2+}-dependent dioxygenase. It binds to one O_2 and one HIF-α subunit at the same time, followed by transferring O_2 to the proline 402 and 564 of the HIF-1α subunit (or 405 and 531 of the HIF-2α subunit) (Hashimoto and Shibasaki, 2015), HIF-L-proline + 2-oxoglutarate (α-ketoglutarate) + O_2 $\vec{x}$ HIF-trans-4-hydroxy-L-proline + succinate + CO_2, to hydroxylate the proline residues. The reaction indicates that the accumulation of 2-oxoglutarate (or α-ketoglutarate) promotes the hydroxylation of HIF, and the accumulation of succinate prohibits hydroxylation. Once hydroxylated, the proline residue not only fails to recruit p300/CBP to NAD but also becomes recognizable by von Hippel–Lindau tumor suppressor protein (VHL) E3 ubiquitin ligase, which targets the HIF-α subunit for ubiquitination and a rapid 26S proteasome-dependent degradation (Maxwell et al., 1999; Bruick and McKnight, 2001; Epstein et al., 2001; Ivan et al., 2001; Jaakkola et al., 2001). Consequently, PHDs serve as an oxygen sensor to regulate HIF-α subunit stability in response to the fluctuation of niche oxygen concentration $[O_2]$ (Ivan et al., 2001). In comparison, FIH is an asparaginyl hydroxylase that uses α-ketoglutarate and O_2 to hydroxylate asparagine 803 of the HIF-1α (or 851 of the HIF-2α) (Schofield and Ratcliffe, 2004) and inhibits its transcriptional activity at CTAD (Lando et al., 2002; Sim et al., 2018), rather than degradation, a detailed discussion of which A detailed can be found elsewhere (Masson and Ratcliffe, 2014; Strowitzki et al., 2019). Apart from hydroxylation, the stability and the ability of HIF-1α to translocate into the nucleus depends on phosphorylation, which is primarily mediated by kinases such as glycogen synthase kinase 3β (GSK3β) and MAPKs (the common effectors involved in TGFβ and IGF-1 signaling, for example, extracellular regulated kinases (Erk1/2) and p38 kinase (Richard et al., 1999; Sodhi et al., 2000; Flugel et al., 2007)) (**Figure 2C**). As HIF-1α promotes angiogenesis and glycolysis and HIF-2α helps the maintenance of stemness (**Figure 2A**), it is not surprising that HIFs are dysregulated in tumors. In fact, not only HIF but also PHDs are dysregulated in tumors. PHDs are often overexpressed in tumors by contradicting the expectations, and inhibition of PHDs can impair tumor growth, metastasis, and immune tolerance (Gaete et al., 2021). Thus, HIFs and PHDs have been proposed as therapeutic targets against cancer.

The regulation of HIF stability by FIH and PHD depends on their K_m values for $[O_2]$ association. The K_m value of FIH is ~90–200 μM (Koivunen et al., 2004; Tarhonskaya et al., 2015). In comparison, the K_m value of PHD for $[O_2]$ association is documented as 230–250 μM (Fong and Takeda, 2008) or even higher (250 μM–1.7 mM) (Ehrismann et al., 2007; Dao et al., 2009; Tarhonskaya et al., 2015). In any case, it is above the $[O_2]$ in

air-saturated aqueous buffer at 37°C ([O_2] ~21% (~210 μM)) (Reynafarje et al., 1985; Murphy, 2009), abundantly above the physiological oxygen concentration ([O_2] ~7% (~70 μM)) (Hu et al., 2014), larger than the K_m value of other oxygenases such as collagen PHD (~40 μM) (Hirsila et al., 2003), and far above the oxygen concentration in mitochondria ([O_2] ~3–30 μM) (Turrens, 2003). Such discrepancy reflects that FIH and PHD are designed for different purposes in response to the niche oxygen concentrations (i.e., FIH for differential activation of HIF target genes and PHD for degradation) and suggests that additional mechanisms might exist for the regulation of HIF-α subunits. Indeed, negative feedback mechanisms have been identified. HIF-1α, for example, promotes its degradation by inducing the expression of PHD2-3 and FIH-1 (Marxsen et al., 2004; Kobayashi et al., 2021).

Module Box II: ROS-Dependent Regulation of HIF-α Stability

Recent evidence suggests that ROS contribute to the regulation of HIF-α stability by modulating the activity of PHD (Gerald et al., 2004; Fong and Takeda, 2008; Lee et al., 2016) (**Figure 2C**). The precise mechanism by which ROS regulate PHD is complex and not fully understood. At least three inhibitory and one enhancing mechanisms have been identified. The first inhibitory mechanism is to act by oxidizing the cysteine residues of PHD into disulfide bonds, which cause homo-dimerization and inactivation of PHD (Lee et al., 2016). The second is to act through chelating and oxidizing PHD-bound Fe^{2+} to Fe^{3+}, by which the ability of PHD to bind to O_2 is abolished (Gerald et al., 2004; Fong and Takeda, 2008). The third is to act through seven in absentia homolog 2 (SIAH2), a RING finger-containing E3 ubiquitin ligase targeting PHDs for ubiquitin-mediated proteasome degradation (Nakayama and Ronai, 2004; Qi et al., 2013). SIAH2 can be phosphorylated and activated by several ROS-activated kinases, a detailed review of which can be found elsewhere (Xu and Li, 2021). In contrast, the enhancing mechanism is a long-term effect and acts through redox factor-1 (Ref-1). Prolonged ROS exposure induces Ref-1 expression in an NF-κB- (nuclear factor kappa-light-chain-enhancer of activated B cells-) dependent manner and, in turn, upregulates the transcriptional activity of HIF-1α to promote PHD2 and FIH-1 expressions (Kobayashi et al., 2021), the outcome of which is to downregulate HIF-1α (**Figure 2C**).

Module Box III: The NOX-Derived ROS (X-ROS) Signaling

NOX can be found on the plasma membrane (NOX1-5 and Duox1-2), endoplasmic reticulum (NOX2, NOX4, and NOX5), mitochondrial membrane (NOX4), nuclear membrane (NOX4-5), membrane microdomains such as caveolae and lipid rafts (NOX1), focal adhesions (NOX4), and invadopodia (NOX1 and NOX4) (Brown and Griendling, 2009; Brandes et al., 2014a; b; Fukai and Ushio-Fukai, 2020). The catalytic domains of NOX, homologs of $gp91^{phox}$ β subunit with six transmembrane helices, are anchored to the membrane with the cytoplasmic tails binding to NADPH for electron transfer (Brandes et al., 2014b). Upon activation, the NOX-associated NADPH is oxidized, and electrons are transferred across the $gp91^{phox}$ transmembrane domain to bind to O_2 in the extracellular or intracellular spaces, thereby increasing ROS levels in the niche or inside the cell (Brandes et al., 2014b).

In general, the functionality of NOX requires their catalytic units, the transmembrane $gp91^{phox}$ homolog subunit (each NOX subtype has its own $gp91^{phox}$ homolog), to be in a homodimer (e.g., NOX5) or in a complex with specific membrane scaffolds, namely, NOX1-4 with the membrane scaffold $p22^{phox}$ and Duox1-2 with membrane scaffolds DuoxA1-2, respectively (Brandes et al., 2014b; Skonieczna et al., 2017) (**Figure 3A**). The mechanisms by which NOX are activated vary among the subtypes. NOX5 and Duox1-2, for example, are activated by calcium binding to their cytoplasmic EF-hand calcium-binding motifs, whereas the activation of NOX1-3 requires the assembly and the PTMs of their cytoplasmic regulators (Brown and Griendling, 2009; Brandes et al., 2014b; Skonieczna et al., 2017). By contrast, NOX4 is constitutively active and does not need the association of any cytoplasmic regulators to produce ROS (Ellmark et al., 2005). Still, the activity of NOX4 is modulated by the phosphorylation on its tyrosine reside 491 (in, e.g., IGF-1 stimulation (Xi et al., 2013)) and on the threonine residues of its membrane scaffold $p22^{phox}$ (Regier et al., 1999). Below, we briefly review the regulation of NOX 1-4 and discuss how they are coupled with cytokine and ECM signaling.

As the first example, we use NOX2 to illustrate how the NOX multi-unit assembly is organized and how the PTMs of NOX subunits affect their assembly and functions. The details can be found elsewhere (Brandes et al., 2014b; Rastogi et al., 2016; Skonieczna et al., 2017). As aforementioned, NOX1-3 are inactive when present as a monomer (i.e., with the $gp91^{phox}$ homolog subunit alone) and need to form a complex with the membrane scaffold $p22^{phox}$ for maturation and stabilization (Nakano et al., 2007). The activation of NOX2 further requires recruiting $p21^{Rac1/2}$ (Rho GTPase Rac1/2), $p67^{phox}$, $p40^{phox}$, and $p47^{phox}$ into the $gp91^{phox}$-$p22^{phox}$ complex (Brandes et al., 2014b), where $gp91^{phox}$ is the core subunit and each NOX subtype has its own homolog (**Figure 3C**). Recruiting these molecules consumes high-energy phosphate compounds. For example, the recruitment of Rac needs the Rac guanine nucleotide exchange factor (GEF) to switch Rac from the GDP- to GTP-bound form and expose its prenylated tail for membrane binding (Abo et al., 1994; Diekmann et al., 1994), whereas the recruitment of $p47^{phox}$ requires phosphorylation of $p47^{phox}$ by serine/threonine kinases such as protein kinase B (PKB)/AKT, protein kinase C (PKC), and p21-activated protein kinase (PAK) (Fontayne et al., 2002; Chen et al., 2003; Hoyal et al., 2003; Bey et al., 2004; Martyn et al., 2005). Reciprocally, the association between $p22^{phox}$ and $p47^{phox}$ is enhanced if $p22^{phox}$ is phosphorylated by phosphatidic acid- (PA-) activated protein kinase or PKC (Regier et al., 1999). The phosphorylation of $p47^{phox}$ not only enables its binding to $p67^{phox}$ and $p22^{phox}$ but also exposes its pbox consensus sequence (PX) domain to phosphatidylinositol (4,5)-bisphosphate or phosphatidylinositol (3,4,5)-trisphosphate (PIP_2 or PIP_3) for membrane binding (Ago et al., 2003; Groemping et al., 2003). Such PX domain is also

found in $p40^{phox}$, a regulator that binds to $p67^{phox}$ and stabilizes $p67^{phox}$-$p47^{phox}$ complex formation (Kanai et al., 2001).

The involvement of PIP_2/PIP_3 in NOX2 multi-unit assembly suggests that NOX2 activity is modulated by PI3K and phosphatase and tensin homolog (PTEN), the common effectors in the cytokine/ECM signaling. Likewise, the involvement of phosphorylation-mediated PTMs on the subunit assembly suggests that cytokine/ECM signaling regulates NOX2 activity. These phosphorylation-mediated PTMs are not just for potentiating NOX multi-unit assembly. PKC-mediated phosphorylation in NOX2 and $p67^{phox}$, for example, has been found to maximize the yield of NOX2-derived ROS (Regier et al., 1999; Raad et al., 2009; Brandes et al., 2014b), which in turn can evoke calcium influx (Gorlach et al., 2015). The binding of Ca^{2+} to the C2 domain of PKC then promotes the membrane targeting of PKC (Shirai and Saito, 2002) and the phosphorylation of $p47^{phox}$, $p67^{phox}$, $p40^{phox}$, and Rac through calcium-activated PKC (Cathcart, 2004; Brown and Griendling, 2009; Gorlach et al., 2015; Islam et al., 2018; Tu et al., 2020), leading to a potential feedback amplification along the ROS-Ca^{2+}-PKC signaling axis (**Figure 3C**).

The second example is NOX1 and NOX3, the activation of which requires the assembly of $p47^{phox}$ homolog Noxo1 and the $p67^{phox}$ homolog Noxa1 to NOX1-$p22^{phox}$ and NOX3-$p22^{phox}$ complexes, respectively (Brandes et al., 2014b). Similar to $p67^{phox}$, the activity of Noxa1 is regulated by phosphorylation. Unlike $p67^{phox}$, however, the phosphorylation of Noxa1 can lead to active or inhibitory effects, which involve not only serine/threonine kinases but also protein tyrosine kinases. For example, PKC, steroid receptor coactivator (Src) kinase, and CaMK2 phosphorylate Noxa1 and enhance its association with Noxo1 and NOX1, whereas the phosphorylation of Noxa1 by cAMP-dependent protein kinase or PKA inhibits the association (Kim et al., 2007; Gianni et al., 2010; Kroviarski et al., 2010; Brandes et al., 2014b). Inhibitory phosphorylation also occurs at NOX2 (mediated by casein kinase 2 (CK2)) (Kim et al., 2009) and at $p40^{phox}$, the phosphorylation of which leads to the suppression of NOX activity (Lopes et al., 2004).

The third example is NOX4 (**Figure 3D**). The activation of NOX4 does not explicitly require the multi-unit assembly of cytosolic regulators. Still, NOX4 interacts with several cytosolic molecules to modulate its activity. For example, NOX4 interacts with a chaperon protein, calnexin, to facilitate its maturation (Prior et al., 2016). NOX4 also interacts with a mitochondrial protein, polymerase δ-interacting protein 2 (Poldip2), to increase its activity (Lyle et al., 2009). Poldip2 is a molecule interacting with DNA polymerase δ p50 subunit and with the proteins constituting the mitochondrial DNA nucleoid, through which NOX4 activity is associated with the TCA cycle and metabolic reprogramming (Andjongo et al., 2021; Kulik et al., 2021). In fact, metabolism-related cytokines, such as insulin and IGF-1, are known to increase NOX4 expression (Meng et al., 2008; Schroder et al., 2009; Kim et al., 2012). Cytokine-enhanced upregulation of NOX has also been reported in the TGFβ-mediated pulmonary remodeling (Watson et al., 2016) (**Figure 3B**). In addition to the mitochondria, Poldip2 interacts and activates the Rho GEF, epithelial cell transforming sequence 2 (Ect2), to enhance actin filament polymerization, thereby linking the NOX4 activity to cytoskeletal dynamics (Huff et al., 2019). As for the phosphorylation-mediated PTMs, in contrast to NOX1-3, mostly regulated by serine/threonine kinases, NOX4 is primarily regulated by protein tyrosine kinases (PTKs) such as Src kinase. The phosphorylation of Tyr-491 on NOX4, for example, promotes NOX4 association with Src homology 2- (SH2-) domain-containing protein tyrosine phosphatase (SHP) substrate-1 (SHPS-1), through an adaptor protein, growth factor receptor-bound protein 2 (Grb2) (Xi et al., 2013). SHPS-1 is a transmembrane protein that serves as a scaffold to cluster membrane receptors such as IGF-1 receptor (IGF-1R) with other signaling and adapter molecules, including protein tyrosine kinases, Src family kinase (SrcFK), focal adhesion kinase- (FAK-) related cytosolic kinase, NOX4, SHP-2, Grb2, Janus kinase 2 (Jak2), proline-rich tyrosine kinase 2 (Pyk2), and integrin-associated protein (IAP) (Oshima et al., 2002; Maile et al., 2008; Shen et al., 2009; Xi et al., 2013). Among them, IAP is a transmembrane protein associated with several integrins, including the broadly expressed RGD receptor αvβ3, the platelet-fibrinogen receptor αIIbβ3, and the collagen receptor α2β1. In IGF-1 signaling, the SHPS-1-mediated association of IGF-1R with SHP-2 and Src kinase regulates the lifetime of phosphorylated IGF-1R and the duration of IGF-1 signaling. The association of IGF-1R with IAP enables the crosstalk between IGF-1R and integrin/FAK signaling, by which growth factor stimulation can be coupled with cell–ECM interactions (Maile et al., 2003).

NOX4 is not the only NOX family member that can bind to scaffold proteins involved in cytokine and integrin/ECM signaling. NOX2, for example, can be translocated to the cell front *via* the association of phosphorylated $p47^{phox}$ with scaffold proteins such as tumor necrosis factor (TNF) receptor-associated factor 4 (TRAF4) and Wiskott–Aldrich Syndrome protein (WASP) family verprolin homologous protein 1 (WAVE1) (Wu et al., 2003; Li et al., 2005; Anilkumar et al., 2008; Kim et al., 2017; Fukai and Ushio-Fukai, 2020). Reciprocally, TNFα-induced Erk1/2 activation requires the association of phosphorylated $p47^{phox}$ with TRAF4 (Li et al., 2005). Likewise, vascular EGF- (VEGF-) induced JNK activation needs the interaction of $p47^{phox}$ with WAVE1 (Wu et al., 2003). The TRAF4-$p47^{phox}$ association also plays an important role in the TRAF4-mediated thrombosis, suppressed by NOX2 inhibition (Arthur et al., 2011). These lines of evidence suggest not only spatial confinement of X-ROS to the vicinity of signaling targets (as the lifetime of ROS is short (Marklund, 1976)) but also crosstalk between X-ROS and cytokine/ECM signaling that leads to feedback amplification or suppression. The feedback signal could occur at multiple levels, including genetic regulations (e.g., TGFβ, insulin, and IGF-1 are known to increase NOX4 expression (Ning et al., 2002; Meng et al., 2008; Schroder et al., 2009; Kim et al., 2012; Watson et al., 2016; Liu W. J. et al., 2021; Yazaki et al., 2021)), PTMs (e.g., phosphorylation- and oxidation-mediated regulations), and ligand-receptor interactions. One example of ligand-receptor interactions is TGFβ signaling, where ROS produced by NOX4 promotes the activation of

latent TGFβ, an inactive form of TGFβ secreted and bound to ECM (Watson et al., 2016). The activated ligands, in turn, can stimulate not only the ROS-producing cells but also nearby non-ROS-producing cells, leading to a multi-scale (i.e., autonomous and non-autonomous) niche response in the TGFβ-ROS signaling. Another example is integrin, the most abundant receptor for cell–ECM interactions. Growing evidence suggests that integrins are redox-sensitive, and NOX4-derived ROS can activate integrins through the cleavage of integrin α subunits (Wang et al., 1997; Ushio-Fukai, 2009; de Rezende et al., 2012; Eble and de Rezende, 2014).

Module Box IV: Mechanics for the Regulation of Organ Size and Shape

To control cell shape and tissue topology, for decades, the dogma has been the interactions of diffusive extracellular cytokines and intracellular signaling molecules. It is suggested that the dynamic instability of interacting molecules can create spatiotemporal patterns to direct the assembly and remodeling of cytoskeleton and ECM, the mechanical output of which shapes cell and tissue boundaries and, in turn, determines cell fate. Conversely, little is known about whether the shape of cell and tissue boundary can spontaneously emerge through the mechanical instability of cytoskeleton and ECM and, in turn, direct the spatiotemporal patterns of signaling molecules and cytokines. Regardless of whether the chemical or the mechanical factors serve as the initial cues, cells need to continuously produce and respond to mechanical forces for the creation and maintenance of cell shape and tissue topology and often do so in synchrony with other cells (Cai D. et al., 2014). Unlike chemical signals, mechanical forces lack specificity and can be integrated, independent of the origins. Further, forces can be transmitted between and across cells through cytoskeletons, membranes, intercellular adhesions (Ragsdale et al., 1997; Vaezi et al., 2002), and ECM (Reinhart-King et al., 2008). Unlike the isotropic diffusion of cytokines, the transmission of forces within the boundary depends on the topology and structure of materials and hence can be fast, long-range, and highly anisotropic. Cells can likely take advantage of these properties to create long-range regulators and/or communicators. In fact, it has been shown that cells use membrane tension as a long-range inhibitor to regulate their polarization and morphology (Toriyama et al., 2010; Houk et al., 2012). We have also shown that epithelial cells create forces at collagen-based ECM and use them as a long-range coordinator to guide the self-assembly of tubular patterns (Guo et al., 2012).

Following the laws of thermodynamics, cell shape and tissue topology are determined by minimizing the surface free energy, which creates local forces at the boundaries, such as shear and/or normal stresses, that in turn evoke signaling activities to change cell fate. Shear stress, for example, is known to facilitate the respiratory barrier function and renal tubulogenesis, and failure in these processes leads to an abnormality such as polycystic kidney diseases (Sidhaye et al., 2008; Cattaneo et al., 2011). Similarly, normal stress that stretches the boundary between cells and ECM can lead to cell proliferation, whereas compression can lead to stem cell differentiation, as in the formation of teeth and cartilages (Terraciano et al., 2007; Mammoto et al., 2011; Aragona et al., 2013). In both cases, the forces are transduced into chemical signaling, such as the expression or nuclear translocation of transcriptional factors, Pax9, Sox-9, and/or YAP (Terraciano et al., 2007; Dupont et al., 2011; Mammoto et al., 2011). In this regard, cell mechanics and cytokine signaling appear to be both upstream and downstream of each other, with cell mechanics as a double-edged sword to facilitate organ development and potentiate cancer progression.

From the physics perspective, cell mechanics contains the passive components and the active elements, corresponding to the mechanical structures/properties of cells and the forces created therein, respectively. In general, forces created or acting at the cell include isotropic ones, such as osmotic pressure regulated by ion channels/pumps and water channels, and anisotropic ones, such as shear stress, cytoskeletal polymerization-mediated expansion, actomyosin-mediated retraction, and adhesions at the cell–cell and cell–ECM interfaces. For osmotic pressure, one example is the NOX2-mediated activation of ENaC, in which NOX2 produces ROS to activate the nearby ENaC (*via* cysteine oxidization) and induce sodium influx (Takemura et al., 2010; Goodson et al., 2012). A similar effect has been found in peroxynitrite ($OONO^-$, created by $NO + O_2^-$) mediated inhibitory cysteine glutathionylation on the sodium-potassium pump (Na^+-K^+ ATPase), which causes intracellular sodium retention (Brown and Griendling, 2009; Figtree et al., 2009). The increment of intracellular sodium concentration, in turn, brings water into the cell through the water channels and aquaporin and induces calcium influx through the reverse mode of the sodium-calcium exchanger (NCX) (Tykocki et al., 2012; Ma and Liu, 2013; Yan et al., 2015; Chifflet and Hernandez, 2016) (**Figures 3B,C**). Depending on the cell type, calcium influx can activate NOX5, Duox1-2 (Brandes et al., 2014b; a), and/or PKC (Shirai and Saito, 2002), which can phosphorylate $p47^{phox}$, $p67^{phox}$, $p40^{phox}$, Rac, and NOX2 (Cathcart, 2004; Brown and Griendling, 2009; Gorlach et al., 2015), leading to a positive feedback amplification on ROS-Ca^{2+} signaling. Calcium and the activated Rac1 can further promote actomyosin association and actin filament polymerization, respectively, thereby connecting the feedback with cell mechanics.

Rac1 is not the only ROS-activated effector in cytoskeletal dynamics. SrcFK, for example, can be activated by ROS through cysteine oxidization to phosphorylate the Rho GEF ARHGEF1 and the Rho-associated protein kinase (ROCK), thereby promoting RhoA activation for actin filament polymerization and myosin light chain (MLC) phosphorylation for actomyosin contraction (MacKay et al., 2017). *Via* cysteine oxidization, ROS also enables the association of Ras GTPase-activating-like protein or IQ motif-containing GTPase activating protein 1, IQGAP1, with NOX2 and cytokine receptors such as VEGF receptor (VEGFR) at the lamellipodial leading edge (Ikeda et al., 2005; Kaplan et al., 2011) (**Figure 4A**). IQGAP1-3 are scaffold proteins interacting with more than 100 molecules. These molecules include CD44, Rac1, Cdc42, formin mDia1, inverted formin-2

(INF-2), WASP, microtubule plus-end binding protein CAP-GLY domain-containing linker protein 1 (CLIP1), and cytoplasmic linker associated protein 1 (CLASP1), adenomatous polyposis coli (APC), β-catenin, Mek1/2 kinase, Erk1/2, Src kinase, integrin-linked kinase (ILK), 5′ AMP-activated protein kinase (AMPK), PTP, and ezrin (Brandt et al., 2007; Le Clainche et al., 2007; Watanabe et al., 2009; Malarkannan et al., 2012; White et al., 2012; Widmaier et al., 2012; Liu et al., 2014; Smith et al., 2015; Bartolini et al., 2016; Sayedyahossein et al., 2016; Hedman et al., 2021). IQGAPs also bind to CLASP2, YAP, and the regulators of YAP in the Hippo pathway, MST2, and LATS1 (Watanabe et al., 2009; Sayedyahossein et al., 2016; Quinn et al., 2021). Through these binding capacities, the cytokine-NOX2 signaling can confine microtubule plus end, ROS signals, kinase activities, and actin filament polymerization at the cell leading edge, by which it not only directs the microtubule transport-delivered surface receptors and signaling molecules to the moving front but also interferes with YAP-dependent mechanotransduction.

IQGAP1 is involved in microtubule dynamics. To date, the most well-studied system for the coupling of X-ROS and microtubule dynamics is the cardiomyocytes. These cells are huge (with cell volume ≥40,000 μm^3), in a rod shape packed with dense cytoskeletal networks that can be divided into two groups—the contractile actomyosin arrays organized into myofibrils and the viscoelastic microtubule bundles aligned in the longitudinal direction of the cells. Given the long persistence length of microtubules (~0.5–1.5 mm^2 (Gittes et al., 1993; van Mameren et al., 2009)), it is plausible that microtubules serve as the mechanical sensor to detect the conformational change of the cell as a whole. In fact, it was shown that physiologic stretch elicits a rapid activation of NOX2 in these cells, likely through the release of microtubule-bound Rac1-GTP (Best et al., 1996) by mechanical deformation to activate nearby NOX2. NOX2-derived ROS then sensitize nearby sarcoplasmic reticulum (SR) calcium channels, ryanodine receptors (RyRs), by cysteine oxidation to release calcium ions in response to the mechanical stretch as a rapid and localized mechano-chemo transduction process (Prosser et al., 2011). Conversely, in muscle contraction, microtubules buckle to bear the mechanical load created by the actomyosin contraction. The buckling not only elicits X-ROS signaling but also provides resistance against the contraction (Robison et al., 2016). The amount of elicited X-ROS signals depends on the PTMs of microtubules. It was shown that detyrosinated microtubules, a stable microtubule subpopulation, are responsible for muscle stiffness and X-ROS generation during contraction (Robison et al., 2016). As a result, suppressing microtubule detyrosination provides a therapeutic strategy to treat patients with hypertrophic or dilated cardiomyopathies, both of which carry a higher amount of detyrosinated microtubules than normal (Chen et al., 2018).

With the cytoskeletal dynamics and NOX activity mutually influencing each other, it is plausible that NOX is subject to the mechanical modulation in cell morphogenesis and involved in cell mechanotransduction. Indeed, recent studies have shown that cyclic stretch increases mitochondria-released ROS, FAK phosphorylation at Tyr397, and PKC activity (Ali et al., 2006). PKC and the released ROS, in turn, activate (through phosphorylation and/or cysteine oxidization) $p47^{phox}$, $p67^{phox}$, $p40^{phox}$, Rac, NOX2, SrcFK, and NOX4 (Shirai and Saito, 2002; Cathcart, 2004; Brown and Griendling, 2009; Xi et al., 2013; Gorlach et al., 2015) to enhance ROS production, whereas FAK recruits Src kinase to the integrin cytoplasmic tails and forms a complex therein to induce multiple responses including PI3K-AKT activation, actin filament polymerization, and focal adhesion complex formation (Bolos et al., 2010; Zhao and Guan, 2011). The cysteine-oxidized SrcFK then activates ARHGEF1 and ROCK to enhance MLC phosphorylation, stress fiber assembly, and force generation at the cell–ECM interface (Tominaga et al., 2000; MacKay et al., 2017), by which the mechanical stretch between cells and the ECM could be reinforced (**Figure 2C**). In addition, mechanical stretch can induce persistent calcium influx *via* microtubule-dependent activation of NOX2 to generate ROS, which acts on redox-sensitive transient receptor potential (TRP) channels (Song et al., 2011; Taylor-Clark, 2016; Pires and Earley, 2017; Pratt et al., 2020; Singh et al., 2021) such as TRPA1, TRPM2, TRPV4, and TRPC6 to evoke or prolong calcium signaling, thereby enhancing PKC activity (Shirai and Saito, 2002) and actomyosin assembly and contractility (through, e.g., activating the CaM (calmodulin)/MLCK-signaling pathway (Zergane et al., 2021)). The integration of these effects can lead to a self-perpetuated amplification of the cellular mechanical responses, which might serve as a switch for the selection of stem cell fate. One example is the cyclic stretch-induced cardiomyogenesis of mouse embryonic stem cells in the presence of Wnt/β-catenin signaling (Heo and Lee, 2011). At the genetic level, mechanical stretch can modulate NOX and HIF-1α expressions (Grote et al., 2003; Schmelter et al., 2006; Sauer et al., 2008; Zhang et al., 2015). However, the effect is exposure time- and pattern-dependent (Goettsch et al., 2009) and can lead to positive or negative feedback regulations, a detailed review of which can be found elsewhere (Brandes et al., 2014a).

Module Box V: Merlin, YAP, and Angiomotin as Transducers for Cell Mechanics and Tissue Topology

YAP/TAZ boost organ growth and are suppressed by the Hippo pathway (Wang et al., 2009; Zhao et al., 2010a; Li et al., 2010; Lian et al., 2010; Dupont et al., 2011; Yu et al., 2015; Panciera et al., 2017; Totaro et al., 2018b). YAP is referred to as WW domain-containing transcription coactivator Yes-associated protein (Sudol, 1994), TAZ is referred to as transcriptional coactivator with PDZ-binding motif, also known as WW domain-containing transcription regulator 1 (WWTR1) (Sarmasti Emami et al., 2020), and the Hippo pathway, also known as the Salvador–Warts–Hippo (SWH) pathway, is a pathway that controls organ size by restraining cell proliferation and promoting apoptosis (Piccolo et al., 2014). Herein, PDZ stands for post-synaptic density 95, Discs large, and Zonula occludens-1, whereas the WW domain, named after the presence of two tryptophan (W) residues and also known as the rsp5-domain or WWP repeating motif, is a modular protein domain

preferentially binding to proline-rich, for example, PPXY and LPXY, or phosphor-serine/threonine-containing (e.g., p-SP/p-TP) motifs (Chen and Sudol, 1995; Sudol et al., 1995; Macias et al., 1996; Lu et al., 1999). YAP/TAZ has a critical role in stem cell self-renewal and tissue-specific progenitor cell self-expansion (Dong et al., 2007; Zhao et al., 2011b; Anton and Wandosell, 2021), where YAP/TAZ is accumulated and active in the cell nucleus (Camargo et al., 2007; Cao et al., 2008; Schlegelmilch et al., 2011; Silvis et al., 2011; Lavado et al., 2013). Moreover, as hyperactive YAP/TAZ leads to uncontrolled cell growth, a growing interest has been raised in the roles of YAP/TAZ in cancer progression (Saucedo and Edgar, 2007; Xu et al., 2009; Pan, 2010; Johnson and Halder, 2014; Mo et al., 2014; Lee Y. A. et al., 2018). In fact, YAP/TAZ contributes not only to tumor growth but also to drug resistance (Lai et al., 2011; Zhao and Yang, 2015). Likewise, self-sustained YAP activity has been found in CAFs, through mutually enhanced cell contractility and "inside-out" ECM stiffening, to remodel the niche mechano-environment (i.e., the tumor microenvironment (TME)), thereby promoting tumor progression (Calvo et al., 2013; Piccolo et al., 2014). To date, the regulation of YAP/TAZ has been intensively studied. Herein, we focus on X-ROS-dependent cytokine/ECM signaling in the regulation of the Hippo pathway. In order to proceed, a short introduction of the Hippo pathway is given below. More details of this pathway can be found elsewhere (Pan, 2010; Yu and Guan, 2013; Piccolo et al., 2014; Zanconato et al., 2016a; Zanconato et al., 2016b; Meng et al., 2016; Panciera et al., 2017; Zheng and Pan, 2019; Sarmasti Emami et al., 2020; Zhao et al., 2020; Wang et al., 2021).

The Hippo pathway is processed by several serine/threonine kinases and cofactors in a multiplexed, sequential manner. These molecules include the mammalian Ste20-like protein kinase 1/2 (MST1/2), the Salvador family WW domain-containing protein 1 (SAV1), the large tumor suppressor kinase 1/2 (LATS1/2), and the Mps one binder (MOB) kinase activator-like 1 (MOB1) (Piccolo et al., 2014; Sarmasti Emami et al., 2020) (**Figure 4B**). The signaling starts from the association of MST1/2 with SAV1 into a hetero-tetramer complex (2 MST and 2 SAV1), by which MST1/2 perform auto-activation (at T180). Activated MST1/2-SAV1 then phosphorylate MOB1 and LATS1/2 (in a complex form) to induce LATS1/2 auto-phosphorylation and auto-activation (LATS1 at T1079 and LATS2 at T1041 (Ma et al., 2019; Sarmasti Emami et al., 2020)). Other kinases that act in parallel to MST1/2 and activate LATS1/2 include mitogen-activated protein kinase kinase kinase kinases (MAP4Ks) (Meng et al., 2015) and serine/threonine kinase 25 (STK25) (Lim et al., 2019). Once activated, LATS1/2 phosphorylate YAP at S61, S109, S127, S381, and S397 (Zhao et al., 2010b; Mo et al., 2014; Piccolo et al., 2014; Ni et al., 2015; Elisi et al., 2018; Mana-Capelli and Mccollum, 2018; Sarmasti Emami et al., 2020), which is counteracted by the protein phosphatase magnesium-dependent 1A (PPM1A or PP2Cα) (Zhou et al., 2021), PP1A (Li et al., 2016), and PP2A (Schlegelmilch et al., 2011), or the pre-phosphorylation of YAP at S128 by Nemo-like kinase (NLK) (Hong et al., 2017; Moon et al., 2017). YAP with phosphorylation at S127 is a target of 14-3-3 proteins, whereas phosphorylation at YAP S381 or S397 creates a phosphor-degron motif for the subsequent phosphorylation by casein kinase 1 (CK1) and binding of Skp1-Cullin-1-F-box protein (SCF) type of E3 ubiquitin ligase, $SCF^{\beta\text{-}TrCP}$, which catalyzes the ubiquitination and degradation of YAP (Hao et al., 2008; Zhao et al., 2010b; Liu et al., 2010; Iwasa et al., 2013; He et al., 2016). The association of YAP with 14-3-3 proteins sequesters YAP in the cytoplasm or at the adherens junctions (AJs) (*via* the association of AJ α-catenin with 14-3-3 proteins and YAP (through its WW-domain)) (Schlegelmilch et al., 2011; Yu and Guan, 2013). In epithelial organs, 14-3-3 protein-potentiated association of YAP with α-catenin depends on the cell density and the maturation of AJs. When the cells are at low-density states or with immature AJs, α-catenin fails to sequester YAP at AJs, and the cytoplasmic 14-3-3 protein-YAP complex is subject to the PPM1A/PP2A-mediated dephosphorylation at YAP S127 (Schlegelmilch et al., 2011; Zhou et al., 2021).

14-3-3 proteins are not the only molecules to sequester YAP. Switch/sucrose non-fermentable (SWI/SWF), an ATP-dependent chromatin remodeling complex, can bind to YAP in the nucleus through AT-rich interactive domain-containing protein 1A (ARID1A), thereby inactivating the transcriptional activity of YAP (Chang et al., 2018). Dishevelled (DVL), a scaffold molecule in the Wnt pathway (Barry et al., 2013), can sequester pS127-YAP in the cytoplasm (Lee Y. et al., 2018). Angiomotin (AMOT), a PDZ domain-binding protein, can bind to and sequester YAP in the cytoplasm and/or at the tight junctions (TJs), but the association acts through the YAP WW domain without YAP S127 phosphorylation (Zhao et al., 2011a; Yi et al., 2013; Moleirinho et al., 2017; Wang et al., 2021) and depends on actin dynamics because actin filaments and YAP compete for the same binding site at AMOT (Yi et al., 2011; Li et al., 2015). Likewise, protein tyrosine phosphatase non-receptor type 14 (PTPN14) can bind to YAP through the WW domains of YAP and sequester YAP at AJs or in the cytoplasm without YAP S127 phosphorylation (Poernbacher et al., 2012; Wilson et al., 2014). Other molecules that can sequester YAP without YAP S127 phosphorylation include axin (Azzolin et al., 2014) and IQGAP1 (Quinn et al., 2021), both of which are the scaffold molecules for β-catenin. Axin, a scaffold that assembles APC, β-catenin, and GSK3β into the destruction complex of β-catenin in the Wnt signaling pathway, can bind to and sequester YAP in the cytoplasm (Azzolin et al., 2014) or the multi-vesicular body (MVB) (Gargini et al., 2016; Rivas et al., 2018; Anton and Wandosell, 2021). In comparison, the association of IQGAP1 and YAP occurs through the DNA-binding domain for the transcriptional enhancer factor TEF-1, TEC1, and AbaA (TEA domain- (TEAD-)) binding domain of YAP and does not explicitly sequester YAP into the nucleus or the cytoplasm. Instead, its major effect is to block YAP-TEAD nuclear interaction (Sayedyahossein et al., 2016). A similar mechanism is AMPK-mediated phosphorylation on YAP S94, which disrupts the YAP-TEAD association (Mo et al., 2015) in metabolic and nutrient-sensing regulations (Santinon et al., 2016). Intriguingly, IQGAP1 can bind to and suppress the activity of MST2 and LATS1 (Quinn et al., 2021), and as a result, it suppresses both the Hippo pathway and YAP signaling (**Figures 4B,C**).

YAP sequestered by 14-3-3 proteins or β-catenin destruction complex in the cytoplasm is subject to degradation *via* the ubiquitin-proteasome pathway (Zhao et al., 2020). By contrast, YAP molecules sequestered in the MVB, with IQGAP1, or at the AJs/TJs are prevented from degradation or nuclear translocation. Only free YAP (with or without S127 phosphorylation) can translocate into the nucleus for the transcription of target genes (Zhao et al., 2020) such as PD-L1 (Janse van Rensburg et al., 2018), connective tissue growth factor (CTGF), fibroblast growth factor 1 (FGF1), receptor tyrosine kinase AXL, BMP4, and pro-apoptotic or pro-survival genes (Kim M.-K. et al., 2018; Sarmasti Emami et al., 2020; Quinn et al., 2021). These genes are involved in not only organ development but also tumorigenesis, including enhanced cell migration and immune evasion. The nuclear accumulation of YAP, however, is counteracted by the neurofibromatosis type 2 (NF2, a 4.1 protein, ezrin, radixin, and moesin (FERM) domain-containing molecule, also known as moesin/ezrin/radixin-like protein (Merlin) or schwannomin (Bretscher et al., 2002; Baser et al., 2003; McClatchey, 2003)) which exports YAP out of the nucleus *via* its nuclear localization signal (NLS) sequence and nuclear export signal (NES) sequences (Gladden et al., 2010; Furukawa et al., 2017). Such Merlin-assisted nuclear export of YAP acts independently of the Hippo pathway or other related molecules such as AMOT. Instead, it requires cells at high densities or with high intercellular tension (Furukawa et al., 2017). Another molecule for YAP nuclear export is DVL, which acts only when YAP S127 is phosphorylated (Barry et al., 2013; Lee Y. et al., 2018).

These lines of evidence indicate that the regulation of the Hippo pathway and YAP signaling occurs through PTMs (e.g., phosphorylation and ubiquitination) and compartmentalization. The question is how these processes are linked to the organ size and shape, or more explicitly, to the ROS-dependent cytokine/ECM signaling and the cell mechanics in organ development, repair, and malignancy. Mechanistically, MST1 and MST2 share functional redundancy. They contain an N-terminal kinase domain and a C-terminal coiled-coil SAV/Ras-association domain family (RASSF)/HPO (SARAH) domain with a flexible linker in between (Jin et al., 2012; Ni et al., 2013). SARAH domains are self-associable. Through SARAH-domain self-association, MST1/2 form homodimers and undergo trans-autophosphorylation at T180 (in the kinase domain) and at T325, T336, and T378 (in the linker region) (Bae et al., 2017). The trans-phosphorylation of T180 leads to MST1/2 auto-activation. The trans-phosphorylation of the linker, however, inhibits MST1/2 by recruiting a multi-subunit PP2A complex, striatin- (STRN-) interacting phosphatase and kinase (STRIPAK), through an adaptor, sarcolemmal membrane-associated protein (SLMAP), to dephosphorylate T180 and counteract MST1/2 auto-activation (Bae et al., 2017). Initially defined as a non-canonical PP2A regulatory subunit (B subunit) (Moreno et al., 2000), STRN has a caveolin-binding domain, a coiled-coil domain, a Ca^{2+}-calmodulin- (CaM-) binding domain, and a tryptophan–aspartate- (WD-) repeat domain, by which it can recruit and bind to multiple partners (Hwang and Pallas, 2014). The resulting complex, STRIPAK, contains a PP2A catalytic subunit (PP2AC), scaffolding subunit (PP2AA), and the STRN regulatory subunit that recruits STRN-interacting protein (STRIP1/2), SLMAP, and members of the STE20 family of kinases (e.g., MST1/2) (Couzens et al., 2013).

The ability to auto-activate and recruit inhibitors to deactivate itself at the same time, as in the case of MST1/2 and STRIPAK, is not rare in biology. POPX2, for example, forms a trimeric complex with the Rac1/Cdc42 guanine nucleotide exchange factor ARHGEF7 (also known as the p21-activated protein kinase-exchange factor β (βPIX)) and PAK, wherein Rac1-activated PAK is subject to immediate dephosphorylation by POPX2 (Kim P. R. et al., 2020). Another example is the complex formation of the scaffold molecule, muscle-selective A-kinase anchoring proteins (mAKAP), with cAMP-specific phosphodiesterase (PDE)-4D3 (PDE4D3) and PKA, wherein the PKA activity is subject to the downregulation of cAMP level by PDE4D3 (Sette and Conti, 1996; Lim et al., 1999; Rababa'h et al., 2013). From the thermodynamics point of view, having the auto-activation and auto-inhibition occur at the same time places the complex in a highly unstable state. However, from the evolutionary point of view, this scenario provides an ability to create instant Hippo "on/off" signals in response to tissue injury or remodeling. The inhibitory effect of STRIPAK on MST1/2 is antagonized by the association of SAV1, which contains an N-terminal flexible region, a tandem repeat of two WW domains, and a C-terminal SARAH domain (Bae et al., 2017). The N-terminal region of SAV1 has a FERM domain-binding motif to bind to FERM-domain proteins such as Merlin and Expanded (Ex) (Bretscher et al., 2002; Baser et al., 2003; McClatchey, 2003) and a protein interaction domain (PID) to bind to and suppress STRIPAK (Bae et al., 2017). Similar to the SARAH domains, the WW domains of SAV1 are self-associable (Ohnishi et al., 2007) but act through a domain-swapping mechanism between two SAV1s (Lin et al., 2020). *Via* the intermolecular association of SARAH and WW domains, two SAV1 and two MST1/2s can form a hetero-tetramer, thereby bringing the N-terminal of SAV1 to the proximity of STRIPAK to antagonize the phosphatase. However, the binding affinity between the SAV1 N-terminal and STRIPAK is low (with K_m ~100 μM (Bae et al., 2017)). Additional modulators are thus needed to facilitate the suppression.

The AJ- and TJ-associated factors, including WW domain and C2 domain-containing proteins (WWC), such as kidney and brain expressed protein (KIBRA /WWC1 (Hoffken et al., 2021)); PDZ-domain proteins, such as AMOT; and FERM domain proteins, such as Merlin, Ex, and PTPN14 appear to be the key modulators. Predominantly expressed in the kidney and the brain, the first key molecule, KIBRA, contains two WW domains (Kremerskothen et al., 2003), a potential coiled-coil domain, a C2 domain responsible for Ca^{2+}-sensitive interaction with phospholipids, a class III PDZ-binding motif ADDV, and an atypical protein kinase C (aPKC) binding region (Baumgartner et al., 2010; Genevet et al., 2010; Yu et al., 2010; Boggiano and Fehon, 2012; Zhang et al., 2014; Su et al., 2017). More than 20 binding partners of KIBRA have been identified. These molecules include Merlin, Ex, FRM6 (FERM domain-containing protein 6), AMOT, PALS1- (protein associated with Caenorhabditis elegans

Lin-7 protein 1-) associated tight junction protein (PATJ), PTPN14, PP1, SAV1, LATS1/2, the mitotic serine/threonine kinase Aurora-A, PKCζ, and the apical polarity complexes PAR3/PAR6β (partition-defective 3/partition-defective 6β) (Xiao et al., 2011a; Xiao et al., 2011b; Zhang et al., 2014; Zhou et al., 2017). At mature TJs, KIBRA forms a complex with Merlin, Ex, and AMOT to interact with MST1/2-SAV1 and LATS1/2-MOB1, thereby promoting LATS auto-activation and YAP phosphorylation (Zhang et al., 2014) (**Figure 4D**). By having such a complex formation, Merlin can likely be placed at the SAV1-STRIPAK binding interface, thereby stabilizing SAV1-STRIPAK interaction and suppressing STRIPAK activity (Bae et al., 2017). However, the association of Merlin with KIBRA is inhibited by Aurora-mediated phosphorylation at KIBRA S539, which is counteracted by PP1 and PTPN14 (Xiao et al., 2011b; Poernbacher et al., 2012; Wang W. et al., 2014), suggesting a link between cell mitosis and the Hippo pathway. In the presence of apicobasal polarity, KIBRA-Merlin-FRMD6 complex formation competes with Par3-aPKC- KIBRA complex formation (Suzuki and Ohno, 2006; Yoshihama et al., 2009; Zhou et al., 2017), and KIBRA directly suppresses aPKC and aPKC-mediated apical exocytosis (Yoshihama et al., 2011), by which cells can limit the expansion of apical surface, an important feature in stem cell homeostasis and absent in tumorigenesis.

The second key molecule, AMOT, is an AJ/TJ-associable PDZ-domain protein that plays an important role in regulating the partitioning of Merlin and YAP, as shown in the differentiation of human pluripotent stem cells (Zaltsman et al., 2019). AMOT possesses an N-terminal domain, which contains a WW domain- and actin-binding motif (157–191) that YAP and actin filaments compete binding to, followed by a coiled-coil domain that can bind to Merlin (Yi et al., 2011; Li et al., 2015), and a C-terminal PDZ domain that can bind to TJs (Hirate and Sasaki, 2014; Mana-Capelli et al., 2014). The competition of YAP and actin filaments with AMOT appears to depend on the "structural code" of the cells. In blastocysts, for example, the embryonic cells are segregated into an outer layer with cells forming apicobasal polarity and an inner layer without polarity formation. AMOT localizes to the AJs of non-polarized cells at the inner layer, with S176 phosphorylated by LATS, which inhibits actin binding, stabilizes the AMOT-LATS interaction (Dai et al., 2013; Hirate et al., 2013; Hirate and Sasaki, 2014), promotes AMOT-YAP association, and enables YAP phosphorylation (Mana-Capelli et al., 2014). By contrast, AMOT is unphosphorylated and sequestered to the apical actin at the outer layer, thereby releasing YAP for nuclear signaling (Hirate et al., 2013) (**Figure 4D**).

The third key molecule, Merlin, contains an N-terminal FERM domain (sequence 19–313), followed by one α-helical domain (314–507) and one C-terminal domain (508–595) (Muranen et al., 2007; Li et al., 2015). The α helical domain possesses a coiled-coil motif that can bind to AMOT (Yi et al., 2011; Li et al., 2015), whereas the N-terminal and the C-terminal can self-associate (McClatchey, 2003) with K_m ~3 μM, a much weaker affinity than that of ERM proteins (K_m ~0.016 μM) (Li et al., 2015). Merlin has many binding partners (Hennigan et al., 2019) through which it can associate with or dissociate from AJs. The selection of binding partners is primarily modulated by Merlin PTMs such as phosphorylation and ubiquitination (Laulajainen et al., 2011). These PTMs displace the self-associated C-terminal and N-terminal of Merlin away from each other, thereby exposing the binding sites to, for example, MST1/2-SAV1, LATS1/2, YAP, AKT, paxillin, FAK, and integrin β1 (Obremski et al., 1998; Fernandez-Valle et al., 2002; James et al., 2004; Tang et al., 2007; Yamauchi et al., 2008; Flaiz et al., 2009; Yi et al., 2011; Yin et al., 2013; Li et al., 2015; Bae et al., 2017). Alternatively, Merlin can bind to PIP_2 through its FERM domain, by which Merlin adopts an expanded conformation to expose the binding sites (Ali Khajeh et al., 2014). Thus, Merlin "with" and "without" PTMs (and/or PIP_2 binding) are often referred to as the "open" and "close" states, respectively. Historically, in the "close" state, Merlin has been known as the tumor suppressor (Li et al., 2015). For the "open" state, major phosphorylation sites include S10 and S518 by PKA (Laulajainen et al., 2008); S10, T230, and S315 by AKT (Tang et al., 2007; Laulajainen et al., 2011); and S518 by PAK (Shaw et al., 2001). Phosphorylating Merlin at S518 prevents Merlin from participating in the Hippo pathway and sequesters Merlin on the cell membrane through the association with the C-terminal of cell surface receptors such as CD44 (Morrison et al., 2001; Sherman and Gutmann, 2001) and/or bind to tubulin to enhance microtubule polymerization (Muranen et al., 2007). Merlin S518 phosphorylation is counteracted by myosin phosphatase target subunit 1- (MYPT1-) regulated PP1c, the phosphatase for MLC (Jin et al., 2006). MYPT1 is inactivated by ILK or ROCK-mediated phosphorylation at T696 (by ILK/RCOK) and S854/T855 (by ROCK) (Serrano et al., 2013; Hartmann et al., 2015), which occurs during cell migration or spreading on stiff substrates. Alternatively, MYPT1 can be sequestered by phosphorylated MLC when cells are spreading on stiff substrates (Joo and Yamada, 2014). These lines of evidence provide an explanation for how stiff microenvironments might disable Merlin-mediated tumor suppression, enhance YAP nuclear translocation, and promote tumor invasion (Paszek et al., 2005; Guo et al., 2012).

In contrast to phosphorylation at S518, Merlin phosphorylated at S10, T230, and/or S315 is subject to ubiquitination and proteasome-mediated degradation (Laulajainen et al., 2011), which, however, requires S518 to be dephosphorylated (Li et al., 2015; Wei et al., 2020), suggesting that Merlin phosphorylated at S518 and Merlin phosphorylated at S10, T230, and/or S315 are two functionally exclusive states (**Figure 4D**). Merlin ubiquitination is mediated by the E3 ubiquitin ligase, neural precursor cell expressed developmentally downregulated protein 4 (NEDD4), which conjugates one or two ubiquitin molecules at Merlin K396 and K159 by the aid of AMOT (Wei et al., 2020). In this process, AMOT serves as a scaffold protein to bind to Merlin through their mutual coiled-coil domains (Yi et al., 2011; Li et al., 2015) and bind to NEDD4 through the association of its two PPXY motifs with the WW domains of NEDD4 (Skouloudaki and Walz, 2012). Although Merlin ubiquitination promotes the degradation of the Merlin-AMOT complex, it is required for MST-mediated LATS phosphorylation (Wei et al., 2020). The ubiquitinated

Merlin-AMOT complex can bind to the N-terminal FERM-binding domain (FBD) of LATS through the Merlin FERM domain (K_m ~1.4 μM (Yin et al., 2013; Li et al., 2015)). Other associations include those between SAV1 and MOB-1 (Yin et al., 2013), between the Merlin FERM domain and the N-terminal FERM domain-binding motif of SAV1 (Bretscher et al., 2002; Baser et al., 2003; McClatchey, 2003; Bae et al., 2017), between the extreme N-terminal end of Merlin and α-catenin (Cole et al., 2008), and between AMOT and YAP (at the N-terminal actin-binding motif of AMOT (157–191)) (Mana-Capelli et al., 2014). Through these molecular associations, the ubiquitinated Merlin-AMOT complex likely promotes the clustering of YAP, LATS-MOB1, and MST-SAV1 at AJs (by Merlin-α-catenin-AJ association) or TJs (by AMOT PDZ domain-TJ association), wherein MST1/2 potentiate LATS1/2 auto-activation (Gladden et al., 2010; Hansen et al., 2015) (**Figures 4B,D**). In addition, independent of MST, AMOT can act along with MOB1 to promote LATS autophosphorylation and auto-activation (Mana-Capelli and Mccollum, 2018). Activated LATS phosphorylates not only YAP but also AMOT (at S175/S176), the phosphorylation of which suppresses actin binding to AMOT and stabilizes the binding between LATS-MOB1 and Merlin-AMOT (Dai et al., 2013; Hirate and Sasaki, 2014; Mana-Capelli et al., 2014; Moleirinho et al., 2017; Mana-Capelli and Mccollum, 2018) (**Figure 4D**). As a result, the Merlin-AMOT complex can likely promote LATS activation and YAP phosphorylation in a self-sustained manner.

The fourth key molecule, an AJ-associable FERM domain protein for YAP modulation, is PTPN14 (Wang et al., 2012; Huang et al., 2013; Liu et al., 2013; Wilson et al., 2014). PTPN14 contains an N-terminal FERM domain, followed by two PPXY motifs which are essential for the interactions with YAP and KIBRA through their WW domains (Poernbacher et al., 2012), and a C-terminal PTP catalytic domain which is essential to counteract Src kinase- or receptor tyrosine kinase- (RTK-) mediated phosphorylation at β-catenin Y654 and VE-cadherin, thereby stabilizing AJs (Van Veelen et al., 2011; Fu et al., 2020). Along with the PPXY motifs, the PTP domain of PTPN14 is required for the interactions with KIBRA (Wilson et al., 2014). Further, PTPN14 can bind to LATS1/2 and acts independently or cooperatively with KIBRA to enhance LATS1/2 auto-activation and YAP S127 phosphorylation, even in the absence of MST1/2 (Wilson et al., 2014). Thus, the KIBRA-AMOT-Merlin complex and KIBRA-PTPN14 complex can act in parallel to modulate YAP phosphorylation and sequestration at AJs (**Figure 4D**).

Module BOX VI: The HIF/YAP/Notch Triad and PD-L1

YAP/TAZ forms complexes with HIF-1α and functions as the transcription activator of HIF-1α to enhance expressions of molecules involved in organ development, tissue homeostasis, and tumorigenesis (Xiang et al., 2015; Zhao et al., 2020). Under hypoxia, YAP binds to nuclear HIF-1α and sustains its stability, thereby promoting the expression of pyruvate kinase isozymes M2 (PKM2), a key enzyme of glycolysis, in, for example, hepatocellular carcinoma cells (HCCs) (Zhang X. et al., 2018), whereas in the cytoplasm, YAP enhances HIF-1α stability by inhibiting VHL-dependent degradation of hydroxylated HIF-1α (Ma et al., 2015; Zhao et al., 2020) (**Figure 1A**). Likewise, HIF-2α, another hypoxia responding subunit, has been found to increase YAP1 expression and activity, yet it does so without the involvement of Src kinase, PI3K, ERK, or MAPK signaling pathways (Ma et al., 2017). No direct association between YAP and HIF-2α was observed either (Ma et al., 2017). In addition to glycolysis, the YAP-HIF-1α complex promotes the transcription of genes involved in angiogenesis and cell growth (Zhao et al., 2020). Genes containing HREs that H1F-1α can bind to also include *WWTR1* (i.e., TAZ) and *SIAH1* (Zhao et al., 2020), and the TAZ-HIF-1α complex has been shown to promote the transcription of SIAH1 (Xiang et al., 2014; Xiang et al., 2015; Zhao et al., 2020). Similar to SIAH2 (Ma et al., 2015), SIAH1 induces LATS2 degradation and, in turn, TAZ nuclear localization (Xiang et al., 2014; Xiang et al., 2015; Zhao et al., 2020). Thus, positive feedback exists along the YAP/TAZ-HIF/SIAH axis (**Figure 5A**). In the development of growth plate, for example, HIF-1α was found to promote YAP activation and, in turn, upregulate the expression of sex-determining region-box 9tbox9 protein (SOX-9), a marker of stemness, for the maintenance of chondrogenic phenotype (Li H. et al., 2018).

Notch signaling is a highly conserved cell–cell communication mechanism by which cells regulate organ development, homeostasis, and repair through lateral inhibition (or "trans-inhibition") between neighboring cells (Kopan and Ilagan, 2009; Guruharsha et al., 2012; Kovall et al., 2017; Siebel and Lendahl, 2017). Notch is a cell surface receptor. Upon ligand binding, Notch is cleaved to release Notch intracellular domain (NICD), which translocates into the nucleus to bind to CSL (the transcriptional repressor CBF1/suppressor of hairless/Lag-1) or the human homolog RBPJ (recombination signal-binding protein for immunoglobulin κJ region, also known as CBF1) to facilitate the transcription of Notch target genes (Kopan and Ilagan, 2009). In tumorigenesis, Notch signaling promotes the CSC formation by reducing their proliferation yet increasing their resistance to therapies, thereby potentiating cancer cell dormancy and relapse (Janghorban et al., 2018). Moreover, Notch has been proposed as a mechanical sensor based on the observation that Notch can be activated by mechanical stretch and shear stress (Gordon et al., 2015; Chowdhury et al., 2016; Mack et al., 2017; Loerakker et al., 2018) and that Notch participates in mechanics-dependent periodic feather branch pattern formation (Cheng et al., 2018). For proper organ development, the specification of cell fate must be spatiotemporally coordinated with tissue morphogenesis. Therefore, it is plausible that the signaling of the "messengers" for tissue structure and mechanics (i.e., YAP/TAZ) is linked to Notch signaling pathways, by which cells can sense the mechanical changes in the niche through (e.g., cell–ECM adhesions and cell–cell contacts) and make a correspondent decision on the cell fate.

Several examples support the idea that YAP/TAZ and Notch signaling pathways are coupled (Totaro et al., 2018a). This coupling can be positive or negative, with YAP/TAZ acting upstream of, downstream of, or in parallel with Notch signaling. Such versatility is achieved by having YAP/TAZ and

Notch synergistically co-regulate shared target genes, having YAP/TAZ act upstream to regulate the expression of Notch ligands or receptors (thereby downregulating or upregulating Notch activity, respectively), or having Notch act upstream to upregulate or downregulate YAP activity (Totaro et al., 2018a). An example of the synergistic coupling is the control of smooth muscle differentiation from neural crest cells (Manderfield et al., 2015), where YAP/TAZ forms a complex with NICD to promote the transcription of Notch target genes for smooth muscle fate (Manderfield et al., 2012). Another example is the binary cell fate decision in the embryonic transition from morula to blastocyst. In this case, the binary decision occurs between cells becoming inner cell mass or outer-layer trophectoderm (TE) (Nishioka et al., 2009; Hirate et al., 2013; Leung and Zernicka-Goetz, 2013; Engel-Pizcueta and Pujades, 2021). In this case, Notch and YAP/TAZ act in parallel and non-redundantly to drive the specification of the TE fate gene, *Cdx2*, by having Notch elicit the onset of Cdx2 expression and YAP maintain the expression of Cdx2, respectively (Watanabe et al., 2017). For YAP/TAZ acting upstream to upregulate Notch, one example is the binary cell fate decision made between cholangiocytes and hepatocytes in liver development (Kodama et al., 2004; Zong et al., 2009). In this case, YAP drives *Notch2* expression and cholangiocyte specification and proliferation (Wu et al., 2017). Another is between the tip and stalk cells in angiogenesis, where YAP/TAZ suppresses the β-catenin-NICD-mediated expression of Notch ligand and endothelial Delta-like 4 (Dll4) protein in the tip cells (Yasuda et al., 2019). For YAP acting upstream to downregulate Notch, the example is the homeostasis of the epidermis, where Notch signaling is required for the transition of keratinocytes from the basal to the suprabasal layers (Siebel and Lendahl, 2017; Totaro et al., 2018a). In this case, the segregation of cell fate at different layers is achieved by spatially confining the Notch activity throughout the entire epidermis. Cells in the basal layer mainly express the Notch ligands Delta-like 1 (Dll1) and Jagged-2 (Jag2), whereas cells in the suprabasal layers mainly express the Notch receptors. Mechanical stretch and/or ECM stiffness in the basal layer activates YAP/TAZ signaling, which suppresses Notch activity by upregulating the expression of Notch ligands to counteract Notch activity through the "cis-inhibition," that is, having the Notch ligand and receptor co-expressed on the same cell surface to suppress the Notch activity (Totaro et al., 2018a). Conversely, for Notch acting upstream of YAPTAZ, an example is the symmetric stem cell division in the embryonic brain development, where Notch upregulates YAP expression by the binding of NICD-RBPJ complex to the YAP promoter, thereby promoting neural stem cell symmetric proliferation (Li et al., 2012).

Recent studies on glioblastoma stem cells revealed the differential roles of HIF-1α and HIF-2α on Notch signaling. It was observed that these two HIF subunits bind to NICD in a competitive manner (Hu et al., 2014). When HIF-1α binds to NICD and Notch-responsive promoters, Notch signaling is activated and cell differentiation is suppressed (Hu et al., 2014), thereby maintaining the undifferentiated cell state in various stem cells and precursor cells (Gustafsson et al., 2005). In contrast, when HIF-2α binds to NICD, Notch signaling is repressed, leading to cell differentiation and stem cell exhaustion (Hu et al., 2014). The coupling of NICD and HIF with the intracellular transducers of niche factor signaling is indeed a common behavior. In TGF-β signaling, for example, both NICD and HIF-1α can bind to the intracellular transducer of TGF-β signals (Blokzijl et al., 2003; Huang Y. et al., 2021), smad3 (mothers against decapentaplegic homolog 3), and the association of HIF-1α and smad3 has been shown to switch the functionality of TGF-β signaling to glycolysis in non-small cell lung cancer (NSCLC) (Huang Y. et al., 2021).

Recently, applying blockade antibodies against PD-1 and its ligand PD-L1 has become a promising strategy for treating advanced cancers (Brahmer et al., 2012; Topalian et al., 2012). The capacity of immune suppression is also one essential feature in the mesenchymal stem cell- (MSC-) based cell therapy (Ankrum et al., 2014; Jiang and Xu, 2020). A growing interest has thus been focused on the interplay of PD-L1 and HIF/Notch/YAP signaling pathways due to the exclusive involvement of HIF/Notch/YAP signaling in the development and homeostasis of stem cells and in the progression of cancers. In particular, YAP can bind to the PD-L1 enhancer region to promote PD-L1 expression, independent of any existing signaling factors and pathways known to upregulate PD-L1, such as EGFR, AKT, MAPK, and interferon- (IFN-) γ (Kim M. H. et al., 2018). In addition to being hypoxic, the TME contains multiple inflammatory factors such as interleukin-6 (IL-6) and remodeling factors such as TGF-β, which can activate signal transducer and activator of transcription 3 (STAT3) to increase the synthesis of HIF-1α and bind to NICD for a synergistic operation on Notch target genes, including the upregulation of PD-L1 expression (Blokzijl et al., 2003; Lee et al., 2009; Yu et al., 2009; Fan et al., 2013; Kitamura et al., 2017; Gupta et al., 2018; Kunnumakkara et al., 2018; Wen et al., 2020). Thus, the pharmaceutical targeting on YAP/Notch/HIF signaling pathways has been proposed as a potential adjunct therapy for cancer treatment, along with the conventional chemotherapy and immune therapy (Janghorban et al., 2018).

AUTHOR CONTRIBUTIONS

C-LG prepared and wrote the entire manuscript, including the figures and Math Box.

FUNDING

This work was supported by the Taiwan Ministry of Science and Technology *via* Grant MOST 107-2112-M-001-040-MY3, MOST 110-2112-M-001-039, and MOST 110-2314-B-001-004 and by Academia Sinica *via* Grant AS-TP-109-M04.

ACKNOWLEDGMENTS

C-LG acknowledged the thoughtful discussion with Rita Yen-Hua Huang at the Taiwan Medical University and the support from the Institute of Physics, Academia Sinica.

REFERENCES

Abdollahi, H., Harris, L. J., Zhang, P., Mcilhenny, S., Srinivas, V., Tulenko, T., et al. (2011). The Role of Hypoxia in Stem Cell Differentiation and Therapeutics. *J. Surg. Res.* 165, 112–117. doi:10.1016/j.jss.2009.09.057

Abe, J.-i., Kusuhara, M., Ulevitch, R. J., Berk, B. C., and Lee, J.-D. (1996). Big Mitogen-Activated Protein Kinase 1 (BMK1) Is a Redox-Sensitive Kinase. *J. Biol. Chem.* 271, 16586–16590. doi:10.1074/jbc.271.28.16586

Abo, A., Webb, M. R., Grogan, A., and Segal, A. W. (1994). Activation of NADPH Oxidase Involves the Dissociation of P21rac from its Inhibitory GDP/GTP Exchange Protein (rhoGDI) Followed by its Translocation to the Plasma Membrane. *Biochem. J.* 298, 585–591. doi:10.1042/bj2980585

Aceto, N., Bardia, A., Miyamoto, D. T., Donaldson, M. C., Wittner, B. S., Spencer, J. A., et al. (2014). Circulating Tumor Cell Clusters Are Oligoclonal Precursors of Breast Cancer Metastasis. *Cell* 158, 1110–1122. doi:10.1016/j.cell.2014.07.013

Ago, T., Kuribayashi, F., Hiroaki, H., Takeya, R., Ito, T., Kohda, D., et al. (2003). Phosphorylation of P47 Phox Directs Phox Homology Domain from SH3 Domain toward Phosphoinositides, Leading to Phagocyte NADPH Oxidase Activation. *Proc. Natl. Acad. Sci. U.S.A.* 100, 4474–4479. doi:10.1073/pnas.0735712100

Aikawa, R., Komuro, I., Yamazaki, T., Zou, Y., Kudoh, S., Tanaka, M., et al. (1997). Oxidative Stress Activates Extracellular Signal-Regulated Kinases through Src and Ras in Cultured Cardiac Myocytes of Neonatal Rats. *J. Clin. Invest.* 100, 1813–1821. doi:10.1172/jci119709

Al-Eisa, A., and Dhaunsi, G. S. (2017). NOX-mediated Impairment of PDGF-Induced DNA Synthesis in Peripheral Blood Lymphocytes of Children with Idiopathic Nephrotic Syndrome. *Pediatr. Res.* 82, 629–633. doi:10.1038/pr.2017.122

Ali Khajeh, J., Ju, J. H., Atchiba, M., Allaire, M., Stanley, C., Heller, W. T., et al. (2014). Molecular Conformation of the Full-Length Tumor Suppressor NF2/Merlin-A Small-Angle Neutron Scattering Study. *J. Mol. Biol.* 426, 2755–2768. doi:10.1016/j.jmb.2014.05.011

Ali, M. H., Mungai, P. T., and Schumacker, P. T. (2006). Stretch-induced Phosphorylation of Focal Adhesion Kinase in Endothelial Cells: Role of Mitochondrial Oxidants. *Am. J. Physiology-Lung Cell. Mol. Physiology* 291, L38–L45. doi:10.1152/ajplung.00287.2004

Álvarez-Santos, M. D., Álvarez-González, M., Estrada-Soto, S., and Bazán-Perkins, B. (2020). Regulation of Myosin Light-Chain Phosphatase Activity to Generate Airway Smooth Muscle Hypercontractility. *Front. Physiol.* 11, 701. doi:10.3389/fphys.2020.00701

Ancel, J., Birembaut, P., Dewolf, M., Durlach, A., Nawrocki-Raby, B., Dalstein, V., et al. (2019). Programmed Death-Ligand 1 and Vimentin: A Tandem Marker as Prognostic Factor in NSCLC. *Cancers (Basel)* 11. doi:10.3390/cancers11101411

Andjongo, É., Benhamouche, S., Bouraoui, A., and Baciou, L. (2021). PolDIP2, une protéine clé de la régulation du fonctionnement mitochondrial et du métabolisme cellulaire. *Med. Sci. Paris.* 37, 97–100. doi:10.1051/medsci/2020263

Andre, L., Fauconnier, J., Reboul, C., Feillet-Coudray, C., Meschin, P., Farah, C., et al. (2013). Subendocardial Increase in Reactive Oxygen Species Production Affects Regional Contractile Function in Ischemic Heart Failure. *Antioxidants Redox Signal.* 18, 1009–1020. doi:10.1089/ars.2012.4534

Andreyev, A. Y., Kushnareva, Y. E., and Starkov, A. A. (2005). Mitochondrial Metabolism of Reactive Oxygen Species. *Biochem. Mosc.* 70, 200–214. doi:10.1007/s10541-005-0102-7

Anilkumar, N., Weber, R., Zhang, M., Brewer, A., and Shah, A. M. (2008). Nox4 and Nox2 NADPH Oxidases Mediate Distinct Cellular Redox Signaling Responses to Agonist Stimulation. *Atvb* 28, 1347–1354. doi:10.1161/atvbaha.108.164277

Ankrum, J. A., Ong, J. F., and Karp, J. M. (2014). Mesenchymal Stem Cells: Immune Evasive, Not Immune Privileged. *Nat. Biotechnol.* 32, 252–260. doi:10.1038/nbt.2816

Anraku, Y. (1988). Bacterial Electron Transport Chains. *Annu. Rev. Biochem.* 57, 101–132. doi:10.1146/annurev.bi.57.070188.000533

Antón, I. M., and Wandosell, F. (2021). WIP, YAP/TAZ and Actin Connections Orchestrate Development and Transformation in the Central Nervous System. *Front. Cell Dev. Biol.* 9, 673986. doi:10.3389/fcell.2021.673986

Aponte, P. M., and Caicedo, A. (2017). Stemness in Cancer: Stem Cells, Cancer Stem Cells, and Their Microenvironment. *Stem Cells Int.* 2017, 5619472. doi:10.1155/2017/5619472

Aragona, M., Panciera, T., Manfrin, A., Giulitti, S., Michielin, F., Elvassore, N., et al. (2013). A Mechanical Checkpoint Controls Multicellular Growth through YAP/TAZ Regulation by Actin-Processing Factors. *Cell* 154, 1047–1059. doi:10.1016/j.cell.2013.07.042

Artavanis-Tsakonas, S., Rand, M. D., and Lake, R. J. (1999). Notch Signaling: Cell Fate Control and Signal Integration in Development. *Science* 284, 770–776. doi:10.1126/science.284.5415.770

Arthur, J. F., Shen, Y., Gardiner, E. E., Coleman, L., Kenny, D., Andrews, R. K., et al. (2011). TNF Receptor-Associated Factor 4 (TRAF4) Is a Novel Binding Partner of Glycoprotein Ib and Glycoprotein VI in Human Platelets. *J. Thromb. Haemost.* 9, 163–172. doi:10.1111/j.1538-7836.2010.04091.x

Au, H.-K., Peng, S.-W., Guo, C.-L., Lin, C.-C., Wang, Y.-L., Kuo, Y.-C., et al. (2021). Niche Laminin and IGF-1 Additively Coordinate the Maintenance of Oct-4 through CD49f/IGF-1r-Hif-2α Feedforward Loop in Mouse Germline Stem Cells. *Front. Cell Dev. Biol.* 9, 646644. doi:10.3389/fcell.2021.646644

Azimi, I., Petersen, R. M., Thompson, E. W., Roberts-Thomson, S. J., and Monteith, G. R. (2017). Hypoxia-induced Reactive Oxygen Species Mediate N-Cadherin and SERPINE1 Expression, EGFR Signalling and Motility in MDA-MB-468 Breast Cancer Cells. *Sci. Rep.* 7, 15140. doi:10.1038/s41598-017-15474-7

Azzolin, L., Panciera, T., Soligo, S., Enzo, E., Bicciato, S., Dupont, S., et al. (2014). YAP/TAZ Incorporation in the β-Catenin Destruction Complex Orchestrates the Wnt Response. *Cell* 158, 157–170. doi:10.1016/j.cell.2014.06.013

Bae, S. J., Ni, L., Osinski, A., Tomchick, D. R., Brautigam, C. A., and Luo, X. (2017). SAV1 Promotes Hippo Kinase Activation through Antagonizing the PP2A Phosphatase STRIPAK. *Elife* 6. doi:10.7554/elife.30278

Bailly, C. (2020). Regulation of PD-L1 Expression on Cancer Cells with ROS-Modulating Drugs. *Life Sci.* 246, 117403. doi:10.1016/j.lfs.2020.117403

Balistreri, C. R., Madonna, R., Melino, G., and Caruso, C. (2016). The Emerging Role of Notch Pathway in Ageing: Focus on the Related Mechanisms in Age-Related Diseases. *Ageing Res. Rev.* 29, 50–65. doi:10.1016/j.arr.2016.06.004

Barry, E. R., Morikawa, T., Butler, B. L., Shrestha, K., De La Rosa, R., Yan, K. S., et al. (2013). Restriction of Intestinal Stem Cell Expansion and the Regenerative Response by YAP. *Nature* 493, 106–110. doi:10.1038/nature11693

Barsoum, I. B., Smallwood, C. A., Siemens, D. R., and Graham, C. H. (2014). A Mechanism of Hypoxia-Mediated Escape from Adaptive Immunity in Cancer Cells. *Cancer Res.* 74, 665–674. doi:10.1158/0008-5472.can-13-0992

Bartolini, F., Andres-Delgado, L., Qu, X., Nik, S., Ramalingam, N., Kremer, L., et al. (2016). An mDia1-INF2 Formin Activation Cascade Facilitated by IQGAP1 Regulates Stable Microtubules in Migrating Cells. *MBoC* 27, 1797–1808. doi:10.1091/mbc.e15-07-0489

Baser, M. E., R. Evans, D. G., and Gutmann, D. H. (2003). Neurofibromatosis 2. *Curr. Opin. Neurology* 16, 27–33. doi:10.1097/00019052-200302000-00004

Basu, S., Totty, N. F., Irwin, M. S., Sudol, M., and Downward, J. (2003). Akt Phosphorylates the Yes-Associated Protein, YAP, to Induce Interaction with 14-3-3 and Attenuation of P73-Mediated Apoptosis. *Mol. Cell* 11, 11–23. doi:10.1016/s1097-2765(02)00776-1

Basu, U., Case, A. J., Liu, J., Tian, J., Li, Y.-L., and Zimmerman, M. C. (2019). Redox-sensitive Calcium/calmodulin-dependent Protein Kinase IIα in Angiotensin II Intra-neuronal Signaling and Hypertension. *Redox Biol.* 27, 101230. doi:10.1016/j.redox.2019.101230

Battelli, M. G., Polito, L., Bortolotti, M., and Bolognesi, A. (2016a). Xanthine Oxidoreductase-Derived Reactive Species: Physiological and Pathological Effects. *Oxid. Med. Cell Longev.* 2016, 3527579. doi:10.1155/2016/3527579

Battelli, M. G., Polito, L., Bortolotti, M., and Bolognesi, A. (2016b). Xanthine Oxidoreductase in Cancer: More Than a Differentiation Marker. *Cancer Med.* 5, 546–557. doi:10.1002/cam4.601

Baumgartner, R., Poernbacher, I., Buser, N., Hafen, E., and Stocker, H. (2010). The WW Domain Protein Kibra Acts Upstream of Hippo in Drosophila. *Dev. Cell* 18, 309–316. doi:10.1016/j.devcel.2009.12.013

Bays, J. L., Campbell, H. K., Heidema, C., Sebbagh, M., and Demali, K. A. (2017). Linking E-Cadherin Mechanotransduction to Cell Metabolism through Force-Mediated Activation of AMPK. *Nat. Cell Biol.* 19, 724–731. doi:10.1038/ncb3537

Bedard, K., and Krause, K.-H. (2007). The NOX Family of ROS-Generating NADPH Oxidases: Physiology and Pathophysiology. *Physiol. Rev.* 87, 245–313. doi:10.1152/physrev.00044.2005

Ben Mahdi, M. H., Andrieu, V., and Pasquier, C. (2000). Focal Adhesion Kinase Regulation by Oxidative Stress in Different Cell Types. *IUBMB Life* 50, 291–299. doi:10.1080/15216540051081038

Bergert, M., Lembo, S., Sharma, S., Russo, L., Milovanović, D., Gretarsson, K. H., et al. (2021). Cell Surface Mechanics Gate Embryonic Stem Cell Differentiation. *Cell Stem Cell* 28, 209–216. doi:10.1016/j.stem.2020.10.017

Besse-Patin, A., and Estall, J. L. (20142014). An Intimate Relationship between ROS and Insulin Signalling: Implications for Antioxidant Treatment of Fatty Liver Disease. *Int. J. Cell Biol.* 2014, 519153. doi:10.1155/2014/519153

Best, A., Ahmed, S., Kozma, R., and Lim, L. (1996). The Ras-Related GTPase Rac1 Binds Tubulin. *J. Biol. Chem.* 271, 3756–3762. doi:10.1074/jbc.271.7.3756

Bey, E. A., Xu, B., Bhattacharjee, A., Oldfield, C. M., Zhao, X., Li, Q., et al. (2004). Protein Kinase Cδ Is Required for p47phoxPhosphorylation and Translocation in Activated Human Monocytes. *J. Immunol.* 173, 5730–5738. doi:10.4049/jimmunol.173.9.5730

Bleier, L., and Dröse, S. (2013). Superoxide Generation by Complex III: From Mechanistic Rationales to Functional Consequences. *Biochimica Biophysica Acta (BBA) - Bioenergetics* 1827, 1320–1331. doi:10.1016/j.bbabio.2012.12.002

Block, K., Eid, A., Griendling, K. K., Lee, D.-Y., Wittrant, Y., and Gorin, Y. (2008). Nox4 NAD(P)H Oxidase Mediates Src-dependent Tyrosine Phosphorylation of PDK-1 in Response to Angiotensin II. *J. Biol. Chem.* 283, 24061–24076. doi:10.1074/jbc.m803964200

Blokzijl, A., Dahlqvist, C., Reissmann, E., Falk, A., Moliner, A., Lendahl, U., et al. (2003). Cross-talk between the Notch and TGF-β Signaling Pathways Mediated by Interaction of the Notch Intracellular Domain with Smad3. *J. Cell Biol.* 163, 723–728. doi:10.1083/jcb.200305112

Boggiano, J. C., and Fehon, R. G. (2012). Growth Control by Committee: Intercellular Junctions, Cell Polarity, and the Cytoskeleton Regulate Hippo Signaling. *Dev. Cell* 22, 695–702. doi:10.1016/j.devcel.2012.03.013

Bolós, V., Gasent, J. M., Lopez-Tarruella, S., and Grande, E. (2010). The Dual Kinase Complex FAK-Src as a Promising Therapeutic Target in Cancer. *Ott* 3, 83–97. doi:10.2147/ott.s6909

Bonner, M. Y., and Arbiser, J. L. (2012). Targeting NADPH Oxidases for the Treatment of Cancer and Inflammation. *Cell. Mol. Life Sci.* 69, 2435–2442. doi:10.1007/s00018-012-1017-2

Boral, D., Vishnoi, M., Liu, H. N., Yin, W., Sprouse, M. L., Scamardo, A., et al. (2017). Molecular Characterization of Breast Cancer CTCs Associated with Brain Metastasis. *Nat. Commun.* 8, 196. doi:10.1038/s41467-017-00196-1

Brahmer, J. R., Tykodi, S. S., Chow, L. Q. M., Hwu, W.-J., Topalian, S. L., Hwu, P., et al. (2012). Safety and Activity of Anti-PD-L1 Antibody in Patients with Advanced Cancer. *N. Engl. J. Med.* 366, 2455–2465. doi:10.1056/nejmoa1200694

Brandes, R. P., Weissmann, N., and Schröder, K. (2014a). Nox Family NADPH Oxidases in Mechano-Transduction: Mechanisms and Consequences. *Antioxidants Redox Signal.* 20, 887–898. doi:10.1089/ars.2013.5414

Brandes, R. P., Weissmann, N., and Schröder, K. (2014b). Nox Family NADPH Oxidases: Molecular Mechanisms of Activation. *Free Radic. Biol. Med.* 76, 208–226. doi:10.1016/j.freeradbiomed.2014.07.046

Brandt, D. T., Marion, S., Griffiths, G., Watanabe, T., Kaibuchi, K., and Grosse, R. (2007). Dia1 and IQGAP1 Interact in Cell Migration and Phagocytic Cup Formation. *J. Cell Biol.* 178, 193–200. doi:10.1083/jcb.200612071

Bretscher, A., Edwards, K., and Fehon, R. G. (2002). ERM Proteins and Merlin: Integrators at the Cell Cortex. *Nat. Rev. Mol. Cell Biol.* 3, 586–599. doi:10.1038/nrm882

Brown, D. I., and Griendling, K. K. (2009). Nox Proteins in Signal Transduction. *Free Radic. Biol. Med.* 47, 1239–1253. doi:10.1016/j.freeradbiomed.2009.07.023

Bruick, R. K., and Mcknight, S. L. (2001). A Conserved Family of Prolyl-4-Hydroxylases that Modify HIF. *Science* 294, 1337–1340. doi:10.1126/science.1066373

Buricchi, F., Giannoni, E., Grimaldi, G., Parri, M., Raugei, G., Ramponi, G., et al. (2007). Redox Regulation of Ephrin/integrin Cross-Talk. *Cell Adhesion Migr.* 1, 33–42. doi:10.4161/cam.3911

Burtenshaw, D., Hakimjavadi, R., Redmond, E. M., and Cahill, P. A. (2017). Nox, Reactive Oxygen Species and Regulation of Vascular Cell Fate. *Antioxidants (Basel)* 6. doi:10.3390/antiox6040090

Cai, D., Chen, S.-C., Prasad, M., He, L., Wang, X., Choesmel-Cadamuro, V., et al. (2014a). Mechanical Feedback through E-Cadherin Promotes Direction Sensing during Collective Cell Migration. *Cell* 157, 1146–1159. doi:10.1016/j.cell.2014.03.045

Cai, W.-X., Liang, L., Wang, L., Han, J.-T., Zhu, X.-X., Han, H., et al. (2014b). Inhibition of Notch Signaling Leads to Increased Intracellular ROS by Up-Regulating Nox4 Expression in Primary HUVECs. *Cell. Immunol.* 287, 129–135. doi:10.1016/j.cellimm.2013.12.009

Cai, X., Wang, K.-C., and Meng, Z. (2021). Mechanoregulation of YAP and TAZ in Cellular Homeostasis and Disease Progression. *Front. Cell Dev. Biol.* 9, 673599. doi:10.3389/fcell.2021.673599

Caliceti, C., Nigro, P., Rizzo, P., and Ferrari, R. (2014). ROS, Notch, and Wnt Signaling Pathways: Crosstalk between Three Major Regulators of Cardiovascular Biology. *Biomed. Res. Int.* 2014, 318714. doi:10.1155/2014/318714

Calvo, F., Ege, N., Grande-Garcia, A., Hooper, S., Jenkins, R. P., Chaudhry, S. I., et al. (2013). Mechanotransduction and YAP-dependent Matrix Remodelling Is Required for the Generation and Maintenance of Cancer-Associated Fibroblasts. *Nat. Cell Biol.* 15, 637–646. doi:10.1038/ncb2756

Camargo, F. D., Gokhale, S., Johnnidis, J. B., Fu, D., Bell, G. W., Jaenisch, R., et al. (2007). YAP1 Increases Organ Size and Expands Undifferentiated Progenitor Cells. *Curr. Biol.* 17, 2054–2060. doi:10.1016/j.cub.2007.10.039

Cao, X., Pfaff, S. L., and Gage, F. H. (2008). YAP Regulates Neural Progenitor Cell Number via the TEA Domain Transcription Factor. *Genes Dev.* 22, 3320–3334. doi:10.1101/gad.1726608

Caporizzo, M. A., Chen, C. Y., and Prosser, B. L. (2019). Cardiac Microtubules in Health and Heart Disease. *Exp. Biol. Med. (Maywood)* 244, 1255–1272. doi:10.1177/1535370219868960

Caporizzo, M. A., Chen, C. Y., Salomon, A. K., Margulies, K. B., and Prosser, B. L. (2018). Microtubules Provide a Viscoelastic Resistance to Myocyte Motion. *Biophysical J.* 115, 1796–1807. doi:10.1016/j.bpj.2018.09.019

Cathcart, M. K. (2004). Regulation of Superoxide Anion Production by NADPH Oxidase in Monocytes/Macrophages. *Atvb* 24, 23–28. doi:10.1161/01.atv.0000097769.47306.12

Cattaneo, I., Condorelli, L., Terrinoni, A. R., Antiga, L., Sangalli, F., and Remuzzi, A. (2011). Shear Stress Reverses Dome Formation in Confluent Renal Tubular Cells. *Cell Physiol. Biochem.* 28, 673–682. doi:10.1159/000335813

Chakraborty, S., Njah, K., Pobbati, A. V., Lim, Y. B., Raju, A., Lakshmanan, M., et al. (2017). Agrin as a Mechanotransduction Signal Regulating YAP through the Hippo Pathway. *Cell Rep.* 18, 2464–2479. doi:10.1016/j.celrep.2017.02.041

Chang, L., Azzolin, L., Di Biagio, D., Zanconato, F., Battilana, G., Lucon Xiccato, R., et al. (2018). The SWI/SNF Complex Is a Mechanoregulated Inhibitor of YAP and TAZ. *Nature* 563, 265–269. doi:10.1038/s41586-018-0658-1

Chang, Y.-L., Yang, C.-Y., Lin, M.-W., Wu, C.-T., and Yang, P.-C. (2016). High Co-expression of PD-L1 and HIF-1α Correlates with Tumour Necrosis in Pulmonary Pleomorphic Carcinoma. *Eur. J. Cancer* 60, 125–135. doi:10.1016/j.ejca.2016.03.012

Chao, H.-C. A., Chung, C.-L., Pan, H.-A., Liao, P.-C., Kuo, P.-L., and Hsu, C.-C. (2011). Protein Tyrosine Phosphatase Non-receptor Type 14 Is a Novel Sperm-Motility Biomarker. *J. Assist. Reprod. Genet.* 28, 851–861. doi:10.1007/s10815-011-9602-0

Chattopadhyay, R., Raghavan, S., and Rao, G. N. (2017). Resolvin D1 via Prevention of ROS-Mediated SHP2 Inactivation Protects Endothelial Adherens Junction Integrity and Barrier Function. *Redox Biol.* 12, 438–455. doi:10.1016/j.redox.2017.02.023

Chen, C. S., Mrksich, M., Huang, S., Whitesides, G. M., and Ingber, D. E. (1997). Geometric Control of Cell Life and Death. *Science* 276, 1425–1428. doi:10.1126/science.276.5317.1425

Chen, C. Y., Caporizzo, M. A., Bedi, K., Vite, A., Bogush, A. I., Robison, P., et al. (2018). Suppression of Detyrosinated Microtubules Improves Cardiomyocyte Function in Human Heart Failure. *Nat. Med.* 24, 1225–1233. doi:10.1038/s41591-018-0046-2

Chen, H., Houshmand, G., Mishra, S., Fong, G.-H., Gittes, G. K., and Esni, F. (2010). Impaired Pancreatic Development in Hif2-Alpha Deficient Mice. *Biochem. Biophysical Res. Commun.* 399, 440–445. doi:10.1016/j.bbrc.2010.07.111

Chen, H. I., and Sudol, M. (1995). The WW Domain of Yes-Associated Protein Binds a Proline-Rich Ligand that Differs from the Consensus Established for Src

Homology 3-binding Modules. *Proc. Natl. Acad. Sci. U.S.A.* 92, 7819–7823. doi:10.1073/pnas.92.17.7819

Chen, Q., Powell, D. W., Rane, M. J., Singh, S., Butt, W., Klein, J. B., et al. (2003). Akt Phosphorylates P47phoxand Mediates Respiratory Burst Activity in Human Neutrophils. *J. Immunol.* 170, 5302–5308. doi:10.4049/jimmunol.170.10.5302

Chen, S., and Sang, N. (2016). Hypoxia-Inducible Factor-1: A Critical Player in the Survival Strategy of Stressed Cells. *J. Cell. Biochem.* 117, 267–278. doi:10.1002/jcb.25283

Chen, W.-J., Ho, C.-C., Chang, Y.-L., Chen, H.-Y., Lin, C.-A., Ling, T.-Y., et al. (2014). Cancer-associated Fibroblasts Regulate the Plasticity of Lung Cancer Stemness via Paracrine Signalling. *Nat. Commun.* 5, 3472. doi:10.1038/ncomms4472

Chen, X., Song, M., Zhang, B., and Zhang, Y. (2016). Reactive Oxygen Species Regulate T Cell Immune Response in the Tumor Microenvironment. *Oxid. Med. Cell Longev.* 2016, 1580967. doi:10.1155/2016/1580967

Cheng, D., Yan, X., Qiu, G., Zhang, J., Wang, H., Feng, T., et al. (2018). Contraction of Basal Filopodia Controls Periodic Feather Branching via Notch and FGF Signaling. *Nat. Commun.* 9, 1345. doi:10.1038/s41467-018-03801-z

Chiarugi, P., Pani, G., Giannoni, E., Taddei, L., Colavitti, R., Raugei, G., et al. (2003). Reactive Oxygen Species as Essential Mediators of Cell Adhesion. *J. Cell Biol.* 161, 933–944. doi:10.1083/jcb.200211118

Chifflet, S., and Hernandez, J. A. (2016). The Epithelial Sodium Channel and the Processes of Wound Healing. *Biomed. Res. Int.* 2016, 5675047. doi:10.1155/2016/5675047

Cho, Y., Park, M. J., Kim, K., Kim, S. W., Kim, W., Oh, S., et al. (2020). Reactive Oxygen Species-Induced Activation of Yes-Associated Protein-1 through the C-Myc Pathway Is a Therapeutic Target in Hepatocellular Carcinoma. *Wjg* 26, 6599–6613. doi:10.3748/wjg.v26.i42.6599

Chong, H. C., Tan, M. J., Philippe, V., Tan, S. H., Tan, C. K., Ku, C. W., et al. (2009). Regulation of Epithelial-Mesenchymal IL-1 Signaling by PPARβ/δ Is Essential for Skin Homeostasis and Wound Healing. *J. Cell Biol.* 184, 817–831. doi:10.1083/jcb.200809028

Chowdhury, F., Li, I. T. S., Ngo, T. T. M., Leslie, B. J., Kim, B. C., Sokoloski, J. E., et al. (2016). Defining Single Molecular Forces Required for Notch Activation Using Nano Yoyo. *Nano Lett.* 16, 3892–3897. doi:10.1021/acs.nanolett.6b01403

Cole, B. K., Curto, M., Chan, A. W., and Mcclatchey, A. I. (2008). Localization to the Cortical Cytoskeleton Is Necessary for Nf2/merlin-dependent Epidermal Growth Factor Receptor Silencing. *Mol. Cell Biol.* 28, 1274–1284. doi:10.1128/mcb.01139-07

Cosset, É., Ilmjärv, S., Dutoit, V., Elliott, K., Von Schalscha, T., Camargo, M. F., et al. (2017). Glut3 Addiction Is a Druggable Vulnerability for a Molecularly Defined Subpopulation of Glioblastoma. *Cancer cell* 32, 856–868. doi:10.1016/j.ccell.2017.10.016

Couzens, A. L., Knight, J. D., Kean, M. J., Teo, G., Weiss, A., Dunham, W. H., et al. (2013). Protein Interaction Network of the Mammalian Hippo Pathway Reveals Mechanisms of Kinase-Phosphatase Interactions. *Sci. Signal* 6, rs15. doi:10.1126/scisignal.2004712

Covello, K. L., Kehler, J., Yu, H., Gordan, J. D., Arsham, A. M., Hu, C.-J., et al. (2006). HIF-2α Regulates Oct-4: Effects of Hypoxia on Stem Cell Function, Embryonic Development, and Tumor Growth. *Genes Dev.* 20, 557–570. doi:10.1101/gad.1399906

Cummins, E. P., Keogh, C. E., Crean, D., and Taylor, C. T. (2016). The Role of HIF in Immunity and Inflammation. *Mol. Aspects Med.* 47-48, 24–34. doi:10.1016/j.mam.2015.12.004

Cummins, E. P., Selfridge, A. C., Sporn, P. H., Sznajder, J. I., and Taylor, C. T. (2014). Carbon Dioxide-Sensing in Organisms and its Implications for Human Disease. *Cell. Mol. Life Sci.* 71, 831–845. doi:10.1007/s00018-013-1470-6

Dai, X., She, P., Chi, F., Feng, Y., Liu, H., Jin, D., et al. (2013). Phosphorylation of Angiomotin by Lats1/2 Kinases Inhibits F-Actin Binding, Cell Migration, and Angiogenesis. *J. Biol. Chem.* 288, 34041–34051. doi:10.1074/jbc.m113.518019

Danovi, S. A., Rossi, M., Gudmundsdottir, K., Yuan, M., Melino, G., and Basu, S. (2008). Yes-associated Protein (YAP) Is a Critical Mediator of C-jun-dependent Apoptosis. *Cell Death Differ.* 15, 217–219. doi:10.1038/sj.cdd.4402226

Dao, J. H., Kurzeja, R. J. M., Morachis, J. M., Veith, H., Lewis, J., Yu, V., et al. (2009). Kinetic Characterization and Identification of a Novel Inhibitor of Hypoxia-Inducible Factor Prolyl Hydroxylase 2 Using a Time-Resolved Fluorescence Resonance Energy Transfer-Based Assay Technology. *Anal. Biochem.* 384, 213–223. doi:10.1016/j.ab.2008.09.052

Davalli, P., Mitic, T., Caporali, A., Lauriola, A., and D'arca, D. (2016). ROS, Cell Senescence, and Novel Molecular Mechanisms in Aging and Age-Related Diseases. *Oxid. Med. Cell Longev.* 2016, 3565127. doi:10.1155/2016/3565127

De Gaetano, A., Gibellini, L., Zanini, G., Nasi, M., Cossarizza, A., and Pinti, M. (2021). Mitophagy and Oxidative Stress: The Role of Aging. *Antioxidants (Basel)* 10. doi:10.3390/antiox10050794

De Rezende, F. F., Martins Lima, A., Niland, S., Wittig, I., Heide, H., Schröder, K., et al. (2012). Integrin α7β1 Is a Redox-Regulated Target of Hydrogen Peroxide in Vascular Smooth Muscle Cell Adhesion. *Free Radic. Biol. Med.* 53, 521–531. doi:10.1016/j.freeradbiomed.2012.05.032

Di Meo, S., Reed, T. T., Venditti, P., and Victor, V. M. (20162016). Role of ROS and RNS Sources in Physiological and Pathological Conditions. *Oxid. Med. Cell Longev.* 2016, 1245049. doi:10.1155/2016/1245049

Diebold, I., Petry, A., Hess, J., and Görlach, A. (2010). The NADPH Oxidase Subunit NOX4 Is a New Target Gene of the Hypoxia-Inducible Factor-1. *MBoC* 21, 2087–2096. doi:10.1091/mbc.e09-12-1003

Diekmann, D., Abo, A., Johnston, C., Segal, A. W., and Hall, A. (1994). Interaction of Rac with P67 Phox and Regulation Pf Phagocytic NADPH Oxidase Activity. *Science* 265, 531–533. doi:10.1126/science.8036496

Discher, D. E., Mooney, D. J., and Zandstra, P. W. (2009). Growth Factors, Matrices, and Forces Combine and Control Stem Cells. *Science* 324, 1673–1677. doi:10.1126/science.1171643

Dong, J., Feldmann, G., Huang, J., Wu, S., Zhang, N., Comerford, S. A., et al. (2007). Elucidation of a Universal Size-Control Mechanism in Drosophila and Mammals. *Cell* 130, 1120–1133. doi:10.1016/j.cell.2007.07.019

Dupont, S., Morsut, L., Aragona, M., Enzo, E., Giulitti, S., Cordenonsi, M., et al. (2011). Role of YAP/TAZ in Mechanotransduction. *Nature* 474, 179–183. doi:10.1038/nature10137

Durán, R. V., Mackenzie, E. D., Boulahbel, H., Frezza, C., Heiserich, L., Tardito, S., et al. (2013). HIF-independent Role of Prolyl Hydroxylases in the Cellular Response to Amino Acids. *Oncogene* 32, 4549–4556. doi:10.1038/onc.2012.465

Dustin, C. M., Heppner, D. E., Lin, M.-C. J., and Van Der Vliet, A. (2020). Redox Regulation of Tyrosine Kinase Signalling: More Than Meets the Eye. *J. Biochem.* 167, 151–163. doi:10.1093/jb/mvz085

Eble, J. A., and De Rezende, F. F. (2014). Redox-Relevant Aspects of the Extracellular Matrix and its Cellular ContactsviaIntegrins. *Antioxidants Redox Signal.* 20, 1977–1993. doi:10.1089/ars.2013.5294

Ehrismann, D., Flashman, E., Genn, D. N., Mathioudakis, N., Hewitson, K. S., Ratcliffe, P. J., et al. (2007). Studies on the Activity of the Hypoxia-Inducible-Factor Hydroxylases Using an Oxygen Consumption Assay. *Biochem. J.* 401, 227–234. doi:10.1042/bj20061151

Elisi, G. M., Santucci, M., D'arca, D., Lauriola, A., Marverti, G., Losi, L., et al. (2018). Repurposing of Drugs Targeting YAP-TEAD Functions. *Cancers (Basel)* 10. doi:10.3390/cancers10090329

Ellmark, S., Dusting, G., Ngtangfui, M., Guzzopernell, N., and Drummond, G. (2005). The Contribution of Nox4 to NADPH Oxidase Activity in Mouse Vascular Smooth Muscle. *Cardiovasc. Res.* 65, 495–504. doi:10.1016/j.cardiores.2004.10.026

Emerling, B. M., Platanias, L. C., Black, E., Nebreda, A. R., Davis, R. J., and Chandel, N. S. (2005). Mitochondrial Reactive Oxygen Species Activation of P38 Mitogen-Activated Protein Kinase Is Required for Hypoxia Signaling. *Mol. Cell Biol.* 25, 4853–4862. doi:10.1128/mcb.25.12.4853-4862.2005

Engel-Pizcueta, C., and Pujades, C. (2021). Interplay between Notch and YAP/TAZ Pathways in the Regulation of Cell Fate during Embryo Development. *Front. Cell Dev. Biol.* 9, 711531. doi:10.3389/fcell.2021.711531

Epstein, A. C. R., Gleadle, J. M., Mcneill, L. A., Hewitson, K. S., O'rourke, J., Mole, D. R., et al. (2001). *C. elegans* EGL-9 and Mammalian Homologs Define a Family of Dioxygenases that Regulate HIF by Prolyl Hydroxylation. *Cell* 107, 43–54. doi:10.1016/s0092-8674(01)00507-4

Ezashi, T., Das, P., and Roberts, R. M. (2005). Low O 2 Tensions and the Prevention of Differentiation of hES Cells. *Proc. Natl. Acad. Sci. U.S.A.* 102, 4783–4788. doi:10.1073/pnas.0501283102

Fan, Y., Mao, R., and Yang, J. (2013). NF-κB and STAT3 Signaling Pathways Collaboratively Link Inflammation to Cancer. *Protein Cell* 4, 176–185. doi:10.1007/s13238-013-2084-3

Feno, S., Butera, G., Vecellio Reane, D., Rizzuto, R., and Raffaello, A. (2019). Crosstalk between Calcium and ROS in Pathophysiological Conditions. *Oxid. Med. Cell Longev.* 2019, 9324018. doi:10.1155/2019/9324018

Fernandez-Valle, C., Tang, Y., Ricard, J., Rodenas-Ruano, A., Taylor, A., Hackler, E., et al. (2002). Paxillin Binds Schwannomin and Regulates its Density-dependent Localization and Effect on Cell Morphology. *Nat. Genet.* 31, 354–362. doi:10.1038/ng930

Figtree, G. A., Liu, C.-C., Bibert, S., Hamilton, E. J., Garcia, A., White, C. N., et al. (2009). Reversible Oxidative Modification. *Circulation Res.* 105, 185–193. doi:10.1161/circresaha.109.199547

Flaiz, C., Ammoun, S., Biebl, A., and Hanemann, C. O. (2009). Altered Adhesive Structures and Their Relation to RhoGTPase Activation in Merlin-Deficient Schwannoma. *Brain Pathol.* 19, 27–38. doi:10.1111/j.1750-3639.2008.00165.x

Flügel, D., Görlach, A., Michiels, C., and Kietzmann, T. (2007). Glycogen Synthase Kinase 3 Phosphorylates Hypoxia-Inducible Factor 1alpha and Mediates its Destabilization in a VHL-independent Manner. *Mol. Cell Biol.* 27, 3253–3265. doi:10.1128/MCB.00015-07

Folkman, J., and Moscona, A. (1978). Role of Cell Shape in Growth Control. *Nature* 273, 345–349. doi:10.1038/273345a0

Fong, G.-H., and Takeda, K. (2008). Role and Regulation of Prolyl Hydroxylase Domain Proteins. *Cell Death Differ.* 15, 635–641. doi:10.1038/cdd.2008.10

Fontayne, A., Dang, P. M.-C., Gougerot-Pocidalo, M.-A., and El Benna, J. (2002). Phosphorylation of P47phox Sites by PKC α, βII, δ, and ζ: Effect on Binding to P22phox and on NADPH Oxidase Activation. *Biochemistry* 41, 7743–7750. doi:10.1021/bi011953s

Force, T., and Woodgett, J. R. (2009). Unique and Overlapping Functions of GSK-3 Isoforms in Cell Differentiation and Proliferation and Cardiovascular Development. *J. Biol. Chem.* 284, 9643–9647. doi:10.1074/jbc.r800077200

Fu, P., Ramchandran, R., Shaaya, M., Huang, L., Ebenezer, D. L., Jiang, Y., et al. (2020). Phospholipase D2 Restores Endothelial Barrier Function by Promoting PTPN14-Mediated VE-Cadherin Dephosphorylation. *J. Biol. Chem.* 295, 7669–7685. doi:10.1074/jbc.ra119.011801

Fujii, M., Toyoda, T., Nakanishi, H., Yatabe, Y., Sato, A., Matsudaira, Y., et al. (2012). TGF-β Synergizes with Defects in the Hippo Pathway to Stimulate Human Malignant Mesothelioma Growth. *J. Exp. Med.* 209, 479–494. doi:10.1084/jem.20111653

Fukai, T., and Ushio-Fukai, M. (2020). Cross-Talk between NADPH Oxidase and Mitochondria: Role in ROS Signaling and Angiogenesis. *Cells* 9. doi:10.3390/cells9081849

Funato, Y., and Miki, H. (2010). Redox Regulation of Wnt Signalling via Nucleoredoxin. *Free Radic. Res.* 44, 379–388. doi:10.3109/10715761003610745

Funato, Y., Terabayashi, T., Sakamoto, R., Okuzaki, D., Ichise, H., Nojima, H., et al. (2010). Nucleoredoxin Sustains Wnt/β-Catenin Signaling by Retaining a Pool of Inactive Dishevelled Protein. *Curr. Biol.* 20, 1945–1952. doi:10.1016/j.cub.2010.09.065

Furukawa, K. T., Yamashita, K., Sakurai, N., and Ohno, S. (2017). The Epithelial Circumferential Actin Belt Regulates YAP/TAZ through Nucleocytoplasmic Shuttling of Merlin. *Cell Rep.* 20, 1435–1447. doi:10.1016/j.celrep.2017.07.032

Gabrilovich, D. I., and Nagaraj, S. (2009). Myeloid-derived Suppressor Cells as Regulators of the Immune System. *Nat. Rev. Immunol.* 9, 162–174. doi:10.1038/nri2506

Gaete, D., Rodriguez, D., Watts, D., Sormendi, S., Chavakis, T., and Wielockx, B. (2021). HIF-prolyl Hydroxylase Domain Proteins (PHDs) in Cancer-Potential Targets for Anti-tumor Therapy? *Cancers* 13, 988. doi:10.3390/cancers13050988

Gao, Y., Nihira, N. T., Bu, X., Chu, C., Zhang, J., Kolodziejczyk, A., et al. (2020). Acetylation-dependent Regulation of PD-L1 Nuclear Translocation Dictates the Efficacy of Anti-PD-1 Immunotherapy. *Nat. Cell Biol.* 22, 1064–1075. doi:10.1038/s41556-020-0562-4

Gargini, R., Escoll, M., García, E., García-Escudero, R., Wandosell, F., and Antón, I. M. (2016). WIP Drives Tumor Progression through YAP/TAZ-Dependent Autonomous Cell Growth. *Cell Rep.* 17, 1962–1977. doi:10.1016/j.celrep.2016.10.064

Gau, D., and Roy, P. (2018). SRF'ing and SAP'ing - the Role of MRTF Proteins in Cell Migration. *J. Cell Sci.* 131. doi:10.1242/jcs.218222

Ge, H., Tian, M., Pei, Q., Tan, F., and Pei, H. (2021). Extracellular Matrix Stiffness: New Areas Affecting Cell Metabolism. *Front. Oncol.* 11, 631991. doi:10.3389/fonc.2021.631991

Genevet, A., Wehr, M. C., Brain, R., Thompson, B. J., and Tapon, N. (2010). Kibra Is a Regulator of the Salvador/Warts/Hippo Signaling Network. *Dev. Cell* 18, 300–308. doi:10.1016/j.devcel.2009.12.011

Gerald, D., Berra, E., Frapart, Y. M., Chan, D. A., Giaccia, A. J., Mansuy, D., et al. (2004). JunD Reduces Tumor Angiogenesis by Protecting Cells from Oxidative Stress. *Cell* 118, 781–794. doi:10.1016/j.cell.2004.08.025

Gerhardt, H., and Betsholtz, C. (2003). Endothelial-pericyte Interactions in Angiogenesis. *Cell Tissue Res.* 314, 15–23. doi:10.1007/s00441-003-0745-x

Ghio, A. J., Nozik-Grayck, E., Turi, J., Jaspers, I., Mercatante, D. R., Kole, R., et al. (2003). Superoxide-Dependent Iron Uptake. *Am. J. Respir. Cell Mol. Biol.* 29, 653–660. doi:10.1165/rcmb.2003-0070oc

Gianni, D., Taulet, N., Dermardirossian, C., and Bokoch, G. M. (2010). c-Src-mediated Phosphorylation of NoxA1 and Tks4 Induces the Reactive Oxygen Species (ROS)-dependent Formation of Functional Invadopodia in Human Colon Cancer Cells. *MBoC* 21, 4287–4298. doi:10.1091/mbc.e10-08-0685

Giannoni, E., Taddei, M. L., and Chiarugi, P. (2010). Src Redox Regulation: Again in the Front Line. *Free Radic. Biol. Med.* 49, 516–527. doi:10.1016/j.freeradbiomed.2010.04.025

Gilkes, D. M., Bajpai, S., Chaturvedi, P., Wirtz, D., and Semenza, G. L. (2013). Hypoxia-inducible Factor 1 (HIF-1) Promotes Extracellular Matrix Remodeling under Hypoxic Conditions by Inducing P4HA1, P4HA2, and PLOD2 Expression in Fibroblasts. *J. Biol. Chem.* 288, 10819–10829. doi:10.1074/jbc.m112.442939

Gittes, F., Mickey, B., Nettleton, J., and Howard, J. (1993). Flexural Rigidity of Microtubules and Actin Filaments Measured from Thermal Fluctuations in Shape. *J. Cell Biol.* 120, 923–934. doi:10.1083/jcb.120.4.923

Gladden, A. B., Hebert, A. M., Schneeberger, E. E., and Mcclatchey, A. I. (2010). The NF2 Tumor Suppressor, Merlin, Regulates Epidermal Development through the Establishment of a Junctional Polarity Complex. *Dev. Cell* 19, 727–739. doi:10.1016/j.devcel.2010.10.008

Goettsch, C., Goettsch, W., Arsov, A., Hofbauer, L. C., Bornstein, S. R., and Morawietz, H. (2009). Long-term Cyclic Strain Downregulates Endothelial Nox4. *Antioxidants Redox Signal.* 11, 2385–2397. doi:10.1089/ars.2009.2561

Gomez, E. W., Chen, Q. K., Gjorevski, N., and Nelson, C. M. (2010). Tissue Geometry Patterns Epithelial-Mesenchymal Transition via Intercellular Mechanotransduction. *J. Cell Biochem.* 110, 44–51. doi:10.1002/jcb.22545

Gong, J., Yao, Y., Zhang, P., Udayasuryan, B., Komissarova, E. V., Chen, J., et al. (2015). The C2 Domain and Altered ATP-Binding Loop Phosphorylation at Ser 359 Mediate the Redox-dependent Increase in Protein Kinase C-δ Activity. *Mol. Cell Biol.* 35, 1727–1740. doi:10.1128/mcb.01436-14

Goodson, P., Kumar, A., Jain, L., Kundu, K., Murthy, N., Koval, M., et al. (2012). Nadph Oxidase Regulates Alveolar Epithelial Sodium Channel Activity and Lung Fluid Balance In Vivo via O2− Signaling. *Am. J. Physiology-Lung Cell. Mol. Physiology* 302, L410–L419. doi:10.1152/ajplung.00260.2011

Gordan, J. D., Bertout, J. A., Hu, C.-J., Diehl, J. A., and Simon, M. C. (2007). HIF-2α Promotes Hypoxic Cell Proliferation by Enhancing C-Myc Transcriptional Activity. *Cancer cell* 11, 335–347. doi:10.1016/j.ccr.2007.02.006

Gordon, W. R., Zimmerman, B., He, L., Miles, L. J., Huang, J., Tiyanont, K., et al. (2015). Mechanical Allostery: Evidence for a Force Requirement in the Proteolytic Activation of Notch. *Dev. Cell* 33, 729–736. doi:10.1016/j.devcel.2015.05.004

Görlach, A., Bertram, K., Hudecova, S., and Krizanova, O. (2015). Calcium and ROS: A Mutual Interplay. *Redox Biol.* 6, 260–271. doi:10.1016/j.redox.2015.08.010

Greenwald, R. J., Freeman, G. J., and Sharpe, A. H. (2005). The B7 Family Revisited. *Annu. Rev. Immunol.* 23, 515–548. doi:10.1146/annurev.immunol.23.021704.115611

Gregg, D., De Carvalho, D. D., and Kovacic, H. (2004). Integrins and Coagulation: A Role for ROS/redox Signaling? *Antioxidants Redox Signal.* 6, 757–764. doi:10.1089/1523086041361604

Groemping, Y., Lapouge, K., Smerdon, S. J., and Rittinger, K. (2003). Molecular Basis of Phosphorylation-Induced Activation of the NADPH Oxidase. *Cell* 113, 343–355. doi:10.1016/s0092-8674(03)00314-3

Grosberg, A., Kuo, P.-L., Guo, C.-L., Geisse, N. A., Bray, M.-A., Adams, W. J., et al. (2011). Self-organization of Muscle Cell Structure and Function. *PLoS Comput. Biol.* 7, e1001088. doi:10.1371/journal.pcbi.1001088

Grote, K., Flach, I., Luchtefeld, M., Akin, E., Holland, S. M., Drexler, H., et al. (2003). Mechanical Stretch Enhances mRNA Expression and Proenzyme

Release of Matrix Metalloproteinase-2 (MMP-2) via NAD(P)H Oxidase-Derived Reactive Oxygen Species. *Circ. Res.* 92, e80–6. doi:10.1161/01.RES.0000077044.60138.7C

Guo, C.-L., Ouyang, M., Yu, J.-Y., Maslov, J., Price, A., and Shen, C.-Y. (2012). Long-range Mechanical Force Enables Self-Assembly of Epithelial Tubular Patterns. *Proc. Natl. Acad. Sci. U.S.A.* 109, 5576–5582. doi:10.1073/pnas.1114781109

Guo, R., Li, Y., Wang, Z., Bai, H., Duan, J., Wang, S., et al. (2019). Hypoxia-inducible Factor-1α and Nuclear factor-κB Play Important Roles in Regulating Programmed Cell Death Ligand 1 Expression by Epidermal Growth Factor Receptor Mutants in Non-small-cell Lung Cancer Cells. *Cancer Sci.* 110, 1665–1675. doi:10.1111/cas.13989

Gupta, S. C., Kunnumakkara, A. B., Aggarwal, S., and Aggarwal, B. B. (2018). Inflammation, a Double-Edge Sword for Cancer and Other Age-Related Diseases. *Front. Immunol.* 9, 2160. doi:10.3389/fimmu.2018.02160

Guruharsha, K. G., Kankel, M. W., and Artavanis-Tsakonas, S. (2012). The Notch Signalling System: Recent Insights into the Complexity of a Conserved Pathway. *Nat. Rev. Genet.* 13, 654–666. doi:10.1038/nrg3272

Gustafsson, M. V., Zheng, X., Pereira, T., Gradin, K., Jin, S., Lundkvist, J., et al. (2005). Hypoxia Requires Notch Signaling to Maintain the Undifferentiated Cell State. *Dev. Cell* 9, 617–628. doi:10.1016/j.devcel.2005.09.010

Halligan, D. N., Murphy, S. J. E., and Taylor, C. T. (2016). The Hypoxia-Inducible Factor (HIF) Couples Immunity with Metabolism. *Seminars Immunol.* 28, 469–477. doi:10.1016/j.smim.2016.09.004

Han, Y., Ishibashi, S., Iglesias-Gonzalez, J., Chen, Y., Love, N. R., and Amaya, E. (2018). Ca2+-Induced Mitochondrial ROS Regulate the Early Embryonic Cell Cycle. *Cell Rep.* 22, 218–231. doi:10.1016/j.celrep.2017.12.042

Hansen, C. G., Moroishi, T., and Guan, K.-L. (2015). YAP and TAZ: a Nexus for Hippo Signaling and beyond. *Trends Cell Biol.* 25, 499–513. doi:10.1016/j.tcb.2015.05.002

Hao, Y., Chun, A., Cheung, K., Rashidi, B., and Yang, X. (2008). Tumor Suppressor LATS1 Is a Negative Regulator of Oncogene YAP. *J. Biol. Chem.* 283, 5496–5509. doi:10.1074/jbc.m709037200

Harris, A. L. (2002). Hypoxia - a Key Regulatory Factor in Tumour Growth. *Nat. Rev. Cancer* 2, 38–47. doi:10.1038/nrc704

Hartmann, S., Ridley, A. J., and Lutz, S. (2015). The Function of Rho-Associated Kinases ROCK1 and ROCK2 in the Pathogenesis of Cardiovascular Disease. *Front. Pharmacol.* 6, 276. doi:10.3389/fphar.2015.00276

Hashimoto, T., and Shibasaki, F. (2015). Hypoxia-inducible Factor as an Angiogenic Master Switch. *Front. Pediatr.* 3, 33. doi:10.3389/fped.2015.00033

Hayward, M.-K., Muncie, J. M., and Weaver, V. M. (2021). Tissue Mechanics in Stem Cell Fate, Development, and Cancer. *Dev. Cell* 56, 1833–1847. doi:10.1016/j.devcel.2021.05.011

He, M., Zhou, Z., Shah, A. A., Hong, Y., Chen, Q., and Wan, Y. (2016). New Insights into Posttranslational Modifications of Hippo Pathway in Carcinogenesis and Therapeutics. *Cell Div.* 11, 4. doi:10.1186/s13008-016-0013-6

Hecht, D., and Zick, Y. (1992). Selective Inhibition of Protein Tyrosine Phosphatase Activities by H2O2 and Vanadate In Vitro. *Biochem. Biophysical Res. Commun.* 188, 773–779. doi:10.1016/0006-291x(92)91123-8

Hecker, L., Cheng, J., and Thannickal, V. J. (2012). Targeting NOX Enzymes in Pulmonary Fibrosis. *Cell. Mol. Life Sci.* 69, 2365–2371. doi:10.1007/s00018-012-1012-7

Heddleston, J. M., Li, Z., Lathia, J. D., Bao, S., Hjelmeland, A. B., and Rich, J. N. (2010). Hypoxia Inducible Factors in Cancer Stem Cells. *Br. J. Cancer* 102, 789–795. doi:10.1038/sj.bjc.6605551

Hedman, A. C., Li, Z., Gorisse, L., Parvathaneni, S., Morgan, C. J., and Sacks, D. B. (2021). IQGAP1 Binds AMPK and Is Required for Maximum AMPK Activation. *J. Biol. Chem.* 296, 100075. doi:10.1074/jbc.ra120.016193

Helms, M. N., Jain, L., Self, J. L., and Eaton, D. C. (2008). Redox Regulation of Epithelial Sodium Channels Examined in Alveolar Type 1 and 2 Cells Patch-Clamped in Lung Slice Tissue. *J. Biol. Chem.* 283, 22875–22883. doi:10.1074/jbc.m801363200

Hennigan, R. F., Fletcher, J. S., Guard, S., and Ratner, N. (2019). Proximity Biotinylation Identifies a Set of Conformation-specific Interactions between Merlin and Cell Junction Proteins. *Sci. Signal* 12. doi:10.1126/scisignal.aau8749

Heo, J. S., and Lee, J.-C. (2011). β-Catenin Mediates Cyclic Strain-Stimulated Cardiomyogenesis in Mouse Embryonic Stem Cells through ROS-dependent and Integrin-Mediated PI3K/Akt Pathways. *J. Cell. Biochem.* 112, 1880–1889. doi:10.1002/jcb.23108

Heppner, D. E., Dustin, C. M., Liao, C., Hristova, M., Veith, C., Little, A. C., et al. (2018). Direct Cysteine Sulfenylation Drives Activation of the Src Kinase. *Nat. Commun.* 9, 4522. doi:10.1038/s41467-018-06790-1

Heppner, D. E. (2021). Structural Insights into Redox-Active Cysteine Residues of the Src Family Kinases. *Redox Biol.* 41, 101934. doi:10.1016/j.redox.2021.101934

Hikage, F., Atkins, S., Kahana, A., Smith, T. J., and Chun, T.-H. (2019). HIF2A-LOX Pathway Promotes Fibrotic Tissue Remodeling in Thyroid-Associated Orbitopathy. *Endocrinology* 160, 20–35. doi:10.1210/en.2018-00272

Hiraga, R., Kato, M., Miyagawa, S., and Kamata, T. (2013). Nox4-derived ROS Signaling Contributes to TGF-β-Induced Epithelial-Mesenchymal Transition in Pancreatic Cancer Cells. *Anticancer Res.* 33, 4431–4438.

Hirate, Y., Hirahara, S., Inoue, K.-i., Suzuki, A., Alarcon, V. B., Akimoto, K., et al. (2013). Polarity-dependent Distribution of Angiomotin Localizes Hippo Signaling in Preimplantation Embryos. *Curr. Biol.* 23, 1181–1194. doi:10.1016/j.cub.2013.05.014

Hirate, Y., and Sasaki, H. (2014). The Role of Angiomotin Phosphorylation in the Hippo Pathway during Preimplantation Mouse Development. *Tissue Barriers* 2, e28127. doi:10.4161/tisb.28127

Hirsilä, M., Koivunen, P., Günzler, V., Kivirikko, K. I., and Myllyharju, J. (2003). Characterization of the Human Prolyl 4-hydroxylases that Modify the Hypoxia-Inducible Factor. *J. Biol. Chem.* 278, 30772–30780. doi:10.1074/jbc.m304982200

Hoare, M., and Narita, M. (2018). Notch and Senescence. *Adv. Exp. Med. Biol.* 1066, 299–318. doi:10.1007/978-3-319-89512-3_15

Höffken, V., Hermann, A., Pavenstädt, H., and Kremerskothen, J. (2021). WWC Proteins: Important Regulators of Hippo Signaling in Cancer. *Cancers (Basel)* 13. doi:10.3390/cancers13020306

Holmström, K. M., and Finkel, T. (2014). Cellular Mechanisms and Physiological Consequences of Redox-dependent Signalling. *Nat. Rev. Mol. Cell Biol.* 15, 411–421. doi:10.1038/nrm3801

Hong, A. W., Meng, Z., Yuan, H. X., Plouffe, S. W., Moon, S., Kim, W., et al. (2017). Osmotic Stress-induced Phosphorylation by NLK at Ser128 Activates YAP. *EMBO Rep.* 18, 72–86. doi:10.15252/embr.201642681

Horowitz, A., Murakami, M., Gao, Y., and Simons, M. (1999). Phosphatidylinositol-4,5-bisphosphate Mediates the Interaction of Syndecan-4 with Protein Kinase C. *Biochemistry* 38, 15871–15877. doi:10.1021/bi991363i

Houk, A. R., Jilkine, A., Mejean, C. O., Boltyanskiy, R., Dufresne, E. R., Angenent, S. B., et al. (2012). Membrane Tension Maintains Cell Polarity by Confining Signals to the Leading Edge during Neutrophil Migration. *Cell* 148, 175–188. doi:10.1016/j.cell.2011.10.050

Hoyal, C. R., Gutierrez, A., Young, B. M., Catz, S. D., Lin, J.-H., Tsichlis, P. N., et al. (2003). Modulation of P47 PHOX Activity by Site-specific Phosphorylation: Akt-dependent Activation of the NADPH Oxidase. *Proc. Natl. Acad. Sci. U.S.A.* 100, 5130–5135. doi:10.1073/pnas.1031526100

Hu, J. K.-H., Du, W., Shelton, S. J., Oldham, M. C., Dipersio, C. M., and Klein, O. D. (2017). An FAK-YAP-mTOR Signaling Axis Regulates Stem Cell-Based Tissue Renewal in Mice. *Cell Stem Cell* 21, 91–106. doi:10.1016/j.stem.2017.03.023

Hu, Y.-Y., Fu, L.-A., Li, S.-Z., Chen, Y., Li, J.-C., Han, J., et al. (2014). Hif-1α and Hif-2α Differentially Regulate Notch Signaling through Competitive Interaction with the Intracellular Domain of Notch Receptors in Glioma Stem Cells. *Cancer Lett.* 349, 67–76. doi:10.1016/j.canlet.2014.03.035

Huang, J.-M., Nagatomo, I., Suzuki, E., Mizuno, T., Kumagai, T., Berezov, A., et al. (2013). YAP Modifies Cancer Cell Sensitivity to EGFR and Survivin Inhibitors and Is Negatively Regulated by the Non-receptor Type Protein Tyrosine Phosphatase 14. *Oncogene* 32, 2220–2229. doi:10.1038/onc.2012.231

Huang, J. H., Co, H. K., Lee, Y. C., Wu, C. C., and Chen, S. H. (2021a). Multistability Maintains Redox Homeostasis in Human Cells. *Mol. Syst. Biol.* 17, e10480. doi:10.15252/msb.202110480

Huang, S., and Ingber, D. E. (1999). The Structural and Mechanical Complexity of Cell-Growth Control. *Nat. Cell Biol.* 1, E131–E138. doi:10.1038/13043

Huang, Y., Chen, Z., Lu, T., Bi, G., Li, M., Liang, J., et al. (2021b). HIF-1α Switches the Functionality of TGF-β Signaling via Changing the Partners of Smads to Drive Glucose Metabolic Reprogramming in Non-small Cell Lung Cancer. *J. Exp. Clin. Cancer Res.* 40, 398. doi:10.1186/s13046-021-02188-y

Huang, Y., Lin, D., and Taniguchi, C. M. (2017). Hypoxia Inducible Factor (HIF) in the Tumor Microenvironment: Friend or Foe? *Sci. China Life Sci.* 60, 1114–1124. doi:10.1007/s11427-017-9178-y

Hubbi, M. E., and Semenza, G. L. (2015). Regulation of Cell Proliferation by Hypoxia-Inducible Factors. *Am. J. Physiology-Cell Physiology* 309, C775–C782. doi:10.1152/ajpcell.00279.2015

Huff, L. P., Kikuchi, D. S., Faidley, E., Forrester, S. J., Tsai, M. Z., Lassègue, B., et al. (2019). Polymerase-δ-interacting Protein 2 Activates the RhoGEF Epithelial Cell Transforming Sequence 2 in Vascular Smooth Muscle Cells. *Am. J. Physiology-Cell Physiology* 316, C621–C631. doi:10.1152/ajpcell.00208.2018

Hulikova, A., Harris, A. L., Vaughan-Jones, R. D., and Swietach, P. (2013). Regulation of Intracellular pH in Cancer Cell Lines under Normoxia and Hypoxia. *J. Cell. Physiol.* 228, 743–752. doi:10.1002/jcp.24221

Hwang, J., and Pallas, D. C. (2014). STRIPAK Complexes: Structure, Biological Function, and Involvement in Human Diseases. *Int. J. Biochem. Cell Biol.* 47, 118–148. doi:10.1016/j.biocel.2013.11.021

Ikeda, S., Yamaoka-Tojo, M., Hilenski, L., Patrushev, N. A., Anwar, G. M., Quinn, M. T., et al. (2005). IQGAP1 Regulates Reactive Oxygen Species-dependent Endothelial Cell Migration through Interacting with Nox2. *Atvb* 25, 2295–2300. doi:10.1161/01.atv.0000187472.55437.af

Inamori, M., Mizumoto, H., and Kajiwara, T. (2009). An Approach for Formation of Vascularized Liver Tissue by Endothelial Cell-Covered Hepatocyte Spheroid Integration. *Tissue Eng. Part A* 15, 2029–2037. doi:10.1089/ten.tea.2008.0403

Irrcher, I., Ljubicic, V., and Hood, D. A. (2009). Interactions between ROS and AMP Kinase Activity in the Regulation of PGC-1α Transcription in Skeletal Muscle Cells. *Am. J. Physiology-Cell Physiology* 296, C116–C123. doi:10.1152/ajpcell.00267.2007

Islam, S. M. A., Patel, R., and Acevedo-Duncan, M. (2018). Protein Kinase C-ζ Stimulates Colorectal Cancer Cell Carcinogenesis via PKC-ζ/Rac1/Pak1/β-Catenin Signaling Cascade. *Biochimica Biophysica Acta (BBA) - Mol. Cell Res.* 1865, 650–664. doi:10.1016/j.bbamcr.2018.02.002

Ivan, M., Kondo, K., Yang, H., Kim, W., Valiando, J., Ohh, M., et al. (2001). HIFα Targeted for VHL-Mediated Destruction by Proline Hydroxylation: Implications for O 2 Sensing. *Science* 292, 464–468. doi:10.1126/science.1059817

Iwasa, H., Maimaiti, S., Kuroyanagi, H., Kawano, S., Inami, K., Timalsina, S., et al. (2013). Yes-associated Protein Homolog, YAP-1, Is Involved in the Thermotolerance and Aging in the Nematode *Caenorhabditis elegans*. *Exp. Cell Res.* 319, 931–945. doi:10.1016/j.yexcr.2013.01.020

Jaakkola, P., Mole, D. R., Tian, Y.-M., Wilson, M. I., Gielbert, J., Gaskell, S. J., et al. (2001). Targeting of HIF-α to the von Hippel-Lindau Ubiquitylation Complex by O 2 -Regulated Prolyl Hydroxylation. *Science* 292, 468–472. doi:10.1126/science.1059796

Jaalouk, D. E., and Lammerding, J. (2009). Mechanotransduction Gone Awry. *Nat. Rev. Mol. Cell Biol.* 10, 63–73. doi:10.1038/nrm2597

Jaccard, A., and Ho, P.-C. (2020). The Hidden Side of PD-L1. *Nat. Cell Biol.* 22, 1031–1032. doi:10.1038/s41556-020-0568-y

James, M. F., Beauchamp, R. L., Manchanda, N., Kazlauskas, A., and Ramesh, V. (2004). A NHERF Binding Site Links the βPDGFR to the Cytoskeleton and Regulates Cell Spreading and Migration. *J. Cell Sci.* 117, 2951–2961. doi:10.1242/jcs.01156

Janghorban, M., Xin, L., Rosen, J. M., and Zhang, X. H.-F. (2018). Notch Signaling as a Regulator of the Tumor Immune Response: To Target or Not to Target? *Front. Immunol.* 9, 1649. doi:10.3389/fimmu.2018.01649

Janse Van Rensburg, H. J., Azad, T., Ling, M., Hao, Y., Snetsinger, B., Khanal, P., et al. (2018). The Hippo Pathway Component TAZ Promotes Immune Evasion in Human Cancer through PD-L1. *Cancer Res.* 78, 1457–1470. doi:10.1158/0008-5472.can-17-3139

Javadov, S. (2015). The Calcium-ROS-pH Triangle and Mitochondrial Permeability Transition: Challenges to Mimic Cardiac Ischemia-Reperfusion. *Front. Physiol.* 6, 83. doi:10.3389/fphys.2015.00083

Ji, F., Wang, Y., Qiu, L., Li, S., Zhu, J., Liang, Z., et al. (2013). Hypoxia Inducible Factor 1α-Mediated LOX Expression Correlates with Migration and Invasion in Epithelial Ovarian Cancer. *Int. J. Oncol.* 42, 1578–1588. doi:10.3892/ijo.2013.1878

Jiang, F., Liu, G.-S., Dusting, G. J., and Chan, E. C. (2014). NADPH Oxidase-dependent Redox Signaling in TGF-β-Mediated Fibrotic Responses. *Redox Biol.* 2, 267–272. doi:10.1016/j.redox.2014.01.012

Jiang, W., and Xu, J. (2020). Immune Modulation by Mesenchymal Stem Cells. *Cell Prolif.* 53, e12712. doi:10.1111/cpr.12712

Jin, H., Sperka, T., Herrlich, P., and Morrison, H. (2006). Tumorigenic Transformation by CPI-17 through Inhibition of a Merlin Phosphatase. *Nature* 442, 576–579. doi:10.1038/nature04856

Jin, Y., Dong, L., Lu, Y., Wu, W., Hao, Q., Zhou, Z., et al. (2012). Dimerization and Cytoplasmic Localization Regulate Hippo Kinase Signaling Activity in Organ Size Control. *J. Biol. Chem.* 287, 5784–5796. doi:10.1074/jbc.m111.310334

Johnson, R., and Halder, G. (2014). The Two Faces of Hippo: Targeting the Hippo Pathway for Regenerative Medicine and Cancer Treatment. *Nat. Rev. Drug Discov.* 13, 63–79. doi:10.1038/nrd4161

Joo, E. E., and Yamada, K. M. (2014). MYPT1 Regulates Contractility and Microtubule Acetylation to Modulate Integrin Adhesions and Matrix Assembly. *Nat. Commun.* 5, 3510. doi:10.1038/ncomms4510

Juan, C. A., Pérez de la Lastra, J. M., Plou, F. J., and Pérez-Lebeña, E. (2021). The Chemistry of Reactive Oxygen Species (ROS) Revisited: Outlining Their Role in Biological Macromolecules (DNA, Lipids and Proteins) and Induced Pathologies. *Int. J. Mol. Sci.* 22. doi:10.3390/ijms22094642

Kanai, F., Liu, H., Field, S. J., Akbary, H., Matsuo, T., Brown, G. E., et al. (2001). The PX Domains of P47phox and P40phox Bind to Lipid Products of PI(3)K. *Nat. Cell Biol.* 3, 675–678. doi:10.1038/35083070

Kang, X., Wei, X., Jiang, L., Niu, C., Zhang, J., Chen, S., et al. (2016). Nox2 and Nox4 Regulate Self-Renewal of Murine Induced-Pluripotent Stem Cells. *IUBMB Life* 68, 963–970. doi:10.1002/iub.1574

Kaplan, N., Urao, N., Furuta, E., Kim, S.-J., Razvi, M., Nakamura, Y., et al. (2011). Localized Cysteine Sulfenic Acid Formation by Vascular Endothelial Growth Factor: Role in Endothelial Cell Migration and Angiogenesis. *Free Radic. Res.* 45, 1124–1135. doi:10.3109/10715762.2011.602073

Kawahara, T., Quinn, M. T., and Lambeth, J. D. (2007). Molecular Evolution of the Reactive Oxygen-Generating NADPH Oxidase (Nox/Duox) Family of Enzymes. *BMC Evol. Biol.* 7, 109. doi:10.1186/1471-2148-7-109

Kawano, Y., Fukata, Y., Oshiro, N., Amano, M., Nakamura, T., Ito, M., et al. (1999). Phosphorylation of Myosin-Binding Subunit (MBS) of Myosin Phosphatase by Rho-Kinase In Vivo. *J. Cell Biol.* 147, 1023–1038. doi:10.1083/jcb.147.5.1023

Keith, B., and Simon, M. C. (2007). Hypoxia-inducible Factors, Stem Cells, and Cancer. *Cell* 129, 465–472. doi:10.1016/j.cell.2007.04.019

Kerr, J. P., Robison, P., Shi, G., Bogush, A. I., Kempema, A. M., Hexum, J. K., et al. (2015). Detyrosinated Microtubules Modulate Mechanotransduction in Heart and Skeletal Muscle. *Nat. Commun.* 6, 8526. doi:10.1038/ncomms9526

Kessler, M., Hoffmann, K., Brinkmann, V., Thieck, O., Jackisch, S., Toelle, B., et al. (2015). The Notch and Wnt Pathways Regulate Stemness and Differentiation in Human Fallopian Tube Organoids. *Nat. Commun.* 6, 8989. doi:10.1038/ncomms9989

Khairallah, R. J., Shi, G., Sbrana, F., Prosser, B. L., Borroto, C., Mazaitis, M. J., et al. (2012). Microtubules Underlie Dysfunction in Duchenne Muscular Dystrophy. *Sci. Signal* 5, ra56. doi:10.1126/scisignal.2002829

Khurana, A., Nakayama, K., Williams, S., Davis, R. J., Mustelin, T., and Ronai, Z. e. (2006). Regulation of the Ring Finger E3 Ligase Siah2 by P38 MAPK. *J. Biol. Chem.* 281, 35316–35326. doi:10.1074/jbc.m606568200

Kim, E., Kim, W., Lee, S., Chun, J., Kang, J., Park, G., et al. (2017). TRAF4 Promotes Lung Cancer Aggressiveness by Modulating Tumor Microenvironment in Normal Fibroblasts. *Sci. Rep.* 7, 8923. doi:10.1038/s41598-017-09447-z

Kim, E. Y., Anderson, M., and Dryer, S. E. (2012). Insulin Increases Surface Expression of TRPC6 Channels in Podocytes: Role of NADPH Oxidases and Reactive Oxygen Species. *Am. J. Physiology-Renal Physiology* 302, F298–F307. doi:10.1152/ajprenal.00423.2011

Kim, G. S., Jung, J. E., Niizuma, K., and Chan, P. H. (2009). CK2 Is a Novel Negative Regulator of NADPH Oxidase and a Neuroprotectant in Mice after Cerebral Ischemia. *J. Neurosci.* 29, 14779–14789. doi:10.1523/jneurosci.4161-09.2009

Kim, J.-S., Diebold, B. A., Babior, B. M., Knaus, U. G., and Bokoch, G. M. (2007). Regulation of Nox1 Activity via Protein Kinase A-Mediated Phosphorylation of NoxA1 and 14-3-3 Binding. *J. Biol. Chem.* 282, 34787–34800. doi:10.1074/jbc.m704754200

Kim, M.-K., Jang, J.-W., and Bae, S.-C. (2018b). DNA Binding Partners of YAP/TAZ. *BMB Rep.* 51, 126–133. doi:10.5483/bmbrep.2018.51.3.015

Kim, M. H., Kim, C. G., Kim, S.-K., Shin, S. J., Choe, E. A., Park, S.-H., et al. (2018a). YAP-induced PD-L1 Expression Drives Immune Evasion in BRAFi-

Resistant Melanoma. *Cancer Immunol. Res.* 6, 255–266. doi:10.1158/2326-6066.cir-17-0320

Kim, P. R., Zhang, S., Rahmat, M. B., and Koh, C.-G. (2020a). Partners in Crime: POPX2 Phosphatase and its Interacting Proteins in Cancer. *Cell Death Dis.* 11, 840. doi:10.1038/s41419-020-03061-0

Kim, S., Lee, M., and Choi, Y. K. (2020b). The Role of a Neurovascular Signaling Pathway Involving Hypoxia-Inducible Factor and Notch in the Function of the Central Nervous System. *Biomol. Ther.* 28, 45–57. doi:10.4062/biomolther.2019.119

Kim, W., Youn, H., Kang, C., and Youn, B. (2015). Inflammation-induced Radioresistance Is Mediated by ROS-dependent Inactivation of Protein Phosphatase 1 in Non-small Cell Lung Cancer Cells. *Apoptosis* 20, 1242–1252. doi:10.1007/s10495-015-1141-1

Kiss, A., Erdődi, F., and Lontay, B. (2019). Myosin Phosphatase: Unexpected Functions of a Long-Known Enzyme. *Biochimica Biophysica Acta (BBA) - Mol. Cell Res.* 1866, 2–15. doi:10.1016/j.bbamcr.2018.07.023

Kitamura, H., Ohno, Y., Toyoshima, Y., Ohtake, J., Homma, S., Kawamura, H., et al. (2017). Interleukin-6/STAT3 Signaling as a Promising Target to Improve the Efficacy of Cancer Immunotherapy. *Cancer Sci.* 108, 1947–1952. doi:10.1111/cas.13332

Kobayashi, Y., Oguro, A., and Imaoka, S. (2021). Feedback of Hypoxia-Inducible Factor-1alpha (HIF-1alpha) Transcriptional Activity via Redox Factor-1 (Ref-1) Induction by Reactive Oxygen Species (ROS). *Free Radic. Res.* 55, 154–164. doi:10.1080/10715762.2020.1870685

Kodama, R., Kato, M., Furuta, S., Ueno, S., Zhang, Y., Matsuno, K., et al. (2013). ROS-generating Oxidases Nox1 and Nox4 Contribute to Oncogenic Ras-Induced Premature Senescence. *Genes cells.* 18, 32–41. doi:10.1111/gtc.12015

Kodama, Y., Hijikata, M., Kageyama, R., Shimotohno, K., and Chiba, T. (2004). The Role of Notch Signaling in the Development of Intrahepatic Bile Ducts. *Gastroenterology* 127, 1775–1786. doi:10.1053/j.gastro.2004.09.004

Kohchi, C., Inagawa, H., Nishizawa, T., and Soma, G. (2009). ROS and Innate Immunity. *Anticancer Res.* 29, 817–821.

Koivunen, P., Hirsilä, M., Günzler, V., Kivirikko, K. I., and Myllyharju, J. (2004). Catalytic Properties of the Asparaginyl Hydroxylase (FIH) in the Oxygen Sensing Pathway Are Distinct from Those of its Prolyl 4-hydroxylases. *J. Biol. Chem.* 279, 9899–9904. doi:10.1074/jbc.m312254200

Kono, K., Saeki, Y., Yoshida, S., Tanaka, K., and Pellman, D. (2012). Proteasomal Degradation Resolves Competition between Cell Polarization and Cellular Wound Healing. *Cell* 150, 151–164. doi:10.1016/j.cell.2012.05.030

Kopan, R., and Ilagan, M. X. G. (2009). The Canonical Notch Signaling Pathway: Unfolding the Activation Mechanism. *Cell* 137, 216–233. doi:10.1016/j.cell.2009.03.045

Koudelková, L., Brábek, J., and Rosel, D. (2021). Src Kinase: Key Effector in Mechanosignalling. *Int. J. Biochem. Cell Biol.* 131, 105908. doi:10.1016/j.biocel.2020.105908

Koundouros, N., and Poulogiannis, G. (2018). Phosphoinositide 3-Kinase/Akt Signaling and Redox Metabolism in Cancer. *Front. Oncol.* 8, 160. doi:10.3389/fonc.2018.00160

Kovall, R. A., Gebelein, B., Sprinzak, D., and Kopan, R. (2017). The Canonical Notch Signaling Pathway: Structural and Biochemical Insights into Shape, Sugar, and Force. *Dev. Cell* 41, 228–241. doi:10.1016/j.devcel.2017.04.001

Kracke, F., Vassilev, I., and KrÃ¶mer, J. O. (2015). Microbial Electron Transport and Energy Conservation Â€" the Foundation for Optimizing Bioelectrochemical Systems. *Front. Microbiol.* 6, 575. doi:10.3389/fmicb.2015.00575

Kremerskothen, J., Plaas, C., Büther, K., Finger, I., Veltel, S., Matanis, T., et al. (2003). Characterization of KIBRA, a Novel WW Domain-Containing Protein. *Biochem. Biophysical Res. Commun.* 300, 862–867. doi:10.1016/s0006-291x(02)02945-5

Krock, B. L., Skuli, N., and Simon, M. C. (2011). Hypoxia-induced Angiogenesis: Good and Evil. *Genes & Cancer* 2, 1117–1133. doi:10.1177/1947601911423654

Kroviarski, Y., Debbabi, M., Bachoual, R., Pe´rianin, A., Gougerot-Pocidalo, M. A., El-Benna, J., et al. (2010). Phosphorylation of NADPH Oxidase Activator 1 (NOXA1) on Serine 282 by MAP Kinases and on Serine 172 by Protein Kinase C and Protein Kinase A Prevents NOX1 Hyperactivation. *FASEB J.* 24, 2077–2092. doi:10.1096/fj.09-147629

Kulik, A. A., Maruszczak, K. K., Thomas, D. C., Nabi-Aldridge, N. L. A., Carr, M., Bingham, R. J., et al. (2021). Crystal Structure and Molecular Dynamics of Human POLDIP2 , a Multifaceted Adaptor Protein in Metabolism and Genome Stability. *Protein Sci.* 30, 1196–1209. doi:10.1002/pro.4085

Kulisz, A., Chen, N., Chandel, N. S., Shao, Z., and Schumacker, P. T. (2002). Mitochondrial ROS Initiate Phosphorylation of P38 MAP Kinase during Hypoxia in Cardiomyocytes. *Am. J. Physiology-Lung Cell. Mol. Physiology* 282, L1324–L1329. doi:10.1152/ajplung.00326.2001

Kunnumakkara, A. B., Sailo, B. L., Banik, K., Harsha, C., Prasad, S., Gupta, S. C., et al. (2018). Chronic Diseases, Inflammation, and Spices: How Are They Linked? *J. Transl. Med.* 16, 14. doi:10.1186/s12967-018-1381-2

Lai, D., Ho, K. C., Hao, Y., and Yang, X. (2011). Taxol Resistance in Breast Cancer Cells Is Mediated by the Hippo Pathway Component TAZ and its Downstream Transcriptional Targets Cyr61 and CTGF. *Cancer Res.* 71, 2728–2738. doi:10.1158/0008-5472.can-10-2711

Lamari, F., Braut-Boucher, F., Pongnimitprasert, N., Bernard, M., Foglietti, M.-J., Derappe, C., et al. (2007). Cell Adhesion and Integrin Expression Are Modulated by Oxidative Stress in EA.Hy 926 Cells. *Free Radic. Res.* 41, 812–822. doi:10.1080/10715760701390027

Lando, D., Peet, D. J., Gorman, J. J., Whelan, D. A., Whitelaw, M. L., and Bruick, R. K. (2002). FIH-1 Is an Asparaginyl Hydroxylase Enzyme that Regulates the Transcriptional Activity of Hypoxia-Inducible Factor. *Genes Dev.* 16, 1466–1471. doi:10.1101/gad.991402

Lasky, J. L., and Wu, H. (2005). Notch Signaling, Brain Development, and Human Disease. *Pediatr. Res.* 57, 104R–109R. doi:10.1203/01.pdr.0000159632.70510.3d

Laulajainen, M., Muranen, T., Carpén, O., and Grönholm, M. (2008). Protein Kinase A-Mediated Phosphorylation of the NF2 Tumor Suppressor Protein Merlin at Serine 10 Affects the Actin Cytoskeleton. *Oncogene* 27, 3233–3243. doi:10.1038/sj.onc.1210988

Laulajainen, M., Muranen, T., Nyman, T. A., Carpén, O., and Grönholm, M. (2011). Multistep Phosphorylation by Oncogenic Kinases Enhances the Degradation of the NF2 Tumor Suppressor Merlin. *Neoplasia* 13, 643–652. doi:10.1593/neo.11356

Lavado, A., He, Y., Paré, J., Neale, G., Olson, E. N., Giovannini, M., et al. (2013). Tumor Suppressor Nf2 Limits Expansion of the Neural Progenitor Pool by Inhibiting Yap/Taz Transcriptional Coactivators. *Development* 140, 3323–3334. doi:10.1242/dev.096537

Le Clainche, C., Schlaepfer, D., Ferrari, A., Klingauf, M., Grohmanova, K., Veligodskiy, A., et al. (2007). IQGAP1 Stimulates Actin Assembly through the N-WASP-Arp2/3 Pathway. *J. Biol. Chem.* 282, 426–435. doi:10.1074/jbc.m607711200

Lecuit, T., and Lenne, P.-F. (2007). Cell Surface Mechanics and the Control of Cell Shape, Tissue Patterns and Morphogenesis. *Nat. Rev. Mol. Cell Biol.* 8, 633–644. doi:10.1038/nrm2222

Lee, B. S., Park, D. I., Lee, D. H., Lee, J. E., Yeo, M.-k., Park, Y. H., et al. (2017). Hippo Effector YAP Directly Regulates the Expression of PD-L1 Transcripts in EGFR-TKI-Resistant Lung Adenocarcinoma. *Biochem. Biophysical Res. Commun.* 491, 493–499. doi:10.1016/j.bbrc.2017.07.007

Lee, G., Won, H.-S., Lee, Y.-M., Choi, J.-W., Oh, T.-I., Jang, J.-H., et al. (2016). Oxidative Dimerization of PHD2 Is Responsible for its Inactivation and Contributes to Metabolic Reprogramming via HIF-1α Activation. *Sci. Rep.* 6, 18928. doi:10.1038/srep18928

Lee, H. B., Yu, M. R., Song, J. S., and Ha, H. (2004a). Reactive Oxygen Species Amplify Protein Kinase C Signaling in High Glucose-Induced Fibronectin Expression by Human Peritoneal Mesothelial Cells. *Kidney Int.* 65, 1170–1179. doi:10.1111/j.1523-1755.2004.00491.x

Lee, H., Herrmann, A., Deng, J.-H., Kujawski, M., Niu, G., Li, Z., et al. (2009). Persistently Activated Stat3 Maintains Constitutive NF-Kb Activity in Tumors. *Cancer cell* 15, 283–293. doi:10.1016/j.ccr.2009.02.015

Lee, I.-T., Shih, R.-H., Lin, C.-C., Chen, J.-T., and Yang, C.-M. (2012). Role of TLR4/NADPH oxidase/ROS-Activated P38 MAPK in VCAM-1 Expression Induced by Lipopolysaccharide in Human Renal Mesangial Cells. *Cell Commun. Signal* 10, 33. doi:10.1186/1478-811x-10-33

Lee, J.-W., Bae, S.-H., Jeong, J.-W., Kim, S.-H., and Kim, K.-W. (2004b). Hypoxia-inducible Factor (HIF-1)α: its Protein Stability and Biological Functions. *Exp. Mol. Med.* 36, 1–12. doi:10.1038/emm.2004.1

Lee, Y. A., Noon, L. A., Akat, K. M., Ybanez, M. D., Lee, T.-F., Berres, M.-L., et al. (2018b). Autophagy Is a Gatekeeper of Hepatic Differentiation and Carcinogenesis by Controlling the Degradation of Yap. *Nat. Commun.* 9, 4962. doi:10.1038/s41467-018-07338-z

Lee, Y., Kim, N. H., Cho, E. S., Yang, J. H., Cha, Y. H., Kang, H. E., et al. (2018a). Dishevelled Has a YAP Nuclear Export Function in a Tumor Suppressor Context-dependent Manner. *Nat. Commun.* 9, 2301. doi:10.1038/s41467-018-04757-w

Lennicke, C., and Cochemé, H. M. (2021a). Redox Metabolism: ROS as Specific Molecular Regulators of Cell Signaling and Function. *Mol. Cell* 81, 3691–3707. doi:10.1016/j.molcel.2021.08.018

Lennicke, C., and Cochemé, H. M. (2021b). Redox Regulation of the Insulin Signalling Pathway. *Redox Biol.* 42, 101964. doi:10.1016/j.redox.2021.101964

Leung, C. Y., and Zernicka-Goetz, M. (2013). Angiomotin Prevents Pluripotent Lineage Differentiation in Mouse Embryos via Hippo Pathway-dependent and -independent Mechanisms. *Nat. Commun.* 4, 2251. doi:10.1038/ncomms3251

Levental, K. R., Yu, H., Kass, L., Lakins, J. N., Egeblad, M., Erler, J. T., et al. (2009). Matrix Crosslinking Forces Tumor Progression by Enhancing Integrin Signaling. *Cell* 139, 891–906. doi:10.1016/j.cell.2009.10.027

Lewis, B., and Aitken, R. J. (2001). A Redox-Regulated Tyrosine Phosphorylation Cascade in Rat Spermatozoa. *J. Androl.* 22, 611–622.

Li, H., Li, X., Jing, X., Li, M., Ren, Y., Chen, J., et al. (2018a). Hypoxia Promotes Maintenance of the Chondrogenic Phenotype in Rat Growth Plate Chondrocytes through the HIF-1α/YAP Signaling Pathway. *Int. J. Mol. Med.* 42, 3181–3192. doi:10.3892/ijmm.2018.3921

Li, J.-M., Fan, L. M., Christie, M. R., and Shah, A. M. (2005). Acute Tumor Necrosis Factor Alpha Signaling via NADPH Oxidase in Microvascular Endothelial Cells: Role of P47 Phox Phosphorylation and Binding to TRAF4. *Mol. Cell Biol.* 25, 2320–2330. doi:10.1128/mcb.25.6.2320-2330.2005

Li, P., Silvis, M. R., Honaker, Y., Lien, W.-H., Arron, S. T., and Vasioukhin, V. (2016). Αe-catenin Inhibits a Src-YAP1 Oncogenic Module that Couples Tyrosine Kinases and the Effector of Hippo Signaling Pathway. *Genes Dev.* 30, 798–811. doi:10.1101/gad.274951.115

Li, Y., Hibbs, M. A., Gard, A. L., Shylo, N. A., and Yun, K. (2012). Genome-wide Analysis of N1ICD/RBPJ Targets In Vivo Reveals Direct Transcriptional Regulation of Wnt, SHH, and Hippo Pathway Effectors by Notch1. *Stem Cells* 30, 741–752. doi:10.1002/stem.1030

Li, Y., Wu, L., Yu, M., Yang, F., Wu, B., Lu, S., et al. (2018b). HIF-1α Is Critical for the Activation of Notch Signaling in Neurogenesis during Acute Epilepsy. *Neuroscience* 394, 206–219. doi:10.1016/j.neuroscience.2018.10.037

Li, Y., Zhou, H., Li, F., Chan, S. W., Lin, Z., Wei, Z., et al. (2015). Angiomotin Binding-Induced Activation of Merlin/NF2 in the Hippo Pathway. *Cell Res.* 25, 801–817. doi:10.1038/cr.2015.69

Li, Z., Zhao, B., Wang, P., Chen, F., Dong, Z., Yang, H., et al. (2010). Structural Insights into the YAP and TEAD Complex. *Genes Dev.* 24, 235–240. doi:10.1101/gad.1865810

Lian, I., Kim, J., Okazawa, H., Zhao, J., Zhao, B., Yu, J., et al. (2010). The Role of YAP Transcription Coactivator in Regulating Stem Cell Self-Renewal and Differentiation. *Genes Dev.* 24, 1106–1118. doi:10.1101/gad.1903310

Lim, J., Pahlke, G., and Conti, M. (1999). Activation of the cAMP-specific Phosphodiesterase PDE4D3 by Phosphorylation. *J. Biol. Chem.* 274, 19677–19685. doi:10.1074/jbc.274.28.19677

Lim, S.-O., Gu, J.-M., Kim, M. S., Kim, H.-S., Park, Y. N., Park, C. K., et al. (2008). Epigenetic Changes Induced by Reactive Oxygen Species in Hepatocellular Carcinoma: Methylation of the E-Cadherin Promoter. *Gastroenterology* 135, 2128–2140. doi:10.1053/j.gastro.2008.07.027

Lim, S., Hermance, N., Mudianto, T., Mustaly, H. M., Mauricio, I. P. M., Vittoria, M. A., et al. (2019). Identification of the Kinase STK25 as an Upstream Activator of LATS Signaling. *Nat. Commun.* 10, 1547. doi:10.1038/s41467-019-09597-w

Limbu, S., Hoang-Trong, T. M., Prosser, B. L., Lederer, W. J., and Jafri, M. S. (2015). Modeling Local X-ROS and Calcium Signaling in the Heart. *Biophysical J.* 109, 2037–2050. doi:10.1016/j.bpj.2015.09.031

Lin, Z., Xie, R., Guan, K., and Zhang, M. (2020). A WW Tandem-Mediated Dimerization Mode of SAV1 Essential for Hippo Signaling. *Cell Rep.* 32, 108118. doi:10.1016/j.celrep.2020.108118

Liu, C.-Y., Zha, Z.-Y., Zhou, X., Zhang, H., Huang, W., Zhao, D., et al. (2010). The Hippo Tumor Pathway Promotes TAZ Degradation by Phosphorylating a Phosphodegron and Recruiting the SCFβ-TrCP E3 Ligase. *J. Biol. Chem.* 285, 37159–37169. doi:10.1074/jbc.m110.152942

Liu, F., Lagares, D., Choi, K. M., Stopfer, L., Marinković, A., Vrbanac, V., et al. (2015). Mechanosignaling through YAP and TAZ Drives Fibroblast Activation and Fibrosis. *Am. J. Physiology-Lung Cell. Mol. Physiology* 308, L344–L357. doi:10.1152/ajplung.00300.2014

Liu, J., Guidry, J. J., and Worthylake, D. K. (2014). Conserved Sequence Repeats of IQGAP1 Mediate Binding to Ezrin. *J. Proteome Res.* 13, 1156–1166. doi:10.1021/pr400787p

Liu, J., Quan, J., Feng, J., Zhang, Q., Xu, Y., Liu, J., et al. (2016a). High Glucose Regulates LN Expression in Human Liver Sinusoidal Endothelial Cells through ROS/integrin αvβ3 Pathway. *Environ. Toxicol. Pharmacol.* 42, 231–236. doi:10.1016/j.etap.2016.01.021

Liu, L., Tao, T., Liu, S., Yang, X., Chen, X., Liang, J., et al. (2021a). An RFC4/Notch1 Signaling Feedback Loop Promotes NSCLC Metastasis and Stemness. *Nat. Commun.* 12, 2693. doi:10.1038/s41467-021-22971-x

Liu, Q., Luo, Q., Ju, Y., and Song, G. (2020a). Role of the Mechanical Microenvironment in Cancer Development and Progression. *Cancer Biol. Med.* 17, 282–292. doi:10.20892/j.issn.2095-3941.2019.0437

Liu, Q. P., Luo, Q., Deng, B., Ju, Y., and Song, G. B. (2020b). Stiffer Matrix Accelerates Migration of Hepatocellular Carcinoma Cells through Enhanced Aerobic Glycolysis via the MAPK-YAP Signaling. *Cancers (Basel)* 12. doi:10.3390/cancers12020490

Liu, W. J., Huang, Y. X., Wang, W., Zhang, Y., Liu, B. J., Qiu, J. G., et al. (2021b). NOX4 Signaling Mediates Cancer Development and Therapeutic Resistance through HER3 in Ovarian Cancer Cells. *Cells* 10. doi:10.3390/cells10071647

Liu, X., Long, X., Gao, Y., Liu, W., Hayashi, T., Mizuno, K., et al. (2020c). Type I Collagen Inhibits Adipogenic Differentiation via YAP Activation In Vitro. *J. Cell. Physiology* 235, 1821–1837. doi:10.1002/jcp.29100

Liu, X., Yang, N., Figel, S. A., Wilson, K. E., Morrison, C. D., Gelman, I. H., et al. (2013). PTPN14 Interacts with and Negatively Regulates the Oncogenic Function of YAP. *Oncogene* 32, 1266–1273. doi:10.1038/onc.2012.147

Liu, Y., Jiang, B.-J., Zhao, R.-Z., and Ji, H.-L. (2016b). Epithelial Sodium Channels in Pulmonary Epithelial Progenitor and Stem Cells. *Int. J. Biol. Sci.* 12, 1150–1154. doi:10.7150/ijbs.15747

Liu, Z.-J., Tan, Y., Beecham, G. W., Seo, D. M., Tian, R., Li, Y., et al. (2012). Notch Activation Induces Endothelial Cell Senescence and Pro-inflammatory Response: Implication of Notch Signaling in Atherosclerosis. *Atherosclerosis* 225, 296–303. doi:10.1016/j.atherosclerosis.2012.04.010

Loehr, J. A., Wang, S., Cully, T. R., Pal, R., Larina, I. V., Larin, K. V., et al. (2018). NADPH Oxidase Mediates Microtubule Alterations and Diaphragm Dysfunction in Dystrophic Mice. *Elife* 7. doi:10.7554/eLife.31732

Loerakker, S., Stassen, O. M. J. A., Ter Huurne, F. M., Boareto, M., Bouten, C. V. C., and Sahlgren, C. M. (2018). Mechanosensitivity of Jagged-Notch Signaling Can Induce a Switch-type Behavior in Vascular Homeostasis. *Proc. Natl. Acad. Sci. U. S. A.* 115, E3682–E3691. doi:10.1073/pnas.1715277115

Lopes, L. R., Dagher, M.-C., Gutierrez, A., Young, B., Bouin, A.-P., Fuchs, A., et al. (2004). Phosphorylated p40PHOX as a Negative Regulator of NADPH Oxidase. *Biochemistry* 43, 3723–3730. doi:10.1021/bi035636s

Low, I. C. C., Loh, T., Huang, Y., Virshup, D. M., and Pervaiz, S. (2014). Ser70 Phosphorylation of Bcl-2 by Selective Tyrosine Nitration of PP2A-B56δ Stabilizes its Antiapoptotic Activity. *Blood* 124, 2223–2234. doi:10.1182/blood-2014-03-563296

Lu, P.-J., Zhou, X. Z., Shen, M., and Lu, K. P. (1999). Function of WW Domains as Phosphoserine- or Phosphothreonine-Binding Modules. *Science* 283, 1325–1328. doi:10.1126/science.283.5406.1325

Lv, Y., Chen, C., Zhao, B., and Zhang, X. (2017). Regulation of Matrix Stiffness on the Epithelial-Mesenchymal Transition of Breast Cancer Cells under Hypoxia Environment. *Sci. Nat.* 104, 38. doi:10.1007/s00114-017-1461-9

Lyle, A. N., Deshpande, N. N., Taniyama, Y., Seidel-Rogol, B., Pounkova, L., Du, P., et al. (2009). Poldip2, a Novel Regulator of Nox4 and Cytoskeletal Integrity in Vascular Smooth Muscle Cells. *Circulation Res.* 105, 249–259. doi:10.1161/circresaha.109.193722

Ma, B., Cheng, H., Gao, R., Mu, C., Chen, L., Wu, S., et al. (2016). Zyxin-Siah2-Lats2 axis Mediates Cooperation between Hippo and TGF-β Signalling Pathways. *Nat. Commun.* 7, 11123. doi:10.1038/ncomms11123

Ma, B., Chen, Y., Chen, L., Cheng, H., Mu, C., Li, J., et al. (2015). Hypoxia Regulates Hippo Signalling through the SIAH2 Ubiquitin E3 Ligase. *Nat. Cell Biol.* 17, 95–103. doi:10.1038/ncb3073

Ma, S., Meng, Z., Chen, R., and Guan, K.-L. (2019). The Hippo Pathway: Biology and Pathophysiology. *Annu. Rev. Biochem.* 88, 577–604. doi:10.1146/annurev-biochem-013118-111829

Ma, T., and Liu, Z. (2013). Functions of Aquaporin 1 and α-epithelial Na+ Channel in Rat Acute Lung Injury Induced by Acute Ischemic Kidney Injury. *Int. Urol. Nephrol.* 45, 1187–1196. doi:10.1007/s11255-012-0355-1

Ma, X., Zhang, H., Xue, X., and Shah, Y. M. (2017). Hypoxia-inducible Factor 2α (HIF-2α) Promotes Colon Cancer Growth by Potentiating Yes-Associated Protein 1 (YAP1) Activity. *J. Biol. Chem.* 292, 17046–17056. doi:10.1074/jbc.m117.805655

Macias, M. J., Hyvönen, M., Baraldi, E., Schultz, J., Sudol, M., Saraste, M., et al. (1996). Structure of the WW Domain of a Kinase-Associated Protein Complexed with a Proline-Rich Peptide. *Nature* 382, 646–649. doi:10.1038/382646a0

Mack, J. J., Mosqueiro, T. S., Archer, B. J., Jones, W. M., Sunshine, H., Faas, G. C., et al. (2017). NOTCH1 Is a Mechanosensor in Adult Arteries. *Nat. Commun.* 8, 1620. doi:10.1038/s41467-017-01741-8

Mackay, C. E., Shaifta, Y., Snetkov, V. V., Francois, A. A., Ward, J. P. T., and Knock, G. A. (2017). ROS-dependent Activation of RhoA/Rho-Kinase in Pulmonary Artery: Role of Src-Family Kinases and ARHGEF1. *Free Radic. Biol. Med.* 110, 316–331. doi:10.1016/j.freeradbiomed.2017.06.022

Maile, L. A., Badley-Clarke, J., and Clemmons, D. R. (2003). The Association between Integrin-Associated Protein and SHPS-1 Regulates Insulin-like Growth Factor-I Receptor Signaling in Vascular Smooth Muscle Cells. *MBoC* 14, 3519–3528. doi:10.1091/mbc.e03-04-0239

Maile, L. A., Capps, B. E., Miller, E. C., Aday, A. W., and Clemmons, D. R. (2008). Integrin-associated Protein Association with SRC Homology 2 Domain Containing Tyrosine Phosphatase Substrate 1 Regulates Igf-I Signaling In Vivo. *Diabetes* 57, 2637–2643. doi:10.2337/db08-0326

Majmundar, A. J., Wong, W. J., and Simon, M. C. (2010). Hypoxia-inducible Factors and the Response to Hypoxic Stress. *Mol. Cell* 40, 294–309. doi:10.1016/j.molcel.2010.09.022

Malarkannan, S., Awasthi, A., Rajasekaran, K., Kumar, P., Schuldt, K. M., Bartoszek, A., et al. (2012). IQGAP1: a Regulator of Intracellular Spacetime Relativity. *J. I.* 188, 2057–2063. doi:10.4049/jimmunol.1102439

Mammoto, A., and Ingber, D. E. (2009). Cytoskeletal Control of Growth and Cell Fate Switching. *Curr. Opin. Cell Biol.* 21, 864–870. doi:10.1016/j.ceb.2009.08.001

Mammoto, T., Mammoto, A., Torisawa, Y.-s., Tat, T., Gibbs, A., Derda, R., et al. (2011). Mechanochemical Control of Mesenchymal Condensation and Embryonic Tooth Organ Formation. *Dev. Cell* 21, 758–769. doi:10.1016/j.devcel.2011.07.006

Mana-Capelli, S., and Mccollum, D. (2018). Angiomotins Stimulate LATS Kinase Autophosphorylation and Act as Scaffolds that Promote Hippo Signaling. *J. Biol. Chem.* 293, 18230–18241. doi:10.1074/jbc.ra118.004187

Mana-Capelli, S., Paramasivam, M., Dutta, S., and Mccollum, D. (2014). Angiomotins Link F-Actin Architecture to Hippo Pathway Signaling. *MBoC* 25, 1676–1685. doi:10.1091/mbc.e13-11-0701

Manderfield, L. J., Aghajanian, H., Engleka, K. A., Lim, L. Y., Liu, F., Jain, R., et al. (2015). Hippo Signaling Is Required for Notch-dependent Smooth Muscle Differentiation of Neural Crest. *Development* 142, 2962–2971. doi:10.1242/dev.125807

Manderfield, L. J., High, F. A., Engleka, K. A., Liu, F., Li, L., Rentschler, S., et al. (2012). Notch Activation of Jagged1 Contributes to the Assembly of the Arterial Wall. *Circulation* 125, 314–323. doi:10.1161/circulationaha.111.047159

Mansour, F. A., Al-Mazrou, A., Al-Mohanna, F., Al-Alwan, M., and Ghebeh, H. (2020). PD-L1 Is Overexpressed on Breast Cancer Stem Cells through notch3/mTOR axis. *Oncoimmunology* 9, 1729299. doi:10.1080/2162402x.2020.1729299

Marazita, M. C., Dugour, A., Marquioni-Ramella, M. D., Figueroa, J. M., and Suburo, A. M. (2016). Oxidative Stress-Induced Premature Senescence Dysregulates VEGF and CFH Expression in Retinal Pigment Epithelial Cells: Implications for Age-Related Macular Degeneration. *Redox Biol.* 7, 78–87. doi:10.1016/j.redox.2015.11.011

Marklund, S. (1976). Spectrophotometric Study of Spontaneous Disproportionation of Superoxide Anion Radical and Sensitive Direct Assay for Superoxide Dismutase. *J. Biol. Chem.* 251, 7504–7507. doi:10.1016/s0021-9258(17)32878-8

Martyn, K. D., Kim, M.-J., Quinn, M. T., Dinauer, M. C., and Knaus, U. G. (2005). p21-activated Kinase (Pak) Regulates NADPH Oxidase Activation in Human Neutrophils. *Blood* 106, 3962–3969. doi:10.1182/blood-2005-03-0859

Marxsen, J. H., Stengel, P., Doege, K., Heikkinen, P., Jokilehto, T., Wagner, T., et al. (2004). Hypoxia-inducible Factor-1 (HIF-1) Promotes its Degradation by Induction of HIF-α-Prolyl-4-Hydroxylases. *Biochem. J.* 381, 761–767. doi:10.1042/bj20040620

Masoud, G. N., and Li, W. (2015). HIF-1α Pathway: Role, Regulation and Intervention for Cancer Therapy. *Acta Pharm. Sin. B* 5, 378–389. doi:10.1016/j.apsb.2015.05.007

Masson, N., and Ratcliffe, P. J. (2014). Hypoxia Signaling Pathways in Cancer Metabolism: the Importance of Co-selecting Interconnected Physiological Pathways. *Cancer Metab.* 2, 3. doi:10.1186/2049-3002-2-3

Matsuno, Y., Coelho, A. L., Jarai, G., Westwick, J., and Hogaboam, C. M. (2012). Notch Signaling Mediates TGF-B1-Induced Epithelial-Mesenchymal Transition through the Induction of Snai1. *Int. J. Biochem. Cell Biol.* 44, 776–789. doi:10.1016/j.biocel.2012.01.021

Maxwell, P. H., Wiesener, M. S., Chang, G.-W., Clifford, S. C., Vaux, E. C., Cockman, M. E., et al. (1999). The Tumour Suppressor Protein VHL Targets Hypoxia-Inducible Factors for Oxygen-dependent Proteolysis. *Nature* 399, 271–275. doi:10.1038/20459

Maydan, M., Mcdonald, P. C., Sanghera, J., Yan, J., Rallis, C., Pinchin, S., et al. (2010). Integrin-Linked Kinase Is a Functional Mn2+-dependent Protein Kinase that Regulates Glycogen Synthase Kinase-3β (GSK-3β) Phosphorylation. *PloS one* 5, e12356. doi:10.1371/journal.pone.0012356

Mazumdar, J., Dondeti, V., and Simon, M. C. (2009). Hypoxia-inducible Factors in Stem Cells and Cancer. *J. Cell Mol. Med.* 13, 4319–4328. doi:10.1111/j.1582-4934.2009.00963.x

Mcclatchey, A. I. (2003). Merlin and ERM Proteins: Unappreciated Roles in Cancer Development? *Nat. Rev. Cancer* 3, 877–883. doi:10.1038/nrc1213

Meng, D., Lv, D.-D., and Fang, J. (2008). Insulin-like Growth Factor-I Induces Reactive Oxygen Species Production and Cell Migration through Nox4 and Rac1 in Vascular Smooth Muscle Cells. *Cardiovasc. Res.* 80, 299–308. doi:10.1093/cvr/cvn173

Meng, Z., Moroishi, T., and Guan, K.-L. (2016). Mechanisms of Hippo Pathway Regulation. *Genes Dev.* 30, 1–17. doi:10.1101/gad.274027.115

Meng, Z., Moroishi, T., Mottier-Pavie, V., Plouffe, S. W., Hansen, C. G., Hong, A. W., et al. (2015). MAP4K Family Kinases Act in Parallel to MST1/2 to Activate LATS1/2 in the Hippo Pathway. *Nat. Commun.* 6, 8357. doi:10.1038/ncomms9357

Miao, J., Hsu, P.-C., Yang, Y.-L., Xu, Z., Dai, Y., Wang, Y., et al. (2017). YAP Regulates PD-L1 Expression in Human NSCLC Cells. *Oncotarget* 8, 114576–114587. doi:10.18632/oncotarget.23051

Mo, J.-S., Meng, Z., Kim, Y. C., Park, H. W., Hansen, C. G., Kim, S., et al. (2015). Cellular Energy Stress Induces AMPK-Mediated Regulation of YAP and the Hippo Pathway. *Nat. Cell Biol.* 17, 500–510. doi:10.1038/ncb3111

Mo, J. S., Park, H. W., and Guan, K. L. (2014). The Hippo Signaling Pathway in Stem Cell Biology and Cancer. *EMBO Rep.* 15, 642–656. doi:10.15252/embr.201438638

Moeller, B. J., Cao, Y., Li, C. Y., and Dewhirst, M. W. (2004). Radiation Activates HIF-1 to Regulate Vascular Radiosensitivity in Tumors. *Cancer cell* 5, 429–441. doi:10.1016/s1535-6108(04)00115-1

Moi, P., Chan, K., Asunis, I., Cao, A., and Kan, Y. W. (1994). Isolation of NF-E2-Related Factor 2 (Nrf2), a NF-E2-like Basic Leucine Zipper Transcriptional Activator that Binds to the Tandem NF-E2/ap1 Repeat of the Beta-Globin Locus Control Region. *Proc. Natl. Acad. Sci. U.S.A.* 91, 9926–9930. doi:10.1073/pnas.91.21.9926

Moleirinho, S., Hoxha, S., Mandati, V., Curtale, G., Troutman, S., Ehmer, U., et al. (2017). Regulation of Localization and Function of the Transcriptional Co-activator YAP by Angiomotin. *Elife* 6. doi:10.7554/eLife.23966

Moon, S., Kim, W., Kim, S., Kim, Y., Song, Y., Bilousov, O., et al. (2017). Phosphorylation by NLK Inhibits YAP -14-3-3-interactions and Induces its Nuclear Localization. *EMBO Rep.* 18, 61–71. doi:10.15252/embr.201642683

Morel, F., Rousset, F., Vu Chuong Nguyen, M., Trocme, C., Grange, L., and Lardy, B. (2015). La NADPH Oxydase Nox4, Une Cible Thérapeutique Potentielle Dans L'arthrose. *Bull. l'Académie Natl. Médecine* 199, 673–687. doi:10.1016/s0001-4079(19)30941-0

Moreno, C. S., Park, S., Nelson, K., Ashby, D., Hubalek, F., Lane, W. S., et al. (2000). WD40 Repeat Proteins Striatin and S/G2 Nuclear Autoantigen Are Members of a Novel Family of Calmodulin-Binding Proteins that Associate with Protein Phosphatase 2A. *J. Biol. Chem.* 275, 5257–5263. doi:10.1074/jbc.275.8.5257

Morrison, H., Sherman, L. S., Legg, J., Banine, F., Isacke, C., Haipek, C. A., et al. (2001). The NF2 Tumor Suppressor Gene Product, Merlin, Mediates Contact Inhibition of Growth through Interactions with CD44. *Genes Dev.* 15, 968–980. doi:10.1101/gad.189601

Muranen, T., Grönholm, M., Lampin, A., Lallemand, D., Zhao, F., Giovannini, M., et al. (2007). The Tumor Suppressor Merlin Interacts with Microtubules and Modulates Schwann Cell Microtubule Cytoskeleton. *Hum. Mol. Genet.* 16, 1742–1751. doi:10.1093/hmg/ddm122

Murphy, M. P. (2009). How Mitochondria Produce Reactive Oxygen Species. *Biochem. J.* 417, 1–13. doi:10.1042/bj20081386

Nagarkoti, S., Dubey, M., Awasthi, D., Kumar, V., Chandra, T., Kumar, S., et al. (2018). S-glutathionylation of P47phox Sustains Superoxide Generation in Activated Neutrophils. *Biochimica Biophysica Acta (BBA) - Mol. Cell Res.* 1865, 444–454. doi:10.1016/j.bbamcr.2017.11.014

Nakano, Y., Banfi, B., Jesaitis, A. J., Dinauer, M. C., Allen, L.-A. H., and Nauseef, W. M. (2007). Critical Roles for P22phox in the Structural Maturation and Subcellular Targeting of Nox3. *Biochem. J.* 403, 97–108. doi:10.1042/bj20060819

Nakayama, K., and Ronai, Z. e. (2004). Siah: New Players in the Cellular Response to Hypoxia. *Cell Cycle* 3, 1345–1347. doi:10.4161/cc.3.11.1207

Nelson, C. M., Vanduijn, M. M., Inman, J. L., Fletcher, D. A., and Bissell, M. J. (2006). Tissue Geometry Determines Sites of Mammary Branching Morphogenesis in Organotypic Cultures. *Science* 314, 298–300. doi:10.1126/science.1131000

Nguyen Dinh Cat, A., Montezano, A. C., Burger, D., and Touyz, R. M. (2013). Angiotensin II, NADPH Oxidase, and Redox Signaling in the Vasculature. *Antioxidants Redox Signal.* 19, 1110–1120. doi:10.1089/ars.2012.4641

Ni, L., Li, S., Yu, J., Min, J., Brautigam, C. A., Tomchick, D. R., et al. (2013). Structural Basis for Autoactivation of Human Mst2 Kinase and its Regulation by RASSF5. *Structure* 21, 1757–1768. doi:10.1016/j.str.2013.07.008

Ni, L., Zheng, Y., Hara, M., Pan, D., and Luo, X. (2015). Structural Basis for Mob1-dependent Activation of the Core Mst-Lats Kinase Cascade in Hippo Signaling. *Genes Dev.* 29, 1416–1431. doi:10.1101/gad.264929.115

Ning, W., Song, R., Li, C., Park, E., Mohsenin, A., Choi, A. M. K., et al. (2002). TGF-β1stimulates HO-1 via the P38 Mitogen-Activated Protein Kinase in A549 Pulmonary Epithelial Cells. *Am. J. Physiology-Lung Cell. Mol. Physiology* 283, L1094–L1102. doi:10.1152/ajplung.00151.2002

Nishioka, N., Inoue, K.-i., Adachi, K., Kiyonari, H., Ota, M., Ralston, A., et al. (2009). The Hippo Signaling Pathway Components Lats and Yap Pattern Tead4 Activity to Distinguish Mouse Trophectoderm from Inner Cell Mass. *Dev. Cell* 16, 398–410. doi:10.1016/j.devcel.2009.02.003

Noguchi, S., Saito, A., and Nagase, T. (2018). YAP/TAZ Signaling as a Molecular Link between Fibrosis and Cancer. *Int. J. Mol. Sci.* 19. doi:10.3390/ijms19113674

Noguchi, S., Saito, A., Mikami, Y., Urushiyama, H., Horie, M., Matsuzaki, H., et al. (2017). TAZ Contributes to Pulmonary Fibrosis by Activating Profibrotic Functions of Lung Fibroblasts. *Sci. Rep.* 7, 42595. doi:10.1038/srep42595

Noman, M. Z., Desantis, G., Janji, B., Hasmim, M., Karray, S., Dessen, P., et al. (2014). PD-L1 Is a Novel Direct Target of HIF-1α, and its Blockade under Hypoxia Enhanced MDSC-Mediated T Cell Activation. *J. Exp. Med.* 211, 781–790. doi:10.1084/jem.20131916

Novianti, T., Juniantito, V., Jusuf, A. A., Arida, E. A., Sadikin, M., and Jusman, S. W. A. (2020). High Expressions of the Cytoglobin and PGC-1α Genes during the Tissue Regeneration of House Gecko (Hemidactylus Platyurus) Tails. *BMC Dev. Biol.* 20, 11. doi:10.1186/s12861-020-00214-4

Obremski, V. J., Hall, A. M., and Fernandez-Valle, C. (1998). Merlin, the Neurofibromatosis Type 2 Gene Product, and ?1 Integrin Associate in Isolated and Differentiating Schwann Cells. *J. Neurobiol.* 37, 487–501. doi:10.1002/(sici)1097-4695(199812)37:4<487::aid-neu1>3.0.co;2-b

Ohnishi, S., Güntert, P., Koshiba, S., Tomizawa, T., Akasaka, R., Tochio, N., et al. (2007). Solution Structure of an Atypical WW Domain in a Novel β-clam-like Dimeric Form. *FEBS Lett.* 581, 462–468. doi:10.1016/j.febslet.2007.01.008

Oshima, K., Ruhul Amin, A. R. M., Suzuki, A., Hamaguchi, M., and Matsuda, S. (2002). SHPS-1, a Multifunctional Transmembrane Glycoprotein. *FEBS Lett.* 519, 1–7. doi:10.1016/s0014-5793(02)02703-5

Pan, D. (2010). The Hippo Signaling Pathway in Development and Cancer. *Dev. Cell* 19, 491–505. doi:10.1016/j.devcel.2010.09.011

Panciera, T., Azzolin, L., Cordenonsi, M., and Piccolo, S. (2017). Mechanobiology of YAP and TAZ in Physiology and Disease. *Nat. Rev. Mol. Cell Biol.* 18, 758–770. doi:10.1038/nrm.2017.87

Park, J., Kim, D.-H., Shah, S. R., Kim, H.-N., KshitizKim, P., Kim, P., et al. (2019). Switch-like Enhancement of Epithelial-Mesenchymal Transition by YAP through Feedback Regulation of WT1 and Rho-Family GTPases. *Nat. Commun.* 10, 2797. doi:10.1038/s41467-019-10729-5

Paszek, M. J., Zahir, N., Johnson, K. R., Lakins, J. N., Rozenberg, G. I., Gefen, A., et al. (2005). Tensional Homeostasis and the Malignant Phenotype. *Cancer cell* 8, 241–254. doi:10.1016/j.ccr.2005.08.010

Paul, M. K., Bisht, B., Darmawan, D. O., Chiou, R., Ha, V. L., Wallace, W. D., et al. (2014). Dynamic Changes in Intracellular ROS Levels Regulate Airway Basal Stem Cell Homeostasis through Nrf2-dependent Notch Signaling. *Cell Stem Cell* 15, 199–214. doi:10.1016/j.stem.2014.05.009

Peng, G., and Liu, Y. (2015). Hypoxia-inducible Factors in Cancer Stem Cells and Inflammation. *Trends Pharmacol. Sci.* 36, 374–383. doi:10.1016/j.tips.2015.03.003

Peng, J.-J., Xiong, S.-Q., Ding, L.-X., Peng, J., and Xia, X.-B. (2019). Diabetic Retinopathy: Focus on NADPH Oxidase and its Potential as Therapeutic Target. *Eur. J. Pharmacol.* 853, 381–387. doi:10.1016/j.ejphar.2019.04.038

Perillo, B., Di Donato, M., Pezone, A., Di Zazzo, E., Giovannelli, P., Galasso, G., et al. (2020). ROS in Cancer Therapy: the Bright Side of the Moon. *Exp. Mol. Med.* 52, 192–203. doi:10.1038/s12276-020-0384-2

Pervaiz, S., Taneja, R., and Ghaffari, S. (2009). Oxidative Stress Regulation of Stem and Progenitor Cells. *Antioxidants Redox Signal.* 11, 2777–2789. doi:10.1089/ars.2009.2804

Petruzzelli, R., Christensen, D. R., Parry, K. L., Sanchez-Elsner, T., and Houghton, F. D. (2014). HIF-2α Regulates NANOG Expression in Human Embryonic Stem Cells Following Hypoxia and Reoxygenation through the Interaction with an Oct-Sox Cis Regulatory Element. *PloS one* 9, e108309. doi:10.1371/journal.pone.0108309

Piccolo, S., Dupont, S., and Cordenonsi, M. (2014). The Biology of YAP/TAZ: Hippo Signaling and beyond. *Physiol. Rev.* 94, 1287–1312. doi:10.1152/physrev.00005.2014

Pietruczuk, P., Jain, A., Simo-Cheyou, E. R., Anand-Srivastava, M. B., and Srivastava, A. K. (2019). Protein Kinase B/AKT Mediates Insulin-like Growth Factor 1-induced Phosphorylation and Nuclear Export of Histone Deacetylase 5 via NADPH Oxidase 4 Activation in Vascular Smooth Muscle Cells. *J. Cell. Physiology* 234, 17337–17350. doi:10.1002/jcp.28353

Pires, P. W., and Earley, S. (2017). Redox Regulation of Transient Receptor Potential Channels in the Endothelium. *Microcirculation* 24. doi:10.1111/micc.12329

Poernbacher, I., Baumgartner, R., Marada, S. K., Edwards, K., and Stocker, H. (2012). Drosophila Pez Acts in Hippo Signaling to Restrict Intestinal Stem Cell Proliferation. *Curr. Biol.* 22, 389–396. doi:10.1016/j.cub.2012.01.019

Poon, E., Harris, A. L., and Ashcroft, M. (2009). Targeting the Hypoxia-Inducible Factor (HIF) Pathway in Cancer. *Expert Rev. Mol. Med.* 11, e26. doi:10.1017/s1462399409001173

Prabhakar, N. R., and Semenza, G. L. (2012). Adaptive and Maladaptive Cardiorespiratory Responses to Continuous and Intermittent Hypoxia Mediated by Hypoxia-Inducible Factors 1 and 2. *Physiol. Rev.* 92, 967–1003. doi:10.1152/physrev.00030.2011

Pratt, S. J. P., Lee, R. M., Chang, K. T., Hernández-Ochoa, E. O., Annis, D. A., Ory, E. C., et al. (2020). Mechanoactivation of NOX2-Generated ROS Elicits Persistent TRPM8 Ca 2+ Signals that Are Inhibited by Oncogenic KRas. *Proc. Natl. Acad. Sci. U.S.A.* 117, 26008–26019. doi:10.1073/pnas.2009495117

Prior, K.-K., Wittig, I., Leisegang, M. S., Groenendyk, J., Weissmann, N., Michalak, M., et al. (2016). The Endoplasmic Reticulum Chaperone Calnexin Is a NADPH Oxidase NOX4 Interacting Protein. *J. Biol. Chem.* 291, 7045–7059. doi:10.1074/jbc.m115.710772

Prosser, B. L., Khairallah, R. J., Ziman, A. P., Ward, C. W., and Lederer, W. J. (2013). X-ROS Signaling in the Heart and Skeletal Muscle: Stretch-dependent Local ROS Regulates [Ca2+]i. *J. Mol. Cell. Cardiol.* 58, 172–181. doi:10.1016/j.yjmcc.2012.11.011

Prosser, B. L., Ward, C. W., and Lederer, W. J. (2011). X-ROS Signaling: Rapid Mechano-Chemo Transduction in Heart. *Science* 333, 1440–1445. doi:10.1126/science.1202768

Qi, J., Kim, H., Scortegagna, M., and Ronai, Z. e. A. (2013). Regulators and Effectors of Siah Ubiquitin Ligases. *Cell Biochem. Biophys.* 67, 15–24. doi:10.1007/s12013-013-9636-2

Qiang, L., Wu, T., Zhang, H.-W., Lu, N., Hu, R., Wang, Y.-J., et al. (2012). HIF-1α Is Critical for Hypoxia-Mediated Maintenance of Glioblastoma Stem Cells by Activating Notch Signaling Pathway. *Cell Death Differ.* 19, 284–294. doi:10.1038/cdd.2011.95

Quinn, N. P., Garcia-Gutierrez, L., Doherty, C., Von Kriegsheim, A., Fallahi, E., Sacks, D. B., et al. (2021). IQGAP1 Is a Scaffold of the Core Proteins of the Hippo Pathway and Negatively Regulates the Pro-apoptotic Signal Mediated by This Pathway. *Cells* 10. doi:10.3390/cells10020478

Raad, H., Paciet, M.-H., Boussetta, T., Kroviarski, Y., Morel, F., Quinn, M. T., et al. (2009). Regulation of the Phagocyte NADPH Oxidase Activity: Phosphorylation of gp91phox/NOX2 by Protein Kinase C Enhances its Diaphorase Activity and Binding to Rac2, P67phox, and P47phox. *FASEB J.* 23, 1011–1022. doi:10.1096/fj.08-114553

Rababa'h, A., Craft, J. W., Jr., Wijaya, C. S., Atrooz, F., Fan, Q., Singh, S., et al. (2013). Protein Kinase A and phosphodiesterase-4D3 Binding to Coding Polymorphisms of Cardiac Muscle Anchoring Protein (mAKAP). *J. Mol. Biol.* 425, 3277–3288. doi:10.1016/j.jmb.2013.06.014

Ragsdale, G. K., Phelps, J., and Luby-Phelps, K. (1997). Viscoelastic Response of Fibroblasts to Tension Transmitted through Adherens Junctions. *Biophysical J.* 73, 2798–2808. doi:10.1016/s0006-3495(97)78309-7

Raman, D., and Pervaiz, S. (2019). Redox Inhibition of Protein Phosphatase PP2A: Potential Implications in Oncogenesis and its Progression. *Redox Biol.* 27, 101105. doi:10.1016/j.redox.2019.101105

Rao, R. K., and Clayton, L. W. (2002). Regulation of Protein Phosphatase 2A by Hydrogen Peroxide and Glutathionylation. *Biochem. Biophysical Res. Commun.* 293, 610–616. doi:10.1016/s0006-291x(02)00268-1

Rastogi, R., Geng, X., Li, F., and Ding, Y. (2016). NOX Activation by Subunit Interaction and Underlying Mechanisms in Disease. *Front. Cell Neurosci.* 10, 301. doi:10.3389/fncel.2016.00301

Ray, P. D., Huang, B.-W., and Tsuji, Y. (2012). Reactive Oxygen Species (ROS) Homeostasis and Redox Regulation in Cellular Signaling. *Cell. Signal.* 24, 981–990. doi:10.1016/j.cellsig.2012.01.008

Regier, D. S., Waite, K. A., Wallin, R., and Mcphail, L. C. (1999). A Phosphatidic Acid-Activated Protein Kinase and Conventional Protein Kinase C Isoforms Phosphorylate P22 , an NADPH Oxidase Component. *J. Biol. Chem.* 274, 36601–36608. doi:10.1074/jbc.274.51.36601

Reinhart-King, C. A., Dembo, M., and Hammer, D. A. (2008). Cell-cell Mechanical Communication through Compliant Substrates. *Biophysical J.* 95, 6044–6051. doi:10.1529/biophysj.107.127662

Reynafarje, B., Costa, L. E., and Lehninger, A. L. (1985). O2 Solubility in Aqueous Media Determined by a Kinetic Method. *Anal. Biochem.* 145, 406–418. doi:10.1016/0003-2697(85)90381-1

Richard, D. E., Berra, E., Gothié, E., Roux, D., and Pouysségur, J. (1999). p42/p44 Mitogen-Activated Protein Kinases Phosphorylate Hypoxia-Inducible Factor 1α (HIF-1α) and Enhance the Transcriptional Activity of HIF-1. *J. Biol. Chem.* 274, 32631–32637. doi:10.1074/jbc.274.46.32631

Rivas, S., Antón, I. M., and Wandosell, F. (2018). WIP-YAP/TAZ as A New Pro-oncogenic Pathway in Glioma. *Cancers (Basel)* 10. doi:10.3390/cancers10060191

Robison, P., Caporizzo, M. A., Ahmadzadeh, H., Bogush, A. I., Chen, C. Y., Margulies, K. B., et al. (2016). Detyrosinated Microtubules Buckle and Bear Load in Contracting Cardiomyocytes. *Science* 352, aaf0659. doi:10.1126/science.aaf0659

Rohwer, N., and Cramer, T. (2011). Hypoxia-mediated Drug Resistance: Novel Insights on the Functional Interaction of HIFs and Cell Death Pathways. *Drug Resist. Updat.* 14, 191–201. doi:10.1016/j.drup.2011.03.001

Rosenbluh, J., Nijhawan, D., Cox, A. G., Li, X., Neal, J. T., Schafer, E. J., et al. (2012). β-Catenin-Driven Cancers Require a YAP1 Transcriptional Complex for Survival and Tumorigenesis. *Cell* 151, 1457–1473. doi:10.1016/j.cell.2012.11.026

Rudolph, J. (2005). Redox Regulation of the Cdc25 Phosphatases. *Antioxidants Redox Signal.* 7, 761–767. doi:10.1089/ars.2005.7.761

Saito, S., Lin, Y.-C., Tsai, M.-H., Lin, C.-S., Murayama, Y., Sato, R., et al. (2015). Emerging Roles of Hypoxia-Inducible Factors and Reactive Oxygen Species in Cancer and Pluripotent Stem Cells. *Kaohsiung J. Med. Sci.* 31, 279–286. doi:10.1016/j.kjms.2015.03.002

Sánchez-de-Diego, C., Valer, J. A., Pimenta-Lopes, C., Rosa, J. L., and Ventura, F. (2019). Interplay between BMPs and Reactive Oxygen Species in Cell Signaling and Pathology. *Biomolecules* 9. doi:10.3390/biom9100534

Santabárbara-Ruiz, P., López-Santillán, M., Martínez-Rodríguez, I., Binagui-Casas, A., Pérez, L., Milán, M., et al. (2015). ROS-induced JNK and P38 Signaling Is Required for Unpaired Cytokine Activation during Drosophila Regeneration. *PLoS Genet.* 11, e1005595. doi:10.1371/journal.pgen.1005595

Santinon, G., Pocaterra, A., and Dupont, S. (2016). Control of YAP/TAZ Activity by Metabolic and Nutrient-Sensing Pathways. *Trends Cell Biol.* 26, 289–299. doi:10.1016/j.tcb.2015.11.004

Santos, C. X., Hafstad, A. D., Beretta, M., Zhang, M., Molenaar, C., Kopec, J., et al. (2016). Targeted Redox Inhibition of Protein Phosphatase 1 by Nox4 Regulates eIF 2α-mediated Stress Signaling. *EMBO J.* 35, 319–334. doi:10.15252/embj.201592394

Sarkar, T. R., Sharan, S., Wang, J., Pawar, S. A., Cantwell, C. A., Johnson, P. F., et al. (2012). Identification of a Src Tyrosine Kinase/SIAH2 E3 Ubiquitin Ligase Pathway that Regulates C/EBPδ Expression and Contributes to Transformation of Breast Tumor Cells. *Mol. Cell Biol.* 32, 320–332. doi:10.1128/mcb.05790-11

Sarmasti Emami, S., Zhang, D., and Yang, X. (2020). Interaction of the Hippo Pathway and Phosphatases in Tumorigenesis. *Cancers (Basel)* 12. doi:10.3390/cancers12092438

Sarti, P., Antonini, G., Malatesta, R., Vallone, B., and Brunori, M. (1988). Is the Internal Electron Transfer the Rate-Limiting Step in the Catalytic Cycle of Cytochrome C Oxidase? *Ann. N. Y. Acad. Sci.* 550, 161–166. doi:10.1111/j.1749-6632.1988.tb35332.x

Sasai, Y. (2013). Cytosystems Dynamics in Self-Organization of Tissue Architecture. *Nature* 493, 318–326. doi:10.1038/nature11859

Saucedo, L. J., and Edgar, B. A. (2007). Filling Out the Hippo Pathway. *Nat. Rev. Mol. Cell Biol.* 8, 613–621. doi:10.1038/nrm2221

Sauer, H., Ruhe, C., Müller, J. P., Schmelter, M., D'Souza, R., and Wartenberg, M. (2008). Reactive Oxygen Species and Upregulation of NADPH Oxidases in Mechanotransduction of Embryonic Stem Cells. *Methods Mol. Biol.* 477, 397–418. doi:10.1007/978-1-60327-517-0_30

Sayedyahossein, S., Li, Z., Hedman, A. C., Morgan, C. J., and Sacks, D. B. (2016). IQGAP1 Binds to Yes-Associated Protein (YAP) and Modulates its Transcriptional Activity. *J. Biol. Chem.* 291, 19261–19273. doi:10.1074/jbc.m116.732529

Scarborough, E. A., Uchida, K., Vogel, M., Erlitzki, N., Iyer, M., Phyo, S. A., et al. (2021). Microtubules Orchestrate Local Translation to Enable Cardiac Growth. *Nat. Commun.* 12, 1547. doi:10.1038/s41467-021-21685-4

Schieber, M., and Chandel, N. S. (2014). ROS Function in Redox Signaling and Oxidative Stress. *Curr. Biol.* 24, R453–R462. doi:10.1016/j.cub.2014.03.034

Schlegelmilch, K., Mohseni, M., Kirak, O., Pruszak, J., Rodriguez, J. R., Zhou, D., et al. (2011). Yap1 Acts Downstream of α-Catenin to Control Epidermal Proliferation. *Cell* 144, 782–795. doi:10.1016/j.cell.2011.02.031

Schmelter, M., et al.Schmelter, M., Ateghang, B., Helmig, S., Wartenberg, M., Sauer, H. (2006). Embryonic Stem Cells Utilize Reactive Oxygen Species as Transducers of Mechanical Strain-induced Cardiovascular Differentiation. *FASEB J.* 20, 1182–1184. doi:10.1096/fj.05-4723fje

Schofield, C. J., and Ratcliffe, P. J. (2004). Oxygen Sensing by HIF Hydroxylases. *Nat. Rev. Mol. Cell Biol.* 5, 343–354. doi:10.1038/nrm1366

Schöning, J. P., Monteiro, M., and Gu, W. (2017). Drug Resistance and Cancer Stem Cells: the Shared but Distinct Roles of Hypoxia-inducible Factors HIF 1α and HIF 2α. *Clin. Exp. Pharmacol. Physiol.* 44, 153–161. doi:10.1111/1440-1681.12693

Schröder, K., Wandzioch, K., Helmcke, I., and Brandes, R. P. (2009). Nox4 Acts as a Switch between Differentiation and Proliferation in Preadipocytes. *Arterioscler. Thromb. Vasc. Biol.* 29, 239–245. doi:10.1161/ATVBAHA.108.174219

Schröder, K. (2014). NADPH Oxidases in Redox Regulation of Cell Adhesion and Migration. *Antioxidants Redox Signal.* 20, 2043–2058. doi:10.1089/ars.2013.5633

Selfridge, A. C., Cavadas, M. A. S., Scholz, C. C., Campbell, E. L., Welch, L. C., Lecuona, E., et al. (2016). Hypercapnia Suppresses the HIF-dependent Adaptive Response to Hypoxia. *J. Biol. Chem.* 291, 11800–11808. doi:10.1074/jbc.m116.713941

Seltana, A., Basora, N., and Beaulieu, J.-F. o. (2010). Intestinal Epithelial Wound Healing Assay in an Epithelialâ€"mesenchymal Co-culture System. *Wound Repair Regen.* 18, 114–122. doi:10.1111/j.1524-475x.2009.00554.x

Semenza, G. L. (2010). HIF-1: Upstream and Downstream of Cancer Metabolism. *Curr. Opin. Genet. Dev.* 20, 51–56. doi:10.1016/j.gde.2009.10.009

Semenza, G. L. (2003). Targeting HIF-1 for Cancer Therapy. *Nat. Rev. Cancer* 3, 721–732. doi:10.1038/nrc1187

Serrano, I., Mcdonald, P. C., Lock, F., Muller, W. J., and Dedhar, S. (2013). Inactivation of the Hippo Tumour Suppressor Pathway by Integrin-Linked Kinase. *Nat. Commun.* 4, 2976. doi:10.1038/ncomms3976

Seth, D., and Rudolph, J. (2006). Redox Control of Cell Cycle Progression via Cdc25 Phosphatase (Mih1p) in *S. cerevisiae*. *Cell Cycle* 5, 2172–2173. doi:10.4161/cc.5.18.3252

Sette, C., and Conti, M. (1996). Phosphorylation and Activation of a cAMP-specific Phosphodiesterase by the cAMP-dependent Protein Kinase. *J. Biol. Chem.* 271, 16526–16534. doi:10.1074/jbc.271.28.16526

Settleman, J., and Baum, B. (2008). Cell Shape and Tissue Morphogenesis. *Seminars Cell & Dev. Biol.* 19, 213–214. doi:10.1016/j.semcdb.2008.02.002

Sharma, S., Sirin, Y., and Susztak, K. (2011). The Story of Notch and Chronic Kidney Disease. *Curr. Opin. Nephrol. Hypertens.* 20, 56–61. doi:10.1097/mnh.0b013e3283414c88

Shaw, R. J., Paez, J. G., Curto, M., Yaktine, A., Pruitt, W. M., Saotome, I., et al. (2001). The Nf2 Tumor Suppressor, Merlin, Functions in Rac-dependent Signaling. *Dev. Cell* 1, 63–72. doi:10.1016/s1534-5807(01)00009-0

Shen, X., Xi, G., Radhakrishnan, Y., and Clemmons, D. R. (2009). Identification of Novel SHPS-1-Associated Proteins and Their Roles in Regulation of Insulin-like Growth Factor-dependent Responses in Vascular Smooth Muscle Cells. *Mol. Cell. Proteomics* 8, 1539–1551. doi:10.1074/mcp.m800543-mcp200

Sherman, L. S., and Gutmann, D. H. (2001). Merlin: Hanging Tumor Suppression on the Rac. *Trends Cell Biol.* 11, 442–444. doi:10.1016/s0962-8924(01)81334-9

Shin, S. Y., Kim, C. G., Jho, E.-H., Rho, M.-S., Kim, Y. S., Kim, Y.-H., et al. (2004). Hydrogen Peroxide Negatively Modulates Wnt Signaling through Downregulation of β-catenin. *Cancer Lett.* 212, 225–231. doi:10.1016/j.canlet.2004.03.003

Shirai, Y., and Saito, N. (2002). Activation Mechanisms of Protein Kinase C: Maturation, Catalytic Activation, and Targeting. *J. Biochem.* 132, 663–668. doi:10.1093/oxfordjournals.jbchem.a003271

Sick, S., Reinker, S., Timmer, J., and Schlake, T. (2006). WNT and DKK Determine Hair Follicle Spacing through a Reaction-Diffusion Mechanism. *Science* 314, 1447–1450. doi:10.1126/science.1130088

Sidhaye, V. K., Schweitzer, K. S., Caterina, M. J., Shimoda, L., and King, L. S. (2008). Shear Stress Regulates Aquaporin-5 and Airway Epithelial Barrier Function. *Proc. Natl. Acad. Sci. U.S.A.* 105, 3345–3350. doi:10.1073/pnas.0712287105

Siebel, C., and Lendahl, U. (2017). Notch Signaling in Development, Tissue Homeostasis, and Disease. *Physiol. Rev.* 97, 1235–1294. doi:10.1152/physrev.00005.2017

Silver, B. B., Wolf, A. E., Lee, J., Pang, M.-F., and Nelson, C. M. (2020). Epithelial Tissue Geometry Directs Emergence of Bioelectric Field and Pattern of Proliferation. *MBoC* 31, 1691–1702. doi:10.1091/mbc.e19-12-0719

Silvis, M. R., Kreger, B. T., Lien, W. H., Klezovitch, O., Rudakova, G. M., Camargo, F. D., et al. (2011). α-Catenin Is a Tumor Suppressor that Controls Cell Accumulation by Regulating the Localization and Activity of the Transcriptional Coactivator Yap1. *Sci. Signal* 4, ra33. doi:10.1126/scisignal.2001823

Sim, J., Cowburn, A. S., Palazon, A., Madhu, B., Tyrakis, P. A., Macías, D., et al. (2018). The Factor Inhibiting HIF Asparaginyl Hydroxylase Regulates Oxidative Metabolism and Accelerates Metabolic Adaptation to Hypoxia. *Cell Metab.* 27, 898–913. doi:10.1016/j.cmet.2018.02.020

Singh, R., Adhya, P., and Sharma, S. S. (2021). Redox-sensitive TRP Channels: a Promising Pharmacological Target in Chemotherapy-Induced Peripheral Neuropathy. *Expert Opin. Ther. Targets* 25, 529–545. doi:10.1080/14728222.2021.1956464

Sirin, Y., and Susztak, K. (2012). Notch in the Kidney: Development and Disease. *J. Pathol.* 226, 394–403. doi:10.1002/path.2967

Skonieczna, M., Hejmo, T., Poterala-Hejmo, A., Cieslar-Pobuda, A., and Buldak, R. J. (2017). NADPH Oxidases: Insights into Selected Functions and Mechanisms of Action in Cancer and Stem Cells. *Oxid. Med. Cell Longev.* 2017, 9420539. doi:10.1155/2017/9420539

Skouloudaki, K., and Walz, G. (2012). YAP1 Recruits C-Abl to Protect Angiomotin-like 1 from Nedd4-Mediated Degradation. *PloS one* 7, e35735. doi:10.1371/journal.pone.0035735

Smith, J. M., Hedman, A. C., and Sacks, D. B. (2015). IQGAPs Choreograph Cellular Signaling from the Membrane to the Nucleus. *Trends Cell Biol.* 25, 171–184. doi:10.1016/j.tcb.2014.12.005

Smoot, R. L., Werneburg, N. W., Sugihara, T., Hernandez, M. C., Yang, L., Mehner, C., et al. (2018). Platelet-derived Growth Factor Regulates YAP Transcriptional Activity via Src Family Kinase Dependent Tyrosine Phosphorylation. *J. Cell. Biochem.* 119, 824–836. doi:10.1002/jcb.26246

Sodhi, A., Montaner, S., Patel, V., Zohar, M., Bais, C., Mesri, E. A., et al. (2000). The Kaposi's Sarcoma-Associated Herpes Virus G Protein-Coupled Receptor Up-Regulates Vascular Endothelial Growth Factor Expression and Secretion through Mitogen-Activated Protein Kinase and P38 Pathways Acting on Hypoxia-Inducible Factor 1alpha. *Cancer Res.* 60, 4873–4880.

Song, M. Y., Makino, A., and Yuan, J. X.-J. (2011). Role of Reactive Oxygen Species and Redox in Regulating the Function of Transient Receptor Potential Channels. *Antioxidants Redox Signal.* 15, 1549–1565. doi:10.1089/ars.2010.3648

Spiegelman, B. M., and Ginty, C. A. (1983). Fibronectin Modulation of Cell Shape and Lipogenic Gene Expression in 3T3-Adipocytes. *Cell* 35, 657–666. doi:10.1016/0092-8674(83)90098-3

Sporn, M. B., and Liby, K. T. (2012). NRF2 and Cancer: the Good, the Bad and the Importance of Context. *Nat. Rev. Cancer* 12, 564–571. doi:10.1038/nrc3278

Sprouse, M. L., Welte, T., Boral, D., Liu, H. N., Yin, W., Vishnoi, M., et al. (2019). PMN-MDSCs Enhance CTC Metastatic Properties through Reciprocal Interactions via ROS/Notch/Nodal Signaling. *Int. J. Mol. Sci.* 20. doi:10.3390/ijms20081916

Stegen, S., Laperre, K., Eelen, G., Rinaldi, G., Fraisl, P., Torrekens, S., et al. (2019). HIF-1α Metabolically Controls Collagen Synthesis and Modification in Chondrocytes. *Nature* 565, 511–515. doi:10.1038/s41586-019-0874-3

Steinberg, S. F. (2015). Mechanisms for Redox-Regulation of Protein Kinase C. *Front. Pharmacol.* 6, 128. doi:10.3389/fphar.2015.00128

Strowitzki, M. J., Cummins, E. P., and Taylor, C. T. (2019). Protein Hydroxylation by Hypoxia-Inducible Factor (HIF) Hydroxylases: Unique or Ubiquitous? *Cells* 8. doi:10.3390/cells8050384

Su, T., Ludwig, M. Z., Xu, J., and Fehon, R. G. (2017). Kibra and Merlin Activate the Hippo Pathway Spatially Distinct from and Independent of Expanded. *Dev. Cell* 40, 478–490. doi:10.1016/j.devcel.2017.02.004

Sudol, M. (1994). Yes-associated Protein (YAP65) Is a Proline-Rich Phosphoprotein that Binds to the SH3 Domain of the Yes Proto-Oncogene Product. *Oncogene* 9, 2145–2152.

Sudol, M., Chen, H. I., Bougeret, C., Einbond, A., and Bork, P. (1995). Characterization of a Novel Protein-Binding Module - the WW Domain. *FEBS Lett.* 369, 67–71. doi:10.1016/0014-5793(95)00550-s

Sugihara, T., Werneburg, N. W., Hernandez, M. C., Yang, L., Kabashima, A., Hirsova, P., et al. (2018). YAP Tyrosine Phosphorylation and Nuclear Localization in Cholangiocarcinoma Cells Are Regulated by LCK and Independent of LATS Activity. *Mol. Cancer Res.* 16, 1556–1567. doi:10.1158/1541-7786.mcr-18-0158

Suzuki, A., and Ohno, S. (2006). The PAR-aPKC System: Lessons in Polarity. *J. Cell Sci.* 119, 979–987. doi:10.1242/jcs.02898

Taddei, M. L., Parri, M., Mello, T., Catalano, A., Levine, A. D., Raugei, G., et al. (2007). Integrin-mediated Cell Adhesion and Spreading Engage Different Sources of Reactive Oxygen Species. *Antioxidants Redox Signal.* 9, 469–481. doi:10.1089/ars.2006.1392

Takemura, Y., Goodson, P., Bao, H. F., Jain, L., and Helms, M. N. (2010). Rac1-mediated NADPH Oxidase Release of O2− Regulates Epithelial Sodium Channel Activity in the Alveolar Epithelium. *Am. J. Physiology-Lung Cell. Mol. Physiology* 298, L509–L520. doi:10.1152/ajplung.00230.2009

Tamura, M., Itoh, K., Akita, H., Takano, K., and Oku, S. (2006). Identification of an Actin-Binding Site in P47phoxan Organizer Protein of NADPH Oxidase. *FEBS Lett.* 580, 261–267. doi:10.1016/j.febslet.2005.11.080

Tang, X., Jang, S.-W., Wang, X., Liu, Z., Bahr, S. M., Sun, S.-Y., et al. (2007). Akt Phosphorylation Regulates the Tumour-Suppressor Merlin through

Ubiquitination and Degradation. *Nat. Cell Biol.* 9, 1199–1207. doi:10.1038/ncb1641

Tannahill, G. M., Curtis, A. M., Adamik, J., Palsson-Mcdermott, E. M., Mcgettrick, A. F., Goel, G., et al. (2013). Succinate Is an Inflammatory Signal that Induces IL-1β through HIF-1α. *Nature* 496, 238–242. doi:10.1038/nature11986

Tarhonskaya, H., Hardy, A. P., Howe, E. A., Loik, N. D., Kramer, H. B., Mccullagh, J. S. O., et al. (2015). Kinetic Investigations of the Role of Factor Inhibiting Hypoxia-Inducible Factor (FIH) as an Oxygen Sensor. *J. Biol. Chem.* 290, 19726–19742. doi:10.1074/jbc.m115.653014

Tawadros, A. I. F., and Khalafalla, M. M. M. (2018). Expression of Programmed Death-Ligand 1 and Hypoxia-Inducible Factor-1α Proteins in Endometrial Carcinoma. *J. Cancer Res. Ther.* 14, S1063–S1069. doi:10.4103/0973-1482.202891

Taylor-Clark, T. E. (2016). Role of Reactive Oxygen Species and TRP Channels in the Cough Reflex. *Cell Calcium* 60, 155–162. doi:10.1016/j.ceca.2016.03.007

Teo, Y. V., Rattanavirotkul, N., Olova, N., Salzano, A., Quintanilla, A., Tarrats, N., et al. (2019). Notch Signaling Mediates Secondary Senescence. *Cell Rep.* 27, 997–1007. doi:10.1016/j.celrep.2019.03.104

Terraciano, V., Hwang, N., Moroni, L., Park, H. B., Zhang, Z., Mizrahi, J., et al. (2007). Differential Response of Adult and Embryonic Mesenchymal Progenitor Cells to Mechanical Compression in Hydrogels. *Stem Cells* 25, 2730–2738. doi:10.1634/stemcells.2007-0228

Terry, S., Buart, S., and Chouaib, S. (2017). Hypoxic Stress-Induced Tumor and Immune Plasticity, Suppression, and Impact on Tumor Heterogeneity. *Front. Immunol.* 8, 1625. doi:10.3389/fimmu.2017.01625

Tian, H., Mcknight, S. L., and Russell, D. W. (1997). Endothelial PAS Domain Protein 1 (EPAS1), a Transcription Factor Selectively Expressed in Endothelial Cells. *Genes Dev.* 11, 72–82. doi:10.1101/gad.11.1.72

Tominaga, T., Sahai, E., Chardin, P., Mccormick, F., Courtneidge, S. A., and Alberts, A. S. (2000). Diaphanous-related Formins Bridge Rho GTPase and Src Tyrosine Kinase Signaling. *Mol. Cell* 5, 13–25. doi:10.1016/s1097-2765(00)80399-8

Tong, W. W., Tong, G. H., and Liu, Y. (2018). Cancer Stem Cells and Hypoxia-Inducible Factors (Review). *Int. J. Oncol.* 53, 469–476. doi:10.3892/ijo.2018.4417

Topalian, S. L., Hodi, F. S., Brahmer, J. R., Gettinger, S. N., Smith, D. C., Mcdermott, D. F., et al. (2012). Safety, Activity, and Immune Correlates of Anti-PD-1 Antibody in Cancer. *N. Engl. J. Med.* 366, 2443–2454. doi:10.1056/nejmoa1200690

Toriyama, M., Sakumura, Y., Shimada, T., Ishii, S., and Inagaki, N. (2010). A Diffusion-based Neurite Length-sensing Mechanism Involved in Neuronal Symmetry Breaking. *Mol. Syst. Biol.* 6, 394. doi:10.1038/msb.2010.51

Totaro, A., Castellan, M., Di Biagio, D., and Piccolo, S. (2018a). Crosstalk between YAP/TAZ and Notch Signaling. *Trends Cell Biol.* 28, 560–573. doi:10.1016/j.tcb.2018.03.001

Totaro, A., Panciera, T., and Piccolo, S. (2018b). YAP/TAZ Upstream Signals and Downstream Responses. *Nat. Cell Biol.* 20, 888–899. doi:10.1038/s41556-018-0142-z

Touyz, R. M., and Briones, A. M. (2011). Reactive Oxygen Species and Vascular Biology: Implications in Human Hypertension. *Hypertens. Res.* 34, 5–14. doi:10.1038/hr.2010.201

Tu, X., Yasuda, R., and Colgan, L. A. (2020). Rac1 Is a Downstream Effector of PKCα in Structural Synaptic Plasticity. *Sci. Rep.* 10, 1777. doi:10.1038/s41598-020-58610-6

Tung, J.-N., Lin, P.-L., Wang, Y.-C., Wu, D.-W., Chen, C.-Y., and Lee, H. (2018). PD-L1 Confers Resistance to EGFR Mutation-independent Tyrosine Kinase Inhibitors in Non-small Cell Lung Cancer via Upregulation of YAP1 Expression. *Oncotarget* 9, 4637–4646. doi:10.18632/oncotarget.23161

Turing, A. (1952). The Chemical Basis of Morphogenesis. *Phil. Trans. Roy. Soc. Lond. B Biol. Sci.* 237, 37.

Turrens, J. F. (2003). Mitochondrial Formation of Reactive Oxygen Species. *J. Physiology* 552, 335–344. doi:10.1113/jphysiol.2003.049478

Tykocki, N. R., Jackson, W. F., and Watts, S. W. (2012). Reverse-mode Na+/Ca2+ Exchange Is an Important Mediator of Venous Contraction. *Pharmacol. Res.* 66, 544–554. doi:10.1016/j.phrs.2012.08.004

Uchida, K., Scarborough, E. A., and Prosser, B. L. (2021). Cardiomyocyte Microtubules: Control of Mechanics, Transport, and Remodeling. *Annu. Rev. Physiol.* 10, 257–283. doi:10.1146/annurev-physiol-062421-040656

Ushio-Fukai, M. (2009). Compartmentalization of Redox Signaling through NADPH Oxidase-Derived ROS. *Antioxidants Redox Signal.* 11, 1289–1299. doi:10.1089/ars.2008.2333

Vaezi, A., Bauer, C., Vasioukhin, V., and Fuchs, E. (2002). Actin Cable Dynamics and Rho/Rock Orchestrate a Polarized Cytoskeletal Architecture in the Early Steps of Assembling a Stratified Epithelium. *Dev. Cell* 3, 367–381. doi:10.1016/s1534-5807(02)00259-9

Valle-Prieto, A., and Conget, P. A. (2010). Human Mesenchymal Stem Cells Efficiently Manage Oxidative Stress. *Stem cells Dev.* 19, 1885–1893. doi:10.1089/scd.2010.0093

Van Mameren, J., Vermeulen, K. C., Gittes, F., and Schmidt, C. F. (2009). Leveraging Single Protein Polymers to Measure Flexural Rigidity. *J. Phys. Chem. B* 113, 3837–3844. doi:10.1021/jp808328a

Van Veelen, W., Le, N. H., Helvensteijn, W., Blonden, L., Theeuwes, M., Bakker, E. R. M., et al. (2011). -catenin Tyrosine 654 Phosphorylation Increases Wnt Signalling and Intestinal Tumorigenesis. *Gut* 60, 1204–1212. doi:10.1136/gut.2010.233460

Veith, A., and Moorthy, B. (2018). Role of Cytochrome P450s in the Generation and Metabolism of Reactive Oxygen Species. *Curr. Opin. Toxicol.* 7, 44–51. doi:10.1016/j.cotox.2017.10.003

Violi, F., and Pignatelli, P. (2014). Platelet NOX, a Novel Target for Anti-thrombotic Treatment. *Thromb. Haemost.* 111, 817–823. doi:10.1160/TH13-10-0818

Voet, D., and Voet, J. G. (2011). *Biochemistry*. Hoboken, NJ: John Wiley & Sons.

Wang, C.-Y., Yang, T.-T., Chen, C.-L., Lin, W.-C., and Lin, C.-F. (2014a). Reactive Oxygen Species-Regulated Glycogen Synthase Kinase-3β Activation Contributes to All-Trans Retinoic Acid-Induced Apoptosis in Granulocyte-Differentiated HL60 Cells. *Biochem. Pharmacol.* 88, 86–94. doi:10.1016/j.bcp.2013.12.021

Wang, G. L., Jiang, B. H., Rue, E. A., and Semenza, G. L. (1995). Hypoxia-inducible Factor 1 Is a Basic-Helix-Loop-Helix-PAS Heterodimer Regulated by Cellular O2 Tension. *Proc. Natl. Acad. Sci. U.S.A.* 92, 5510–5514. doi:10.1073/pnas.92.12.5510

Wang, K., Degerny, C., Xu, M., and Yang, X.-J. (2009). YAP, TAZ, and Yorkie: a Conserved Family of Signal-Responsive Transcriptional Coregulators in Animal Development and Human diseaseThis Paper Is One of a Selection of Papers Published in This Special Issue, Entitled CSBMCB's 51st Annual Meeting - Epigenetics and Chromatin Dynamics, and Has Undergone the Journal's Usual Peer Review Process. *Biochem. Cell Biol.* 87, 77–91. doi:10.1139/o08-114

Wang, M., Dai, M., Wang, D., Xiong, W., Zeng, Z., and Guo, C. (2021). The Regulatory Networks of the Hippo Signaling Pathway in Cancer Development. *J. Cancer* 12, 6216–6230. doi:10.7150/jca.62402

Wang, R., Peterson, J., Aster, R. H., and Newman, P. J. (1997). Disruption of a Long-Range Disulfide Bond between Residues Cys406 and Cys655 in Glycoprotein IIIa Does Not Affect the Function of Platelet Glycoprotein IIb-IIIa. *Blood* 90, 1718–1719. doi:10.1182/blood.v90.4.1718.1718_1718_1719

Wang, W., Huang, J., Wang, X., Yuan, J., Li, X., Feng, L., et al. (2012). PTPN14 Is Required for the Density-dependent Control of YAP1. *Genes Dev.* 26, 1959–1971. doi:10.1101/gad.192955.112

Wang, W., Li, X., Huang, J., Feng, L., Dolinta, K. G., and Chen, J. (2014b). Defining the Protein-Protein Interaction Network of the Human Hippo Pathway. *Mol. Cell. Proteomics* 13, 119–131. doi:10.1074/mcp.m113.030049

Wang, Z., Da Silva, T. G., Jin, K., Han, X., Ranganathan, P., Zhu, X., et al. (2014c). Notch Signaling Drives Stemness and Tumorigenicity of Esophageal Adenocarcinoma. *Cancer Res.* 74, 6364–6374. doi:10.1158/0008-5472.can-14-2051

Watanabe, T., Noritake, J., Kakeno, M., Matsui, T., Harada, T., Wang, S., et al. (2009). Phosphorylation of CLASP2 by GSK-3β Regulates its Interaction with IQGAP1, EB1 and Microtubules. *J. Cell Sci.* 122, 2969–2979. doi:10.1242/jcs.046649

Watanabe, Y., Miyasaka, K. Y., Kubo, A., Kida, Y. S., Nakagawa, O., Hirate, Y., et al. (2017). Notch and Hippo Signaling Converge on Strawberry Notch 1 (Sbno1) to Synergistically Activate Cdx2 during Specification of the Trophectoderm. *Sci. Rep.* 7, 46135. doi:10.1038/srep46135

Watson, W. H., Ritzenthaler, J. D., and Roman, J. (2016). Lung Extracellular Matrix and Redox Regulation. *Redox Biol.* 8, 305–315. doi:10.1016/j.redox.2016.02.005

Wei, Y., Yee, P. P., Liu, Z., Zhang, L., Guo, H., Zheng, H., et al. (2020). NEDD4L-mediated Merlin Ubiquitination Facilitates Hippo Pathway Activation. *EMBO Rep.* 21, e50642. doi:10.15252/embr.202050642

Wen, Q., Han, T., Wang, Z., and Jiang, S. (2020). Role and Mechanism of Programmed Death-Ligand 1 in Hypoxia-Induced Liver Cancer Immune Escape. *Oncol. Lett.* 19, 2595–2601. doi:10.3892/ol.2020.11369

Weng, M.-S., Chang, J.-H., Hung, W.-Y., Yang, Y.-C., and Chien, M.-H. (2018). The Interplay of Reactive Oxygen Species and the Epidermal Growth Factor Receptor in Tumor Progression and Drug Resistance. *J. Exp. Clin. Cancer Res.* 37, 61. doi:10.1186/s13046-018-0728-0

Werner, E., and Werb, Z. (2002). Integrins Engage Mitochondrial Function for Signal Transduction by a Mechanism Dependent on Rho GTPases. *J. Cell Biol.* 158, 357–368. doi:10.1083/jcb.200111028

White, C. D., Erdemir, H. H., and Sacks, D. B. (2012). IQGAP1 and its Binding Proteins Control Diverse Biological Functions. *Cell. Signal.* 24, 826–834. doi:10.1016/j.cellsig.2011.12.005

Widmaier, M., Rognoni, E., Radovanac, K., Azimifar, S. B., and Fässler, R. (2012). Integrin-linked Kinase at a Glance. *J. Cell Sci.* 125, 1839–1843. doi:10.1242/jcs.093864

Wikström, M., and Springett, R. (2020). Thermodynamic Efficiency, Reversibility, and Degree of Coupling in Energy Conservation by the Mitochondrial Respiratory Chain. *Commun. Biol.* 3, 451. doi:10.1038/s42003-020-01192-w

Wilkinson, H. N., and Hardman, M. J. (2020). Wound Healing: Cellular Mechanisms and Pathological Outcomes. *Open Biol.* 10, 200223. doi:10.1098/rsob.200223

Wilkinson-Berka, J. L., Rana, I., Armani, R., and Agrotis, A. (2013). Reactive Oxygen Species, Nox and Angiotensin II in Angiogenesis: Implications for Retinopathy. *Clin. Sci. (Lond)* 124, 597–615. doi:10.1042/cs20120212

Wilson, C., and González-Billault, C. (2015). Regulation of Cytoskeletal Dynamics by Redox Signaling and Oxidative Stress: Implications for Neuronal Development and Trafficking. *Front. Cell. Neurosci.* 9, 381. doi:10.3389/fncel.2015.00381

Wilson, K. E., Li, Y.-W., Yang, N., Shen, H., Orillion, A. R., and Zhang, J. (2014). PTPN14 Forms a Complex with Kibra and LATS1 Proteins and Negatively Regulates the YAP Oncogenic Function. *J. Biol. Chem.* 289, 23693–23700. doi:10.1074/jbc.m113.534701

Wozniak, M. A., and Chen, C. S. (2009). Mechanotransduction in Development: a Growing Role for Contractility. *Nat. Rev. Mol. Cell Biol.* 10, 34–43. doi:10.1038/nrm2592

Wu, L., Li, Y., Yu, M., Yang, F., Tu, M., and Xu, H. (2018). Notch Signaling Regulates Microglial Activation and Inflammatory Reactions in a Rat Model of Temporal Lobe Epilepsy. *Neurochem. Res.* 43, 1269–1282. doi:10.1007/s11064-018-2544-5

Wu, N., Nguyen, Q., Wan, Y., Zhou, T., Venter, J., Frampton, G. A., et al. (2017). The Hippo Signaling Functions through the Notch Signaling to Regulate Intrahepatic Bile Duct Development in Mammals. *Lab. Invest* 97, 843–853. doi:10.1038/labinvest.2017.29

Wu, R. F., Gu, Y., Xu, Y. C., Nwariaku, F. E., and Terada, L. S. (2003). Vascular Endothelial Growth Factor Causes Translocation of P47 to Membrane Ruffles through WAVE1. *J. Biol. Chem.* 278, 36830–36840. doi:10.1074/jbc.m302251200

Xi, G., Shen, X.-C., Wai, C., and Clemmons, D. R. (2013). Recruitment of Nox4 to a Plasma Membrane Scaffold Is Required for Localized Reactive Oxygen Species Generation and Sustained Src Activation in Response to Insulin-like Growth Factor-I. *J. Biol. Chem.* 288, 15641–15653. doi:10.1074/jbc.m113.456046

Xiang, L., Gilkes, D. M., Hu, H., Luo, W., Bullen, J. W., Liang, H., et al. (2015). HIF-1α and TAZ Serve as Reciprocal Co-activators in Human Breast Cancer Cells. *Oncotarget* 6, 11768–11778. doi:10.18632/oncotarget.4190

Xiang, L., Gilkes, D. M., Hu, H., Takano, N., Luo, W., Lu, H., et al. (2014). Hypoxia-inducible Factor 1 Mediates TAZ Expression and Nuclear Localization to Induce the Breast Cancer Stem Cell Phenotype. *Oncotarget* 5, 12509–12527. doi:10.18632/oncotarget.2997

Xiao, L., Chen, Y., Ji, M., and Dong, J. (2011a). KIBRA Regulates Hippo Signaling Activity via Interactions with Large Tumor Suppressor Kinases. *J. Biol. Chem.* 286, 7788–7796. doi:10.1074/jbc.m110.173468

Xiao, L., Chen, Y., Ji, M., Volle, D. J., Lewis, R. E., Tsai, M.-Y., et al. (2011b). KIBRA Protein Phosphorylation Is Regulated by Mitotic Kinase Aurora and Protein Phosphatase 1. *J. Biol. Chem.* 286, 36304–36315. doi:10.1074/jbc.m111.246850

Xie, Q., Chen, J., Feng, H., Peng, S., Adams, U., Bai, Y., et al. (2013). YAP/TEAD-mediated Transcription Controls Cellular Senescence. *Cancer Res.* 73, 3615–3624. doi:10.1158/0008-5472.can-12-3793

Xiu, M., Wang, Y., Li, B., Wang, X., Xiao, F., Chen, S., et al. (2021). The Role of Notch3 Signaling in Cancer Stemness and Chemoresistance: Molecular Mechanisms and Targeting Strategies. *Front. Mol. Biosci.* 8, 694141. doi:10.3389/fmolb.2021.694141

Xu, D., and Li, C. (2021). Regulation of the SIAH2-HIF-1 Axis by Protein Kinases and its Implication in Cancer Therapy. *Front. Cell Dev. Biol.* 9, 646687. doi:10.3389/fcell.2021.646687

Xu, M. Z., Yao, T.-J., Lee, N. P. Y., Ng, I. O. L., Chan, Y.-T., Zender, L., et al. (2009). Yes-associated Protein Is an Independent Prognostic Marker in Hepatocellular Carcinoma. *Cancer* 115, 4576–4585. doi:10.1002/cncr.24495

Xu, Q., Huff, L. P., Fujii, M., and Griendling, K. K. (2017). Redox Regulation of the Actin Cytoskeleton and its Role in the Vascular System. *Free Radic. Biol. Med.* 109, 84–107. doi:10.1016/j.freeradbiomed.2017.03.004

Xu, X., Shen, X., Wang, J., Feng, W., Wang, M., Miao, X., et al. (2021a). YAP Prevents Premature Senescence of Astrocytes and Cognitive Decline of Alzheimer's Disease through Regulating CDK6 Signaling. *Aging Cell* 20, e13465. doi:10.1111/acel.13465

Xu, Z., Liang, Y., Delaney, M. K., Zhang, Y., Kim, K., Li, J., et al. (2021b). Shear and Integrin Outside-In Signaling Activate NADPH-Oxidase 2 to Promote Platelet Activation. *Atvb* 41, 1638–1653. doi:10.1161/atvbaha.120.315773

Yamauchi, J., Miyamoto, Y., Kusakawa, S., Torii, T., Mizutani, R., Sanbe, A., et al. (2008). Neurofibromatosis 2 Tumor Suppressor, the Gene Induced by Valproic Acid, Mediates Neurite Outgrowth through Interaction with Paxillin. *Exp. Cell Res.* 314, 2279–2288. doi:10.1016/j.yexcr.2008.03.019

Yan, F., Wang, Y., Wu, X., Peshavariya, H. M., Dusting, G. J., Zhang, M., et al. (2014). Nox4 and Redox Signaling Mediate TGF-β-Induced Endothelial Cell Apoptosis and Phenotypic Switch. *Cell Death Dis.* 5, e1010. doi:10.1038/cddis.2013.551

Yan, Z.-Y., Ban, T., Fan, Y., Chen, W.-R., Sun, H.-L., Chen, H., et al. (2015). Na+-induced Ca2+ Influx through Reverse Mode of Na+-Ca2+ Exchanger in Mouse Ventricular Cardiomyocyte. *Oncotarget* 6, 23272–23280. doi:10.18632/oncotarget.4878

Yang, M., Soga, T., Pollard, P. J., and Adam, J. (2012). The Emerging Role of Fumarate as an Oncometabolite. *Front. Oncol.* 2, 85. doi:10.3389/fonc.2012.00085

Yasuda, D., Kobayashi, D., Akahoshi, N., Ohto-Nakanishi, T., Yoshioka, K., Takuwa, Y., et al. (2019). Lysophosphatidic Acid-Induced YAP/TAZ Activation Promotes Developmental Angiogenesis by Repressing Notch Ligand Dll4. *J. Clin. Invest* 129, 4332–4349. doi:10.1172/jci121955

Yazaki, K., Matsuno, Y., Yoshida, K., Sherpa, M., Nakajima, M., Matsuyama, M., et al. (2021). ROS-Nrf2 Pathway Mediates the Development of TGF-B1-Induced Epithelial-Mesenchymal Transition through the Activation of Notch Signaling. *Eur. J. Cell Biol.* 100, 151181. doi:10.1016/j.ejcb.2021.151181

Yeo, C. D., Kang, N., Choi, S. Y., Kim, B. N., Park, C. K., Kim, J. W., et al. (2017). The Role of Hypoxia on the Acquisition of Epithelial-Mesenchymal Transition and Cancer Stemness: a Possible Link to Epigenetic Regulation. *Korean J. Intern Med.* 32, 589–599. doi:10.3904/kjim.2016.302

Yi, C., Shen, Z., Stemmer-Rachamimov, A., Dawany, N., Troutman, S., Showe, L. C., et al. (2013). The P130 Isoform of Angiomotin Is Required for Yap-Mediated Hepatic Epithelial Cell Proliferation and Tumorigenesis. *Sci. Signal* 6, ra77. doi:10.1126/scisignal.2004060

Yi, C., Troutman, S., Fera, D., Stemmer-Rachamimov, A., Avila, J. L., Christian, N., et al. (2011). A Tight Junction-Associated Merlin-angiomotin Complex Mediates Merlin's Regulation of Mitogenic Signaling and Tumor Suppressive Functions. *Cancer cell* 19, 527–540. doi:10.1016/j.ccr.2011.02.017

Yin, F., Yu, J., Zheng, Y., Chen, Q., Zhang, N., and Pan, D. (2013). Spatial Organization of Hippo Signaling at the Plasma Membrane Mediated by the Tumor Suppressor Merlin/NF2. *Cell* 154, 1342–1355. doi:10.1016/j.cell.2013.08.025

Yoshihama, Y., Hirai, T., Ohtsuka, T., and Chida, K. (2009). KIBRA Co-localizes with Protein Kinase Mζ (PKMζ) in the Mouse Hippocampus. *Biosci. Biotechnol. Biochem.* 73, 147–151. doi:10.1271/bbb.80564

Yoshihama, Y., Sasaki, K., Horikoshi, Y., Suzuki, A., Ohtsuka, T., Hakuno, F., et al. (2011). KIBRA Suppresses Apical Exocytosis through Inhibition of aPKC

Kinase Activity in Epithelial Cells. *Curr. Biol.* 21, 705–711. doi:10.1016/j.cub.2011.03.029

Yu, F.-X., and Guan, K.-L. (2013). The Hippo Pathway: Regulators and Regulations. *Genes Dev.* 27, 355–371. doi:10.1101/gad.210773.112

Yu, F.-X., Zhao, B., and Guan, K.-L. (2015). Hippo Pathway in Organ Size Control, Tissue Homeostasis, and Cancer. *Cell* 163, 811–828. doi:10.1016/j.cell.2015.10.044

Yu, H., Pardoll, D., and Jove, R. (2009). STATs in Cancer Inflammation and Immunity: a Leading Role for STAT3. *Nat. Rev. Cancer* 9, 798–809. doi:10.1038/nrc2734

Yu, J., Zheng, Y., Dong, J., Klusza, S., Deng, W.-M., and Pan, D. (2010). Kibra Functions as a Tumor Suppressor Protein that Regulates Hippo Signaling in Conjunction with Merlin and Expanded. *Dev. Cell* 18, 288–299. doi:10.1016/j.devcel.2009.12.012

Zaltsman, Y., Masuko, S., Bensen, J. J., and Kiessling, L. L. (2019). Angiomotin Regulates YAP Localization during Neural Differentiation of Human Pluripotent Stem Cells. *Stem Cell Rep.* 12, 869–877. doi:10.1016/j.stemcr.2019.03.009

Zanconato, F., Battilana, G., Cordenonsi, M., and Piccolo, S. (2016a). YAP/TAZ as Therapeutic Targets in Cancer. *Curr. Opin. Pharmacol.* 29, 26–33. doi:10.1016/j.coph.2016.05.002

Zanconato, F., Cordenonsi, M., and Piccolo, S. (2016b). YAP/TAZ at the Roots of Cancer. *Cancer cell* 29, 783–803. doi:10.1016/j.ccell.2016.05.005

Zeller, K. S., Riaz, A., Sarve, H., Li, J., Tengholm, A., and Johansson, S. (2013). The Role of Mechanical Force and ROS in Integrin-dependent Signals. *PloS one* 8, e64897. doi:10.1371/journal.pone.0064897

Zergane, M., Kuebler, W. M., and Michalick, L. (2021). Heteromeric TRP Channels in Lung Inflammation. *Cells* 10. doi:10.3390/cells10071654

Zhang, H.-M., Chen, W., Liu, R.-N., and Zhao, Y. (2018a). Notch Inhibitor Can Attenuate Apparent Diffusion Coefficient and Improve Neurological Function through Downregulating NOX2-ROS in Severe Traumatic Brain Injury. *Dddt* 12, 3847–3854. doi:10.2147/dddt.s174037

Zhang, J., Yang, P. L., and Gray, N. S. (2009). Targeting Cancer with Small Molecule Kinase Inhibitors. *Nat. Rev. Cancer* 9, 28–39. doi:10.1038/nrc2559

Zhang, L., Wu, J., Duan, X., Tian, X., Shen, H., Sun, Q., et al. (2016). NADPH Oxidase: A Potential Target for Treatment of Stroke. *Oxid. Med. Cell Longev.* 2016, 5026984. doi:10.1155/2016/5026984

Zhang, L., Yang, S., Wennmann, D. O., Chen, Y., Kremerskothen, J., and Dong, J. (2014). KIBRA: In the Brain and beyond. *Cell. Signal.* 26, 1392–1399. doi:10.1016/j.cellsig.2014.02.023

Zhang, R., Pan, Y., Fanelli, V., Wu, S., Luo, A. A., Islam, D., et al. (2015). Mechanical Stress and the Induction of Lung Fibrosis via the Midkine Signaling Pathway. *Am. J. Respir. Crit. Care Med.* 192, 315–323. doi:10.1164/rccm.201412-2326oc

Zhang, X., Li, Y., Ma, Y., Yang, L., Wang, T., Meng, X., et al. (2018b). Yes-associated Protein (YAP) Binds to HIF-1α and Sustains HIF-1α Protein Stability to Promote Hepatocellular Carcinoma Cell Glycolysis under Hypoxic Stress. *J. Exp. Clin. Cancer Res.* 37, 216. doi:10.1186/s13046-018-0892-2

Zhao, B., Li, L., Lei, Q., and Guan, K.-L. (2010a). The Hippo-YAP Pathway in Organ Size Control and Tumorigenesis: an Updated Version. *Genes Dev.* 24, 862–874. doi:10.1101/gad.1909210

Zhao, B., Li, L., Lu, Q., Wang, L. H., Liu, C.-Y., Lei, Q., et al. (2011a). Angiomotin Is a Novel Hippo Pathway Component that Inhibits YAP Oncoprotein. *Genes Dev.* 25, 51–63. doi:10.1101/gad.2000111

Zhao, B., Li, L., Tumaneng, K., Wang, C.-Y., and Guan, K.-L. (2010b). A Coordinated Phosphorylation by Lats and CK1 Regulates YAP Stability through SCFβ-TRCP. *Genes Dev.* 24, 72–85. doi:10.1101/gad.1843810

Zhao, B., Tumaneng, K., and Guan, K.-L. (2011b). The Hippo Pathway in Organ Size Control, Tissue Regeneration and Stem Cell Self-Renewal. *Nat. Cell Biol.* 13, 877–883. doi:10.1038/ncb2303

Zhao, C., Zeng, C., Ye, S., Dai, X., He, Q., Yang, B., et al. (2020). Yes-associated Protein (YAP) and Transcriptional Coactivator with a PDZ-Binding Motif (TAZ): a Nexus between Hypoxia and Cancer. *Acta Pharm. Sin. B* 10, 947–960. doi:10.1016/j.apsb.2019.12.010

Zhao, X., and Guan, J.-L. (2011). Focal Adhesion Kinase and its Signaling Pathways in Cell Migration and Angiogenesis. *Adv. Drug Deliv. Rev.* 63, 610–615. doi:10.1016/j.addr.2010.11.001

Zhao, Y., and Yang, X. (2015). The Hippo Pathway in Chemotherapeutic Drug Resistance. *Int. J. Cancer* 137, 2767–2773. doi:10.1002/ijc.29293

Zheng, Y., and Pan, D. (2019). The Hippo Signaling Pathway in Development and Disease. *Dev. Cell* 50, 264–282. doi:10.1016/j.devcel.2019.06.003

Zhong, H., De Marzo, A. M., Laughner, E., Lim, M., Hilton, D. A., Zagzag, D., et al. (1999). Overexpression of Hypoxia-Inducible Factor 1alpha in Common Human Cancers and Their Metastases. *Cancer Res.* 59, 5830–5835.

Zhou, L., Cha, G., Chen, L., Yang, C., Xu, D., and Ge, M. (2019). HIF1α/PD-L1 axis Mediates Hypoxia-Induced Cell Apoptosis and Tumor Progression in Follicular Thyroid Carcinoma. *Ott* 12, 6461–6470. doi:10.2147/ott.s203724

Zhou, P.-J., Xue, W., Peng, J., Wang, Y., Wei, L., Yang, Z., et al. (2017). Elevated Expression of Par3 Promotes Prostate Cancer Metastasis by Forming a Par3/aPKC/KIBRA Complex and Inactivating the Hippo Pathway. *J. Exp. Clin. Cancer Res.* 36, 139. doi:10.1186/s13046-017-0609-y

Zhou, R., Wu, Q., Wang, M., Irani, S., Li, X., Zhang, Q., et al. (2021). The Protein Phosphatase PPM1A Dephosphorylates and Activates YAP to Govern Mammalian Intestinal and Liver Regeneration. *PLoS Biol.* 19, e3001122. doi:10.1371/journal.pbio.3001122

Zong, Y., Panikkar, A., Xu, J., Antoniou, A., Raynaud, P., Lemaigre, F., et al. (2009). Notch Signaling Controls Liver Development by Regulating Biliary Differentiation. *Development* 136, 1727–1739. doi:10.1242/dev.029140

Zorov, D. B., Juhaszova, M., and Sollott, S. J. (2014). Mitochondrial Reactive Oxygen Species (ROS) and ROS-Induced ROS Release. *Physiol. Rev.* 94, 909–950. doi:10.1152/physrev.00026.2013

Conflict of Interest: The author declares that the research was conducted in the absence of any commercial or financial relationships that could be construed as a potential conflict of interest.

GLOSSARY

AEC2, anion exchange protein 2

AJ, adherens junction

AKAP, A-kinase anchoring protein

ALK5, activin A receptor type II-like kinase, 53kDa, transforming growth factor β receptor I

AMOT, angiomotin

Ang II,

angiotensin II

AMPK, 5′ AMP-activated protein kinase

APC, adenomatous polyposis coli

aPKC, atypical protein kinase C

AQP, aquaporin

ARHGEF, Rho-guanine nucleotide exchange factor

ARID1A, AT-rich interactive domain-containing protein 1A

BMK1/Erk5, big MAP kinase

BMP, bone morphogenic protein

BNIP, BCL2/adenovirus E1B 19 kDa protein-interacting protein

βPIX, p21-activated protein kinase-exchange factor β

CAF, cancer-associated fibroblast

CaMK2, Ca^{2+}/calmodulin-dependent kinase 2

CaMKP, CaMK phosphatase

CBP, cyclic adenosine monophosphate response element-binding protein-binding protein, also named CREB-binding protein (CREBBP)

CK1, casein kinase 1

CK2, casein kinase 2

CLASP1, cytoplasmic linker associated protein 1

CLIP1, CAP-GLY domain-containing linker protein 1

CREBBP, cyclic adenosine monophosphate response element-binding protein-binding protein, also named CBP

CSC, cancer stem cell

CSC-like, cancer stem cell-like

CSL, the transcriptional repressor CBF1/suppressor of hairless/Lag-1

CTC, circulating tumor cell

CTGF, connective tissue growth factor

Dll1, Delta-like 1

Dll4, Delta-like 4

DVL, Dishevelled

ECM, extracellular matrix

Ect2, epithelial cell transforming sequence 2

EGF, epidermal growth factor (EGF)

EMI, epithelial-mesenchymal interaction

EMT, epithelial-mesenchymal transition

ENaC, epithelial sodium channels

ENO1, enolase 1

ErK1/2, extracellular regulated kinases 1/2

ETC, electron transfer chain

Ex, Expanded

FAD, flavin adenine dinucleotide

$FADH_2$, the reduced form of FAD

FAK, focal adhesion kinase

FBD, FERM-binding domain

FERM, 4.1 protein, ezrin, radixin, and moesin

FGF, fibroblast growth factor

FIH, the factor inhibiting HIF

FRM6, FERM domain-containing protein 6

GEF, guanine-nucleotide exchange factor

GLUT, glucose transporter

Grb2, growth factor receptor-bound protein 2

GSK3β, glycogen synthase kinase 3β

HCC, hepatocellular carcinoma cell

HIF, hypoxia-inducible factor

HK, hexokinase

HPH, HIF prolyl hydroxylases

HRE, hypoxia-responsive element

IAP, integrin-associated protein

IFN, interferon

IGF-1, insulin-like growth factor-1

IGF-1R, IGF-1 receptor

IκBα, nuclear factor of kappa light polypeptide gene enhancer in B-cells inhibitor, alpha

IL, interleukin

ILK, integrin-linked kinase

INF-2, inverted formin-2

IQGAP1, IQ motif-containing GTPase activating protein 1

Jag2, Jagged-2

JaK2, Janus kinase 2

JNK, Jun N-terminal kinase

KIBRA, kidney and brain expressed protein

Keap1, Kelch-like ECH-associated protein 1

LATS1/2, large tumor suppressor kinase 1/2

LDHA, lactate dehydrogenase A

LMW-PTP, low molecular weight protein tyrosine phosphatase

LOX, lysyl oxidase

LOXL, LOX-like enzymes

mAKAP, muscle-selective A-kinase anchoring protein

MAP4K, mitogen-activated protein kinase kinase kinase kinase

MAPK, mitogen-activated protein kinase

MDSC, myeloid-derived suppressor cell

Merlin, moesin/ezrin/radixin-like protein

Mito, mitochondria

MLC, myosin light chain

MOB1, Mps one binder (MOB) kinase activator-like 1

MSC, mesenchymal stem cell

MST1/2, mammalian Ste20-like protein kinase 1/2

MVB, multi-vesicular body

MYPT1, myosin phosphatase target subunit 1

NAD^+, nicotinamide adenine dinucleotide

$NADP^+$, nicotinamide adenine dinucleotide phosphate

NADPH, the reduced form of nicotinamide adenine dinucleotide phosphate

NCX, sodium-calcium exchanger

NEDD4, neural precursor cell expressed developmentally downregulated protein 4

NES, nuclear export signal

NF2, neurofibromatosis type 2

NF-κB, nuclear factor kappa-light-chain-enhancer of activated B cells

NICD, Notch intracellular domain

NLK, Nemo-like kinase

NLS, nuclear localization signal

NOS, nitric oxide synthase

NOX, NADPH oxidases

Nrf2, nuclear factor erythroid-derived 2-related factor 2

NRX, nucleoredoxin

NSCLC, non–small cell lung cancer

p300, E1A binding protein p300

PA, phosphatidic acid

PAK, P21-activated protein kinase

PALS1, protein associated with Caenorhabditis elegans Lin-7 protein 1

PAR3, partition-defective 3

PAR6β, partition-defective 6β

PATJ, PALS1-associated tight junction protein

PD-1, programmed death-1

PDE, phosphodiesterase

PDGF, platelet-derived growth factor

PDK, pyruvate dehydrogenase kinase (PDK)

PD-L1, programmed death ligand-1

PDZ, Post-synaptic density 95, Discs large, and Zonula occludens-1

PHD prolyl hydroxylase domain-containing proteins

PID, protein interaction domain

PI3K, phosphatidyl-inositol-3-kinase

PIP_2, phosphatidylinositol (4,5)-bisphosphate

PIP_3, phosphatidylinositol (3,4,5)-trisphosphate

PIX, p21-activated protein kinase exchange factor

PKA, cAMP-dependent protein kinase

PKB, protein kinase B

PKC, protein kinase C

PKG, cGMP-dependent protein kinase

PKM2, pyruvate kinase isozymes M2

Poldip2, polymerase δ-interacting protein 2

POPX2, partner of PIX 2, also known as protein phosphatase 2C-like domain-containing metal-dependent protein phosphatase (PPM), PPM1F, or CaMK phosphatase (CaMKP)

PP2AC, PP2A catalytic subunit

PPM, protein phosphatase 2C-like domain-containing metal-dependent protein phosphatase

PPM1A, protein phosphatase, Mg^{2+}/Mn^{2+}-dependent 1A

PPM1F, protein phosphatase, Mg^{2+}/Mn^{2+}-dependent 1F

PPP, protein serine/threonine phosphatases

PTEN, phosphatase and tensin homolog

PTK protein tyrosine kinase

PTM, post-translational modification

PTP, protein tyrosine phosphatases

PTPN14, protein tyrosine phosphatase non-receptor type 14

PX, pbox consensus sequence

Pyk2, proline-rich tyrosine kinase 2

Rac1, Ras-related C3 botulinum toxin substrate 1

RASSF, Ras-association domain family

RBPJ, recombination signal-binding protein for immunoglobulin κJ region

Ref-1, redox factor-1

RhoA, Ras homolog family member A

ROCK, Rho-associated protein kinase

RyR, ryanodine receptor

SARAH, SAV/RASSF/HPO

SAV1, Salvador family WW domain-containing protein 1

SCF, Skp1-Cullin-1-F-box protein

$SCF^{β\text{-}TrCP}$, SCF type of E3 ubiquitin ligase

SCLC, small cell lung cancer

SH2, Src homology 2

SHP, SH2 domain-containing protein tyrosine phosphatase

SHPS-1, SHP substrate-1

SIAH1/2, seven in absentia homolog 1/2

SLMAP, sarcolemmal membrane-associated protein

Smad3, mothers against decapentaplegic homolog 3

SNF, sucrose non-fermentable

SR, sarcoplasmic reticulum

Src, steroid receptor coactivator

SrcFK, Src family kinase

STAT3, signal transducer and activator of transcription 3

STK25, serine/threonine kinase 25

STRIP1/2, STRN-interacting protein 1/2

STRIPAK, STRN-interacting phosphatase and kinase

STRN, striatin

SWH, Salvador–Warts–Hippo

SWI, switch

TAZ, transcriptional coactivator with PDZ-binding motif

TE, trophectoderm

TEAD, the transcriptional enhancer factor TEF-1, TEC1, and AbaA (TEA) domain

TGFβ, transforming growth factor-β

TGFβR, transforming growth factor-β receptor

TJ, tight junction

TME, tumor microenvironment

TNF, tumor necrosis factor

TRAF4, TNF receptor-associated factor 4

TRP, transient receptor potential

VEGF, vascular EGF

VEGFR, VEGF receptor

VHL, von Hippel–Lindau tumor suppressor protein E3 ubiquitin ligase

WASP, Wiskott–Aldrich syndrome protein

WAVE1, WASP family verprolin homologous protein 1

WWC, WW domain and C2 domain-containing protein

WWTR1, WW domain-containing transcription regulator 1

X-ROS, NOX-derived ROS

YAP, Yes-associated protein

Yes, Src family, non-receptor proto-oncogene tyrosine-protein kinase.

Advantages of publishing in Frontiers

OPEN ACCESS
Articles are free to read for greatest visibility and readership

FAST PUBLICATION
Around 90 days from submission to decision

HIGH QUALITY PEER-REVIEW
Rigorous, collaborative, and constructive peer-review

TRANSPARENT PEER-REVIEW
Editors and reviewers acknowledged by name on published articles

Frontiers
Avenue du Tribunal-Fédéral 34
1005 Lausanne | Switzerland

Visit us: www.frontiersin.org
Contact us: frontiersin.org/about/contact

REPRODUCIBILITY OF RESEARCH
Support open data and methods to enhance research reproducibility

DIGITAL PUBLISHING
Articles designed for optimal readership across devices

FOLLOW US
@frontiersin

IMPACT METRICS
Advanced article metrics track visibility across digital media

EXTENSIVE PROMOTION
Marketing and promotion of impactful research

LOOP RESEARCH NETWORK
Our network increases your article's readership